

Institut für Nutzpflanzenwissenschaften und Ressourcenschutz
- Pflanzenernährung -

**The Role of Lipids in the Formation of Beneficial
Interactions Between Plant Roots and Soil
Microbiota under Heat Stress**

Dissertation

zur Erlangung des Grades

Doctor of Philosophy (Ph.D.)

der Landwirtschaftlichen Fakultät
der Rheinischen Friedrich-Wilhelms-Universität Bonn

von

Allene Andaya Macabuhay

aus

Masbate, Philippinen

Bonn 2024

Referent: Prof. Dr. Gabriel Schaaf

Korreferentin: Prof. Dr. Ute Roessner

Tag der mündlichen Prüfung: 25.10.2023

Angefertigt mit Genehmigung der Landwirtschaftlichen Fakultät der Universität Bonn

Thesis abstract

Climate change, which is characterized by the rise of global atmospheric temperatures known as global warming, has serious detrimental effects on crop production because of the direct influence of elevated temperature on plant development. One novel strategy to increase crop productivity while mitigating heat stress is the use of soil microbes, which is slowly gaining popularity because of its low-cost approach, availability, sustainability, and quick turnover. Specific soil microbes can form symbiotic relationships with the roots, whose beneficial effects on plant growth and development, as well as on plant responses to biotic and abiotic stresses, lead to improved plant performance. The plant-microbe interaction is complex and involves below-ground communication, followed by modifications of molecular, biochemical, and morphological processes in the plant. Plant roots display extreme plasticity in adapting to a range of environmental stimuli and are therefore important indicators of plant-level responses to microbial colonization, via changes in architecture and metabolic processes. Lipids, which are essential constituents of the plasma membrane with diverse functions in cellular processes and homeostasis, have been proposed to play significant roles in the rhizosphere. Because heat stresses have a profound effect on membrane stability and lipid composition, rising global temperatures are likely to impact the formation of plant-microbe symbiosis.

This study aimed to characterize and quantify the bacteria-induced growth promotion and heat tolerance in plants, and to investigate how plant root lipid profiles are altered under both bacteria and high-temperature conditions. For that, advanced phenotyping and lipidomics technology were employed to monitor plant responses to developmental and environmental changes. By using the high-resolution, high-throughput phenotyping platform GrowScreen-Agar II, an open-top plant-bacteria co-cultivation system was optimized utilizing the model plant *Arabidopsis thaliana* and the plant-growth-promoting rhizobacteria (PGPR) *Paraburkholderia phytofirmans* PsJN. This allowed for in-depth, tissue- and time-specific root-and-shoot morphological trait characterization, which elucidated the dynamics of bacterial promotion on plant growth. We have quantified the magnitude of bacterial-induced plant stimulation between ambient and elevated temperatures, confirming the excellent benefit of the PGPR in ameliorating the adverse effects of heat stress. These morphological traits were also associated with the root lipid profile using *state-of-the-art* lipidomics technology, which revealed specific lipid species and their functions in this tripartite interaction. Knowledge gained from this study, besides being fundamental in the understanding of plant-microbe interactions, can also inform research agenda of future directions for microbial studies as potential agricultural and biotechnological solutions in the endeavor to address global food security under climate change.

Zusammenfassung

Der Klimawandel, der durch den auch als Erderwärmung bezeichneten Anstieg der globalen atmosphärischen Temperaturen gekennzeichnet ist, hat schwerwiegende negative Auswirkungen auf die Nutzpflanzenproduktion, da sich höhere Temperaturen direkt auf die Pflanzenentwicklung auswirken. Eine neuartige Strategie zur Steigerung der Pflanzenproduktivität bei gleichzeitiger Abschwächung von Hitzestress ist der Einsatz von Bodenmikroben, der aufgrund ihrer geringen Kosten, ihrer Verfügbarkeit, ihrer Nachhaltigkeit und ihres schnellen Umsatzes langsam an Popularität gewinnt. Einige dieser Mikroorganismen gehen mit Wurzeln symbiotische Beziehungen ein, die sich positiv auf Pflanzenwachstum und -entwicklung auswirken, Schutz vor biotischen und abiotischen Stressfaktoren bieten und hierdurch zu einer verbesserten Pflanzenleistung führen. Die Interaktion zwischen Pflanzen und Mikroben ist ein komplexer Prozess, der durch Kommunikationsprozesse im Boden sowie morphologische, molekulare und biochemische Veränderungen in der Pflanze gekennzeichnet ist. Wurzeln, mit ihrer hohen Plastizität in Anpassung an eine Vielzahl von Umweltreizen, sind wichtige Indikatoren für die Reaktionen der Pflanzen auf mikrobielle Besiedlung, wie sich durch Veränderungen in der Architektur und verschiedener Stoffwechselprozesse zeigt. Lipide, die wesentliche Bestandteile der Plasmamembranen sind und vielfältige Funktionen bei zellulären Prozessen und der Zellhomöostase erfüllen, spielen eine wichtige Rolle in der Rhizosphäre. Steigende globale Temperaturen werden wegen ihres Einflusses auf Membranstabilität und Lipidzusammensetzung wahrscheinlich große Auswirkungen auf die Bildung von Symbiosen zwischen Pflanzen und Mikroben haben.

Ziel dieser Studie war es, bakterieninduzierte Wachstumsförderung und Hitzetoleranz bei Pflanzen zu charakterisieren und zu untersuchen, wie sich die Lipidprofile von Pflanzenwurzeln durch Bakterien und erhöhte Temperaturen verändern. Um die Reaktionen der Pflanzen auf Entwicklungs- und Umweltveränderungen zu untersuchen, wurden moderne Phänotypisierungs- und Lipidomik-Technologien eingesetzt. Mit Hilfe der hochauflösenden Hochdurchsatz-Phänotypisierungsplattform GrowScreen-Agar II wurde ein offenes Pflanzen-Bakterien-Kokultivierungssystem mit der Modellpflanze *Arabidopsis thaliana* und der pflanzenwachstumsfördernden Rhizobakterie (PGPR) *Paraburkholderia phytofirmans* PsJN optimiert. Dies ermöglichte eine eingehende, gewebe- und zeitaufgelöste Charakterisierung der morphologischen Eigenschaften von Wurzel und Spross, wodurch die Dynamik der bakteriellen Förderung des Pflanzenwachstums aufgeklärt werden konnte. Hierbei wurde das Ausmaß der bakteriell induzierten Pflanzenstimulation zwischen ambienter und erhöhter Temperatur quantifiziert und damit ein grosser Nutzen der PGPR bei der Abschwächung der negativen Auswirkungen von Hitzestress bestätigt. Morphologische Merkmale wurden auch mit dem Wurzellipidprofil in Verbindung gebracht, wobei die modernste Lipidomik-Technologie, die spezifische Lipidspezies und ihre Funktionen in dieser dreiteiligen Interaktion aufzeigte.

Die aus dieser Studie gewonnenen Erkenntnisse sind nicht nur für das Verständnis der Wechselwirkungen zwischen Pflanzen und Mikroben von grundlegender Bedeutung, sondern können in zukünftige mikrobielle Studien einfließen und damit potenzielle landwirtschaftliche und biotechnologische Lösungen für die Bewältigung der globalen Ernährungssicherheit im Klimawandel bieten.

Declaration

This is to certify that

- i. the thesis comprises only my original work towards the PhD
- ii. due acknowledgement has been made in the text to all other material used; and
- iii. the thesis is fewer than 100,000 words in length, exclusive of tables, maps, bibliographies and appendices.

Allene Andaya Macabuhay
School of BioSciences
The University of Melbourne
Parkville, Victoria 3010

Preface

The candidate has contributed to more than 50% of the content of this thesis and is the primary author of all publications derived from this thesis.

The growing of plants and bacteria, optimization of the co-cultivation system, measurements and periodic phenotyping of plants, time-course harvest, sample preparation, lipid extraction, mass spectrometric data analysis, results interpretation, and statistical analysis were carried out by the candidate. Project supervisors, Prof. Ute Roessner, Prof. Michelle Watt., A/Prof Alexander Johnson, Dr. Robert Walker, and Dr. Borjana Arsova were involved in the design of experiments and supervision of the candidate. Prof. Gabriel Schaaf supervised the candidate remotely from the University of Bonn.

Chapter 2 – A/Prof. Maria Josefina Poupin Swinburn (Universidad Adolfo Ibanez, Chile) provided the bacterial strain *Paraburkholderia phytofirmans* PsJN used at the University of Melbourne.

Chapter 3 – Prof. Michelle Watt and Dr. Borjana Arsova supervised the experimentation conducted at the Forschungszentrum Juelich. Anna Galinski provided training for the root analysis software (GrowScreen-Root). Dr. Bernd Kastenholz assisted in the plant cultivation for GrowScreen-Agar I and II platform. Dr. Kerstin Nagel and her team from the JPPC group (Dr. Henning Lenz, Dr. Alexander Putz, Dr. Sascha Adels, and Dr. Mark Mueller-Linow) developed the GrowScreen-Agar platforms, provided training, technical drawings, shoot analysis, and technical assistance throughout the use of the platform. Dr. Jana Kelm performed PCR analysis for 16S rRNA sequencing.

Chapter 4 – Dr. Atul Bhatnagar performed the LC-MS untargeted lipid data acquisition from the Sydney Mass Spectrometry facility. Dr. Cheka Kehelpannala assisted in the lipid extraction and provided training for the MS-DIAL lipid analysis.

All authors discussed the results and their implications and provided feedback on the manuscript at all stages.

Acknowledgement

First and foremost, I would like to say a heartfelt thanks to the Almighty for His benevolent love and constant reassurance that I am not alone in my struggles.

My PhD journey has been both challenging and rewarding. Through all of this, I am thankful for the people who have been a part of this bittersweet journey.

First, I would like to express my sincerest gratitude to my primary supervisor Prof. Ute Roessner, who has given me the rare opportunity of being a part of her group and working on her project. As an academic, her passion for research is infectious and motivating. Her support, time, and concern for everyone get her working even from a hospital bed, and even at surprising times and days. I am proud to have known such an inspiration, who has shown guidance and compassion throughout my PhD journey. I would also like to thank my FZJ supervisors Prof. Michelle Watt and Dr. Borjana Arsova who have shown support and assistance during my stay in Juelich, Germany. My overseas JUMPA experience has been excellent thanks to their careful management and assistance.

I would also like to thank my Melbourne supervisors, A/Prof Alex Johnson, for letting me be a part of and sharing his group's interests, and Dr. Robert Walker, who has been a delightful presence and support in the lab. Thank you for the insightful discussions and feedback, and for always responding whenever I need urgent help. Finally, I would like to acknowledge Prof. Gabriel Schaaf, who may have come late into the picture (as with my later University of Bonn enrolment as part of the JUMPA agreement), but who has certainly expressed concern over my welfare and provided valuable insights on my research, university, and career.

My deepest thanks and gratitude as well to the people at the Forschungszentrum Juelich – Helena, Stefan, Kelvin, Jana, and Tanya, who have taken me under their wings and made Germany a (third) home. Thank you for the chitchats, the bike rides, the lifts, the shared coffee breaks, and even the (failed) attempts to teach me the language.

I am also grateful to the people from the Roessner group, Martino, Sibel, Sneha, and Carl, whom I have shared many struggles with, particularly during the challenging times of the pandemic. I am particularly thankful for people who went out of their way to share a burden, to give a hand, and help me out, even if it was just to say, “How are you?..” “It’s ok..” Can I help?” For this, I would like to thank Tannaz, Cheka, and Pipob.

I am always thankful to my family who constantly checks on me and who always makes sure that I prioritize my health. They know how much it’s overlooked when I am drowning with work. It is hard being away from your loved ones, but it is a comfort to know that they are

together and have each other. To my relatives here and back home, who get worried when they do not hear from me (or from my social media), I am grateful to all of them.

Last but not the least, I would like to thank my partner, for his patience and understanding during this seemingly “unending” journey. He has been very supportive throughout my study, from Masters to PhD. I rarely cry when faced with hardships, but it is always a comfort to know that I have a cuddly chest to cry on when I need to. I can be difficult and demanding at times, especially during stressful situations during my PhD, but he stood by me and weathered my moods. Special mention to my furbaby, Thor, who kept me company during times when I had to burn the midnight (and dawn) candles.

Publications

Published articles

Macabuhay, A., Arsova, B., Walker, R., Johnson, A., Watt, M., & Roessner, U. (2022, 2022/02/01/). Modulators or facilitators? Roles of lipids in plant root–microbe interactions. *Trends in Plant Science*, 27(2), 180-190. <https://doi.org/10.1016/j.tplants.2021.08.004>

Presented in the Appendices

Macabuhay, A., Arsova, B., Watt, M., Nagel, K. A., Lenz, H., Putz, A., Adels, S., Müller-Linow, M., Kelm, J., Johnson, A. A. T., Walker, R., Schaaf, G., & Roessner, U. (2022). Plant Growth Promotion and Heat Stress Amelioration in *Arabidopsis* Inoculated with *Paraburkholderia phytofirmans* PsJN Rhizobacteria Quantified with the GrowScreen-Agar II Phenotyping Platform. *Plants*, 11(21), 2927. <https://doi.org/10.3390/plants11212927>

Presented in Chapter 3

Publication-in-progress

Macabuhay, A., Kehelpannala, C., Bhatnagar, A., Arsova, B., Walker, R., Johnson, A., Watt, M., Schaaf, G., & Roessner, U. Exploring lipid-mediated beneficial interactions between *Arabidopsis thaliana* roots and PGPR *Paraburkholderia phytofirmans* PsJN: Implications for plant growth promotion and heat stress resilience (*from Chapter 4*)

Abbreviations

$^1\text{O}_2$	singlet oxygen
2D or 3D	two/ three dimensional
ABA	abscisic acid
AHL	acylated homoserine lactones
AMF	arbuscular mycorrhizal fungi
AOS	activated oxygen species
APCI	atmospheric pressure chemical ionization
ATP	adenosine triphosphate
AzA	azelaic acid
BHT	butylated hydroxytoluene
CCD	carotenoid cleavage dioxygenases
CDP-DAG	cytidine diphosphate-diacylglycerol
CDPK	calcium dependent protein kinase
Cer	ceramide
CFC	chlorofluorocarbons
CH_4	Methane
CHCl_3	chloroform
CL	cardiolipin
CO_2	carbon dioxide
CoQ	coenzyme Q
CV	coefficient of variance
DAPG	2,4-Diacetylphloroglucinol
DBI	double bond index
DCA	α,ω -dicarboxylic acids
DG	diacylglycerol
DGDG	digalactosyldiacylglycerol
DGTS	diacylglyceryl trimethylhomoserine
DKP	diketopiperazines
DSF	diffusible signal factors
ENSO	El Niño–Southern Oscillation
EPS	exopolysaccharide
ERT	Electrical Resistance Tomography
ESI	electro-spray ionization
ETI	effector-triggered immunity
FA	fatty acyls
FC	fold change
GC	gas chromatography
GC-MS	gas chromatography - mass spectrometry
GL	Glycerolipids
GlcCer	glucosylceramides
GP	glycerophospholipids

GPI-PLC	glycosylphosphatidylinositol
Gro3P	glycerol-3-phosphate
GS	genome selection
GWAS	genome-wide association studies
H ₂ O ₂	hydrogen peroxide
HCl	hydrochloric acid
HexCer	hexosylceramides
HFC	hydrofluorocarbons
HPLC	high-performance liquid chromatography
HR	hypersensitive response
HRMS	high-resolution mass spectrometry
HSP	heat shock protein
IPCC	Intergovernmental Panel on Climate Change
ISR	induced systemic response
ISRD	internal standards
IUPAC-IUBMB	International Union of Pure and Applied Chemists and the International Union of Biochemistry
JA	jasmonic acid
LC	liquid chromatography
LCB	long-chain base
LC-MS	liquid chromatography - mass spectrometry
LC-MS/MS	liquid chromatography - tandem mass spectrometry
LCO	lipo-chitooligosaccharides
LEA	late embryogenesis abundant
LIPID MAPS	Lipid Metabolites and Pathways Strategy
LLE	liquid-liquid extraction
LPC	lysophosphatidylcholines
LPE	lysophosphatidylethanolamines
LPG	lysophosphatidylglycerol
MAMP	microbe-associated molecular patterns
MAPK	mitogen activated protein kinase
MAS	marker-assisted selection
MDMS	multi-dimensional MS
MeOH	methanol
MESA	methyl-salicylic acid
MG	monoacylglycerol
MGDG	monogalactosyldiacylglycerol
MiSSP7	mycorrhiza-induced small secreted protein 7
MON	monocillin I
MPK6	mitogen-activated protein kinase 6
MRM	multiple reaction monitoring
MS	mass spectrometry
MS/MS	tandem MS
MSI	mass spectrometry imaging

N ₂ O	nitrous oxide
NAE	N-acylethanolamines
nano-SIMS	nano-secondary ion mass spectrometry
NMR	nuclear magnetic resonance
O ²⁻	superoxide radical
OD ₆₀₀	optical density
OH ⁻	hydroxyl radical
OHFA	ω-hydroxy
OL	ornithine lipids
PA	phosphatidic acid
PAMP	pathogen-associated molecular pattern
PBS	phosphate buffered saline
PC	phosphatidylcholine
PCA	principal component analysis
PCD	programmed cell death
PE	phosphatidylethanolamine
PG	phosphatidylglycerol
PGPM	plant growth-promoting microorganisms
PGPR/F	plant growth-promoting rhizobacteria/ fungi
PI	phosphatidylinositol
PIP	phosphatidylinositol-4-monophosphate
PIP2	phosphatidylinositol-4,5-bisphosphate
PK	Polyketides
PLA/PLC PLD	Phospholipase A/C/D
PR	prenol lipids
PRM	parallel reaction monitoring
PRR	pattern recognition receptors
PS	phosphatidylserine
PSAT1	phospholipid acyltransferase 1
QqQ	triple quadrupole
QS	quorum sensing
QTRAP	quadrupole linear-iron trap
RAD	radiciol
RAM2	reduced arbuscular mycorrhiza 2
ROS	reactive oxygen species
RSA	root system architecture
SA	salicylic acid
SAR	systemic acquired response
SF ₆	sulfur hexafluoride
SL	Saccharolipids
SOD	superoxide dismutase protein
SP	Sphingolipids
SPE	solid-phase extraction

SQ	squalene
SQDG	sulfoquinovosyldiacylglycerol
ST	sterol lipids
SWATH-MS	Sequential Window Acquisition of All Theoretical Mass Spectra
TG	triacylglycerol
TLC	thin-layer chromatography
TOF	time-of-flight
UHPLCS	ultra-high performance liquid chromatography
UNFCCC	United Nations Framework Convention on Climate Change
USEPA	U.S. Environmental Protection Agency
USGCRP	U.S. Global Change Research Program
VOC	volatile organic compounds
ANOVA	analysis of variance

List of Figures

Figure 1. 1 Changes in atmospheric CO₂ and global surface temperature (relative to 1850–1900) from the deep past to the next 300 years. This figure attempts to show that CO₂ and temperatures are similar to those only from many millions of years ago. CO₂ concentrations from millions of years ago are reconstructed from multiple proxy records. CO₂ levels for the last 800,000 years through the mid-20th century are from air trapped in polar ice; recent values are from direct air measurements. Global surface temperature before 1850 is estimated from marine oxygen isotopes, one of the multiple sources of evidence used to assess paleo temperatures. The temperature of the past 170 years is the Sixth Assessment Report (AR6) assessed mean. CO₂ levels and global surface temperature change for the future are shown for three Shared Socio-economic Pathway (SSP) scenarios through 2300 CE, using Earth system model emulators calibrated to the assessed global surface temperatures. [Source: Image and description adapted from (Arias, 2021).]4

Figure 1. 2 Key greenhouse gases emitted by human activities based on global emissions from 2010 (Left). Top global CO₂ producers in 2014 (Right). Left figure shows the percentage of each gas comprising the global greenhouse gas, with corresponding sources mainly for CO₂. Right figure shows CO₂ emissions from fossil fuel combustion and some industrial processes such as cement manufacturing and gas flaring from different countries. [Sources: Figures and description adapted from IPCC (2014) and Boden et al. (2017)]5

Figure 1. 3 Atmospheric carbon dioxide (CO₂) concentration (ppm) at Mauna Loa, Hawaii from pre-industrial period (<1700), through 1979 until 2021. CO₂ concentration was mostly stable at 285 ppm before the 1700s (Industrial Revolution) and has increased rapidly since then. [Source: Interactive video from National Oceanic and Atmospheric Administration (NOAA), Earth System Research Laboratory (ESRL), Global Monitoring Division].....6

Figure 1. 4 Classification of plants based on heat tolerance. [Source: Image adapted from Hasanuzzaman et al. (2013)]9

Figure 1. 5 Different adaptation mechanisms of plants to high temperature: A. Avoidance, T: Tolerance. [Source: Image adapted from Hasanuzzaman et al. (2013).] 15

Figure 1. 6 Proposed mechanisms of heat stress tolerance in plants. MAPK, mitogen-activated protein kinases; CDPK, calcium-dependent protein kinase; HSK, histidine kinase; ROS, reactive oxygen species; HSPs, heat shock proteins. [Source: Image and description adapted from Wahid et al. (2007).] 17

Figure 1. 7 Schematic representation of a longitudinal section of a growing root showing the six major sites of rhizodeposition: (1) loss of root cap and border cells, (2) loss of insoluble mucilage, (3) loss of soluble root exudates, (4) loss of volatile organic C, (5) loss of C to symbionts (e.g. arbuscular mycorrhizas), and (6) loss of C due to death and lysis of root epidermal and cortical cells. [Source: Image and description adapted from Jones et al. (2009).] 20

Figure 1. 8 Cross and longitudinal section of a dicot root structure. [Source: Image by Dave Carlson - <https://www.carlsonstockart.com/photo/root-structure-monocot-dicot-cross-longitudinal-section/>] 29

Figure 1. 9 2D imaging of plant roots. (a) GLO-Roots. Arabidopsis plant expressing a luminescent reporter imaged on each side of the rhizotron (colored green and magenta respectively) at 21 days after sowing (DAS). (b) GROWSCREEN-Rhizo. A high-throughput automated root phenotyping platform using soil-filled rhizotrons. (c) Pouch system for cereal seedlings (left panel). RootNav analysis software (right panel). (d) Phytomorph. A high-throughput robotic imaging platform for Arabidopsis growing on agar plates. [Source: Image and description adapted from Atkinson et al. (2019).] ... 33

Figure 1. 10 3D tomographic imaging of plant roots. (a) X-ray CT micrograph of a wheat seedling 12 DAS. (b) MRI imaging of a maize root system at 6, 9, 12, and 15 DAS. Upper panel, MRI data (2D maximum intensity projection). Lower panel, 3D surface rendering. Scale bar: 20 mm. (c) Maize roots imaged using MRI-PET. Two plants are growing in the same pot. The greyscale image is MRI, the color is 11C PET data following application to a leaf of one plant. (d) OpenSimRoot simulation using output from (a) to model rhizosphere N depletion. (e) Maize root imaged at 9 DAS using optical projection tomography (OPT) and PET. The black and white image is OPT, the

color is 11C PET data. [Source: Image and description adapted from Atkinson et al. (2019).]34

Figure 1. 11 Automated root image analysis software. (a) DIRT measures traits based on the ‘shovelomics’ approach. Root systems are washed and imaged from above in front of a dark background. Root systems are separated from the background via thresholding, and RSA traits are derived from each segmented object. (b) Root-soil segmentation in X-Ray CT. Root and soil pixels are identified via a Support Vector Machine classifier trained on deep-learned features. Images show the ground truth, original image, and SVM classifier output. (c) End-to-end deep learning for root tip identification. A deep network trained on thousands of instances of root tips and negative samples can be passed over an entire image to obtain likely root tip locations. [Source: Image and description adapted from Atkinson et al. (2019).]35

Figure 1. 12 Representative structure of each lipid category. The LIPID MAPS consortium has subdivided lipids into eight principal categories based on their functions, chemical characteristics, and specificities. A more consistent format for representing lipid structures has been proposed by Fahy et. al [84] in which, in the simplest case of the fatty acid derivatives, the acid group (or equivalent) is drawn on the right hand while the hydrophobic hydrocarbon chain is on the left, with some notable exceptions. Fatty acyls [FA]- have aliphatic chain of methylene groups and can be subdivided into saturated or unsaturated; Glycerolipids [GL]- characterized by the number of glycerol groups; Glycerophospholipids [GP]- amphipathic with a polar glycerol and phosphate group and non-polar hydrocarbon; Sphingolipids [SP]- have a sphingoid backbone; Sterol lipids [ST]- with sterol nucleus composed of four tightly fused carbon rings and a hydroxyl group attached to the first ring; Prenol lipids [PR]- synthesized from the five-carbon precursors (isopentyl diphosphate and dimethylallyl diphosphate); Saccharolipids [SL]- has fatty acid and a sugar backbone; Polyketides [PK]- has various structural forms, often as cyclic molecules with modifications such as methyl group or hydroxyl groups. [Image created with Biorender.com.].....40

Figure 1. 13 Lipid components and signaling in the plasma membrane. (A) Lipids in the plasma membrane. The plasma membrane is primarily comprised of glycerophospholipids (GP), sphingolipids (SP), and sterol lipids (ST) – with functions that maintain the structure, stability, and regulation of essential cell processes. (B) The five major glycerophospholipids that predominate in the plasma membrane are

phosphatidylethanolamine (PE), phosphatidylserine (PS), phosphatidylcholine (PC), sphingomyelin (SM), and phosphatidylinositol (PI). Together they constitute more than half the mass of lipids in most membranes. Their distribution, variable within the two monolayers, leads to the bilayer asymmetry which is crucial in cell signaling and protein binding. (C) Membrane phospholipids have specific functions in cell signaling. (C-1) In response to extracellular signals, cytosolic proteins such as protein kinase C (PKC) are activated and bind to the cytosolic face of the membrane where the negatively-charged PS concentrated in this area, are required for their activity. (C-2) Extracellular signals can activate phosphatidylinositol kinase (PI 3-kinase), leading to phosphorylated inositol phospholipids in the plasma membrane. Various intracellular signaling molecules are then attracted and bind to the phosphorylated lipids in the membrane, where they interact and help relay the signal into the cell. (C-3) Other extracellular signals activate phospholipases (e.g. phospholipase C) that cleave phospholipids. These lipid fragments then act as separate signaling molecules to relay signals into the cell – the tail retained in the membrane help activate protein kinase C while the head is released into the cytosol. [Image created with Biorender.com.]47

Figure 1. 14 Lipids as chemical signals in rhizosphere interactions and signaling. Plants initiate signaling through the release of rhizodeposits from the roots in a process called rhizodeposition. Rhizodeposits can originate from various sources including root cap (RC), border cells (BC), root exudates (E), volatile organic carbon (VOC), carbon from symbionts or microbes (M), and carbon loss due to lysates (L) from epidermal and cortical cells. The release of rhizodeposits also comes with a variety of substances, including lipids, which act as chemical signals that are then perceived by the microbes. Plant-secreted substances influence cell-cell signaling among different microorganisms which are not in proximity to plants. Microbes also produce communication signals for population and behavior coordination, including quorum sensing (QS) such as N-acyl homoserine lactones (AHL), diffusible signal factors (DSF), pyrones, dialkylresorcinol, peptides; antimicrobials (at low and non-inhibitory concentrations); alcohols; and volatile organic compounds (VOC). As a response to signals perceived from among themselves (intraspecies), other microorganisms (interspecies), or plants, microbes release diverse signaling molecules such as effector proteins (microbe/pathogen-associated molecular patterns, MAMPs/PAMPs), which can induce plant defense or immunity responses, i.e. by priming, induced systemic resistance

(ISR), and systemic acquired resistance (SAR). Microbes also release similar compounds to plants. These microbe-released compounds can affect plant gene expression, hormonal balance, development, metabolism, and stress responses. They can also interfere with and suppress plant immunity to successfully colonize plant tissues. (Red texts are lipid categories: FA- fatty acids, ST- sterol lipids, PR- prenol lipids, PK- polyketide, SL- saccharolipids). [Image created with Biorender].57

Figure 1. 15 Lipid roles in the microbial colonization of roots. Lipids are involved in the different stages of microbial colonization of plant roots. (A) Lipid roles can be traced back from the recruitment and shaping of the microbiome through the release of rhizodeposits, where lipids act as chemical signals released by the plants, perceived and utilized by microbes to regulate intra- and interspecies behavior, and released by microbes into the roots to influence plant responses. (B) Successful recruitment of microbes leads to the formation of microbial biofilms on root surfaces. Lipids in the plasma membrane mediate the interaction of the plant roots and microorganisms. (C) Different lipid species perform various functions during signal reception, transduction, and downstream response mechanism of plants to microbial attack or beneficial symbiosis. Some of the lipids involved are phospholipids and phospholipases, glycerolipids, sphingolipids, galactolipids, fatty acids, sterol lipids, and oxylipins. (Pe- pericycle, Xy- xylem, CS- Casparian strip, Ph- pith, En- endodermis, Ex- exodermis, Ep- epidermis, RH- root hairs, PAMP/MAMP- pathogen/microbe-associated molecular pattern, PLD/PLC/PLA- phospholipase D/C/A, PA- phosphatidic acid, RAM2- reduced arbuscular mycorrhiza 2, LOX- lipoxygenase, ROS- reactive oxygen species, TAG- triglyceride, JA-Ile- jasmonyl isoleucine, JA-Trp- jasmonyl tryptophan, Gro3P- glycerol-3-phosphate, AzA- azelaic acid, NO- nitric oxide, ETI- effector triggered immunity, SA- salicylic acid, SAR- systemic acquired resistance, LCB- long chain base, LOH 1/2/3- Longevity assurance gene one homologs (1/2/3), PCD- programmed cell death, DGDG- digalactosyldiacylglycerol, MGDG- monogalactosyldiacylglycerol). [Image created with Biorender.com.].....63

Figure 1. 16 MS-based plant lipidomics workflow. A typical lipidomics workflow for analysing plant lipids consists of harvesting different plant tissues (e.g. roots, stems, leaves, florets, siliques, seeds). Depending on the biological sample and analytical techniques to be employed, sample pre-treatment and lipid extraction is performed. In general, these methods can be categorized as liquid-liquid extraction (LLE) – most

predominant lipid extraction method with the strongest applicability, solid-phase extraction (SPE) – utilizes a stationary phase that selectively retains specific molecular classes with similar properties, and those which require chemical derivation to improve detection sensitivity, selectivity, chromatographic performance, and separation efficiency. Data from biological samples are then generated using mass spectrometry (MS) that is hyphenated with analytical techniques broadly grouped into direct infusion (shotgun lipidomics), chromatography-based acquisition, and MS imaging. Acquired data are then processed and subjected to qualitative and quantitative analysis, lipid identification, and performing bioinformatics and statistical analysis. As lipidomics produces a large amount of data, proper calculation tools, databases, and algorithms for efficient mining of data are utilized to understand the biological significance of the data set. (BUME- butanol methanol, MTBE- methyl-tert-butyl ether, HRMS- high-resolution MS, MDMS- multi-dimensional MS, LC-MS- liquid chromatography MS, GC-MS- gas chromatography MS, TLC- thin-layer chromatography, SFC- supercritical fluid chromatography, CE- Capillary electrophoresis, MALDI-MS- matrix-assisted laser desorption/ionization MS, DESI-MS- desorption electrospray ionization MS, SIMS-MS- secondary ion mass spectrometry MS.....69

Figure 2. 1 Different growth systems used – “closed-plate” (at UoM), “open-top” (FZJ), and modified growth systems (at UoM), to establish plant-bacteria cultivation protocols 83

Figure 2. 2 Workflow of methods for plant and bacterial co-cultivation in a “closed-plate” system89

Figure 2. 3 Workflow protocol for culturing bacteria.....90

Figure 2. 4 Sample streaking technique (A) and an actual bacterial streaked plate (B)92

Figure 2. 5 Overnight liquid cultures of some trial bacteria and a control93

Figure 2. 6 Plated serial dilution of a bacterial inoculum94

Figure 2. 7 Horizontally grown (A) and vertically grown (B) Arabidopsis plants at 30 days after sowing95

Figure 2. 8 Sowing individual seeds onto the agar surface using a 1 mL pipette.....97

Figure 2. 9 GrowScreen-Agar, mechanical setup for automated imaging roots and shoots of plants grown in agar-filled plates. The Petri dishes are fixed in red holders, which are

moved in a rectangular frame by using pneumatic cylinders (a, b). At one position of the setup, Petri dishes (b) are optically accessible and images of root and shoot are taken (c, d). Representative original color image of four Arabidopsis shoots taken by the top camera (c); part of an original greyscale root image taken by the bottom camera (e) and color-coded image (quantified with the image-based software GROWSCREEN-ROOT) with primary root (green) and lateral roots (red) of an Arabidopsis plant (f). In total 70 Petri dishes containing up to 280 Arabidopsis plants fit into the GrowScreen-Agar system. During image acquisition, the opening above the bottom camera (a) is closed by a cover panel. [Source: Image and description adapted from Nagel et al. (2020).] 100

Figure 2. 10 Workflow of experimentation at Forschungszentrum Juelich..... 102

Figure 2. 11 Customization of the small Petri plates for the GrowScreen-Agar I. a) Positioning and aligning the plates. b) Covering the top part of the bottom dish in preparation for drilling holes. c) Drilling holes into the plates using metal stencils. d) Cutting the top part of the lid to allow plant shoots to grow outside the holes of the plates. [Source: Images (except for the first one) taken from Becker and Kastenholz (2020).] 103

Figure 2. 12 Dispensing a single Arabidopsis seed into each hole of the customized plates. [Source: Image taken from (Becker & Kastenholz, 2020).]..... 106

Figure 2. 13 (Left to right) Rack designed for GrowScreen-Agar I (“Root Carousel”) customized plates (a) and re-adjusting some seedlings on the “open-top” system to grow directly outside of the holes (b). Some seeds managed to grow their plants under the plate, making them trapped and unable to expand their shoots. Other seedlings were stuck inside the agar so the use of a needle or tweezer was sometimes necessary. [Source: Images adapted and description modified from (Becker & Kastenholz, 2020).] 107

Figure 2. 14 A sample customized plate being placed into a red cassette ready to be imaged by the GrowScreen-Agar I platform. [Source: Images adapted from (Becker & Kastenholz, 2020).]..... 108

Figure 2. 15 Position of the imaging system within the GrowScreen-Agar II platform. Details and specifications of the system are illustrated in Chapter 3 and supplements..... 109

Figure 2. 16 Inclined plates to address the problem of harvesting roots growing inside the agar. 111

Figure 2. 17 Modified “open-top” system using customized square Petri plates and racks 112

Figure 2. 18 Plate customization and plant-bacteria cultivation in a modified “open-top” system. 114

Figure 2. 19 Arabidopsis plants in an open plate and corresponding image from WinRhizo 115

Figure 3. 1 GrowScreen-Agar II: Plant cultivation setup and root/shoot image acquisition and analysis. a) Arabidopsis plants growing in customized plates and magazine (product specification on Figs. S1 and S2, respectively). Black plate collars provide the background for the growing shoots outside of the plates while at the same time, they exclude light entering the top of the metal magazine (bottom panel) to provide dark environment for the roots. b) Overview of a single plate that is manually transferred to an imaging system (Fig. S3) equipped with cameras for imaging the shoots and the roots, generating two images: top view of the shoot(s) and the whole root system. c) (Top) Analysed image of a rosette using the Colour segmentation tool that computes the sum of white pixels as a proxy to compute the projected leaf area {Müller-Linow, 2022 #1665}. (Bottom) Analysed image of a root system using the GrowScreen-Root {Nagel, 2020 #1244}. Different root types are distinguished by colour: green for primary roots, red for 1st order lateral roots, and blue for 2nd order lateral roots. The whole image area can also be divided horizontally into several sections to extract root length density per layer..... 126

Figure 3. 2 Morphological traits of different root types. Traits were measured from plants with or without bacteria PsJN inoculation under ambient or high temperature conditions from 5 to 21 days after inoculation (DAI) in the GrowScreen-Agar II platform. Root lengths: a) total, b) primary, c) 1st order lateral roots, d) 2nd order lateral roots; Growth rates: f) total, g) primary, h) 1st order lateral roots, i) 2nd order lateral roots; Number of lateral roots: e) 1st order lateral roots, j) 2nd order lateral roots. Temperature - black and circle symbol (ambient), red and triangle symbol (high temperature); Bacterial application – empty symbol (control), filled symbol (PsJN-inoculated). Treatments: Amb-Ctl (control plants under ambient), Amb-PsJN (PsJN-inoculated plants under ambient), HT-Ctl (control plants under high temperature), and HT-PsJN (PsJN-inoculated plants under high temperature). All points are the mean ± standard error of

n= 12 (Amb-Ctl), 15 (Amb-PsJN), 12 (HT-Ctl), 8 (HT-PsJN) samples within each treatment. Asterisks: Black – significant difference between mean of PsJN-inoculated and control plants under ambient condition, red - significant difference between mean of PsJN-inoculated and control plants under high temperature condition, based on the Student’s t-test with $p < 0.05$ 131

Figure 3. 3 Root system morphological traits. Traits were measured from plants with or without bacteria PsJN inoculation under ambient or high temperature conditions from 5 to 21 days after inoculation (DAI) in the GrowScreen-Agar II platform. a) Root system depth, b) root system width, c) convex hull area, and d) branching angle of 1st order lateral roots. Temperature - black and circle symbol (ambient), red and triangle symbol (high temperature); Bacterial application – empty symbol (control), filled symbol (PsJN-inoculated). Treatments: Amb-Ctl (control plants under ambient), Amb-PsJN (PsJN-inoculated plants under ambient), HT-Ctl (control plants under high temperature), and HT-PsJN (PsJN-inoculated plants under high temperature). All points are the mean \pm standard error of n= 12 (Amb-Ctl), 15 (Amb-PsJN), 12 (HT-Ctl), 8 (HT-PsJN) samples within each treatment. Asterisks: Black – significant difference between mean of PsJN-inoculated and control plants under ambient condition, red - significant difference between mean of PsJN-inoculated and control plants under high temperature condition, based on the Student’s t-test with $p < 0.05$ 132

Figure 3. 4 Root length distribution across different depths through time. Length distribution of plant roots from all treatments across different depths or layers (20 horizontal sections) at several timepoints (9, 12, 14, 16, 19, and 21 DAI). Treatments: [black points, open symbols] - Amb-Ctl (control plants under ambient), [black points, closed symbols] - Amb-PsJN (PsJN-inoculated plants under ambient), [red points, open symbols] - HT-Ctl (control plants under high temperature), and [red points, closed symbols] - HT-PsJN (PsJN-inoculated plants under high temperature). All points are the mean \pm standard error of n= 12 (Amb-Ctl), 15 (Amb-PsJN), 12 (HT-Ctl), 8 (HT-PsJN) samples within each treatment. 135

Figure 3. 5 Correlation analysis for lateral roots a) Correlation between the length of the primary roots (Fig. 2b) and the number of 1st order lateral roots (Fig. 2e). b) Correlation between the number of 1st and 2nd order lateral roots of plants from all treatments. Treatments: Amb-Ctl (control plants under ambient) – grey, empty circle; Amb-PsJN (PsJN-inoculated plants under ambient) – black, filled circle; HT-Ctl (control plants

under high temperature) – pink, empty triangle; and HT-PsJN (PsJN-inoculated plants under high temperature) – red, filled triangles. Trendlines follow similar colour as their corresponding treatments. Points were taken at different time intervals (5, 7, 9, 12, 14, 16, 19, and 21). 136

Figure 3. 6 Projected leaf area and dry weight. a) Measured projected leaf area of *Arabidopsis* rosettes growing outside of the agar-filled plates with or without bacteria PsJN inoculation under ambient or high temperature conditions. Temperature - black and circle symbol (ambient), red and triangle symbol (high temperature); bacterial application – empty symbol (control), filled symbol (PsJN-inoculated). b) Dry weights of shoots from all treatments during invasive harvest. Treatments: Amb-Ctl (control plants under ambient), Amb-PsJN (PsJN-inoculated plants under ambient), HT-Ctl (control plants under high temperature), and HT-PsJN (PsJN-inoculated plants under high temperature). All points are the mean \pm standard error of n= 12 (Amb-Ctl), 15 (Amb-PsJN), 12 (HT-Ctl), 8 (HT-PsJN) samples within each treatment. Asterisks: Black – significant difference between mean of PsJN-inoculated and control plants under ambient condition, red - significant difference between mean of PsJN-inoculated and control plants under high temperature condition, based on the Student’s t-test with $p < 0.05$ 137

Figure 4. 1 Number of apparent lipids detected and annotated in *Arabidopsis* root. Cer – ceramides, CL – cardiolipin, CoQ – coenzyme Q, DG – diacylglycerols, DGDG – digalactosyldiacylglycerols, DGGG – diacylglyceryl glucuronides, HexCer – hexosylceramides, LPC – lysophosphatidylcholines, LPE – lysophosphatidylethanolamines, MG – monoacylglycerols, MGDG – monogalactosyldiacylglycerols, NAE – N-acylethanolamines, PC – glycerophosphocholines, PE – glycerophosphoethanolamines, PG – glycerophosphoglycerols, PI – glycerophosphoinositol, PS – glycerophosphoserines, SQDG – sulfoquinovosyldiacylglycerols, ST – sterols, TG - triacylglycerols 168

Figure 4. 2 Principal component analysis (PCA) score plot of the annotated lipids detected from control and PsJN-inoculated roots subjected to ambient and high-temperature conditions. Treatments: ATC – ambient-control, ATP – ambient- PsJN-inoculated, HTC – high temperature- control, HTP – high-temperature- PsJN -inoculated, pooled biological quality control (PBQC) samples. Numbers at the start of each treatment

name refers to measurements or harvest times at 7, 14, and 21 days after inoculation (DAI). Coloured ellipses around samples display 95% confidence areas. 169

Figure 4.3 Principal component analysis (PCA) plots of the annotated lipids (A) and unknown features (B) detected from control and PsJN-inoculated roots subjected to ambient and high-temperature conditions. Legend: ATC – ambient-control, ATP – ambient- PsJN-inoculated, HTC – high temperature- control, HTP – high-temperature- PsJN -inoculated. Measurements were taken at (a) 7 (top), (b) 14 (middle), and (c) 21 (bottom) days after inoculation (DAI). Coloured ellipses around samples display 95% confidence areas. 172

Figure 4.4 Hierarchical clustering coupled with heatmap of the annotated lipids (A) and unknown features (B) detected from control and PsJN-inoculated roots subjected to ambient and high-temperature conditions. Legend on the upper right side: ATC – ambient-control, ATP – ambient- PsJN-inoculated, HTC – high temperature- control, HTP – high-temperature- PsJN -inoculated. Measurements were taken at (a) 7 (top), (b) 14 (middle), and (c) 21 (bottom) days after inoculation (DAI). Label at the bottom refers to the replicates; and for each replicate (column), blue and red colours signify the lower and higher abundance of specific lipids as compared to the other replicates, with darker colours indicating more pronounced differences. Dendrogram at the top indicates the main lipid clusters represented with branches of different colours. 174

Figure 4.5 Analysis of variance (ANOVA) of the annotated lipids and unknown features detected from control and PsJN-inoculated roots subjected to ambient and high-temperature conditions. Red dots – lipid species showing significant differences, green dots – lipid species showing no significant differences. (a), (b), and (c) represents the time points 7, 14, and 21 days after inoculation (DAI). 175

Figure 4.6 Principal component analysis (PCA) (a), PCA loading plot (b), and log₂ fold change comparison (c) of the levels of lipid classes between control and PsJN-inoculated roots subjected under ambient (A) and high-temperature (B) conditions at 7 days after inoculation (DAI). Treatments: ATC – ambient-control, ATP – ambient-PsJN-inoculated, HTC – high temperature- control, HTP – high-temperature- PsJN-inoculated. Coloured ellipses around samples display 95% confidence areas. 181

Figure 4.7 Principal component analysis (PCA) (a), PCA loading plot (b), and log₂ fold change comparison (c) of the levels of lipid classes between control and PsJN-

inoculated roots subjected under ambient (A) and high-temperature (B) conditions at 14 days after inoculation (DAI). Treatments: ATC – ambient-control, ATP – ambient-PsJN-inoculated, HTC – high temperature- control, HTP – high-temperature- PsJN-inoculated. Coloured ellipses around samples display 95% confidence areas. 183

Figure 4. 8 Principal component analysis (PCA) (a), PCA loading plot (b), and log₂ fold change comparison (c) of the levels of lipid classes between control and PsJN-inoculated roots subjected under ambient (A) and high-temperature (B) conditions at 21 days after inoculation (DAI). Treatments: ATC – ambient-control, ATP – ambient-PsJN-inoculated, HTC – high temperature- control, HTP – high-temperature- PsJN-inoculated. Coloured ellipses around samples display 95% confidence areas. 185

Figure 4. 9 Volcano plots of significantly altered lipids in the comparison between control and PsJN-inoculated roots under ambient (A) and high-temperature (B) conditions at 7 (a), 14 (b), and 21 (c) DAI. Fold change direction is ATP/ATC. Horizontal axis plots the fold change between two groups (on a log₂ scale), while vertical axis shows the $P < 0.05$ for a t-test differences between samples (on a negative log scale). Red dots represent significantly increased lipid species with an FC threshold of 1.2, while blue dots represent significantly decreased lipid species, based on the two-factor t-test $P > 0.05$ 188

Figure 4. 10 Principal component analysis (PCA) plots between ambient-grown and heat-stressed roots at three timepoints. Treatments: ATC – ambient-control and HTC – high temperature- control. Measurements were taken at 7, 14, and 21 days after inoculation (DAI). Coloured ellipses around samples display 95% confidence areas. 192

Figure 4. 11 Analysis of variance (ANOVA) between ambient-grown and heat stressed roots at all three time points. Red dots – lipid species showing significant differences, green dots – lipid species showing no significant differences. 192

Figure 4. 12 Hierarchical clustering coupled with heatmap between ambient-grown and heat-stressed roots at three different timepoints. Treatments: ATC – ambient-control and HTC – high temperature- control. Measurements were taken at 7, 14, and 21 days after inoculation (DAI). Label at the bottom refers to the replicates; and for each replicate (column), blue and red colours signify the lower and higher abundance of specific lipids as compared to the other replicates, with darker colours indicating more pronounced

differences. Dendrogram at the top indicates the main lipid clusters represented with branches of different colours. 193

Figure 4. 13 Volcano plots of significantly altered lipids in the comparison between ambient-grown and heat-stressed roots taken at 7 (a), 14 (b), and 21 (c) DAI. Fold change direction is HTC/ATC. Horizontal axis plots the fold change between two groups (on a log₂ scale), while vertical axis shows the $P < 0.05$ for a t-test differences between samples (on a negative log scale). Red dots represent significantly increased lipid species with an FC threshold of 1.2, while blue dots represent significantly decreased lipid species, based on the two-factor t-test $P > 0.05$ 194

List of Tables

Table 1. 1 Threshold high temperatures for some crop plants	7
Table 2. 1 The concentrations of compounds in Milli-Q water as a solvent for the preparation of nutrient stock solutions which are used in GrowScreen-Agar (Nagel et al., 2020).	104
Table 4. 1 Components and concentrations of the SPLASH LipidoMIX™ Internal Standard	164
Table 4. 2 Loadings of the first two principal components of the four treatments (control roots under ambient, PsJN-inoculated roots at ambient, control roots at high temperature, and PsJN-inoculated roots at high temperature) at 7 days after inoculation (DAI).	176
Table 4. 3 Loadings of the first two principal components of the four treatments (control roots under ambient, PsJN-inoculated roots at ambient, control roots at high temperature, and PsJN-inoculated roots at high temperature) at 14 days after inoculation (DAI).	177
Table 4. 4 Loadings of the first two principal components of the four treatments (control roots under ambient, PsJN-inoculated roots at ambient, control roots at high temperature, and PsJN-inoculated roots at high temperature) at 21 days after inoculation (DAI).	178
Table 4. 5 Loadings of the first two principal components of control and PsJN-inoculated roots under two temperatures and three time points.....	186
Table 4. 6 Number of changed (increased or decreased) lipid classes (with a $P < 0.05$ and ≥ 1.2 -fold change) corresponding to the peak areas between control and PsJN-inoculated roots under two temperatures and three time points. Red and bold texts indicate significantly changed.	187
Table 4. 7 Number of significantly changed (increased or decreased) lipid species (with a $P < 0.05$ and ≥ 1.2 -fold change) corresponding to the peak areas between control and PsJN-inoculated roots under two temperatures and three time points. Treatments: ATC – ambient-control, ATP – ambient- PsJN-inoculated, HTC – high temperature- control, HTP – high temperature- PsJN-inoculated.	190

Table 4. 8 Number of significantly changed (increased or decreased) lipid species (with a $P < 0.05$ and ≥ 1.2 -fold change) corresponding to the peak areas between ambient-grown and heat-stressed roots at three time points. Treatments: ATC – ambient-control and HTC – high temperature- control.195

List of Supplementary Figures

Figure S 1 WinRhizo analysed root lengths and root and shoot biomass. Root lengths quantified using WinRhizo analysis in a closed-plate experiment: (a) Total root lengths, (b) primary root length, and (c) branched root lengths. Temperature - black and circle symbol (ambient), red and triangle symbol (high temperature); bacterial application – empty symbol (control), filled symbol (PsJN-inoculated). Plant biomass taken at harvest: (d) shoot dry weight and (e) root dry weight. (f) Sample images of 16-day old seedlings from each of the four treatments. Treatments: Amb-Ctl (control plants under ambient), Amb-PsJN (PsJN-inoculated plants under ambient), HT-Ctl (control plants under high temperature), and HT-PsJN (PsJN-inoculated plants under high temperature). All points are the mean \pm standard error of $n=6$ samples within each treatment. Asterisks: Black – significant difference between mean of PsJN-inoculated and control plants under ambient condition, red - significant difference between mean of PsJN-inoculated and control plants under high temperature condition, based on the Student's t-test with $p<0.05$223

Figure S 2 Root sampling and bacterial colonization confirmation. (a) Brief procedure for sampling of root tissues for the determination of bacterial colonization. (A) Cutting about 1-2 cm of the root tip, placing into pre-prepared Eppendorf tube with LB (no NaCl) media, and washing/agitating the root using a vortex to get the root surface bacteria. (B-2) Aliquoting from the LB surface washing fraction. (C) Performing serial dilution of the bacterial inoculum, aliquoting from each dilution, and plating. (B-1) Removal of the washed root and transfer into a separate clean tube for maceration. (D) Adding LB media (no NaCl) to the macerated root and mixing using a vortex to extract the bacteria inside the root tissue. (E) Aliquoting from the washing to transfer to tubes for serial dilution and then plating each of the dilutions (F). (C) corresponds to **rhizoplane** colonization while (F) yields **endophytic** colonization of bacteria (image created with BioRender.com). (b) Sample plated dilutions at 21 DAI. Left two columns show rhizoplane colonization and right two columns show endophytic colonization of the bacteria. 1st and 3rd columns are from non-inoculated roots showing no growth, indicating sterility of system; while 2nd and 4th are from inoculated roots, showing growth from the bacterial strain PsJN. (c) PCR of single bacterial colonies from macerated root tips which have been plated out on LB media. The PCR products were

sequenced, and the ones identified as *Parabulkoholderia* sp. are indicated with a green asterix “*”. Minimum of 3 plants of each treatment were sampled. Note that the three high temperature control roots and one ambient temperature control root showed no colonies at all on the plate - thus no PCR products, whereas the products in the 2 ambient temperature controls was identified as a *Paenibacillus* sp. “+”- positive control for the universal bacterial primers, “-“ – negative control for the PCR reaction, Ctl-control, PsJN- Roots inoculated with PsJN bacteria.225

Figure S 3 Sample root images generated by the GrowScreen-Agar II. Images of plant roots from the four treatments at 16 DAI taken by the root camera of the GrowScreen-Agar II imaging system. Treatments (from left to right): Amb-Ctl (control or non-inoculated plants under ambient), Amb-PsJN (PsJN-inoculated plants under ambient), HT-Ctl (control or non-inoculated plants under high temperature), and HT-PsJN (PsJN-inoculated plants under high temperature).226

Figure S 4 Agar plates for GrowScreen-Agar II. Technical drawings of three components of the agar plate: 1) an opaque cover with an anti-fog agent which prevents water droplets, 2) a transparent back plate with holes on top which allows root imaging and the shoot to grow outside of the plate, and 3) a black top part (“collar”) also with three holes as background for shoot imaging, keeping light out of the root zone and mechanical support for leaves. The technical drawings show the assembly of the three components (a), different side views (b, c), top view (d), while figure e) shows an original photo of the assembled plate. The dimensions are given in mm (b-d). ‘Agar: 11,5’ represents the filling height of the agar (c) and ‘R’ the radius of the holes (d).227

Figure S 5 Magazines for GrowScreen-Agar II. The plates are positioned vertically and maintained for plant cultivation in fabricated metal magazines accommodating up to 10 plates. The design of the magazines allows the roots to grow in the dark. The technical drawings show a side view (a), top view (b), and front view (c) of the magazine, while figure (d) shows an original photo of the magazine, each loaded with 9 plates and 1 open slot. In figure (a) the side wall of the magazine is partly removed to show the plates inside the magazine and one plate is lifted in (a) and (b). The dimensions are given in mm.228

Figure S 6 Imaging station of GrowScreen-Agar II. For imaging roots and shoots, the plates are placed in the imaging station of the phenotyping platform GrowScreen-Agar II. The imaging system features a metal housing equipped with one root and two shoot cameras aiming at a slot for inserting the plate. The root camera takes images of the whole agar area (20 x 10 cm) while the shoot cameras take a side view and a top view image of the shoots. The technical drawings show a side view **(a)**, top view **(b)**, and front view **(c)** of the imaging station, while the original photo shows nearly a side view **(d)**. The black background **(c, d)** provides a good contrast for shoot image analysis. Root illumination is achieved from the back while leaves are illuminated for imaging by using LED rings placed around the objective lenses of the shoot camera **(a-d)**229

Figure S 7 Published section of Chapter 1 (section 1.5 to 1.6) in the journal Trends in Plant Science with the title “Modulators or facilitators? Roles of lipids in plant root–microbe interactions. (Macabuhay, A., Arsova, B., Walker, R., Johnson, A., Watt, M., & Roessner, U. (2022, 2022/02/01/). Modulators or facilitators? Roles of lipids in plant root–microbe interactions. Trends in Plant Science, 27(2), 180-190. <https://doi.org/https://doi.org/10.1016/j.tplants.2021.08.004>).....230

List of Supplementary Tables

Table S 1 Mean values and standard error of different root type morphological traits	242
Table S 2 Mean values and standard error of different root system traits describing distribution and spread	243

Table of Contents

Referent.....	ii
Thesis abstract.....	iii
Zusammenfassung.....	iv
Declaration.....	v
Preface.....	vi
Acknowledgement	vii
Publications.....	ix
Abbreviations.....	x
List of Figures.....	xiv
List of Tables	xxvii
List of Supplementary Figures.....	xxix
List of Supplementary Tables	xxxii
Table of Contents.....	xxxiii
CHAPTER 1	1
Plant root-microbe interactions in a changing climate	1
Preface to Chapter 1.....	2
1.1. Climate change: drivers and impacts	3
1.1.1. Implications of climate change to agriculture	6
1.2. High temperature (heat) stress in plants.....	8
1.2.1. Plant responses to heat stress.....	9
1.2.1.1. Morphological responses.....	10
1.2.1.2. Anatomical responses.....	11
1.2.1.3. Phenological responses.....	11
1.2.1.4. Physiological responses	12
1.2.1.5. Molecular responses.....	13

1.2.2. Plant mechanisms for heat tolerance:	14
1.2.2.1. Avoidance mechanisms.....	14
1.2.2.2. Induction of heat tolerance	15
1.2.3. Strategies for heat tolerance and plant adaptation	17
1.2.3.1. Crop management	17
1.2.3.2. Conventional breeding technique	18
1.2.3.3. Genetic engineering and biotechnology	18
1.2.3.4. Microbe applications	19
1.3. Rhizosphere and the resident “plant-friendly” microorganisms	19
1.3.1. Plant growth-promoting rhizobacteria.....	22
1.3.2. High-temperature effects on soil microbes.....	23
1.3.3. Mechanisms by which microbes enhance thermotolerance in plant	24
1.3.3.1. Induction of heat shock protein (HSP).....	25
1.3.3.2. Production of plant growth regulators	25
1.3.3.3. Mediation of ROS.....	26
1.3.3.4. Defense through EPS or biofilm formation.....	26
1.3.3.5. Moderation of protective molecules	27
1.3.3.6. Nutrient and water uptake	27
1.4 Plant roots – The hidden half	28
1.4.1. Root system architecture	30
1.4.1.1. Microbial effect on the RSA	30
1.4.1.1. High temperature stress effect on the RSA	31
1.4.2. Root Phenotyping	31
1.5. Biochemical nature of plant root-microbe interactions.....	36
1.5.1. Lipids at the forefront of biochemical research.....	36
1.5.2. Lipids: Description, categories, and nomenclature	38
1.5.2.1. Categories of lipids:.....	38
1.5.2.2. Lipid nomenclature	39
1.5.3. General functions of lipids	41
1.5.3.1. The plasma membrane and the lipids regulating its functions.....	42
1.5.3.1.1. Roles of lipids in the structural formation and integrity of the plasma membrane	43

1.5.3.1.2. Roles of lipids in nutrient transport (permeability) across the plasma membrane:	44
1.5.3.1.3. Roles of plasma membrane lipids in cell signaling (reception, transduction, and response)	45
1.5.4. Main lipids in plants and microbes and their associated functions	48
1.5.4.1. Plant lipids	48
1.5.4.2. Fungal lipids	50
1.5.4.3. Bacterial lipids	50
1.5.5. Lipids: The chemical language during rhizosphere interactions	51
1.5.5.1. Plant root to microbe signaling through rhizodeposition	52
1.5.5.2. Microbe perception of plant root-released compounds and other microbial signals	53
1.5.5.3. Signaling response from microbes back to the plant	55
1.5.6. Plant lipids during pathogenic and symbiotic interactions with microorganisms	58
1.5.7. Plant lipids under high-temperature stress	64
1.6. Approaches in plasma membrane lipid visualization and advances in MS-based plant lipidomics	66
1.6.1. Visualizing lipids in the plasma membrane	66
1.6.2. Lipidomics: The science of the lipidome	67
1.6.3. Mass spectrometry (MS)-based lipidomics	68
1.6.3.1. Sample preparation	68
1.6.3.2. Homogenization	69
1.6.3.3. Addition of standards	70
1.6.3.4. Lipid extraction	70
1.6.3.5. Mass-spectrometry-based analysis	71
1.6.3.6. Data curation	72
1.7. Conclusion	73
1.8. Significance of the Study	74
1.9. Objectives of the study and biological samples used	76
1.9.1. Biological samples	76
1.9.1.1. Arabidopsis thaliana Col-0	77
1.9.1.2. Paraburkholderia phytofirmans PsJN	78
1.9.2. Chapter synopsis (with COVID-19 impacts)	79

CHAPTER 2	82
Methods development for plant-bacteria co-cultivation and phenotyping with the “closed-plate” and “open-top” growth systems	82
Preface to Chapter 2.....	83
2.1. Introduction	84
2.2. Growth protocols and methods optimization	87
2.2.1. Establishing protocols for optimized plant and bacterial growth conditions and co-cultivation using the traditional “closed-plate” system (University of Melbourne).....	88
2.2.1.1. Selection and sourcing of microbial strain for the experiment	89
2.2.1.2. Culturing of <i>Paraburkholderia phytofirmans</i> PsJN	90
2.2.1.2.1. Bacterial media preparation, pouring, and plating.....	90
2.2.1.2.2. Streaking and bacterial isolation on LB agar plate.....	91
2.2.1.2.3. Overnight liquid culturing	92
2.2.1.2.4. OD ₆₀₀ determination, serial dilution, and colony counting.....	92
2.2.1.3. Arabidopsis plant cultivation	94
2.2.1.3.1. Plant media preparation, pouring, and plating.....	94
2.2.1.3.2. Surface sterilization and stratification of seeds.....	96
2.2.1.3.3. Sowing of seeds	96
2.2.1.4. Plant inoculation with the <i>P. phytofirmans</i> PsJN.....	97
2.2.1.4.1. Radicle length checking.....	97
2.2.1.4.2. Preparing bacterial culture in MS liquid media for plant inoculation	97
2.2.1.4.3. Root inoculation.....	98
2.2.1.5. Growth in the climate/ growth chamber.....	98
2.2.1.6. Plant phenotyping.....	99
2.2.1.7. Harvest and analysis	99
2.2.2. Optimization methods for “open-top” plant cultivation using the GrowScreen-Agar phenotyping platform (Forschungszentrum Juelich (FZJ))	99
2.2.2.1. Petri plate customization for the GrowScreen-Agar 1 platform:.....	102
2.2.2.2. Preparation of the plant agar media and pouring into customized plates.....	103
2.2.2.3. Arabidopsis plant and PsJN bacterial cultivation	105
2.2.2.4. Bacterial inoculation of Arabidopsis seeds	106
2.2.2.5. Growth of plants in the climate chambers	106
2.2.2.6. Plant phenotyping and data acquisition	107

2.2.2.7. Harvest	108
2.2.2.8. Experimentation using the GrowScreen-Agar II platform	108
2.2.2.8.1. First experimentation – Replicating the plant phenotypes	109
2.2.2.8.2. Second experimentation – Testing repeatability and addressing contamination	110
2.2.2.8.3. Third experimentation – Root harvest optimization	110
2.2.2.8.4. Last experimentation – Preventing agar drying.....	111
2.2.3. Optimization methods to replicate the “open-top” system of the GrowScreen-Agar II platform but utilizing the conventional agar-plate protocols (University of Melbourne)	111
2.2.3.1. Optimization experiments replicating the open-top system at FZJ but using traditional plant cultivation materials	112
2.2.3.2. Final experiments reverting to the traditional “closed-plate” growing system but using the plant-bacteria cultivation protocols established at the FZJ	115
CHAPTER 3	116
Plant growth promotion and heat stress amelioration in <i>Arabidopsis</i> inoculated with <i>Paraburkholderia phytofirmans</i> PsJN rhizobacteria quantified with the GrowScreen-Agar II phenotyping platform.....	116
Preface to Chapter 3	117
Plant growth promotion and heat stress amelioration in <i>Arabidopsis</i> inoculated with <i>Paraburkholderia phytofirmans</i> PsJN rhizobacteria quantified with the GrowScreen-Agar II phenotyping platform.....	119
Abstract.....	119
Keywords	120
3.1 Introduction	120
3.2. Results	124
3.2.1. Increased plant growth and higher plant biomass at 21 days post-inoculation with bacteria PsJN in a “closed-plate” system	124
3.2.2. In-depth root characterization shows PsJN-imparted growth promotion on root system architecture (RSA) as influenced by temperature and time.....	125
3.2.3. High temperature negatively impacts the root system distribution, but PsJN buffers this effect through improvements on individual root types.....	131

3.2.4. Root length per depth is influenced through time by bacterial inoculation and high temperature	133
3.2.5. Growth association between root types varies under each treatment.....	135
3.2.6. Bacterial inoculation under different temperatures influences the leaf area and dry weights with different magnitude	136
3.3. Discussion	138
3.3.1. Changes in the root system architecture are modulated by intrinsic factors and different root-environment interactions.....	138
3.3.2. <i>P. phytofirmans</i> PsJN induces modifications of the components of the root system architecture contributing to improved plant growth.....	140
3.3.3. Positive bacteria-imparted root modifications correlate with shoot responses at ambient temperature and are time-dependent.....	141
3.3.4. The extent of bacterial stimulation effect in roots and shoots varies depending on the temperature condition	142
3.3.5. Temporal effects of bacterial inoculation show accelerated growth rates at the early stage of plant growth depending on root type and temperature condition	143
3.3.6. The GrowScreen-Agar II is an efficient platform for plant cultivation, non-invasive phenotyping, and root and shoot trait characterization.....	144
3.4. Materials and Methods:.....	146
3.4.1. Customized agar-plate preparation.....	146
3.4.2. Seed sterilization, sowing, and stratification	147
3.4.3. Bacterial cultivation and inoculation	147
3.4.4. Plant growth conditions	148
3.4.4.1. GrowScreen-Agar II platform specifications	148
3.4.4.2. Growth optimization using a traditional “closed-plate” system	149
3.4.5. Time course image analysis.....	149
3.4.6. End-point harvest and validation of bacterial colonization	150
3.4.7. Statistical analysis.....	151
3.5. Conclusions and future perspectives	151

3.6. Supplementary Materials.....	152
3.7. Author contributions	152
3.8. Funding.....	153
3.9. Acknowledgments.....	153
3.10. Conflict of interest.....	153
CHAPTER 4	154
The lipidome of <i>Arabidopsis thaliana</i> roots at different stages of interaction with the endophytic plant growth-promoting rhizobacteria <i>Paraburkholderia phytofirmans</i> PsJN under heat stress.....	154
Preface to Chapter 4.....	155
4.1. Introduction	157
4.2. Materials and Methods	161
4.2.1. Growth protocols for Arabidopsis plants and its co-cultivation with P. phytofirmans PsJN bacteria plants.....	161
4.2.2. Sample collection and lipid extraction	163
4.2.2.1. Extraction from plant roots.....	163
4.2.2.2. Extraction from bacteria	164
4.2.3. Lipid analysis by Liquid Chromatography–Mass Spectrometry (LC-MS).....	165
4.2.4. Data processing.....	166
4.2.5. Statistical analysis.....	166
4.3. Results	167
4.3.1. Confirmation of bacterial colonization of the rhizoplane and root tissues.....	167
4.3.2. Lipid profiling of control and PsJN-inoculated Arabidopsis roots under ambient and high temperature conditions and three time points.....	167
4.3.3. Comparison of annotated lipids and unknown features profile of Arabidopsis roots under four treatments and three timepoints	170
4.3.4. Comparison of lipid class profiles of control and PsJN-inoculated roots under each treatment and time point	179

4.3.5. Specific lipid species altered when control and PsJN-inoculated roots were subjected to different temperatures and at different time points	187
4.3.6. Comparison of lipid profiles of ambient-grown and heat-stressed roots at different time points.	191
4.4. Discussion	196
4.4.1. High temperature altered several annotated lipid species and manifested similar dynamic changes in unknown features	197
4.4.2. Bacteria-induced changes to the lipid profile is prominent under high temperature	200
4.4.3. Specific lipid species with specific behaviour and fold change comparison of control and inoculated roots.....	203
4.5. Conclusion.....	205
CHAPTER 5	207
General discussion and conclusion	207
5.1. Introduction	208
5.2. Relevance of the study	211
5.3. Thesis outline and main insights	211
5.4. Synthesis.....	216
5.4. Concluding remarks and future perspectives	218
Appendices.....	222
References.....	244

CHAPTER 1

Plant root-microbe interactions in a changing climate

Preface to Chapter 1

This chapter of the thesis introduces the complex underground interactions between plant roots and the soil microbes under the climate-change driven elevated global atmospheric temperatures. The first part of the chapter describes the different components of this tripartite interaction such as the drivers and impacts of climate change and heat stress, the nature of plant roots and how they respond to the biotic and abiotic environment, and the potential of soil microbes for improving plant growth and tolerating high temperature stress. The second part of the chapter (sections 1.5. to 1.5.6) was published in the journal *Trends in Plant Science* with the title “Modulators or facilitators? Roles of lipids in plant root–microbe interactions” (Macabuhay, A., Arsova, B., Walker, R., Johnson, A., Watt, M., & Roessner, U. (2022, 2022/02/01/). Modulators or facilitators? Roles of lipids in plant root–microbe interactions. *Trends in Plant Science*, 27(2), 180-190. <https://doi.org/https://doi.org/10.1016/j.tplants.2021.08.004>) as a compressed review article and is presented in the Appendices. I contributed 80% of the work, which includes the survey of the literature and the writing of the manuscript. At the end of the chapter, the specific objectives of the PhD project and the chapter synopsis (with COVID-19 impacts) are also presented.

1.1. Climate change: drivers and impacts

Though people often think that it is a future problem, the effects of climate change are already happening now. Global climate change has long been predicted by scientists to cause occurrences such as the shrinking of glaciers and ice sheets, accelerated rise of the sea level, shifting of plant and animal geographic ranges, deep ocean acidification, and longer and more intense heat waves. According to the National Oceanic and Atmospheric Administration (NOAA), climate change is more than just an increase in global atmospheric temperatures. It also involves the changes in weather patterns leading to drought, wildfires, extreme rainfall, and flooding, including the El Niño–Southern Oscillation (ENSO) climate pattern (with La Niña as the colder counterpart) (<https://www.noaa.gov/education/resource-collections/climate/climate-change-impacts>) – all of which can have detrimental impacts on the environment and the agricultural sector.

As defined in the Fifth Assessment Report (AR5) of the Intergovernmental Panel on Climate Change (IPCC), climate change is the “alteration in the state of the climate that can be identified by changes in the mean and/or the variability of its properties, attributed to both natural phenomena and anthropogenic activities, and which persists for an extended period” (IPCC, 2014, p.5). On the other hand, the Framework Convention on Climate Change (UNFCCC), made a distinction between climate-related changes attributable to human activities altering the composition of the global atmosphere, and climate variability due to natural causes observed over comparable period of time (IPCC, 2014).

Before the Industrial Revolution in the 1700s, climate change was caused by natural processes such as changes in the solar energy, volcanic eruption, and natural changes in greenhouse gases (IPCC, 2013). However, climate-induced variability that occurred after the Industrial Revolution could not be explained alone by natural causes but instead has been ascribed to likely been dominantly caused by human activities (Arias, 2021). Nowadays, according to the report, although natural causes are still influencing the Earth’s climate, humans are increasingly affecting it, to the point where we are now the main cause of recent and projected climate-related changes. Human activities contributing to climate change include burning fossil fuels for energy and heat, clearing the forests, use of fertilizers in crops, storing waste materials in landfills, raising livestock, use of transportation, and production of industrial products.

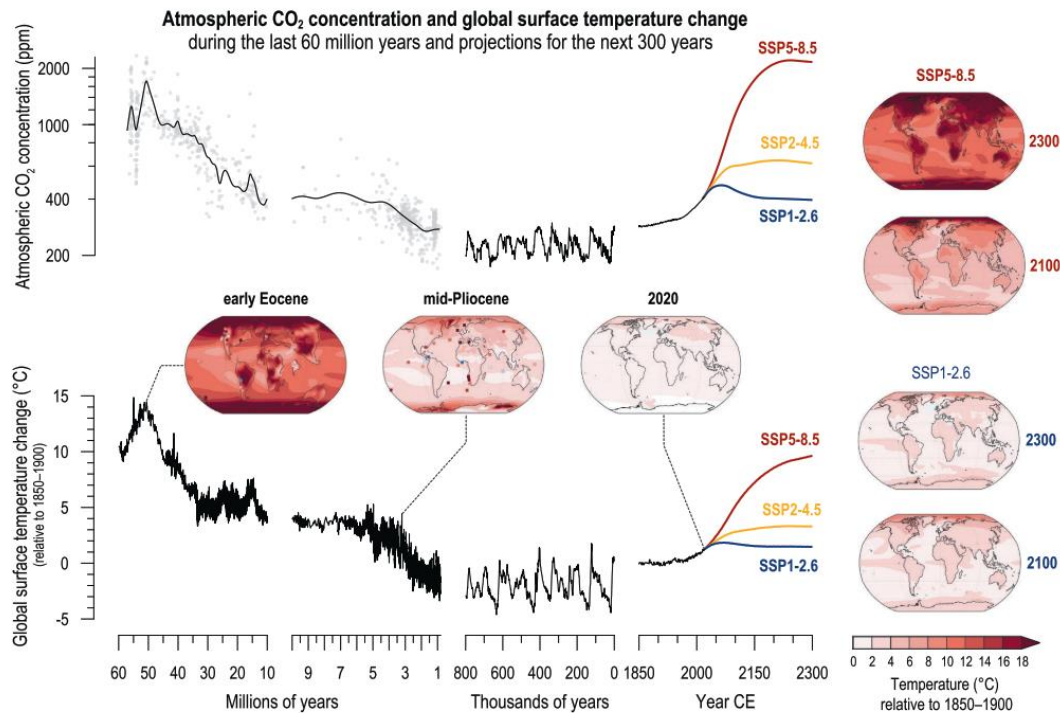


Figure 1.1 Changes in atmospheric CO₂ and global surface temperature (relative to 1850–1900) from the deep past to the next 300 years. This figure attempts to show that CO₂ and temperatures are similar to those only from many millions of years ago. CO₂ concentrations from millions of years ago are reconstructed from multiple proxy records. CO₂ levels for the last 800,000 years through the mid-20th century are from air trapped in polar ice; recent values are from direct air measurements. Global surface temperature before 1850 is estimated from marine oxygen isotopes, one of the multiple sources of evidence used to assess paleo temperatures. The temperature of the past 170 years is the Sixth Assessment Report (AR6) assessed mean. CO₂ levels and global surface temperature change for the future are shown for three Shared Socio-economic Pathway (SSP) scenarios through 2300 CE, using Earth system model emulators calibrated to the assessed global surface temperatures. [Source: Image and description adapted from (Arias, 2021).]

According to the U.S. Environmental Protection Agency (USEPA), changes imposed by the drivers of climate change are quantified by effective radiative forcing (ERF), which is a measure of influence on the Earth’s energy balance (in Wm^{-2}), where warming of the planet’s surface is considered a positive radiative forcing (Arias, 2021). Some examples of ERF are greenhouse gases (GHG), aerosols, or land use change. The report specified that the main contributor to the total radiative forcing is the increase in greenhouse gases. Since 1950, greenhouse gas emissions have been the cause of most warming. These gases make up the thin atmospheric layer that acts as a blanket covering and blocking sunlight from escaping or being reflected back in space, thus making the Earth’s surface and lower atmosphere a habitable

environment in a process known as the “greenhouse effect”. Gases that comprise the greenhouse gases include carbon dioxide (CO₂), methane (CH₄), nitrous oxide (N₂O), ozone (O₃), and fluorinated gases (F-gases) such as chlorofluorocarbons (CFC), hydrofluorocarbons (HFC), and sulfur hexafluoride (SF₆). Among these gases, atmospheric CO₂, which has the largest concentration and the longest lifetime, significantly contributes to the largest forcing that is slowly heating the Earth’s surface. CO₂ can come from the following sources: carbon cycle emissions (e.g. volcanic eruptions and ocean-atmospheric exchange), plant and animal respiration, anthropogenic activities such as the burning of fossil fuels (coal, oil, natural gas), and land use changes such as deforestation, land clearings for agriculture, and soil degradation (Arias, 2021).

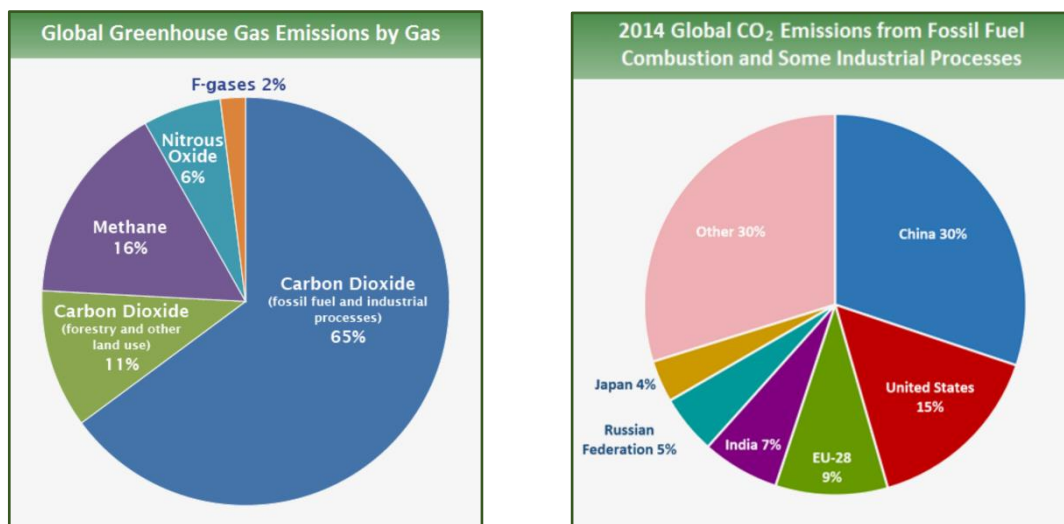


Figure 1. 2 Key greenhouse gases emitted by human activities based on global emissions from 2010 (Left). Top global CO₂ producers in 2014 (Right). Left figure shows the percentage of each gas comprising the global greenhouse gas, with corresponding sources mainly for CO₂. Right figure shows CO₂ emissions from fossil fuel combustion and some industrial processes such as cement manufacturing and gas flaring from different countries. [Sources: Figures and description adapted from IPCC (2014) and Boden et al. (2017)]

The increase in the concentration of atmospheric CO₂, along with other greenhouse gases, is responsible for most of the surface warming, in the so-called “enhanced greenhouse effect” or global warming, which is characterized by a significant increase in global atmospheric temperatures (IPCC, 2014). IPCC (2014) predicted an average increase in the global temperature of approximately 3.5°C (5.4°F), or 2°C by 2050 and about 4°C by the end of the century. Should global emissions of CO₂ continue to rise, there will be more drastic incidences

of extreme temperatures or heat stress and extreme weather events such as heat waves, which are projected to continue and accelerate significantly (IPCC, 2021).

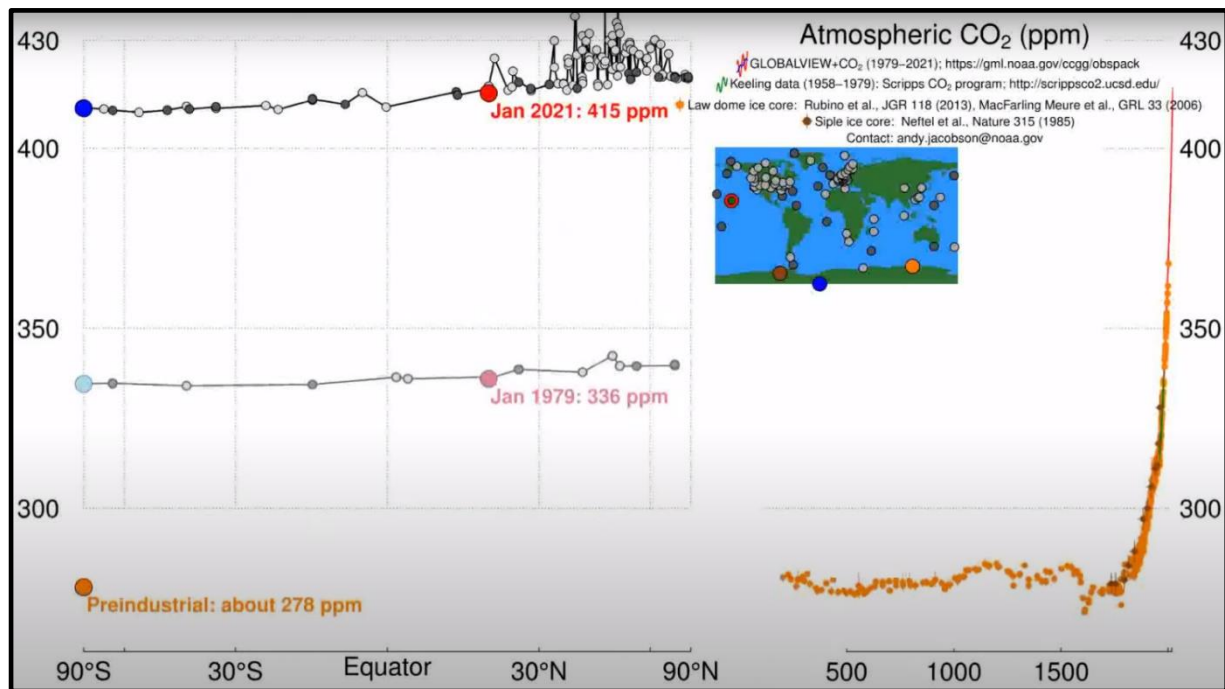


Figure 1.3 Atmospheric carbon dioxide (CO₂) concentration (ppm) at Mauna Loa, Hawaii from pre-industrial period (<1700), through 1979 until 2021. CO₂ concentration was mostly stable at 285 ppm before the 1700s (Industrial Revolution) and has increased rapidly since then. [Source: Interactive video from National Oceanic and Atmospheric Administration (NOAA), Earth System Research Laboratory (ESRL), Global Monitoring Division]

1.1.1. Implications of climate change to agriculture

The range of available scientific evidence indicates that the net damage of climate change is likely to increase over time. The effects of climate change, together with associated environmental variations, are mainly estimated by the number of stress spells, their impacts on daily life, as well as damage to agricultural crops (WHO, 2018). High temperatures, in particular, are already felt in many sectors and are expected to become even more disruptive throughout the century, with variable intensities and impacts (Arias, 2021). Based on the National Climate Assessment of the U.S. Global Change Research Program (USGCRP), agriculture is one of the sectors most susceptible to elevated global temperatures mainly because of the agricultural system's critical dependency on climate and the latter's complex role in the social and economic system – on the local, national, and global scale (USGCRP, 2017). As a side effect of the negative impacts of climate change on agriculture, there will be

global food insecurity through changes in crop yields. This is because an important prerequisite to attaining food security is crop production (Brown et al., 2015). With the unprecedented increase in the world population (projected to grow to about 9 billion in 2050), reduced availability of fertile agricultural lands, and high-input low-variability cropping systems, the reduction in crop productivity due to climate change-induced elevated temperatures can pose significant threat to food security (Raza, Razzaq, et al., 2019). In developing countries, where the effects of high temperatures are predominant, scientists have been forced to devise new strategies to cope with adverse environmental challenges, including the development and production of new climate-smart crop cultivars (Wheeler & von Braun, 2013).

Under normal environmental conditions, plants are subjected to abiotic stresses, such as waterlogging, drought, heat, cold, and salinity – all of which can be exacerbated by climate-related changes (Ashraf et al., 2018). The cultivation of agricultural crops and their yields is highly dependent on changes in temperature, as well as the intensity and frequency of weather conditions. On some level, increasing temperatures, simultaneous with elevated CO₂ concentrations, may have positive effects on crop yields depending on optimal growth requirements (variable across different developmental stages), the type of crop in a specific area, and the farmer’s utilization of warm weather in crop selection (Ziska et al., 2016). However, several conditions must be met in order to gain these benefits, including nutrient levels, soil moisture, and water availability. Conversely, a decline in crop yield will follow once the optimum temperature is exceeded. The optimum threshold temperatures of some crop plants are tabulated in Table 1.

Table 1. 1 Threshold high temperatures for some crop plants

Crop plants	Threshold temperature (°C)	Growth stage	References
Wheat	26	Post-anthesis	Stone and Nicolás (1994)
Corn	38	Grain filling	Thompson (1986)
Cotton	45	Reproductive	Rehman et al. (2004)
Pearl millet	35	Seedling	Ashraf and Hafeez (2004)
Tomato	30	Emergence	Camejo et al. (2005)
Brassica	29	Flowering	Morrison and Stewart (2002)
Cool season pulses	25	Flowering	Siddique et al. (1999)
Groundnut	34	Pollen production	Vara Prasad et al. (2000)
Cowpea	41	Flowering	Patel and Hall (1990)
Rice	34	Grain yield	Morita et al. (2004)

[Source: Table adapted from Wahid et al. (2007)]

Based on the study conducted by Lobell and Gourdji (2012), high temperatures can influence crop yields and responses through five main pathways. First, crops accelerate their development leading to shorted crop duration, generally associated with lower yields (Stone,

2001). Second, depending on the current temperature relative to optimum (with C₄ plants having higher optimum temperatures), the rates of photosynthesis, respiration, and grain-filling of both C₃ and C₄ crops are adjusted (Crafts-Brandner & Salvucci, 2002). Third, there is an observed exponential increase in the saturation vapor pressure of the air which is the vapor pressure deficit (VPD) between the air and the leaf, a condition that results in reduced water-use efficiency as plants lose more water per unit of carbon gain (Ray et al., 2002). Fourth, during the critical reproductive periods, increased probability of hot extremes and reduced probability of cold extremes will impose direct damage to plant cells, leading to sterility, lower yields, and the risk of complete crop failure (Teixeira et al., 2013). Finally, increased temperatures will favor an increase in the growth and survival of many pests and diseases specific to agricultural crops (Ziska et al., 2011).

1.2. High temperature (heat) stress in plants

Heat stress is defined as the rise in temperature beyond a threshold level for a period of time that is sufficient to cause irreversible damage to plant growth and development (Wahid et al., 2007). Accordingly, a transient elevation in temperature of about 10-15°C above the optimum ambient temperature requirement of a plant can generally be considered heat stress (also “heat shock”). This phenomenon is a complex function of intensity, duration, and rate of increase in temperature. Extremely high temperatures can cause cellular injury and even cell death within minutes, while moderately high temperatures can cause direct injuries including protein denaturation and aggregation, and increased fluidity of the membrane only after long exposure (Schöffl et al., 1999; Shinozaki & Yamaguchi-Shinozaki, 1999). The occurrence of heat stress in specific climatic zones depends on the probability and period of high temperatures that happen during the day and/or night (Wahid et al., 2007). While others believe that night temperatures are the major limiting factors, many argue that day and night temperatures are not independently affecting plants and that the diurnal mean temperature is a better predictor of plant response to elevated temperature (Willits & Peet, 1998).

Many crops and plant species have upper and lower developmental threshold temperatures – the daily mean temperatures that mark the beginning at which detectable reduction in growth begins when subjected to heat stress, which can vary in plant species belonging to different habitats (Siddique et al., 1999). Lower developmental threshold or base temperature is one below at which plant growth and development stop. In contrast, upper developmental threshold varies depending on plant species and genotypes within species and is affected by different

environmental conditions. In tropical and subtropical climates, the determination of high-temperature sensitivity, which varies on the plant's developmental stage, is particularly important as heat stress has the potential to become a major limiting factor for field crop production (Wahid et al., 2007). For example, brief exposure of certain plants to high temperatures during the grain-filling period can accelerate senescence, diminish seed set and seed weight, as well as reduce yield. This is because plants tend to divert resources that limit the availability of photosynthates for reproductive development. Heat stress can also induce sterility when imposed immediately before or after anthesis or flowering and can cause severe yield losses through flower drop or pod abortion, as with the case of pulse legumes (Siddique et al., 1999). Therefore, determining the threshold temperatures can help prevent damage throughout the plant's ontogeny due to unfavorable temperatures.

1.2.1. Plant responses to heat stress

Whether transitory or constant, high temperature or heat stress elicits an array of responses in plants, and this can be through physiological, morpho-anatomical, molecular, or biochemical changes, which directly affect plant growth and productivity. Plants can be classified into three groups based on their preferred temperature of growth: Psychrophiles, which grow optimally at low temperatures between 0°C and 10°C; Mesophytes, which favor moderate temperature and grow well between 10 and 30°C; and the Thermophytes, which grow well between 30 to 65°C.

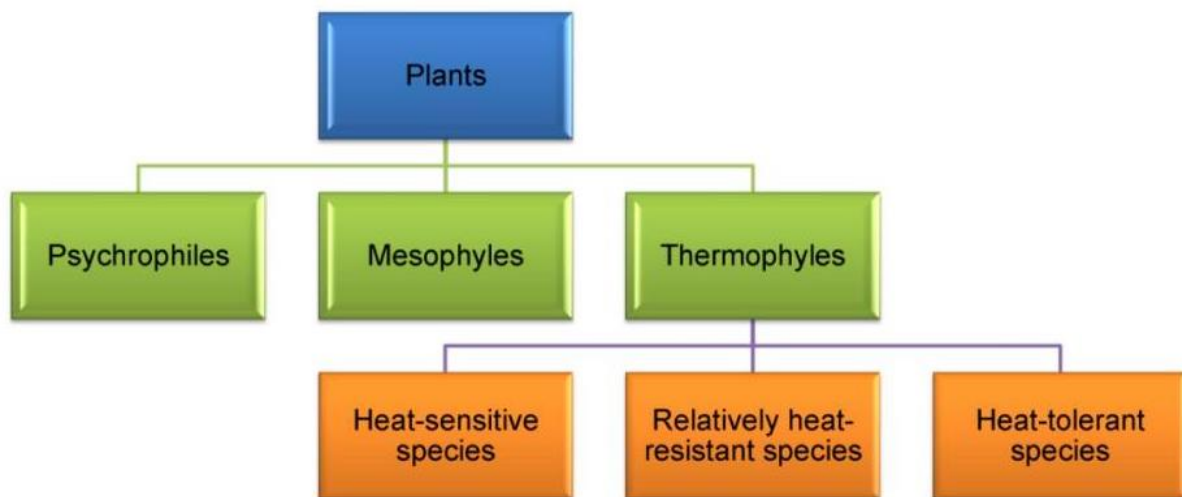


Figure 1. 4 Classification of plants based on heat tolerance. [Source: Image adapted from Hasanuzzaman et al. (2013)]

1.2.1.1. Morphological responses

Morphologically, heat stress can cause scorching of leaves and twigs, sunburns on leaves, branches, and stems, leaf senescence and abscission, shoot and root growth inhibition, and fruit discoloration and damage, leading to reduced yield and dry matter accumulation (Vollenweider & Günthardt-Goerg, 2005). These responses may be direct as with existing physiological processes or indirect in altering the pattern of development. In addition, these responses vary among plant species and from one phenological stage to another. For example, during seed development, a long-term application of heat stress can cause delayed germination or loss of vigor, which can ultimately lead to reduced emergence and seedling establishment. At seedling emergence, coleoptile growth in maize was reduced at 40°C and ultimately ceased at 45°C due to diurnally variable temperatures (Weaich et al., 1996). On established plants, heat stress can have the following morphological effects: a significant decline in shoot dry mass, relative growth rate, and net assimilation rates (in maize, pearl millet, and sugarcane), although with minimal effect on leaf expansion (Ashraf & Hafeez, 2004). A major impact of heat stress on shoot growth is the severe reduction in the length of the first internode, as with the case of sugarcane which exhibited smaller internodes but increased tillering, early senescence, and reduced total biomass (Hall, 1992).

During anthesis and grain-filling, heat stress can critically affect many cereal crops in temperate regions. For example, heat stress has been known to reduce kernel growth leading to a reduction of kernel density and weight in spring wheat (Guilioni et al., 2003); reduction in starch, protein, and oil contents in maize kernel (Wilhelm et al., 1999) and grain quality in other cereals (Maestri et al., 2002); reduction in both grain weight and grain number in wheat (Ferris et al., 1998). Reproductive organs and processes are also adversely affected by high temperature, including meiosis in both female and male organs, pollen germination and pollen tube growth, ovule viability, stigmata and style positions, number of pollen grains retained by the stigma, fertilization and post-fertilization processes, growth of the endosperms, pre-embryo and fertilized embryo (as reviewed by Foolad (2005). The review also mentioned that the reproductive phases most vulnerable to high-temperature stress are gametogenesis (8-9 days before anthesis) and fertilization (1-3 days after anthesis). High temperatures can also induce poor fruit set due to the reduction in the levels of carbohydrates and growth regulators released in the plant sink tissues (Kinet & Peet, 1997). Overall, previous studies and available resources show that plant morphological responses to high temperature or heat stress vary with plant species and specific phenological stages.

1.2.1.2. Anatomical responses

Anatomical responses in plants include a greater tendency for reduced cell size, closure of stomata to curtail water loss, increased stomatal and trichotomous densities, and greater xylem vessels of both roots and shoots (Bañon et al., 2004). A study on grapes revealed that heat stress severely damaged the mesophyll cells and increased the permeability of the plasma membrane (Zhang et al., 2005). The onset of a high-temperature regime was also found to induce the formation of polymorphic leaves and a reduction in transpirational water loss via bimodal stomatal behavior in *Zygophyllum qatarense* (Sayed, 1996). High temperature also caused changes on a sub-cellular level, such as the modifications in the chloroplast, which ultimately result in reduced photosynthetic activities. Chloroplast modifications include changes in the structural organization of the thylakoids, loss of grana stacking or its swelling, the re-shaping of the chloroplast (into a round shape), swelling of the stroma lamellae, and clumping of the vacuole contents (Zhang et al., 2005). In addition, there are also disruptions of the cristae and the emptying of the mitochondria, which lead to decreased respiratory activities. In general, these show that high temperature considerably affects anatomical structures not only on the tissue and cellular level but also at the sub-cellular level; and that cumulative effects of these changes imposed by high temperature may result in poor plant growth and productivity (Wahid et al., 2007).

1.2.1.3. Phenological responses

During the plant's ontogeny, different phenological stages differ in their sensitivity to high temperature; however, this depends on species and genotype as there are great inter- and intra-specific variations (Wollenweber et al., 2003). The effect of heat stress is evident in the rate of plant development, which may be increasing to a certain limit and decreasing afterward (Howarth, 2005). Different developmental stages in plants have varying sensitivity to high-temperature stress. It is still unknown, however, whether the damaging effects of heat episodes from different developmental stages are cumulative (Wollenweber et al., 2003). The most sensitive stages of plant growth to high temperatures are the vegetative and reproductive stages, although germination is also highly susceptible. During the vegetative stage, plants are most vulnerable to damaged photosynthetic machinery, particularly involving the leaf gas exchange properties.

At the reproduction stage, heat stress can cause significant increases in the abortion of floral buds and opened flowers, impairment of pollen and anther development that leads to decreased fruit or grain set, and damage to fertilization and seed production (Guilioni et al., 2003). During grain-filling, high temperatures can cause modification in the flour and bread quality, and other physicochemical properties of grain crops (Perrotta et al., 1998), including the protein content of the flour. It is an advantageous trait for plants to have earlier heading to retain more green leaves at anthesis, leading to a smaller reduction in yield under high temperatures (Tewolde et al., 2006). Therefore, knowledge of the developmental stages and plant processes most vulnerable to high temperatures is crucial for crop production under high-temperature conditions.

1.2.1.4. Physiological responses

High temperature is frequently associated with a reduction in water availability, as with heat stress and drought, particularly observed in field conditions. In plants, physiological responses are those associated with photosynthesis, water relations, and cell membrane thermostability – where the water status is significantly influenced by fluctuating temperatures. Under sufficient water conditions, plants can maintain a stable tissue water status regardless of temperature; however, when there is limited moisture, high temperature can severely impair this process. This was observed by Bañon et al. (2004) when the elevated night temperatures caused a reduction in the leaf water potential of water-stressed *Lotus criticus* plants compared with unstressed ones; while similar occurrence in sugarcane under sufficient water supply and relative humidity implied the effect of heat stress on root hydraulic conductance. On the other hand, Tsukaguchi et al. (2003) found that high temperatures seem to cause more water loss during daytime than nighttime, and this can be attributed to enhanced transpiration during daytime that induces water deficiency in plants, leading to reduced water potential and perturbation of many physiological processes.

While any constraint in photosynthesis can limit plant growth at high temperatures, alterations in the photosynthetic attributes can be good indicators of thermotolerance in plants as they show a correlation with growth (Wahid et al., 2007). Episodes of high temperature affect the photochemical reactions (thylakoid lamellae), carbon metabolism (stroma of chloroplast), chlorophyll fluorescence (the ratio of variable fluorescence to maximum fluorescence, F_v/F_m), and base fluorescence (Wise et al., 2004). These changes in chlorophyll or the photosynthetic apparatus were suggested to be associated with the production of active

oxygen species (Camejo et al., 2006). As a consequence of heat stress, there occurs an imbalance in photosynthesis and respiration, where the rate of photosynthesis decreases, while the dark- and photo-respiration rates increase considerably. In addition, the rate of biochemical reactions decreases, and enzyme activation and denaturation takes place as the temperature increases leading to severely reduced photosynthesis (Nakamoto & Hiyama, 1999).

The cell membrane thermostability is also affected by high temperature since the latter accelerates the kinetic energy and movement of molecules across membranes, thereby loosening chemical bonds within molecules of biological membranes (Savchenko et al., 2014). This makes the lipid bilayer of biological membranes more fluid through either denaturation of proteins or an increase in unsaturated fatty acids. Such alterations of the membrane enhance their permeability, which can also be observed from the increased loss of electrolytes – also known as solute leakage, which is an indirect measure of heat stress tolerance in diverse plant species (Ashraf & Hafeez, 2004; Wahid et al., 2012).

1.2.1.5. Molecular responses

Aside from tissue dehydration that elicits several physiological responses, heat stress may also induce oxidative stress, such as the generation of activated oxygen species (AOS) including singlet oxygen ($^1\text{O}_2$), superoxide radical (O^{2-}), hydrogen peroxide (H_2O_2) and hydroxyl radical (OH^-), which are indicators of cellular injury (Liu & Huang, 2000). AOS is responsible for the autocatalytic peroxidation of membrane lipids and pigments, which leads to the loss of membrane semi-permeability and the modifications of its functions (Xu et al., 2006). Individually, O^{2-} and H_2O_2 are not that toxic; however, these two combine to form OH^- in the presence of trace amounts of Fe^{2+} and Fe^{3+} by the Haber–Weiss reaction (Sairam & Tyagi, 2004). OH^- can damage chlorophyll, protein, DNA, lipids, and other important macromolecules, thus fatally affecting plant metabolism and limiting growth and yield.

To protect cells from oxidative damage, plants have developed a series of enzymatic and non-enzymatic detoxification systems to counteract AOS, such as the overexpression of superoxide dismutase protein (SOD) that affects several physiological phenomena (Scandalios, 1993). Stressed tissues have decreased antioxidant activity resulting in higher levels of AOS, therefore, protection against oxidative stress is an important component in determining the survival of heat-stressed plants. Enhanced synthesis of antioxidants such as ascorbate and glutathione, and more studies on some signaling molecules that can increase the antioxidant capacity of cells, will be useful in the acclimation of plants to heat stress (Xu et al., 2006).

Another important adaptation mechanism of plants to cope with environmental stresses such as high temperature is the expression of stress proteins, which presumably assist in stress tolerance via the hydration of cellular structures due to their solubility in water (Nakamoto & Hiyama, 1999). Heat shock proteins (HSPs) and other proteins are implicated in the heat-stress response of plants. Production of HSPs is increased whenever plants experience either an abrupt or gradual increase in temperature (Schöffl et al., 1999), and this is a universal response to heat stress also observed in other organisms ranging from bacteria to humans (Vierling, 1991). HSP-triggered thermotolerance is attributed to the observations that (a) their induction coincides with the organism under stress, (b) their biosynthesis is extremely fast and intensive, and (c) they are induced in a wide variety of cells and organisms (Nakamoto & Hiyama, 1999).

1.2.2. Plant mechanisms for heat tolerance:

Plants employ a variety of adaptation mechanisms to survive in hot and dry environments. According to Hasanuzzaman et al. (2013), there are two specific ways by which plants adapt, through avoidance and tolerance mechanisms, dependent on high-temperature duration, which both utilize several strategies.

1.2.2.1. Avoidance mechanisms

For short-duration high-temperature conditions, plants may exhibit avoidance or acclimation mechanisms. Acclimation strategies may include stomatal closure to reduce water loss, increased stomatal and trichomatous densities, and enlarged xylem vessels; while avoidance strategies include early maturation of crops to escape the hot spells during harvests, reduction in the absorption of solar radiation through the process of paraheliotropism (when leaf blades position themselves parallel to the sun rays), leaf blade rolling to increase water metabolism (as is the case with wheat during high temperature), and limiting transpiration with the use of the same anatomical and physiological adaptive mechanisms employed during water deficit (Adams et al., 2001; Rodríguez et al., 2005). On the other hand, plants that have been constantly subjected to high temperatures have evolved life histories allowing them to avoid the hottest period of the season. This is achieved through mechanisms such as the abscission of the leaf, leaving buds that are heat resistant, or early completion of the entire reproductive cycle during the cooler months (as with desert annuals). Such adaptations in morphology and phenology are commonly associated with net photosynthesis under high temperatures (particularly C4 and CAM photosynthetic pathways) (Fitter & Hay, 2012).

Tolerance to heat in plants can be described as the ability to grow and produce economic yield even under high temperatures (Wang et al., 2004). This trait has high specificity, causing closely related species, even various tissues and organs of the same plant, to exhibit some variations. Some major tolerance mechanisms that plants exploit to counteract the effects of heat stress are ion transporters, late embryogenesis abundant (LEA) proteins, osmoprotectants, antioxidant defense, and mechanisms implicated in signaling cascades and transcriptional control (Rodríguez et al., 2005).

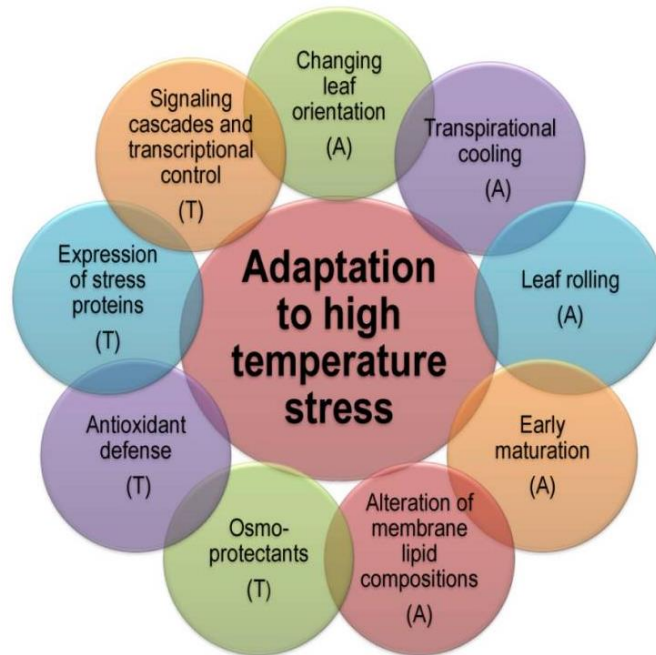


Figure 1. 5 Different adaptation mechanisms of plants to high temperature: A. Avoidance, T: Tolerance. [Source: Image adapted from Hasanuzzaman et al. (2013).]

1.2.2.2. Induction of heat tolerance

Plant stress tolerance mechanisms are first induced by the initial stress signals, which could be ionic or osmotic effects or alterations in membrane fluidity. These signals then trigger the downstream signaling processes and transcription controls, causing the stress-responsive mechanisms to activate and re-establish homeostasis and protect and repair the damaged membranes and proteins (Vinocur & Altman, 2005). These initial steps are crucial in that inadequate responses at one or more steps of the signaling and gene activation processes might result in irreversible damage to cellular homeostasis and destruction of functional and structural proteins and membranes, leading to cell death (Bohnert et al., 2006; Vinocur & Altman, 2005).

A series of response mechanisms to cope with high-temperature stress, beginning with heat perception and signaling and metabolite production, have been proposed. The effects of heat stress are prominent at several levels, originating from the plasma membrane and progressing down to the cytosol or cytoplasmic organelles through the operation of biochemical pathways (Sung et al., 2003). Wahid et al. (2007) summarized the induction of the heat tolerance process (Figure 6). The initial effect of heat stress is detected on the plasmalemma, which exhibits a more fluid lipid bilayer. This change in fluidity then induces the Ca^{2+} influx and cytoskeletal reorganization, which results in the upregulation of the mitogen-activated protein kinase (MAPK) and calcium-dependent protein kinase (CDPK). This signaling cascade ultimately leads to the production of antioxidants and compatible osmolytes for cell water balance and osmotic adjustment. Another effect of heat stress that is of great significance for signaling, is the production of reactive oxygen species (ROS) in the organelles such as the chloroplast and mitochondria (Bohnert et al., 2006), the consequence of which is also the induction of antioxidant defense mechanism. In accordance with this, the capacity to acquire thermotolerance was correlated with the activities of catalase and superoxide dismutase, higher ascorbic acid content, and less oxidative damage in a set of wheat genotypes (Sairam & Tyagi, 2004). Finally, one of the most investigated thermotolerance mechanisms is the induction of HSP from protein denaturation, involving several conserved families of proteins with unique chaperone mechanisms and activities. The HSP's protective effects can be attributed to the concerted actions of a network of chaperone machinery, which interact with other stress-response mechanisms (Wang et al., 2004), such as signal transductions and gene activation, redox state regulation, and production of osmolytes and antioxidants (Arrigo, 1998; Nollen & Morimoto, 2002; Panchuk et al., 2002).

Although the study is still in its infancy, changes in the membrane lipid levels are considered an important element in high-temperature tolerance. For example, heat treatment in a heat-resistant mutant line was found to increase the relative quantities of linolenic acid (among galactolipids) and *trans*-3-hexaldecanoic acid (among phospholipids), when compared with its wildtype (Behl et al., 1996). The contribution of lipids, which are major structural components and contributes to several membrane functions, needs to be further explored, particularly under high-temperature stress.

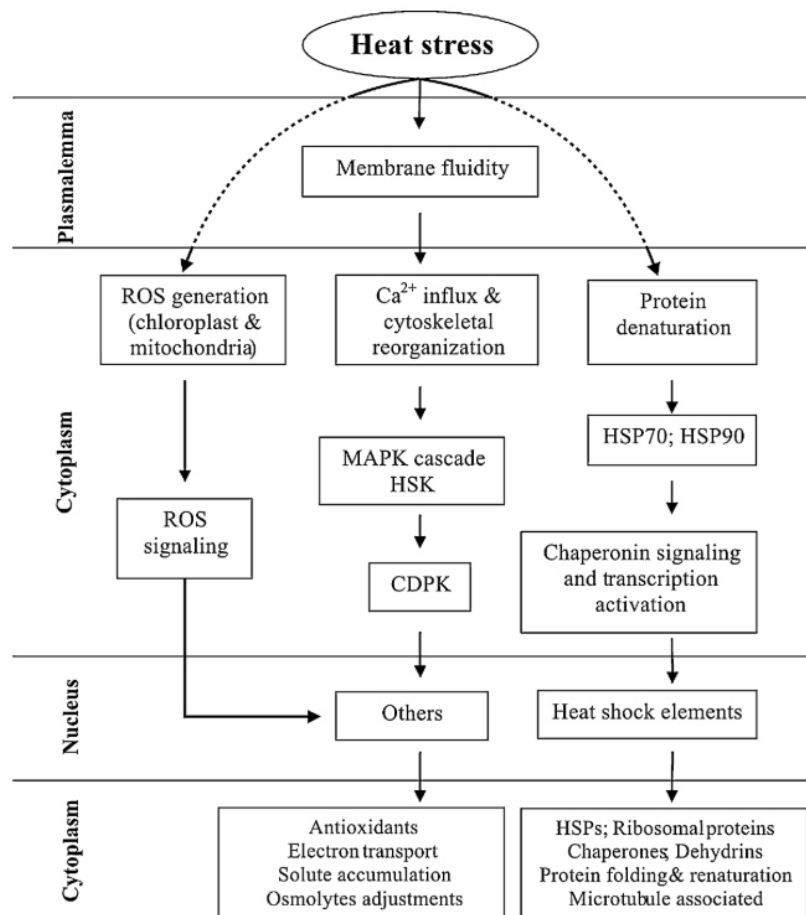


Figure 1. 6 Proposed mechanisms of heat stress tolerance in plants. MAPK, mitogen-activated protein kinases; CDPK, calcium-dependent protein kinase; HSK, histidine kinase; ROS, reactive oxygen species; HSPs, heat shock proteins. [Source: Image and description adapted from Wahid et al. (2007).]

1.2.3. Strategies for heat tolerance and plant adaptation

Because of the variation in the environment due to climate change, which has a lasting influence on agriculture, several adaptation strategies for crops have emerged.

1.2.3.1. Crop management

One approach employed to combat climate-related stresses in agriculture is the use of crop management techniques to enhance crop development under various environmental stresses. This includes the alteration of planting and harvesting time, utilization of crops with shorter life cycles, application of crop rotation and irrigation methods, as well as varying the cropping schemes (Raza, Razzaq, et al., 2019). Additional crop management techniques used are seed priming, where seeds are placed in an osmotic solution at moderate temperatures before drying;

deep placement, which counters the emergence problem of plants due to very hot soil surface; and shading with foliage, which prevents intense direct solar radiation and high temperature.

1.2.3.2. Conventional breeding technique

Another approach is the use of conventional techniques through plant breeding (Blum, 2018). This allows plants to tolerate harsh weather conditions, particularly during their crucial growth phases. However, the direct selection process can have some serious difficulties, particularly in the field, where it is challenged by uncontrolled environmental factors that throw off the precision and repeatability of trials. A common method of selecting plants for heat tolerance studies has been to grow breeding materials in a targeted hot environment and identify and screen for high-yielding individuals or lines (Ehlers & Hall, 1998). Another technique used to define accomplished breeding is genetic divergence analysis, a technique used for the development of new cultivars based on genetic similarities and distance, which is used for polymorphism, inbreeding, assessment, assortment, and recombination to develop climate-smart plants (Raza, Mehmood, et al., 2019).

1.2.3.3. Genetic engineering and biotechnology

Finally, there are also genetics and genomics strategies, which include omics-led breeding and marker-assisted selection (MAS) that provide resources to elucidate biological functions of any genetic information from crop upgrading and development (Stinchcombe & Hoekstra, 2008). Genome-wide association studies (GWAS) is a powerful tool for understanding the complete set of genetic variants in various crop cultivars to associate alleles with any specific trait (Manolio, 2010). Genome selection (GS) is done by using high-throughput phenotyping and marker densities to screen elite germplasm for improving polygenic traits (Kumar et al., 2018). There is also genetic engineering through the use of biotechnology for genetic manipulation of the genome to develop genetically-engineered plants demonstrating resistance against climate variations (Reynolds et al., 2015).

Although plant breeding and plant engineering have been powerful tools in improving plant tolerance to abiotic stresses such as high temperature (Araus et al., 2008; Mittler & Blumwald, 2010; Sangam et al., 2009), these are met with several challenges. The gaps in our knowledge of the complex mechanisms involved in stress tolerance (physiological, developmental, biochemical, genetic) and the difficulty of combining target alleles to create improved and high-yielding genotypes pose major constraints in improving the heat stress tolerance of crops.

In addition, most of the transgenic plant experiments are conducted under controlled greenhouse conditions, with only a few translated into field trials. It is a crucial requirement that transgenic plants be evaluated, and how the proof-of-concept of gene effect in studied model plant species can be adapted to crop species, particularly in close-to-field conditions (Bhatnagar-Mathur et al., 2008). Unfortunately, amidst breakthroughs and advancements in plant molecular and breeding techniques for abiotic stress tolerance, these approaches did not bring promising results in farmers' fields (Bhatnagar-Mathur et al., 2008; Wang et al., 2003), except for notable exceptions (Munns et al., 2006). Whilst essential, these techniques entail a long and expensive process (Etesami et al., 2015).

1.2.3.4. Microbe applications

A new strategy that is slowly gaining momentum because of its sustainability, e.g., avoidance of indiscriminate use of fertilizers and agrochemicals (to increase crop production or to address pest/insect attacks that are exacerbated by hot and dry/humid conditions), is the use of beneficial soil microorganisms and their interactions with plants. According to Cheng et al. (2019), some rhizobacteria and endophytes could alleviate the adverse effects of high-temperature stress on plants, and at the same time, expand the plant's ability to grow at wider temperature ranges. Studies on abiotic stress tolerance, as with salinity by Shrivastava and Kumar (2015) and Dodd and Pérez-Alfocea (2012) have shown that microbial inoculants can alleviate plant stress and can offer a possible cost-effective, environment-friendly, agricultural input, which has a quicker turnover than new plant germplasm. Thus, there is a need to investigate the diverse beneficial microorganisms, their unique characteristics of heat tolerance, the mechanisms by which they impart thermotolerance in plants, and the resulting response reaction of the interacting partners against high-temperature stress.

1.3. Rhizosphere and the resident “plant-friendly” microorganisms

The area immediately surrounding the plant roots, also known as the rhizosphere, represents a critical hotspot for biogeochemical transformation that underlies the different processes involved in soil formation, carbon cycling, and the complex interaction of the Earth's terrestrial ecosystems (Zhalnina et al., 2018). Within the rhizosphere, a dynamic and intricate interaction between plant roots and diverse networks of organisms, particularly microorganisms, have long existed and been shaped by over 450 million years of cohabitation. Several specific

characteristics have been named and associated with the enrichment of the rhizosphere, including the presence of secretory systems, phage defense, adhesion, iron mobilization, and sugar transport (Bulgarelli et al., 2015; Pini et al., 2011). This specific soil region, which is highly influenced by plant roots, offers an environment that is rich in nutrients for the survival of microorganisms (Bais et al., 2006).

Although roots release both inorganic and organic compounds, the release of the latter significantly influences the biological, physical, and chemical nature of the soil; and this process is known as rhizodeposition. Bulgarelli et al. (2013) defined rhizodeposition as the process responsible for the formation of a distinctive rhizosphere microbiota. This involves the intertwined processes of plant development and secretory activities of the root system. According to Jones et al. (2009), there are several rhizodeposition processes by which carbon enters the soil, including from the loss of root cap and border cell loss, death and lysis of root cells (cortex, root hairs, etc), flow of C to root-associated symbionts living in the soil (e.g. mycorrhizas), gaseous losses, leakage of solutes from living cells (root exudates), and insoluble polymer secretion from living cells (mucilage) (Figure 7).

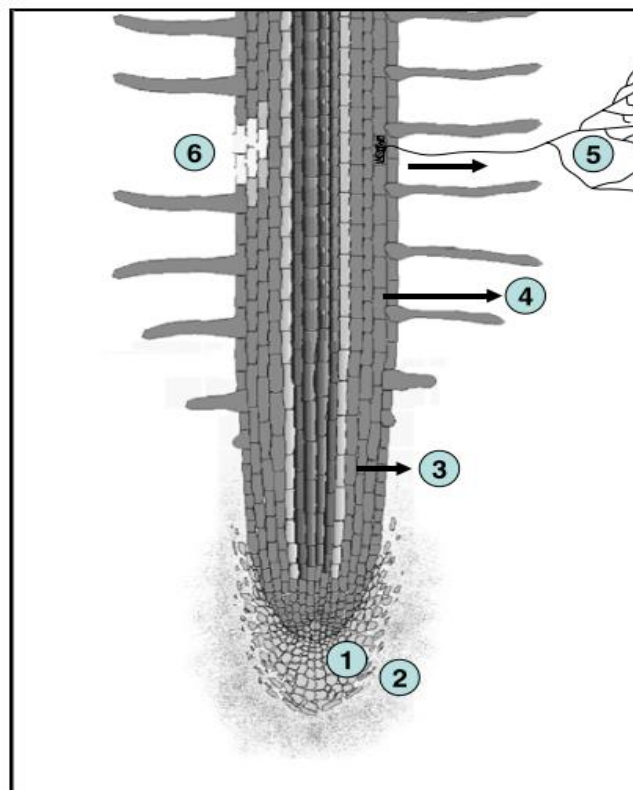


Figure 1. 7 Schematic representation of a longitudinal section of a growing root showing the six major sites of rhizodeposition: (1) loss of root cap and border cells, (2) loss of insoluble mucilage, (3) loss of soluble root exudates, (4) loss of volatile organic C, (5) loss of C to symbionts (e.g. arbuscular

mycorrhizas), and (6) loss of C due to death and lysis of root epidermal and cortical cells. [Source: Image and description adapted from Jones et al. (2009).]

The release of rhizodeposits also comes with an array of compounds such as organic acids (e.g. citric, malic, lactic, succinic, oxalic, and pyruvic acids), sugars (e.g. glucose, fructose, xylose, maltose, sucrose, and ribose), as well as nucleotides, amino acids, putrescine, vitamins, and fatty acids (Bais et al., 2006). It has been estimated that about 11% (Jones et al., 2009) - 20% (el Zahar Haichar et al., 2016; Tian et al., 2020) of the photosynthetically-fixed carbons are exuded by plant roots into the rhizosphere.

Because of their chemotactic nature, microbes are attracted to rhizodeposits for nutrition (Lugtenberg & Kamilova, 2009). It has been suggested that plants enrich or select microbes that are beneficial to their health and growth through the release of rhizodeposits, thereby shaping the composition of microbial communities (Sessitsch et al., 2002). Therefore, the recruitment of the rhizosphere microbes is highly influenced by rhizodeposition and often through bacterial chemotaxis and motility (Tian et al., 2020). This detectable influence on the shape and diversity of the microbial community in the rhizosphere was found not only in distinct plant species but even in unique cultivars. The structure of the microbial community in the rhizosphere is the outcome of a complex series of plant and microbe feedback and interaction, as well as the physical and chemical soil characteristics (Zhalnina et al., 2018).

Although some microbes are found primarily outside of the roots (epiphytes), those that are found in the intercellular sites within the roots (endophytes) may have a greater impact and more advantage for colonization and nutrient exchange due to their proximity to the plant tissues (Sessitsch et al., 2002). The diverse microorganisms in the soil also influence the chemical setting of the rhizosphere by secreting an array of compounds, including their waste products, enzymes, secondary metabolites (e.g. acidic metabolites that facilitate solubilization of insoluble minerals and absorption of phosphorous and other nutrients for the plants), and phytohormones and growth stimulants, which have been found to influence plant growth and defense against biotic factors (Ortiz-Castro et al., 2011), and affect productivity and resistance against abiotic stresses (Etesami et al., 2015).

The rhizosphere is comprised of soil microorganisms that thrive with the plant's resources and include bacteria, fungi, oomycete, algae, and protozoan (Sohrabi et al., 2017). Microbiota is the term used to describe the totality of microbes in a particular environment (Bulgarelli et al., 2015). The multitudes of microbes present in the rhizosphere are in various forms of interactions with the plant roots; while some are in mutualistic association and benefit each

other, others are under commensalism, parasitism, or in a pathogenic relationship. Although the diversity of microorganisms is high in the bulk soil, the amount of diversity in the rhizosphere is considered to be a few to dozens of times more. Hao and Xiao (2017) mentioned that the most predominant microbes in the rhizosphere are the bacteria, with the Gram-negative bacteria more prevalent such as *Pseudomonas*, *Flavobacterium*, *Alcaligenes*, *Agrobacterium*, *Chromobacterium*, and the like. On the other hand, Gram-positive bacteria such as *Brevibacterium*, coccus, and *Bacillus*, are found in less abundance in the rhizosphere. Conspicuous as well are the effects of interacting fungi and actinobacteria. In general, the microbiota of the rhizosphere is of high specificity, even between different cultivars of the same species (Leff et al., 2015).

Most of the rhizosphere microbes are beneficial to plants; and in the absence of environmental stressors, have been found to impart growth promotion in plants (Bulgarelli et al., 2015). They are generally referred to as plant growth-promoting rhizobacteria (PGPR) or plant growth-promoting fungi (PGPF) but can be more generically called plant growth-promoting microorganisms (PGPM) (Etesami et al., 2015). Exceptions to this are the arbuscular mycorrhizal fungi (AMF) and symbiotic nitrogen-fixing bacteria, which provide significant benefits to plants but are generally not regarded as PGPMs (Franche et al., 2009).

1.3.1. Plant growth-promoting rhizobacteria

Plant growth-promoting rhizobacteria or PGPRs are among the beneficial soil microbes - colonizing the plant rhizosphere and developing close physical, molecular, and biochemical contacts with plant roots (Lugtenberg & Kamilova, 2009). PGPRs include bacteria of diverse genera such as *Arthrobacter*, *Azotobacter*, *Azospirillum*, *Bacillus*, *Enterobacter*, *Pseudomonas*, *Rhizobium*, and *Serratia* (Gray & Smith, 2005), as well as *Streptomyces* spp. (Dimkpa et al., 2009).

In general, the proposed roles of PGPRs can be summarised as 1) reinforcing plant protection, e.g., through competition for growth space and essential nutrients and production of a wide range of antibiotics and enzymes (e.g. proteases and chitinases) which offset harmful microorganisms (Niazi et al., 2014); 2) production of siderophores (small metal-binding molecules) to solubilize and scavenge iron and other micronutrients from the environment, thereby making them unavailable for detrimental microbes while making them available for plants (Whipps, 2001); 3) stimulation of growth through the production of phytohormones such as auxins, gibberellins, and cytokinin (Hayat et al., 2010) and other plant growth promoting

substances (Singh, 2013); and 4) increasing yield by changing the morphology and architecture of the root system (Asari et al., 2017). A unique and novel benefit of some microbes is their influence on a plant's mechanistic responses against abiotic stresses like drought (Cohen et al., 2015), chilling injury (Grover et al., 2011), salinity (Pinedo et al., 2015), metal toxicity (Khan, 2005), and extremely hot weather conditions (McLellan et al., 2007). This is through mechanisms such as the induction of osmoprotectants and heat shock proteins (Nuria et al., 2018) and the production of exopolysaccharides and other determinants (Yang et al., 2009).

PGPRs affect root phenotypes by either inhibiting or lengthening the primary roots and proliferation of lateral roots and root hairs (Ryu et al., 2005), ultimately leading to increased shoot biomass. These induced changes in root development phenotypes are due to the modulation of plant-endogenous mechanisms regulating root development, which can include regulation of plant hormones such as auxin (Grieneisen et al., 2007) and cytokinin (Moubayidin et al., 2013), and positive alteration of the reactive oxygen species (ROS) through transcriptional regulation of the transition from cell proliferation to cell differentiation in roots (Schmidt & Schippers, 2015).

1.3.2. High-temperature effects on soil microbes

The occurrence of heat stress or heat waves, which is becoming more common and intense, is massively impacting the agricultural systems. Such heat events affect the plants as well as the microbial communities within the soil. The soil is a dynamic and complex biophysical body that is predominantly constituted of microbes, which could be held responsible for its biogeochemical changes (Maitra et al., 2021). The majority of soil microbes, which are mesophilic by nature, can experience detrimental effects from high air and soil temperatures. According to Kumar and Verma (2018), prolonged exposure to high soil temperatures modifies the soil microbial community, thereby replacing the native mesophilic soil microbes with heat-tolerant (thermophilic) ones. However, exposure to short-term heat stress may be tolerated by some microbial groups through genotypic and phenotypic heat acclimations.

In general, high temperatures can induce severe loss of cell water content, leading to dehydration of microbial cells (Maitra et al., 2021). High temperatures (e.g. those above 50°C) may also induce some damage to the genetic material, protein structures, and enzymatic activities in microbes, which can be lethal. To tolerate high temperatures, microbes utilize several defensive strategies to counter the detrimental effects. This may include, but is not limited to, the production of HSPs, DNA repair mechanisms, production of the EPS-based

biofilm, use of molecular chaperones, and sporulation to stimulate the production of dormant spores (Maitra et al., 2021). These changes in the microbial community throughout the duration of the high temperatures persisted even after the removal of heat stress (Pettersson & Bååth, 2003). Due to the continuous rise of the global mean temperatures, as much as the increasing events of high soil temperatures, the study of thermotolerant microbes is becoming increasingly useful. Previous investigations of beneficial microbes worldwide have identified several thermotolerant strains.

Some of the commonly identified thermotolerant organisms include *Alicylobacillus acidoterrestris*, *Pseudomonas cerdrina*, *Pseudomonas putida*, *Pseudomonas aeruginosa*, *Brevundimonas terrae*, *Anthrobacter nicotinae*, *Burkholderia phytofirmans* (now *Paraburkholderia phytofirmans*), and others (Bensalim et al., 1998). Notable examples are the bacteria from the *Geobacillus* genus and other closely-related genera, which were able to grow up to 70°C in laboratory settings. Previous studies (Marchant et al., 2008; Santana & Gonzalez, 2015) found that these bacteria were commonly placed in soils within the mesophilic range as vegetative spores. Other examples were that of thermotolerant *Bacillus cereus* SA1, which has shown positive impacts on soybeans (Khan et al., 2020); actinomycetes from the *Actinokineospora* genus identified in China, which can tolerate up to 55°C (Tang et al., 2012). Furthermore, phosphate-solubilizing thermotolerant bacteria such as *Bacillus coagulans* C45, *B. licheniformis* A3, and *B. smithi* F18 were able to tolerate up to 75°C in lab conditions; while the fungus *Aspergillus fumigants* O4 and NTU-132 strains were reported to be active up to a temperature of 65°C with undamaged enzymatic activities (Chang & Yang, 2009).

1.3.3. Mechanisms by which microbes enhance thermotolerance in plant

Microbes are biological agents that can be utilized to combat heat stress when inoculated in plants. The beneficial effects of root microbes on plant growth and the suppression of diseases in plants have been exhaustively studied. However, due to advancements in technology and scientific knowledge, a growing number of studies have identified microbes that can also assist plants in combating abiotic stress conditions. This shows the symbiotic relationship of the host plants with the rhizosphere microbes. The growth and performance of the rhizosphere microbe community are dependent on the easy carbon source provided through the plant root's rhizodeposits; therefore, microbes must invest in the survival and proper functioning of the plant under normal and stress conditions (Maitra et al., 2021).

1.3.3.1. Induction of heat shock protein (HSP)

Microbes can mediate heat tolerance through the induction of heat shock proteins. In particular, heat shock protein 90 (HSP90), which is a molecular chaperone involved in the plant-microbe crosstalk, has been proven to impart some degree of thermotolerance to plants (Picard, 2002; Pratt & Toft, 2003). As demonstrated by several studies, manipulation of the levels of HSP90 may result in phenotypic alterations as well as heritable genetic changes due to epigenetic changes (Queitsch et al., 2002; Sollars et al., 2003). A study on the rhizospheric fungus *Paraphaeosphaeria quadrisepata* by McLellan et al. (2007), which showed heat tolerance in *Arabidopsis* and wheat plants through the modulation of HSP90 chaperone with HSP90-specific inhibitor monocillin I (MON) and radiciol (RAD), led to the upregulation and expression of major heat responsive elements (e.g. HSP70 and HASP101).

1.3.3.2. Production of plant growth regulators

Another mechanism that is utilized by microbes to assist plants in responding to environmental stress conditions is the production of plant growth regulators. Ahammed and Yu (2016) indicated that all of the major plant growth regulators and phytohormones, such as auxin, gibberellin, cytokinin, ethylene, ABA, and brassinosteroid, as well as the signaling molecules salicylic acid and jasmonic acid, take essential roles in the heat tolerance of plants. These growth regulators have specific functions and consequences. For example, auxin has been found to interact with HSPs and plant heat transcription factors in *Arabidopsis* (R. Wang et al., 2016). Gibberellin reduction is associated with the accumulation of DELA proteins (Hedden & Thomas, 2012), which results in the inhibition of growth but enhancement of stress tolerance. Cytokinins are involved with the promotion of cell division, regulation of redox potentials, maintenance of meristematic activity (Gupta & Rashotte, 2012), maintenance of stomatal conductance that induces transpirational cooling (Macková et al., 2013), and with specific roles in HASP metabolism (Sobol et al., 2014) during heat stress. ABA has the following roles: as a signaling molecule, inducer of HSP, acts as a growth regulator, and is also involved in stomatal regulation in plants, to induce heat tolerance (Hsieh et al., 2013; Li et al., 2015; Tang et al., 2008). Some of the studied microbes that produce plant growth regulators imparting heat tolerance are bacterial strains *Azospirillum brasilense* Sp245 (auxin and cytokinin) in wheat (Choudhary et al., 2016), *Achromobacter piechaudii* ARV8 (ACC deaminase enzyme) in

pepper (Gururani et al., 2013), and *Bacillus cereus* SA1 (auxin and gibberellins) in soybeans (Khan et al., 2020).

1.3.3.3. Mediation of ROS

Microbes mediate the production of ROS. ROS, mainly the by-products of the plant's metabolism under normal conditions, include a range of active radicles such as hydroxyl radicles, peroxide radicles, singlet oxygen, superoxide radicles, and more (Gupta et al., 2017). Under normal conditions, plants can handle these radicles; however, during stresses, the ROS production exceeds the optimum levels, leading to a cascade of effects such as membrane leakage, lipid peroxidation, denaturation of proteins, pigment, and food storage material degradation, and cell damage (Bose et al., 2014; Van Ruyskensvelde et al., 2018). Several studies suggest the active involvement of rhizosphere microbes in ROS metabolism under heat-stress conditions. For example, thermotolerant strain *Pseudomonas mendoina* reduced membrane damage due to increased SOD, POX, APX, and antioxidant enzymes (Maitra et al., 2021); *Azospirillum brasilense* showed lower heat damage as indicated by low oxidative damage, cell leakage, etc. in maize crops (Maitra et al., 2021); IAA-overproducing heat-tolerant rhizobacteria in *Medicago* showed enhanced antioxidant activities (Maitra et al., 2021); and the thermotolerant strains *Azospirillum brasilense* NO40 and *Bacillus amyloliquefaciens* UCMB5113 resulted in higher antioxidant activities in young wheat seedlings (Abd El-Daim et al., 2014).

1.3.3.4. Defense through EPS or biofilm formation

Exopolysaccharides or EPS serve as the extracellular environment for the microbes, often ranging from 40-95% of the total cell weight as with bacteria (Flemming & Wingender, 2001). Microbe-produced EPS are nearly 97% water in a complex polymer matrix, which is advantageous during desiccation events. This matrix is generally released by microbes as cell exudates for competition and defense, as with *Pseudomonas* (Sandhya et al., 2009). The production of EPS is particularly high during incidences of stresses (e.g. heat, salinity, drought). EPS are active components of the soil organic matter; and as such, are known to physically impact the soil properties by increasing its water-holding capacity, therefore, delaying the onset of water stress. Soil structure is improved through the EPS' excellent binding properties of the polysaccharides (Morcillo & Manzanera, 2021). With an improved soil structure due to EPS, water is not a limiting factor in plant growth and if this balance is

maintained, transpirational cooling will be effective enough against the deleterious effects of heat stress. The thermotolerant strains *Bacillus cereus* P2 and *Planomicrobium chinense* P1 have been found to produce enough EPS to counter the negative effects of drought and temperature stress on rainfed wheat (Khan & Bano, 2019). Naseem and Bano (2014) also found the same trend in drought- and heat-stressed maize plants with thermotolerant strains *Proteus penneri* PP1, *Pseudomonas aeruginosa* PA2, and *Alcaligenes faecalis* AF3.

1.3.3.5. Moderation of protective molecules

Diverse small and large molecular weight compounds within the plant's system have active roles in the mitigation of heat stress, most of which are nitrogenous compounds, small organic molecules, and non-protein amino acids (Parida & Das, 2005). Several studies have also reported that the accumulation of proline and glycine betaine is involved in the plant's stress response (Basu et al., 2021; Szabados & Saviouré, 2010; Verbruggen & Hermans, 2008). Moreover, the application of thermotolerant PGPR has increased these two compounds in plants; and these enhancements were through direct absorption of microbial origin compounds, or via the up-regulation of the genetic control for increased production of said molecules (Ait Barka et al., 2006; Singh et al., 2019).

1.3.3.6. Nutrient and water uptake

Heat stress, which is usually accompanied by water stress, results in oxidative stress and nutrient deficiency in plants (Sattar et al., 2020; Zhou et al., 2017). During thermo-stress, one of the highly impacted physiological processes in plants is photosynthesis. Once this is impaired, energy-consuming processes such as active uptake of nutrients are nearly stopped, causing the reduction of nutrients in the plant. This can be worsened by the development of water stress in the soil, leading to further reduction in nutrient availability to the plant roots (Bista et al., 2018). If the plant's nutritional status is negatively impacted, this will weaken the plant's performance under stress conditions. Thermotolerant bacteria have gained attention due to their potential for mitigating heat stress in plants through involvement in the availability of soil phosphorous. Some thermotolerant strains were reported to be involved in phosphorous mineralization through organic acid production (Rodríguez & Fraga, 1999). This includes the thermotolerant strains from *Erwinia*, *Bacillus*, *Rhizobium*, and *Pseudomonas* genera. Other thermotolerant strains *Bacillus smithi*, *Bacillus coagulans*, *Bacillus licheniformis*, *Aspergillus fumigatus*, and *Streptomyces thermophiles* were also good at phosphate solubilizing activity

that they have now commercialized biofertilizers for high-temperature soils (Chang & Yang, 2009). Finally, some of the microbe root dwellers can secrete siderophores, thus, increasing the availability of iron and zinc (Carmen & Roberto, 2011).

With all the mechanisms by which microbes assist plants in tolerating high-temperature stress, it is no wonder they are considered an excellent alternative strategy for mitigating heat stress effects, particularly in agriculture. Since the survival and the ability to impart tolerance to heat stress of the rhizosphere microbes rely heavily on the health and nutrients provided by the plants, it is, therefore, necessary to have a good working interaction between the soil microbes and the host plant roots.

1.4 Plant roots – The hidden half

Plant roots are intricate structures with anatomical and morphological features that exhibit diverse interactions with their niche and other living organisms with which they cohabitate. They are mainly involved with plant anchorage, water uptake, nutrient absorption, and the production and storage of essential compounds for plant growth. At the initial growth stage, roots show three distinct types of tissue systems – the epidermis (dermal tissue system), which contains the root hairs; the ground tissues (comprised of the cortex and endodermis), which occupies the largest volume of most roots; and the vascular tissues (vascular tissue system), which consist of the xylem (water transport) and phloem (nutrient transport) and is surrounded by the pericycle where lateral root formation arise (Smith, 2007). The roots undergo extension (of the root axes from the apical meristems) and branching (of lateral roots from the pericycle) to expand the resource base and anchorage of the plant. The primary root can be divided into three developmental zones: the meristematic (surrounded by the root cap, which has the gravity sensing part at the tip – the columella), elongation, and differentiation (maturation) zones (Verbon & Liberman, 2016) (Figure 8).

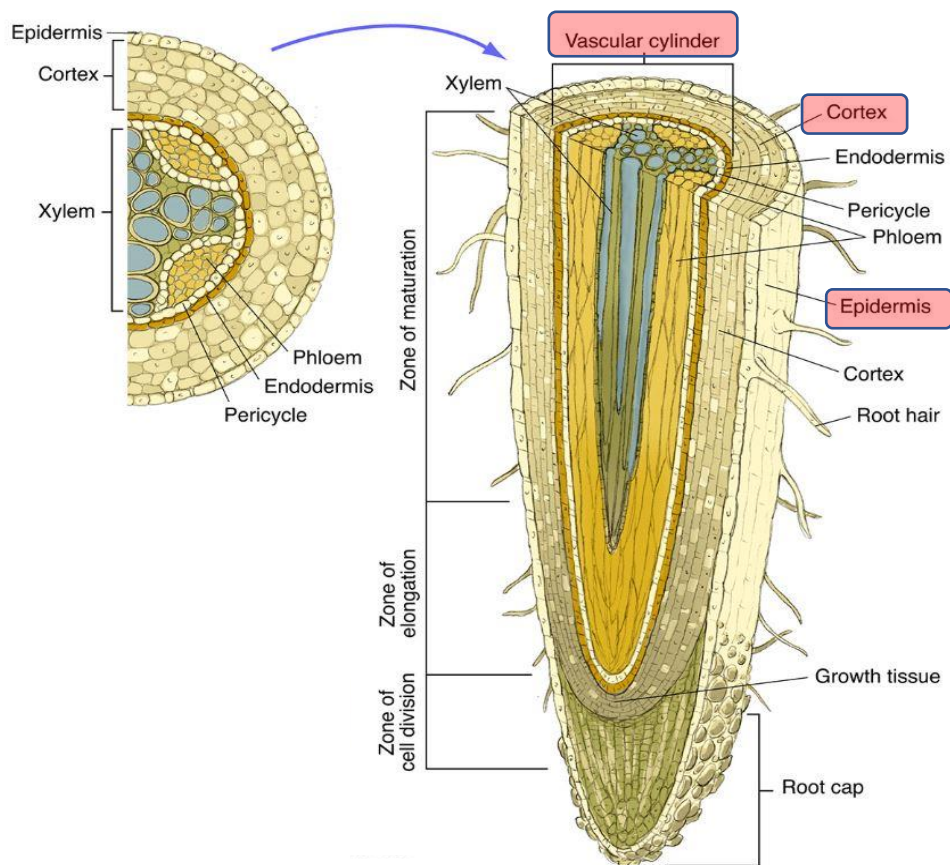


Figure 1.8 Cross and longitudinal section of a dicot root structure. [Source: Image by Dave Carlson - <https://www.carlsonstockart.com/photo/root-structure-monocot-dicot-cross-longitudinal-section/>]

There are generally two types of roots: those that are formed in the embryo such as the tap or primary and seminal roots (Khan et al., 2016); and those that are formed post-embryonically, such as adventitious roots that form from consecutive nodes on shoots, basal roots, nodal roots, and lateral roots (Lynch & Brown, 2012). Primary roots, which comprise the basic component of the root system, are initiated during embryogenesis and develop shortly after germination (Qin et al., 2019). The growth of primary roots is maintained by two basal developmental processes: cell proliferation in the root apical meristem and cell elongation in the elongation zone. These processes are centrally regulated by phytohormones including auxin, ethylene, abscisic acid, gibberellins, cytokinins, jasmonic acid, strigolactones, and brassinosteroids, which play vital roles in the regulation of primary root growth (Li et al., 2015; Pacifici et al., 2015). On the other hand, lateral roots are formed from the pericycle through auxin-dependent cell cycle activation, which produces the founder cells that undergo several rounds of cell

division (Overvoorde et al., 2010). The development and growth dynamics of the individual component of the root system, including the elongation of the root types, formation of the growth angles from the main axis, together with the branching of the lateral roots, are determined by genetics, physiological, and environmental factors (Lynch & Brown, 2012).

1.4.1. Root system architecture

Root system traits have long been a target of interest by many researchers and plant breeders since many of the traits required in future crops and sustainable plant production are associated with root properties (Tracy et al., 2020).

An important feature of the root in the soil, to cope with heterogeneously distributed resources, is its architecture. Roots change their architecture, direction, and rate of growth in response to a wide range of stimuli, including gravity, light, water, nutrient availability, toxic metals, and microorganisms. They tend to grow towards nutrients and water, however, this mechanistic growth pattern changes when these factors are in interaction with each other. For example, root gravitropic responses are influenced by hydrotropism (Takahashi, 1997) and the presence of toxic metals (Hawes et al., 2002).

All the root components make up the dynamic root system architecture (RSA). The RSA is characterized by the spatial configuration of the root system or the explicit deployment of the root axes and is also described as the topological or geometric measure of the root shape (Bucksch et al., 2017).

1.4.1.1. Microbial effect on the RSA

Under a changing environment, the RSA exhibits plasticity and responds to diverse external conditions, which in this study, are the presence of microorganisms and high-temperature conditions. For example, PGPRs have been described to affect post-embryonic root development by altering cell division and differentiation within the primary root as well as affecting root hair formation and lateral root development (Verbon & Liberman, 2016). The most common PGPR-induced root phenotype is either the inhibition of primary root growth coupled with the proliferation of lateral roots and root hairs (Ryu et al., 2005), leading to increased shoot biomass; or the increase in primary root growth that is coupled with an increase in plant biomass (Schenk et al., 2012).

1.4.1.1. High temperature stress effect on the RSA

On the other hand, high-temperature stress induces several morphological responses in roots including changes in the RSA, such as the decrease in primary root length; reduction in the number, length, and emergence angle of lateral roots; increase in diameter and number of the second and third order laterals; and increase in the density of root hairs (Calleja-Cabrera et al., 2020). In general, the modulating effects of high temperature on the RSA limit the volume that roots may access for the uptake of water and nutrients (Koevoets et al., 2016).

Through its direct effects on growth and development, as well as on metabolic processes, temperature affects the expansion of the root system. Reduced or even no growth below the minimum temperature, maximal growth at optimum temperature (usually a broad range), and reduced to no growth again above the maximum temperature are the common responses of a root system. Both soil and air temperatures have a marked effect on root axes development, as with the increase in the number of root axes and lateral roots with accumulated temperature at the meristems (Vincent & Gregory, 1989). The effect of temperature on growth can be seen in terms of root length, with the rate of root expansion increasing faster approaching optimum temperature and decreasing thereafter (Seiler, 1998), and root mass, which also depends on assimilate supply or light interception (Stone & Taylor, 1983). Temperature also affects the orientation of the roots, as with root pleiotropism (angled growth from the vertical), and the rate and duration of metabolic processes such as water and nutrient transport. As the development progresses, root metabolism becomes more temperature-sensitive due to the decreasing mobilization of seed reserve during early seedling growth. Responses to the temperature at different organization levels (e.g. changes in lipid composition and carrier activity at the membrane level and size and morphology on the root system level) within the plant usually manifest after prolonged exposure with the end goal of ensuring efficient nutrient uptake and transport (McMichael & Burke, 1994).

1.4.2. Root Phenotyping

The target of doubling crop production by 2050, to address the increasing global population, is challenged by the impacts of climate change on water availability and the drive to reduce fertilizer inputs for a more sustainable agriculture (Atkinson et al., 2019). It has been proposed that developing crops with enhanced nutrient and water uptake efficiency, essentially improving the belowground root system traits (known as the “second green revolution”) will provide an alternative solution (Lynch, 2007). Root system traits have long been a target of

interest by many researchers and plant breeders since many of the traits required in future crops and sustainable plant production are associated with root properties (Tracy et al., 2020).

Tracy et al. (2020) highlighted the root traits selected to be incorporated into new germplasms for plant breeders. These traits are either directly involving roots or indirectly with shoots. Some of the desired traits include the phenotype for deep water captures such as deeper and more extensive root growth and steeper roots (wide angle to soil surface). For better water conservation, a good trait is having a narrow xylem anatomy. For maintained, if not, greater yield in drought-prone areas, thicker tap roots can be selected, along with optimal leaf width. For greater use of phosphorous, shallower roots can be utilized. Another preferred trait involves malate exudation through the identification of malate transporters at root tips, within the roots, and the leaf sheaths. In gist, the functional root types were selected to confer: increased water acquisition (Hurd, 1974), enhanced water use efficiency (WUE) (Richards & Passioura, 1989), heat and drought tolerant (Caradus & Woodfield, 1998), access to phosphorous (Wissuwa et al., 2016), and tolerance to high soil Al (Sasaki et al., 2005), NA (Munns et al., 2012), and cereal cyst nematodes (Ogbonnaya et al., 2001).

Elucidating the RSA could help in improving agricultural productivity and understanding how plants respond and adapt to changing environmental conditions. However, evaluating the plant root systems poses several challenges, mainly because of their hidden nature. In early studies, the root system could not be assessed without destroying or losing part of it to invasive measurement and harvest. Moreover, studying the ideal root systems for crop growth under natural conditions is complicated due to the variations in the environment. Despite these challenges, specific root traits have been incorporated into crops. RSA studies were made possible owing to the advancements in root phenotyping and analytical software development (Takahashi & Pradal, 2021).

Root system trait phenotyping has some challenges and (Atkinson et al., 2019) tried to summarize them and mentioned the different techniques and technological innovations. First of all, in natural conditions, the opaque nature of soils makes in situ phenotyping of the root systems challenging as compared to measuring and analyzing the shoots. Traditional non-destructive techniques employed under controlled laboratory conditions included the use of transparent or artificial growth media, growth pouches, and rhizotrons. These, however, only generated 2D images, and if the soil is used, there is the difficulty of capturing the complete RSA as it gets occluded by soil particles. This was addressed with the use of soil-free techniques (artificial media) such as gel plates, hydroponics, aeroponics, and growth pouches, which provided greater contrast between root and substrate, although results can vary with

actual soil setting (Kuijken et al., 2015). Examples of 2D soil and artificial media system are the high-throughput phenotyping platforms GrowScreen-Rhizo (Nagel et al., 2012), Phytomorph (Subramanian et al., 2013), GrowScreen-PaGe (Gioia et al., 2016), RADIX (Le Marié et al., 2016), and RhizoTubes (Jeudy et al., 2016) (Figure 9).

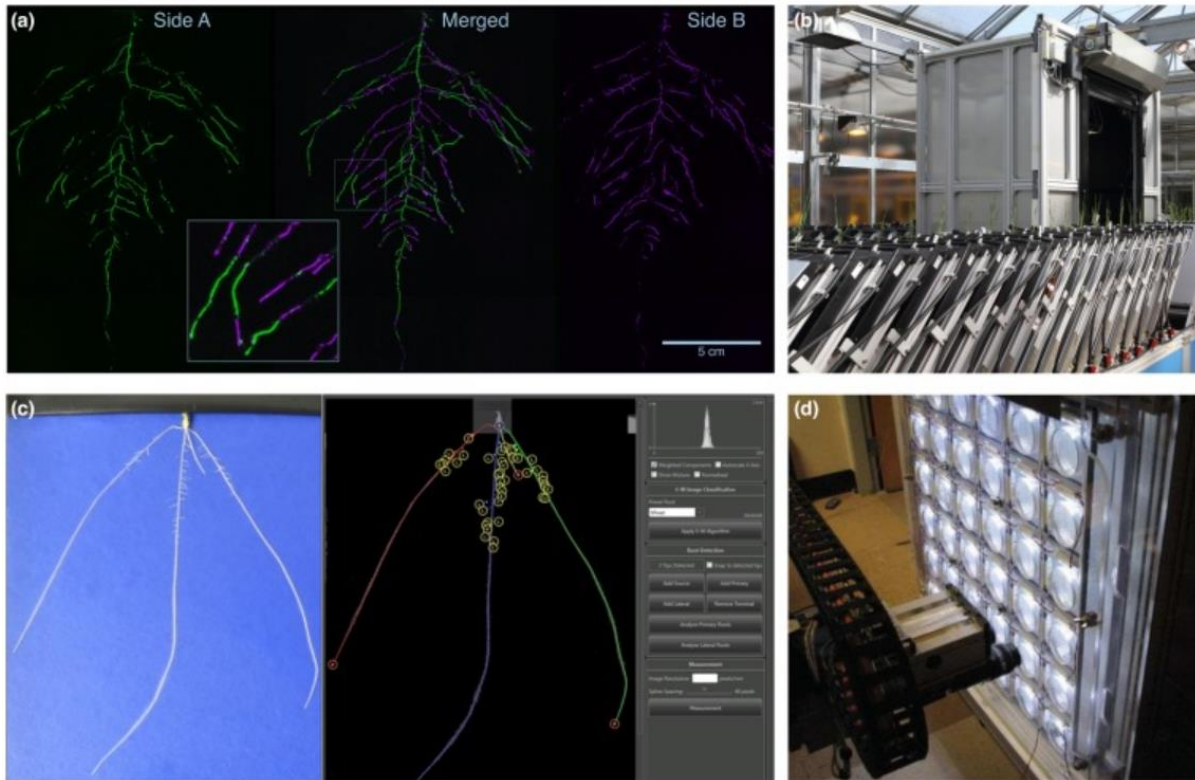


Figure 1.9 2D imaging of plant roots. (a) GLO-Roots. Arabidopsis plant expressing a luminescent reporter imaged on each side of the rhizotron (colored green and magenta respectively) at 21 days after sowing (DAS). (b) GROWSCREEN-Rhizo. A high-throughput automated root phenotyping platform using soil-filled rhizotrons. (c) Pouch system for cereal seedlings (left panel). RootNav analysis software (right panel). (d) Phytomorph. A high-throughput robotic imaging platform for Arabidopsis growing on agar plates. [Source: Image and description adapted from Atkinson et al. (2019).]

Another issue with root phenotyping is that plant root systems are three-dimensional (3D) structures with many features difficult to quantify in 2D (Topp et al., 2013). Some of these features include the arrangement of seminal roots at the root crown of cereals, the angle of the roots, and the number of roots and root whorls in maize crowns. An advantage of 3D is its capability to capture dynamic growth responses such as gravitropism and circumnutation (Clark et al., 2011). Currently, 3D non-invasive phenotyping of roots in soil is achieved using three tomographic techniques originally developed for medical applications: X-ray computed tomography (X-ray CT), magnetic resonance imaging (MRI), and positron emission

tomography (PET) (Figure 10). Both X-ray CT and MRI can be used continuously to monitor root system development, with no adverse effect due to periodic scanning (van Dusschoten et al., 2016).

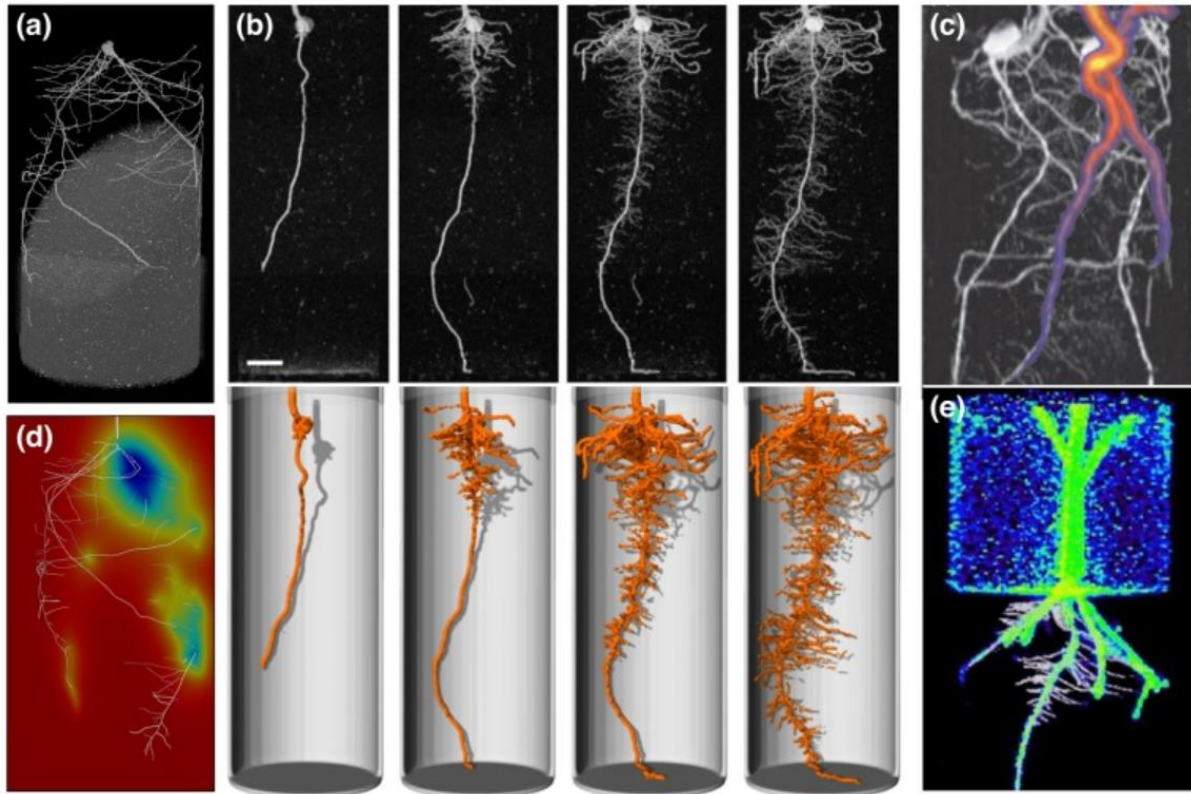


Figure 1. 10 3D tomographic imaging of plant roots. (a) X-ray CT micrograph of a wheat seedling 12 DAS. (b) MRI imaging of a maize root system at 6, 9, 12, and 15 DAS. Upper panel, MRI data (2D maximum intensity projection). Lower panel, 3D surface rendering. Scale bar: 20 mm. (c) Maize roots imaged using MRI-PET. Two plants are growing in the same pot. The greyscale image is MRI, the color is ¹¹C PET data following application to a leaf of one plant. (d) OpenSimRoot simulation using output from (a) to model rhizosphere N depletion. (e) Maize root imaged at 9 DAS using optical projection tomography (OPT) and PET. The black and white image is OPT, the color is ¹¹C PET data. [Source: Image and description adapted from Atkinson et al. (2019).]

Because of the challenge of belowground imaging in the field, phenotyping for root system traits is met with difficulties, thus the lag in technological advancements. Some of the classic methods used for field-based phenotyping include soil core break, which is currently being improved by employing UV illumination and fluorescence spectroscopy for enhanced soil and root contrast (Wasson et al., 2016). Another popular high-throughput method is shovelomics or root crown phenotyping. This method generates a number of key RSA parameters including root crown number angle and number (Trachsel et al., 2011). There are also geophysical

methods to study the root and the soil profile, such as the Electrical Resistance Tomography (ERT), which measures soil water profiles to analyze large diameter root profiles (Amato et al., 2008); and ground penetrating radar, which uses high-frequency waves to detect and quantify tree roots (Liu et al., 2016).

Root phenotyping does not only involve imaging and measurement, but also root trait digitization and quantification (Takahashi & Pradal, 2021). Due to the large number of datasets generated by the high-throughput capture of root systems, there is a need for fast and accurate root trait characterization software solutions to reliably derive traits. Several tools have emerged fairly recently, which exhibit a mixture of manual approaches. This includes DART (Le Bot et al., 2010), the semi-automated SmartRoots (Lobet et al., 2011) and RootNav (Pound et al., 2013), and the fully automated EZ-Rhizo (Armengaud, 2009), GiA Roots (Galkovskyi et al., 2012), and DIRT (Bucksch et al., 2014).

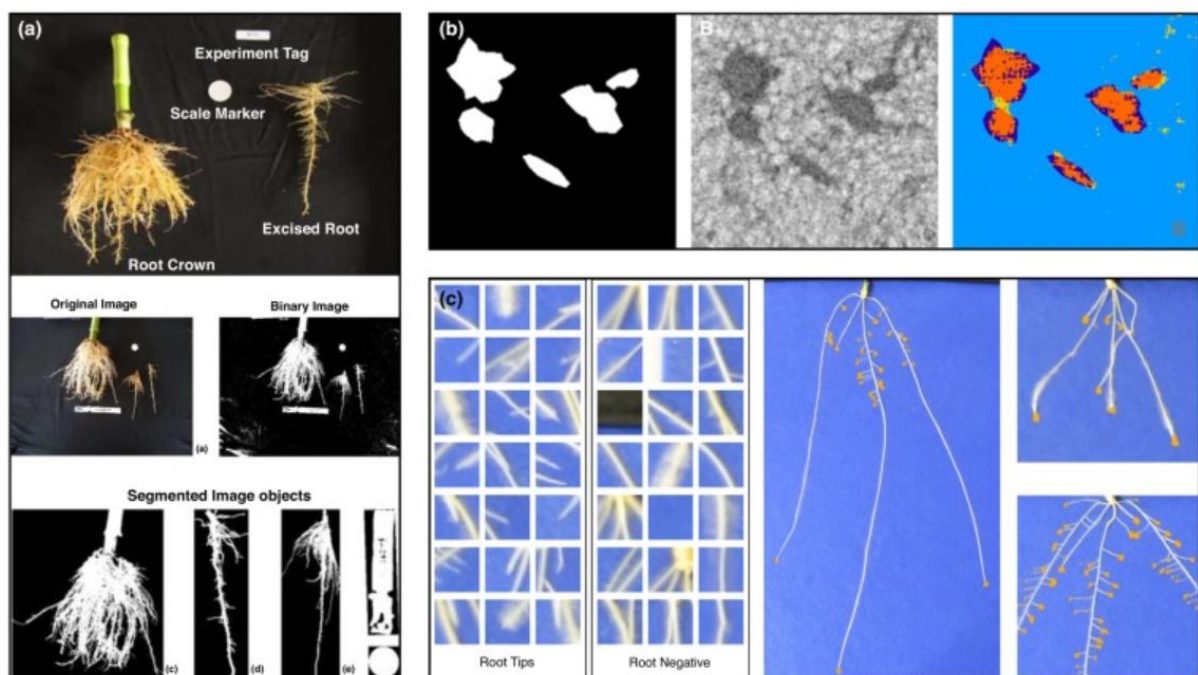


Figure 1. 11 Automated root image analysis software. (a) DIRT measures traits based on the ‘shovelomics’ approach. Root systems are washed and imaged from above in front of a dark background. Root systems are separated from the background via thresholding, and RSA traits are derived from each segmented object. (b) Root-soil segmentation in X-Ray CT. Root and soil pixels are identified via a Support Vector Machine classifier trained on deep-learned features. Images show the ground truth, original image, and SVM classifier output. (c) End-to-end deep learning for root tip identification. A deep network trained on thousands of instances of root tips and negative samples can be passed over an entire image to obtain likely root tip locations. [Source: Image and description adapted from Atkinson et al. (2019).]

To address some of the shortcomings of the root software analysis tools, deep machine learning is slowly being utilized. This is a standard technique for many computer vision problems with the availability of large datasets. Deep learning is aimed at reducing the reliance on the high user input in order to increase both the throughput and quality of the phenotypic data (Atkinson et al., 2017)

1.5. Biochemical nature of plant root-microbe interactions

1.5.1. Lipids at the forefront of biochemical research

For a long time, the focus of scientific research has been on the accepted dogma of biology: DNA (genomics), RNA (transcriptomics), and proteins (proteomics) to resolve mechanistic investigations of cell functions (Stephenson et al., 2017). The study and characterization of endogenous small molecules – metabolites (metabolomics), which are substrates and products of biochemical reactions that reveal the interconnectivity of biological pathways, has also rapidly emerged (Zhang et al., 2013). As primary metabolites, lipids maintain cellular functions and are involved in primary metabolic processes. However, amid the precipitous growth of scientific knowledge and databases that can be attributed to unprecedented progress in genome sequencing and annotation, protein function interpretation, and metabolome profiling, studies on lipids have been considerably less (Shevchenko & Simons, 2010). To gain a complete understanding of cellular physiology and metabolic homeostasis, a comprehensive analysis of lipids is essential, therefore prompting lipid biology to be a major research target of systems biology (Fahy et al., 2005).

Lipids are a diverse and ubiquitous class of biomolecules and major constituents of eukaryotic and prokaryotic cell membranes (Fahy et al., 2011; van Meer et al., 2008). They play essential roles in maintaining the structure and function of the plasma membrane (Horn & Jaiswal, 2019) and intracellular membranes (Casares et al., 2019). They provide various biological functions in energy and carbon storage, serve as mediators in cell signaling pathways, and regulate stress responses (Welti et al., 2007). Because of diverse roles in cellular functions, systemic effects of lipid homeostasis and lipid metabolism can reflect the greater biochemical changes of the whole system, influencing the overall health status of an organism (Boutte & Jaillais, 2020; Wu et al., 2020).

Plants are exposed to their surrounding environment, thereby, in constant interaction with a multitude of organisms. Numerous studies on aboveground plant-microbe interactions have already been documented; however, rhizosphere studies have been restricted due to limitations in the application of “omics” profiling techniques (Downie et al., 2015) and difficulties in simulating a natural underground ecosystem (Sergaki et al., 2018). Although these interactions have been mostly investigated at metabolic and transcriptomic levels, there are still many open questions on the biochemical interaction, resource exchange, and communication between the involved organisms. Rhizosphere-related phenomena such as rhizodeposition, microbial chemotaxis, and plant-microbe signaling are some important underground processes that still need to be further explored (Mendes et al., 2013), and in which lipids are highly involved (Cassim et al., 2019; Niu & Xiang, 2018).

In the rhizosphere, whenever plant roots communicate with or contact microbes, molecular information is exchanged. During this interaction, the plasma membrane acts as the interface, either allowing advantageous resource exchange or inhibiting interaction through downstream signaling cascades (Cacas et al., 2016; Lodish et al., 2008). The plasma membrane serves as a critical player in signaling responses to external stimuli, initial microbe recognition, and multiple downstream responses, which the microbes attempt to manipulate to suppress plant defense responses (Cacas et al., 2016; Lodish et al., 2008). Overcoming these defense responses leads to successful colonization and procurement of nutrients from plants (Boon & Smith, 2002).

As major components of the plasma membrane, lipids establish the physical barrier on the living cell surfaces, modulate the communication between the host and microbe, and serve as signaling molecules or providers of elicitors for pathogen recognition, thereby influencing the establishment or prevention of microbial colonization (Abdel-Mawgoud & Stephanopoulos, 2018; Siebers et al., 2016). The isolation and characterization of a vast number of lipids have been a challenging task, requiring a cohort of multi-level and interdisciplinary studies, and leading to the emergence of the research field of lipidomics (Wu et al., 2020). With advancements in molecular identification and quantification methods brought by the development and availability of highly sensitive analytical technologies, our knowledge of the roles of lipids in rhizospheric interactions has tremendously expanded. This section will highlight the various roles of lipids in plants and at the different stages of plant root-microbe interactions: from (i) signaling and resource exchange; to (ii) pattern-recognition, signal transduction, and downstream defense response mechanisms during perception and contact; leading to (iii) the establishment of symbiosis that can either impart plant growth-promotion

and stress tolerance or cause diseases and death. This will also provide an overview of the recent developments in visualizing and characterizing lipid components in membranes and plant tissues. Moreover, we will also look into the advances in the lipidomics workflow, including sample extraction protocols, mass-spectrometry-based techniques, biostatistical data analysis, and lipidomic data interpretation.

1.5.2. Lipids: Description, categories, and nomenclature

Lipids have been initially defined as biological substances that are generally hydrophobic, which, in many cases, can be soluble in organic solvents (Smith, 2000). They have also been broadly subdivided into two groups: “simple” lipids, those that yield at most two types of hydrolysis products (e.g., fatty acids, sterols, and acylglycerols), and “complex” lipids, yielding three or more products (e.g. glycerophospholipids and glycosphingolipids) (Fahy et al., 2005). However, for a comprehensive and standardized classification, Fahy et al. (2005) broadly defined lipids as “hydrophobic or amphipathic small molecules that originate entirely or in part by carbanion-based condensation of thioesters and/or by carbocation-based condensation of isoprene units”. The production, transport, and recognition of lipids are performed by the concerted actions of numerous enzymes, binding proteins, and receptors ((Fahy et al., 2005).

To deal with the massive amounts of data generated by the growing lipid research community and to facilitate international communication, a comprehensive and standardized classification with a common platform compatible with informatics requirements has been developed. The Lipid Metabolites and Pathway Strategy (LIPID MAPS), founded to “unify the field of lipidomics”, is a web portal designed to be a gateway for Lipidomics resources (Fahy et al., 2009), which includes a relational database that encompasses structures and annotations of biologically-relevant lipids (Sud et al., 2007).

1.5.2.1. Categories of lipids:

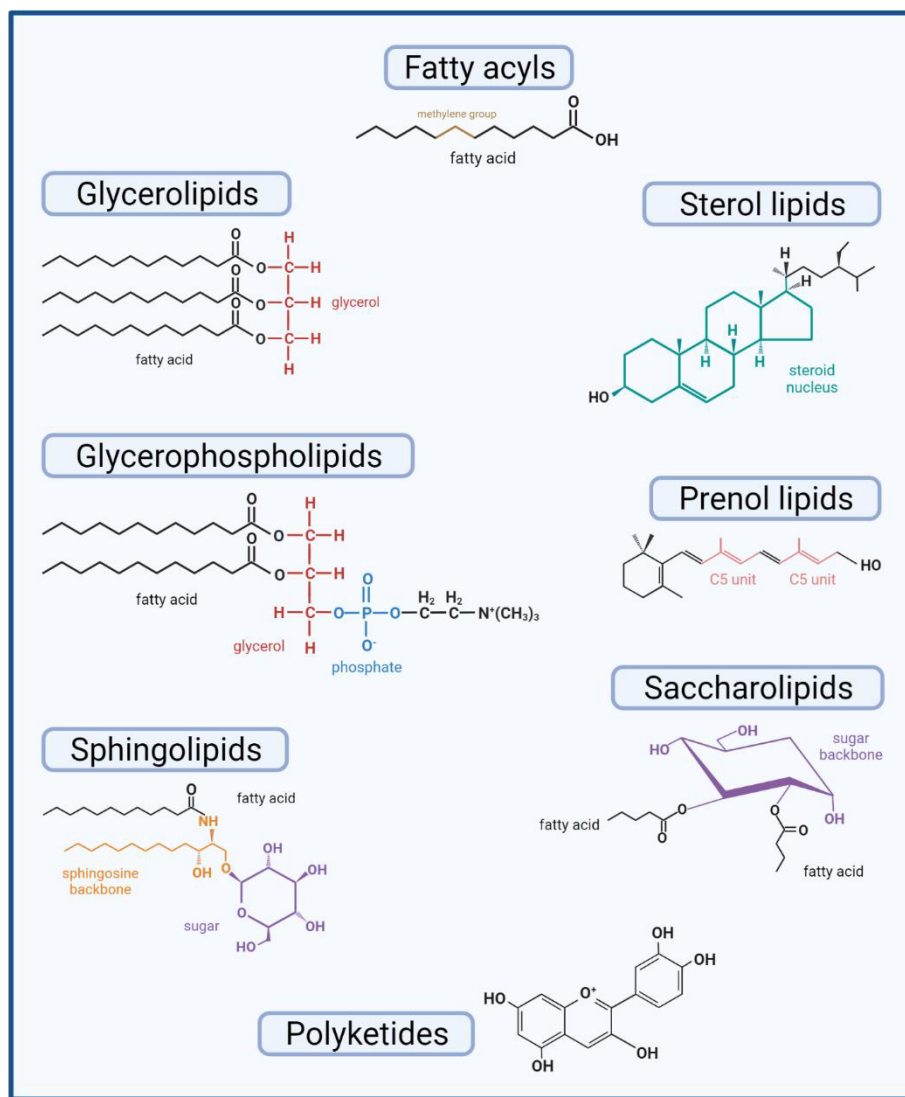
The Lipid Maps consortium has divided lipids into eight principal categories based on their functions (https://www.lipidmaps.org/data/classification/LM_classification_exp.php). **Fatty acyls (FA)** represent the major building block of complex lipids, and therefore, are one of the most fundamental categories of biological lipids. They are characterized by a series of methylene groups imparting their hydrophobic characteristic and are subdivided depending on the existence of double bonds in their hydrocarbon chains. Common examples include fatty acid esters such as wax monoesters and diesters and lactones. **Glycerolipids (GL)** are mainly

composed of mono-, di-, and tri-substituted glycerols; the most well-known of which are triglycerides (TAG). They comprise the bulk of oil storage in plant tissues. **Glycerophospholipids (GP)**, also known as phospholipids, are amphipathic molecules with a polar head consisting of glycerol and a phosphate group, and a non-polar tail made of hydrocarbon chains. As key components of the plasma membrane bilayer, they act as binding sites for intra- and intercellular proteins and are involved in cell metabolism and signaling. **Sphingolipids (SP)** are a family of compounds sharing a common structural feature – a sphingoid base backbone synthesized *de novo* from serine and a long-chain fatty acyl-CoA then converted into products such as ceramides, phosphosphingolipids, glycosphingolipids, and other derivative species. They have protective functions and play important roles in cellular signaling. **Sterol lipids (ST)** are important components of the cell membrane, participating in signal transduction. The most well-known examples are phytosterol in plants, and cholesterol and derivatives, such as steroids that have specific roles as hormones and signaling molecules. **Prenol lipids (PR)** are synthesized from the 5-carbon precursors, isopentenyl diphosphate and dimethyl diphosphate, which are mainly produced via the mevalonic acid (MVA) pathway. They are essential for immune response and some regulatory functions, e.g. carotenoids that function as antioxidants and precursors of Vitamin A and E. **Saccharolipids (SL)** are composed of a fatty acid linked to a sugar backbone, forming structures that are compatible with membrane lipid bilayers. They can be found in the Lipid A component of lipopolysaccharides (LPS) in gram-negative bacteria as acylated glucosamine precursors. Finally, **Polyketides (PK)** have great structural diversity and comprise a very large number of secondary metabolites. They are often cyclic molecules whose backbones are further modified by glycosylation, methylation, hydroxylation, oxidation, and/or other processes. PKs are found in anti-microbial, anti-parasitic, and anti-cancer agents, such as erythromycins, tetracyclines, and avermectins (Fig. 1.5.2.)

1.5.2.2. Lipid nomenclature

Once the classification of lipids was established, the next step was to have a systematic way of naming them. The requirement for naming lipids was to have an unambiguous definition of the lipid structure that is equally amenable to chemists, biologists, and medical researchers. Therefore, in conjunction with the classification scheme, Fahy et al. (2005) also provided a systematic naming scheme for the various classes and subclasses of lipids. This closely followed the existing rules of the International Union of Pure and Applied Chemists and the

International Union of Biochemistry (IUPAC-IUBMB), except for a few differences. Based on LIPID MAPS, the lipid nomenclature falls into two main categories, systematic and common trivial names; the latter of which includes abbreviations to conveniently define acyl/alkyl chains in glycerolipids, sphingolipids, and glycerophospholipids.



Created with BioRender.com

Figure 1. 12 Representative structure of each lipid category. The LIPID MAPS consortium has subdivided lipids into eight principal categories based on their functions, chemical characteristics, and specificities. A more consistent format for representing lipid structures has been proposed by Fahy et. al [84] in which, in the simplest case of the fatty acid derivatives, the acid group (or equivalent) is drawn on the right hand while the hydrophobic hydrocarbon chain is on the left, with some notable exceptions. Fatty acyls [FA]- have aliphatic chain of methylene groups and can be subdivided into saturated or unsaturated; Glycerolipids [GL]- characterized by the number of glycerol groups; Glycerophospholipids [GP]- amphipathic with a polar glycerol and phosphate group and non-polar hydrocarbon; Sphingolipids [SP]- have a sphingoid backbone; Sterol lipids [ST]- with sterol nucleus

composed of four tightly fused carbon rings and a hydroxyl group attached to the first ring; Prenol lipids [PR]- synthesized from the five-carbon precursors (isopentyl diphosphate and dimethylallyl diphosphate); Saccharolipids [SL]- has fatty acid and a sugar backbone; Polyketides [PK]- has various structural forms, often as cyclic molecules with modifications such as methyl group or hydroxyl groups. [Image created with Biorender.com.]

1.5.3. General functions of lipids

In general, lipids have various complex biological functions. As main components of a eukaryotic cell membrane, they perform essential roles in maintaining its form and physiological processes. Glycerophospholipids mainly comprise the structure of biological membranes such as the plasma membrane and the intracellular membranes of the cell organelles (Casares et al., 2019; Horn & Jaiswal, 2019). These lipids in biological membranes are also involved in the formation of the bilayers, which are energetically preferred processes under an aqueous environment that utilize strategic lipid alignment and behavior (Alberts et al., 2002). Lipids also function as energy storage, as with triacylglycerols (TAG) located in adipose (fat) tissues in mammals (Ahmadian et al., 2007). The continuous synthesis and breakdown of this product are mainly controlled by the activation of the enzyme called hormone-sensitive lipase. Fatty acid breakdown provides more calorific content (about 9kcal/g) as compared to the breakdown of carbohydrates and proteins (4 kcal/g), which is associated with considerable hydration of water, making fat a more efficient storage of energy (Stryer, 1995). Lipid signaling is also a vital component of cell signaling, which may be controlled and activated by several receptors and lipids identified as signaling molecules and messengers (Okazaki & Saito, 2014). In plants, there are several lipid signaling molecules, which have low abundance at less than 1% of the total lipids and a fast turnover (Hou et al., 2016). Hou et al. (2016) enumerated some of the common groups of signaling lipids: phosphatidic acid, which is a diacyl glycerophospholipid that serves as a precursor for the biosynthesis of complex lipids (Munnik & Testerink, 2009); phosphoinositides, signaling molecules important in membrane trafficking, cytoskeleton organization, growth of the polar tip, and stress responses (Di Paolo & De Camilli, 2006; Munnik, 2010), sphingolipids, representing a heterogenous group of compounds that are involved in a variety of cellular processes and environmental responses such as the modulation of PCD (Liang et al., 2003); lysophospholipids, minor membrane compounds which have been found to accumulate in response to freezing, wounding, pathogen infection, or elicitor application (Welti et al., 2002); and oxylipins, which are involved in plant development and response to environmental cues,

with JA as the most common example (Savchenko et al., 2014). Other signaling lipids were identified and characterized, although this was done through animal studies. Examples are the N-acylethanolamine, found most abundant in desiccated seeds and which are implicated in plant growth and pathogen defense (Y.-S. Wang et al., 2006); alkamides, which are structurally similar to NAE with similar functions in plant development that intersect with jasmonate and cytokinin signaling pathway (López-Bucio et al., 2006); and free fatty acids, derived from triglycerides, phospholipids, sphingolipids, or NAEs, which were suggested to have direct involvement with biotic and abiotic stress responses in plants (e.g. study of Mandal et al. (2012) on oleic acids). Lipids have also other functions, particularly in humans. For example, 1) fat-soluble vitamins A, D, E, and K serve as essential nutrients stored in the liver and fatty tissues as with isoprene-based lipids (Kono & Arai, 2015); 2) acyl-carnitines are involved in the transport and metabolism of fatty acids in and out of the mitochondria (Jones et al., 2010); 3) polyprenols and phosphorylated derivatives are involved in the oligosaccharide transport across membranes (Akhtar et al., 2017); and 4) polyprenol phosphate and di-phosphate sugars function in extra-cytoplasmic glycosylation reactions and eukaryotic protein N-glycosylation (Eichler & Guan, 2017). The next sections discuss the functions of lipids particularly in the plasma membrane and during interactions between plants and microbes.

1.5.3.1. The plasma membrane and the lipids regulating its functions

The plasma membrane is a highly-ordered key biological structure that separates the interior of the cell from the extracellular medium – and which functions mainly in cell protection, nutrient exchange regulation, and signaling mediation (Xue et al., 2009). It functions like a sensor that regulates cellular activities and with an intricate pathway that orchestrates reception, signal transduction, and appropriate response mechanisms against a continuously changing environment. Because of these inherent functions, the plasma membrane needs to be both stable and robust – to maintain structural stability, while being fluid and adaptable – to cope with external factors and changes (Cassim et al., 2019). The remarkable molecular organization of the plasma membrane, which is constituted of a huge diversity of proteins and lipids in an asymmetric proteo-lipidic matrix, is what allows for its short-term dynamics and long-term stability. Given that the protein-to-lipid ratio (mass/mass) was determined to be close to 1.3, as with the case in the tobacco plasma membrane (Cacas et al., 2016), it can only be deduced that lipids largely contribute to the organization and composition of the plasma membrane, which is responsible for maintaining essential processes of plant cell physiology, abiotic stress

adaptation, intra- and intercellular communication, nutrient exchange, and plant-microbe interactions (Xue et al., 2009).

1.5.3.1.1. Roles of lipids in the structural formation and integrity of the plasma membrane

The structure of the plasma membrane is attributed to the unique properties of the lipid molecules, allowing them to assemble spontaneously in bilayers in an aqueous environment. The main lipid components found in the plasma membrane are glycerophospholipids, sphingolipids (SP), and sterol (ST) lipids (Cassim et al., 2019).

The plasma membrane is mostly composed of molecules that are amphipathic (or amphiphilic) - characterized by a hydrophilic (“water-loving”) polar end and a hydrophobic (“water-fearing”) non-polar end (Lodish et al., 2008). Among these, glycerophospholipids which have polar head groups and two hydrophobic hydrocarbon tails, are the most abundant. Their tails are made up of fatty acids which can differ in length (most commonly within 14-24 carbon atoms); with saturated and unsaturated (with one or more *cis*-double bonds that create a kink) tails (Alberts et al., 2002). The fluidity of the membrane is highly influenced by the differences in the length and desaturation degree of these fatty acid tails, as these affect the packing of the lipid molecules against one another (Alberts et al., 2002). Another factor influencing the fluidity of the bilayer is the mobility of the lipid molecules within each monolayer (also called a leaflet) and between them. Using electron spin resonance (ESR) spectroscopy, the principles of which are similar to that of nuclear magnetic resonance (NMR), the motion and orientation of a spin-labeled lipid were determined to be 1) “flip-flop” – lipid migration from one leaflet to another (occurs <once a month); and 2) “flexion”, “rotation”, or “lateral diffusion” – movement within the same leaflet (occurs $\sim 10^7$ times per second) (Liu & Conboy, 2005). This illustrates the flexibility of the hydrocarbon chains and the rapid rotation of individual lipid molecules around their long axis. The lipid composition, as well as temperature, also affect the fluidity and viscosity of the bilayer (Uemura et al., 2006). For example, the temperature can induce a phase transition, changing the liquid state of the bilayer to a two-dimensional rigid crystalline (or gel) state at a characteristic freezing point, depending on the length of the hydrocarbon chains and the presence of double bonds. Shorter chain lengths prevent the interaction of hydrocarbon tails with one another, while the *cis*-double bonds prevent packing, letting the membrane remain fluid even at lower temperatures (Seelig & Seelig, 1977). As such, some organisms have learned to adapt to fluctuating environmental

temperatures, by changing the proportion of and synthesizing fatty acids with more *cis*-double bonds (Seelig & Seelig, 1977).

Aside from phospholipids, however, the bilayer is also composed of sterols that enhance and maintain the permeability-barrier properties of the lipid bilayer (Hartmann, 1998). Sterols tend to make the bilayer less fluid because of their 1:1 proportion with phospholipid molecules. This is due to the orientation of their hydroxyl group and steroid rings against the polar head and first hydrocarbon chains of phospholipids, respectively, which causes rigidity and less permeability, as well as their high concentrations in most eukaryotic plasma membranes. However, they also prevent the packing and crystallizing of the hydrocarbon chains which inhibits potential phase transition. Since the plasma membrane is not only composed of the lipid bilayer but also of embedded membrane proteins – integral and peripheral, other lipids also play crucial roles in maintaining the order in the membrane (Brown & London, 2000). Because of their long and saturated fatty hydrocarbon chains, van der Waals attractive forces tend to hold sphingolipids together in small microdomains known as “lipid rafts” (also rich in sterols) (Brown & London, 2000). The lipid rafts are thicker than the other parts of the bilayer, allowing them to accommodate and organize certain membrane proteins – either to concentrate them for small vesicle transport or to enable the simultaneous functioning of proteins, e.g. during extracellular signal conversion to intracellular ones. Depending on their shape, lipid molecules can spontaneously aggregate to bury their hydrophobic tail in the interior while exposing the hydrophilic heads to water (Dowhan & Bogdanov, 2002). This is done in either of two ways: wedge-shaped lipid molecules forming a spherical micelle (tails inwards) or cylinder-shaped phospholipid molecules forming a bilayer (hydrophobic tails sandwiched between hydrophilic head groups). Both the cylindrical shape and amphipathic nature of glycerophospholipids contribute to the plasma membrane stability, allowing a self-healing property where a tear in the bilayer can be spontaneously repaired (Kozlov et al., 2014) [plasma membrane structure illustrated in Fig. 1.6.3.1-A].

1.5.3.1.2. Roles of lipids in nutrient transport (permeability) across the plasma membrane:

According to Lodish et al. (2008), one of the amazing characteristics of the plasma membrane is its ability to regulate the entry and concentration of essential substances into and out of the cell. This includes ions such as Ca^{++} , Na^+ , K^+ , and Cl^- , and nutrients including glucose, fatty acids, and amino acids. The plasma membrane also maintains the metabolic intermediates within the cell and removes the waste and toxic products from the cell, particularly carbon

dioxide (CO₂) or Na⁺. Therefore, this selective permeability of the plasma membrane allows the cell to maintain a constant internal environment. Lodish et al. (2008) also mentioned that because of its non-polar tails, the glycerophospholipid bilayer can only move relatively small, non-polar materials such as other lipids, oxygen (O₂) and carbon dioxide (CO₂) gases, and alcohol. It is essentially impermeable to water-soluble molecules such as glucose and amino acids, and electrolytes. Their movement is generally mediated by transport proteins associated with the bilayer - the specificity of which depends on the cell type and the required low-molecular-weight compounds (Lodish et al., 2008). The diffusion of substances through the lipid bilayer is categorized based on whether energy is required. Passive transport describes the movement without the expenditure of cellular energy by following a concentration gradient such as *diffusion* (e.g. O₂ and CO₂) and *facilitated diffusion* (e.g. large polar glucose molecule which requires a specialized glucose transporter) (Mueckler & Thorens, 2013; Yang & Hinner, 2015). On the other hand, active transport involves the movement of substances across the bilayer against a concentration gradient using energy from adenosine triphosphates (ATP) such as the *use of protein pumps* (e.g. sodium-potassium pump or Na⁺/K⁺ ATPase), *endocytosis* (which can be phagocytosis, pinocytosis, or receptor-regulated endocytosis), or *exocytosis* (Cooper et al., 2007).

1.5.3.1.3. Roles of plasma membrane lipids in cell signaling (reception, transduction, and response)

The bilayer of eukaryotic membranes contains a variety of glycerophospholipids, with head groups that differ in size, shape, and charge (Alberts et al., 2002). This variability is essential as some membrane proteins can function only in the presence of specific head groups, just as several enzymes in aqueous solution require specific ions for activity. Moreover, to be recruited and concentrated into specific membrane sites in the cytosolic leaflet of the bilayer, some enzymes only bind to specific phospholipid head groups. Notable as well is the asymmetric distribution of the lipid composition in the two leaflets of the bilayer (Boon & Smith, 2002). The external leaflet of the bilayer is enriched primarily with choline-containing lipids, phosphatidylcholine (PC), and sphingomyelin (SM); whereas the cytoplasmic leaflet is preferentially enriched with amine-containing glycerophospholipids such as phosphatidylethanolamine (PE) and phosphatidylserine (PS) (Daleke, 2003). Minor glycerophospholipids such as phosphatidic acid (PA), phosphatidylinositol (PI), phosphatidylinositol-4-monophosphate (PIP), and phosphatidylinositol-4,5-bisphosphate

(PIP₂), are also found on the cytoplasmic leaflet of the membrane (Daleke, 2003) [Fig. 1.6.3.1-B]. These membrane phospholipids have important implications in cellular signaling as described by (Alberts et al., 2002). Because of the negative charge of PS, the leaflets of the bilayer have a significant charge difference which is functionally important in the direct binding of cytosolic proteins (e.g. enzyme protein kinase C (PKC)) to the plasma membrane as a signaling response. In other cases, protein-binding sites are created at a particular time and place only after the lipid head groups are modified. For example, the phosphorylation of PI via lipid kinases (e.g., phosphatidylinositol kinase (PI 3-kinase) activated as a response to extracellular signals) then leads to the recruitment of proteins from the cytosol into the cytosolic leaflet of the membrane. Another way is by the cleavage of specific glycerophospholipid molecules by phospholipases that generate fragments acting as short-lived intracellular mediators. An example would be the cleaving of inositol phospholipid by phospholipase C leading to its separation into two fragments: the tail, which remains in the membrane that helps activate protein kinase C; and the head, released into the cytosol that stimulates the release of Ca²⁺ from the endoplasmic reticulum (ER) [Fig. 1.5.3.1.3. B-C].

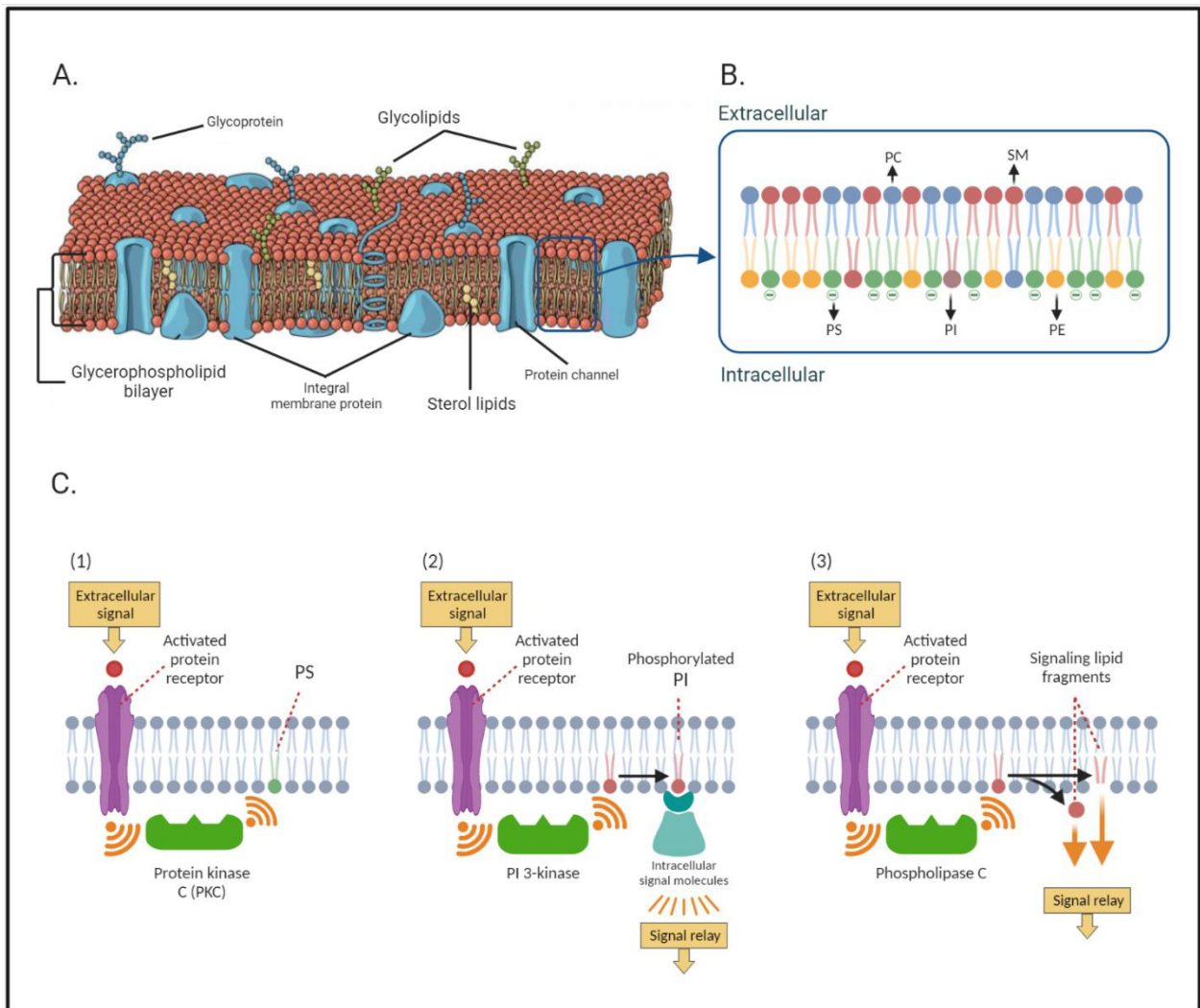


Figure 1.13 Lipid components and signaling in the plasma membrane. (A) Lipids in the plasma membrane. The plasma membrane is primarily comprised of glycerophospholipids (GP), sphingolipids (SP), and sterol lipids (ST) – with functions that maintain the structure, stability, and regulation of essential cell processes. (B) The five major glycerophospholipids that predominate in the plasma membrane are phosphatidylethanolamine (PE), phosphatidylserine (PS), phosphatidylcholine (PC), sphingomyelin (SM), and phosphatidylinositol (PI). Together they constitute more than half the mass of lipids in most membranes. Their distribution, variable within the two monolayers, leads to the bilayer asymmetry which is crucial in cell signaling and protein binding. (C) Membrane phospholipids have specific functions in cell signaling. (C-1) In response to extracellular signals, cytosolic proteins such as protein kinase C (PKC) are activated and bind to the cytosolic face of the membrane where the negatively-charged PS concentrated in this area, are required for their activity. (C-2) Extracellular signals can activate phosphatidylinositol kinase (PI 3-kinase), leading to phosphorylated inositol phospholipids in the plasma membrane. Various intracellular signaling molecules are then attracted and bind to the phosphorylated lipids in the membrane, where they interact and help relay the signal into the cell. (C-3) Other extracellular signals activate phospholipases (e.g. phospholipase C) that cleave phospholipids. These lipid fragments then act as separate signaling molecules to relay signals into the

cell – the tail retained in the membrane help activate protein kinase C while the head is released into the cytosol. [Image created with Biorender.com.]

Depending on the specific lipid components (whether in abundance or small quantities) in individual organisms, lipids may play diverse roles both in the maintenance of inherent cell functions, as well as in the interaction with other organisms. The next section highlights the main lipids, with their associated functions, found in plants, fungi, and bacteria – which are major players in the rhizospheric interactions.

1.5.4. Main lipids in plants and microbes and their associated functions

Plants are sessile organisms whose tasks are not only to manage their growth and development but also to regulate their complex metabolic and biosynthetic processes to adapt against biotic and abiotic environmental stressors (Liu et al., 2019). Lipids, being the primary components of biological membranes, have important roles in their growth regulation and either symbiotic relationship with symbionts or defense response mechanisms against microbial attack (Siebers et al., 2016). Major lipids directly involved in these processes are glycerophospholipids and associated lipid-modifying enzymes such as phospholipases D, C, and A, glycolipids, free fatty acids, oxylipins, sterol lipids, carotenoids, and apocarotenoids (Siebers et al., 2016).

1.5.4.1. Plant lipids

Plant glycerophospholipids, predominantly synthesized at the endoplasmic reticulum, are mainly comprised of PC and PE, with palmitic and linoleic acids as the main acyl chains; while minor components include that of PG, PI, PA, and PS. PS species are the only ones associated with a high proportion of very long fatty acid chains such as behemic C22 and lignoceric C24 acid (Grison et al., 2015). Phospholipases are instrumental in catalyzing the conversion of phospholipids into fatty acids and lysophospholipids, diacylglycerol (DAG), or PA, depending on their positional specificity (Pleskot et al., 2013). During pathogen attack, both phospholipases and glycerophospholipid-derived molecules in plant membranes are involved in cell signaling and induction of immunity responses (Arisz et al., 2009). Glycolipids can be mainly found in the chloroplasts of plants, including that of algae and cyanobacteria, and in some bacterial phyla (Abdel-Mawgoud & Stephanopoulos, 2018). The most common glycolipids found in plants are galactolipids, mainly 50% mono monogalactosyldiacylglycerol (MGDG) and 20% digalactosyldiacylglycerol (DGDG), while a minor proportion is comprised

of sulfolipid sulfoquinovosyldiacylglycerol (Hölzl & Dörmann, 2007). Fatty acids are major structural constituents of the cell as they are a component of glycerolipids (Mandal et al., 2012). Together with fatty acid metabolites, they are important modulators of many signal transduction pathways in response to variable stresses as well as plant-microbe interactions. Before they are converted into lipid mediators, fatty acids are first either produced by *de novo* synthesis or released from glycerolipids by lipases. Oxylipins in plants refer to a diverse class of lipid metabolites, which are important signaling molecules derived from the oxidation of unsaturated fatty acids, mostly during oxidative stress (Mosblech et al., 2009). Commonly found oxylipins in plants are fatty acid hydroperoxides, hydroxy-, oxo-, or keto-fatty acids, divinyl ethers, volatile aldehydes, or the plant hormone jasmonic acid (JA). They perform various biological roles as secondary messengers or even as bactericidal agents during defense response. The cytosol in plant cells is where sterol lipids are synthesized via the isoprenoid pathway (Wewer et al., 2011). Major sterols found in plants (also called phytosterols) are stigmasterol, β -sitosterol, and campesterol, while cholesterol can be found in low abundance. Sterols can either occur in their free form (free sterols) or are derivatized at the C3 hydroxy group to form conjugated sterols. While some sterols in plants are of low amounts (e.g. sterol esters), their relative abundance can be influenced by biotic or abiotic stresses. Carotenoids are C40 polyenes that are present in all photosynthetic organisms and serve as accessory pigments in the light-harvesting complex, both as photoprotectants and antioxidants (Mohammadi et al., 2012). The presence of β -carotene in membranes has been postulated to also assist during initial xylem and leaf colonization of sweet corn by the pathogen *Pantoea stewartii* subsp. *Stewartii*. Apocarotenoids, on the other hand, are isoprenoids derived by the cleavage from C40 carotenoid precursors catalyzed by carotenoid cleavage dioxygenases (CCDs) (Alder et al., 2012). Most plant hormones, such as abscisic acid (ABA), strigolactones, the acyclic C14 polyene mycorradicin, the cyclic C13 cyclohexenone, as well as hydroxylated and glycosylated derivatives of the latter, are comprised of apocarotenoids (Walter, 2013). Sphingolipids, which contain amino alcohol (long-chain base, LCB) instead of a glycerol backbone, are crucial for the integrity of the membrane bilayer and membrane raft formation (Siebers et al., 2016). The two major sphingolipid classes in plants, synthesized using ceramide as a substrate, are glucosylceramides (GlcCer) and glycosylinositol phosphoceramides (GIPC). Both are abundant components of the plasma membrane, ER membrane, and tonoplast; and together with sterols, maintain the lipid raft formation. Sphingolipids are also implicated in signaling and programmed cell death (PCD), which is a defense response mechanism against pathogen attack (Luttgeharm et al., 2015).

1.5.4.2. Fungal lipids

As with most eukaryotic cells, fungal membranes contain huge amounts of glycerophospholipids, mainly PC, PE, and PA, including phosphatidylglycerol (PG) and cardiolipin (CL) (Beccaccioli et al., 2019). Their membranes also contain sterol lipids; however, instead of phytosterols that are found in plants, they accumulate ergosterol which has shown to have important roles during plant-fungal interactions (Siebers et al., 2016). Sphingolipids are also found in considerable amounts in their membranes, although they have a different set of LCB to that of plants (Warnecke & Heinz, 2003). Two complex sphingolipids are found in fungi: phosphoinositol sphingolipids and glucosylceramides (GlcCer), which show a distinct feature of having a C-9 methyl group on the LCB, that are particularly important for pathogenesis and induction of various plant defense mechanisms. Fatty acids such as palmitvaccenic acid, which are found abundantly in mycorrhizal fungi in the form of triacylglycerol (thus the term “oleaginous fungi”), can serve as a biomarker for the evaluation of mycorrhizal colonization (Bago et al., 2000). It is not yet clear though whether mycorrhizal fungi synthesize their fatty acids from plant-derived carbon sources such as hexose, or if these were provided by the host plant (Bago et al., 2000; Trépanier et al., 2005; Wewer et al., 2014). What has been found was that fungal *de novo* fatty acid synthesis was influenced by plant nutrient supply and that it was restricted to the intraradical mycelium (Trépanier et al., 2005). Lysophosphatidylcholine (LPC) is another lipid that may perform signaling functions during mycorrhizal symbioses, such as the upregulation of the expression of the phosphate transporter *PT4* in plants (Vijayakumar et al., 2016). Ergosterol is one of the microbe-associated-molecular patterns (MAMPs) that act as an elicitor of the microbe-triggered immunity (MTI) upon contact with plants, leading to responses such as ROS production, changes in proton fluxes, and potential of the plasma membrane, and activation of isoprenoid synthesis inducing phytoalexin production (Tugizimana et al., 2014).

1.5.4.3. Bacterial lipids

Bacterial membranes are mainly composed of glycerophospholipids (PE, PG, and CL), the synthesis of which begins with the conversion of PA to cytidine diphosphate-diacylglycerol (CDP-DAG) by the CDP-DAG synthase CdsA with CTP as co-substrate (Parsons & Rock, 2013). Bacteria that produce PC are often symbionts or pathogens of plants (Sohlenkamp & Geiger, 2015). Bacteria also produce a high variety of phosphate-free membrane lipids, including glycolipids found in cyanobacteria and gram-negative bacteria, which serve as

membrane anchors for lipoteichoic acids and in nodule-forming bacteria or plant pathogens (Diercks et al., 2015; Hölzl & Dörmann, 2007). Other examples of bacterial lipids are betaine lipids such as diacylglyceryl trimethylhomoserine (DGTS) which are specific to α -proteobacteria, although homologs of enzymes in DGTS synthesis are encoded in the genomes of other bacterial groups (Sohlenkamp & Geiger, 2015), and ornithine lipids (OLs) which are common in bacteria, but absent in eukaryotes (Diercks et al., 2015). Another example of phosphate-free membrane lipids are hopanoids, which are specific lipids that play a role during nitrogen fixation of *Frankia sp.* and various *Bradyrhizobium* species (Silipo et al., 2014), and during plant-microbe interaction of *B. diazoefficiens* with its native host soybean and symbiosis with different species of the tropical legume *Aeschynomene* (Kulkarni et al., 2015). Bacterial membranes also have oleic acid-derived oxylipins, which function as autoinducers for the novel quorum sensing system by controlling the cell-density gene expression (Martínez et al., 2019). The most common class of autoinducers in gram-negative bacteria are the N-acyl homoserine lactones (AHLs) (Schuster et al., 2013). However, other bacterial species – gram-negative and positive alike, possess alternative quorum-sensing mediators such as alkylquinolones, α -hydroxyketones, peptides, and fatty acid-like molecules. Quorum-sensing systems regulate important biological processes including bioluminescence, DNA transfer, antibiotic resistance, motility, biofilm formation, and virulence (Williams et al., 2007).

1.5.5. Lipids: The chemical language during rhizosphere interactions

Plant roots are surrounded and highly influenced by the rhizosphere – a complex ecosystem of nutrient-rich soil (Verbon & Liberman, 2016). This thin strip of soil is enriched with an assortment of root secretions including primary metabolites (e.g. organic acids, carbohydrates, and amino acids) and secondary metabolites (e.g. alkaloids, terpenoids, and phenolics), which come at a significant carbon (C)-cost for the plant, but with ultimate importance in driving all types of rhizospheric interactions. Because of their organotrophic nature, a multitude of microorganisms including bacteria, fungi, and protists, densely populate this area (van Dam & Bouwmeester, 2016). This allows microorganisms to either extend the plant's performance and capacity to adapt to the environment or utilize nutrients at the plant's expense through niche colonization. The behavior and impact of these microbes are believed to rely heavily on the compounds, which mediate interactions through the release and perception of signaling molecules secreted by both plants and microbes (Mendes et al., 2013). This process is known in general terms as signaling or communication highway, underground interaction, rhizosphere

chemical language, or complex plant-microbe interaction (Bais et al., 2004; Mendes et al., 2013). The rhizospheric interactions can be grouped into three signaling categories: 1) signaling from plant roots to microbes, which is facilitated by small-secreted molecules; 2) intra- and interspecies signaling mainly occurring via quorum sensing (QS) to synchronize microbial behaviors; and 3) signaling from microbes to plants through the release of compounds affecting plant gene expression, root architecture, and defense responses (Venturi & Keel, 2016). This section focuses on rhizosphere interkingdom signaling, which is divided into three consecutive stages (Fig 1.5.5).

1.5.5.1. Plant root to microbe signaling through rhizodeposition

The first stage in any rhizospheric interaction is the recruitment of the rhizobiome into the plant vicinity, which is highly influenced by rhizodeposition. Shaping the rhizosphere chemistry is stimulated by rhizodeposits, a collective term for C-containing compounds released by the roots, which can have various origins: at root apices, from sloughed-off root cells, border cells, and tissues; mucilage released from the root caps and root hairs; root exudates, which likely decrease with distance from root apices due to microbial mineralization; volatile organic compounds (VOCs); lysates released by senescing epidermal and cortical cells; and altered root-derived C by microbes or symbionts (e.g. C released by the extensive hyphal networks of arbuscular mycorrhiza) (Bais et al., 2004; Dennis et al., 2010). The release of rhizodeposits comes with a wide variety of substances such as sugars (e.g. glucose, oligosaccharides, deoxyribose), amino acids (e.g. α - and β -alanine, glutamine, methionine), organic acids (e.g. acetic, benzoic, oxaloacetic acids), enzymes (e.g. amylase, invertase, peroxidase), growth factors and vitamins (choline, pyridoxine, riboflavin), flavonones and purines/nucleotides (e.g. adenine, guanine, uridine/cytidine), and miscellaneous substances (e.g. auxins, glucosides, inositol and myo-inositol-like compounds, inorganic ions and gaseous molecules such as CO_2 , H_2 , H^+ , O^- , HCO_3^-) (Uren, 2007).

Lipids in various forms such as fatty acids (e.g. linoleic, linolenic, oleic, palmitic, stearic acids) and sterols (e.g. campesterol, cholesterol, sitosterol, stigmasterol) are also among these essential compounds that enrich the rhizosphere chemistry (Uren, 2007). Plants initiate an interaction by secreting (sending) out these substances (“chemical” signals) into the rhizosphere. Specific examples are plant-produced flavonoids such as 2-phenyl-1,4-benzopyrone derivatives involved in root nodule formation (Maillet et al., 2011), inhibitory flavonoids such as phytoalexin, medicarpin, and glyceollin (Costa et al., 2021), and the volatile

organic compound (VOC) (E)- β -caryophyllene that functions as plant bioprotectant against herbivores and pathogens and as an attractant for organisms preying on root-feeding herbivores from maize roots (Degenhardt et al., 2009; Dudareva et al., 2006). These chemotactic attractors can facilitate the recruitment, nutrition, shaping, and tuning of the microbial communities from a reservoir of microorganisms present in the soil – by encouraging, limiting, or inhibiting microbial activity and proliferation (Bais et al., 2004; Costa et al., 2021; van Dam & Bouwmeester, 2016).

1.5.5.2. Microbe perception of plant root-released compounds and other microbial signals

The second stage of the rhizosphere interaction is the perception or detection of low molecular weight compounds, such as lipid molecules, released by the plant roots (or other microbes) by microbes, which results in the catabolism, transformation, or rejection of the perceived compound (Venturi & Keel, 2016). Perception of these compounds then leads to the stimulation of regulatory or signaling cascades that cause various responses in the microbes.

In the case of legumes and their rhizobial symbiont, the first signals exchanged are the plant-produced flavonoid compound, which induces the bacterial *nod* genes that are responsible for the secretion of lipo-chitooligosaccharides (LCOs) (Maillet et al., 2011). These are also known as nodulation (Nod) factors (Nod-LCOs), which are the central signal molecules for initiating nodule formation in the roots (Lerouge et al., 1990). Similar signaling is also utilized by mycorrhiza (named Myc-LCOs), although mycorrhizal symbiosis has long been established with the earliest plants (Parniske, 2008). This led to the conclusion that the chemical dialogue is continuous and conserved, and that most likely during evolution rhizobia co-opted the mycorrhizal signaling machinery. The strigolactone plant hormones, which are involved with *in planta* functions (e.g. auxin transport and cell protection, respectively), also act as *ex-planta* stimuli for mycorrhizal hyphae and AMF stimulation, as with cutin monomers (Akiyama et al., 2005; Waldie et al., 2014). These molecules, however, are examples of plant signals perceived not just by beneficial, but also by opportunistic pathogenic organisms, e.g. detection of strigolactone by root-parasitic plants *Strigga* spp. and *Orobranche* spp, for seed germination and perception of cutin monomers as elicitors by aerial fungal pathogens for appressorial formation (Liu et al., 2011; Ruyter-Spira et al., 2013). Plants also produce an array of volatile compounds, estimated to constitute about 1% of their secondary metabolites, that freely cross the membrane and disperse into the soil (Dudareva et al., 2006). Low molecular

weight compounds from plants have also been shown to bind to a subfamily of LuxR proteins in some bacterial strains (e.g. some pathogenic xanthomonads and beneficial pseudomonads), to elicit QS-mimicking response (González & Venturi, 2013). These are only but a few of the numerous plant molecules which are sensed and responded to, in terms of gene expression regulation, by microbes.

Root-secreted substances have also been thought to influence the gene expression of different microorganisms in the rhizosphere (cell-cell signaling) which are not in proximity and association with plants. A well-known process that many bacteria undergo is the cell density-dependent signaling mechanism – quorum sensing, which is driven by the production and response to quorum levels of chemical signals (Fuqua et al., 1994). This QS mechanism is instrumental for the regulation of microbial phenotypes such as biofilm formation, virulence, conjugation, secretion of hydrolytic enzymes, and production of secondary metabolites – increasing rhizosphere competence that leads to successful colonization (Newton & Fray, 2004). A variety of rhizosphere proteobacteria produce and/or respond to the QS signal N-acyl homoserine lactone (AHL), including strains from the genera of *Pseudomonas*, *Burkholderia*, *Serratia*, *Erwinia*, and *Ralstonia*, as well as rhizobial species (Ferluga et al., 2008). There are several other types of recently discovered QS signals: from gram-negative bacteria are pyrones and dialkylresorcinols (Brameyer et al., 2015) and diffusible signal factor (DSF, which are *cis*-2-saturated fatty acids) family (Ryan et al., 2015); from gram-positive bacteria are peptides (known as pheromones) (Monnet et al., 2016); antibiotics at low and non-inhibitory concentrations (Andersson & Hughes, 2014); and from fungal species (mostly ascomycetes) are some alcohols, particularly associated with development processes (Leeder et al., 2011). A wide range of bacterial and fungal species also release an array of VOCs (usually alkenes, benzenoids, aldehydes, and ketones) which are believed to play crucial roles in long-distance rhizosphere interactions (Bitas et al., 2013). Among microbial communities, these compounds can act like chemical weapons, exhibiting antimicrobial activity, or interfere with other QS systems (interspecies); and they can coordinate gene expression and influence intraspecies behaviors such as biofilm formation, virulence, and stress tolerance (Audrain et al., 2015). All these QS signals and VOCs released by microorganisms can also act as interkingdom signals – influencing plant gene expression and immunity; and affecting plant root architecture, growth, and development (Bitas et al., 2013; Venturi & Keel, 2016).

1.5.5.3. Signaling response from microbes back to the plant

The third stage in the rhizosphere interaction involves the release of diverse signaling molecules from microorganisms to their plant host, as a response to signals perceived from among themselves (intraspecies), other microorganisms (interspecies), or plants. The most studied rhizosphere microorganisms are rhizobial bacteria – plant growth-promoting bacteria (PGPR, from the genera *Pseudomonas*, *Bacillus*, *Azospirillum*), as well as mycorrhiza and plant growth-promoting fungi (PGPF, such as *Trichoderma* and non-pathogenic *Fusaria*) (Pieterse et al., 2014). Conserved microbe-specific molecules known as microbe-associated molecular patterns (MAMPs), such as lipopolysaccharides (which have the active Lipid A), peptidoglycans, flagellin, and chitin, are detected by dedicated pattern recognition receptors (PRRs) from plants (Zamioudis & Pieterse, 2012). This detection triggers a local basal systemic defense response controlled by regulatory networks that involve signaling pathways via plant hormones including salicylic acid (SA), jasmonic acid (JA), and ethylene (Pieterse et al., 2014; Vos et al., 2013). The plant defense response can be induced systemic resistance (ISR), systemic acquired resistance (SAR), or priming. ISR is usually induced by beneficial colonizing PGPF and PGPR against foliar pathogens and leaf-feeding insects, which initiate JA and SA signaling pathways (Pieterse et al., 2014). SAR, on the other hand, is commonly induced by pathogen attack, which triggers SA signaling (Vos et al., 2013). Plants also exhibit an innate immune response triggered by beneficial microbes, called priming, that helps the plants to react more efficiently against biotic and abiotic stimuli (Balmer et al., 2015). Although these mechanisms are designed to prevent potential attacks, beneficial rhizosphere microbes have developed countermeasures for immune recognition, leading to successful plant colonization. The signaling and mechanisms involved, however, are still subject to more investigation but are an area of great interest that is rapidly evolving (Zamioudis & Pieterse, 2012).

Aside from effector proteins secreted directly into the plant cell and MAMPs/PAMPS, microbes also release other diverse signaling molecules. These molecules are not only used for intra- and interspecies signaling but also in interacting with plants. Previously cited examples are Nod- and Myc-LCO factors released by rhizobia and mycorrhiza, respectively, which suppress SA-dependent defense response to initiate the symbiosis signaling pathway (Oldroyd, 2013). Some mycorrhiza, e.g. *Laccaria bicolor* and *Rhizophagus intraradices*, also produce small secreted proteins (SSPs) which act as mutualistic effectors that alter plant hormone signaling pathways to establish symbiosis (Plett et al., 2014). QS molecules such as AHL from

PGPR, diffusible signal factors (DSF) and cyclodipeptides from *Xanthomonas*, and diketopiperazines (DKP) from *Pseudomonas aeruginosa* also serve as interkingdom signaling molecules which elicit effects on plants (Grandclément et al., 2016; Sieper et al., 2014). They can change the gene expression and protein profile of plant roots and shoots; influence root development, plant defense, and stress responses; and regulate metabolic activity and hormone balance. Certain antimicrobials at sub-inhibitory concentration can induce systemic plant responses, such as the 2,4-Diacetylphloroglucinol (DAPG) and pyocyanin, which trigger ISR (via SA and ethylene signaling) against fungal and bacterial leaf pathogen (Weller et al., 2012) and affect root development via auxin-dependent signaling pathway (Ortiz-Castro et al., 2014). Other examples of pseudomonad-released antimicrobials, which also act as intra- and interspecies signals, are phloroglucinols and phenazines (Powers et al., 2015). Other microbial signaling molecules belong to VOCs which can act as plant growth promoters or inhibitors, and as priming agents or elicitors of systemic plant defense and stress tolerance. An example of VOC is 2,3-Butanediol (2,3-BD) released by bacteria (from the genera *Bacillus*, *Pseudomonas*, and *Enterobacter*), which induces plant growth and ISR against plant-pathogens and assists in a plant's tritrophic interaction with herbivores and their parasitoid (D'Alessandro et al., 2014). Indole, produced by various PGPRs, is another bacterial VOC which affects root development by auxin-signaling pathway (Bailly et al., 2014). Phytohormone-like compounds such as auxins, gibberellins, and cytokinins belong to a further class of microbial signaling molecules produced not only by beneficial (PGPR and PGPF), but also by pathogenic fungal and bacterial microbes; which influence hormone signaling pathways, immune response, and plant growth and development (Dreccer et al., 2014; Venturi & Keel, 2016) (Lipid roles in rhizosphere interactions summarized in Fig. 2).

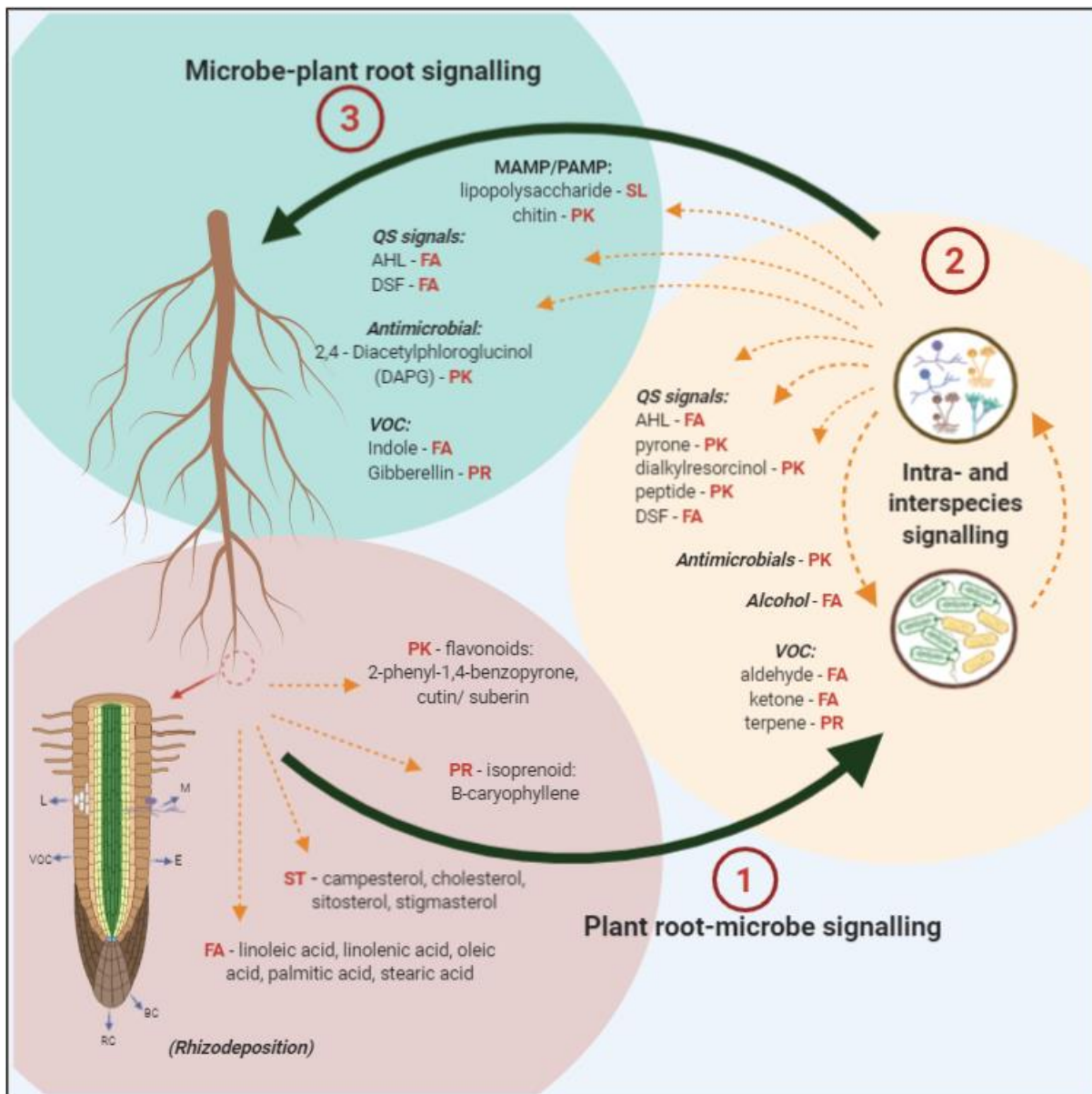


Figure 1. 14 Lipids as chemical signals in rhizosphere interactions and signaling. Plants initiate signaling through the release of rhizodeposits from the roots in a process called rhizodeposition. Rhizodeposits can originate from various sources including root cap (RC), border cells (BC), root exudates (E), volatile organic carbon (VOC), carbon from symbionts or microbes (M), and carbon loss due to lysates (L) from epidermal and cortical cells. The release of rhizodeposits also comes with a variety of substances, including lipids, which act as chemical signals that are then perceived by the microbes. Plant-secreted substances influence cell-cell signaling among different microorganisms which are not in proximity to plants. Microbes also produce communication signals for population and behavior coordination, including quorum sensing (QS) such as N-acyl homoserine lactones (AHL), diffusible signal factors (DSF), pyrones, dialkylresorcinol, peptides; antimicrobials (at low and non-inhibitory concentrations); alcohols; and volatile organic compounds (VOC). As a response to signals perceived from among themselves (intraspecies), other microorganisms (interspecies), or plants, microbes release diverse signaling molecules such as effector proteins (microbe/pathogen-associated

molecular patterns, MAMPs/PAMPs), which can induce plant defense or immunity responses, i.e. by priming, induced systemic resistance (ISR), and systemic acquired resistance (SAR). Microbes also release similar compounds to plants. These microbe-released compounds can affect plant gene expression, hormonal balance, development, metabolism, and stress responses. They can also interfere with and suppress plant immunity to successfully colonize plant tissues. (Red texts are lipid categories: FA- fatty acids, ST- sterol lipids, PR- prenol lipids, PK- polyketide, SL- saccharolipids). [Image created with Biorender].

1.5.6. Plant lipids during pathogenic and symbiotic interactions with microorganisms

Apart from acting as chemical signals in rhizosphere signaling, lipids are also involved in diverse functions during pathogen attacks or infection and mutualistic or symbiotic interactions with beneficial microorganisms. Specific lipids have particular functions, such as in host-specific pathogen recognition, signaling in the cells from the site of infection or interaction, and transfer of infection signals to distal organs of the plants during defense responses (Lim et al., 2017; Mandal et al., 2010; Siebers et al., 2016). Signal-inducing compounds from microbes or elicitors are recognized by the plant's innate immune system, which results in the induction of defense responses (Jones & Dangl, 2006) or invasion of host tissues (Rossi et al., 2020).

According to Siebers et al. (2016), lipids in the plasma membrane play key roles in plant cell responses to microbial attacks and interactions with beneficial microbes. These lipids are synthesized, modified, or re-allocated upon upregulation of several genes encoding enzymes of lipid metabolism. This indicates the importance of lipid-modifying enzymes as regulators of the spatial and temporal production of lipid metabolites that are involved in signaling and membrane proliferation for the establishment of intracellular compartments or compositional changes of the bilayer. **Phospholipase D (PLD)**, which forms PA by cleaving the terminal phosphodiester bond of phospholipids, is involved in lipid metabolism and hormone signaling (abscisic acid, ABA; JA) as well as during biotic and abiotic stress responses (J. W. Wang et al., 2006). For example, PLD β 1 positively regulates the production of JA and plant resistance to necrotrophic fungal pathogen *Botrytis cinerea* in Arabidopsis, downregulates the SA-dependent signaling pathway, and increases tolerance to *Pseudomonas syringae* tomato pv DC3000 (Pst DC3000) (Zhao, 2015). PLD β 1-deficient mutants also show the accumulation of lysophospholipids, including lysophosphatidylethanolamine (LPE), lysophosphatidylcholine (LPC), and lysophosphatidylglycerol (LPG), which are important signaling molecules mediating plant defense responses (Zhao et al., 2013). Activation of **phospholipase C (PLC)** or the DAG kinase pathway (DGK) is triggered by pathogen-associated molecular pattern

(PAMP) recognition, leading also to the accumulation of PA (Arisz & Munnik, 2013). PLC in plants can be divided into 3 categories based on substrate specificity and cellular function: 1) PC-PLCs or non-specific PLCs that hydrolyze PC and other phospholipids, 2) phosphatidylinositol-4,5-bisphosphate (PIP₂)-PLC (PI-PLC) that acts on phosphoinositides, and 3) glycosylphosphatidylinositol (GPI-PLCs) that hydrolyzes GPI anchors on proteins. PLCs play a role in the elicitor recognition processes, act as second messengers stimulated during pathogen infection, and are involved in downstream disease resistance signaling (Vossen et al., 2010). **Phospholipase A (PLA)** catalyzes the hydrolysis of acyl bonds of phospholipids to yield FA and lysophospholipids, the latter of which are involved in systemic responses after wounding (PLA₂-derived LPC and LPE) (Rietz et al., 2010). PLA is involved in plant growth regulation, root and pollen development, stress responses, and defense signaling. It is also linked to plant immunity because of its roles in oxylipin and JA biosynthesis; is considered important during the oxidative burst induced by biotic elicitors, and is known to protect against plant pathogens (Rietz et al., 2010). During microbial attack or plant-pathogen interaction, these lipid-hydrolyzing enzymes induce the production of defense-signaling molecules such as oxylipins, including JA and the potent second messenger PA (Arisz et al., 2009). **Plant-derived PA**, which often binds to proteins leading to alterations of protein localization or enzyme activity, regulates a range of different physiological processes such as activities of kinases, phosphatases, phospholipases, and proteins involved in membrane trafficking, CA²⁺ signaling, or the oxidative burst (Siebers et al., 2016). PA acts as a precursor for lipid intermediates such as LPA, DAG, and FA and serves as a specific membrane-binding docking site for PA-binding proteins. PA levels were increased during pathogen attack or elicitor treatment in several plants (Suzuki et al., 2007).

Systemic acquired resistance (SAR), which is based on previous infections that lead to enhanced resistance in subsequent infections, represents a whole plant defense response directed against a wide spectrum of pathogens (Gao et al., 2014). At the site of infection, small molecules that serve as initial signals of the effector-triggered immunity (ETI) response, such as **methyl-salicylic acid (MESA)**, are produced and then moved to the distal plant organs where they are hydrolyzed into SA that trigger SAR (Gao et al., 2014). Other signal molecules such as glycerol-3-phosphate (Gro3P), azelaic acid (AZA), and nitric oxide (NO) function as inducers of SAR. **Gro3P**, a product of glycerophosphodiesterases produced from PLA and lyso-PLA enzymatic activities, can also be synthesized through the glycerol kinase pathway, while its accumulation is highly conserved in different organisms (Venugopal et al., 2009). In plants, Gro3P is proposed to regulate plant defense signaling and is an important component of diverse

energy-producing reactions and the precursor for glycerolipid biosynthesis (Chanda et al., 2008). **AzA**, which is a C-9 dicarboxylic acid and a general oxidative stress signal implicated in SAR, is produced from the oxidative cleavage of unsaturated FA (18:1, 18:2, 18:3) during pathogen infection (Yu et al., 2013). AzA-induced SAR depends on Gro3P, but in turn, AzA accumulation can also induce Gro3P synthesis, even in the absence of pathogen infection. On the other hand, mutualistic or symbiotic interactions with beneficial, plant growth-promoting microorganisms, can stimulate the plant immune system which results in the induced systemic resistance (ISR) that mediates resistance to a wide array of diseases (Pieterse et al., 2014). While SAR and ISR partly overlap and share common signaling components, ISR in distal organs is mainly based on the activities of the phytohormone JA in contrast to SAR which is based on SA.

Galactolipids, which make up the major glycolipid fraction, have important roles in signal transduction, cell communication, and pathogen responses (Gaude et al., 2004). Galactolipids have different functions in SAR, with **MGDG** regulating the biosynthesis of AzA and Gro3P, while **DGDG** affects the biosynthesis of NO and SA. Aside from SAR, galactolipids are also involved in other plant-microbe interactions, e.g. in the peribacteroid membrane formed during root-nodule symbiosis, which helps to save phosphate because of reduced requirements for phospholipids.

A key step in **FA** biosynthesis in Arabidopsis, catalyzed by a stearyl-acyl-carrier protein desaturase (SSI2), is the desaturation of **18:0** (stearic acid) to **18:1** (oleic acid), with the latter acting as a signal of biotic stress responses via NO (Mandal et al., 2012). Changes in the levels of oleic acid lead to the alterations of SA-and JA-mediated defense responses (Kachroo et al., 2005). Trienoic FAs (16:3, 18:3), which are the most abundant FA in plant membranes, particularly in Arabidopsis' galactolipids, also play important roles in plant defense response. The **18:3** (alpha-linolenic acid) works against avirulent bacterial pathogens; and low levels of this, such as in Arabidopsis fad7fad8 mutants deficient in two ω -3 desaturases (FADs), led to a decrease in ROS accumulation, cell death initiation, and resistance to avirulent strains of *P. syringae* (Yaeno et al., 2004).

During arbuscular mycorrhizal formation (AMF), regulation of several genes is also involved in plant lipid metabolism, such as the upregulation of genes encoding enzymes for FA synthesis from plastid and glycerolipid synthesis, indicating the increased production of lipids during root mycorrhization (Wewer et al., 2014). This could be because of the requirement of phospholipids to establish a large surface of the periarbuscular membrane (Vijayakumar et al., 2016). Lipid-derived signals were also found to be involved in AM

formation such as **reduced arbuscular mycorrhiza 2 (RAM2)**, which shows sequence similarities with Gro3P acyltransferase genes GPAT5 (suberin biosynthesis) and GPAT6 (cutin biosynthesis) from Arabidopsis (E. Wang et al., 2012). RAM2 is involved in the synthesis of ω -hydroxy (OHFAs) and α,ω -dicarboxylic acids (DCAs) – FAs associated with suberin and cutin, which are important in AM formation.

A process that plays an important role in signal transduction and programmed cell death (PCD), which can be induced by both biotic and abiotic stresses, is lipid peroxidation (Siebers et al., 2016). This process can be mediated via enzymatic pathways (lipoxygenase, LOX) or non-enzymatic pathways (ROS). Lipids that can be subjected to peroxidation are **galactolipids**, **free FA**, or **acyl groups** bound to **TAG**, and this leads to the generation of jasmonate (JA) during defense response (Nakashima et al., 2011). **JA-related oxylipins**, derived from the 13-lipoxygenase reaction of 18:2, 18:3, or 16:3, have signaling functions in plants. JAs are particularly produced during wounding, e.g. after herbivore attack and microbe infection, and are important for defense response to different fungal and bacterial pathogens (Scalschi et al., 2015).

Because some fungi (e.g. *Aspergillus*) produce a set of oxylipins related to that of plants, such as **8-hydroxyoleic acid**, **8-hydroxylinoleic acid**, **8-hydroxylinolenic acid**, **leukotrienes**, and **prostaglandins**, it is speculated that plants and fungi “communicate” via the oxylipin language (Christensen & Kolomiets, 2011). AMF colonization led to the accumulation of JA in barley roots showing upregulation of the expression of JA biosynthetic genes (allene oxide cyclase, AOC; allene oxide synthase, AOS) (Isayenkov et al., 2005). In tomatoes, AMF infection results in the upregulation of expression of AOS1, methyl jasmonate esterase (JAME), and the jasmonate ZIM domain 2 (JAZ2) genes, which are involved in the 13-lipoxygenase pathway that leads to oxophytodienoic acid (OPDA) and JA production (López-Ráez et al., 2010). The colonization of *Populus* by the ectomycorrhizal fungus *Laccaria bicolor* also showed upregulation of JA-regulated genes, with JA application affecting fungal colonization. This fungus developed a countermeasure to suppress the negative impact of JA on its colonization of poplar by producing the mycorrhiza-induced small secreted protein 7 (MiSSP7) which binds with the JAZ6 protein of poplar, protecting it from JA-dependent degradation (Plett et al., 2014).

Sterol lipids also play significant roles in plant-microbe interactions. K. Wang et al. (2012) showed how **stigmasterol** was vital during the resistance of Arabidopsis to virulent and avirulent *P. syringae* strains. That found that infection with this pathogen stimulated the stigmasterol synthesis via the desaturation of **β -sitosterol**. The ratio between stigmasterol to β -

sitosterol increased in membranes at the site of infection which rendered Arabidopsis plants susceptible to primary bacterial infections; however, SAR was not affected indicating that SAR was independent of stigmasterol. This indicated a correlation between the stigmasterol:β-sitosterol ratio and bacterial virulence due to changes in membrane integrity as a result of a shift in sterol lipids. Moreover, the accumulation of stigmasterol upon *P. syringae* infection also showed the defense response of plants to prevent unwanted nutrient efflux, therefore inhibiting bacterial proliferation in the apoplast (K. Wang et al., 2012). **Sterol esters**, which are synthesized from free sterols using phospholipid as an acyl donor by the enzyme phospholipid acyltransferase 1 (PSAT1), are also involved in pathogen recognition, as demonstrated by Kopischke et al. (2013). They observed that Arabidopsis PSAT1 mutant infected with pathogens showed hyperaccumulation of callose and enhanced cell death, preventing the proliferation of pathogens. When the sterol-specific fluorochrome stain Filipin was applied to the appressorial tip of germ tubes and septum of *B. graminis*, it showed circular enrichment in the epidermis cells beneath appressoria, which was concluded to be the aggregation of sterol lipids and proteins in the plasma membrane forming microdomains (lipid rafts) (Bhat et al., 2005).

Sphingolipids have been shown to be involved in PCD, which is a defense reaction against pathogen attack (Dickman & Fluhr, 2013). The expression of ceramide synthases in Arabidopsis (LOH1, LOH2, and LOH3) showed that while overexpression of LOH1 and LOH3 increases plant growth, overexpression of LOH2 results in dwarfing and the constitutive expression of hypersensitive response (HR) genes and PCD (Luttgeharm et al., 2015). An aspect in many studies is the accumulation of SA in sphingolipids mutants, which led to the proposal of a putative interaction between sphingolipid metabolism and SA signaling during PCD and HR (Sánchez-Rangel et al., 2015). The proposed sphingolipid molecules involved in SA biosynthesis are **LCBs** and **ceramides**; and four possible candidates for signal transduction from alterations of sphingolipid content to SA biosynthesis were MPK6 (mitogen-activated protein kinase 6), ROS, CA²⁺, and NO (Sánchez-Rangel et al., 2015).

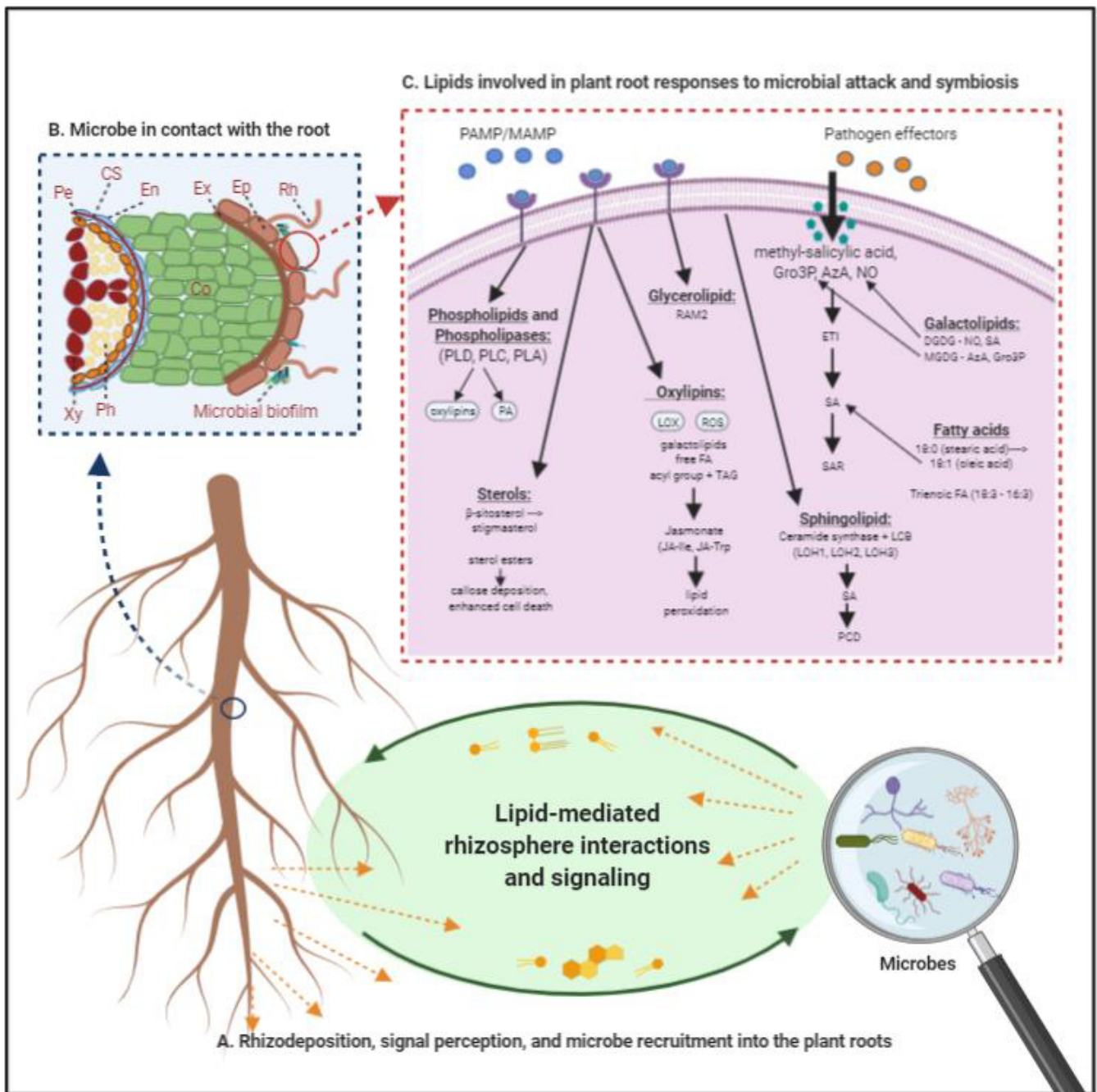


Figure 1. 15 Lipid roles in the microbial colonization of roots. Lipids are involved in the different stages of microbial colonization of plant roots. (A) Lipid roles can be traced back from the recruitment and shaping of the microbiome through the release of rhizodeposits, where lipids act as chemical signals released by the plants, perceived and utilized by microbes to regulate intra- and interspecies behavior, and released by microbes into the roots to influence plant responses. (B) Successful recruitment of microbes leads to the formation of microbial biofilms on root surfaces. Lipids in the plasma membrane mediate the interaction of the plant roots and microorganisms. (C) Different lipid species perform various functions during signal reception, transduction, and downstream response mechanism of plants to microbial attack or beneficial symbiosis. Some of the lipids involved are phospholipids and

phospholipases, glycerolipids, sphingolipids, galactolipids, fatty acids, sterol lipids, and oxylipins. (Pe-pericycle, Xy- xylem, CS- Casparian strip, Ph- pith, En- endodermis, Ex- exodermis, Ep- epidermis, RH- root hairs, PAMP/MAMP- pathogen/microbe-associated molecular pattern, PLD/PLC/PLA- phospholipase D/C/A, PA- phosphatidic acid, RAM2- reduced arbuscular mycorrhiza 2, LOX- lipoxygenase, ROS- reactive oxygen species, TAG- triglyceride, JA-Ile- jasmonyl isoleucine, JA-Trp- jasmonyl tryptophan, Gro3P- glycerol-3-phosphate, AzA- azelaic acid, NO- nitric oxide, ETI- effector triggered immunity, SA- salicylic acid, SAR- systemic acquired resistance, LCB- long chain base, LOH 1/2/3- Longevity assurance gene one homologs (1/2/3), PCD- programmed cell death, DGDG- digalactosyldiacylglycerol, MGDG- monogalactosyldiacylglycerol). [Image created with Biorender.com.]

With all the essential functions of lipids, designated to different lipid categories with unique chemical characteristics allowing a wide-range of performances, this could be the reason why they evolved as signal molecules for communication between host plants and microorganisms, in pathogenic and mutualistic interactions. Therefore, comprehensive lipidomic studies are required to further identify additional lipids and novel lipid functions. Substantial improvements in analytical techniques can enhance our understanding of plant lipid metabolism and its interaction with the biotic environment.

1.5.7. Plant lipids under high-temperature stress

Lipid molecules have essential functions and are building blocks for every living cell membrane, which are sites for many specific activities of enzymes, transport ions, metabolites, and hormonal receptors (Wang & Lin, 2006). Temperature during plant growth has profound influence on membrane lipids. During stress conditions, membrane lipids undergo several changes such as the alteration of the fatty acid composition and degree of unsaturation. The regulation of membrane lipid composition and fatty acid saturation levels are often the mechanisms utilized by plants to adjust their cellular membranes to maintain stability and functions (Welti et al., 2007). These changes suggested the potential mechanisms for plant acclimation or adaptation to stress-induced changes, and these were made possible through detailed, quantitative lipid profiling elucidating lipid modifications in structure and components (Welti et al., 2007).

One of the prime targets of high-temperature stress was proposed to be plant cellular membranes. For example, as the host to the photosynthetic apparatuses, the chloroplast membranes are thought to be highly susceptible to heat stress-induced damage (Berry & Bjorkman, 1980; Quinn, 1988). As a major constituent of membranes, the composition of

glycerolipids is adjusted to maintain the integrity and optimal fluidity of the membranes (Zheng et al., 2011). High temperatures also cause a reduction in the degree of unsaturation of fatty acids, as was shown by Falcone et al. (2004) in the study of *Arabidopsis* at 36°C, where there was a decrease of 39% on the double bond index (DBI) from 17°C. Murakami et al. (2000) also found that a decrease in this unsaturation enhances thermotolerance in tobacco. Moreover, they discovered that galactolipids harbored more trienoic fatty acids than other membrane phospholipids, making them major contributors to membrane unsaturation. The desaturation of lipids is mediated by a series of desaturases located in the endoplasmic reticulum and chloroplasts, which have similar catalytic sequences within their active sites (Buchanan et al., 2002). This process usually starts with 16:0 and 18:0 fatty acids (Wallis & Browse, 2002). Desaturation and its reverse process involve oxidation-reduction and consume energy and additional resources, though, to date, little is known of the reverse enzymatic mechanisms (Harwood & Harwood, 1998).

Membrane lipids also serve as substrates for the production of several signaling lipids such as phosphatidic acid, phosphoinositide, sphingolipids, lysophospholipids, oxylipins, N-acyl ethanolamines, free fatty acids, and others (Wang, 2004). Essentially, the formation of lipid-signaling molecules marks the onset of the signaling cascades from stress perception to adaptive metabolism; subsequently affecting the localization, conformation, and activities of intracellular proteins and metabolites. According to Hou et al. (2016), any stress stimuli can rapidly activate the enzymatic production and metabolism of the signaling molecules due to their tight regulation. Specifically, temperature stress can trigger lipid-dependent signaling cascades that control the expression of gene clusters to activate adaptation mechanisms in plants. Because of their roles as intermediates of signal transduction pathways, the signaling roles of lipids are gaining interest (Hou et al., 2016). Some lipid-signaling responses found under high temperatures include: the activation of PLD leading to increased PA levels in tobacco BY-2 cells, *Arabidopsis*, and rice seedlings (Mishkind et al., 2009); activation of phosphatidylinositol phosphate kinase (PIP2K) that initiate the accumulation of phosphatidylinositol 4,5-bisphosphate (PtdIns(4,5)P₂) (Mishkind et al., 2009); and activation of PLC/DGK pathways upon heat stress accompanied by a depletion of PIs (Gao et al., 2014). The fluidity of the plasma membrane is also increased by heat stress, which induces the Ca²⁺ influx into the cytoplasm, leading to the phosphorylation of heat shock transcription factors and expression of downstream genes (Balogh et al., 2013). Furthermore, LCB phosphates also contribute to heat stress tolerance by promoting the survival of *Arabidopsis* cells under heat stress, thus, being considered the regulators of thermotolerance (Alden et al., 2011).

Although many microorganisms have been investigated that impart thermotolerance to plants, little is known about the consequence of their interactions on the lipid profile and composition, though microbial growth-promotion effects have been well-documented. Only a few studies have reported beneficial microorganisms being utilized for addressing heat stress in plants.

1.6. Approaches in plasma membrane lipid visualization and advances in MS-based plant lipidomics

Although plant root-microbe interaction studies have come a long way, there is still a wide area of research that will likely be the subject of many future studies. In particular, there is the investigation of lipids in microbial exudates, including signaling molecules, as well as the biochemical changes undergone by plants throughout the interaction process. Recent advances in analytical technologies have enabled the visualization of lipids, through the localization of their spatial distribution in the plasma membrane, as well as the quantification and characterization of their diverse nature, which shows specificity in identity and function in different cellular organelle membranes (Cassim et al., 2019). Moreover, comprehensive profiling, identification, and quantification of lipids in plant tissues are now possible because of lipidomics' enabling technology – mass spectrometry.

1.6.1. Visualizing lipids in the plasma membrane

Early visualization of the plasma membrane was done by obtaining highly purified right side out (RSO) plasma membrane vesicles using a two-phase aqueous polymer partition system from various plants, with enzymatic reactions or western blotting for addressing contaminants and purity of the plasma membrane fractions (Larsson et al., 1994). For *in vivo* visualization of lipids, strategies have been developed using biosensors, which show affinity for lipids, and lipidomics imaging, although the resolution is not yet high enough to allow characterization of lipids inside a given membrane (Woodfield et al., 2017). A study by Ellis et al. (2018) reported a lipidome-per-pixel approach that identified hundreds of lipid molecular species and their spatial locations using tandem mass spectrometry in parallel with high-resolution mass spectrometry imaging (MSI). The use of labeled lipids in nano-secondary ion mass spectrometry (nano-SIMS) has also allowed the deciphering of lipid segregation in the plasma membrane. Although these high-resolution methods are promising in plant lipid studies, access

to the plasma membrane can be impaired by the plant's cell wall (Cassim et al., 2019). The transbilayer distribution and asymmetry of lipids in the plasma membrane have also been a source of interest and have led to the development of several methods including biochemical, histochemical, and freeze-fractured replica immunoelectron microscopy techniques (Murate & Kobayashi, 2016). In parallel with visualization studies of lipids, the development of high-throughput lipidomic methods made way for the comprehensive characterization of the molecular species of lipids present in the plant plasma membrane – giving such levels of details as the fatty acid positions for GL, LCB for sphingolipids, and the many phytosterols (Samarakoon et al., 2012; Yu et al., 2018).

1.6.2. Lipidomics: The science of the lipidome

Lipidomics refers to the science that analyses the complete set of lipid species in a cell, tissue, or biological system (called the lipidome) through the application of analytical chemistry principles and techniques (Fahy et al., 2011). In general, lipidomics aims to characterize the structures of lipid species, quantify the level of individual lipid species in biological samples, and determine the interactions of individual lipid species with other lipids, metabolites, and proteins *in vivo* (Wang et al., 2019). There are two principal approaches in lipidomics: targeted which focuses on a limited number of defined lipids to accurately determine their absolute abundances, and non-targeted which screens lipid species without preselection within a biological sample, resulting in a high number of unknown mass signals for comparative studies (Lee & Yokomizo, 2018; Wu et al., 2020). Non-targeted lipidomics approaches require chemometric methods to reveal relevant signals and subsequent database searches; however, it is restricted by the data processing and data interpretation complexity as well as the availability of comprehensive databases for identification (Cajka & Fiehn, 2016).

Lipidomics is made possible because of the *state-of-the-art* analytical technologies available for the study of either individual lipids or the lipidome. Each technology has its advantages and limitations, and familiarity with these is essential in choosing the appropriate technique to answer specific lipid-related questions. Developments in lipidomics have been largely driven by the rapid advancements in technologies such as chromatography, nuclear magnetic resonance (NMR) spectroscopy, and mass spectrometry (Correia et al., 2018). Among these, MS has by far been the most dominant analytical platform and widely used technique because of its excellent qualitative and quantitative capabilities (Cajka & Fiehn, 2016).

1.6.3. Mass spectrometry (MS)-based lipidomics

Mass spectrometry (MS) is a powerful technique used to quantify known and identify unknown chemical and biological compounds, including the products of chemical synthesis or degradation, biological molecules such as proteins, nucleic acids, lipids, or natural large- or small molecular weight compounds, by elucidating their structure and chemical properties (Prados-Rosales et al., 2019). In lipidomics, continuous advancements and technical refinements in mass spectrometry, which significantly improved its sensitivity and throughput, have been customized for the detection of mass signals of known lipids and identification of unknown lipids (Poole, 2018). A typical MS-based lipidomic workflow consists of biological sample collection or harvest, lipid extraction and sample pre-treatment, MS-data acquisition, and data processing and biological interpretation (Wu et al., 2020) (Fig. 1.6.3.). Given the complexity of the structure and diversity of lipid molecules, there is still room for improvement – from sample preparation to data processing (Cajka & Fiehn, 2016).

1.6.3.1. Sample preparation

Plants can be grown in various media, e.g. soil, liquid, agar, or vermiculite; therefore, harvested tissues are first washed rapidly in iced-cold water to remove potential contaminants or residues that can affect the mass spectrometry analysis. The critical consideration for the harvest is that the lipidome profile of the tissues is preserved throughout the sample handling process. Lipids are susceptible to degradation, including oxidation, peroxidation, and hydrolysis, although this can be prevented by various physical and chemical strategies (Rustam & Reid, 2018). Although most lipid species are stable at room temperature, plant tissue samples (including their extracts) are immediately quenched or snap frozen with liquid nitrogen (at -80 C) to inhibit any lipid metabolic and enzymatic activity before the extraction process (Rupasinghe & Roessner, 2018). Plant tissues contain a substantial amount of lipid catabolic enzymes such as lipases, lipoxygenases, and acyltransferases, which can enhance the decomposition of lipid species leading to a significant decrease in phospholipid content and increase in oxylipin and acyl-MGDG content (Nilsson et al., 2015) when samples are allowed to thaw. To minimize potential degradation induced by reactive oxygen species, one strategy is the addition of antioxidants such as butylated hydroxytoluene (BHT) at low concentrations of 0.1 to 0.01% into all solvents used in the extraction process (Pizarro et al., 2016).

1.6.3.2. Homogenization

In general, sampling or harvesting plants is rather laborious (as compared to biofluids) because of the additional homogenization step for tissues or cells before lipid extraction. Rupasinghe and Roessner (2018) stipulated that the homogenization processes are operated under low temperatures (as low as -18 °C) because the force generated by the beads in cryo-mills or mortar and pestles results in heat generation, which can release acyl fatty acids leaving lyso-lipid species. However, the lipid extraction solvent of the frozen homogenized samples is carried out at room temperature, due to the lipids' poor cold temperature solubility.

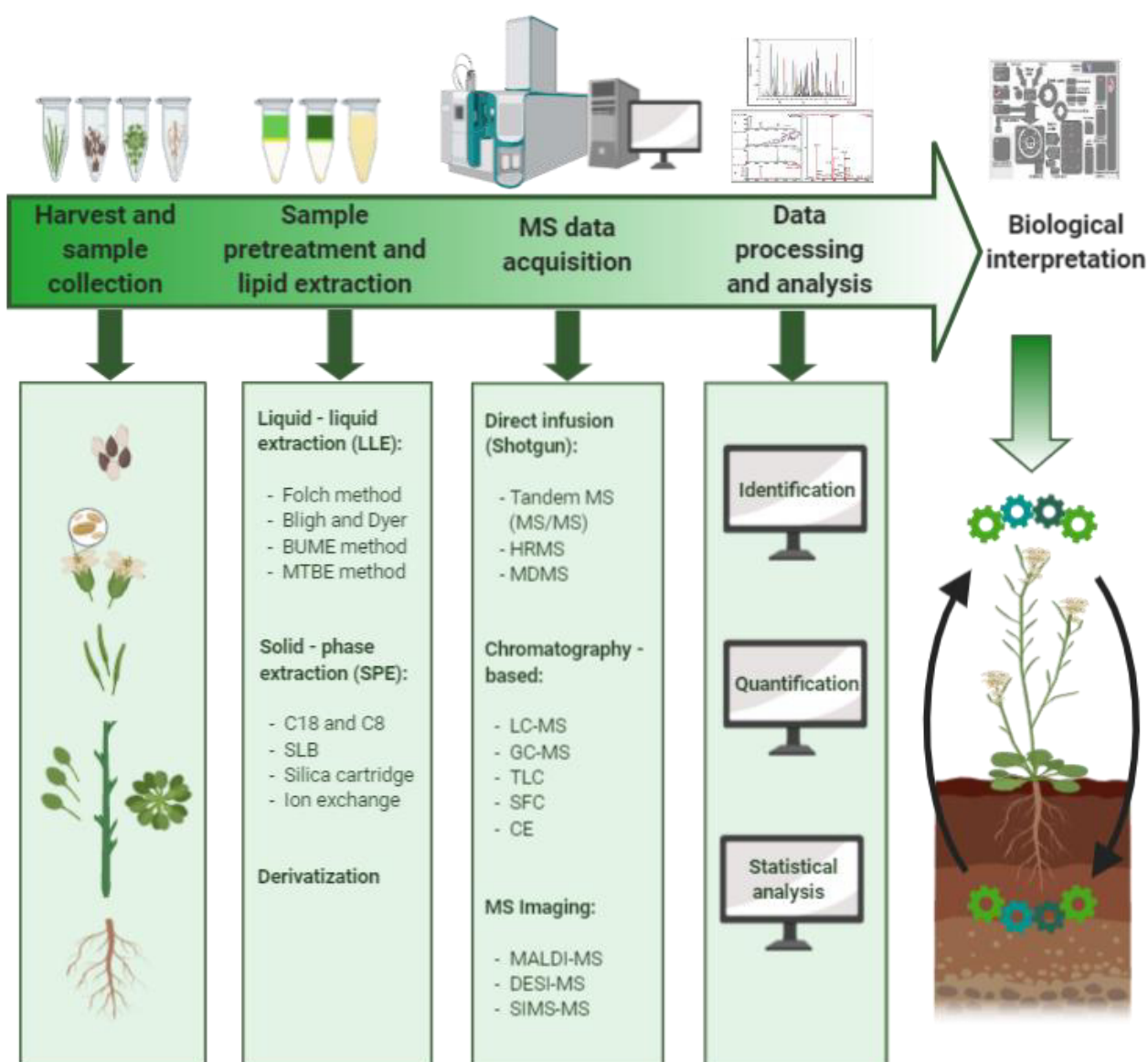


Figure 1. 16 MS-based plant lipidomics workflow. A typical lipidomics workflow for analysing plant lipids consists of harvesting different plant tissues (e.g. roots, stems, leaves, florets, siliques,

seeds). Depending on the biological sample and analytical techniques to be employed, sample pre-treatment and lipid extraction is performed. In general, these methods can be categorized as liquid-liquid extraction (LLE) – most predominant lipid extraction method with the strongest applicability, solid-phase extraction (SPE) – utilizes a stationary phase that selectively retains specific molecular classes with similar properties, and those which require chemical derivation to improve detection sensitivity, selectivity, chromatographic performance, and separation efficiency. Data from biological samples are then generated using mass spectrometry (MS) that is hyphenated with analytical techniques broadly grouped into direct infusion (shotgun lipidomics), chromatography-based acquisition, and MS imaging. Acquired data are then processed and subjected to qualitative and quantitative analysis, lipid identification, and performing bioinformatics and statistical analysis. As lipidomics produces a large amount of data, proper calculation tools, databases, and algorithms for efficient mining of data are utilized to understand the biological significance of the data set. (BUME- butanol methanol, MTBE- methyl-tert-butyl ether, HRMS- high-resolution MS, MDMS- multi-dimensional MS, LC-MS- liquid chromatography MS, GC-MS- gas chromatography MS, TLC- thin-layer chromatography, SFC- supercritical fluid chromatography, CE- Capillary electrophoresis, MALDI-MS- matrix-assisted laser desorption/ionization MS, DESI-MS- desorption electrospray ionization MS, SIMS-MS- secondary ion mass spectrometry MS).

1.6.3.3. Addition of standards

The sample preparation stage also involves the addition of quality control samples and internal standards. Quality control samples, which can be classified into either pooled or reference standards, maintain the reliability, stability, and reproducibility of the analytical data within a large-scale lipidomic study; whereas, internal standards, which are isotopically labeled or structured analogs, are used to achieve sample consistency and standard signal responses (Wang et al., 2017). Due to the various factors that can influence the “relative”, “semiquantitative”, and “absolute” quantification of lipids from different experimental workflows, Wang et al. (2017) has provided a defined set of guidelines for the use and selection of internal standards. Generally, two or more internal standards are required for relatively accurate (+10%) absolute quantification of lipid species within a given class or subclass, with their exact concentration empirically determined for each sample (Rustam & Reid, 2018).

1.6.3.4. Lipid extraction

Analysis of lipid compounds from various biological samples begins with the extraction of lipids, which are mostly embedded in complex matrices, using various methods catering to either niche or broad-spectrum applications, to ensure the success of subsequent analyses. According to Hu and Zhang (2018), the most commonly used extraction methods in lipidomics include **liquid-liquid extraction (LLE)** and **solid-phase extraction (SPE)**, with LLE as the

most predominant method having the strongest applicability to all kinds of biological samples. This method makes use of two immiscible organic solvents to achieve lipid separation from the more polar matrix. The first and considered “gold” standard of LLE extraction was based on Folch extraction which utilized chloroform-methanol-water to extract full-lipid compounds (Folch et al., 1957). This method, however, was developed for animal lipid extractions, thus, may not be as effective for extracting plant lipids (Bowen-Forbes & Goldson-Barnaby, 2017). Over the years, several methods have been adapted from the Folch protocol: the Bligh-Dyer method which uses a monophasic extraction before a biphasic system (Bligh & Dyer, 1959), the BUME (butanol-methanol) method which shortens the extraction time by half by using only one round of extraction (Löfgren et al., 2012), and the MTBE (methyl tert-butyl ether) method which is a simplified extraction with high recovery rate because of the lipid-containing organic phase sitting at the top of the mixture (Matyash et al., 2008). Other modified protocols also branched out from these methods, e.g. those conducted by Welti et al. (2007), Shiva et al. (2018), and Burgos et al. (2011), although the extraction efficiency and reproducibility still need to be tested on various plant tissues. A recent study by Kehelpannala et al. (2020) comparing several established extraction methods using different Arabidopsis plant tissues has found the most efficient and least laborious method, utilizing a single-step extraction within 24 hours using chloroform-isopropanol-methanol-water mixture. Scientists have also explored the use of SPE, which utilizes a stationary phase that selectively retains specific classes of molecules with similar properties. This method is mainly used to enrich signaling lipid molecules that are less physiologically abundant such as eicosanoid, steroid hormones, and fatty acid esters of hydroxy fatty acids (FAHFAs) (López-Bascón et al., 2016). Others also looked into automation and other technologies such as microwave-assisted extraction and supercritical fluid extraction. In the end, the traditional liquid-liquid extraction is still used, especially for quantitative lipidomics, because of its extraction efficiency for most lipid compounds (Wang et al., 2019).

1.6.3.5. Mass-spectrometry-based analysis

MS-based analysis of some lipid species (e.g. FAs, eicosanoids, steroids, and fatty aldehydes) can be quite challenging due to their specific lipid properties: poor MS ionization efficiency, low endogenous abundances, chemical instability, poor chromatography performance, and susceptibility to interference from matrix components. Chemical derivatization solved these challenges, by enhancing detection sensitivity, selectivity,

chromatographic performance, and separation efficiency (Zhao et al., 2014). MS is usually used in combination with other techniques in what is so-called hyphenated bioanalytical methods (Shulaev & Chapman, 2017). Three of the most dominant combinations are that of MS coupled with 1) prior chromatographic separation such as thin-layer chromatography (TLC), gas chromatography (GC), and liquid chromatography (LC); 2) direct infusion or shotgun MS such as tandem MS (MS/MS), high-resolution MS (HRMS), and multi-dimensional MS (MDMS); and 3) mass spectrometry imaging (MSI), e.g. matrix-assisted laser desorption/ionization (MALDI), desorption electrospray ionization (DESI), and secondary ion MS (SIMS) (Wang et al., 2019). **GC-MS** has been used to analyze simple lipids such as FAs and sterols, both requiring a chemical derivatization pre-treatment for esterification or silylation (Zhao et al., 2014). **LC-MS** is well suited for analyzing heat-labile metabolites and complex lipid classes like glycerolipids, glycerophospholipids, and glycolipids (Okazaki & Saito, 2018). Because of its excellent separation efficiency, high sensitivity, and strong specificity, LC-MS has become the most mainstream and widely used method (Wang et al., 2017).

For targeted lipidomics, the traditional approach used is multiple reaction monitoring (MRM) on a triple quadrupole (QQQ) or quadrupole linear-ion trap (QTRAP) that is coupled to high-performance liquid chromatography (HPLC) or ultra-high performance liquid chromatography (UHPLC). For untargeted lipidomics, the common techniques employed are high-resolution mass spectrometry (HRMS) using time-of-flight (TOF), Fourier-transform ion cyclotron resonance (FT-ICR), or Orbitrap platforms, that utilize high resolution and high mass accuracy to resolve isobaric lipid species having similar nominal mass but different exact masses (Cajka & Fiehn, 2016; Yu et al., 2018). A recent acquisition strategy, parallel reaction monitoring (PRM) has been developed to integrate targeted and untargeted data by combining HPLC with quadrupole-equipped HRMS (Yu et al., 2018).

1.6.3.6. Data curation

Lipidomics studies generate large amounts of data that have to be annotated and analyzed using biostatistical methods. The processing of raw data files represents a crucial step in the overall workflow. The complexity of raw data, limited spectral and reference biochemical databases, and incomplete knowledge of plant lipid metabolism and its regulation, pose significant challenges in the analysis of global lipidomics profiling data (Hartler et al., 2013). While direct infusion MS data pre-processing is greatly simplified because there is no need for peak finding

and feature alignments, LC-MS data processing pipelines follow several stages such as filtering, feature detection, peak alignment, and (if needed) data normalization. Final data output show information on extracted m/z values, retention times, and corresponding intensity for all detected peaks (Cajka & Fiehn, 2016).

Many commercial and open-source software automatizing data analyses have been made available for both lipid identification and quantification. Some of the available commercial software are *LipidSearch* (ThermoFisher), *LipidView* (SCIEX), *Lipidizer* Platform (SCIEX), *SimLipid* (PREMIER Biosoft); including vendor-proprietary software. *GeneData* is an example of software from independent developers. Many open-source software were also developed including *XCMS*, *MZmine 2*, *MS-DIAL*, *MetAlign*, *IDEOM Lipid Profiler*, *LipidInspector*, *LipidQA*, *LIMSA*, *Fatty Acid Analysis Tool* (FAAT), *Analysis of Lipid Experiments* (ALEX), and *LipID* (Shulaev & Chapman, 2017; Theodoridis et al., 2012). LIPID MAPS is an open-source general lipid database that provides critical chemical information of diverse lipids for compound annotation – necessary components for lipidomics analysis (Sud et al., 2007).

With the continuous and rapid advances in analytical techniques, lipidomics is now faced with fewer obstacles due to analytical methods. Optimization of these methods now enables the visualization, profiling, and quantification of a large number of lipids, although there are still challenges such as sensitivity for low-abundance lipids from small sample sizes. There is also the challenge of integrating lipidomics with other “omics” technologies – exploring the whole lipid metabolic pathways while elucidating their effects on the gene and protein levels (Hu & Zhang, 2018). With a huge room for improvements in analytical techniques, much can still be done on plant lipid research, which can further our understanding of plant metabolism and its interaction with the biotic environment.

1.7. Conclusion

Within the complex underground ecosystem of soil and plants, the rhizomicrobiome can play significant roles in the dynamics of plant growth promotion and stress tolerance activities. Proper and comprehensive knowledge of such organisms and their plant stimulatory mechanisms may help to cope with the fluctuations in the climate and environment, being experienced and yet to be experienced in the future. With the threat of increasing temperatures, the advent of the widening horizons of knowledge on rhizospheric microorganisms may come

as a boon from nature toward maintaining a sustainable agricultural system, while buffering the adverse effects of changing climate scenarios (Maitra et al., 2021).

It has already been established that complex underground interactions occur between plant roots and soil microorganisms. Plants actively shape the microbiome inhabiting the rhizosphere and the subsequent colonization of their root tissues. We now know that complex plant root-microbe interactions are governed by three stages: plant root-to-microbe, microbe-to-microbe, and microbe-to-plant root interfaces. On all accounts of these interactions, lipids have been found to play essential roles, whether as the “chemical language” that facilitates the exchange of resources or as signaling molecules that modulate the cell responses against pathogen attack and enhance microbial symbiosis. Although a considerable number of lipids are already known, annotated, and associated with physiological and biochemical roles, there are still many more unknown lipids with corresponding novel functions likely to exist, which may play pivotal roles in determining or shaping the rhizomicrobiome. Further information on naturally-occurring lipids and their diverse roles or responses to various stimuli will be elucidated by recent advances in analytical techniques, particularly in liquid and gas chromatography coupled with the powerful mass spectrometry.

This large-scale analysis of lipids can then be combined with the other omics studies, i.e., genomics, transcriptomics, and proteomics, to begin to uncover the genes involved in the fundamental processes of plants and microbes and during the various stages of their interactions. The integration of the combined omics studies will be useful in the holistic interpretation of biological systems such as plants, and how they respond to biotic and abiotic environmental stimuli.

As part of the rhizospheric signaling and interaction studies between plants and beneficial microorganisms, research on lipids can therefore open new avenues to increase crop productivity and tolerance to environmental stresses such as heat stress.

1.8. Significance of the Study

As with the continuous contention on climate change, many people from different backgrounds and levels still discount the already growing impacts of the unprecedented rise of global atmospheric temperatures. Moreover, although there has been a considerable number of studies on the impacts of high temperatures, in small (e.g. growth chamber and greenhouse experiments) and large-scale quantities (e.g. field trials), this number lag behind studies on

other environmental stressors such as drought, salinity, and metal toxicity. As was shown in this chapter, temperature affects all organisms with varying degrees of intensity, from microbes to plants, whether underground or aboveground, and depending on their ontology. It is therefore timely and crucial to look at the interconnectivity among the components of the ecosystem. Importantly, it is necessary to understand how increasing temperatures can influence the biotic interactions between plants and microorganisms, which have long co-existed in various forms of symbiosis.

Many heat stress agronomical studies involved conventional breeding and genetic engineering to identify significant genes to manipulate and ultimately develop more tolerant and resistant crops. However, these studies can be laborious, consequently expensive, and can also take some time; not to mention that genetic modification of crops is still an unacceptable concept in many areas due to sustainability concerns. The proposed strategy of harnessing the use of beneficial microbes like PGPR may be an alternative approach to increase plant performance and productivity while mitigating the damaging effects of heat stress. At the moment, much is already known about plants and microorganisms, *per se*; however, little is still known about the complexities of their interactions, even more so, when subjected to high temperatures. Multitudes of studies have characterized their molecular and genetic components, but not much has been investigated on the biochemical nature of their interactions. Lipids, which are diverse organic compounds that play essential roles and key biological functions in cellular functions and homeostasis, also perform crucial roles during the communication, resource exchange, and metabolic processes of the two interacting organisms. Lipid profiles are also directly linked to the plant's phenotype, which can physically indicate plant responses to any external stimuli, such as the application of microorganisms and increase in temperatures.

This study will first investigate the dynamics of growth promotion imparted by the beneficial microbe through plant morphological responses. The observed phenotypes will then be linked to the lipid profile, to evaluate the various lipid components and lipid-based signaling molecules that are integral participants during plant root-microbe interactions. Moreover, this study is timely and relevant in that it will look at plant-microbe interactions under warming conditions that are projected in the near future. The information generated from this study will be valuable for developing novel strategies to manipulate microbes and/or plants, as well as the rhizosphere interface. Microbial-related solutions can then be used for more sustainable agriculture, e.g., reduced usage of agrochemicals, to enrich the rhizomicrobiome for beneficial

microbes, thereby improving plant performance and resistance to both biotic and abiotic stresses.

1.9. Objectives of the study and biological samples used

The overarching aim of this study was to investigate the dynamics of microbe-imparted growth promotion in plants under high-temperature conditions and link this to the plant lipid profile, to understand how lipid components are affected during plant-microbe interactions and how beneficial microbes can reduce the impact of high-temperature stress.

We hypothesized that i) beneficial soil microbes will induce growth stimulatory effects on plants, that ii) the root lipids will be influenced by the plant root-microbe interactions; and that iii) inoculation of the microbe will ameliorate the negative effects of high temperature or heat stress on the plant-microbe components and their associated lipid profiles.

Specific objectives of the study were to:

1. Develop an optimized system for co-cultivation of plants and microbes that is conducive to periodic imaging and non-invasive plant phenotyping.
2. Characterize and quantify the dynamics of microbe-imparted growth promotion in plants under ambient and high-temperature conditions through measurement of root and shoot morphological responses.
3. Generate lipidomic profiles of both control and inoculated plant roots to identify lipids associated with improved plant growth under control conditions.
4. Compare the lipidomic profiles of control and inoculated plant roots under different temperature conditions to determine how high temperature influences plant root-microbe interactions.
5. Determine the role of lipid-based signaling molecules during key plant-microbe interactions under ambient and high temperature conditions.

1.9.1. Biological samples

To address the given objectives and test the hypothesis of this study, the interaction of specific biological samples was investigated. For plants, we utilized *Arabidopsis*; while for the beneficial soil microbe, we chose the *Paraburkholderia phytofirmans* PsJN, and this was because of their unique characteristics suitable for this research.

1.9.1.1. *Arabidopsis thaliana* Col-0

Arabidopsis thaliana, which belongs to the Cruciferae (family Brassicaceae, Capparales) and is also known as Thale cress, is a widely utilized dicotyledonous plant species (Mitchell-Olds, 2001). Although not a crop, it is considered a model plant because of its many advantages for basic research in the fields of genetics, molecular biology, and genomics. *Arabidopsis* has a “tap root” system which includes a single main primary root that produces branching roots in successive orders (Chochois et al., 2012). The complete sequencing of the *Arabidopsis* genome led to the investigation of several specific gene functions, elucidating diverse information about the growth and development, physiology, and biochemistry of higher plants (Boyes et al., 2001; Hetu et al., 2005; Meinke et al., 1998). There are several characteristics of this plant that make it convenient for plant science studies (<https://www.arabidopsis.org/portals/education/aboutarabidopsis.jsp>). For example, it has a fully sequenced small genome (125 Mb total) from hundreds of ecotypes, with extensive genetic and physical maps of all five chromosomes. It also has a rapid and short life cycle of six to eight weeks from germination to seed set, with prolific seed production (Boyes et al., 2001). It has a small size of 20-25 cm in height and is a self-pollinator that can also be genetically cross-pollinated (Meinke et al., 1998). *Arabidopsis* is also known for its easy cultivation and transformation, with the availability of many mutant lines and genomic resources, as well as access to and availability of a multinational research community. This plant can also be grown on almost any growth media including soil, agar, and hydroponics, making it well-suited for laboratory growth settings (Meinke et al., 1998).

Arabidopsis is also an oilseed plant with triacylglycerols as its major storage oil found in seed (Hsiao et al., 2014), making it suitable for lipid studies. This makes *Arabidopsis* an important plant subject not just for studies on storage oil production that is of interest to the industry, but also for studies on seed oil metabolism for the improvement of composition, yield, and nutritional value of vegetable oils (Napier et al., 2014). Moreover, *Arabidopsis* also has a sequenced microbiome. According to Bulgarelli et al. (2013), the most prominent bacterial phyla and endophyte bacterial assemblages in the *Arabidopsis* root rhizosphere are the *Acidobacteria*, *Actinobacteria*, *Bacteroidetes*, and *Proteobacteria*. From its root endosphere, the common phyla found are *Acidobacteria*, *Firmicutes*, *Bacteroidetes*, and *Proteobacteria*.

1.9.1.2. Paraburkholderia phytofirmans PsJN

Paraburkholderia is a new genus delineated from *Burkholderia* through phylogenetic analysis, as comprised of environment-friendly species demonstrating biocontrol and bioremediation processes (Esmael et al., 2018; Sawana et al., 2014). *Paraburkholderia phytofirmans* PsJN is a Gram-negative, rod-shaped, non-sporulating, and motile bacterium which was first isolated from surface-sterilized onion roots infected with the mycorrhizal fungus *Glomus vesiculiferum* (Sawana et al., 2014). It is a well-studied model and plant growth-promoting endophyte that is known to induce tolerance to environmental stresses. This bacterium has been used in different plant studies against drought, low and high temperature, and salinity (Ait Barka et al., 2006; Bensalim et al., 1998; Nafees et al., 2018; Naveed et al., 2014). This bacterial strain has also been successfully grown and studied on a range of plant species, as compiled by Esmael et al. (2018), including wheat (Naveed et al., 2014), maize (Naveed et al., 2015), brassica (Nafees et al., 2018), grapevine (Compant et al., 2005), switchgrass (Wang et al., 2015), *Arabidopsis* (Poupin et al., 2013), tomato (Pillay & Nowak, 1997), watermelon and cantaloupe (Liu et al., 1993), potato (Bensalim et al., 1998), cucumber and sweet pepper (Nowak et al., 2002).

P. phytofirmans PsJN's beneficial effects on plants are attributed to several mechanisms. This includes the following: modulation of plant phytohormones (Pieterse et al., 2012) such as indole-3-acetic acid (IAA) that is involved in the efficient colonization of *Arabidopsis* roots and improvement of different plant parameters (plant height, biomass, photosynthesis, and chlorophyll content) (Zúñiga et al., 2013), production of 1-aminocyclopropane-1-carboxylate deaminase (ACC) associated with lowering the ethylene level in plants (Glick et al., 1998), facilitation of resource acquisition (Naveed et al., 2014), production of siderophores and secondary metabolites (Esmael et al., 2018), and induction of systemic resistance (ISR) (Miotto-Vilanova et al., 2016), leading to more adaptability to different biotic and abiotic stress conditions (Pieterse et al., 2014). Perception and recruitment of this bacteria are highly influenced by root exudation (Kost et al., 2014) and microbial quorum sensing molecules presented by acylated homoserine lactones (AHLs), which are implicated in early communication with the host plant (Zúñiga et al., 2013). Successful attachment and colonization of the root surface and tissues by *P. phytofirmans* PsJN is attributed to its production of cellulose or exopolysaccharides (EPS) and biofilm formation (Kandel et al., 2017).

1.9.2. Chapter synopsis (with COVID-19 impacts)

Chapter 2 of the thesis was conducted to achieve the first objective to develop a working system where both *Arabidopsis* and the bacterial strain *Paraburkholderia phytofirmans* PsJN can be cultivated together in a sterile environment. The growing protocols for both the plant and the bacteria came from the combined adaptation of previous related investigations and conducted pilot experiments in the present study. Specifically, this chapter aims to optimize the methods by which both biological samples can grow simultaneously while monitoring development throughout the growth period up to the maximum space capacity. Concurrent with the above objective was the adaptation of the growth system to an appropriate phenotyping platform for periodic non-invasive imaging and measurements. This chapter also elucidates the challenges of the conventional growth system for plant-microbe interaction studies, and how the optimized protocols of the phenotyping platform addressed the issues of imaging, tissue harvest, and root trait analysis.

More specifically, described in this chapter are the different adaptations of the established plant cultivation system based on the available phenotyping platform and associated resources within the two research groups (University of Melbourne and Forschungszentrum Juelich). Three rounds of experimentation were conducted. The pilot experiments, which utilized the conventional “closed-plate system”, were performed at the University of Melbourne. The results of these experiments served as the basis for the establishment of the protocols at the Forschungszentrum Juelich, where the new “open-top system” was trialled. However, this part of the research was unfortunately impacted by COVID-19, and therefore, not completed. As a result, the third round of experimentation was conducted at the University of Melbourne, which was adapted from both the “closed-plate” and the “open-top” growth protocols, leading to project re-structure.

Chapter 3 of the thesis talks mainly about the outcome of the experimentation at the Forschungszentrum Juelich and the utilization of the *state-of-the-art* GrowScreen-Agar II phenotyping platform. This chapter addressed the second objective, but more specifically it aimed to verify the i) repeatability of the results of the pilot experiments at a larger scale, ii) transfer and adapt the protocols from the conventional growth system to the new phenotyping platform, and finally, ii) quantify the growth promotion imparted by the bacteria to the *Arabidopsis* plants under both ambient and high-temperature conditions, by characterizing the root and shoot morphological traits. The outcome of experiments described in this chapter

served as the basis for the lipidomics experiments (**Chapter 4**), where the phenotype and morphological responses of plants were then linked to their lipid profiles. This chapter was published in the journal *Plants* (Macabuhay, A., Arsova, B., Watt, M., Nagel, K. A., Lenz, H., Putz, A., Adels, S., Müller-Linow, M., Kelm, J., Johnson, A. A. T., Walker, R., Schaaf, G., & Roessner, U. (2022). Plant Growth Promotion and Heat Stress Amelioration in *Arabidopsis* Inoculated with *Paraburkholderia phytofirmans* PsJN Rhizobacteria Quantified with the GrowScreen-Agar II Phenotyping Platform. *Plants*, 11(21), 2927. <https://doi.org/https://doi.org/10.3390/plants11212927>).

As this chapter was COVID-19 impacted, the planned final experiments at the Institute that were designed for tissue harvest (to be sent to Melbourne for lipid analysis) were, instead, implemented back at the University of Melbourne, as covered in the succeeding chapter. COVID-19 impacts included the Australian border closing, thus, the urgent return to Melbourne, and the partially completed experiments in Germany. Back at the University of Melbourne, analysis of the data generated from these experiments was done remotely and subjected to some IT and computational challenges due to long pandemic-imposed lockdowns.

Chapter 4 describes the lipidomics workflow and technology utilized to address the last three objectives of the thesis, which mainly aimed to generate and characterize the lipidomic profiles of *Arabidopsis* roots subjected to both biotic (bacteria) and abiotic (high temperature) factors. Here, the lipid profiles of control and inoculated plant roots are compared and further associated with their corresponding heat stress profiles. To realize these objectives, illustrated here are the methods employed in the mass-spectrometry (MS)-based lipidomics analysis of plant root tissues; from optimized tissue harvest, sample preparation, and lipid extraction; to performing LC-MS-based sample analysis. The untargeted approach to perform discovery lipidomics and identify all known and novel lipid species involved during the plant root-microbe-heat stress interactions was used. Finally, this chapter also described the data curation, annotation, and analysis done via the MS-Dial software to identify all possible lipid species, within specified limitations and suggestions for future studies, as this experiment and analysis were impacted by the pandemic.

One of the challenges to the experimentation for this chapter during COVID-19 was the lack of the phenotyping platform that was used in Germany. This platform has its associated growth protocols and materials (e.g. customized racks and magazines). Back at the University of Melbourne, there was an initial attempt to simulate the “open-top” growth and imaging system of the GrowScreen-Agar II, but this was challenged by COVID-19 impacts such as

lockdowns, closed workshops and facilities, supply chain issues and delivery delays, and very limited access to the University, and more. As a result, a new experimental design was adapted to accommodate and still realize the objectives of this chapter.

Chapter 5 summarizes and integrates all the outcomes of the previous experimental chapters – characterizing and quantifying the dynamics of spatio-temporal, bacteria-imparted growth promotion in *Arabidopsis* and associating the morphological phenotypes to the changes in the lipidome of the plant roots under ambient and high-temperature conditions. This chapter provides reasoning for the proposed ameliorative effects of microbial application on detrimental heat stress effects in plant roots, connecting morphological phenotypes with biochemical phenotypes. And finally, this chapter also suggests future directions for further studies.

CHAPTER 2

Methods development for plant-bacteria co-cultivation and phenotyping with the “closed-plate” and “open-top” growth systems

Preface to Chapter 2

The first objective of my PhD research was to develop an optimized system for the co-cultivation of plants and microbes that is conducive to periodic imaging and non-invasive plant phenotyping. Explained in this chapter is the rationale behind the experimental design, particularly the selection of the type of system most appropriate for the chosen biological samples, *Arabidopsis* plants and bacterial strain *Paraburkholderia phytofirmans* PsJN, given the parametric traits aimed to be characterized. This chapter also discusses the methods used to establish an optimized growth protocol for the plants and bacteria, their co-cultivation, and the time course imaging and phenotyping protocols in a conventional “closed-plate” system, at the University of Melbourne. With the change in the research facility and, therefore, laboratory and technological resources, established plant-bacteria growth protocols were then adapted and optimized to the “open-top” growth system of the new phenotyping platform at the Forschungszentrum Juelich (Germany). Finally, discussed here are also the alternate methods utilized to conduct the experiments under COVID-19 pandemic restrictions back at the University of Melbourne, when the 12-month planned research in Germany was cut short, significantly altering the original research structure.

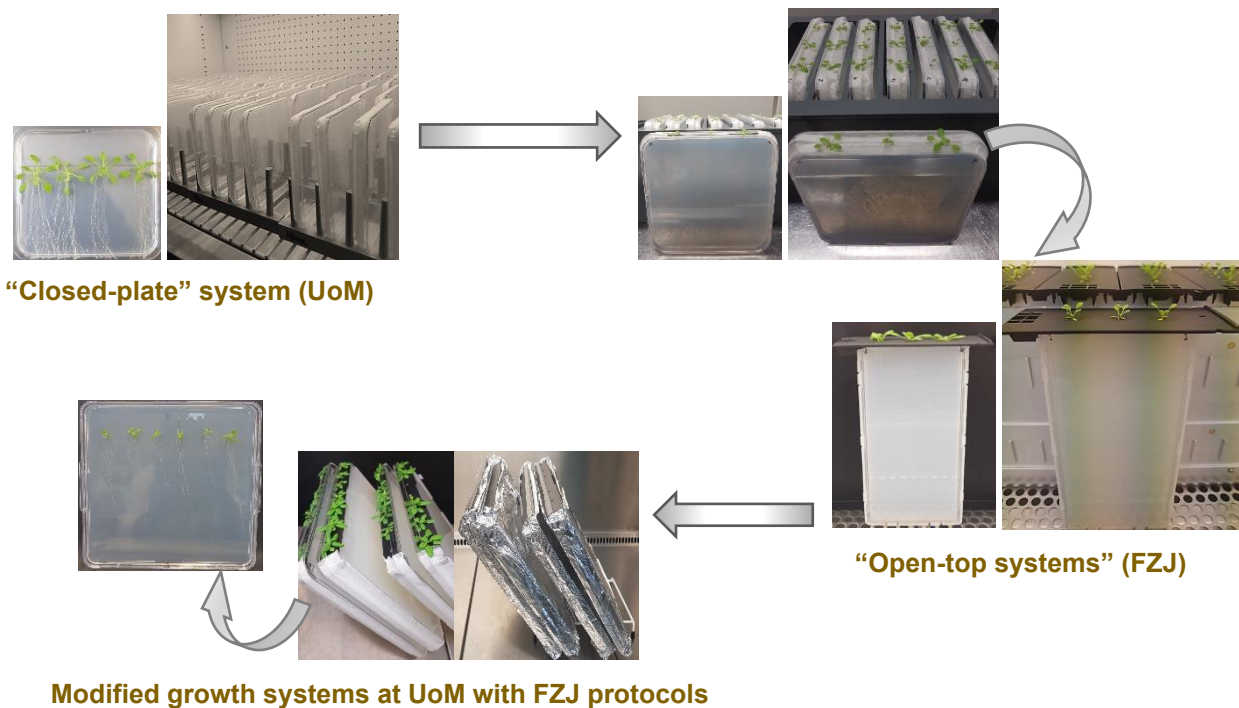


Figure 2. 1 Different growth systems used – “closed-plate” (at UoM), “open-top” (FZJ), and modified growth systems (at UoM), to establish plant-bacteria cultivation protocols

2.1. Introduction

With the increasing global temperatures, beneficial plant root-microbe interactions provide a sustainable biological solution for enhancing crop production while mitigating the adverse effects of heat stress. A significant amount of work has established the importance of rhizosphere microbiota in biogeochemical processes in the soil and plant physiological processes, including plant resistance to diseases and tolerance to abiotic stresses (Hunter, 2016; Van Der Heijden & Hartmann, 2016; Vessey, 2003; Yang et al., 2009). Understanding plant root-microbe interactions in the rhizosphere will likely be the key to enhancing the ecosystem functioning since the root structure serves as the interface for the complex microbial signaling and biochemical exchange (Hartmann et al., 2009; Paterson et al., 2007; Philippot et al., 2013).

Investigations of the mechanisms of plant root-microbe interactions, particularly in field conditions, however, are faced with difficulties due to the unpredictability of the climate and environment, as well as the irreproducibility and complexity of microbiome composition and genetics (Dubey et al., 2016; Gao et al., 2018; Reynolds et al., 2003). Moreover, the examination of the subterranean relationships and their reciprocal responses is challenged by the dynamic nature and complexity of both organisms – hidden, and in the dark. In addition, there is a lack of experimental systems that will facilitate natural root structure development and morphological responses under controlled conditions. There is a need for experimental designs that mimic the naturally-existing plant root-microbe interactions to delineate plant responses to microbial inoculation as well as other external abiotic factors (Nathoo et al., 2017).

A proposed strategy is the construction of a simplified model ecosystem that will allow for controlled, replicated laboratory experiments investigating the complex interactions of plants and microbes, elucidating valuable insights with potential for further testing in the field (Busby et al., 2017; Finkel et al., 2017). This system will utilize the traditional approach, where plants are grown in agar-filled plates or slabs, liquid media, or in soil-filled pots (Nezhad, 2014). Although these artificial growth system approaches will likely remain to be the most widely used, they do not represent natural field conditions. Moreover, these systems do not permit the precise monitoring and manipulation of the growing environment of plants. To address these drawbacks, rhizoboxes and rhizotrons have been developed, designed particularly for the study of below-ground processes (Oburger et al., 2013; Van der Krift & Berendse, 2002). New systems were also built utilizing advanced microfluidic devices for high-throughput analysis, e.g. Plant Chip (Jiang et al., 2014), RootChip (Grossmann et al., 2011), and Root array (Busch et al., 2012). Recently, a new system was also described – a two-layer imaging platform with

microfluidic features, enabling *Arabidopsis* root hair imaging at an early growth stage (Aufrecht et al., 2017).

The effects of high-temperature stress on aerial parts of the plants and their responses are already well documented; however, its corresponding influence on roots has been less explored (Wahid et al., 2007). One way to adapt plants to climate-driven environmental stressors is to take into account and harness their below-ground traits. Roots manifest high plasticity in response to soil and environmental changes, which provide opportunities for manipulation and improvement. To develop better-adapted, climate-smart crops, there is an urgent need for better comprehension of the physiological, morphological, metabolic, and molecular mechanisms governing this plasticity.

Different processes regulate root responses to increasing temperatures. In warmer environments, plants have increased water demand due to water loss by evapotranspiration and decreased water uptake from limited water availability. This leads to an overall water deficit scenario in plants (Heckathorn et al., 2013). High temperatures have been shown to elicit responses through aquaporins, membrane channels that facilitate water transport inside the cell, or by diffusion through the plasma membrane (Maurel et al., 2015). Similar to water, nutrient uptake is also altered by high temperatures, the mechanisms of which are crop-specific (Giri et al., 2017; Tindall et al., 1990). Roots also show mechanisms for temperature sensing, at a molecular and cellular level, that were proposed to be different from the thermomorphogenesis signaling in shoots (Bellstaedt et al., 2019). This temperature sensing can be translated into the activation of several physiological processes indicative of primary temperature-sensing events (Penfield, 2008), that alter membrane and cytoskeleton stability, as well as proteins and nucleic acids (Dai Vu et al., 2019). Under high temperatures, plant hormones that are involved in root development and growth also mediate temperature stress responses in the roots. Notable examples of plant hormones, which trigger signal transduction pathways assisting plants to overcome stress, are salicylic acid, ethylene, abscisic acid, cytokinin, auxin, and gibberellins (Larkindale & Huang, 2004; Lin et al., 2009; Talanova et al., 2003; Vishwakarma et al., 2017). Significant molecular and genetic changes in plants, which include global reprogramming and protein profile changes to adjust plant growth, are also triggered by high temperatures (Bita & Gerats, 2013; Carrera et al., 2018; Jia et al., 2017).

Another mechanism affected by high temperatures in roots is its metabolism, which changes to maintain homeostasis for plant survival, and which is dependent on the sensitivity of key metabolic regulatory enzymes. After experiencing heat stress, main carbohydrates such as glucose, fructose, galactose, sucrose, or xylose, as well as levels of various glycolytic cycle

enzymes are changed (Aidoo et al., 2016; Ribeiro et al., 2014; Sun & Guo, 2016). Within the optimal temperature range, there is an association of the changes in the root:shoot ratio; however, at relatively high temperatures, root development is impaired with alterations of the root system architecture (RSA) and reduction of the root:shoot ratio (Koevoets et al., 2016; Ribeiro et al., 2014). The RSA refers to the organization of the primary, lateral, adventitious, and accessory roots, which is determined by parameters such as length, number, and angle. This feature is crucial in the regulation of water and nutrient uptake because it controls the volume of soil that roots can scavenge at various environmental conditions (Lynch, 1995). In general, some of the prominent morphological responses of roots to supra-optimal temperatures include a decrease in primary root length, number of lateral roots, and angle of emergence; and the initiation of second and third-order lateral roots that are also characterized by larger diameter (Calleja-Cabrera et al., 2020).

The roots' plasticity enables them to adjust to different environmental conditions and display a range of highly variable morphological traits to adapt root architecture and functionality to disadvantageous conditions like high temperatures. According to Atkinson et al. (2019), improvements to the RSA of plant roots promise to deliver higher efficiency in water and nutrient uptake; however, a major bottleneck in this field is profiling the root phenome, i.e., structure and function. Innovations in imaging, sensor, and phenotyping technologies, together with methodological advances in the acquisition, handling, and processing of large datasets are making root phenomic studies possible. Together, these advancements will help drive the selection of the next generation of climate-resilient crops to address global food security under a changing climate (Atkinson et al., 2019).

The majority of phenotyping efforts conducted in the past were focused on shoot traits such as product quality, yield, shoot vigor, and disease resistance, whereas phenotyping of the roots received only meager attention (Kuijken et al., 2015). This situation could be attributed to the technical challenges in accessing the soil when performing non-destructive, phenotyping of root traits. According to Kuijken et al. (2015), the development of the optimal phenotyping platform to quantify the parametric traits of the RSA is often a compromise among a range of platform properties and requirements. Priorities for the design are based on three main processes: plant cultivation, data acquisition, and data processing – which are the essential pipelines of plant phenotyping. Furthermore, for a suitable cultivation system, some desirable considerations are 1) agronomic relevance, 2) the ability to grow plants in several developmental stages, 3) the extent to which experimental noise can be reduced, and 4) the possibility and effort to acquire good quality data. According to Arsova et al. (2019), the current

phenotyping and agronomic robotic technologies open a wider opportunity to discover the dynamic responses of plants to both the biotic and abiotic environment and their improvement and farm utilization.

2.2. Growth protocols and methods optimization

As with any experimental research, the design of the experiment was first considered. The selection of the biological organisms has already been explained and justified in Chapter 1. An important consideration that followed was the type of system that will be most suitable for the following conditions: 1) a sterile environment for the co-cultivation of plants and bacteria, 2) that will allow visible observation of plant development, particularly roots, in a fixed matrix or media, 3) that will be compatible with the available imaging and phenotyping equipment, and 4) that will allow continuous non-invasive measurements of plants.

This research was originally designed to have pilot experiments performed at the University of Melbourne and the final experiments conducted at the Forschungszentrum Juelich to utilize their phenotyping platform, the GrowScreen-Agar. However, due to unforeseen circumstances, as with the COVID-19 pandemic, the experimentation with the platform was only partially completed. New experiments had to be conducted back at the University of Melbourne to fulfill the objectives while getting around the challenges. An initial attempt was made to replicate the “open-top” growth system; however, the lack of available materials (e.g., customizable plates) and the challenges of customizing available ones (due to workshop closures, laboratory restrictions, and ordering delays) made this impossible. Moreover, the “open-top” system was not optimally designed to be imaged in the WinRhizo equipment. Therefore, another attempt to cultivate plants and bacteria, while adapting the growth system for optimized imaging and root tissue harvest, was made.

This chapter is divided into three sections: 1) growth protocols conducted to establish the optimized growth conditions for plants and bacteria cultivation in a conventional “closed-plate” system (conducted at the University of Melbourne); 2) adaptation of the established plant-bacteria co-cultivation growth protocol to the new phenotyping platform, which follows an “open-top” system, with its associated agar-cultivation, imaging, and analysis protocols (performed at the Forschungszentrum Juelich in Germany); 3) optimization methods to adapt the working growth protocols of the “open-top” system, but using available plant cultivation

resources and technology, mainly for growing and harvesting plant tissues for lipid analysis (back at the University of Melbourne).

2.2.1. Establishing protocols for optimized plant and bacterial growth conditions and co-cultivation using the traditional “closed-plate” system (University of Melbourne)

This part of the experimentation has been designed, firstly, to establish the appropriate growing protocols for both *Arabidopsis* plants and bacteria in an enclosed sterile environment. Several growth protocols for *Arabidopsis* plants already existed. However, for this study, some additional considerations were 1) the application of bacteria, therefore the stringent sterility requirement of the system; 2) the simulation of the gravitropic root growth, thus, the need for appropriate orientation of the plates; 3) the periodic observation of root development that requires a matrix to support a fixed root structure, which in turn, dictates the media to be used; and 4) the type of data acquisition method (e.g., use of imaging platform or manual root trait measurements), which also requires specific material for the plate.

To realize these requirements and objectives for *Arabidopsis* co-cultivation with bacteria, the traditional agar-plate (“close-plate”) method was utilized. The sealable condition of the conventional Petri plates maintained the sterile environment required for growing both plants and bacteria while eradicating contamination. The plates were initially orientated in a vertical position to mimic the downward growth of the roots in the soil, which also demonstrated their structural growth. Finally, the use of agar in a transparent plate allowed for the non-invasive, timecourse observation and phenotyping of the roots, elucidating the development of the root system and the individual root architectural components. Whilst an agar-based growth system may not be representative of actual field conditions, this system allows for control of soil/medium heterogeneity, which reduces experimental noise. This system also facilitates easy measurements of the root systems, in response to any applied external factors (e.g. bacteria and high temperature), at varying developmental stages to assess growth and responses over time. A workflow of the methods used is illustrated and described in Figure 2.2.

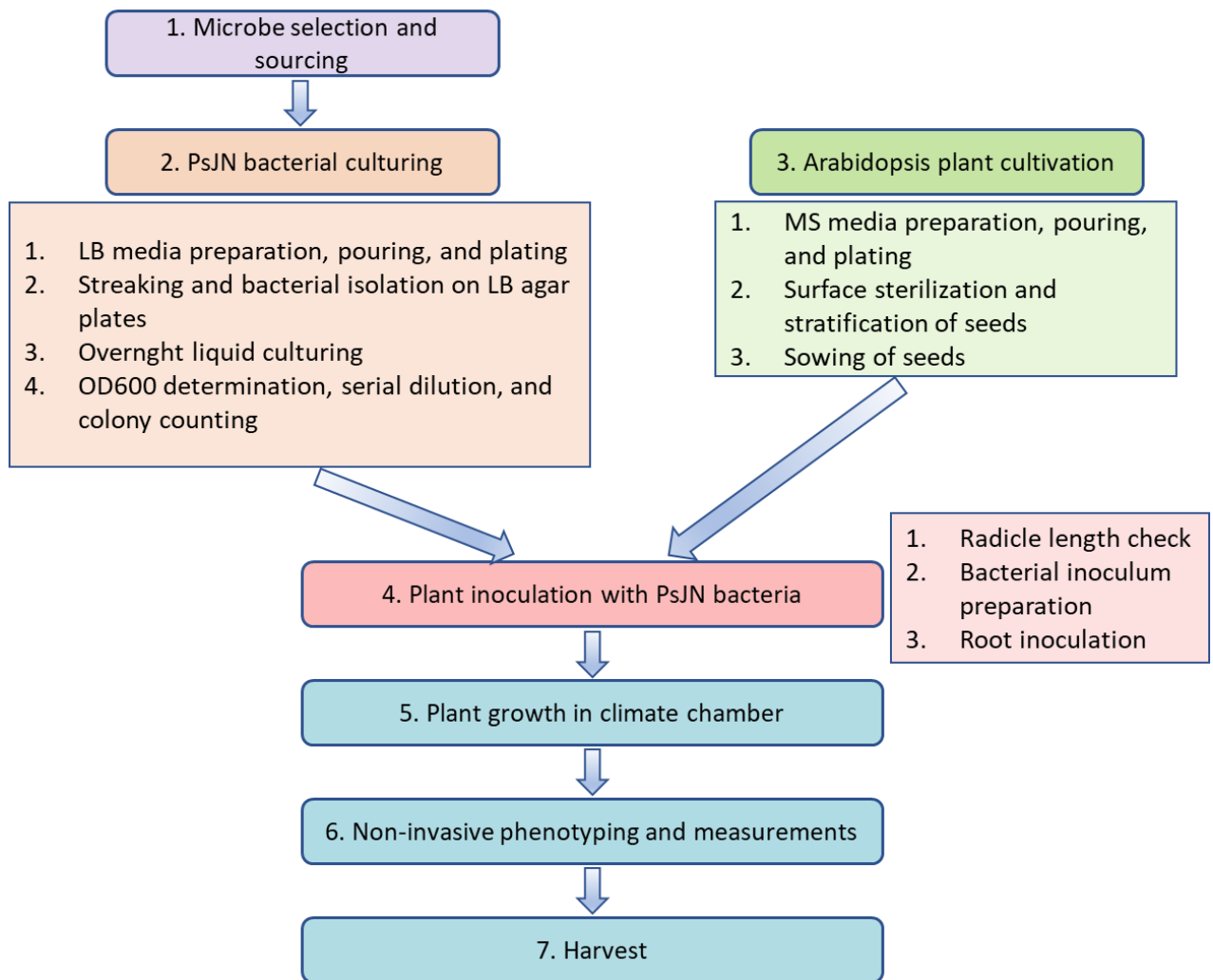


Figure 2. 2 Workflow of methods for plant and bacterial co-cultivation in a “closed-plate” system

2.2.1.1. Selection and sourcing of microbial strain for the experiment

For selecting the specific microbe, some criteria were established for the literature search. First, the microbial strain should be a well-studied or previously experimented plant growth-promoting microbe. It should have been previously investigated and found to confer thermotolerance, if possible, to Arabidopsis, but if not, at least to other plants. Lastly, the chosen strains were checked against those that have been found and sequenced by (Bai et al., 2015) to be naturally occurring in Arabidopsis roots. From the narrowed-down microbial strain list which included: *Bacillus amyloliquefaciens* 5113, *Azospirillum brasilense* NO40, *Pseudomonas putida* NBRI0987, *Trichoderma harzianum* T34, *Rhizophagus irregularis*, *Pseudomonas* sp. strains AKM-P6 and PsJN, *Curvularia protuberata* Cp4666D, and *Paraphaeosphaeria quadriseptata*; the bacteria, *Paraburkholderia phytofirmans* PsJN (previously under *Pseudomonas*, then *Burkholderia* genus) was selected. Aside from having a

fully sequenced genome, this bacterial strain is a well-established plant growth-promoting endophyte that is also known to assist plants against abiotic stresses like high temperature (Bensalim et al., 1998). This strain was kindly provided by a research group in Chile (Poupin et al., 2013) that is actively working on this bacteria.

2.2.1.2. *Culturing of Paraburkholderia phytofirmans PsJN*

Since dealing with the biosecurity issues with the import of the bacteria to the country took several months, time was spent practicing how to culture bacterial strains provided by other colleagues. Said strains were *Azospirillum brasilense* sp7, *Azospirillum brasilense* sp245, and *Herbaspirillum seropedicae* spZ67. With these trials, a workflow was established for culturing the actual bacterial strain. The strain PsJN arrived in a bacterial slant and was immediately revived after it was released from quarantine or biosecurity. A workflow for reviving and culturing bacteria was followed (Figure 2.3.).

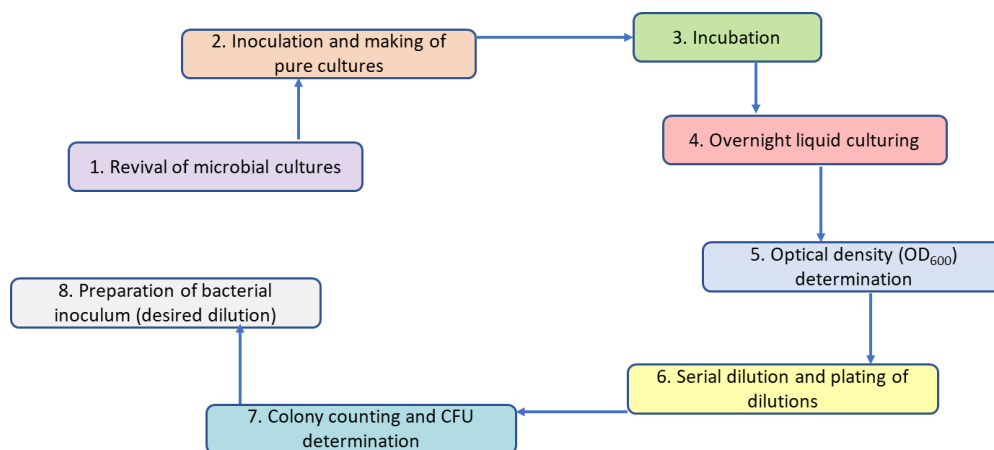


Figure 2.3 Workflow protocol for culturing bacteria

2.2.1.2.1. Bacterial media preparation, pouring, and plating

For culturing the bacteria PsJN, the Luria-Bertani (LB) media was utilized. To make the 500 mL LB agar solution, 2.5 g yeast extract (Oxoid), 5 g BBL™ Trypticase™ Peptone (BD), and 7.5 g Bacto™ agar (BD) were combined and homogenized. This was done by filling a 1 L glass container (Schott bottle) with 500 mL of Milli-Q H2O, placing the solution with a magnetic stirrer in a stir plate, and slowly adding each of the ingredients. Sodium chloride (NaCl) which is a normal component of LB media was omitted because of this bacteria's low halophilic tolerance of only 0.5%. Only half of the container was filled to provide extra volume

when the molten agar solution starts boiling during autoclaving. Once homogenized, the bottle was closed with the lid but not air-tight sealed. Autoclave tape was attached to the cap and a label was created to make indications of successful autoclaving (i.e. sample has spent at least 10 minutes at 121°C). Once autoclaving was completed, the bottle was first dried then the surface was disinfected before being transferred to a sterile bench where plates have been lined in a row, partially covered with lids. Pouring was done by initially using a 50 mL Falcon tube to estimate the amount of media that will go into each plate. The plates were then carefully filled with liquid agar solution. This row of plates was then pushed to the back of the bench to give way for another batch of empty plates to be filled. The agar media was left to harden and solidify for at least an hour before the plates were covered, stacked, and finally bagged in an upside-down (lid down) position to prevent condensation from dripping onto the agar surface. Plates were stored in a cold room maintained at 4 °C.

2.2.1.2.2. Streaking and bacterial isolation on LB agar plate

Before streaking, the plates to be used were removed from the cold room and placed on the sterile bench at ambient temperature. From the bacterial slant that was provided, the bacterial inoculum was touched with a sterilized inoculating loop and carefully spread over a section of the agar medium. This was done by holding the loop at an angle to make broad strokes and touching only the surface, not digging into the agar. This created streak 1. Once the first streak was made, another inoculating loop was used by dragging one end of streak 1 to spread the bacteria over a second section of the plate to create streak 2. Similarly, for streak 3, the same procedure as with the previous streaking was applied; with all the streaks created each time somehow perpendicular and not overlapping with each other except for the dragged ends. When the entire plate has been streaked, it was then covered and sealed with micropore tape (Figure 2.4.). Plates with the newly streaked bacteria were incubated for two days at 30°C. After which, single colonies, which looked like white dots, were then visible. Each dot is composed of millions of genetically identical bacteria that arose from a single bacterium. When the bacteria growth was too dense with no visible single colonies, streaking was repeated onto a new agar plate to create single colonies.

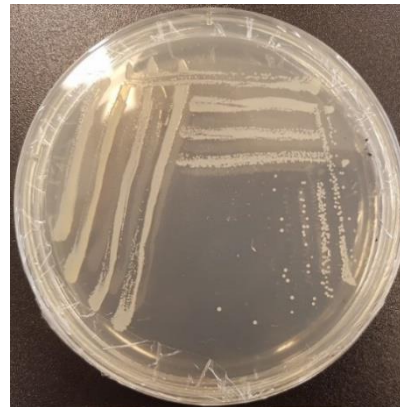


Figure 2. 4 Sample streaking technique (A) and an actual bacterial streaked plate (B)

2.2.1.2.3. Overnight liquid culturing

Liquid culturing was performed to support a higher density of bacteria and to grow enough culture for the experiment. To do so, the LB liquid solution or broth was first prepared. This was similar to making the bacterial media, except without the agar. That is, in a 1 L Schott bottle, 2.5 g yeast extract (Oxoid) and 5 g BBL™ Trypticase™ Peptone (BD) was added to a 500 mL of Milli-Q H2O to create a 500 mL LB broth. Autoclaving protocols similarly described in section 2.2.1.2.1. were then employed. Once the LB broth was prepared, 10 mL of the solution was aliquoted using a 10 mL Gibson pipette into 50 mL Falcon tubes, ready to be inoculated by the bacteria. From a previously streaked bacterial plate with growing single bacterial colonies, a single colony was picked using a sterile 10 uL pipette tip. This tip was then transferred and dropped into the aliquoted 10 mL LB broth, thereby making the inoculated bacterial media. A controlled comparison was also set up by leaving one tube with 10 mL LB broth uninoculated. Both control and inoculated tubes were covered and placed inside a shaking incubator overnight with the following settings: 30°C and 150 rpm.

2.2.1.2.4. OD₆₀₀ determination, serial dilution, and colony counting

To estimate the concentration of bacteria in the liquid culture, OD₆₀₀ which is an abbreviation indicating an absorbance or optical density of a sample measured at a wavelength of 600 nm, was used. The day after inoculating an LB liquid culture, bacterial growth was checked by looking for a cloudy haze in the inoculated media (Figure 2.5.). In comparison, the sterility of the control was observed with the clear liquid or the natural LB broth hue. To determine the OD₆₀₀ value at the log phase of bacterial growth, the culture was checked several hours earlier

than the estimated complete incubation time. For the bacteria PsJN, the optimum growth value of 0.8 was achieved in about 24 hours, therefore, optical density checks were done starting from 16 hours. Measurements were performed using a spectrophotometer (DS-11 FX Spectrophotometer/ Fluorometer, DeNovix, Inc., DE, USA). This was done by pipetting 1 mL of the bacterial inoculum into a glass cuvette. However, a standard was first set by pipetting 1 mL of the control LB broth. OD₆₀₀ values were then recorded including the time corresponding to the measurement. Once the desired density was reached, the bacterial inoculum was then set aside, ready for serial dilutions and colony counting.

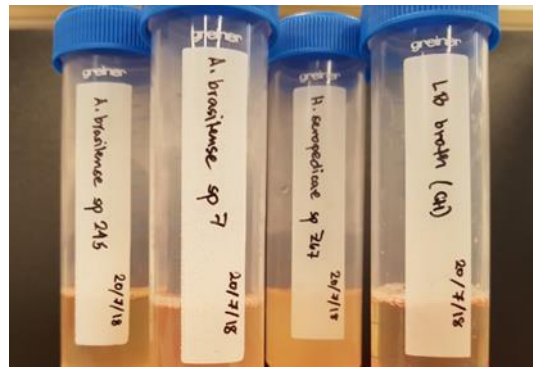


Figure 2.5 Overnight liquid cultures of some trial bacteria and a control

A ten-fold serial dilution was performed to determine the concentration of bacteria, in a colony-forming unit (cfu), present at the specific absorbance of 0.8. This was done by preparing sterile 2 mL Eppendorf tubes, labeled 10^1 to 10^7 corresponding to each dilution factor. Using aseptic techniques, 900 μL of LB broth was pipetted into each of the tubes. From the prepared overnight bacterial inoculum, 100 μL was aliquoted and pipetted out into the first tube labeled 10^1 . This tube was then vortexed, after which, 100 μL was taken out and pipetted into the next tube labeled as 10^2 . This process of serially diluting the inoculum continued until the last tube with the 10^7 dilutions.

Once the serial dilutions were ready, plating and colony counting ensued (Figure 2.6). Briefly, seven agar plates were prepared and labeled corresponding to the serially diluted tubes. 100 μL was pipetted out from each dilution tube and placed in the middle of the plate. Using a spreader, the diluted inoculum was distributed evenly on the surface of the agar. The inoculum on plates was first allowed to dry out or be absorbed before the plates were sealed with micropore tape, turned upside down, then placed in an incubator for about two days. Bacterial growth was then checked, and the single colonies were counted. As a rule, the accepted number of colonies on the plate was between 30 to 300 cfu. More than or less than that was tagged

either too many to count (TMTC) or too little to count (TLTC), respectively. Calculations were done to determine the number of bacteria per mL (cfu/mL) or the total number of bacteria in the original inoculum.

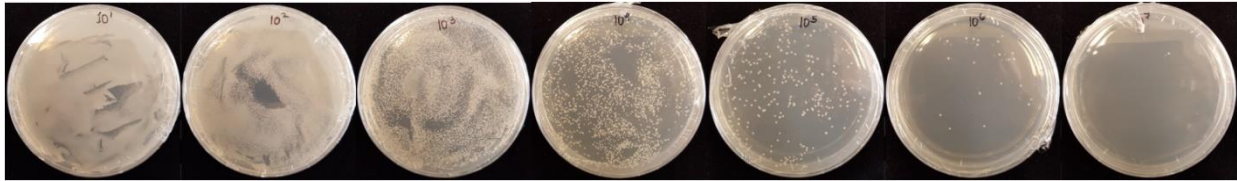


Figure 2. 6 Plated serial dilution of a bacterial inoculum

2.2.1.3. Arabidopsis plant cultivation

2.2.1.3.1. Plant media preparation, pouring, and plating

For the pilot closed-plate experiment, the media used for *Arabidopsis* cultivation was comprised of Murashige and Skoog (MS), 2-(N-morpholino) ethanesulfonic acid (MES), and agar powder. Briefly, in a large beaker with 1 L of distilled H₂O and a magnetic stirrer, 2.2 g MS, 0.5 g MES, and 1% sucrose were added. The beaker was placed on top of a stir plate where the solution was mixed and homogenized. While being mixed, the pH of the solution was also adjusted using a pH meter, to about 5.6 to 5.8 by adding several drops of 1 N KOH using a glass Pasteur pipette and rubber. When the desired pH was reached, the solution was then transferred to a separate 1 L glass container (Schott bottle), containing 9 g of agar powder. This amount varied depending on the orientation of the agar plate. For vertical growth, 9 g of agar was used to reinforce its strength against gravity; whilst for horizontal growth, only 7 g of agar was enough. The container was then capped, but not tightly sealed, equipped with autoclave tape, and then placed in the autoclave for sterilization. After autoclaving the solution, it was transferred to the sterile bench where all the plates had been previously laid out, partly covered with their lids. Using a 50 mL Falcon tube, about 45 mL of the agar media was poured into each plate. Once everything was filled, the plates were then allowed to cool down for a couple of hours before the lids were replaced. Plates were stacked up, placed inside their original bag, and turned upside down (lid down) before the bag was sealed. They were placed and stored in the cold room at 4°C until ready for sowing.

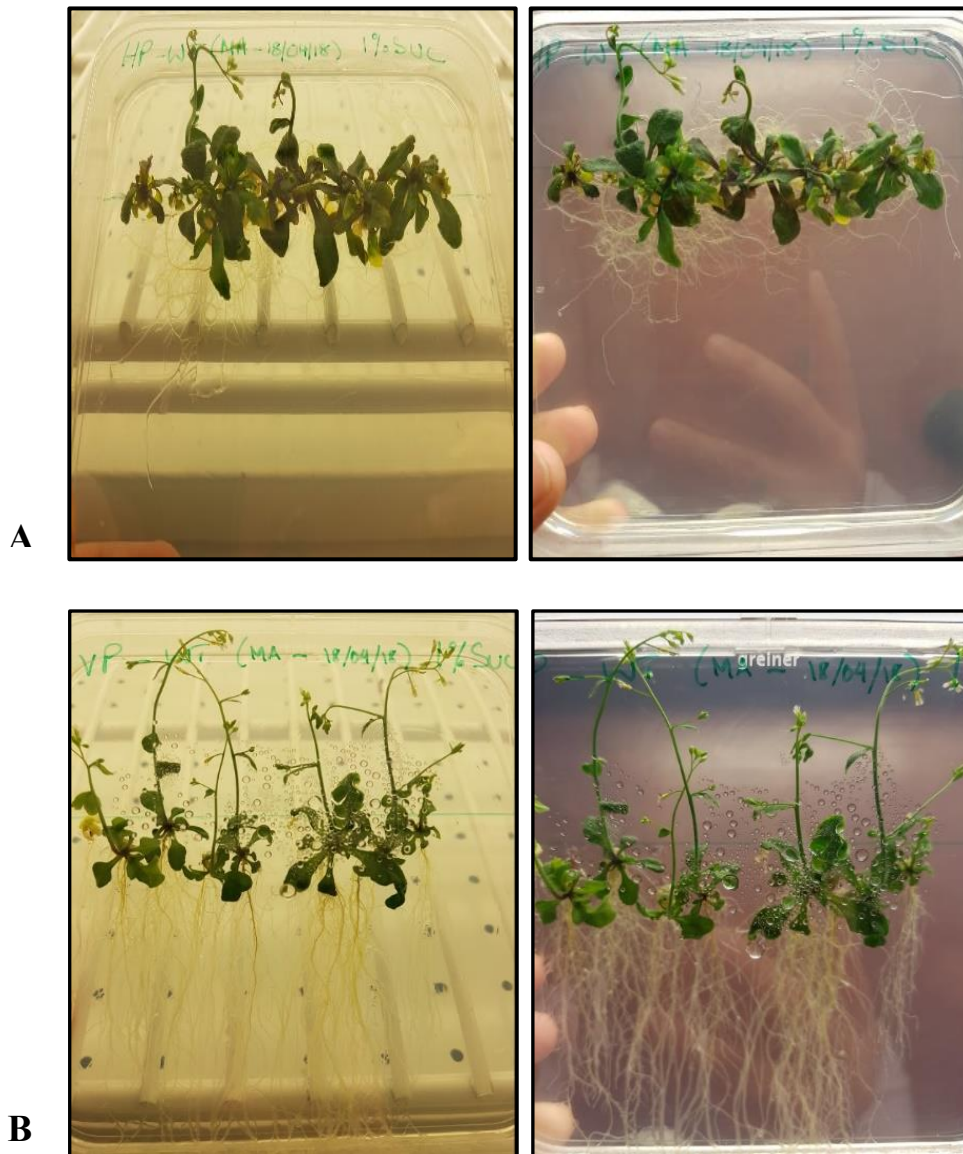


Figure 2.7 Horizontally grown (A) and vertically grown (B) Arabidopsis plants at 30 days after sowing

The suitability of the plate growing orientation was tested as seen in Figure 2.7. Vertical agar growing was chosen because of the representative plant root growth. Sucrose was only used during the initial plant cultivation, however, for the succeeding experiments where plants were inoculated with the bacteria PsJN, the addition of sucrose was omitted altogether because of the latter's affinity for sugar. This was also to eliminate potential interference with the plant's morphologic responses to bacterial colonization.

2.2.1.3.2. Surface sterilization and stratification of seeds

To eliminate the presence of any microorganisms, Arabidopsis Col-0 seeds were surface sterilized with 70% ethanol and 12.5% Sodium hypochlorite solution with 1 mL Triton x-100. Briefly, the seeds in an Eppendorf tube were initially washed by adding 1 mL of 70% ethanol and turning the tube for 5 minutes. The ethanol was then removed, and the seeds were subjected to second washing with sodium hypochlorite (5 mL of 12.5% sodium hypochlorite and 45 mL of distilled H₂O). To facilitate uniform washing of the seeds, the tube was placed in a thermoshaker for 10 minutes; after which, the solution was pipetted out. Finally, the seeds were washed with sterile distilled H₂O five times to eliminate traces of sodium hypochlorite which can be toxic to seedlings if not completely washed off. The last wash was left on the tube for the seeds to be suspended during stratification.

Stratification, which is a method of breaking seed dormancy to promote uniform germination, was done by placing the tube of sterilized seeds in a cold room maintained in the dark at 4 °C for four days.

2.2.1.3.3. Sowing of seeds

For sowing with the “closed-plate” system, the entire lid had to be removed, which exposed the surface of the agar, before the seeds were sown on the marked area of the plate. In this protocol, both the prepared agar plates and recently stratified seeds from the cold room were placed on the sterile bench. Before sowing, a distinct horizontal line (2 cm from the top) was measured and drawn at the back of each plate to determine the point where the seeds will be sown. The plate was also divided accordingly to accommodate four seeds at equal distances from each other and the sides of the plate. As this posed considerable time during sowing, an alternative method was thought of. This made use of a single empty bottom part of the plate, clearly drawn with a sowing line and the location of the seeds also marked. This was then used as a template sitting (open-face down) at the bottom of the agar plate. The goal during sowing was to get only one seed from the Eppendorf tube and to dispense it into the marked location on the plate. Sowing was performed by using a 1 mL pipette, with the index finger operating the suction and release of each seed (Figure 2.8). Once all the seeds were sown, the plates were sealed with micropore tape to allow air exchange during germination, and then placed into two separate growth chambers, with ambient and heat-stress conditions, until ready for inoculation (growth chamber settings in the next section).



Figure 2. 8 Sowing individual seeds onto the agar surface using a 1 mL pipette

2.2.1.4. Plant inoculation with the *P. phytofirmans* PsJN

This stage of the plant cultivation protocol is comprised of three steps; the first two of which were performed simultaneously.

2.2.1.4.1. Radicle length checking

The plants in the growth chamber were checked every day for the appearance and growth of the radicle. Once the radicle reached a length of 2 to 5 mm, inoculation of the bacteria was then performed. The timing of inoculation to the radicle length was of great importance; such that simultaneous to the daily observation of the radicle development was the preparation for the overnight liquid culture, so that the bacterial inoculum was ready at the same time when the radicles reached the required range of lengths.

2.2.1.4.2. Preparing bacterial culture in MS liquid media for plant inoculation

According to a previous study by Poupin et al. (2013), the number of PsJN bacteria for colonization necessary for optimum plant development was determined to be 10^4 cfu/mL. As the method employed in this study was a direct application of the bacteria into the radicles, only a small amount of the inoculum was applied. A 10 μ L inoculum was found to be sufficient

to cover the radicle area. Calculations were made to determine which dilution will yield the required number of bacteria in a 10 μL aliquot. This dilution then became the final bacterial inoculum for the root inoculation.

One important factor considered before the inoculation was the effect of the bacterial medium (LB) on the plant agar media (MS). Another factor was the presence of chemicals released by the bacteria in the medium during growth which could influence early plant responses. Therefore, to eliminate these potential effects, washing was performed after the overnight liquid culture preparation (see section 2.2.1.2.3) and before the serial dilution (section 2.2.1.2.4). Briefly, liquid culture at an OD_{600} of 0.8 in a Falcon tube was spun down using a centrifuge at 10,000 $\times g$ for 10 minutes to get the bacterial pellets. This allowed for the removal of the LB media. A similar amount of MS media was then added to resuspend the pellets. This new solution was again spun down, and the media was removed as with the previous procedure. Finally, the bacterial pellets were resuspended in the MS media, and the OD_{600} was measured. The MS-washed bacterial culture was then serially diluted and the dilution that was previously calculated was set aside as the final bacterial inoculum for root inoculation.

2.2.1.4.3. Root inoculation

Once both the radicles and the bacterial inoculum were ready, bacterial inoculation of the roots was performed. The plates from the growth chamber were transported into the sterile bench and opened for bacterial application. Briefly, the bacteria PsJN was applied by pipetting 10 μL of the prepared dilution of bacterial inoculum directly into the radicles of the Arabidopsis seedlings. The liquid was left to be absorbed into the agar before the plates were closed and sealed with micropore tape.

2.2.1.5. Growth in the climate/ growth chamber

After root inoculation, the plates were placed into wooden racks and transferred into two separate climate chambers with different temperature conditions: ambient and heat stress. Before the transfer, the chambers (or sections within the chamber) were first cleaned and disinfected. As there was limited availability of growth chambers (and most were already shared by two or more researchers depending on their plants' growth requirements), two different growth chambers were used. To minimize, if not eliminate, potential variations due to the difference in the type (e.g. type of light source) and specification of the growth chambers,

the light intensity on the level of the plates was measured using a photometer. Where the intensity was at below-optimum condition, adjustments were made on the location of the plates. The rest of the environmental conditions were easily set as per equipment protocol.

The following were the specified growth settings: Temperature - 22 °C/ 18 °C (ambient), 30 °C / 24 °C (heat stress) day/night; light intensity - 120-150 $\mu\text{mol m}^{-2} \text{s}^{-1}$; photoperiod - 16 hr/ 8 hr light/dark; humidity – 70%.

2.2.1.6. Plant phenotyping

The plants were grown inside the growth chambers while being phenotyped non-destructively at different time intervals: 2, 7, 9, 12, 14, 16, 19, and 21 days after inoculation (DAI). Plant phenotyping was performed by removing the plates from the growth chamber, placing them into a darkened and sealed container during transport, and imaging them individually using WinRhizo™. Once the image was captured, analysis was run on a per-plate basis. Root parameters measured were total root length, primary root length, and branched (combined first and second-order lateral) root length. It is to be noted that because of the software limitation for detecting the primary root whenever there was a crossing or intersection of roots, image tracing by hand was performed before analysis.

2.2.1.7. Harvest and analysis

At 21 days after inoculation, plates were removed from the growth chambers and opened for removing the plant tissues. Shoots were cut from the plants and set aside for measuring fresh weight. Roots were slowly removed from the agar, by holding the top of the root and slowly pulling the rest. Since some parts of the roots were growing inside the plates, there were losses in the harvested tissues. The fresh weight of root tissues was then measured.

The condition where roots grew inside the plates, making harvest a challenge was addressed and the methods optimized at the succeeding experiments conducted at the Forschungszentrum Juelich.

2.2.2. Optimization methods for “open-top” plant cultivation using the GrowScreen-Agar phenotyping platform (Forschungszentrum Juelich (FZJ))

Once the growth conditions and protocols for Arabidopsis and bacteria co-cultivation from the agar or “closed-plate” system was established, the next step was to adapt these protocols to the

phenotyping platform, GrowScreen-Agar. Two types of GrowScreen-Agar equipment were present at the institute.

The original platform, GrowScreen-Agar I (also called the “Root Carousel”) was designed for high-throughput imaging and phenotyping of conventional square Petri plates (120 x 120 mm). This platform is compatible with agar plates sown with plants growing in an “open-top” system, where shoots are growing outside through customized holes made at the top part of the plates. The carousel provides an opportunity for dynamic phenotyping through a non-invasive imaging platform that allows for unobstructed shoot growth and more robust root development while facilitating convenient top and side imaging (for shoots and roots, respectively). The two cameras attached to the carousel also connect to software for rosette area measurement, which works well for *Arabidopsis*, and software for root parameter measurement, the GrowScreen-Root, where manual input may be necessary (Nagel et al., 2009; Nagel et al., 2020). This platform’s high-throughput imaging capability accommodated the imaging of about 70 plates within 15 minutes.

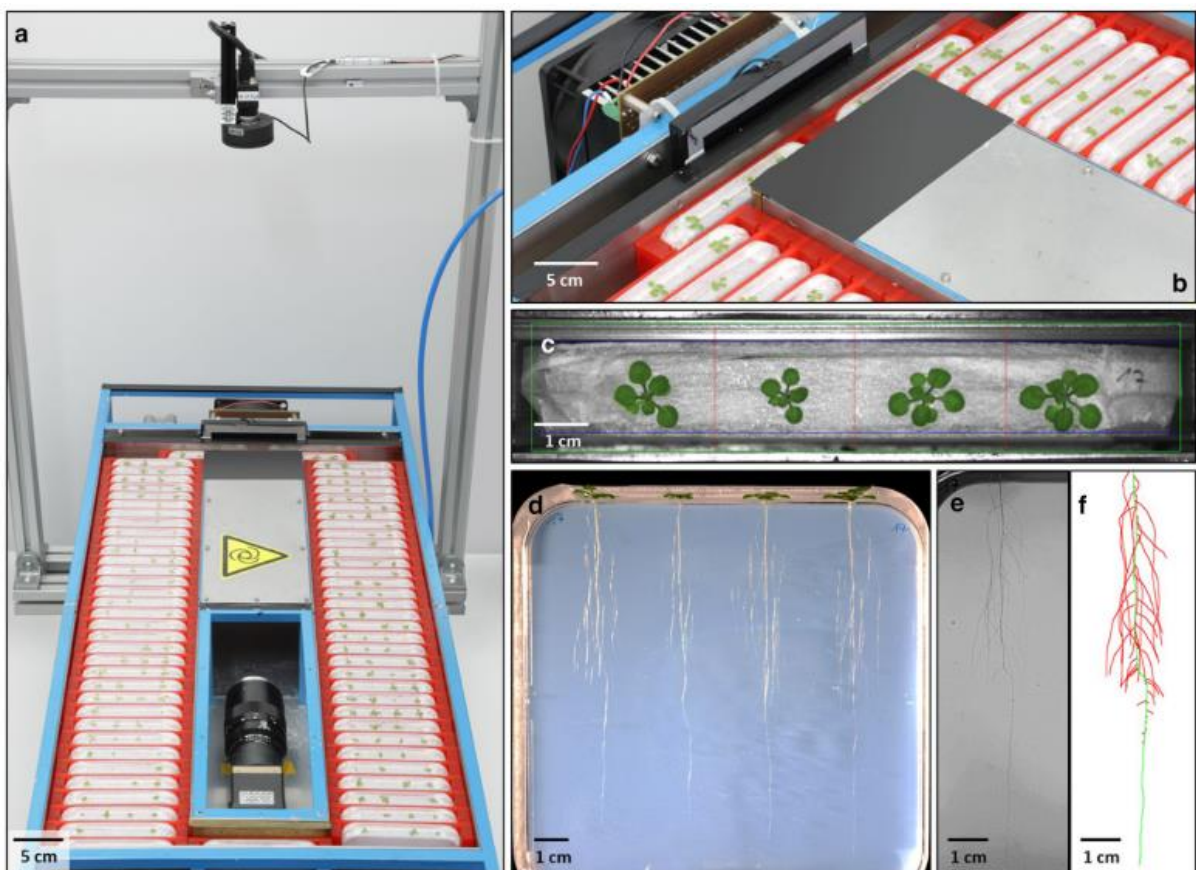


Figure 2. 9 GrowScreen-Agar, mechanical setup for automated imaging roots and shoots of plants grown in agar-filled plates. The Petri dishes are fixed in red holders, which are moved in a rectangular

frame by using pneumatic cylinders (a, b). At one position of the setup, Petri dishes (b) are optically accessible and images of root and shoot are taken (c, d). Representative original color image of four Arabidopsis shoots taken by the top camera (c); part of an original greyscale root image taken by the bottom camera (e) and color-coded image (quantified with the image-based software GROWSCREEN-ROOT) with primary root (green) and lateral roots (red) of an Arabidopsis plant (f). In total 70 Petri dishes containing up to 280 Arabidopsis plants fit into the GrowScreen-Agar system. During image acquisition, the opening above the bottom camera (a) is closed by a cover panel. [Source: Image and description adapted from Nagel et al. (2020).]

The original plan for my experiment was to utilize this already functional and working platform. However, this platform fell short of a crucial requirement of my experiment, which was to grow the plants for a longer period to observe the time-series growth-promotion effects of the bacteria on Arabidopsis roots. At its maximum size, the conventional Petri plate can grow plants for up to about 14 days, before the roots start touching the bottom of the plates. In my pilot experiments, although the bacteria has shown a prominent trend of growth-promotion effects on various root traits within 14 days, the stimulation effects showed an increasing trend, which prompted the objective of growing the plants for a longer time, i.e., 21 days to see more significant effects. Nonetheless, I utilized this system initially to adapt the growth protocols of my plants and bacteria to the specific cultivation protocols associated with the “open-top” feature system of this platform.

The second and upgraded version of this platform, the GrowScreen-Agar II, was designed for longer plates and imaging of the top and side of shoots, as well as the roots, using three strategically-placed cameras (details and images discussed in Chapter 3 and supplements). This platform was also developed for even higher throughput (i.e., several hundreds of plates), with the plan of incorporating the plant cultivation system and the imaging system into one place. That is, this platform was envisioned to be a growth chamber for agar-grown plants, with a built-in imaging system, and with a robotic arm that will manage all handling, transfer, and imaging of the plates, which will be controlled remotely by a computer. Unfortunately, this platform was not yet fully operational during my stay at the institute, and the only functional part was the imaging system. This imaging system was specifically built for designed plates, which are also maintained in customized racks or magazines (specifications discussed and images shown in Chapter 3 and supplements).

Once I had adapted the plant-bacteria growth protocols to the “open-top” system using the original GrowScreen-Agar I, optimization experiments of six plates per treatment using the GrowScreen-Agar II platform were then performed to address several challenges including 1)

contamination due to the open-air nature of the growth system; 2) repeatability of the observed phenotypes ; 3) harvest of roots growing within the agar; and 4) drying of agar at the end of the growth period, particularly at high temperatures. The workflow of experimentation is illustrated in Figure 2.1.0.

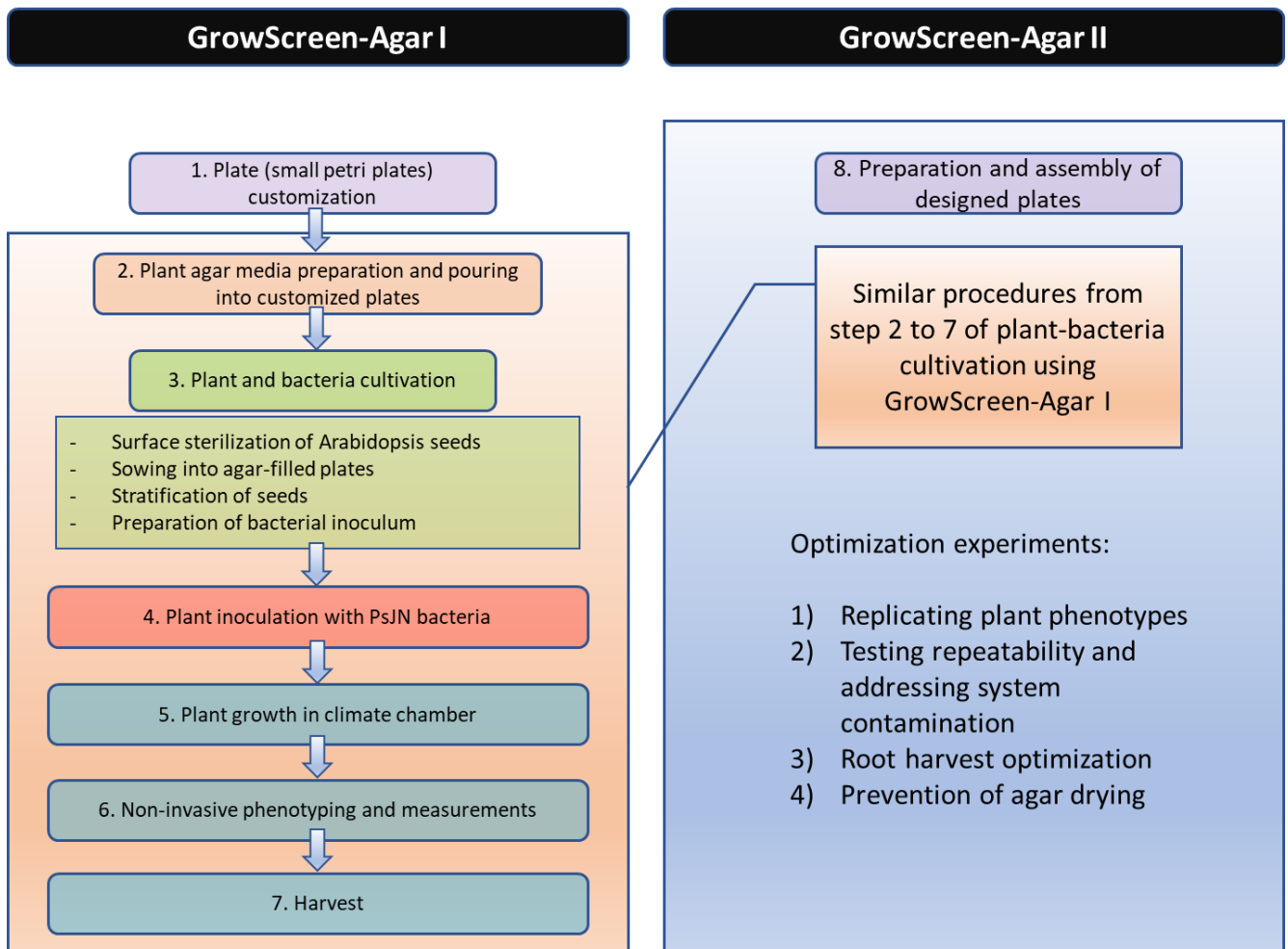


Figure 2. 10 Workflow of experimentation at Forschungszentrum Juelich

2.2.2.1. Petri plate customization for the GrowScreen-Agar 1 platform:

Traditional square Petri dishes (120 x120 x 17mm, Greiner, Solingen) were taken out of the plastic bag and into the cleaned bench inside the biosafety cabinet. First, the lid and bottom dish of the plate were aligned and positioned such that the letterings on the plate will not block the roots during image acquisition. Once the positions of the plate parts were defined, all the bottom dishes were grouped and prepared to be worked on, while the lids were set aside. The top part of the bottom dish (when standing) was covered with micropore tape to mark the area

where the holes will be made. Using an appropriate metal stencil (pre-customized with holes of different numbers and sizes depending on seed type) and a pneumatic drill, the holes for the *Arabidopsis* seeds were then carefully drilled. Afterward, the holes were cleaned and the cuttings were removed using compressed air into a catch tray. Finally, another layer of micropore was placed on top of the drilled one to cover the holes for the succeeding step of pouring media. On the other hand, to obtain a fully open-top Petri plate, the top part of the lids was cut, this time with a hot cutting wire. Caution was observed so as not to touch the hot wire and also to avoid damaging the surface of the lid. Once both sides of the plates were customized, they were then assembled, placed back into the bag, and sealed until the next steps.

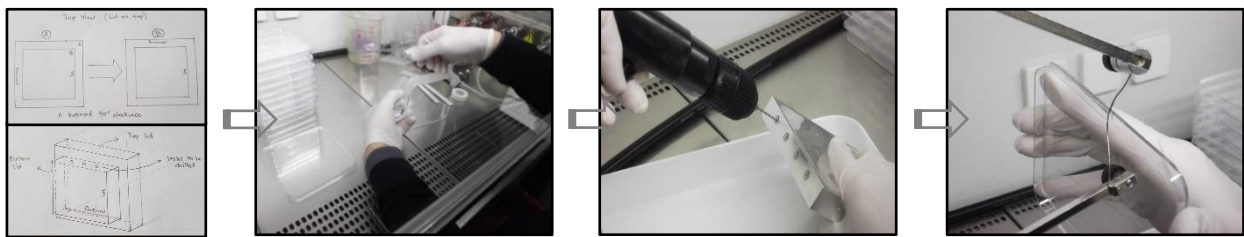


Figure 2. 11 Customization of the small Petri plates for the GrowScreen-Agar I. a) Positioning and aligning the plates. b) Covering the top part of the bottom dish in preparation for drilling holes. c) Drilling holes into the plates using metal stencils. d) Cutting the top part of the lid to allow plant shoots to grow outside the holes of the plates. [Source: Images (except for the first one) taken from Becker and Kastenholz (2020).]

2.2.2.2. Preparation of the plant agar media and pouring into customized plates

Instead of the MS media previously used in the closed-plate experiments, the cultivation system of this platform was optimized for the use of modified Hoagland media. Also, this solution was better suited for biochemical analysis as the chemicals used are controlled and no sugar was present, which was found to influence both plant and bacteria PsJN's behavior. The concentration of compounds used in the preparation of the nutrient stock solution for Hoagland media is tabulated in Table 2.1 (from Nagel et al. (2020)). To make the Hoagland agar media solution, the composition of the solution in a liter of Milli-Q water was specified in Chapter 3.

Table 2. 1 The concentrations of compounds in Milli-Q water as a solvent for the preparation of nutrient stock solutions which are used in GrowScreen-Agar (Nagel et al., 2020).

	Stock solution number	Mass concentration (g/l)	Molar concentration 10^{-3} (mol/l)	Stock solution / litre 10^{-3} (l)	*Full nutrient conc. 10^{-6} (mol/l)
KNO ₃	1	101.103	1000	5	5000
Ca(NO ₃) ₂ · 4 H ₂ O	2	236.149	1000	5	5000
MgSO ₄ · 7 H ₂ O	3	246.475	1000	2	2000
KH ₂ PO ₄	4	136.086	1000	1	1000
MnCl ₂ · 4 H ₂ O	5	1.979	10	1	10
CuSO ₄ · 5 H ₂ O	5	0.250	1	1	1
ZnSO ₄ · 7 H ₂ O	5	0.288	1	1	1
H ₃ BO ₃	5	3.092	50	1	50
Na ₂ MoO ₄ · 2 H ₂ O	5	0.121	0.5	1	0.5
C ₁₀ H ₁₂ FeN ₂ O ₈ ⁻ (Fe-EDTA)	6	30.965	90	1	90
FeSO ₄ · 7 H ₂ O	7	25.021	90	1	90
C ₁₀ H ₁₆ N ₂ O ₈ (EDTA)	8	26.302	90	1	90
H ₂ SO ₄	9	0.1962	2	1	2
KOH	10	15.710	280	1	280

To prevent the cross-reactions and resulting precipitates, the nutrients were separated into six tinted bottles, and the amounts of each element in the six stock solutions were restricted. To create a full-strength nutrient solution, 5 ml of stock solutions 1 and 2, 2 ml of stock solution 3, and 1 ml each of the stock solutions 4, 5, and 6 were filled up to one liter. Iron was available as Fe-EDTA complex in solution 6, with solutions 7 to 10 as reactants for producing the chelate complex (Nagel et al., 2020)).

Once the agar-media solution was autoclaved and ready, a liter of the solution was distributed evenly to ten small customized Petri plates. Briefly, the plates were removed from

the sealed bags, and the bottom dishes were laid flat and evenly on the clean bench, while the lids were set aside. The hot media was allowed to cool down (around 70°C) before being poured evenly onto the dishes. The second layer of micropore tape prevented the poured liquid media from spilling through the holes of the drilled plates. Once the agar solidified, the micropore tapes were then removed from the bottom dishes and the lids placed to cover them. The two parts of the plates were positioned vertically in such a way that the bottoms were flat and aligned before all the sides (except for the top with holes) were sealed with micropore tape. Finally, using a separate strip of micropore tape, the upper sides of the plates were connected without sealing the holes. The assembled sealed plates were either left in the sterile bench for seed sowing or placed back into their plastic bags.

2.2.2.3. Arabidopsis plant and PsJN bacterial cultivation

Arabidopsis seeds were first surface-sterilized to remove any microorganisms. The protocol was slightly different from the one used during the pilot experiments, in that, the solutions used were 70% ethanol (v/v) and 0.5% (v/v) sodium hypochlorite solution with 0.05% (v/v) Tween 20 (5 µL per 10 mL solution). Operating inside the biosafety cabinet, the number of seeds to be used for the experiment was estimated and placed in 2 mL Eppendorf tubes. The seeds were first incubated with 0.5 mL of 70% ethanol solution. Seed suspension and incubation were done by slowly turning the tube for three minutes. After incubation, ethanol was removed by pipetting and replaced with 0.5 mL of 0.5% sodium hypochlorite. The tube was again slowly turned and mixed for the seeds to incubate for about 10 minutes; after which, the solution was pipetted out. After disinfecting the seeds with the solutions, they were washed three times with autoclaved Milli-Q water. After the last washing, the seeds were suspended in another 0.5 mL of autoclaved water and set aside ready for sowing.

While sowing with the “closed-plate” system in the pilot experiments required opening the plates to directly place the seeds into the agar surface, this “open-top” system allowed the individual sowing of the seeds through the drilled holes of the plates, minimizing agar exposure. Firstly, the ten agar-filled plates were arranged and the micropore tapes covering the holes were removed. Using a pipette, a single seed was slowly pipetted out from the sterilized batch and carefully dispensed into the hole of the plate. To make sure that the seed lies in the middle of the hole, a needle was used to position it. When all the holes of the four plates were sown with seeds, the top of the plates was then sealed with parafilm; after which, the plates were placed into plastic bags and sealed aseptically. The bags of plates were then transferred

to a fridge set at 4°C and the seeds were allowed to stratify in the dark for five days to break their dormancy. After the stratification period, the plates were taken back to the biosafety cabinet, the parafilm covering the holes removed, and the seeds ready for bacterial inoculation.



Figure 2. 12 Dispensing a single *Arabidopsis* seed into each hole of the customized plates. [Source: Image taken from (Becker & Kastenholz, 2020).]

Culturing of the bacteria was done similarly as with the pilot experiment, using the same LB media solution and protocols. Plate streaking of the bacteria was periodically done. A day before inoculating the sown seeds, a single bacterial colony from the most recent streaked plate was picked and placed into an LB broth for overnight culturing using an orbital shaker (at 150 rpm) at 30°C. Using a portable spectrophotometer, the optical density of the bacteria was measured; and when the OD₆₀₀ was 0.8 (10⁸ cfu mL⁻¹), the bacterial inoculum was centrifuged down, washed, and serially diluted with Hoagland media to obtain a concentration of 10⁴ cfu mL⁻¹, ready for inoculation to the seeds.

2.2.2.4. Bacterial inoculation of Arabidopsis seeds

Two solutions were prepared for the inoculation of the sown seeds. One was the pre-prepared bacterial inoculum, corresponding to the PsJN-inoculated treatment, and the other was a plain Hoagland solution, as a mock inoculant for application to the control seeds. First, the plates were marked and assigned per treatment. They were then grouped and received the appropriate inoculation. Inoculation was done by pipetting 10 µL of either the PsJN-bacterial inoculum or the Hoagland solution into the seeds. Once all the seeds were inoculated, the holes were sealed with parafilm and the plates transferred to two separate growth or climate chambers.

2.2.2.5. Growth of plants in the climate chambers

The two groups of plant plates, PsJN-inoculated and control, were divided into two growth chambers with either ambient or heat-stress settings. The settings were: Temperature: 22 °C/

18 °C (ambient), 30 °C / 24 °C (heat stress) day/night; light intensity - 120-150 $\mu\text{mol m}^{-2} \text{s}^{-1}$; photoperiod - 16 hr/ 8 hr light/dark; humidity – 70%. To promote uniform lighting received by all plants, the light intensity on the plate level was measured using a photometer; and adjustments were made as necessary. The plates were laid vertically in covered racks that were designed and customized to different plate sizes as seen in Figure 2.1.3. The plants (i.e., holes at the top of the plates), were sealed with parafilm for six days to create a humid greenhouse environment for the establishing seedlings. After six days, the parafilm was removed and the seedlings were then able to grow naturally in the open air.



Figure 2.13 (Left to right) Rack designed for GrowScreen-Agar I (“Root Carousel”) customized plates (a) and re-adjusting some seedlings on the “open-top” system to grow directly outside of the holes (b). Some seeds managed to grow their plants under the plate, making them trapped and unable to expand their shoots. Other seedlings were stuck inside the agar so the use of a needle or tweezers was sometimes necessary. [Source: Images adapted and description modified from (Becker & Kastenholz, 2020).]

2.2.2.6. Plant phenotyping and data acquisition

While growing inside their respective growth chambers, the plates were periodically removed for imaging in the GrowScreen-Agar I. Plates were taken at the following intervals: 5, 7, 9, 12, 14, 16, 19, and 21 days after inoculation. Briefly, plates on racks were transferred to the area where the equipment was. The plates were individually inserted into the red cassettes that come with the GrowScreen-Agar I platform and placed consecutively following the initial marked “0” position, where the cameras were located and bound to start the imaging. The imaging of the plates was controlled by the settings in a computer dedicated to this platform.



Figure 2. 14 A sample customized plate being placed into a red cassette ready to be imaged by the GrowScreen-Agar I platform. [Source: Images adapted from (Becker & Kastenholz, 2020).]

2.2.2.7. Harvest

Three weeks after inoculation or sowing, a trial harvest was performed. Plant roots at this time were already well-branched and occupied the whole plate. Even a week earlier, the roots have already reached the bottom of the plates. Shoots were first cut from the plants and set aside. The plates were then opened and the roots were slowly removed from the surface and inside the agar by holding and pulling from the topmost part of the root. It was observed that the removal of the roots from agar was mostly challenging due to the small and fine root structure of *Arabidopsis* plants completely embedded in the agar, which accounted for considerable loss of root tissues during harvest. This challenge was addressed in the succeeding experimentation using the GrowScreen-Agar II.

2.2.2.8. Experimentation using the GrowScreen-Agar II platform

Except for the customization of plates, this platform utilized the same protocols as with the GrowScreen-Agar I for the cultivation of *Arabidopsis* plants and the culturing of PsJN bacteria. The same inoculation procedure was also followed, as well as the plant phenotyping protocols, although imaging was done with a different system. More specifically, the use of this platform and the methodology employed for addressing the second objective of the thesis were discussed in detail in Chapter 3. A series of experiments were conducted.

The main objective addressed by this platform was to characterize and quantify the bacteria-imparted growth promotion in *Arabidopsis* (root and shoot) plants under ambient and high-temperature conditions using the platform's imaging and root trait analysis software. Specific objectives were set, which also corresponded to the performed experiments.

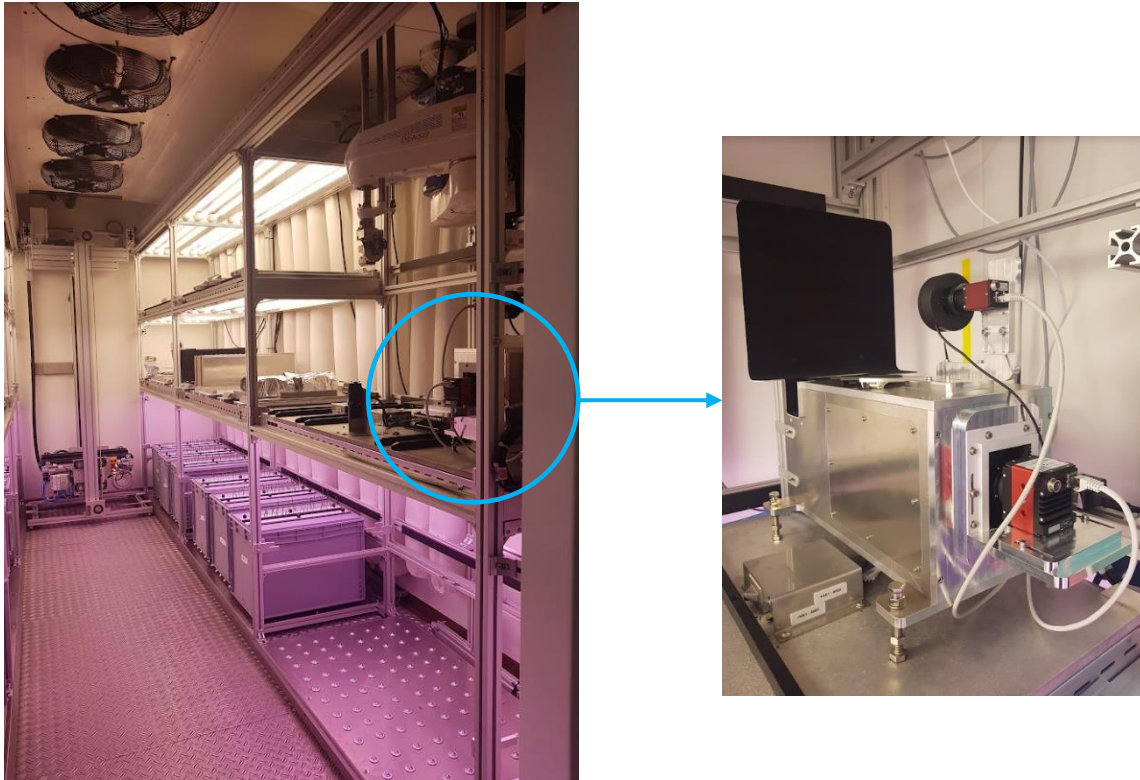


Figure 2. 15 Position of the imaging system within the GrowScreen-Agar II platform. Details and specifications of the system are illustrated in Chapter 3 and supplements.

2.2.2.8.1. First experimentation – Replicating the plant phenotypes

For the first experiment conducted using the GrowScreen-Agar II platform, the objectives were to 1) replicate the phenotype and growth promotion trends found in the previous experiments but on a larger scale to quantify significant effects of the bacteria, 2) determine the duration that the primary roots can grow up to the maximum size of the plate, and 3) determine the harvest time points of the plant tissues for lipid extraction. From this experiment, we were able to establish that 21 days was the maximum time before the roots of *Arabidopsis* start touching the bottom of the designed plates, with a maximum length of 20 cm). The phenotypes of bacteria-imparted growth promotion in plants were also replicated in this first experiment, which ascertained the beneficial effects of the PsJN bacteria. Furthermore, the root trait software also enabled the analysis of the roots down to the 1st and 2nd order lateral roots with higher accuracy. This is superior to the data analysis with WinRhizo, especially for plants at the later stage of development, where the root structures can be intricately entwined. Some notable issues found during this first experiment were the presence of contamination, mostly from fungi species, and the difficulty of removing the roots from agar that dried out.

2.2.2.8.2. Second experimentation – Testing repeatability and addressing contamination

Therefore, the second experiment was conducted with the aims of 1) verifying the repeatability of the phenotypes found in the first experiment using this system, 2) eliminating or reducing the contamination, 3) finding an optimized method to harvest roots from within the agar, and 4) to address the drying of agar at the end of the growth period. We found that the plant responses to bacterial inoculation in this experiment were even stronger than the first one. To address the contamination issue, each step of the entire process was traced back and the methods were performed with even more stringent protocols. Particular attention was placed on the surface sterilization of the seeds, where the disinfecting solutions were re-made fresh; as well as the sowing of seeds, which was then performed very carefully, with minimal hand movement across and above the plates, and avoiding foot traffic close to the biosafety cabinet. Removal of plates from the growth chamber and their transfer to the imaging system (within a growth chamber) was also minimized with a sealed container provided for transport. Unfortunately, the challenge of harvesting roots from agar was not yet addressed in this experiment, rather, in the next one. In the same way, addressing the drying of the agar, particularly on the top part of the roots, was planned in the next experiment.

2.2.2.8.3. Third experimentation – Root harvest optimization

The objective of the third experiment was to optimize the root harvest of *Arabidopsis*, to coax the roots growing inside the agar to come out towards the agar surface. To do this, instead of the pre-made customized racks or magazines that position the plates vertically, an angled metal rack was used. To be consistent with the system's design of roots being maintained in the dark, the plates were individually wrapped in sterile aluminum foil before placing them into the angled rack. The aluminum-covered plates were then placed into the racks set to about 45 to 60 degrees inclined towards the transparent side of the plates. One noticeable effect of the foil was the condensation at the bottom and on the surface of the plates. This brought the issue of contamination originating from the dripping side of the plates where some of the micropore tapes have come loose. This was addressed by carefully cleaning and meticulously disinfecting the bottom side of the plate before and after imaging. A week after the plates were placed in an inclined position, the roots were found growing on the surface of the agar.



Figure 2.16 Inclined plates to address the problem of harvesting roots growing inside the agar.

2.2.2.8.4. Last experimentation – Preventing agar drying

The last experiment was conducted to address the drying of the agar, mostly from the top area of the plate. Here the proposed solution was to double-seal the plate with micropore tape and to try agarose instead of agar. This was done, however, what worked best was filling the plate with the agar media up to its maximum capacity. There was still a reduction in the volume of the agar (thinning from the top), but at the end of the growing period, the thickness was still more than half its original size.

Finally, the system was optimized and the protocols were ready. Unfortunately, the pandemic happened and the final experiments for lipidomics analysis were not performed due to the University-wide call for overseas-based Melbourne students to return to Australia.

2.2.3. Optimization methods to replicate the “open-top” system of the GrowScreen-Agar II platform but utilizing the conventional agar-plate protocols (University of Melbourne)

Back at the University of Melbourne, when the lockdown and pandemic restrictions finally eased, replicating the “open-top” system while using the conventional square “closed-plate” resources was attempted. Since the protocols used at the Forschungszentrum Juelich for Arabidopsis and bacterial cultivation were already established, these were then used in the current experimentation. The objectives were to 1) customize the available plates to demonstrate an “open-top” feature, as with the plant cultivation in the GrowScreen-Agars, 2) perform imaging of the customized plates using the WinRhizo, 3) replicate the phenotype observed for the bacteria-induced plant growth-promotion, and finally, 4) grow the plants and harvest tissues for lipid extraction and analysis.

2.2.3.1. Optimization experiments replicating the open-top system at FZJ but using traditional plant cultivation materials

The first step was to customize the plates. Two sizes of square Petri plates were used, the small (120 x 120 cm) and large (124 x 124 cm) ones for trialing the system. Because the big plates were not available and the supply chain was affected by the pandemic, customization was first attempted on the small square plates. The goal was to make holes on the top part of the plate as with the FZJ protocol. No pneumatic drill was available in the laboratory so an alternative method of making holes was thought of. Using a metal stick and a gas burner, holes were melted on the top side of the bottom dish. Because of the burnt plastic smell and the fumes, this was performed inside a fumehood. Melting the plastic produced some clumped hardened residues. The holes were cleaned off the hardened plastic residues using a pair of long-nose pliers and were endeavored to be smoothed and rounded-shaped. As there was no available cutting wire for this plastic material, the lid was not cut, therefore, partially covering the melted holes from the bottom dish. Since the fumehood is not a sterile place for plant-microbe work, all the customized plates were then washed and dried, before being ethanol- and UV-sterilized in the biosafety cabinet. The Workshop facility of the university was closed at the time of this experiment due to the pandemic. Previous plant and bacteria cultivation protocols were then followed. Images of the growing plants and the plate set-up are illustrated in Figure 2.1.7.



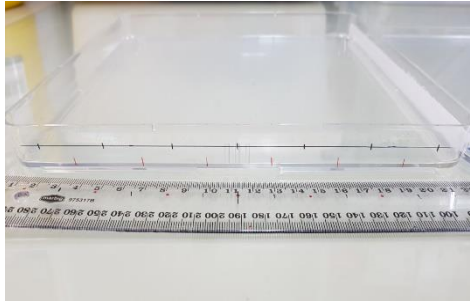
Figure 2. 17 Modified “open-top” system using customized square Petri plates and racks

Once the procedures for customizing the small plates were established, these were then transferred to the big plates (when they finally arrived). The workflow of the procedures, from preparing the plates to sowing and positioning them in the growth chamber, is summarized in

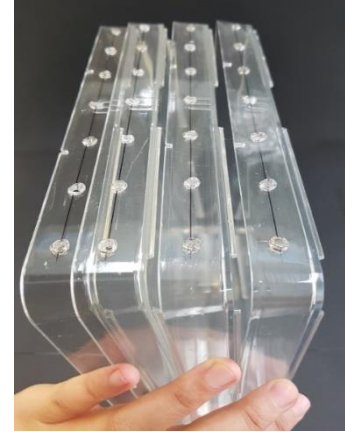
the figure below (Figure 2.1.8.). The protocols for the cultivation of plants and bacteria followed the previously established ones at the FZJ – from sections 2.2.2.2. (Preparation of the plant agar media and pouring into customized plates) to 2.2.2.7. (Harvest).



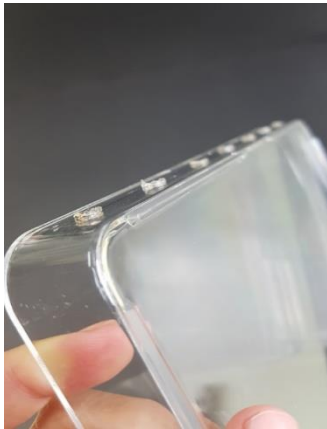
Determining the location of holes for unobstructed growth of plants



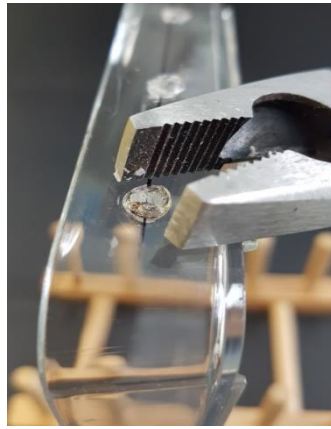
Determining the number of holes (seeds) per plate, measuring, and marking



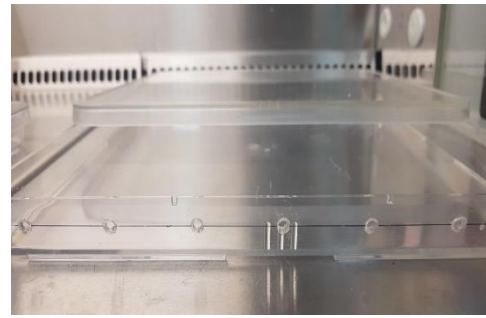
Making holes by melting using a gas burner and a small hot metal stick



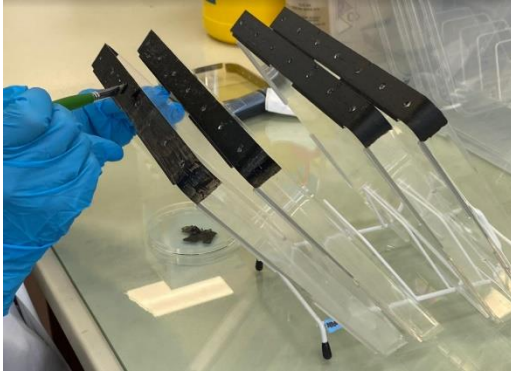
Removing melted plastic fibers/residues and smoothing the surface



Removing protruding burnt/melted plastic using a pair of pliers



Wasing and drying the plates, then sterilizing using ethanol and UV



Painting the top surface to maintain dark root condition throughout the plate



Pouring media, sealing all sides of the plate (except the top) with micropore tape



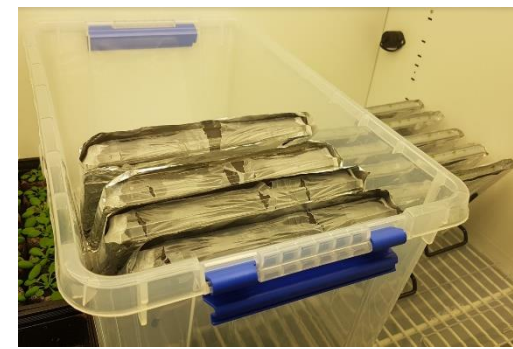
Sowing of individual seeds (after surface sterilization), then sealing with parafilm



Stratifying the seeds on the plates (placed inside a plastic container wrapped in foil) in the cold room for 5 days



Inoculating the seeds with bacteria; sealing the holes with parafilm, arranging the plates in the rack and checking for stability.



Plates/rack set-up placed inside container and into the growth chamber (to prevent contamination and for easy transport).

Figure 2. 18 Plate customization and plant-bacteria cultivation in a modified “open-top” system.

2.2.3.2. Final experiments reverting to the traditional “closed-plate” growing system but using the plant-bacteria cultivation protocols established at the FZJ

Although the customization of the plates worked and the protocols for cultivation were adapted, this system, however, did not work with the phenotyping and imaging equipment on hand. Because of the thickness of the plate and the agar (plates were filled with agar up to maximum capacity) and due to extreme condensation on the surface of the plates, imaging of the roots was made challenging. Moreover, placing the plates horizontally on the scanner of the WinRhizo, as well as closing the lid, was damaging to the shoots growing outside of the plates. As a result, it was decided that the design be reverted to the original “closed-plate” system, while still utilizing the existing plant and bacteria cultivation protocols for the “open-top” system.

The final experiment conducted at the University of Melbourne was aimed at harvesting root tissues for lipid extraction and lipidomics analysis. The tissues were harvested according to the time points previously determined with experiments at the FZJ, which were at 7, 14, and 21 days after inoculation. Moreover, the protocols used for growing *Arabidopsis* plants, for culturing the bacteria PsJN, and their co-cultivation in the chosen sterile system, were the ones already established from the experimentation using the GrowScreen-Agar II platform. To account for the longer root development (and longer phenotyping of plant root-bacterial interactions), the big plates, which were twice the size of the traditional small square Petri plates, were used. The plants were grown entirely inside the agar plates throughout their growth and development, with or without the presence of the PsJN bacteria, and on either ambient or high-temperature conditions.



Figure 2. 19 *Arabidopsis* plants in an open plate and corresponding image from WinRhizo

CHAPTER 3

**Plant growth promotion and heat stress
amelioration in *Arabidopsis* inoculated with
Paraburkholderia phytofirmans PsJN rhizobacteria
quantified with the GrowScreen-Agar II
phenotyping platform**

Preface to Chapter 3

This chapter characterizes and quantifies the dynamics of the growth-promotion and heat tolerance imparted by the bacteria *Paraburkholderia phytofirmans* PsJN to Arabidopsis plants. Specifically, this describes the time- and tissue-specific morphological changes in bacterized plants, using the *state-of-the-art* non-invasive, high-resolution plant phenotyping and imaging platform - GrowScreen-Agar II. This platform is designed with an “open-top” plant cultivation system that allows for shoot growth outside the plate while roots are maintained in the dark, an imaging system that allows for simultaneous capture of shoot (top and front) and root images, and associated root (GrowScreen-Root) and shoot (Colour segmentation) analysis software.



Figure 3. 0 Graphical abstract of the article (used as the issue cover for the journal Plants entitled Hi-Res Root Phenotyping of Bacteria-Ameliorated Plant Response to Heat)

This work has been published in the journal *Plants* with the title “Plant growth promotion and heat stress amelioration in *Arabidopsis* inoculated with *Paraburkholderia phytofirmans* PsJN rhizobacteria quantified with the GrowScreen-Agar II phenotyping platform” (Macabuhay, A., Arsova, B., Watt, M., Nagel, K. A., Lenz, H., Putz, A., Adels, S., Müller-Linow, M., Kelm, J., Johnson, A. A. T., Walker, R., Schaaf, G., & Roessner, U. (2022). Plant Growth Promotion and Heat Stress Amelioration in *Arabidopsis* Inoculated with *Paraburkholderia phytofirmans* PsJN Rhizobacteria Quantified with the GrowScreen-Agar II Phenotyping Platform. *Plants*, 11(21), 2927. <https://doi.org/https://doi.org/10.3390/plants11212927>). It is presented in Chapter 3 in the publication format. I performed 60% of the work, which includes growing the plants and bacteria, optimizing the co-cultivation system, periodic imaging and phenotyping, harvest, analyzing and interpreting the data, and significantly contributed to the writing of the manuscript.

As published in *Plants* (2022)

Plant growth promotion and heat stress amelioration in *Arabidopsis* inoculated with *Paraburkholderia phytofirmans* PsJN rhizobacteria quantified with the GrowScreen-Agar II phenotyping platform

Allene Macabuhay^{1,2,3}, Borjana Arsova^{2*}, Michelle Watt¹, Kerstin A. Nagel², Henning Lenz², Alexander Putz², Sascha Adels², Mark Müller-Linow², Jana Kelm², Alexander A. T. Johnson¹, Robert Walker¹, Gabriel Schaaf³, Ute Roessner^{1,4}

¹ School of BioSciences, University of Melbourne, Parkville, VIC, 3010, Australia

² Institute for Bio- & Geosciences (IBG-2), Plant Sciences, Forschungszentrum Juelich GmbH, 52425 Juelich, Germany

³ Institute of Crop Science and Resource Conservation, Department of Plant Nutrition, University of Bonn, 53115 Bonn, Germany

⁴ Research School of Biology, The Australian National University, Acton, ACT, 2601, Australia

* Correspondence: b.arsova@fz-juelich.de

Abstract

High temperatures inhibit plant growth. A proposed strategy for improving plant productivity under elevated temperatures is the use of plant growth-promoting rhizobacteria (PGPR). While the effects of PGPRs on plant shoots have been extensively explored, roots – particularly their spatial and temporal dynamics, have been hard to study, due to their below-ground nature. Here, we characterized time- and tissue-specific morphological changes in bacterized plants, using a novel non-invasive high-resolution plant phenotyping and imaging platform - GrowScreen-Agar II. The platform uses custom-made agar plates, which allow air exchange

with the agar medium and enable the shoot to grow outside the compartment. The platform provides light protection of roots, exposure of shoots, and non-invasive phenotyping of both organs. *Arabidopsis thaliana*, co-cultivated with *Paraburkholderia phytofirmans* PsJN at elevated and ambient temperature, showed increased length, growth rate, and number of roots. However, the magnitude and direction of growth promotion varied depending on root type, timing, and temperature. Root length and distribution per depth and time was also influenced by bacterization and temperature. Shoot biomass increased at the later stages under ambient temperature in bacterized plants. The study offers insights into the timing of tissue-specific, PsJN-induced morphological changes and should facilitate future molecular and biochemical studies on plant-microbe-environment interactions.

Keywords

Plant growth-promoting rhizobacteria (PGPR), *Paraburkholderia phytofirmans* PsJN, Phenotyping, Root morphology, Root system architecture, High temperature, *Arabidopsis thaliana*, Growth stimulation, Heat tolerance

3.1 Introduction

Plants are constantly challenged by an array of biotic and abiotic constraints that limit their growth and productivity. These include environmental stresses such as drought, flooding, extreme temperatures, metal toxicity, and nutrient deficiency, as well as exposure to phytopathogens and herbivorous insects (Gupta & Pandey, 2019).

Climate-related changes, in particular rising global temperatures, are a serious environmental challenge and of major concern for future crop production. Temperature plays essential roles in all stages of plant development and any exposure outside the optimal range can be stressful or lethal (Barnabas et al., 2008) Plant responses to cope with heat stress vary with the intensity and duration of elevated temperatures (Hasanuzzaman et al., 2013). Aside from directly affecting plants, increased global temperatures also aggravate other existing abiotic stressors such as salinity, drought, or mineral toxicity (Wahid et al., 2007). Two general mechanisms for surviving high temperature conditions are employed by plants. Thermomorphogenesis (responses at moderately high temperatures, (Fonseca de Lima et al., 2021)) induces short-term avoidance, e.g., the elongation of primary roots in search of cooler

soil area and water (Illston & Fiebrich, 2017; Laha et al., 2022; Martins et al., 2017) or acclimation, e.g., changing leaf orientation and transpirational cooling through elongation of the hypocotyl, petioles, and leaves (Casal & Balasubramanian, 2019; Jin & Zhu, 2019; Quint et al., 2016). On the other hand, plants can respond with long-term evolutionary phenological and morphological adaptations (Bohnert et al., 2006; Vinocur & Altman, 2005), associated with heat stress. Heat stress occurs when the rise in temperature for a certain duration exceed a specie-specific threshold level (Barnabas et al., 2008) that is sufficient to cause irreversible damage to plant growth (Wahid et al., 2012).

Plant morphological responses to elevated temperatures are very dynamic (Bucksch et al., 2017). Developmentally, these growth parameters are revealed over the lifetime of a plant through various cellular processes, e.g., cell division, cell expansion, and anisotropic growth (Bucksch et al., 2017; Niklas, 1994). While high temperatures have diverse morphological effects on aboveground plant tissues, such as scorching of the twigs and leaves along with visual symptoms of sunburn, senescence of leaves, growth inhibition, and discoloration of fruits (Vollenweider & Günthardt-Goerg, 2005), belowground, they also cause significant modifications to the root system (Calleja-Cabrera et al., 2020). Moderately elevated temperature leads to root elongation, but this effect stops around 30°C, after which root length decreases (Yang et al., 2017). This is reflected in decreased root growth rate, decreased meristematic zone at 30°C compared to 20°C or 25°C, and decreased number of cells in the elongation zone of the root. Root grown at 30°C also have smaller radii than roots grown at 20-25°C (Yang et al., 2017). Furthermore, another strategy in the RSA to cope with increasing temperatures is the increase in number and length of root hairs, which enhances the root surface area for improved soil exploration of water and nutrients (Pregitzer et al., 2000).

Elevated temperatures often have cumulative effects which result in poor plant growth and performance (Wahid et al., 2007). Consequently, we require novel approaches to mitigate the plant stress response and meet agricultural goals under elevated temperatures (Fahad et al., 2017). Several strategies are already in practice to develop heat-tolerant crop plants, including conventional crop breeding and genetic engineering approaches (Shanmugavel et al., 2020; Verma et al., 2020). The use of plant growth promoting rhizobacteria (PGPR), in addition to the above, is another strategy that can contribute to agricultural sustainability. (Maitra et al., 2021; Sarker et al., 2021).

Unlike obligate symbionts, PGPR can interact with numerous hosts and improve plant health and stress tolerance through a multitude of mechanisms (Adesemoye et al., 2009; Asseng et al., 2015; Ferguson & Mathesius, 2014). PGPR are capable of modulating the root system

architecture (RSA), which can significantly affect crop performance and productivity (Ogawa et al., 2014; Schillaci, Arsova, et al., 2021; Shanmugam et al., 2013). RSA refers to the integrated root system topology, the spatial distribution of the primary and lateral roots, and the number and length of various root types. The RSA is modified by PGPR mainly through their ability to interfere with plant hormonal balance and processes (Vacheron et al., 2013). The implication of the species-specific production of phytohormones, secondary metabolites, and enzymes, leads to changes in the growth rates of primary roots, branching of lateral roots, and density of root hairs (Sukumar et al., 2013; Vacheron et al., 2013).

In the present context of rising global temperatures, it is useful to study PGPRs which also have thermotolerant traits. In the past, several thermotolerant microbial strains were identified (Maitra et al., 2021; Meena et al., 2017), including *Burkholderia phytofirmans* (Bensalim et al., 1998). *Paraburkholderia*, a more recently described genus delineated from *Burkholderia* contains many species that assist plant growth (Esmaeel et al., 2018; Sawana et al., 2014). *Paraburkholderia phytofirmans* PsJN is a well-studied model PGPR that is known to induce tolerance to both biotic and abiotic stresses. This beneficial bacterial endophyte is capable of colonizing a wide range of plants including wheat (Naveed et al., 2014), maize (Naveed et al., 2015), grapevine (Compant et al., 2005), tomato (Pillay & Nowak, 1997), and potato (Bensalim et al., 1998). Its plant-beneficial effects are attributed to several mechanisms including the production or modulation of plant phytohormones (Pieterse et al., 2012), facilitation of resource acquisition (Naveed et al., 2014), production of siderophores and secondary metabolites (Esmaeel et al., 2018), and induction of systemic resistance (ISR) (Miotto-Vilanova et al., 2016). PsJN has been used in different plant studies against drought, low temperature, and salinity (Ait Barka et al., 2006; Nafees et al., 2018; Naveed et al., 2014). Generally, PsJN has increased root biomass in maize, potato, Brassica, and switchgrass; in the latter two also promoting root elongation. It has also been shown to increase the number of root hairs in several species including *Arabidopsis* (Poupin et al., 2013). To our knowledge, however, only two studies to date have utilized this bacterium to protect against high-temperature stress and focused on genotypic responses of potatoes (Bensalim et al., 1998) as well as physiological and biochemical changes in tomato aerial tissue (Issa et al., 2018). In potato (Bensalim et al., 1998), PsJN generally increased the root dry weight of 18 potato clones, compared to non-bacterized plants at elevated temperatures. To our knowledge, the question of adaptation of the root system architecture to elevated temperatures when plants are bacterized with PsJN is still open.

Quantifying plant growth dynamics requires non-invasive phenotyping on the same plant individuals through time. While multiple approaches exist for the aerial part of the plant, roots represent a particular challenge due to their hidden nature (inherently soil). Earlier investigations of plant roots and their interactions with microorganisms only utilized destructive measurements or harvest samplings (e.g. (Casanovas et al., 2002)). Destructive approaches discriminate and fail to capture the diverse growth patterns and dynamics within a plant's ontogeny. To enable an ontogenetic and non-destructive approach, several phenotyping platforms have been employed in plant studies to characterize root traits (Tracy et al., 2020). Now, non-invasive, time-resolved phenotyping is becoming more common to plant root-microorganism processes (Kuang et al., 2022; Schillaci, Arsova, et al., 2021).

Root phenotyping pipelines consist of a plant growth system, root imaging, and root trait digitization (Takahashi & Pradal, 2021). A traditional plant cultivation practice to quantify root growth parameters is the use of a transparent medium such as agar gels (Nagel et al., 2020). Since manual measurements of root traits of agar-grown plants are labor- and time-intensive, there is a necessity for increasing throughput. This is addressed with the use of camera- or scanner-based imaging with varying degrees of automation (Nagel et al., 2020), such as the use of multiple scanners operating in parallel (Adu et al., 2014; Slovak et al., 2014) or the use of a shifting camera operated by moving stages or a robotic gantry system (Men et al., 2012; Nagel et al., 2012; Subramanian et al., 2013). Here we used the 2D imaging system of the novel GrowScreen-Agar II platform and associated image analysis software tools, specifically designed for high-throughput and non-destructive phenotyping of root and shoot development through time. This platform also includes an optimized agar-plate cultivation with the shoots growing outside the plate with the roots kept in the dark to avoid light-related responses, while providing air exchange to the agar surface (Cabrera et al., 2022). Moreover, the GrowScreen-Agar II allows for the observation of plant responses subjected to one or more environmental factors.

This study quantifies the growth stimulation imparted by the plant growth-promoting rhizobacteria *P. phytofirmans* PsJN through the investigation of morphologic and dynamic responses of *Arabidopsis* roots and shoots measured in a three-week period. Additionally, this study examines how the application of the beneficial rhizobacteria can ameliorate the detrimental effects of constant high temperature. In doing so, we provide novel insights on time-specific phytomorphological responses to bacterial inoculation, which enhance the growing knowledge on PGPRs for application in agriculture under future high-temperature

climate conditions. Finally, we describe the technology that can drive knowledge generation by encompassing plant developmental dynamics in plant-microbe-environment interactions.

3.2. Results

3.2.1. Increased plant growth and higher plant biomass at 21 days post-inoculation with bacteria PsJN in a “closed-plate” system

Our pilot experiment utilizing the traditional closed-plate system showed that PsJN promote growth and heat tolerance to *Arabidopsis* plants. For control plants, high temperature resulted in a decrease of total root length, with a reduction ranging from 21% (at 2 DAI) to 76% (at 21 DAI) (Figure S1a). When the total root length was discriminated into primary and branched root components, we found a similar decline in the root lengths by high temperature. Primary root lengths showed a reduction between 21% and 48%, while branched roots showed a higher reduction of 52% to 77% from 2 to 21 DAI, indicating the strong effect of high temperature on the latter root types (Figure S1b, S1c).

Although increased temperature showed detrimental effects on the root lengths, this was ameliorated by the inoculation with PsJN, the magnitude of which varied in the root types. At 21 DAI and high temperature, PsJN-inoculated plants showed 123% increase in total root lengths compared to control plants (Figure S1a). Interestingly, although this positive bacterial inoculation effect on the primary root was strong at the start (at 52%), this declined towards the end of the growing period. Branched roots also showed the same decreasing inoculation effect, from 225% to 136% (Figure S1b, S1c). Under ambient temperature at 21 DAI, bacterial inoculation increased the total root lengths by 37% from control plants, mainly observed from the branched roots. However, this positive effect of bacterial inoculation on the total root lengths under ambient temperature, was 3.3 times lower compared to its effect under high temperature (Figure S1a).

Root and shoot weights were reduced by high temperature compared to ambient temperature (at 50% and 20% reduction, respectively) (Figure S1d, S1e). Bacterial inoculation minimized this reduction under high temperature by increasing the root weights by 6% and shoot weights by 5% compared to control plants. However, a stronger effect of bacterial inoculation was observed under ambient temperature, with an increase of 42% and 16% for root and shoot weights, respectively (Figure S1d, S1e).

The conventional “closed-plate” system, coupled with the WinRhizo imaging platform, allowed plant-bacteria co-cultivation and periodic imaging and trait analysis (Figure S2). However, this system did not allow the natural growth of shoots and roots, but instead enclosed the whole plant inside the plate, providing restrictions on plant development. In addition, the software analysis tool was not sensitive enough to accurately discriminate the higher order root types (1st and 2nd order lateral), particularly at the later stages of root growth. Moreover, it did not enable saving previously analyzed root structures to be appended for succeeding growth stage analysis, which provides a more efficient and accurate way of monitoring root morphologic growth.

3.2.2. In-depth root characterization shows PsJN-imparted growth promotion on root system architecture (RSA) as influenced by temperature and time

The GrowScreen-Agar II platform addressed all of the issues of the traditional “closed plate” approach. First, the customized plates for the imaging system allowed the unobstructed growth of the rosette and the inflorescence (Figure 1a) due to the open holes. The plates were custom-made for the imaging system for consistent plant positioning which is critical for consequent imaging and image superimposition during analysis. The infrared light used for root imaging prevented disturbance or damage to the root tissues. The depth of the system was increased by almost 100% from the closed plates to a maximal 20 cm depth. As a result, Arabidopsis plants grew well, simulating the unobstructed upward growth of the shoots exposed to light and air, and the undisturbed downward growth of the roots in the dark. The dark environment ensured that no skewing occurred during the gravitropic growth process (Figure 1b). Second, with the associated image analysis software, Colour segmentation tool (shoot) and GrowScreen-Root (root), several traits were quantitatively measured; in particular for the roots, which are normally challenging in a time course study (Figure 1c). The GrowScreen-Agar II platform also provided an opportunity to further investigate the architecture of the root system by separating the branched roots into 1st and 2nd order lateral roots and by measuring other quantifiable spatial and temporal parameters highlighting the effects of bacteria under two different temperatures. The platform is suitable for plant-microbe interaction studies, as we could confirm that PsJN inoculated at the germinated seed, was also found in the root-tip regions of 21-day old plants (Figure S2), at the same time the plates looked clean and did not show colony growth on the agar (Figure S3).

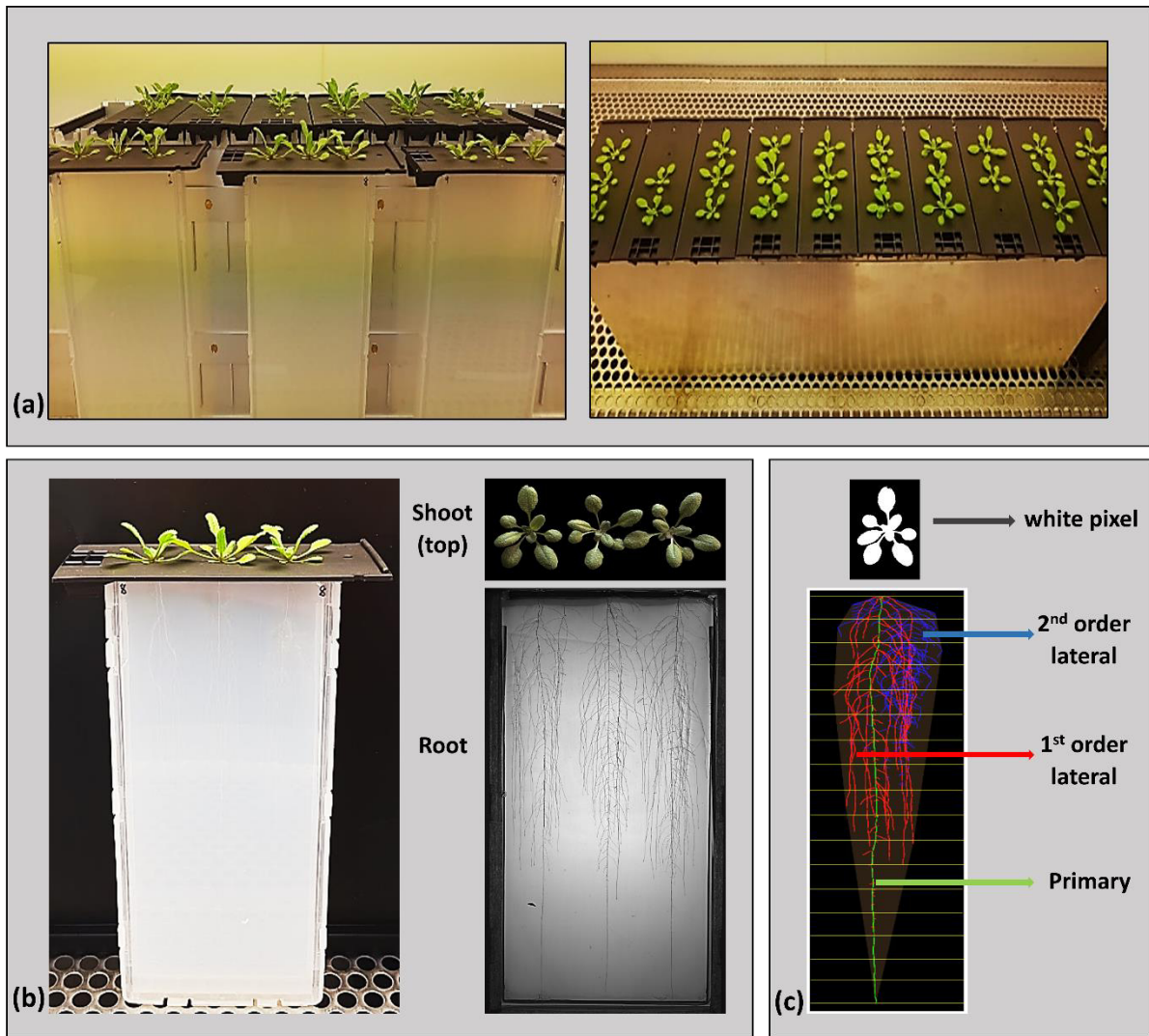


Figure 3. 1 GrowScreen-Agar II: Plant cultivation setup and root/shoot image acquisition and analysis. a) Arabidopsis plants growing in customized plates and magazine (product specification on Figs. S1 and S2, respectively). Black plate collars provide the background for the growing shoots outside of the plates while at the same time, they exclude light entering the top of the metal magazine (bottom panel) to provide dark environment for the roots. b) Overview of a single plate that is manually transferred to an imaging system (Fig. S3) equipped with cameras for imaging the shoots and the roots, generating two images: top view of the shoot(s) and the whole root system. c) (Top) Analysed image of a rosette using the Colour segmentation tool that computes the sum of white pixels as a proxy to compute the projected leaf area (Müller-Linow, 2022). (Bottom) Analysed image of a root system using the GrowScreen-Root (Nagel et al., 2020). Different root types are distinguished by colour: green for primary roots, red for 1st order lateral roots, and blue for 2nd order lateral roots. The whole image area can also be divided horizontally into several sections to extract root length density per layer.

High temperature decreased the **total root lengths** by 63% from ambient temperature, although with inoculation, the decrease was smaller at 43% (Figure 2a). PsJN application

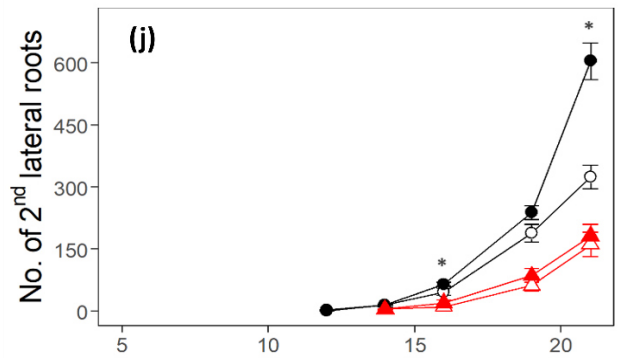
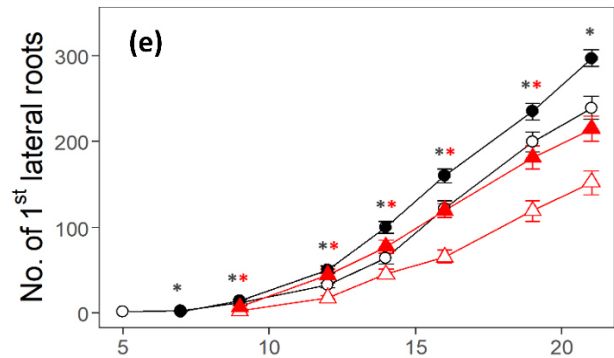
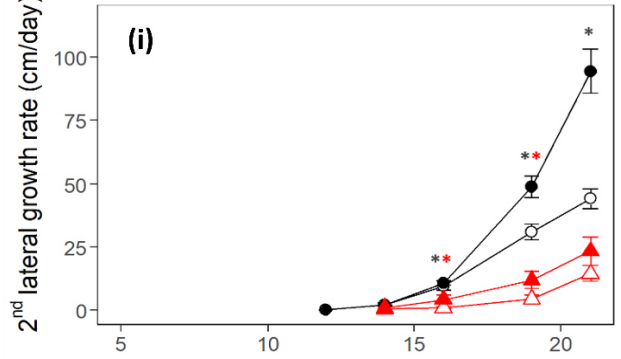
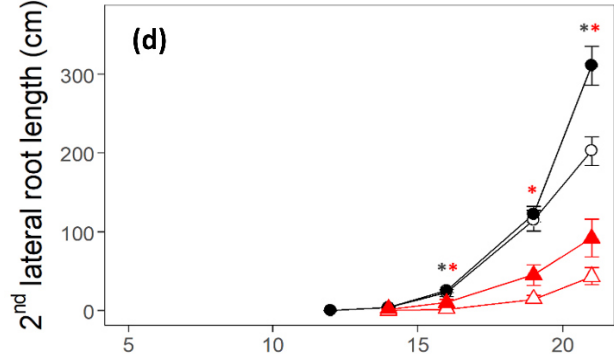
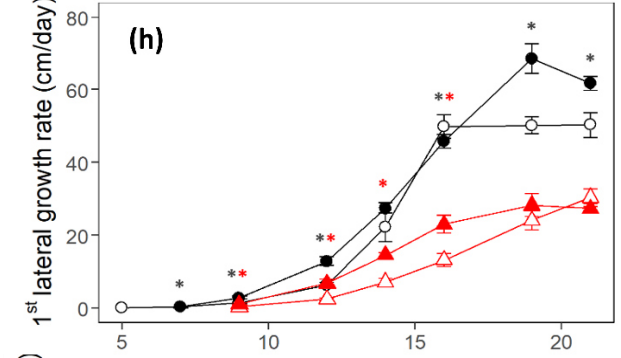
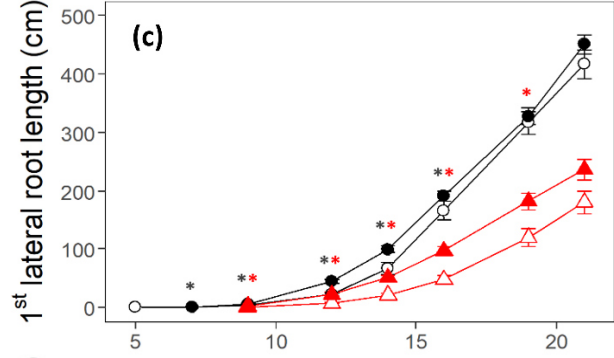
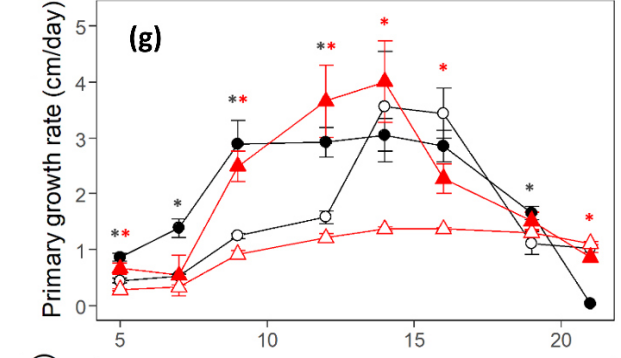
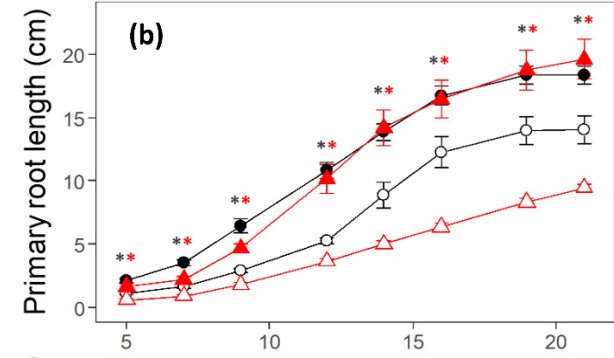
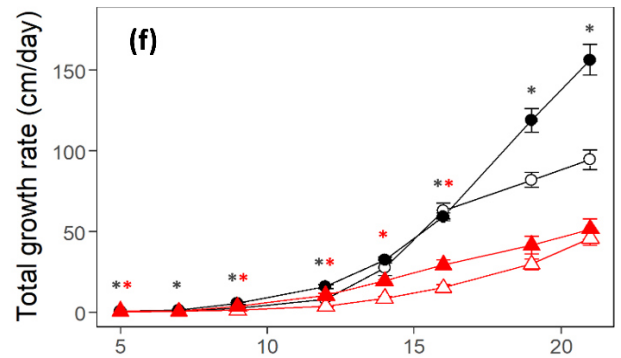
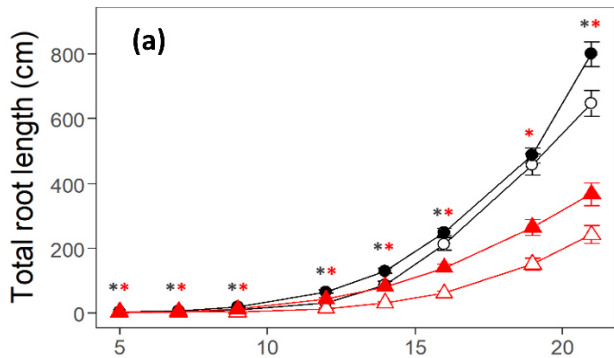
increased the total root lengths of plants under both ambient and high-temperature conditions, and this was shown consistently from 5 DAI up to 21 DAI (Figure 2a). The difference between inoculated and control plants peaked at 12 DAI by 103% for ambient and 202% for high temperature, before slowly dropping afterward. At the end of the growing period under high temperature, bacterial inoculation increased the total root lengths by 52% from control plants. This was twice more than the increase observed under ambient temperature (Figure 2a, Table S1). **Total root growth rates** also indicated the same trend, with high temperature causing a 51% reduction from ambient temperature (Figure 2f). Under high temperature, inoculated plants performed better than control plants with an increase of 178% to 227% from 5 to 9 DAI. On the other hand, this effect was lower at 92% to 121% under ambient temperature. Subsequently, the difference in the growth rates of inoculated and control plants declined such that at 21 DAI, inoculated plants displayed only a 65% and 12% increase on ambient and high temperature, respectively (Figure 2f, Table S1).

To better understand the RSA, we analyzed the roots according to their root types. **Primary roots** were negatively affected by temperature, with high temperature causing an average **length** reduction of 41% from ambient temperature throughout the growth period (Figure 2b). Primary roots also responded to bacterial inoculation at both temperature regimes with varying magnitude. Under high temperature, the primary root lengths of inoculated plants maintained an average increase of 154% from control plants; while at ambient temperature, the stimulation effect of the bacteria decreased from 121% after 9 DAI (Figure 2b). At the end of the growing period, the difference in the primary root lengths between inoculated and control was 3.5 times higher under high temperature (107%) than in ambient condition (31%). Furthermore, under ambient condition, the development of primary roots of both inoculated and control plants, plateaued after 19 DAI (maximal length of 20 cm as with the plate size), whereas, both inoculated and control plants showed a linear increase until the end of the experiment under high-temperature conditions (Figure 2b, Table S1). **Growth rates of primary roots** also showed a response to temperature, with high temperature causing an average reduction of 43% from ambient temperature (until 16 DAI) (Figure 2g). Bacterial inoculation under high temperature countered this through the stimulation of an increase in primary root growth rates up until 14 DAI, before root growth rates rapidly declined. Under ambient condition, bacterial application also increased the primary root growth rates; however, the growth rates of inoculated plants did not change from 9DAI until 14 DAI, when they started declining (Figure 2g, Table S1).

The deleterious effect of high temperature was especially evident in the **length of the 1st order laterals** (from 9 to 21 DAI), with heat-stressed plants showing an average reduction of 70% from ambient plants (Figure 2c). Inoculated plants showed an increase in the length of the 1st order laterals under high temperature. This inoculation effect was present throughout the growth period, although the stimulation effect declined right from the onset of growth (from 584% to 31%). Under ambient condition, in the beginning, there was increased growth until 12 DAI (103%), after which the stimulation decreased (Figure 2c, Table S1). High temperature caused a decrease in the **growth rates of the 1st order lateral** roots from ambient temperature with an average of 65% (Figure 2h). The increase in growth rates of inoculated plants at high temperature was 584% at 9 DAI, but that declined down to 17% at 19 DAI (Table S1). Control plants, however, showed continuous linear growth rates. At ambient temperature, PsJN-inoculation caused an increase in growth rates from control plants up until 12 DAI (by 103%), then declined afterward. Whilst control plants showed increasing growth rates until 16 DAI when their growth rates became constant, inoculated plants showed an almost linear growth up until 19 DAI before their growth declined (Figure 2h). The **number of 1st order lateral roots** was reduced by high temperature with an average of 47% from ambient condition (Figure 2e). Bacterial inoculation also influenced the number of the 1st order laterals, with increases from control plants starting at 9 DAI: 275% under high temperature and 32% under ambient temperature. At the end of the growing period, the difference in the number of 1st order lateral roots between inoculated and control plants under high temperature was twice that of ambient temperature. This illustrates the strong involvement of bacteria PsJN in the emergence of these root parts at both temperatures (Figure 2e, Table S1).

Upon emergence of 2nd order lateral roots, high temperature caused a reduction of 95% (6.5 cm) in the length of these root types, which decreased to 79% (308 cm) at 21DAI (Figure 2d). The positive effect of inoculation under high temperature (from 16 DAI) led to about 6.5 times higher **2nd order lateral root lengths** than control plants (at 9.7 vs. 1.5 cm). At the same timepoint, this bacterial stimulation effect was weaker under ambient temperature, with inoculated plants (25 cm) only about 1.1 times higher than control plants (22.5 cm). At the end of the growing period, the absolute difference in the 2nd order lateral root lengths between heat-stressed inoculated and control plants was 48.5 cm, while under ambient, it was 108.5 cm (Figure 2d, Table S1). High temperature significantly reduced the **2nd order lateral root growth rates**, although this negative effect weakened in time (Figure 2i). At 14 DAI, high temperature caused a reduction of about 18.5 times, whilst at 21 DAI, this reduction was only three times from ambient. Throughout the growing period, the growth rate stimulation by the

bacteria decreased under high temperature (from 8.3 down to 1.6 times), while it was doubled under ambient. At 21 DAI, ambient-grown plants have the highest growth rates of 2nd order laterals, with inoculated and control plants at 94 and 44 cm/day, while heat-stressed plants have 23 and 14 cm/day, respectively (Figure 2i, Table S1). Similarly, the **number of 2nd order lateral roots** was also decreased by high temperature, by 7 times (14 DAI) to 2 times (21 DAI) from ambient temperature (Figure 2j). Surprisingly, the effect of bacterial inoculation was only significant under ambient temperature (16 and 21 DAI). In the end, the positive effect of bacterial inoculation on this root type was quite apparent under ambient with an 86% increase than control. This difference between inoculated and control is about seven times more than in high-temperature condition at 12% (Figure 2j, Table S1).



○ Amb-Ctl ● Amb-PsJN △ HT-Ctl ▲ HT-PsJN

○ Amb-Ctl ● Amb-PsJN △ HT-Ctl ▲ HT-PsJN

Figure 3. 2 Morphological traits of different root types. Traits were measured from plants with or without bacteria PsJN inoculation under ambient or high temperature conditions from 5 to 21 days after inoculation (DAI) in the GrowScreen-Agar II platform. Root lengths: a) total, b) primary, c) 1st order lateral roots, d) 2nd order lateral roots; Growth rates: f) total, g) primary, h) 1st order lateral roots, i) 2nd order lateral roots; Number of lateral roots: e) 1st order lateral roots, j) 2nd order lateral roots. Temperature - black and circle symbol (ambient), red and triangle symbol (high temperature); Bacterial application – empty symbol (control), filled symbol (PsJN-inoculated). Treatments: Amb-Ctl (control plants under ambient), Amb-PsJN (PsJN-inoculated plants under ambient), HT-Ctl (control plants under high temperature), and HT-PsJN (PsJN-inoculated plants under high temperature). All points are the mean \pm standard error of n= 12 (Amb-Ctl), 15 (Amb-PsJN), 12 (HT-Ctl), 8 (HT-PsJN) samples within each treatment. Asterisks: Black – significant difference between mean of PsJN-inoculated and control plants under ambient condition, red - significant difference between mean of PsJN-inoculated and control plants under high temperature condition, based on the Student's t-test with $p < 0.05$.

3.2.3. High temperature negatively impacts the root system distribution, but PsJN buffers this effect through improvements on individual root types

The two temperature regimes showed clear differences in root system distribution, with ambient-grown plants showing greater depths than heat-stressed plants (Figure 3a). In general, high temperature prevented the downward elongation of the roots, causing an average reduction of 28% from ambient temperature. The difference between the two temperature regimes, i.e., Amb-Ctl and HT-Ctl, decreased after 16 DAI, which can be attributed to the faster growth rates of the primary and 1st order lateral roots under ambient temperature (Figure 2g, 2h) that became constant towards the last two timepoints, presumably due to the limitation of the plate. In addition, the slower but continuous growth, particularly the linear growth of the 1st order lateral roots under high temperature (Figure 2g, 2h) towards the end of the growing period also reduced the difference in the depths of heat-stressed and ambient-grown roots (Figure 3a). High temperature also reduced the convex hull area and branching angle of the root system by an average of 69% and 27%, respectively (Figure 3c, 3d). The reduction in the root system width by high temperature may be attributed to the responses of the 1st and 2nd order lateral roots (Figure 2c, 2d, and 2h, 2i), which influence the horizontal extension of the root system. Moreover, the decrease in the number (Figure 2e, 2j), length (Figure 2c, 2d), growth rate (Figure 2h, 2i), and the angle of growth (Figure 3d) of these lateral roots may have contributed to the huge difference between the root system width of heat-stressed and ambient-grown plants (Figure 3b).

In general, the effect of bacterial inoculation only manifested at 16 DAI under ambient temperature on the overall root system depth (Figure 3a), width (Figure 3b), and branching

angle (Figure 3d) (Figure 3a, 3b). Whilst bacterial effects in these cumulative root traits were not found, it could be because there was compensation between the various root types and root traits (Fig. 2). The convex hull area showed a significant bacterial effect under ambient at 7, whereas this effect was evident under high temperature from 5 to 9 DAI (Figure 3c).

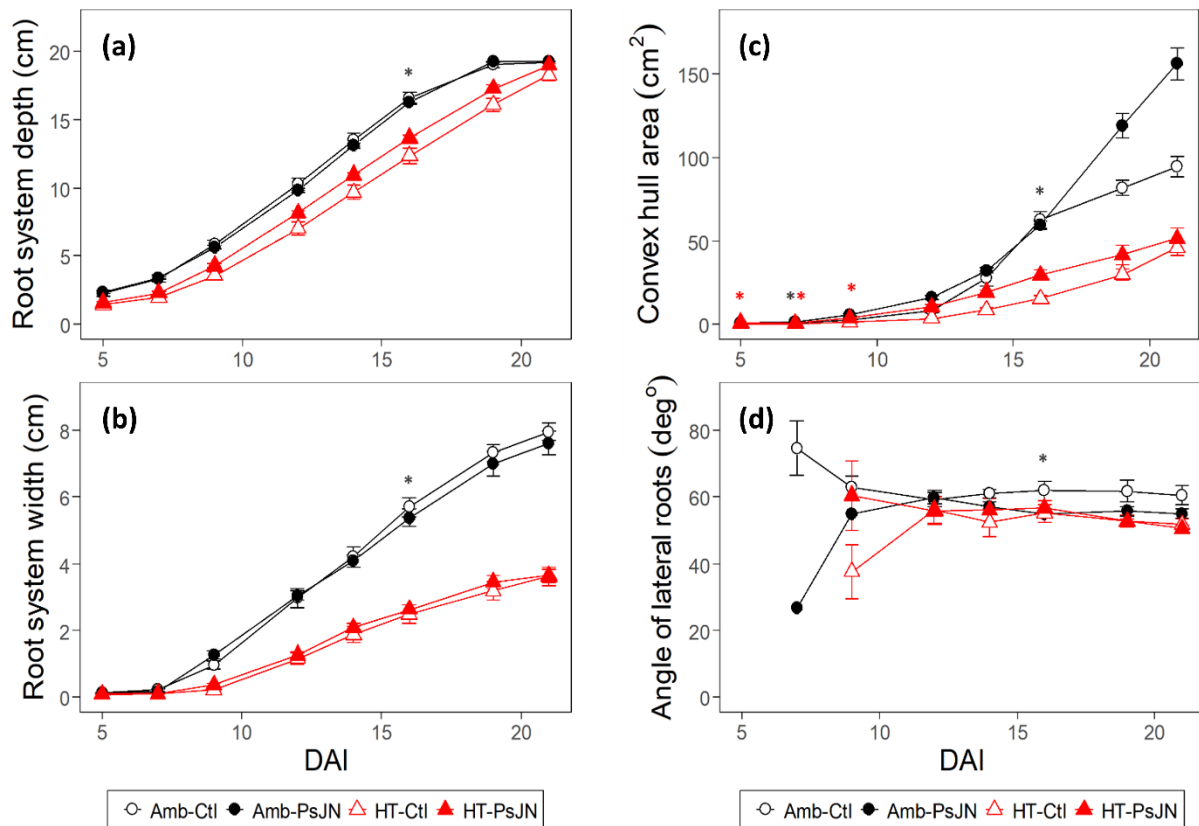


Figure 3.3 Root system morphological traits. Traits were measured from plants with or without bacteria PsJN inoculation under ambient or high temperature conditions from 5 to 21 days after inoculation (DAI) in the GrowScreen-Agar II platform. a) Root system depth, b) root system width, c) convex hull area, and d) branching angle of 1st order lateral roots. Temperature - black and circle symbol (ambient), red and triangle symbol (high temperature); Bacterial application – empty symbol (control), filled symbol (PsJN-inoculated). Treatments: Amb-Ctl (control plants under ambient), Amb-PsJN (PsJN-inoculated plants under ambient), HT-Ctl (control plants under high temperature), and HT-PsJN (PsJN-inoculated plants under high temperature). All points are the mean \pm standard error of $n=12$ (Amb-Ctl), 15 (Amb-PsJN), 12 (HT-Ctl), 8 (HT-PsJN) samples within each treatment. Asterisks: Black – significant difference between mean of PsJN-inoculated and control plants under ambient condition, red - significant difference between mean of PsJN-inoculated and control plants under high temperature condition, based on the Student's t-test with $p<0.05$.

3.2.4. Root length per depth is influenced through time by bacterial inoculation and high temperature

The depth of the agar plate was divided into 20 horizontal layers, referred to here as “depths” from the top or exposed agar surface (0 cm), which divides the root and shoot. The software allowed us to extract the exact length of primary and lateral roots in each of these “depths” and to evaluate the system distribution across root types through depth and time (Figure 4). Plants from all treatments started growing lateral roots from 5 DAI, but a large difference between treatments was not found until 9 DAI when inoculated plants under ambient condition showed the highest total root length (5.6 cm) initiated 1 cm below the open-top plate surface (Figure 4a). At 12 DAI, the effect of bacterial inoculation already started manifesting under high temperature as well, at depths of 1 to 4 cm. Shortly after (around 14 to 16 DAI), high temperature started decreasing the root length distribution at 4 to 8 cm. At the same timepoints, the bacterial stimulation effect on the total root lengths from the upper depths (1 to 9 cm) increased under both temperature regimes (Figure 4a). This effect was also shown in the 1st order lateral root lengths (Figure 4b). For the 2nd order laterals, the effect of inoculation was first observed at 16 DAI under high temperature, from 1 to 3 cm (Figure 4c). At 19 DAI, the stimulation effect of the bacteria on the root lengths (at 1 to 10 cm depth) were more pronounced under high temperature compared to ambient temperature (Figure 4a). This can be attributed to the positive responses of both 1st and 2nd order laterals under high temperature (Figure 4b, 4c). At the end of the growing period (21 DAI), the effect of inoculation on the total root lengths under both ambient and high-temperature condition was prominent from the top down to a 15 cm depth (Figure 4a). This effect was mainly due to the differential effects of the two lateral roots (Figure 4b, 4c). While the effect of bacteria on the 1st order laterals diminished under ambient condition, its effect on the 2nd order laterals increased towards the lower depths (5 to 13 cm). On the other hand, under high temperature, bacterial inoculation caused the 1st and 2nd order lateral roots to display greater root length distribution than control plants, with an almost bimodal curve (Figure 4b, 4c).

Overall, these results show that at all stages and root types, bacterial inoculation increased the root length per depth under both temperatures. While the effect of the inoculation for the 1st order lateral roots under ambient declined through time, the opposite was found on the late-emerging 2nd order laterals. This mainly accounted for the difference between inoculated and control under ambient condition. On the other hand, the effect of bacteria under high temperature can be summed up from the combined effects of the 1st and 2nd order laterals.

(a) Total roots

(b) 1st lateral roots

(c) 2nd lateral roots

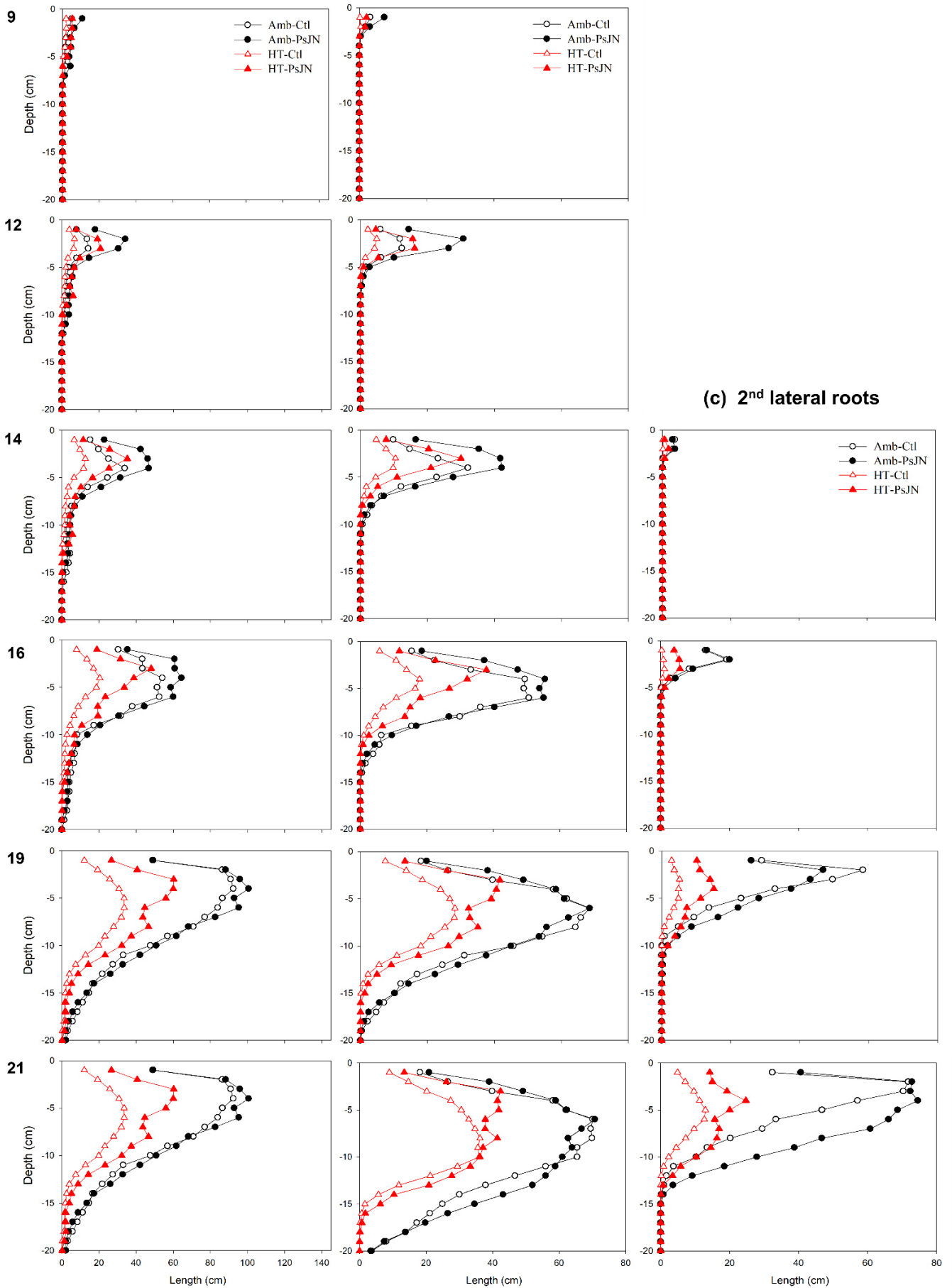


Figure 3. 4 Root length distribution across different depths through time. Length distribution of plant roots from all treatments across different depths or layers (20 horizontal sections) at several timepoints (9, 12, 14, 16, 19, and 21 DAI). Treatments: [black points, open symbols] - Amb-Ctl (control plants under ambient), [black points, closed symbols] - Amb-PsJN (PsJN-inoculated plants under ambient), [red points, open symbols] - HT-Ctl (control plants under high temperature), and [red points, closed symbols] - HT-PsJN (PsJN-inoculated plants under high temperature). All points are the mean \pm standard error of $n= 12$ (Amb-Ctl), 15 (Amb-PsJN), 12 (HT-Ctl), 8 (HT-PsJN) samples within each treatment.

3.2.5. Growth association between root types varies under each treatment

The relationship between the number of 1st order lateral roots and the length of the primary roots, where they branched out from, showed different correlations (Figure 5a). When analyzed for the fitted line per treatment, the association followed that of an exponential relationship between the two given variables. In general, there was an exponential increase in the number of emerging 1st order laterals with the growth of the primary roots. The strongest association was found in control plants at $R^2 = 0.9165$ followed by inoculated plants at $R^2 = 0.8688$, both under ambient condition. Plants subjected to high temperature showed lower correlations, with control plants at $R^2 = 0.814$ and the weakest from inoculated plants at $R^2 = 0.3516$ (Figure 5a).

A polynomial trendline was best fit for the relationship between the number of 2nd order laterals and the corresponding 1st order laterals (Figure 5b). Although showing an increase through time, the number of both lateral roots did not increase at a constant rate. As with the relationship of variables in Figure 5a, the highest association was also found in ambient control plants ($R^2 = 0.8308$), while the lowest was under heat-stressed inoculated plants ($R^2 = 0.4925$) (Figure 5b). The strong correlation of the different roots of inoculated plants under ambient (Amb-PsJN), indicates the already established beneficial effects of the bacteria PsJN for unstressed plants, however, the low correlation found in heat-stressed inoculated plants suggests the changes in the dynamics of growth promotion.

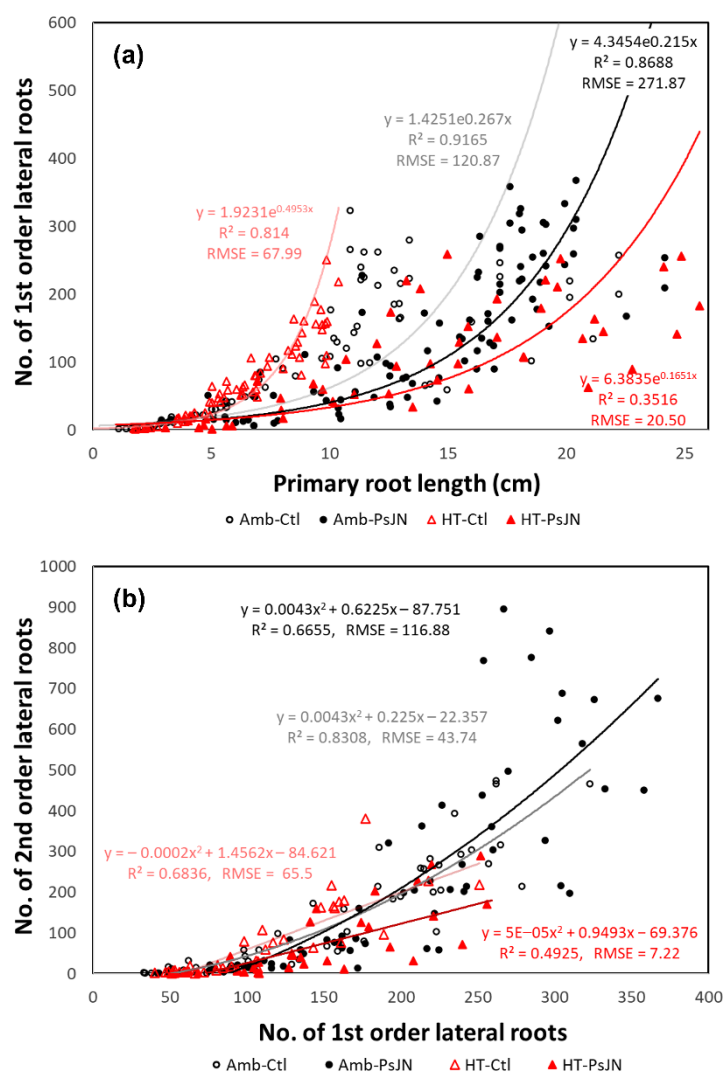


Figure 3. 5 Correlation analysis for lateral roots a) Correlation between the length of the primary roots (Fig. 2b) and the number of 1st order lateral roots (Fig. 2e). b) Correlation between the number of 1st and 2nd order lateral roots of plants from all treatments. Treatments: Amb-Ctl (control plants under ambient) – grey, empty circle; Amb-PsJN (PsJN-inoculated plants under ambient) – black, filled circle; HT-Ctl (control plants under high temperature) – pink, empty triangle; and HT-PsJN (PsJN-inoculated plants under high temperature) – red, filled triangles. Trendlines follow similar colour as their corresponding treatments. Points were taken at different time intervals (5, 7, 9, 12, 14, 16, 19, and 21).

3.2.6. Bacterial inoculation under different temperatures influences the leaf area and dry weights with different magnitude

High temperature caused a decrease of the projected leaf area commencing at 14 DAI (Figure 6a). Overall, high temperature caused a reduction of 51% in shoot dry weights of control plants and a 47% reduction in inoculated plants (compared to ambient control plants) (Figure 6b).

The application of bacteria positively impacted the projected leaf area under ambient temperature; however, this effect was only significantly manifested from 14 DAI (Figure 6a). This stimulation increased leaf area by an average of 29%, about 3 times more than in the high-temperature counterpart. Comparing the dry weights of shoots at harvest, PsJN-inoculated plants have 0.01 g (25%) higher accumulated dry weights than control plants under ambient condition, whereas only a minimal difference of 0.002 g (12%) was found under high-temperature condition (Figure 6b).

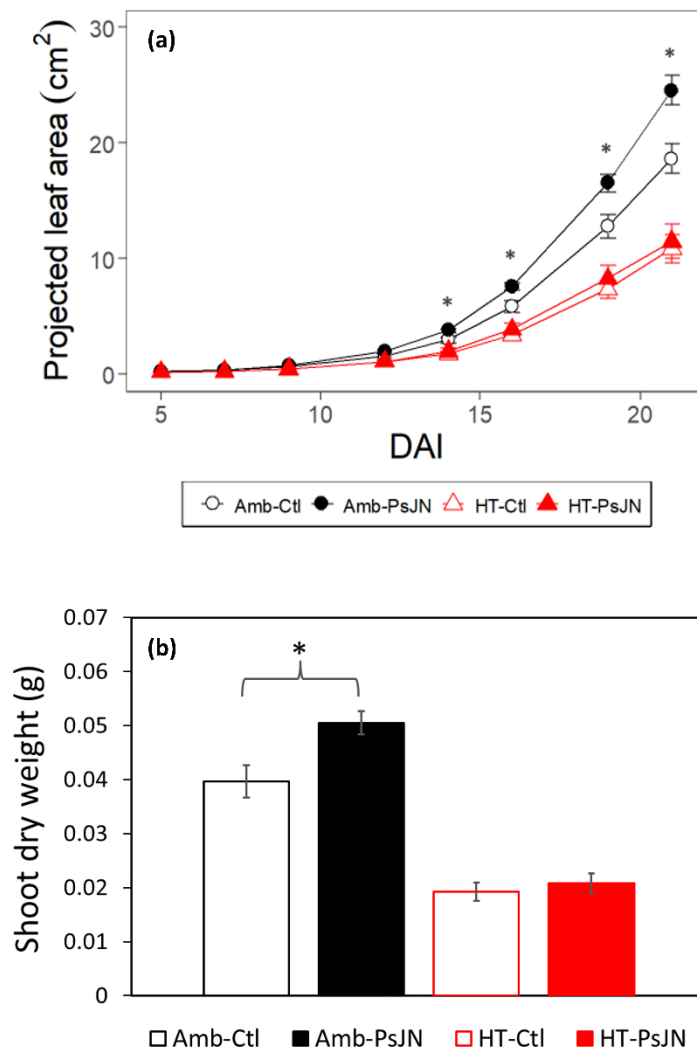


Figure 3. 6 Projected leaf area and dry weight. a) Measured projected leaf area of *Arabidopsis* rosettes growing outside of the agar-filled plates with or without bacteria PsJN inoculation under ambient or high temperature conditions. Temperature - black and circle symbol (ambient), red and triangle symbol (high temperature); bacterial application – empty symbol (control), filled symbol (PsJN-inoculated). b) Dry weights of shoots from all treatments during invasive harvest. Treatments: Amb-Ctl (control plants under ambient), Amb-PsJN (PsJN-inoculated plants under ambient), HT-Ctl

(control plants under high temperature), and HT-PsJN (PsJN-inoculated plants under high temperature). All points are the mean \pm standard error of $n= 12$ (Amb-Ctl), 15 (Amb-PsJN), 12 (HT-Ctl), 8 (HT-PsJN) samples within each treatment. Asterisks: Black – significant difference between mean of PsJN-inoculated and control plants under ambient condition, red - significant difference between mean of PsJN-inoculated and control plants under high temperature condition, based on the Student's t-test with $p<0.05$.

3.3. Discussion

Our studies utilizing both conventional closed-plate and a new open-top system demonstrated the growth stimulatory effects of *P. phytofirmans* PsJN bacteria on the roots and shoots of Arabidopsis plants at ambient and high-temperature conditions. Morphological responses and growth dynamics of the roots and shoots were resolved by monitoring development through non-destructive phenotyping combined with destructive harvest. Here we discuss the changes in the root system architecture of Arabidopsis, in light of known regulatory events by intrinsic factors such as hormones, as well as external biotic and abiotic environmental stimuli. Then we look into the unique characteristics of the bacterial strain PsJN that stimulate plant root architectural changes influencing overall plant development and adaptation to high-temperature stress. We also discuss the advantages of the GrowScreen-Agar II platform over the conventional plant phenotyping pipelines in terms of a strategically-designed plant cultivation system, high-resolution imaging capacity, and streamlined root and shoot trait quantification.

3.3.1. Changes in the root system architecture are modulated by intrinsic factors and different root-environment interactions

The interaction of Arabidopsis with the bacteria PsJN and high temperature altered its RSA. This follows the response of plant roots to the environment involving adjustments to the organization of structural components of the roots, from cellular to whole-plant level (Khan et al., 2016). Arabidopsis has a primary root and several orders of lateral roots (1st and 2nd order lateral roots, investigated here (Figure 2, Figure 4)).

The RSA exhibits plasticity under a changing environment, demonstrating the morphological responses in this study. In agreement with Calleja-Cabrera et al., 2020 (Calleja-Cabrera et al., 2020), high-temperature stress induces several morphological responses in roots including changes such as the decrease in primary root length; reduction in the number, length,

and emergence angle of lateral roots; increase in diameter and number of the second and 3rd order laterals (Figure 2, Figure 3); and increase in the density of root hairs, not investigated here. Plant roots need an optimal temperature range for proper growth rate and functioning (Fonseca de Lima et al., 2021; Koevoets et al., 2016). The response of RSA to increasing temperature can be species-specific since different plants have different optimum temperature requirements for growth (Rogers & Benfey, 2015). An increase in temperature is associated with changes in plant metabolism and nutrient uptake (Radville et al., 2016). This uptake is closely associated with the size, morphology, and functioning of the root system (Alexander et al., 2015). Modifications of the RSA and changes in root growth induced by high temperature can have undesirable effects on the plant's ability to capture resources due to reduced volume of root access (Koevoets et al., 2016). These heat stress-induced alterations to root growth and structure were found to be due to a reduced rate of cell division (Sattelmacher et al., 1990), as well as reduced elongation and cell production rate (Pardales Jr et al., 1992). Changes in the RSA due to high temperature also reduce the root-to-shoot ratio (Ribeiro et al., 2014), linking belowground to aboveground biomass allocation patterns and resource acquisition in plants (Aidoo et al., 2016). This consequence of modified RSA due to high temperature was shown in our study for shoot development (Figure 6). It may be that the root trait response to elevated temperature influenced the carbon fixation and nutrient acquisition, which may have caused the decrease in shoot trait response (Craine et al., 2005; Lynch & Clair, 2004).

PGPRs have been described to affect post-embryonic root development by altering cell division and differentiation within the primary root as well as affecting root hair formation and lateral root development (Verbon & Liberman, 2016). The most common PGPR-induced root phenotype is either the inhibition of primary root growth coupled with the proliferation of lateral roots and root hairs (Ryu et al., 2005), leading to increased shoot biomass; or the increase in primary root growth that is coupled with an increase in plant biomass (Schenk et al., 2012). The PGP bacteria PsJN used in this study had positive effects on the primary, 1st, and 2nd order lateral roots, although we also found that the magnitude and direction of growth stimulation varied depending on the root type and trait, timing, and temperature condition (Figure 2, 3, 4). Unlike obligate symbionts, PGPR can interact with numerous host plants, modifying the RSA to improve plant health and stress tolerance, through a multitude of direct and indirect mechanisms (Adesemoye et al., 2009; Asseng et al., 2015; Ferguson & Mathesius, 2014). These include the formation of biofilms; production of phytohormones (e.g. jasmonic acid, salicylic acid, gibberellins, indole-3-acetic acid (IAA)), exopolysaccharides and 1-aminocyclopropane 1-carboxylic acid (ACC) deaminase (Kasim et al., 2016; Kumar & Verma,

2018); and the production of cell wall degrading enzymes, antibiotics, hydrogen cyanide, siderophores and quorum quenching (Enebe & Babalola, 2018; Maitra et al., 2021). These PGPR-induced modifications of the RSA allow for enhanced functions of different root regions, responsible for soil exploration for nutrient acquisition? (Scheres et al., 2002). The PsJN bacteria used in this study also stimulated the increase in projected leaf area, and this, together with the root growth promotion, may have led to higher shoot dry weight, the magnitude of which varied according to the temperature condition (Figure 6). The simultaneous capture of these time-specific events under bacterial application in two temperature regimes on both root and shoot growth dynamics are some of the new findings of this study not previously reported.

3.3.2. *P. phytostromae* PsJN induces modifications of the components of the root system architecture contributing to improved plant growth

The magnitude of the bacteria-imparted growth promotion on the root architecture varied depending on the specific root type, which to our knowledge has not been dissected before, and was influenced by temperature and time. Significant effects of bacterial inoculation were observed in the root lengths, growth rates, and the number of lateral roots (Figure 2a-2d, 2f-2i, 2e, 2j). These results support other studies showing that PGPRs assist plants by facilitating the elongation of the root tissues and improving their growth rates for optimized absorption of available nutrients (Grover et al., 2021; Vacheron et al., 2013). The increase in the depth of the roots indicates the prominent effect of the bacteria PsJN on the primary roots (Figure 2b, 2g). This can be attributed to the bacteria's involvement in the main processes governing cell division and cell elongation, which are mainly regulated by phytohormones (Pacifici et al., 2015; Qin et al., 2019), ACC deaminase, siderophores, and other secondary metabolites (Naveed et al., 2015; Sun et al., 2009), which have been proposed to act as signaling molecules during plant root-bacteria communication for efficient root colonization (Macabuhay, Arsova, Walker, et al., 2022). On the other hand, the increased formation and elongation of lateral roots (Figure 2c-2d, 2h-2i) with bacterial inoculation may also be due to the alteration of the endogenous pool of growth-regulating hormones such as IAA by the bacteria PsJN (Gupta & Pandey, 2019; Naveed et al., 2015).

This study also showed significant increases in the number of lateral roots with bacterial inoculation (Figure 2e, 2j). This coincides with the outcome of *in vitro* potato plantlets inoculated with a PsJN strain showing better performance in plant growth, likely due to the

development of more secondary roots (Frommel et al., 1991), although our study has further dissected the contribution of 2nd order lateral roots (also known as tertiary roots). The timing and location of the emergence of these lateral roots also contributed to the density and distribution of the roots across different depths and to how the application of bacteria affects the total root lengths (Figure 4a-4c). The increase in the root length distribution towards the deeper or distal part of the root system by the bacteria PsJN indicates the potential for more water and nutrient foraging when the upper edaphic environment turned unfavorable for the roots. Compared to primary roots that traced their origin back from embryogenesis, lateral roots form post-embryonically, allowing for the dynamic acclimation of the whole root system architecture to environmental fluctuations over time (Nagel et al., 2020; Péret et al., 2009). The strong correlation between the number of 1st order laterals against the increase in both the length of the primary roots and the number of 2nd order laterals (Figure 5a-5b) under inoculation indicates the stimulatory effect of the PsJN bacteria on the growth of these roots at ambient condition. This suggests one of PsJN's adaptation benefits to plants. The increase in the number of lateral roots does not only widen the root scavenging area (Yu et al., 2019); this also provides a crucial adaptive response to elevated temperatures, which is generally accompanied by reduced availability of water and nutrients in field settings. Early vigor of these root types can provide an advantage for seedling establishment in preparation for the later growth stages and environmental challenges (Luo et al., 2020).

3.3.3. Positive bacteria-imparted root modifications correlate with shoot responses at ambient temperature and are time-dependent

The positive effects of PsJN on the morphology and growth dynamics of the individual root types manifested early during the root development before declining after certain time points (Figure 4a-d, 4f-i, 4e, 4j). This trend of initial bacterial stimulation and decline was exhibited mainly by the primary and 1st order lateral roots. On the other hand, the 2nd order lateral roots showed a continuous increase from the moment of inoculation, which can be ascribed to the late development of these root types. Contrary to the early growth promotion imparted by PsJN in roots, which started at 5 DAI, the enhancement of the rosette surface area of the shoot came 14 days later (Figure 6a) under ambient conditions. An extended time-series measurement might be needed to fully elucidate the potential of the bacteria PsJN for both root (2nd order laterals) and shoot improvement, as our growth system was limited by the size of the plates.

Whilst they can be found in aboveground tissues of plants, the rhizosphere bacteria *P. phytofirmans* PsJN generally reside inside the root tissues, although some are also located in the rhizoplane (Janssen, 2006). Since plants usually first invest in root growth at the early establishment stage (Radville et al., 2016), the growth promotion imparted by the PGPR strain PsJN may also be reflected in these growing root components. The late-stage significant enhancement of the rosette surface area by the bacteria may just be following this growth trend. It may also be that the plant growth promotion in the shoot is not (only) through the increase in the rosette surface area but from other shoot traits such as growth rates and the number of rosette leaves (Poupin et al., 2013). Results of shoot dry weights at harvest (21 DAI) indicate a strong bacterial stimulation effect, with inoculated plants about 25% heavier than control plants under ambient temperature (Figure 6b). This observed increase in shoot dry matter could be explained by the stimulation of primary root growth and root branching (Frommel et al., 1991), which consequently lead to better nutrient and water uptake. This may indicate that using PsJN will potentially transfer to shoot biomass and be useful for agriculture.

3.3.4. The extent of bacterial stimulation effect in roots and shoots varies depending on the temperature condition

The modulation of growth induced by PsJN on *Arabidopsis* varied in intensity between the two temperatures investigated in our study. Although the beneficial effects of the bacteria were significant under ambient condition on root tissues, these effects were more substantial, with higher relative differences between inoculated and non-inoculated, under heat stress conditions (Figure 2). For example, at the end of the growing period, the difference in the root lengths of inoculated and non-inoculated plants under heat stress condition based on individual root parts was about 3.5 times higher in the primary roots, 3.8 times in the 1st order laterals, and about 2.1 times in the 2nd order laterals, than ambient condition. The strain PsJN is already known for its plant-growth promotion benefits under normal conditions; however, plants can take even more advantage of this bacteria's imparted traits under stressful high-temperature situations when the impacts can be quite deleterious to plants. For example, in potatoes, high temperature caused a reduction in root and shoot development, number of potato tubers, and fresh weight; however, PsJN inoculation showed noticeable beneficial effects on root biomass, and significantly enhanced the tuber number and weight of some cultivars (Bensalim et al., 1998).

The thermotolerant capability imparted by the bacteria might be attributed to its production of ACC deaminase, which has been linked with the alleviation of plant stress because of its

contribution in lowering the ethylene levels, thereby promoting plant growth (Esmaeel et al., 2018; Glick et al., 1998). ACC deaminase-producing bacteria enhance plant growth under different biotic and abiotic environmental conditions such as pathogen attack, drought, salinity, and organic and inorganic contaminants (Glick, 2004; Gupta & Pandey, 2019). Furthermore, microbial deaminases have been shown (or proposed) to be responsible for the dissociation of stress-induced ACC (secreted as root exudates) into ammonia and α -ketobutyrate, thereby eliminating ACC, the precursor for ethylene that has a drastic impact on the physiology, growth, and development of plants (Ali & Kim, 2018; Heydarian et al., 2016; Saleem et al., 2018). Under periods of stresses, ethylene can facilitate the early senescence and abscission of various organs, which are mechanisms to conserve resources (Brown, 1997; Ozga et al., 2017). The role of microbial ACC deaminase producers such as PsJN might be immensely important in today's agricultural systems, where stressed-induced ethylene changes in crops are aggravated by increasing temperature conditions.

Although the PGP effects of the bacteria were strongly demonstrated on several root parameters such as root lengths and growth rates (total, primary, and 1st and 2nd order laterals), as well as the number of 1st and 2nd order lateral roots, these results did not translate in the root system traits (Figure 3a-3d). The conditions in agar where water and nutrients are homogenized, are different from soil where there is a need to expand the volume that is covered by the roots, as there will be very likely heterogenous distribution of edaphic resources. Still, we could show that PsJN causes spatial distribution effects (Figure S6); and that the bacterial enhancements for improved nutrient uptake were manifested in the individual root component, e.g., longer lateral roots (Figure 2), and in the changed root length distribution, e.g., increased root density at the deeper part the roots (Figure 4).

3.3.5. Temporal effects of bacterial inoculation show accelerated growth rates at the early stage of plant growth depending on root type and temperature condition

Although the growth stimulation imparted by the bacteria was a prominent trend, the difference between the inoculated and the control varied at different stages of plant development – initially increasing and then decreasing at certain timepoints. Under ambient condition, the effect of the bacterial inoculation on the root lengths and growth rates showed early in the root development, and the stimulation effect increased up to a certain time depending on the root type (Figure 2b-2d, 2g-2i). For example, the stimulation on the primary roots increased up until 9 DAI and until

12 DAI for 1st order lateral roots, while the 2nd order laterals showed continuous growth and bacterial stimulation until 21 DAI. After these time points (except for 2nd lateral roots), the stimulation effect declined although there were still significant differences between the inoculated and non-inoculated plants.

This outcome, in part, corroborates the result found by Poupin et al., 2013 (Poupin et al., 2013). They found drastic changes, including accelerated plant growth in *Arabidopsis*, with their inoculation at 13 days after sowing. However, although the strain PsJN accelerated the growth rate during the first half of plant development, the growth rates then levelled off and the plant size converged with the non-inoculated plants. In our study, it may be as well that if the plants were allowed to grow further, a similar outcome might take place. For shoots, their study demonstrated that the larger rosette areas of PsJN-inoculated plants during the first half of their life cycles are correlated with larger leaf areas, rather than an increase in the number of leaves. This illustrated that bacteria PsJN acted as a PGPR by accelerating growth rates and producing bigger plants (Poupin et al., 2013). The accelerated growth in the early stages of inoculated plants, which can be attributed to the various mechanistic effects of the bacteria, may provide beneficial effects to the plants including improved nutrient acquisition and/or direct effect on plant metabolism (Poupin et al., 2013). On the other hand, based on the living theory that longevity is negatively correlated with metabolic rate (Issartel & Coiffard, 2011), rapid growth during the early stages of life may be associated with reduced longevity and impaired future performance (Metcalfe & Monaghan, 2003). This may be the case with heat-stressed plants, where accelerated growth rates, particularly during the early growth stage, are generally followed by earlier reproductive and flowering stage.

3.3.6. The GrowScreen-Agar II is an efficient platform for plant cultivation, non-invasive phenotyping, and root and shoot trait characterization

The GrowScreen-Agar II platform provided an efficient growing system that enabled a more natural growth for *Arabidopsis* roots and shoots as compared to the conventional “closed-plate” setup. The previous version of this platform was compared to already existing phenotyping setups in (Nagel et al., 2020). Notably, the strategic design of the agar plates allowed the unobstructed, open-air growth of the shoots which still is a distinguishing feature also in newer systems. This is also a trait in another recent platform GLO-Roots (LaRue et al., 2022; Rellán-Álvarez et al., 2015), which has a similar “open-top” approach, while MultipleXLab (Lube et al., 2022) sticks to the conventional “closed-plate” system. The strategic design of the agar

plates allowed the sterile, unobstructed, open-air growth of the shoots. Access to the leaves opens the potential for non-invasive monitoring of plant physiological parameters such as chlorophyll fluorescence and gas exchange, i.e., net photosynthetic rate, stomatal conductance, and transpiration, which are important indicators of plant response to climate and environment changes (e.g. (Jagadish et al., 2014; Macabuhay et al., 2018; Wahid et al., 2007)). In this study, however, the small size and orientation of *Arabidopsis* rosettes (Figure 1a-1b) restricted the use of gas exchange measuring instruments, which should not be a problem with other species. Aside from the shoot benefits, this platform explicitly addresses the problems of growing and phenotyping roots grown in the dark, which is also accounted for in GLO-Roots, but is still an issue in setups like MultipleXLab.. Moreover, a more detailed and periodic investigation of the different root traits pertaining to the root system architecture was also made possible – a once challenging endeavor for root studies due to the hidden nature of this plant organ. Although this platform is still to be fully automated, it has successfully provided a multi-functional imaging system for non-invasive phenotyping and in-depth characterization of the roots and shoots up to a period of 21 days, by extending the plates. GLO-Roots similarly imaged *Arabidopsis* roots up to 31 days in even longer containers, whereas the automated microscope MultipleXLab only focused on seedlings in the first 4 days. In addition, this phenotyping system made it possible to grow plants subjected to external environmental conditions, such as the addition of the PGPR strain PsJN and the control of temperature. Furthermore GrowScreen-Agar does not require plant transformation or watering with luminescent reagents like in GLO-Roots, but can handle plants of any type of background (as can the light based imaging of MultipleXLab). This also has the potential for investigating more than one gnotobiotic microorganism under combined variable abiotic treatments, which is the direction of plant-microbe interaction studies under future climate challenges (Cheng et al., 2019; Trivedi et al., 2022). This platform's associated image analysis software demonstrated reliable quantification of morphological and dynamic responses of root and shoot traits against combined bacteria and high temperature.

Once completely functional, the GrowScreen-Agar II platform will be a promising solution for high-throughput plant cultivation and non-invasive phenotyping within a fully-automated system. However, despite improvement in the available root space for this study, the platform is still constrained. A limitation of agar-based plant cultivation (both GrowScreen-Agar, MultipleXLab, and others), is the artificial environment that differs greatly from the natural niche of plants and microorganisms in the soil or the field. Here, GLO-Roots that uses soil as a growth medium has a slight advantage with the compromise that soil often obscures root

imaging which could prove challenging at branching points in complex root systems. For all three platforms (similar to findings from all artificial systems) it remains true that while they capture various aspects of plant response mechanisms and quantify the changes, these findings (similar to findings from all artificial systems) need to be further validated in realistic environments, where plants have a larger soil area to scavenge and are exposed to all biotic and abiotic elements.

3.4. Materials and Methods:

3.4.1. Customized agar-plate preparation

The GrowScreen-Agar II platform utilizes specifically designed plates developed in collaboration with and manufactured by the company Happ Kunststoffspritzgusswerk und Formenbau GmbH (Ruppichterath, Germany). Twenty-four plates manufactured by injection molding, which renders them sterile for our use, are comprised of three components: an opaque cover, a transparent back plate with holes on top, and a black top part (“collar”) (Figure S4). The opaque cover consists of polypropylene (PP) and is equipped with an anti-fog agent to prevent water droplets that would disturb root image analysis. The transparent back plate consists of polystyrene (PS) and allows non-invasive imaging of roots growing in the agar. The shoot growth outside of the plate is enabled through 3 holes with a diameter of 5 mm on the short side of the transparent plate (the distance between the holes is 29 mm with one hole exactly in the middle of the short side). The black collar (polypropylene with 30% glass fiber, PP-GF30) has three holes in line with the holes in the transparent back plate but with a reduced diameter to 2 mm. Its primary function is to keep as much light out of the root part of the plate and to provide a proper background for shoot imaging (Figure S4).

Before seed preparation, the holes on the back plates were sealed with micropore tape before being filled with modified Hoagland and agar media [composition in a liter of Milli-Q water: 1.67 mL KNO₃, 1.67 mL Ca(NO₃)₂·4H₂O, 0.67 mL MgSO₄·7H₂O, 0.33 mL KH₂PO₄; 0.33 mL of trace elements (MnCl₂·4H₂O, CuSO₄·5H₂O, ZnSO₄·7H₂O, H₃BO₃, Na₂MoO₄·2H₂O); 0.33 mL [Fe³⁺-EDTA]⁻; and 1% Agar] (Nagel et al., 2020). The media were autoclaved and poured into the plates (approximately 225 mL capacity) inside the biosafety cabinet. Once the agar cooled down and solidified, the opaque covers and collars were attached,

and the assembled plates were stacked and sealed in their original bags to maintain sterility before sowing.

3.4.2. Seed sterilization, sowing, and stratification

Arabidopsis thaliana Col-0 (hereafter referred to as Arabidopsis) seeds were surface sterilized using 70% (v/v) ethanol solution and 0.5% (v/v) sodium hypochlorite solution with 0.05% (v/v) Tween 20 (VWR International GmbH, Darmstadt, Germany) (5 μ L per 10 mL solution). In brief and operating in a biosafety cabinet, Arabidopsis seeds in 2 mL Eppendorf tubes were first incubated with 0.5 mL 70% ethanol for three minutes. After incubation, ethanol was pipetted out and replaced with 0.5 mL of 0.5% sodium hypochlorite solution. The tube was slowly mixed while incubating for 10 minutes. The solution was then pipetted out and the seeds were washed with autoclaved Milli-Q water three times. After washing, the seeds were suspended in 0.5 mL of autoclaved Milli-Q water and set aside for sowing.

To prevent any contamination, sowing was performed inside the biosafety cabinet. Individual Arabidopsis seeds were sown into the pre-prepared agar-filled customized plates. A single seed was slowly pipetted out from the sterilized batch and carefully dispensed into a hole on the plate. When necessary, a sterile syringe needle was used to position the seed into the middle of the hole. When all the holes were sown with seeds, the collars were reapplied then sealed with parafilm; after which, the plates were bagged aseptically and placed horizontally in the fridge at 4°C for five days. Subjecting Arabidopsis seeds to a period of cold temperature breaks dormancy and softens their coat allowing for uniform germination. At the end of the stratification period, the plates were transferred back into the sterile bench and the parafilm was removed for bacterial inoculation.

3.4.3. Bacterial cultivation and inoculation

Paraburkholderia phytofirmans PsJN (DSMZ, Germany) (hereafter referred to as PsJN) was routinely grown on Luria-Bertani (LB) media (1.2% agar w/v with no salt). A day before inoculation, a single bacterial colony from an agar plate was aliquoted into an LB broth and the bacterial solution was cultured overnight in an orbital shaker (150 rpm) at 30°C. The cell suspension was measured for optical density (OD₆₀₀) using a portable spectrophotometer and when an OD₆₀₀ value of 0.8 (equivalent to 10⁸ colony-forming unit (CFU) mL⁻¹) was reached, cells were centrifuged down, washed, and serially diluted with Hoagland media to obtain a concentration of 10⁴ CFU mL⁻¹. A study by Poupin et al., 2013 (Poupin et al., 2013) reported

this bacterial concentration as the optimum for plant-growth promotion in *Arabidopsis*. Inoculation was performed by pipetting 10 μL of either PsJN-bacterial inoculum (inoculated) or Hoagland solution as mock-inoculant (control) onto each seed. After all the seeds received appropriate treatments, the black collars with seed-sown holes were sealed with parafilm, and the inoculated and control plates were transferred to separate growth chambers with varying temperatures.

3.4.4. Plant growth conditions

The number of plates was divided into two groups corresponding to ambient and heat-stress conditions on separate growth chambers, with 22°C/18°C and 30°C/24°C day/night temperatures, respectively. In both climate chambers, the plants were grown under a long day period of 16/8 hours, receiving 120 $\mu\text{mol}/\text{m}^2 \text{ s}^{-1}$ of light and 60% relative humidity. The plates were positioned vertically and maintained in fabricated metal magazines (660 x 210 x 129 mm) fitted for the plates (10 plates per magazine) (Figure S5). This open-top system allowed for the unobstructed, upward, open-air growth of the shoots, whilst simulating the downward growth of the roots in the dark. During the first seven days, the holes remained sealed with parafilm to provide high humidity during germination and early plant development. After this period, the parafilm was removed and, if needed, a syringe needle and/or small tweezer were used to ensure the shoots were growing outside the holes (Figure 1a). The plants were cultivated for 21 days after inoculation (DAI), with routine imaging and phenotyping using the GrowScreen-Agar II imaging system.

3.4.4.1. GrowScreen-Agar II platform specifications

The GrowScreen-Agar II system has been modified from the original GrowScreen-Agar I system (Nagel et al., 2020). GrowScreen-Agar I was designed for imaging traditional square Petri dishes (127 x 127 x 17 mm), having both a top camera for the shoot and a camera with a white backlight for root imaging. The GrowScreen-Agar II was designed for longer (taller) plates (plate: 200 x 100 x 19 mm, collar: 136 x 60 mm), equipped with three cameras for imaging, one for the root (29 MPx Prosilica GT6600, Allied Vision Technologies GmbH, Stadroda, Germany) and two cameras (top and side view) of the shoot (5.1 MPx Mako G-507C, AVT GmbH, as above). Root illumination was achieved from the back with an 850 nm infrared LED panel (EFFI-BL-150T-250-850, EFFILUX, Les Ulis, France), and therefore also an IR-capable lens was used (Xenon Emerald 50/2,2-F-S, Jos. Schneider Optische Werke

GmbH, Bad Kreuznach, Germany). Shoot cameras were equipped with white LED rings (LDR2-70-SW2, CCS Inc., Kyoto, Japan) and standard lenses (LM8JC3M, Kowa Optronics Co. Ltd., Nagoya, Japan and Xenoplan 1.9/3, Jos. Schneider Optische Werke GmbH, Bad Kreuznach, Germany). This imaging system (Figure S6) was strategically positioned inside a growth chamber. In this study, the plates with growing plants were manually transferred into the imaging station. The imaging was driven by a custom software program implemented using the Software Development Kit (SDK).NET based OPC UA Client Server SDK Bundle (Unified Automation GmbH, 90562 Kalchreuth, Germany). After imaging, the plates were placed back into their respective growth temperature chambers (VB 1014, Vötsch Industrietechnik GmbH, 72336 Balingen-Frommern, Germany).

3.4.4.2. Growth optimization using a traditional “closed-plate” system

Before using the “open-top” system, the effects of PsJN were initially investigated in a small experiment using the conventional “closed-plate” set-up. This was used to determine the optimal growth condition for both plant and bacteria, the time-series effect of the inoculation with the corresponding root growth timepoint, and the morphologic responses of the roots to bacteria under ambient and heat stress conditions. In this system, Arabidopsis seeds sown on the surface of agar plates were inoculated with the bacteria PsJN two days after germination, when the radicles were about 2-5 mm. The plates were sealed with micropore, placed in a vertical position, and divided into two growth chambers with ambient and heat stress settings (similar to the abovementioned growth chamber settings). At several timepoints, the plates were removed from the growth chamber and scanned with WinRhizo. Initial analysis was performed using the WinRhizo software.

3.4.5. Time course image analysis

The plates were transferred to the imaging station of the GrowScreen-Agar II and imaged non-destructively at the following time intervals: 5, 7, 9, 12, 14, 16, 19, and 21 days after inoculation, producing the shoot and root images (Figure 1b).

Shoot analysis: The shoot images (.tiff files) captured with the top camera were analyzed with a color space-based segmentation approach to compute the projected leaf area as a proxy for the rosette surface. We used software from a toolbox to estimate leaf angles from stereo images (Müller-Linow et al., 2015), with the revised version of the segmentation tool published separately in (Müller-Linow, 2022). Images were pre-processed to remove chromatic

aberrations, which appear between contrasting regions. In the filtered images, plant pixels were identified by thresholding operations in the HSV color space (Müller-Linow et al., 2015). If not stated, upper thresholds were set to maximum. Lower and upper hue channel (0-360°) thresholds were set to 21° and 222°, and lower thresholds in the saturation and value channels (0-1) were set to 0.11 and 0.17, respectively. The last two dates (19 and 21) were processed with a value channel threshold of 0.08. Two post-processing filters were applied to remove smaller pixel clusters (a group of continuous pixels of category plant or background) resulting from misclassifications in the background and the plants. Pixel clusters of the plant category exceeding a size of 95 pixels were converted to background pixels, while background pixel clusters exceeding a size of 24 pixels were converted to plant pixels. For the last two dates, we increased these thresholds to 502 and 473. The result is a semantic segmentation with white plant pixels and black background pixels. The projected leaf area was computed from the sum of white pixels, which was converted to metric values (Figure 1c (top)).

Root analysis: The root images (.tiff files) were first arranged, processed, and then analyzed using the image analysis software GrowScreen-Root (Nagel et al., 2009; Nagel et al., 2020). The software allows distinguishing between the different root types: the primary roots (green), 1st order lateral roots (red), and 2nd order lateral roots (blue). GrowScreen-Root also measures the following root traits: root lengths (primary, 1st, and 2nd order laterals, and total), convex hull area, root system depth, root system width, number of lateral roots, as well as the branching angle of the laterals (for trait description, see (Nagel et al., 2020) (Figure 1c (bottom))).

3.4.6. End-point harvest and validation of bacterial colonization

At 21 DAI, plates were removed from the growth chambers and the plants were harvested. Plates with root tissues allocated for the determination of bacterial colonization were placed inside the biosafety cabinet. The remaining plates were used for shoot harvest.

Since the PsJN bacterial inoculum was added to the seeds on the open surface of agar plates, we tested whether the bacteria travelled with the downward growth of the roots inside the agar and whether the inoculated samples were colonized by the bacteria at the level of root tips. For rhizoplane colonization, 1-2 cm of the root tip was cut and placed in a 2-ml Eppendorf tube with LB media, washed, vortexed, and the resulting washing was serially diluted and plated. For endophytic colonization, the washed root tissue from the first tube was placed in a separate clean Eppendorf tube where it was first macerated before being resuspended with LB broth.

An aliquot of the resulting mixture was then serially diluted and plated. These bacterial colonization tests were performed on both PsJN-inoculated and control roots, to check for unwanted microbial contaminations (Figure S2). From the plated cultures of the bacteria, a single colony was used for PCR of the 16S rRNA bacterial gene using the universal bacterial primers 27F (5'-AGAGTTTGATCMTGGCTCAG-3') and 1492R (5'-TACGGYTACCTTGTTACGACTT-3'). Part of the PCR product cleaned up and sent for sequencing to check if the sequence matches to PsJN (Figure S2c).

3.4.7. Statistical analysis

The statistical difference of measured parameters between the two treatments, and the effect of microbe application under ambient or heat stress conditions, was analyzed using the Student's *t*-test (two-tailed distribution). In addition, overall treatment effects such as microbial application (microbe), heat stress effect (temperature), and interaction effect per individual day and over the entire growing period were also analyzed using the ANOVA function in R studio. Only those results with a significant *P-value* level of <0.05 were considered reliable enough to reject the *null hypothesis* that the two treatments did not differ for a particular parameter.

3.5. Conclusions and future perspectives

Our study shows that the bacterial endophyte strain *P. phytostromas* PsJN improves shoot and root growth under normal temperature conditions. Depending on the plant tissue and specific trait, this growth enhancement may be more substantial under high-temperature conditions, showing a potential advantage for bacterized plants under future climate change scenarios. We have also demonstrated that depending on the root type and their time of emergence, the stimulation effect imparted by the bacteria may be stronger at the early stages of plant growth and then level off towards the end of plant development. This observation may allow young plants to get well-established roots with more access to water and nutrients, which can assist in later growth stages that are sensitive to environmental fluctuations and challenges. Information about the spatial and temporal effects of this bacteria, particularly in the roots, can inform plant growers about alternative solutions for increasing crop productivity and potential mitigation and adaptive strategies in addressing climate-related impacts on agriculture. Finally, we have demonstrated here the potential of the platform GrowScreen-Agar II in providing a more natural plant growth condition, non-invasive imaging and phenotyping, and trait quantification capability for studying plant morphologic response and growth dynamics.

Crop plant selection is currently being focused on the RSA because of its overarching importance in the plant's ability to acquire edaphic resources, which is limited by suboptimal water and nutrient availability and exacerbated by climate change (Lynch, 2022). Aside from genetic improvement and conventional breeding strategies for improving the RSA, the application of PGPR can be an alternative avenue for developing more productive, resilient, and climate-smart crops. This can be extended to using not just a single but a combination of known beneficial microorganisms. However, further studies on the mechanisms of growth promotion and biotic and abiotic stress tolerance need to be explored to maximize the potential of microbial application to agriculture. In addition, novel growth systems addressing existing plant cultivation limitations and non-invasive high-resolution phenotyping platforms can also be taken advantage of to understand the underlying biochemical mechanisms behind the plant-microbe-environment interactions for future sustainable biotechnological solutions.

3.6. Supplementary Materials

The following supporting information can be downloaded at: www.mdpi.com/xxx/s1, Figure S1: WinRhizo analysed root lengths and root and shoot biomass; Figure S2: Sample root images generated by the GrowScreen-Agar II; Figure S3: Agar plates for GrowScreen-Agar II; Figure S4: Magazines for GrowScreen-Agar II; Figure S5: Imaging station of GrowScreen-Agar II; Figure S6: Root sampling and bacterial colonization confirmation; Table S1: Mean values and standard error of different root type morphological traits; Table S2: Mean values and standard error of different root system traits describing distribution and spread.

3.7. Author contributions

A.M. conducted the experiments, performed data analysis and interpretation, and wrote the manuscript; U.R, M.W., B.A., A.A.T.J., R.W., G.S. conceptualized and advised the experiment, reviewed and edited the manuscript; M.W, B.A. supervised the project at IBG-2 Forschungszentrum Juelich; K.N. assisted with platform utilization and description; K.N., H.L., A.P., S.A. developed the GrowScreen-Agar II phenotyping platform and analysis software; H.L., S.A. provided technical drawings for the platform; K.N., H.L. wrote the description of the components of the platform; M.M-L. developed and performed shoot data analysis and wrote description; J.K. performed PCR and 16s bacterial sequencing. All authors have read, commented, and agreed to the published version of the manuscript.

3.8. Funding

Allene Macabuhay is grateful for the financial support from the University of Melbourne Research Scholarship provided through the Jülich-University of Melbourne Postgraduate Academy (JUMPA) program. Michelle Watt holds the Adrienne Clarke Chair of Botany which is supported through the University of Melbourne Botany Foundation. Borjana Arsova, Kerstin Nagel, Henning Lenz, Alexander Putz, Sascha Adels, and Mark Müller-Linow acknowledge the support of Forschungszentrum Jülich GmbH in the Helmholtz Association. The development of the platform GrowScreen-Agar II was funded by the third-party project of the German Federal Ministry of Education and Research (German-Plant-Phenotyping Network (DPPN), BMBF Fz. 031A053). Gabriel Schaaf acknowledges funding by the Deutsche Forschungsgemeinschaft under Germany's Excellence Strategy – EXC 2070 – 390732324 (PhenoRob).

3.9. Acknowledgments

The authors would like to acknowledge Bernd Kastenholz and Olaf Gardeick for technical help during experiment setup and optimization, Anna Galinski for providing knowledge and training with root analysis software, and Stefan Sanow and Helena Bochmann for assistance in project completion under pandemic conditions (IBG-2, Forschungszentrum Juelich, DE). The authors would also like to thank Maria Josefina Poupin Swinburn (Universidad Adolfo Ibanez, Chile) for providing the bacterial strain *P. phytofirmans* PsJN used for the initial study conducted at the University of Melbourne.

3.10. Conflict of interest

The authors declare no conflict of interest.

CHAPTER 4

**The lipidome of *Arabidopsis thaliana* roots at
different stages of interaction with the endophytic
plant growth-promoting rhizobacteria
Paraburkholderia phytofirmans PsJN under heat
stress**

Preface to Chapter 4

This chapter of the thesis introduces the biochemical nature of the beneficial interactions, specifically focusing on lipids, between the roots of the model plant *Arabidopsis thaliana* and the PGPR *P. phytofirmans* PsJN, under both ambient and high temperature conditions. The interaction was assessed across three stages of the plant root development, while scrutinizing the changes that happen to the root lipidome under the influence of both biotic and abiotic stimuli. The typical “omics” workflow was used as a template (**Figure 4**) in developing the discovery (untargeted) lipidomics workflow and analysis employed in the study.

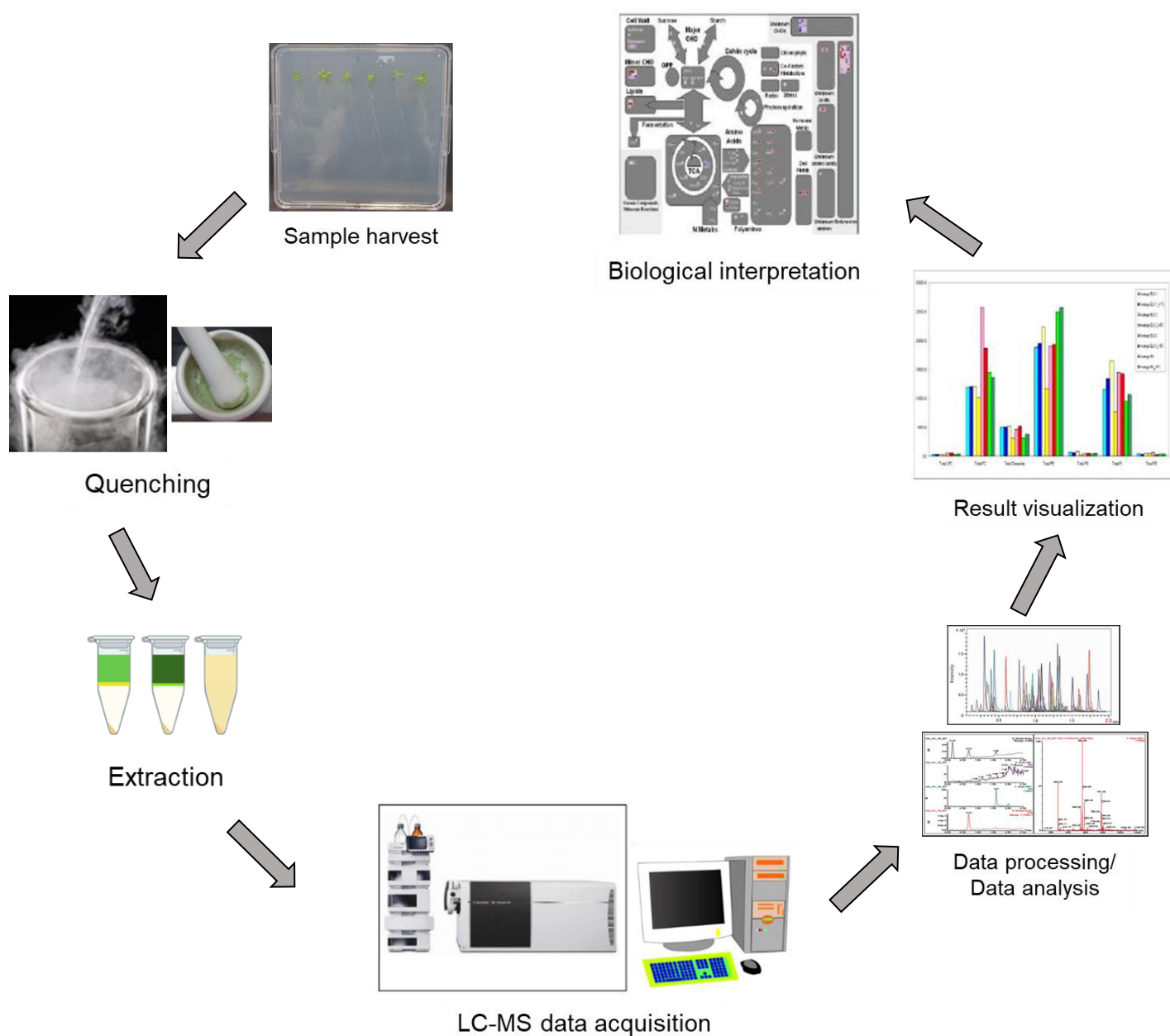


Figure 4 Schematic diagram of the lipidomics workflow employed in this study

This study showed that the plant growth-promoting rhizobacteria *P. phytofirmans* PsJN can induce significant modifications in the lipid profile of roots, which is a rarely investigated organ when compared with the wide array of studies on aboveground plant parts. This also showed the effect of the open-top system for the co-cultivation of plants and bacteria, as shown by the significant changes at the later plant growth development in a natural un-stressed condition. More importantly, the study showed that bacterial application can significantly increase their plant benefits, with earlier emergence, under high temperature stress. High temperature or heat stress is a common detrimental environmental factor to plant growth and this study has demonstrated how alterations in the root lipids under this scenario support the positive effects of the bacteria to plants.

Lipid acronyms used throughout the chapter:

Cer	ceramide
CL	cardiolipin
CoQ	coenzyme Q
DG	diacylglycerol
DGDG	digalactosyldiacylglycerol
FA	fatty acyls
GL	glycerolipids
GP	glycerophospholipids
HexCer	hexosylceramides
LPC	lysophosphatidylcholines
LPE	lysophosphatidylethanolamines
MG	monoacylglycerol
MGDG	monogalactosyldiacylglycerol
NAE	N-acylethanolamines
PA	phosphatidic acid
PC	phosphatidylcholine
PE	phosphatidylethanolamine
PG	phosphatidylglycerol
PI	phosphatidylinositol
PR	prenol lipids
PS	phosphatidylserine
SP	sphingolipids
SQ	squalene
SQDG	sulfoquinovosyldiacylglycerol
ST	sterol lipids
TG	triacylglycerol

4.1. Introduction

Lipids, which are a large group of highly diverse and ubiquitous compounds, are major constituents of eukaryotic and prokaryotic cell membranes (Fahy et al., 2011; Siebers et al., 2016). They are present in all living organisms and perform essential functions such as for energy storage (Welte & Gould, 2017), as structural components of the plasma and intracellular membranes (Quinn et al., 1989), as mediators in signaling transduction pathways and membrane trafficking (Wang, 2004), in maintaining cellular homeostasis (Agmon & Stockwell, 2017), as mitigators of stress responses (Okazaki & Saito, 2014), and as facilitators during various symbiotic interactions with microorganisms (Macabuhay, Arsova, Walker, et al., 2022).

Because of their many functions, any changes in lipids and their metabolism can reflect the biochemical changes of the whole plant system, thereby influencing plant health and development (Boutte & Jaillais, 2020). Notably, plants are in constant exposure to a multitude of microorganisms present in the soil, air, or water, and are in either beneficial (mutualistic) or detrimental (parasitic or pathogenic) forms of interactions.

As the plasma membrane's main component and the interface during the plant's interaction with the surrounding environment, lipids have been the focus of many recent studies investigating plant responses to biotic stimuli (Hou et al., 2016; Siebers et al., 2016). In the rhizosphere, in particular, lipids have important roles; from the formation of symbiotic interactions – as chemical signals released from and perceived by plant roots and microbes, to the establishment of either plant growth-promoting or disease-causing interactions (Macabuhay, Arsova, Walker, et al., 2022). The process of host cell reprogramming allows plant cells to dynamically change their architecture and molecular composition following the encounter with beneficial or pathogenic microbes (Dormann et al., 2014). That is, either for microbial entry or pre-invasive defense, several cell processes are induced, including the breaking of plasma membrane symmetry, tethering of membranes, induction of changes in the lipid composition, and the activation of plasma membrane-to-cytoskeleton signaling (Dormann et al., 2014). Essentially, plasma membrane-associated processes and lipid components mediate the recognition of microbes, the transduction of signals, and the downstream cellular responses.

Although many studies have investigated the roles of lipids in plant-microbe interactions, many of these were focused on pathogenicity (Ali & Kim, 2018; Zhao, 2015), whereas only a few investigations were about beneficial interactions, of which, most were on nitrogen-fixing

bacteria (Santi et al., 2017). Various plant lipids are influenced by mutualistic interactions of plants and microbes. Notable examples are the increase in the concentration of various glycerophospholipids (GP), due to increased membrane GP biosynthesis, whilst a decrease in galactolipids was displayed in the root nodules during the soybean and nitrogen-fixing bacteria symbiosis (Zhang et al., 2020). Inoculation with *Azospirillum* showed a varying effect on GP depending on the plant species – increasing in cowpea calli (Bashan et al., 1992) and decreasing in wheat roots (Pereyra et al., 2006). A study by Castanheira et al. (2017) on the effect of mixed inoculation of beneficial microbes (*Pseudomonas* G1Dc10, *Paenibacillus* G3Ac9, *Sphingomonas azotifigens* DSMZ 18530T) on annual ryegrass has shown a 65% increase in the total fatty acid content, which suggested a dynamic metabolic response and stimulation of membrane lipid biosynthesis. This increase in the total fatty acid was a consequence of the preferential synthesis of saturated palmitic acid (C16:0) and highly unsaturated linoleic (C18:2) and linolenic (C18:3) acids. The synthesis of triacylglycerol (TG) also had conflicting results, decreasing in the nodules during soybean and rhizobia interactions (Zhang et al., 2020), and increasing in shoots with the inoculation of *Bacillus subtilis* into *Brassica indica* grown under salt stress (Abeer et al., 2015).

As sessile organisms, plants are also exposed to the surrounding elements and are frequently subjected to fluctuations in temperature, drought, and soil-nutrient conditions such as salinity, metal toxicity, nutrient scarcity, as well as other environmental stressors. During abiotic stresses, membrane lipids undergo modifications of their fatty acid composition and the degree of unsaturation, which are potential mechanisms to plant acclimation or adaptation to stress-induced changes (Welti et al., 2007). Temperature has a significant influence on membrane lipids during plant growth; and any changes, such as the increase in temperature, can alter the lipid composition and profile (Zheng et al., 2011). In general, high temperatures reduce the degree of unsaturation of fatty acids in plants, as in the case of *Arabidopsis* at 36°C, where the double bond index (DBI) was 1.46 as opposed to 2.39 of plants grown at 17°C (Falcone et al., 2004). Glycerolipids (GL) are the major constituents of membranes; and in response to elevated temperatures, plants can adjust the GL composition to maintain the integrity and optimal fluidity of membranes (Zheng et al., 2011). A study by Higashi et al. (2015) has detected several lipid species in *Arabidopsis* leaves affected by short-term heat stress, which include 1) glycolipids – monogalactosyldiacylglycerol (MGDG), digalactosyldiacylglycerol (DGDG), and sulfoquinovosyldiacylglycerol (SQDG); 2) GPs – phosphatidylglycerol (PG), phosphatidylcholine (PC), phosphatidylethanolamine (PE), and phosphatidylinositol (PI); (3) diacylglycerol (DG), a lipid intermediate; and (4) the storage

lipid TG. This finding was supported by Narayanan et al. (2018) who found that the most responsive lipids to high temperature were the extraplastidic glycerophospholipids (PC, PE, PG, phosphatidylserine (PS), and phosphatidic acid (PA)). In addition, their unsaturation levels were also decreased through the decreases in the levels of 18:3 and increases in the levels of 16:0, 18:1, and 18:2 acyl chains.

The study of lipids and their functions can tell many things about biological systems and their mechanistic responses to external stimuli. Lipids can alter biological functions with even the smallest change in their structure and composition (Harayama & Riezman, 2018). This can be observed in the modification of functions in membrane proteins as well as the changes in the physical structure and physiological properties of the cell membrane, e.g. membrane fluidity and permeability, with changes in the membrane-bound lipids (Guo et al., 2019). It is safe to say that lipids are interlinked with DNA, RNA, proteins, and other metabolites within the central dogma of biology, and, therefore, must be studied as an integral part of the whole system (van Meer, 2005). In addition, it has also been proposed that the study of lipids should involve their time-specific responses and local concentrations (van Meer, 2005).

The cellular lipidome is comprised of hundreds of thousands of lipids (Harkewicz & Dennis, 2011), with diverse functions that may be attributed to various factors such as the head group types, aliphatic chains, and isomerism (M. Wang et al., 2016). It may be possible that the lipid structures exceed 180,000 without even considering all the position isomers, backbone substitutions, and stereochemistry Kehelpannala et al. (2021). For example, the sphingolipidome of plant cells alone may be comprised of at least 500 to perhaps thousands of different species of sphingolipids (Pata et al., 2010). A survey of the plant lipidome in barley roots has identified a total of 49 potential building blocks including 10 polar heads, 18 different fatty acids, 5 long-chain (sphingoid) bases, 11 sphingolipid head groups, and 5 sterols (Yu et al., 2018). A recent publication by Kehelpannala et al. (2021) also generated a comprehensive and detailed tissue-specific lipid map of Arabidopsis plants across selected developmental stages, which has been integrated into an electronic Fluorescent Pictograph (eFP) browser. There are many more studies, making it possible the existence of potentially millions of lipids when all structural differences are taken into account (Koelmel et al., 2017). This only suggests that there are still many more lipid species yet to be discovered and that we are still just scraping the tip of an iceberg when it comes to the complexity and diversity of the plant lipidome. Moreover, when plant studies are combined with microbes, the diversity of the lipid profile is further increased since the microbes have also various and distinct lipids compared to plants.

Because of its still uncharted territory, research on lipids is gaining a lot of attention, more so with the breakthroughs in mass spectrometry. However, despite the many recent advancements in lipidomics and technology, the characterization and profiling of novel lipids and their functions remain a challenging undertaking because of their highly complex and diverse nature. One challenge is that relatively new lipid species are most often of low abundance in complex biological matrices compared to other more common lipids (Bilgin et al., 2016). According to Bilgin et al. (2016), their low abundance will prevent the precursor ions from being selected for fragmentation by data-dependent acquisition methods in liquid chromatography - tandem mass spectrometry (LC-MS/MS) analysis, making identification difficult. Furthermore, the structure identification of all unknown lipids within a biological sample is made challenging by the thousands of unidentified mass spectrometric features (Yu et al., 2018), which are sometimes artifacts generated from in-source fragmentation (Hu et al., 2022), while some peaks could also be the result of solvent masses (Gathungu et al., 2018). Another challenge is associated with the composition of lipids, which varies significantly between organisms, cell types (Welti & Wang, 2004), subcellular organelles (Hölzl & Dörmann, 2007), and microdomains within cell membranes (Gronnier et al., 2018). For example, GPs (mainly structural lipids), are abundantly found in the plasma membrane, tonoplasts, and endoplasmic reticulum (Wewer et al., 2011); DGs such as MGDG, DGDG, and SQDG (involved in photosynthesis), are most prominent in chloroplast membranes (Hölzl & Dörmann, 2007); whilst sterols and sphingolipids (critical functions in signal transduction and cell recognition processes) are found as major components of membrane rafts (Gronnier et al., 2018).

Aside from their differences among cell types, lipid compositions also vary significantly between different plant tissues as with the studies conducted by Narasimhan et al. (2013) on soybean leaf and roots, and by Devaiah et al. (2006) and Kehelpannala et al. (2021) on the different tissues of *Arabidopsis* that includes leaves, flowers, siliques, roots, and seeds. Finally, another challenge for lipid researchers is the dynamics of change in the composition of membrane lipids throughout plant development, season, and even time of day, all of which are further complicated by different environmental conditions (Colin & Jaillais, 2020). Notable examples are PS levels changed throughout root development in *Arabidopsis* (Platre et al., 2019) and the fluctuation in the unsaturation of PC during day and night in *Arabidopsis* flower (Nakamura et al., 2014). The involvement of environmental changes in the remodeling of membrane lipids has also been shown in studies for salinity (Sarabia et al., 2019), low temperature (Barrero-Sicilia et al., 2017; Cheong et al., 2021; Cheong et al., 2019), high

temperature (Higashi & Saito, 2019; Shiva et al., 2020), pathogen and insect attack (Farmer et al., 2003), beneficial microbes (Gupta & Pandey, 2019; Gupta et al., 2021; Schillaci, Kehelpannala, et al., 2021), including physical contacts as with wounding (Vu et al., 2014).

Needless to say, areas of lipid research such as their distribution in different tissues or cell types, their intrinsic functions in various cellular processes, their roles in plant growth and development, as well as their responses to environmental stresses, need to be further explored. In order to do so, mass spectrometric analyses on various complex biological systems can be performed – either using targeted or untargeted lipidomic approaches (Melnik et al., 2017). According to Melnik et al. (2017), targeted analyses, which are focused on pre-defined sets of metabolites, are generally more sensitive and more inclined towards the quantification of lipids; however, it is restricted to only a limited number of compounds to analyze. On the other hand, untargeted analyses, which are ideal for discovery-focused lipidomic approaches, aim to comprehensively capture and profile all detectable compounds in a sample. This provides an unbiased analysis of the changes in the system, allowing for the discovery of novel lipids (Gao et al., 2020). Unfortunately, due to the complexity and huge amount of data retrieved by untargeted methods, as well as the non-specificity or non-standardized nature of the analysis, some analytes tend to go undetected. Nonetheless, this approach is widely used to characterize novel lipids and their functions on different biological systems while in interaction with the biotic and abiotic environment.

In this chapter, the lipid profiles were generated from the lipid compounds extracted from the roots of control and bacteria-inoculated *Arabidopsis* roots grown under ambient and high-temperature conditions. The profiles of the four treatments were then compared among three developmental stages to investigate the effect of time on the dynamics of bacterial growth promotion and lipid alterations from constant high temperatures. Specific lipids that have shown significant changes were then discussed, comparing them with the observed root phenotypes and based on the insights from existing lipid studies.

4.2. Materials and Methods

4.2.1. Growth protocols for *Arabidopsis* plants and its co-cultivation with *P. phytofirmans* PsJN bacteria plants

Arabidopsis thaliana Col-0 seeds were grown on a modified agar-plate system, which utilized large agar Petri plates (245 x 245 x 25 mm, square bioassay dish with handles, Corning, USA),

placed in an inclined position. Agar plates were made with 1% agar and 1/3 modified Hoagland solution, the composition of which was specified in Chapter 3 section 4.1. Seeds were surface-sterilized by washing with 0.5 mL of 70% (v/v) ethanol solution for 5 minutes followed by 0.5 mL of 0.5% (v/v) sodium hypochlorite solution containing 0.05% (v/v) Tween 20 for 10 minutes. Within the incubation time, the tube of seeds was turned slowly, after which, the solutions were pipetted out. The seeds were then thoroughly rinsed five times with 0.5 mL of sterile Milli-Q water and left suspended in another 0.5 mL. Using a pipette, one sterilized seed was drawn out from the tube and carefully sown on marked areas of the plate. A marked guide was prepared beforehand to facilitate equally-distanced sowing and was placed underneath each agar plate. Once all the plates were sown with seeds, they were sealed with wide micropore tape (25 mm, 3M™) to prevent contamination whilst allowing airflow. Plates were placed in sterile plastic containers covered in foil to subject seeds to cold stratification at 4°C for 5 days in a cold chamber, after which inoculation ensued.

P. phytofirmans PsJN was routinely cultured and maintained in Luria-Bertani (LB) media containing 5 g yeast extract (Oxoid), 10 g BBL™ Trypticase™ Peptone (BD), and 15 g Bacto™ agar (BD) in a 1L solution, without sodium chloride due to this bacteria's low halophilic tolerance. A day before the stratifying seeds were taken out of the cold room, overnight bacterial inoculation was performed. Briefly, a single colony was picked from a streaked plate, inoculated in an LB liquid solution, and allowed to incubate overnight in a shaking incubator at 30°C and 180 rpm. Measurement of optical density (OD₆₀₀) using a spectrophotometer (DS-11 FX Spectrophotometer/ Fluorometer, DeNovix, Inc., DE, USA) commenced around 16 hours and every hour afterward to get a value of 0.8 (corresponding to 10⁸ colony-forming units (cfu)/mL). Once the desired OD₆₀₀ was reached, the solution was centrifuged, washed, and serially diluted. A tenfold serial dilution using Hoagland plant media was then performed to get 10⁴ cfu/mL which was found by Poupin et al. (2013) to be the maximum amount of bacteria that yields growth promotion in Arabidopsis. This dilution was set aside as the bacterial inoculum for application to plant roots.

When stratification was over, the plates were placed and opened inside the sterile bench for bacterial inoculation. Briefly, 10 µL of either PsJN-bacterial inoculum or Hoagland liquid solution (mock-inoculant), depending on treatments, was pipetted directly into 2-day-old radicles (about 2-5 mm) of Arabidopsis seedlings. Once all the seeds were inoculated, the plates were double sealed, placed back into the plastic containers in an inclined position (about 30 to 45 degrees from the vertical line), and transferred into separate two growth chambers with varying temperatures. The two chambers were set to either ambient condition at 22°C/18°C or

high temperature at 30°C /24°C. The rest of the climate settings were the same on both growth chambers, i.e., light intensity was at 120-150 $\mu\text{mol m}^{-2} \text{s}^{-1}$; photoperiod maintained was the 16hr/8hr light/dark, and a humidity of 70%. Plants were grown for three weeks (21 days), with the harvesting of assigned plants done on several occasions.

4.2.2. Sample collection and lipid extraction

At three different time points – 7, 14, and 21 days after inoculation, assigned plants had their roots and shoots harvested. Five technical replicates from ten pooled samples of two different plates were prepared at each harvest time point. Shoots were cut along the side of the plate and the roots were harvested by slowly grabbing and removing the top part first (growing inside the agar) first, then gently pulling the rest of the root parts from the agar surface. Harvested tissues were immediately placed into Eppendorf tubes partly submerged in liquid nitrogen to stop any metabolic activity.

4.2.2.1. Extraction from plant roots

For lipid extraction, approximately 30 mg of ground root tissues were transferred into 2 mL tubes and added with 400 μL of -20°C 100% LC-MS grade 2-propanol (Thermo Fisher Scientific, USA) with 0.01% butylated hydroxy toluene (BHT) (Sigma Aldrich, USA). The cold 2-propanol mixture also contained the following internal standards (ISTD): 1 mL of ISTD – PS, PE, PG, Lyso PC, Lyso PG, Lyso PE, DG, MG, cardiolipin (CL), PC, ceramide (Cer), MGDG, DGDG, squalene (SQ) (Avanti Polar Lipids, Inc., USA), 500 μL of Splash LipidoMix (Avanti Polar Lipids, Inc., USA) (individual components in **Table 4.1**), and deuterated cholesterol (Sigma-Aldrich, USA). Root samples with the 2-propanol mixture were subjected to homogenization in a tissue lyzer (Tissue Lyser II, Qiagen), with liquid nitrogen-maintained blocks, for two consecutive 2 min intervals with 30 s pause in between at a frequency of 30 Hz/s. The samples were placed in a thermoshaker set at 1400 rpm and incubated at 75°C for 15 min; after which, they were cooled down to room temperature and added individually with 1200 μL of chloroform (CHCl_3): methanol (MeOH): water mixture (30:41.5:3.5, v/v/v) (reagents from Sigma-Aldrich, USA). A longer incubation of the samples at 25°C for 24 hours, with constant shaking at 300 rpm, followed. After that, the supernatants were transferred to clean 2 mL Eppendorf tubes and were dried down using a speed vacuum concentrator (John Morris Scientific Pty. Ltd., Australia) in preparation for LC-MS analysis.

Table 4. 1 Components and concentrations of the SPLASH LipidoMIX™ Internal Standard

Compound Name	Molecular Weight	Exact Mass	Chemical Formula	Concentration (µg/mL)*
15:0-18:1(d7) PC	753.11	752.61	C41H73D7NO8P	150.6
15:0-18:1(d7) PE	711.03	710.56	C38H67D7NO8P	5.3
15:0-18:1(d7) PS (Na Salt)	777.02	776.53	C39H66D7NNaO10	3.9
15:0-18:1(d7) PG (Na Salt)	764.02	763.54	C39H67D7NaO10P	26.7
15:0-18:1(d7) PI (NH4 salt)	847.13	846.6	C42H75D7NO13P	8.5
15:0-18:1(d7) PA (Na Salt)	689.94	689.5	C36H61D7NaO8P	6.9
18:1(d7) Lyso PC	528.72	528.39	C26H45D7NO7P	23.8
18:1(d7) Lyso PE	486.64	486.35	C23H39D7NO7P	4.9
18:1(d7) Chol Ester	658.16	657.64	C45H71D7O2	329.1
18:1(d7) MG	363.59	363.34	C21H33D7O4	1.8
15:0-18:1(d7) DG	587.98	587.55	C36H61D7O5	8.8
15:0-18:1(d7)-15:0 TG	812.37	811.77	C51H89D7O6	52.8
d18:1-18:1(d9) SM	738.12	737.64	C41H72D9N2O6P	29.6
Cholesterol (d7)	393.71	393.4	C27H39D7O	98.4

Based on Certificate of Analysis from Avanti Polar Lipids, Inc.

* Concentrations are based on the isotopic purity of each individual compound

4.2.2.2. Extraction from bacteria

Lipids were also extracted from PsJN bacteria, which were grown axenically in LB media at 30°C. Having the bacterial profile provided a comparison for the identification of the lipids present in the Arabidopsis root samples and those derived from the bacteria.

At an optical density of 0.8, which was determined to be equivalent to 10⁸ colony forming units (cfu)/mL based on serial dilution and colony counting, the bacterial inoculum was washed twice in sterile phosphate buffered saline (PBS), and cells were harvested by centrifugation at 1000 rpm for 10 min. Cell pellets were then resuspended in 500 µL of -40°C methanol: 0.1 N hydrochloric acid (HCL) (1:1) mixture (both reagents from Sigma-Aldrich), snap frozen in liquid nitrogen, then alternatively dipped into dry ice/ethanol bath and grinding at room temperature until thawed. This freeze-thaw process was repeated ten times to break the bacterial cells. 750 µL of the mixture chloroform: methanol (1:2) containing 1 mM BHT and 50 µM d-cholesterol (Avanti Polar Lipids Inc., US) was added to each sample, before being mixed vigorously with a vortex and then shaken by hand for 5 min at room temperature to extract lipids. Samples were then sonicated for 30 min at room temperature, followed by

centrifugation for 5 min at 13,000 rpm and 0°C. The supernatant (upper phase) was transferred to new 2 mL tubes, while the pellets (lower phase) were mixed with 500 µL chloroform: methanol: 0.1 N HCl (1:2:0.8). The remixed solution was sonicated for 30 min and then centrifuged at 13,000 rpm for 10 min at room temperature; after which, both supernatants were combined. Finally, the combined supernatants were dried using a vacuum concentrator (John Morris Scientific Pty. Ltd., Australia) and prepared for LC-MS analysis.

4.2.3. Lipid analysis by Liquid Chromatography–Mass Spectrometry (LC-MS)

All dried lipid extracts were rehydrated with 200 µL of butanol: MeOH (1:1, v/v) mixture containing 10 mM ammonium formate. Ten pooled biological quality control (PBQC) samples were prepared by aliquoting 10 µL from each lipid sample.

Untargeted lipid analysis of samples was performed using liquid chromatography coupled with mass spectrometry as reported by Kehelpannala et al. (2021). Briefly, an Agilent 1290 HPLC system was utilized for the chromatographic separation of lipids on an Infinity Lab Poroshell 120 EC-C₁₈ 2.1 x 100 mm (2.7-Micron particle size) column (Agilent, USA) operated at 55°C. The samples were placed in the autosampler set at 12°C, with an injection volume of 10 µL and a flow rate of 0.26 mL/min. Elution of samples was performed over 30 min using a binary gradient consisting of acetonitrile (ACN): water (60:40, v/v) (Eluent A) and isopropanol (IPP): ACN (90:10, v/v) (Eluent B), both containing 10 mM ammonium formate. The following gradient was used for Eluent B: 0- 1.5 min isocratic elution at 32%, increased to 45% from 1.5 to 4 min, then to 52% from 4 to 5min, followed by an increase to 58% from 5 to 8 min. Next, the gradient was increased to 66% from 8 to 11 min, then by 70% from 11 to 14 min, and then to 75% from 14 to 18 min. Then, from 18 to 21 min, it was increased to 97% and was maintained at 97% from 21 to 25 min. Finally, solvent B was decreased to 32% in 0.1 min and maintained at 32% for another 4.9 min for column re-equilibration (Hu et al., 2008).

Lipids were then analyzed using a Sciex TOF™ 6600 QqTOF mass spectrometer equipped with a Turbo V™ dual-ion source [electro-spray ionization (ESI) and atmospheric pressure chemical ionization (APCI)] and an automated calibrant delivery system (CDS) using Sequential Window Acquisition of All Theoretical Mass Spectra (SWATH-MS) in positive ion mode (Tsugawa et al., 2018). The parameters set were as follows: MS1 mass range: 100-1700 m/z, SWATH scan range: 300-1700 m/z, MS/MS mass range: 100-1700 m/z, time of flight (TOF) MS accumulation time: 50.0 ms, TOF MS/MS accumulation time: 10 ms, collision

energy: +45 V, collision energy spread: 15V, precursor window: 15 Da and the cycle time: 1042 ms. The following ESI parameters were used: source temperature: 250 °C, curtain gas: 35 psi, Gas 1: 25 psi, Gas 2: 25 psi, declustering potential: +80 V, Ion spray voltage floating: 5500 V. The instrument was calibrated automatically with the CDS delivering APCI calibration solution every five samples.

4.2.4. Data processing

The raw data generated by the LC-MS sample run was first converted into an analysis base file (ABF) format using the Reifycs file converter and then processed through the open-source software MS-DIAL v4.12 (Tsugawa et al., 2015). The features obtained from the SWATH analyses were annotated using the software's internal library. The following were the parameters used: MS1 tolerance = 0.01 Da, MS2 tolerance = 0.05 Da, retention time = 0-30 min, MS1 mass range = 300-1700 Da, and minimum peak height = 1000 amplitude (mass slice width, 0.1 Da; sigma window value, 0.5; amplitude of MS/MS abundance cutoff, 0 and retention time tolerance, 24 min). The lipids were annotated using the following parameters MS1 accurate mass tolerance, 0.01 Da; MS2 accurate mass tolerance, 0.05 Da; identification score cut off, 80% and adduct ion settings, [M+H]⁺, [M+NH₄]⁺, [M+Na]⁺, [M+CH₃OH+H]⁺, [M+K]⁺, [M+ACN+H]⁺, [M+H·H₂O]⁺, [M+2H·H₂O]⁺, [M+2Na·H]⁺, [M+IsoProp+H]⁺, [M+CAN+Na]⁺, [M+2K·H]⁺, [M+DMSO]⁺. The peaks were aligned to a quality control sample using a retention time tolerance of 0.05 min and MS1 tolerance of 0.015 Da. The default values for SWATH-MS or conventional all-ions methods data processing were kept for all other parameters. Identification of lipids was performed using the MS-DIAL internal library database with MS1 accurate mass tolerance of 0.01 Da and MS2 accurate mass tolerance of 0.05 Da (Tsugawa et al., 2015).

4.2.5. Statistical analysis

The output data generated from MS-DIAL consisting of peaks of identified lipids and unidentified features were pre-processed in Microsoft Excel and annotated by cross-referencing against existing lipid databases, e.g., LIPID MAPS, and cleaning off artifacts. Only the lipids and features with a coefficient of variance ($CV = SD(PBQCs)/mean(PBQCs)$) below 20% were included to ensure the reproducibility of the results (Yu et al., 2018). Next, the peaks of identified lipids and unidentified lipid features within the 20% CV were normalized to the fresh weight of each sample, and the file was formatted to the specification of the free web-

based online software, Metaboanalyst 4.0 (www.metaboanalyst.ca/MetaboAnalyst). Before performing statistical analysis, data were screened on Metaboanalyst by filtering-out non-informative variables; after which, features abundance was log-transformed, pareto scaled, and statistically analyzed.

Statistical analyses of the processed data were performed by comparing the treatments against different time points and using different treatment combinations. 2D principal component analysis (PCA) and hierarchical cluster analysis paired with a heatmap were used to illustrate lipid abundances. Student's t-test was used to determine the statistical significance of the difference in the lipid abundance between control and PsJN inoculated plants, under each temperature condition, and at each time point. When comparing the abundance of the features between different treatments or time points, only those with a fold change (FC) threshold of 1.2 and with raw P-value < 0.05 were considered significantly different.

4.3. Results

4.3.1. Confirmation of bacterial colonization of the rhizoplane and root tissues

Arabidopsis thaliana Col-0 roots were inoculated with *P. phytofirmans* PsJN and the rhizoplane and tissue colonization were confirmed using bacterial colonization assays as described (**Figure S2a**). On inoculated samples, bacterial growth was present as seen from the colonies on the agar plates after washing the roots (rhizoplane component) and then macerating the washed roots (endophytic component). The colony PCR and 16S rRNA genomic sequencing also confirmed the identity of the colonies as those belonging to the bacterial strain PsJN. Whilst bacterial colonies were observed on the PsJN-inoculated roots, no growth was present from the washed control roots, which confirmed the sterility of the agar system and the root tissue.

4.3.2. Lipid profiling of control and PsJN-inoculated Arabidopsis roots under ambient and high temperature conditions and three time points

The untargeted analysis of lipids from Arabidopsis roots inoculated with PsJN bacteria produced a total of 13886 features, and of those, 693 were annotated as lipids. The annotated lipid species (with their corresponding number of lipid species) belong to the lipid categories

GP (243), GL (278), SP (130), ST (24), PR (3), and FA (22). GPs were divided into PC (63), PE (76), PG (19), PI (24), PS (22), CL (12), LPC (12), and LPE (10). GLs were comprised of DG (89), DGDG (21), MG (19), DGGGA (14), MGDG (9), TG (120), and SQDG (4). SPs were comprised of Cer (102) and HexCer (28). PR was consisted of CoQ (3), while FAs were comprised of NAE (22). ST has 24 lipid species.

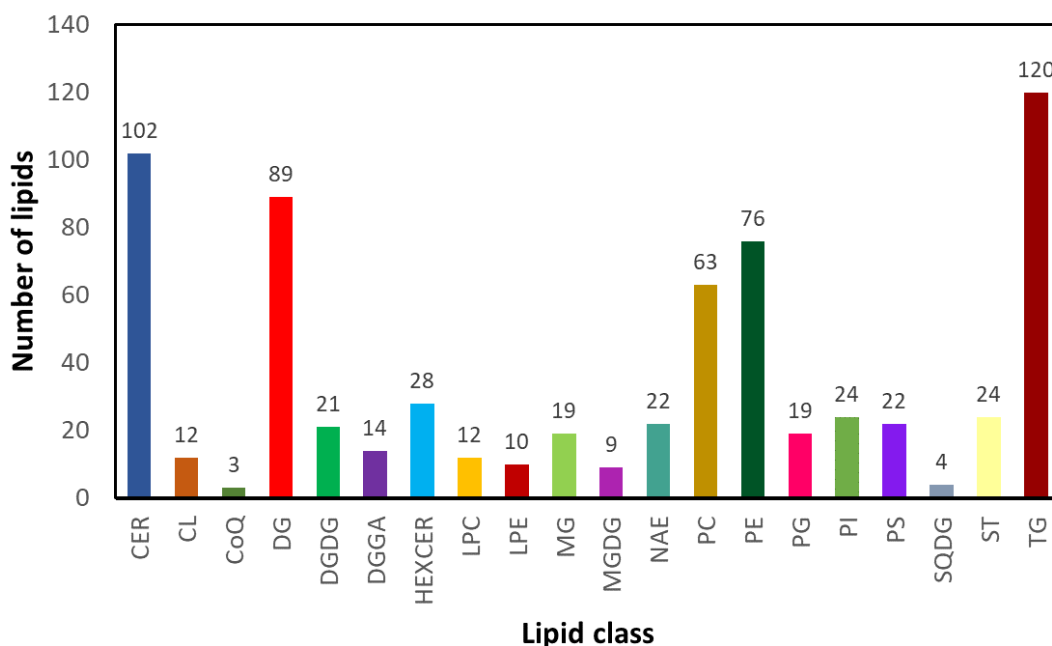


Figure 4. 1 Total number of apparent lipids detected and annotated in Arabidopsis roots subjected to control and PsJN-inoculation and under ambient and high-temperature conditions. Cer – ceramides, CL – cardiolipin, CoQ – coenzyme Q, DG – diacylglycerols, DGDG – digalactosyldiacylglycerols, DGGGA – diacylglyceryl glucuronides, HexCer – hexosylceramides, LPC – lysophosphatidylcholines, LPE – lysophosphatidylethanolamines, MG – monoacylglycerols, MGDG – monogalactosyldiacylglycerols, NAE – N-acylethanolamines, PC – glycerophosphocholines, PE – glycerophosphoethanolamines, PG – glycerophosphoglycerols, PI – glycerophosphoinositol, PS – glycerophosphoserines, SQDG – sulfoquinovosyldiacylglycerols, ST – sterols, TG - triacylglycerols

Out of the individual lipid species annotated belonging to each of the different classes (**Figure 4.1**), 544 lipid annotations were found to be already documented in lipid-based resources such as the LIPID MAPS and the Arabidopsis Lipid Map eFP Browser (https://bar.utoronto.ca/efp_arabidopsis_lipid/cgi-bin/efpWeb.cgi) (Kehelpannala et al., 2021). The remaining features were annotated by cross-referencing the experimental m/z values with accurate masses of an existing list of lipids and by aligning their retention times to the identified

lipids. The rest of the features, labeled in various forms of unknown and unconventional names, were set aside and also subjected to statistical analysis to weigh their significance in explaining the treatment effects or lack thereof. The full list for both data were then filtered down by the calculation of the CV and the acceptance of values below 20% to ascertain the reproducibility of the result (Schillaci, Kehelpannala, et al., 2021).

A data dimension reduction performed by principal component analysis (PCA) showed clear clustering between replicates from all treatments (**Figure 4.2**). The cluster of brown circles evidently separated from the rest on the right side of the quadrant represents the pooled biological quality control samples. This indicates good reproducibility and reliability in the detection by the methods; and therefore, data can be utilized for subsequent analysis, such as subjecting for further lipid identification procedures.

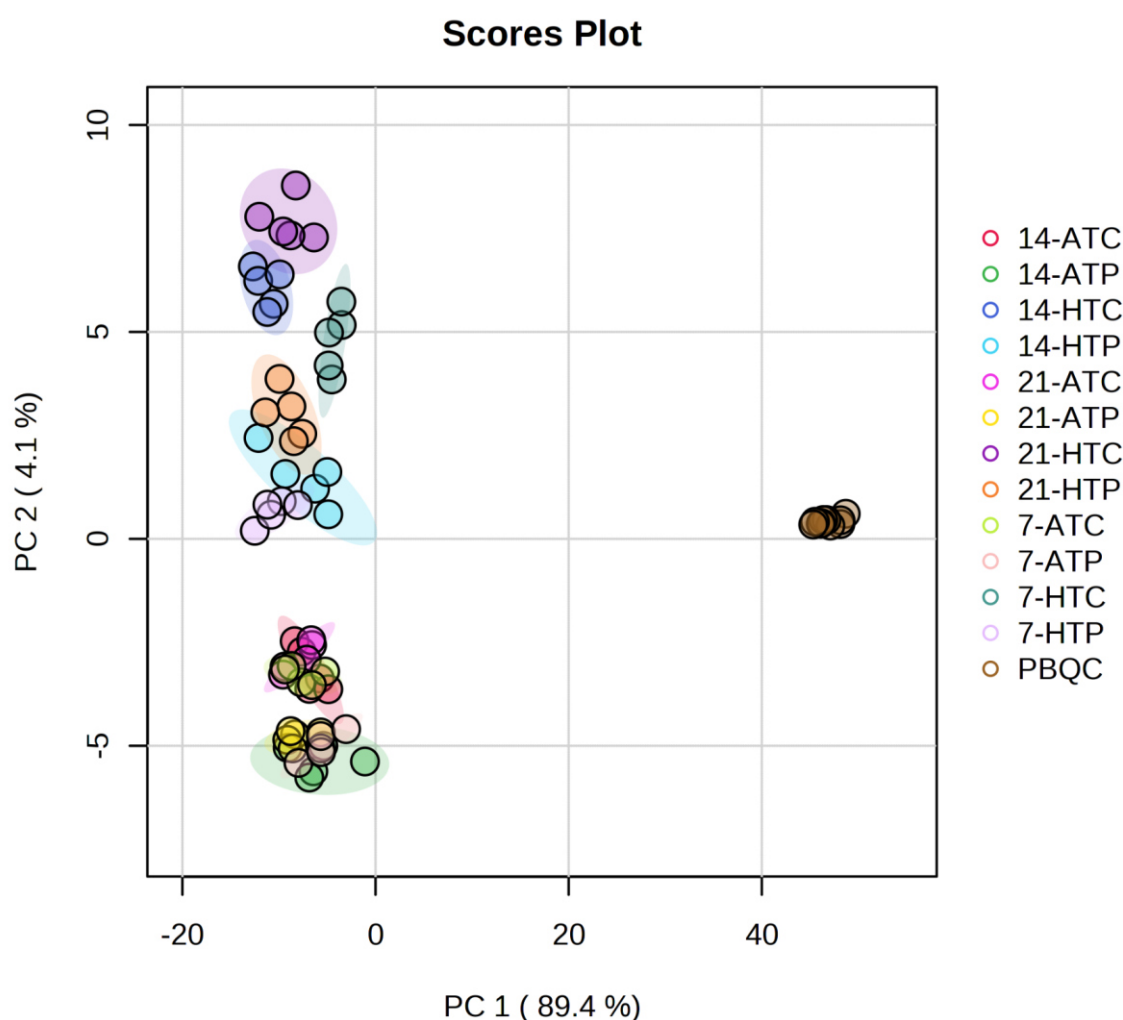


Figure 4.2 Principal component analysis (PCA) score plot of the annotated lipids detected from control and PsJN-inoculated roots subjected to ambient and high-temperature conditions. Treatments: ATC – ambient-control, ATP – ambient- PsJN-inoculated, HTC – high temperature- control, HTP – high-temperature- PsJN -inoculated, pooled biological quality control (PBQC) samples. Numbers at the start

of each treatment name refers to measurements or harvest times at 7, 14, and 21 days after inoculation (DAI). Coloured ellipses around samples display 95% confidence areas.

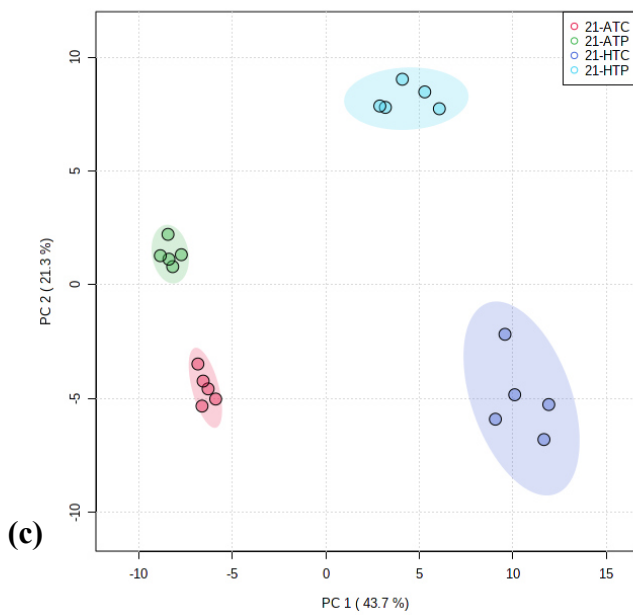
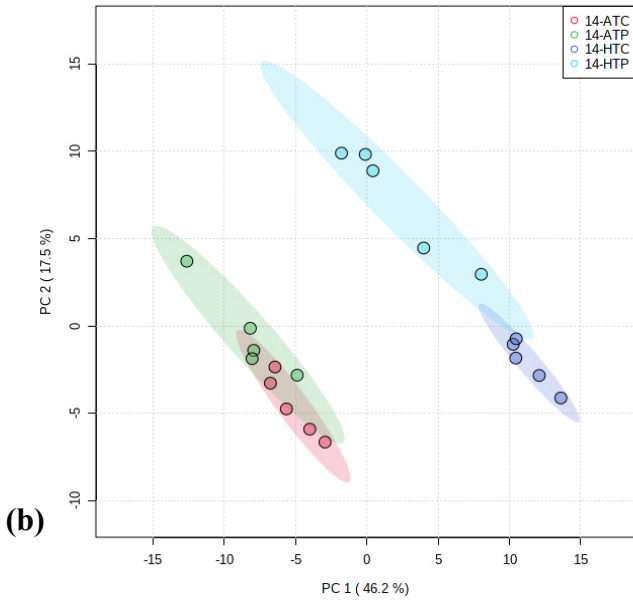
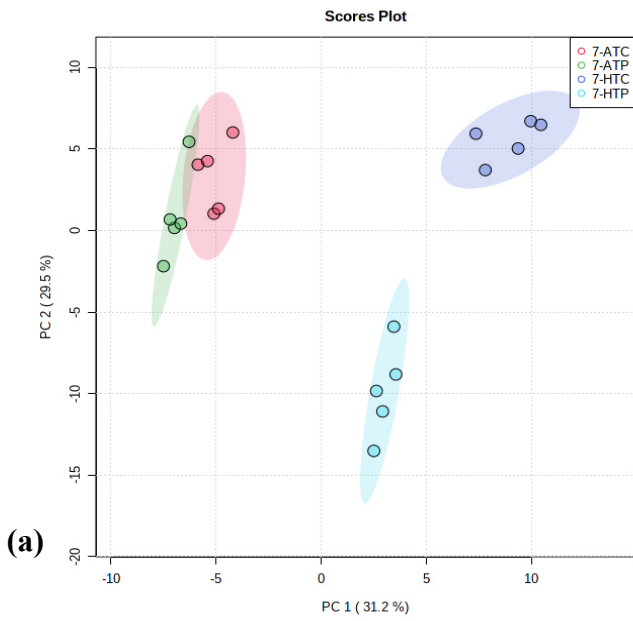
4.3.3. Comparison of annotated lipids and unknown features profile of Arabidopsis roots under four treatments and three timepoints

Further PCA plots were generated for the comparison of all four treatments under each timepoint for both annotated lipids and unknown features. The PCA analysis of the annotated lipid species detected in Arabidopsis control and PsJN-inoculated roots across different time points showed a consistent separation based on temperature, and in some cases (i.e., at 7 and 21 DAI), from the effect of bacterial inoculation, more prominently shown under high-temperature conditions (**Figure 4.3**). The 1st and 2nd PCA accounted for 60.7%, 63.7%, and 65% of the variation of the treatment at 7, 14, and 21 DAI, respectively. The PCA scatterplot for (**Figure 4.3Aa**) and (**Figure 4.3Ac**) showed clustering of treatments ambient–control (ATC) and ambient–PsJN-inoculated (ATP), and separation of treatments high temperature–control (HTC) and high temperature–PsJN-inoculated (HTP).

When compared with the unknown features, the same trend was also observed in the prominent separation between ambient and high temperature treatments. On all time points (7, 14, and 21 DAI) (**Figure 4.3Ba-c**), however, the effect of bacterial inoculation was observed consistently under high temperature from the clear separation of groups HTC and HTP (**Figure 4.3**). The 1st and 2nd PCA accounted for 54.7%, 62%, and 54% of the variation in the treatments at 7, 14, and 21 DAI, respectively. The same clear separation of ambient (ATC and ATP) and high temperature (HTC and HTP) treatments was observed, and on the latter, the separation of control and PsJN-inoculated treatments (HTC vs. HTP).

On both annotated lipids and unknown feature profiles, the effect of bacterial inoculation under ambient conditions appeared inconclusive, i.e., the annotated lipids showed some separation between control and PsJN-inoculated roots only at 21 DAI (**Figure 4.3Ac**), whereas the unknown features showed this bacterial inoculation effect under ambient at 7 DAI (**Figure 4.3Ba**).

(A) Annotated lipids



(B) Unknown features

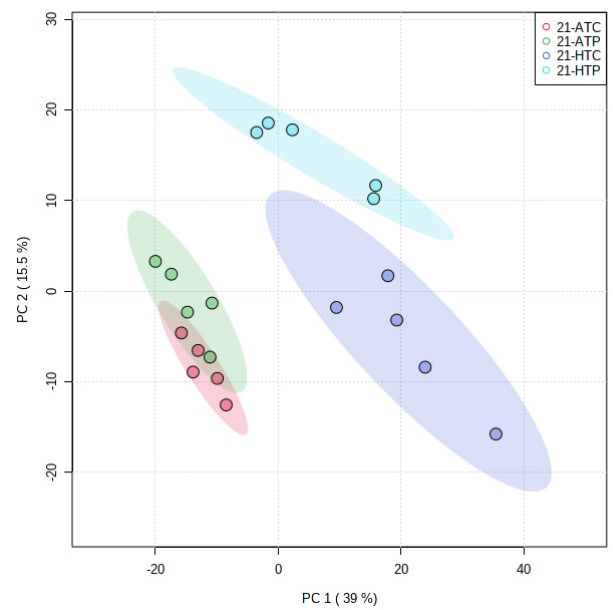
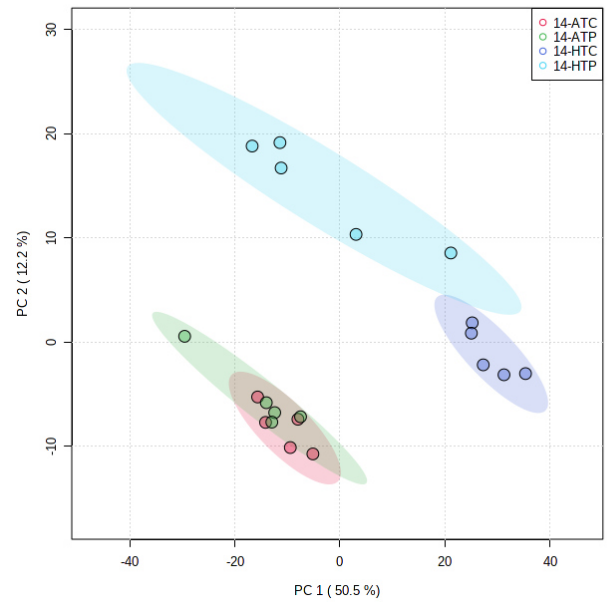
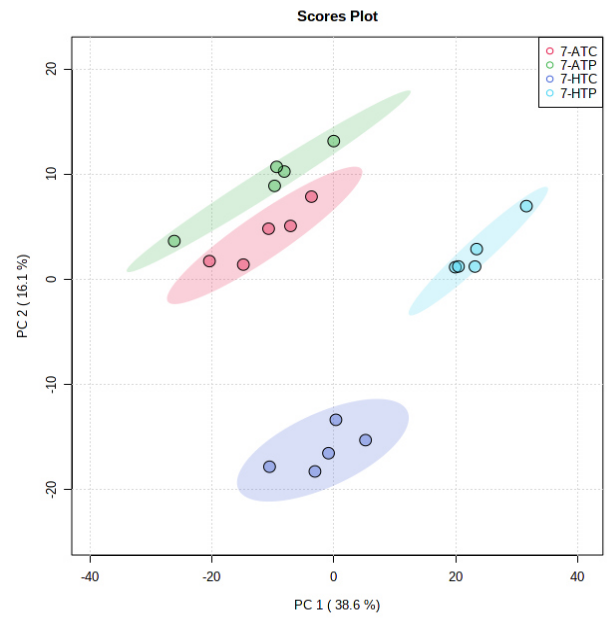
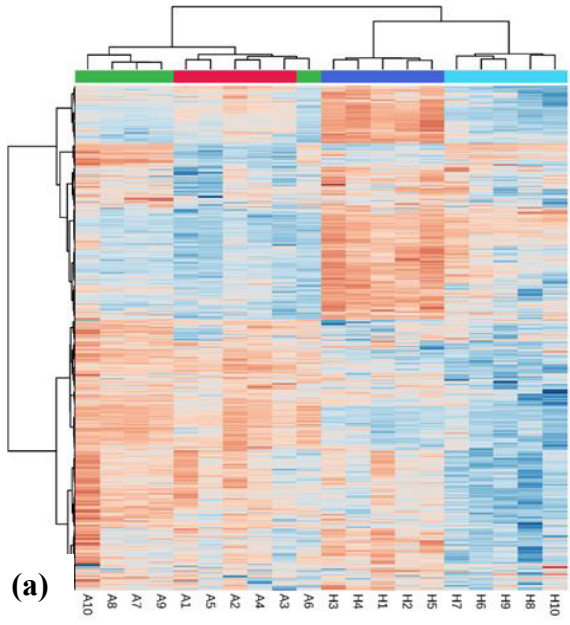


Figure 4.3 Principal component analysis (PCA) plots of the annotated lipids (A) and unknown features (B) detected from control and PsJN-inoculated roots subjected to ambient and high-temperature conditions. Legend: ATC – ambient-control, ATP – ambient- PsJN-inoculated, HTC – high temperature- control, HTP – high-temperature- PsJN -inoculated. Measurements were taken at (a) 7 (top), (b) 14 (middle), and (c) 21 (bottom) days after inoculation (DAI). Coloured ellipses around samples display 95% confidence areas.

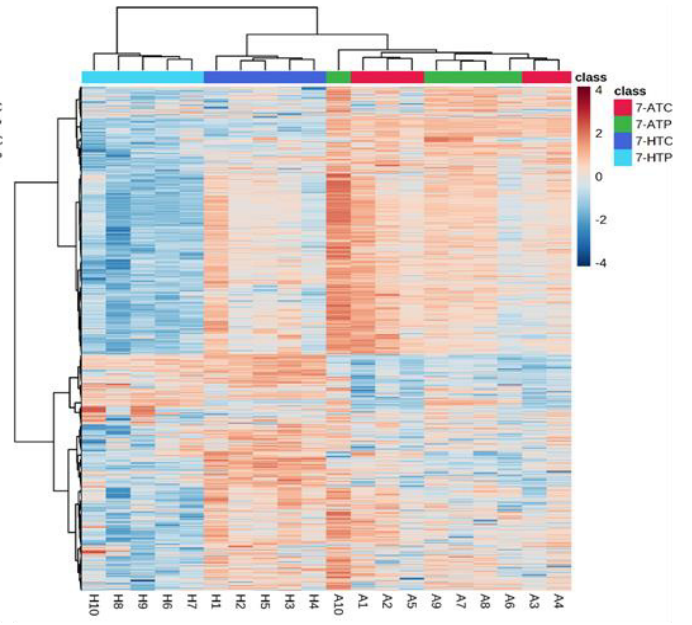
The hierarchical clustering plots, coupled with the heatmap and dendrogram, comparing the four treatments – control and PsJN-inoculated plants under ambient and high-temperature conditions, also showed the separation and relative abundances of the four main lipid clusters on each time point (**Figure 4.4**). In annotated lipids, there were separations in the treatments under each of the three time points. At both 7 and 21 DAI, three distinct clusters were formed – ATC and ATP, HTC, and HTP (**Figure 4.4Aa, Ac**). At 14 DAI, the clustering was not very distinct, though there was an indication of the separation of ambient samples against high temperature treatments (**Figure 4.4Ab**). From the unknown features data, there was a separation of HTP distinctly from the other two treatment groups – HTC and the further clustered subclasses for ATC and ATP at 7 DAI (**Figure 4.4Ba**). At 14 DAI, there were two main separations, one for HTC (though with some samples from HTP), the cluster of ATC and ATP, and finally HTP (**Figure 4.4Bb**). At 21 DAI, there was not a clear separation, although HTC was disconnected from the aggregated clusters of ATC, ATP, and some HTC (**Figure 4.4Bc**).

A one-way analysis of variance (ANOVA) revealed the number of lipid species that were significantly different among the four treatments on both annotated lipids and unknown features (**Figure 4.5**). The number of significantly changed lipid species against nonsignificant (Sig/Unsig) ones from the annotated lipid data were 574/127, 513/188, and 506/195 for 7, 14, and 21 DAI, respectively (**Figure 4.5Aa-c**). For unknown features on the other hand, significant against nonsignificant lipid species from 7 to 21 DAI were 2552/835, 2505/882, and 2033/1354, respectively (**Figure 4.5Ba-c**). Aside from the large difference in the number of significant features between annotated and unknown profile, one notable observation was the decrease in the ratio between significant and nonsignificant lipid species from 7 DAI to 21 DAI. That is, for annotated – from 4.52 to 2.72 down to 2.59; while for unknown – from 3.05 to 2.84, and then down to 1.50 (**Figure 4.5A, B**).

(A) Annotated lipids



(B) Unknown features



(a)

(b)

(c)

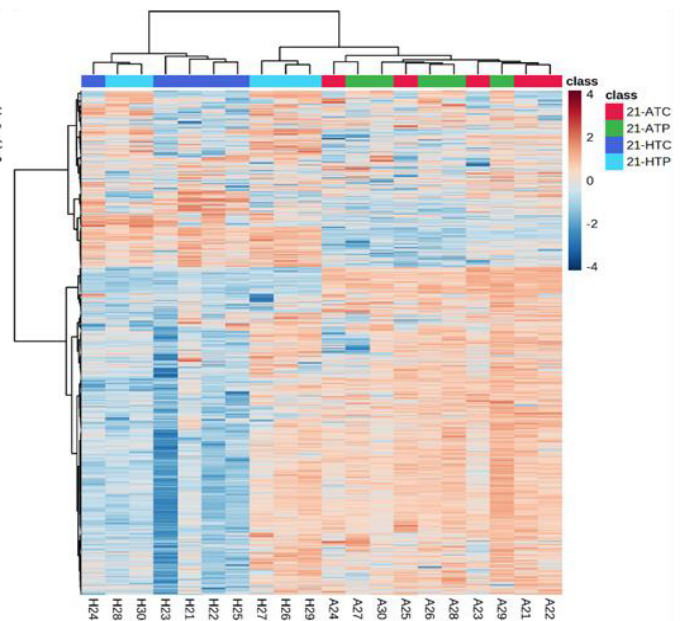
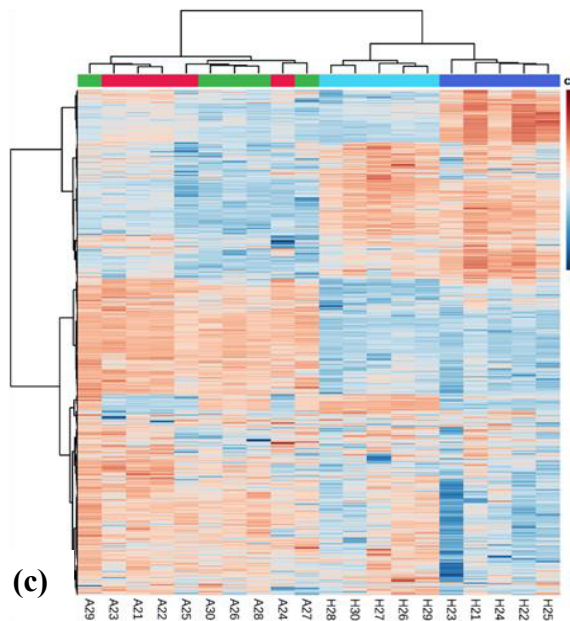
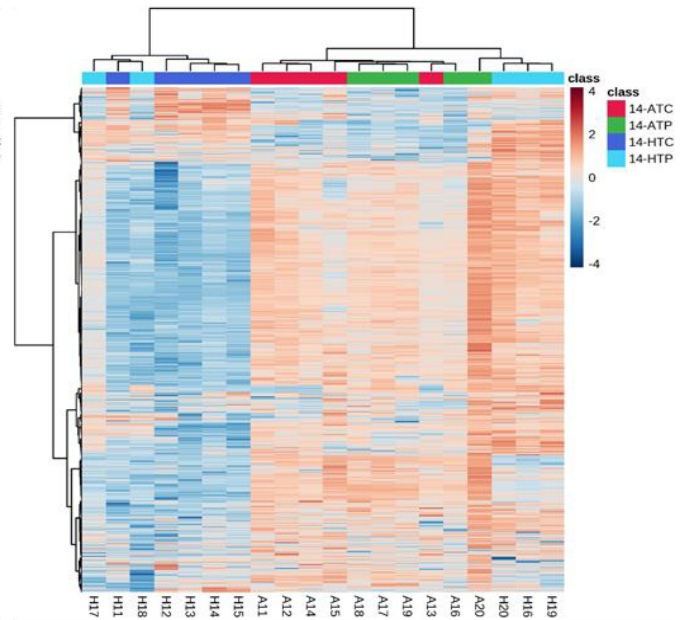
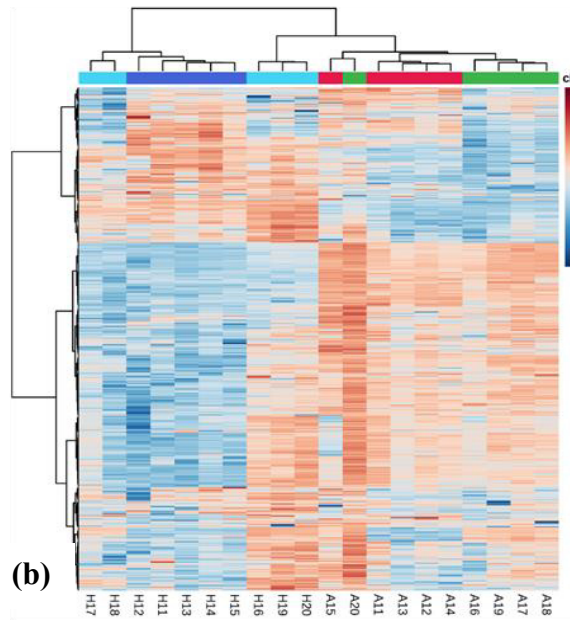


Figure 4. 4 Hierarchical clustering coupled with heatmap of the annotated lipids (A) and unknown features (B) detected from control and PsJN-inoculated roots subjected to ambient and high-temperature conditions. Legend on the upper right side: ATC – ambient-control, ATP – ambient- PsJN-inoculated, HTC – high temperature- control, HTP – high-temperature- PsJN -inoculated. Measurements were taken at (a) 7 (top), (b) 14 (middle), and (c) 21 (bottom) days after inoculation (DAI). Label at the bottom refers to the replicates; and for each replicate (column), blue and red colours signify the lower and higher abundance of specific lipids as compared to the other replicates, with darker colours indicating more pronounced differences. Dendrogram at the top indicates the main lipid clusters represented with branches of different colours.

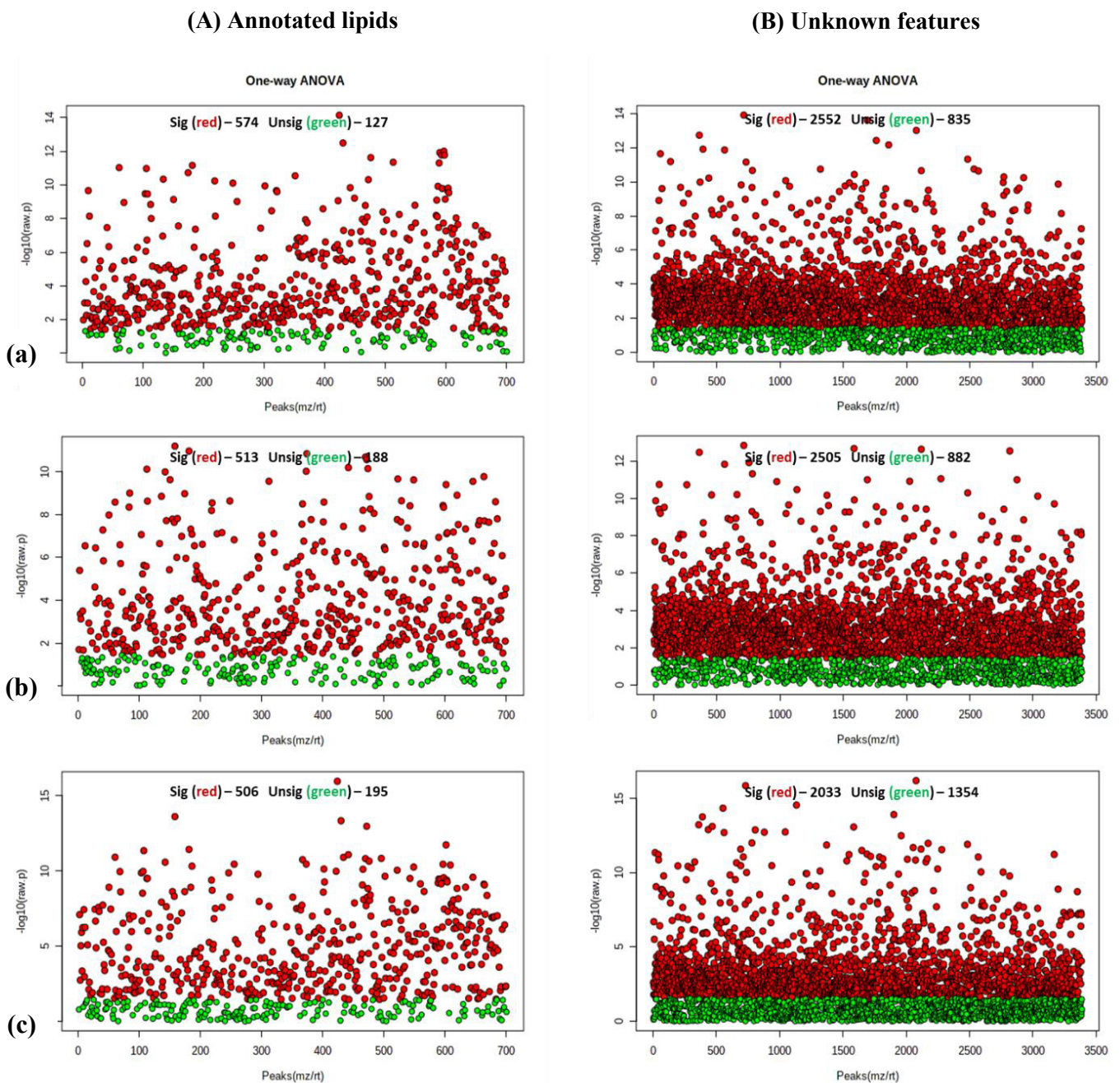


Figure 4. 5 Analysis of variance (ANOVA) of the annotated lipids and unknown features detected from control and PsJN-inoculated roots subjected to ambient and high-temperature conditions. Red dots – lipid species showing significant differences, green dots – lipid species showing no significant differences. (a), (b), and (c) represents the time points 7, 14, and 21 days after inoculation (DAI).

Although the analysis on the unidentified features profile could not provide further information about specific lipids, they have presented insights on the potential contribution of the unknown features to the changes involved among the treatments throughout the plant development. Therefore, to look into the specific contribution of lipids involved in this study's plant root-bacteria-temperature interactions, the annotated lipid profiles (**Figure 4.3A**) were further investigated and dissected.

Looking at the loadings of the first two principal components of the four treatments at each time point, the specific lipids that have strongly influenced the PCA analysis were elucidated (**Table 1 – 3**). In **Figure 4.3A-a**, the highest and lowest loading values indicated the most important lipid species for assigning the principal component 1 (PC1). PC1 explained 31.2% of the variance among the lipid profiles of the four treatments. Examining the loading values indicated that the separation of the treatments is due to higher levels of specific species CL 72:8|CL 36:3_36:5, Cer 42:3;3O|Cer 28:3;2O/14:0;O, Cer 43:3;3O|Cer 29:2;2O/14:1;O, TG 51:5|TG 15:0_18:2_18:3, and MG 38:4 (highest five); and lower levels of CL 72:12|CL 36:6_36:6, LPE 26:0, PE 42:4|PE 26:1_16:3, DG 42:0|DG 20:0_22:0, and HexCer 42:3;3O|HexCer 18:2;2O/24:1;O (lowest five) (the rest of the loadings shown in **Table 2**).

In **Figure 4.3A-b**, the PC1 explained 46.2% of the variance of the four treatments at 14 DAI. Upon examination of the loading values, the specific lipid species that contributed the most to the separation are MG 38:4, Cer 46:4;3O|Cer 18:1;2O/28:3;O, Cer 46:4;3O|Cer 18:1;2O/28:3;O, ST 28:2;O, and Cer 43:3;3O|Cer 29:2;2O/14:1;O as the highest five, while the lowest five was contributed by PI 45:12, CL 72:12|CL 36:6_36:6, PI 47:12, PE 42:4|PE 26:1_16:3, and DG 36:6|DG 18:3_18:3 (the rest of the loadings shown in **Table 3**).

In **Figure 4.3A-c**, the PC1 represented 43.7% of the variance of the compared treatments at 21 DAI. Here, the loadings indicated that the highest five levels of species contributing to the separation were from CL 72:8|CL 36:3_36:5, Cer 42:3;3O|Cer 28:3;2O/14:0;O, Cer 43:3;3O|Cer 29:2;2O/14:1;O, TG 51:5|TG 15:0_18:2_18:3, and MG 38:4, while the lowest five levels were from CL 72:12|CL 36:6_36:6, LPE 26:0, PE 42:4|PE 26:1_16:3, DG 42:0|DG 20:0_22:0, and HexCer 42:3;3O|HexCer 18:2;2O/24:1;O (the rest of the loadings shown in **Table 4**).

Table 4. 2 Loadings of the first two principal components of the four treatments (control roots under ambient, PsJN-inoculated roots at ambient, control roots at high temperature, and PsJN-inoculated roots at high temperature) at 7 days after inoculation (DAI).

Lipid species	PC1	Lipid species	PC2
7 DAI			
<i>Fifteen highest loading values</i>			
CL 72:8 CL 36:3_36:5	0.095	TG 46:3 TG 14:0_14:0_18:3	0.097
Cer 42:3;3O Cer 28:3;2O/14:0;O (a)	0.087	TG 48:3 TG 14:0_16:0_18:3	0.097
Cer 43:3;3O Cer 29:2;2O/14:1;O	0.085	TG 47:3 TG 14:0_15:0_18:3	0.091
TG 51:5 TG 15:0_18:2_18:3 (b)	0.084	TG 49:6 TG 14:0_17:3_18:3	0.091
MG 38:4 (a)	0.082	TG 48:2 TG 14:0_16:0_18:2 (a)	0.090
CL 72:9 CL 36:4_36:5 (a)	0.079	TG 46:2 TG 14:0_14:0_18:2	0.089
PE 41:1 PE 16:0_25:1	0.078	TG 47:2 TG 14:0_15:0_18:2	0.087
TG 58:4 TG 22:0_18:2_18:2	0.078	TG 47:1 TG 15:0_16:0_16:1	0.086
Cer 44:3;3O Cer 18:1;2O/26:2;O	0.078	TG 46:1 TG 14:0_16:0_16:1	0.083
DGDG 35:2 DGDG 17:0_18:2	0.077	TG 50:6 TG 14:0_18:3_18:3 (b)	0.082
DG 43:4 DG 25:1_18:3	0.077	TG 48:4 TG 14:0_16:1_18:3	0.082
Cer 44:3;3O Cer 22:3;2O/22:0;O	0.075	TG 49:3 TG 15:0_16:0_18:3	0.082
PC 30:0 PC 15:0_15:0	0.074	TG 50:5 TG 14:0_18:2_18:3 (a)	0.082
HexCer 40:0;4O HexCer 18:0;3O/22:0;(2OH)	0.073	TG 43:0 TG 14:0_14:0_15:0	0.081
TG 59:4 TG 23:0_18:2_18:2	0.073	TG 54:3 TG 18:1_18:1_18:1	0.081
<i>Fifteen lowest loading values</i>			
PC 34:6	-0.064	TG 52:6 TG 16:0_18:3_18:3 (c) Cer 33:1;4O Cer 17:1;3O/16:0;(2OH)	-0.037
PE 38:3 PE 20:0_18:3	-0.065	PE 32:0 PE 16:0_16:0	-0.038
PG 44:3	-0.065	LPE 17:1 (a)	-0.040
CL 67:2 CL 33:1_34:1	-0.065	PC 32:0 PC 16:0_16:0	-0.041
PE 36:6 PE 18:3_18:3	-0.071	LPE 19:1	-0.055
LPE 25:0	-0.071	PG 38:2 PG 19:1_19:1	-0.067
PE 42:3 PE 24:0_18:3	-0.071	CL 67:3 CL 33:1_34:2	-0.075
PI 35:6	-0.072	PE 35:1 PE 16:0_19:1	-0.077
PE 43:3	-0.074	PE 33:1 PE 16:0_17:1	-0.077
DG 36:6 DG 18:3_18:3	-0.074	PG 35:1 PG 16:0_19:1	-0.085
HexCer 42:3;3O HexCer 18:2;2O/24:1;O	-0.075	PE 32:4	-0.090
DG 42:0 DG 20:0_22:0	-0.075	CL 67:2 CL 33:1_34:1	-0.092
PE 42:4 PE 26:1_16:3	-0.079	CL 68:3 CL 33:1_35:2	-0.093
LPE 26:0	-0.080	CL 65:1 CL 30:0_35:1	-0.096
CL 72:12 CL 36:6_36:6	-0.083		-0.105

Table 4.3 Loadings of the first two principal components of the four treatments (control roots under ambient, PsJN-inoculated roots at ambient, control roots at high temperature, and PsJN-inoculated roots at high temperature) at 14 days after inoculation (DAI).

Lipid species	PC1	Lipid species	PC2
14 DAI			
<i>Fifteen highest loading values</i>			
MG 38:4 (a)	0.074	CL 67:2 CL 33:1_34:1	0.147
Cer 46:4;3O Cer 18:1;2O/28:3;O (c)	0.065	CL 67:3 CL 33:1_34:2	0.146
Cer 46:4;3O Cer 18:1;2O/28:3;O(b)	0.063	CL 65:1 CL 30:0_35:1	0.146
ST 28:2;O (b)	0.060	PE 32:4	0.136
Cer 43:3;3O Cer 29:2;2O/14:1;O	0.059	PG 35:1 PG 16:0_19:1	0.132
PE 41:1 PE 16:0_25:1	0.057	CL 68:3 CL 33:1_35:2	0.130
Cer 44:3;3O Cer 22:3;2O/22:0;O	0.055	PE 33:1 PE 16:0_17:1	0.129
CL 72:8 CL 36:3_36:5	0.055	PE 35:1 PE 16:0_19:1	0.119
Cer 42:3;3O Cer 28:3;2O/14:0;O (a)	0.055	PG 38:2 PG 19:1_19:1	0.115
TG 51:5 TG 15:0_18:2_18:3 (b)	0.052	LPE 19:1	0.105
TG 56:2 TG 16:0_22:0_18:2 (a)	0.052	LPE 17:1 (a)	0.101
TG 58:4 TG 22:0_18:2_18:2	0.052	PE 32:0 PE 16:0_16:0	0.099
TG 59:4 TG 23:0_18:2_18:2	0.051	TG 54:7 TG 18:2_18:2_18:3	0.086
CoQ8	0.050	PE 31:1 PE 14:0_17:1	0.084
TG 60:4 TG 24:0_18:2_18:2	0.049	TG 54:6 TG 18:1_18:2_18:3	0.083
<i>Fifteen lowest loading values</i>			
TG 54:9 TG 18:3_18:3_18:3	-0.072	TG 50:3 TG 16:0_16:0_18:3	-0.059
TG 54:8 TG 18:2_18:3_18:3 (a)	-0.072	TG 50:6 TG 14:0_18:3_18:3 (b)	-0.060
CoQ11	-0.072	TG 49:6 TG 14:0_17:3_18:3	-0.060
PE 43:3	-0.074	DGGA 36:6 DGGA 18:3_18:3 (a)	-0.062
PC 35:6	-0.075	PE 45:2	-0.064
CL 68:3 CL 33:1_35:2	-0.075	DG 42:0 DG 20:0_22:0	-0.064
DGDG 36:8 DGDG 18:4_18:4	-0.076	PS 33:3	-0.064
PE 42:3 PE 24:0_18:3	-0.077	TG 48:2 TG 14:0_16:0_18:2 (a)	-0.064
PC 36:6 PC 18:3_18:3	-0.077	PI 35:6	-0.069
PE 48:8 PE 18:3_30:5	-0.078	PC 35:6	-0.071
DG 36:6 DG 18:3_18:3	-0.079	TG 49:3 TG 15:0_16:0_18:3	-0.074
PE 42:4 PE 26:1_16:3	-0.079	TG 46:3 TG 14:0_14:0_18:3	-0.077
PI 47:12	-0.084	TG 48:5 TG 12:0_18:2_18:3	-0.080
CL 72:12 CL 36:6_36:6	-0.088	TG 49:2 TG 15:0_16:0_18:2	-0.083
PI 45:12	-0.090	TG 48:3 TG 14:0_16:0_18:3	-0.084

Table 4. 4 Loadings of the first two principal components of the four treatments (control roots under ambient, PsJN-inoculated roots at ambient, control roots at high temperature, and PsJN-inoculated roots at high temperature) at 21 days after inoculation (DAI).

Lipid species	PC1	Lipid species	PC2
21 DAI			
<i>Fifteen highest loading values</i>			
CL 72:8 CL 36:3_36:5	0.095	CL 67:3 CL 33:1_34:2	0.172
Cer 42:3;3O Cer 28:3;2O/14:0;O (a)	0.087	CL 67:2 CL 33:1_34:1	0.171
Cer 43:3;3O Cer 29:2;2O/14:1;O	0.085	CL 65:1 CL 30:0_35:1	0.167
TG 51:5 TG 15:0_18:2_18:3 (b)	0.084	CL 68:3 CL 33:1_35:2	0.163
MG 38:4 (a)	0.082	PG 35:1 PG 16:0_19:1	0.160
CL 72:9 CL 36:4_36:5 (a)	0.079	PE 32:4	0.152
PE 41:1 PE 16:0_25:1	0.078	PE 33:1 PE 16:0_17:1	0.136
TG 58:4 TG 22:0_18:2_18:2	0.078	LPE 19:1	0.128
Cer 44:3;3O Cer 18:1;2O/26:2;O	0.078	PG 38:2 PG 19:1_19:1	0.128
DGDG 35:2 DGDG 17:0_18:2	0.077	PE 35:1 PE 16:0_19:1	0.119
DG 43:4 DG 25:1_18:3	0.077	LPE 17:1 (a)	0.111
Cer 44:3;3O Cer 22:3;2O/22:0;O	0.075	MG 32:4 (a)	0.097
PC 30:0 PC 15:0_15:0	0.074	PE 31:1 PE 14:0_17:1	0.092
HexCer 40:0;4O HexCer 18:0;3O/22:0;(2OH)	0.073	CL 66:3 CL 32:1_34:2	0.089
TG 59:4 TG 23:0_18:2_18:2	0.073	PE 32:0 PE 16:0_16:0	0.084
<i>Fifteen lowest loading values</i>			
PC 34:6	-0.064	TG 49:4 TG 14:0_17:2_18:2	-0.087
PE 38:3 PE 20:0_18:3	-0.065	TG 51:4 TG 15:0_18:2_18:2	-0.087
PG 44:3	-0.065	TG 50:2 TG 16:0_16:0_18:2 (a)	-0.089
CL 67:2 CL 33:1_34:1	-0.065	TG 49:5 TG 14:0_17:2_18:3	-0.093
PE 36:6 PE 18:3_18:3	-0.071	TG 49:6 TG 14:0_17:3_18:3	-0.094
LPE 25:0	-0.071	TG 46:2 TG 14:0_14:0_18:2	-0.095
PE 42:3 PE 24:0_18:3	-0.071	TG 47:2 TG 14:0_15:0_18:2	-0.098
PI 35:6	-0.072	TG 50:3 TG 16:0_16:0_18:3	-0.100
PE 43:3	-0.074	TG 50:6 TG 14:0_18:3_18:3 (b)	-0.105
DG 36:6 DG 18:3_18:3	-0.074	TG 47:3 TG 14:0_15:0_18:3	-0.107
HexCer 42:3;3O HexCer 18:2;2O/24:1;O	-0.075	TG 46:3 TG 14:0_14:0_18:3	-0.108
DG 42:0 DG 20:0_22:0	-0.075	TG 48:2 TG 14:0_16:0_18:2 (a)	-0.112
PE 42:4 PE 26:1_16:3	-0.079	TG 49:3 TG 15:0_16:0_18:3	-0.112
LPE 26:0	-0.080	TG 49:2 TG 15:0_16:0_18:2	-0.118
CL 72:12 CL 36:6_36:6	-0.083	TG 48:3 TG 14:0_16:0_18:3	-0.122

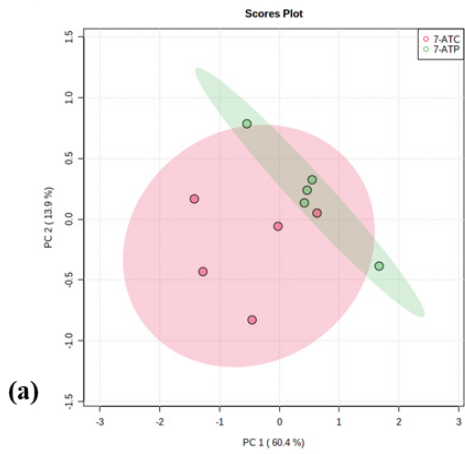
4.3.4. Comparison of lipid class profiles of control and PsJN-inoculated roots under each treatment and time point

To further understand how the lipid profiles of control and PsJN-inoculated roots changes under each temperature treatment and over time, further univariate analysis was performed. Here, we divide the analysis per time point and from each time point, we determine the lipid changes due to the bacterial inoculation under ambient (graph **A** of **Figure 4.6-4.8**) and high temperature (graph **B** of **Figure 4.6-4.8**) conditions. Univariate analysis examines each variable separately and for this, a fold change comparison analysis was constructed. Fold change is used to compare and quantify the changes (as a ratio between two quantities), which in this case, are the increase or decrease of peak areas of lipids, between two compared variables (i.e., control and PsJN-inoculated roots). Described fold changes (with a threshold of 1.2 for this study), was paired with the two-sample *t*-test using the statistical significance level $p < 0.05$ and the Wilcoxon rank-sum tests, to determine whether the increase or decrease in the lipid levels were statistically significant. The fold changes were then \log_2 transformed and plotted in the x-axis against all the lipid classes. For this analysis, lipid class peak areas were calculated by averaging the sum of peak areas of lipid species in each sample.

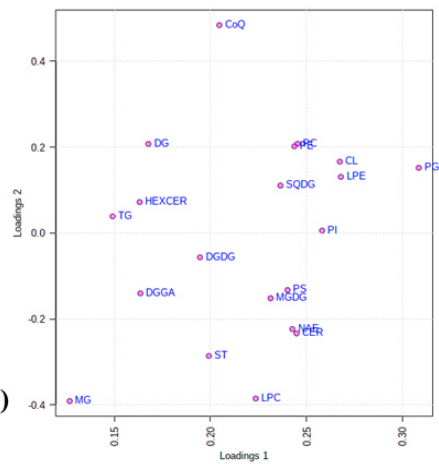
Figure 4.6 describes the various univariate analysis for comparing the lipid classes of control and PsJN-inoculated roots at 7 DAI. Under ambient condition, no clear separation of the two treatments were observed in the PCA score plot (**Figure 4.6Aa**). The PC1 value of 60.4% and PC2 value of 13.9% explained the variance of the lipid profiles between the control and PsJN-inoculated roots. Although not clearly separated, the PCA analysis was partially assigned by the highest and lowest loading values of PC1 and PC2 (**Figure 4.6Ab**, **Table 5**). PC1 consisted of the higher levels of lipid classes CL, LPE, PC, PG, and PI; and the lower levels from the lipid classes DG, DGGA, HexCer, MG and TG. PC2 loadings also showed that higher levels of CL, CoQ, DG, PC, and PE; as well as the lower levels of CER, LPC, MG, NAE, and ST, contributed to the outcome of the PCA analysis (**Table 5**). Fold change analysis showed that, although not significant, the levels of CL, CoQ, LPE, PC, PE, PG, and SQDG were lower in control roots as opposed to PsJN-inoculated roots (**Figure 4.6Ac**).

Under high temperature condition, PCA score plot analysis showed a separation of control and PsJN-inoculated root treatments and the variance was attributed mainly to the PC1 of 75.7% (**Figure 4.6Ba**). Examination of the loading values of PC1 showed that the higher levels (CoQ, DG, DGGA, HexCer, and LPE) and lower levels (CL, MG, MGDG, PI, and TG) of lipid species contributed to this separation observed in the PCA plot (**Figure 4.6Bb**, **Table 5**).

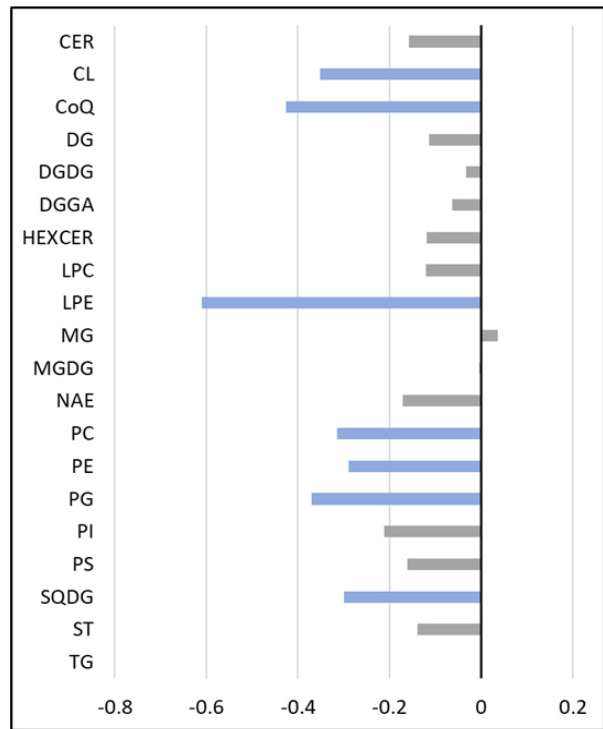
A



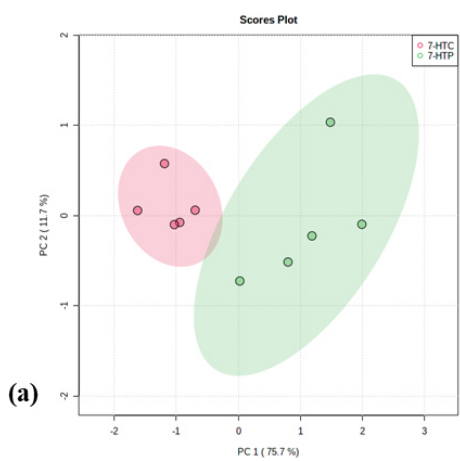
(a)



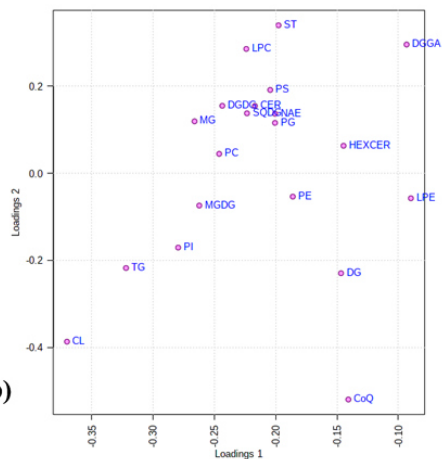
(b)



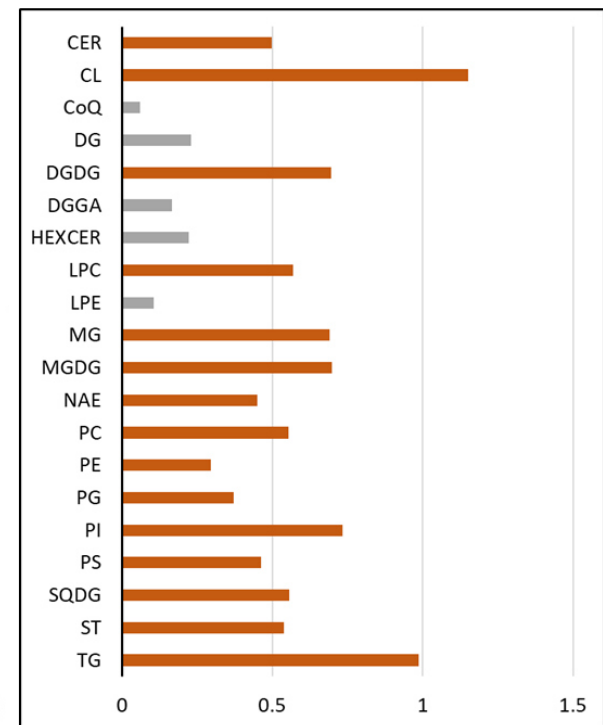
B



(a)



(b)



(c)

Figure 4. 6 Principal component analysis (PCA) (a), PCA loading plot (b), and log₂ fold change comparison (c) of the levels of lipid classes between control and PsJN-inoculated roots subjected under ambient (A) and high-temperature (B) conditions at 7 days after inoculation (DAI). Treatments: ATC – ambient-control, ATP – ambient- PsJN-inoculated, HTC – high temperature- control, HTP – high-temperature- PsJN-inoculated. Coloured ellipses around samples display 95% confidence areas.

Fold changes were calculated by averaging the sum of peak areas of a lipid class by the number of replicates (n=5) per treatment, and then log₂ transformed. The direction of comparison is ATC/ATP. Bar colors: grey – non-significant change, decreased - light blue, dark blue – significantly decreased, light orange – increased, dark orange – significantly increased. Significant differences were determined by two-sample t-test (significance level $p < 0.05$) and the Wilcoxon rank-sum tests. Lipid class abbreviation - refer to page 156.

The fold change analysis shown in **Figure 4.6Bc** revealed that several lipid classes were significantly higher in control roots than PsJN-inoculated roots under high temperature. This consists of CER, CL, DGDG, LPC, MG, MGDG, NAE, PC, PE, PG, PI, PS, SQDG, ST, and TG. This suggests that bacterial inoculation, under the influence of increased temperature, decreased many of the lipid species in Arabidopsis roots at the early development stage of the roots.

At 14 DAI (**Figure 4.7**), both PCA score plots of control and PsJN-inoculated roots under ambient and high temperatures did not show any separation (**Figure 4.7Aa, 4.7Ba**). Under ambient conditions, PC1 and PC2 accounted for 71.2% and 10.3% of variation in the treatments (**Figure 4.7Aa**). The PC1 loading values that contributed to the outcome of the PCA score plot were the higher levels of DGDG, LPC, LPE, SQDG, and ST; and the lower levels of CL, DG, PC, PE, and PG. On the other hand, PC2 higher values came from LPC, MGDG, NAE, PG, and PI; while lower values were from CL, CoQ, DG, LPE, and PE (**Figure 4.7Ab, Table 5**). based on the fold change comparison, the lipid levels of DG, MGDG, and PG were lower in control plants, though not statistically significant (**Figure 4.7Ac**).

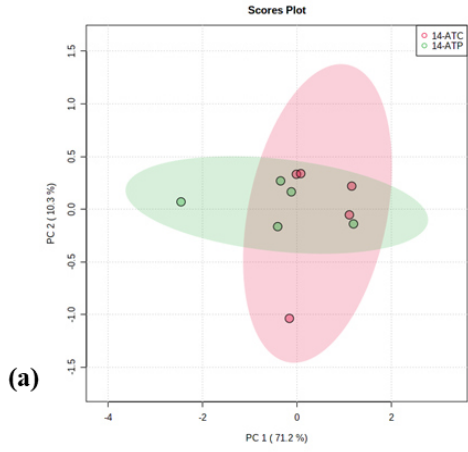
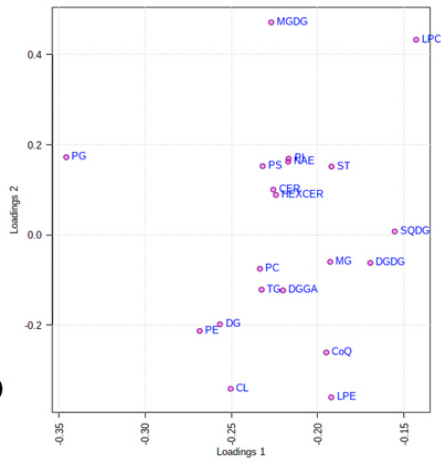
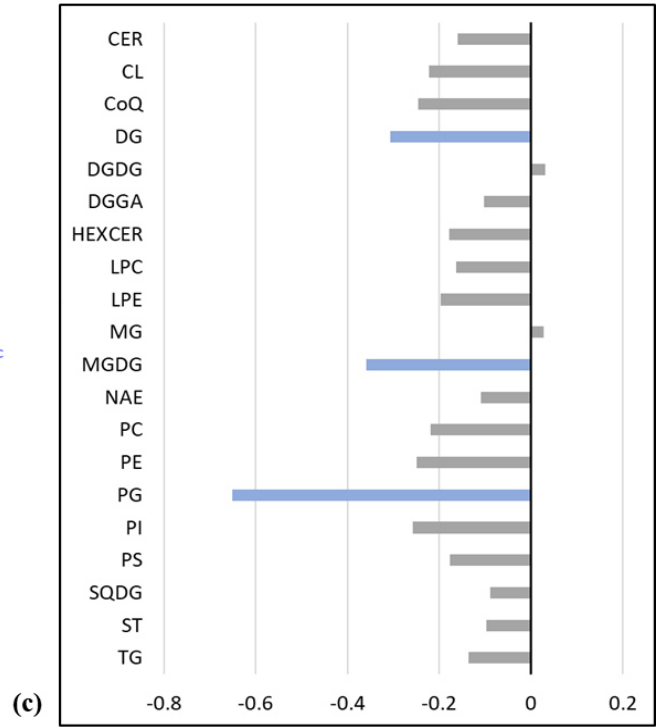
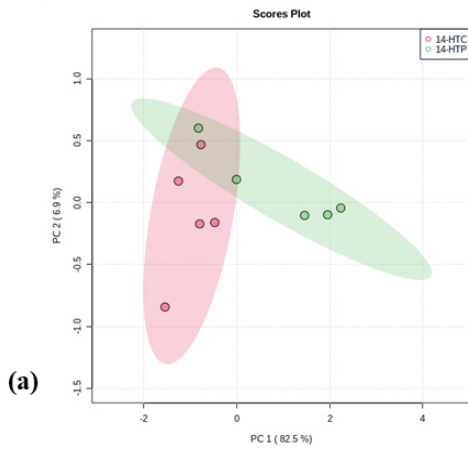
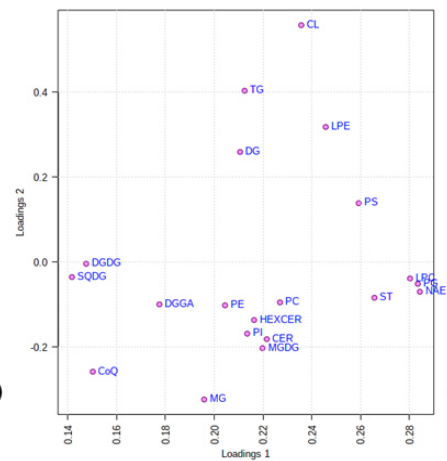
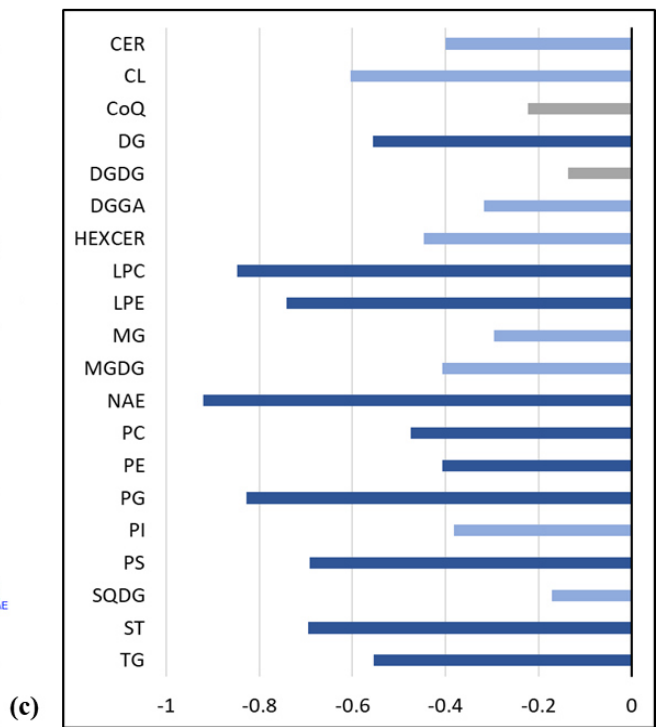
A**(a)****(b)****(c)****B****(a)****(b)****(c)**

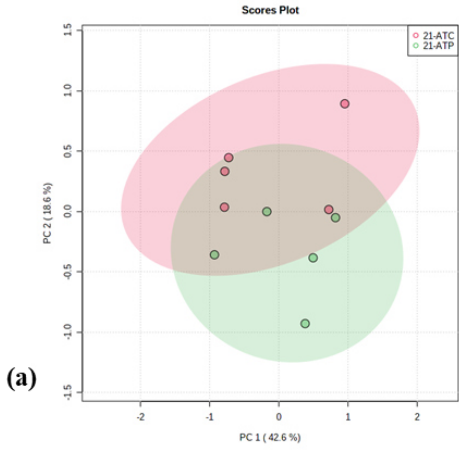
Figure 4. 7 Principal component analysis (PCA) (a), PCA loading plot (b), and log₂ fold change comparison (c) of the levels of lipid classes between control and PsJN-inoculated roots subjected under ambient (A) and high-temperature (B) conditions at 14 days after inoculation (DAI). Treatments: ATC – ambient-control, ATP – ambient- PsJN-inoculated, HTC – high temperature- control, HTP – high-temperature- PsJN-inoculated. Coloured ellipses around samples display 95% confidence areas.

Fold changes were calculated by averaging the sum of peak areas of a lipid class by the number of replicates (n=5) per treatment, and then log₂ transformed. The direction of comparison is ATC/ATP. Bar colors: grey – insignificant change, decreased - light blue, dark blue – significantly decreased, light orange – increased, dark orange – significantly increased. Significant differences were determined by two-sample t-test (significance level $p < 0.05$) and the Wilcoxon rank-sum tests. Lipid class abbreviation - refer to page 156.

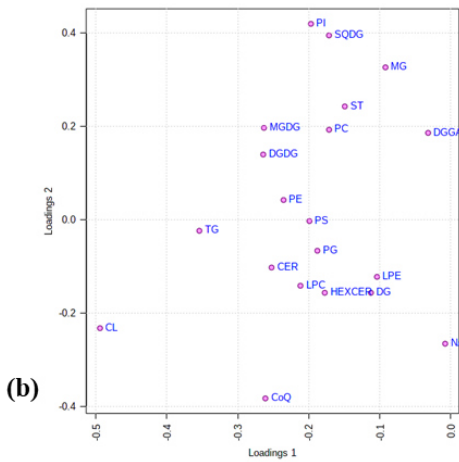
Conditions under high temperature reveal no apparent separation of the two treatments, and that the PC1 (82.5%) and PC2 (16.9%) values accounted for the variances (**Figure 4.7Ba**). The loadings of PC1 showed that separation was caused by the higher levels of LPC, NAE, PG, PS, and ST; and the lower levels of CoQ, DGDG, DGGGA, MG, and SQDG. PC2 loadings showed higher levels (CL, DG, LPE, PS, and TG) and lower levels (CER, CoQ, MG, MGDG, and PI) that account for this result (**Figure 4.7Bb**, **Table 5**). Fold change comparison showed that although many lipid classes under control treatment were lower, only those significantly decreased were from DG, LPC, LPE, NAE, PC, PE, PG, PS, ST, and TG (**Figure 4.7Bc**).

Finally, at 21 DAI (**Figure 4.8**), a separation of control and PsJN-inoculated roots was only detected at high temperature (time x bacteria x temperature interaction, though no separation under ambient, **Figure 4.8Aa**), and this was accounted by the PC1 and PC2 variances of 48% and 22%, respectively (**Figure 4.8Ba**). The lipid classes from PC1 that have the highest levels were of CL, CoQ, DG, MGDG, and TG; while the lowest levels were from CER, DGGGA, LPC, LPE, and NAE. Similarly, for PC2, the separation of the treatments was attributed to higher levels of CoQ, DGGGA, LPE, NAE, and PG; while the lowest levels were from CL, DG, DGDG, MGDG, and TG (**Figure 4.8Bb**). Only the level of the lipid class TG was significantly increased in control roots at this point, although there were some which were decreased, but not significantly.

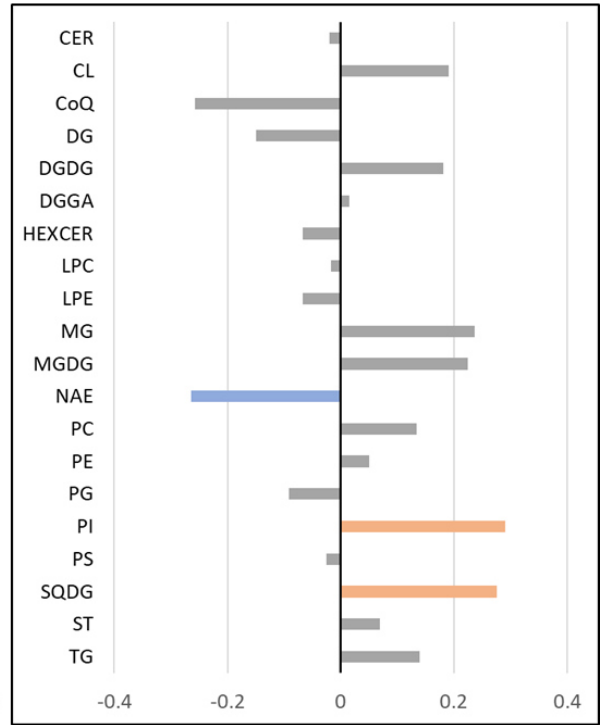
A



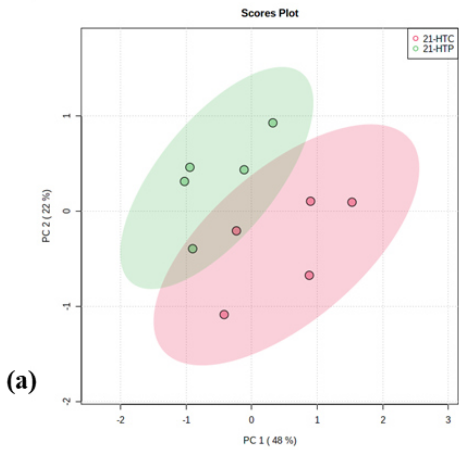
(a)



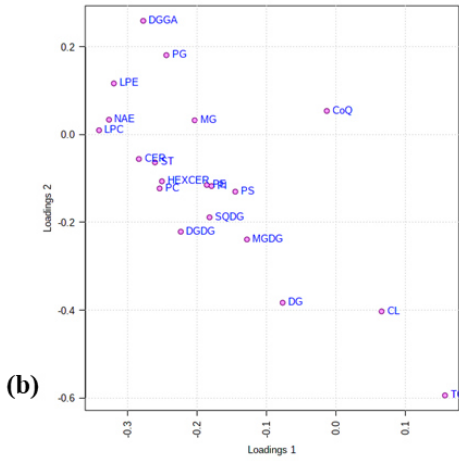
(b)



B



(a)



(b)

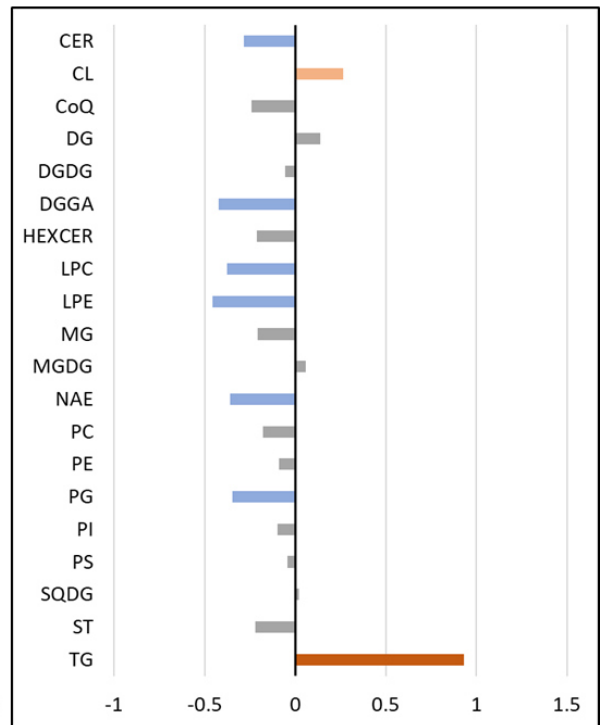


Figure 4. 8 Principal component analysis (PCA) (a), PCA loading plot (b), and log₂ fold change comparison (c) of the levels of lipid classes between control and PsJN-inoculated roots subjected under ambient (A) and high-temperature (B) conditions at 21 days after inoculation (DAI). Treatments: ATC – ambient-control, ATP – ambient- PsJN-inoculated, HTC – high temperature- control, HTP – high-temperature- PsJN-inoculated. Coloured ellipses around samples display 95% confidence areas.

Fold changes were calculated by averaging the sum of peak areas of a lipid class by the number of replicates (n=5) per treatment, and then log₂ transformed. The direction of comparison is ATC/ATP. Bar colors: grey – insignificant change, decreased - light blue, dark blue – significantly decreased, light orange – increased, dark orange – significantly increased. Significant differences were determined by two-sample t-test (significance level $p < 0.05$) and the Wilcoxon rank-sum tests. Lipid class abbreviation - refer to page 156.

Table 6 summarizes all the significantly altered lipid classes ($P < 0.05$) with a ≥ 1.2 -fold change threshold between the control and PsJN-inoculated roots under ambient and high temperature conditions at all three timepoints. This gives the directionality of the changes in the lipid classes as identified by the increase or decrease in the log₂ fold changes. When comparing the number of lipid classes affected, high temperature affected both control and PsJN-inoculated roots more, with control roots showing significantly higher number of increased levels of lipid classes at 7 DAI (15), and higher number of reduced lipid classes at 14 (10) and 21 (6) DAI. Interestingly, under both temperature conditions, the number of affected lipid classes decreased through time. This may suggest that the plants advanced development stage could have made them already hardy against the effect of both bacteria and high temperature. Under ambient, a large number of GPs (PC, PE, PG, LPE, CL) and GLs were affected by bacterial inoculation at 7 DAI. As time progressed, the number of lipid classes from the same category affected were reduced, and at 21 DAI, only the Fatty acyl – NAEs were affected. At high temperature, except for PR lipids, all the lipid classes were significantly higher in control roots. At 14 DAI, however, all the affected lipid classes were already reduced, with only TG significantly increased.

Table 4.5 Loadings of the first two principal components of control and PsJN-inoculated roots under two temperatures and three time points. **Red** texts indicate top five highest loading values, **blue** texts indicate top five lowest loading values.

Lipid class	7 DAI				14 DAI				21 DAI			
	Ambient		High temperature		Ambient		High temperature		Ambient		High temperature	
	PC1	PC2	PC1	PC2	PC1	PC2	PC1	PC2	PC1	PC2	PC1	PC2
CER	0.245	-0.234	-0.217	0.155	-0.226	0.100	0.222	-0.182	-0.252	-0.103	-0.284	-0.056
CL	0.267	0.166	-0.370	-0.387	-0.250	-0.341	0.236	0.558	-0.494	-0.233	0.066	-0.403
CoQ	0.205	0.484	-0.141	-0.519	-0.195	-0.261	0.150	-0.258	-0.261	-0.383	-0.013	0.054
DG	0.168	0.207	-0.147	-0.230	-0.257	-0.198	0.211	0.259	-0.112	-0.157	-0.077	-0.383
DGDG	0.195	-0.057	-0.243	0.155	-0.169	-0.062	0.148	-0.004	-0.264	0.139	-0.223	-0.221
DGGA	0.164	-0.141	-0.093	0.296	-0.220	-0.123	0.178	-0.100	-0.032	0.186	-0.277	0.259
HEXCER	0.163	0.072	-0.145	0.063	-0.224	0.089	0.216	-0.137	-0.177	-0.157	-0.250	-0.106
LPC	0.224	-0.385	-0.224	0.286	-0.143	0.433	0.280	-0.039	-0.212	-0.142	-0.341	0.010
LPE	0.268	0.131	-0.090	-0.057	-0.192	-0.360	0.246	0.318	-0.104	-0.123	-0.320	0.116
MG	0.127	-0.391	-0.266	0.119	-0.193	-0.060	0.196	-0.323	-0.092	0.326	-0.203	0.032
MGDG	0.231	-0.152	-0.262	-0.074	-0.227	0.471	0.220	-0.203	-0.263	0.196	-0.128	-0.239
NAE	0.243	-0.224	-0.200	0.137	-0.217	0.162	0.284	-0.070	-0.008	-0.266	-0.327	0.034
PC	0.245	0.208	-0.246	0.045	-0.233	-0.075	0.227	-0.095	-0.171	0.192	-0.254	-0.123
PE	0.244	0.202	-0.186	-0.054	-0.268	-0.213	0.204	-0.102	-0.235	0.042	-0.186	-0.115
PG	0.308	0.152	-0.201	0.116	-0.346	0.172	0.283	-0.051	-0.188	-0.067	-0.244	0.181
PI	0.258	0.006	-0.279	-0.171	-0.217	0.169	0.214	-0.169	-0.197	0.419	-0.179	-0.117
PS	0.240	-0.133	-0.204	0.191	-0.232	0.153	0.259	0.139	-0.199	-0.003	-0.145	-0.130
SQDG	0.236	0.111	-0.223	0.138	-0.155	0.008	0.142	-0.035	-0.172	0.395	-0.182	-0.189
ST	0.199	-0.286	-0.198	0.340	-0.192	0.152	0.266	-0.084	-0.149	0.242	-0.260	-0.063
TG	0.149	0.039	-0.322	-0.218	-0.233	-0.121	0.212	0.403	-0.354	-0.024	0.157	-0.594

Table 4. 6 Number of changed (increased or decreased) lipid classes (with a $P < 0.05$ and ≥ 1.2 -fold change) corresponding to the peak areas between control and PsJN-inoculated roots under two temperatures and three time points. Red and bold texts indicate significantly changed.

Treatment combination		Number of lipid classes changed by ≥ 1.2 -fold at $P < 0.05$		Lipid classes increased or decreased
		Ambient	High-temperature	
7 DAI				
ATC vs. ATP	Increase			
ATC vs. ATP	Decrease	7		CL, CoQ, LPE, PC, PE, PG, SQDG
HTC vs. HTP	Increase		15 (15)	CER, CL, DGDG, LPC, MG, MGDG, NAE, PC, PE, PG, PI, PS, SQDG, ST, TG
HTC vs. HTP	Decrease			
14 DAI				
ATC vs. ATP	Increase			
ATC vs. ATP	Decrease	3		DG, MGDG, PG
HTC vs. HTP	Increase			
HTC vs. HTP	Decrease		18 (10)	CER, CL, DG , DGGA, HEXCER, LPC, LPE , MG, MGDG, NAE, PC, PE, PG , PI, PS , SQDG, ST, TG
21 DAI				
ATC vs. ATP	Increase	2		PI, SQDG
ATC vs. ATP	Decrease	1		NAE
HTC vs. HTP	Increase		2 (1)	CL, TG
HTC vs. HTP	Decrease		6	CER, DGGA, LPC, LPE, NAE, PG

4.3.5. Specific lipid species altered when control and PsJN-inoculated roots were subjected to different temperatures and at different time points

Although the analysis of the lipid class profile provided insights on the 1) effect of bacterial inoculation under ambient and high temperature condition, 2) number of lipid classes affected by bacterial inoculation and temperature, 3) magnitude of alterations measured in fold changes and the 4) directionality of the changes, whether increasing or decreasing, specific lipid species may behave differently that may cause a drift in the result compared to when all the lipid species were combined into their associated class. As such, a volcano plot analysis was conducted on the individual lipid species. Volcano plots are used to compare the size of the fold change (threshold of 1.2 for this study) with the statistical significance level of $P < 0.05$.

Figure 4.9. illustrates the significantly altered lipid species between the control and PsJN-inoculated roots under ambient and high temperatures and at three time points. Compared to the lipid classes, this information provided more details as to which specific species, and collectively the lipid classes they belong to, were influenced (increased or decreased by) by bacterial inoculation.

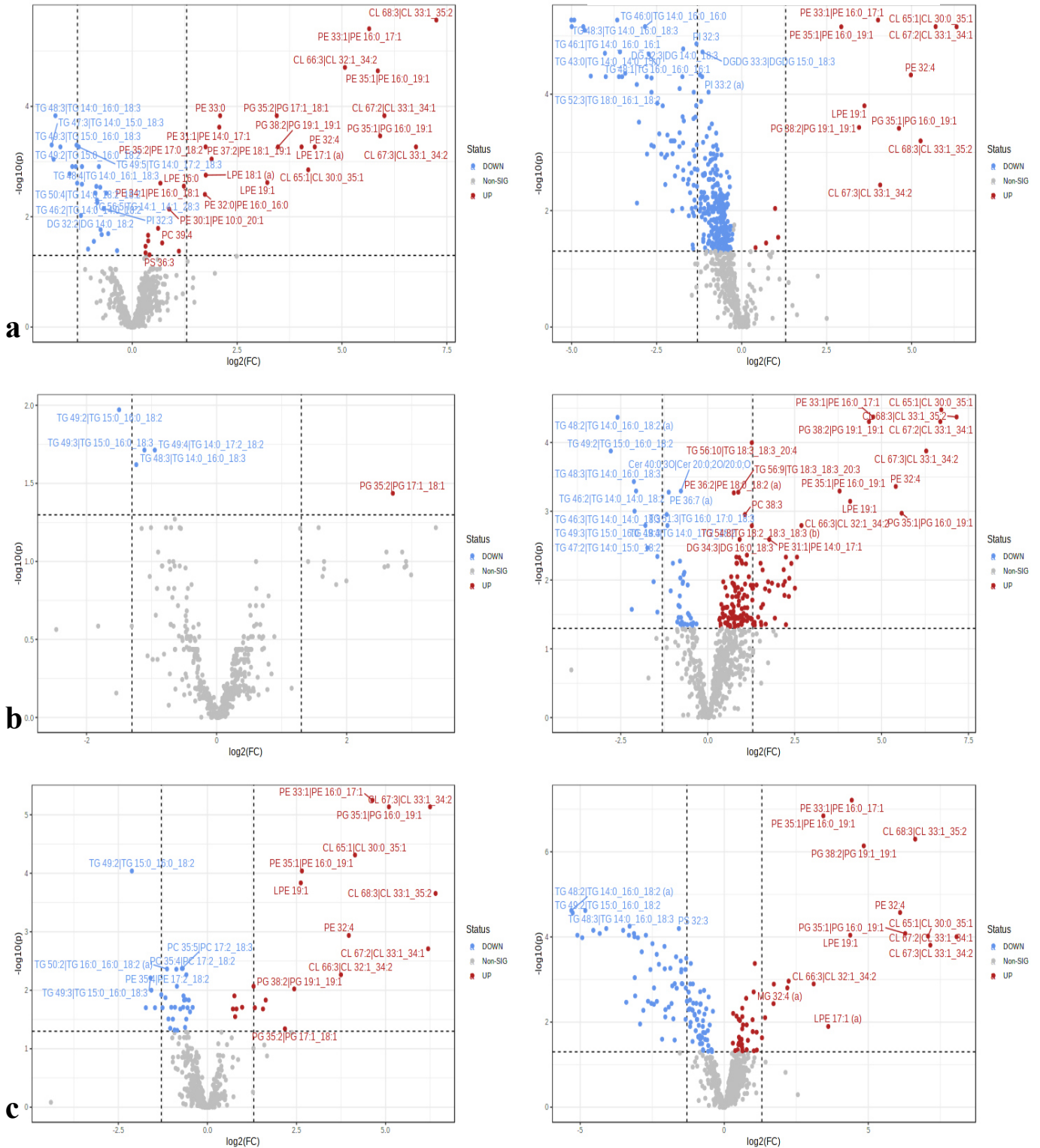
(A) Ambient**(B) High-temperature**

Figure 4.9 Volcano plots of significantly altered lipids in the comparison between control and PsJN-inoculated roots under ambient (A) and high-temperature (B) conditions at 7 (a), 14 (b), and 21 (c) DAI. Fold change direction is ATP/ATC. Horizontal axis plots the fold change between two groups (on a log₂ scale), while vertical axis shows the $P < 0.05$ for a t-test differences between samples (on a negative log scale). Red dots represent significantly increased lipid species with an FC threshold of 1.2, while blue dots represent significantly decreased lipid species, based on the two-factor t-test $P > 0.05$.

When comparing the effect of bacterial inoculation, it was observed that in all time points, high temperature has induced changes in more individual lipid species of PsJN-inoculated roots as compared to those under ambient condition (**Figure 4.9, Table 7**). The increase in the peak area levels was shown in the 14 lipid species at 7 DAI, 147 lipid species at 14 DAI, and 51 lipid species at 21 DAI. On the other hand, decreases in the peak areas were observed in the 338 lipid species at 7 DAI, 44 lipid species at 14 DAI, and 102 lipid species at 21 DAI. Although not as many compared to high temperature, there were also several lipid species that were altered by bacterial inoculation under ambient condition (**Figure 4.9, Table 7**). Increases in the peak area were observed in 30 lipid species at 7 DAI, 1 lipid species at 14 DAI, and 21 lipid species at 21 DAI. On the other hand, decreases were observed in the 27 lipid species at 7 DAI, 4 lipid species at 14 DAI, and 32 lipid species at 21 DAI.

Examination of the significantly changed individual lipid species revealed that the main lipid categories they belong to were GPs, GLs, and SPs, although SPs species were not detected under ambient condition at 14 DAI (**Figure 4.9, Table 7**). Further examination on the effect of bacterial inoculation has shown two very distinct pattern in the 1) highest number of changed lipid species and 2) highest fold change. Counting the number of lipid species that were increased, whether under ambient or high temperature and at any time point, has shown that PE always have the highest number. This is in the same way that TG consistently have the highest number of decreased species. Looking at the fold changes, it was also very evident that, in terms of increases, CLs mainly have the highest fold changes (about 6 to 8 folds) in almost all temperature conditions and time points (except at 14 DAI ambient when it was not detected). What was even more interesting was with the decreases, which consistently illustrated TG species with the highest fold changes (about 1.5 to 5 folds), across all time points and on both temperatures (data not shown).

Table 4. 7 Number of significantly changed (increased or decreased) lipid species (with a $P < 0.05$ and ≥ 1.2 -fold change) corresponding to the peak areas between control and PsJN-inoculated roots under two temperatures and three time points. Treatments: ATC – ambient-control, ATP – ambient- PsJN-inoculated, HTC – high temperature- control, HTP – high temperature- PsJN-inoculated.

Treatment combination		Total number of lipid species		Lipid classes increased or decreased (and number of lipid species per class)	Highest number of changed species	Highest Log ₂ (Fold Change)
		Ambient	High-temperature			
7 DAI						
ATC vs. ATP	Increase	30		CER-1, CL-5, HEXCER-2, LPE-4, PC-1, PE-11, PG-3, PS-1, ST-2	PE-11	CL-7.3
	Decrease	27		DG-4, PC-1, PE-1, PI-1, TG-20	TG-20	TG-1.9
HTC vs. HTP	Increase		14	CL-4, HEXCER-1, LPE-1, PC-1, PE-5, PG-2	PE-5	CL-6.3
	Decrease		338	CER-63, CL-4, DG-55, DGDG-13, DGGA-3, HEXCER-6, LPC-3, MG-8, MGDG-6, NAE-15, PC-24, PE-24, PG-6, PI-15, PS-12, SQDG-3, ST-8, TG-70	TG-70, CER-63	TG-5.0
14 DAI						
ATC vs. ATP	Increase	1		PG-1	PG-1	PG-2.7
	Decrease	4		TG-4	TG-4	TG-1.5
HTC vs. HTP	Increase		147	CER-9, CL-5, DG-27, DGDG-3, DGGA-2, LPC-6, LPE-4, MG-1, MGDG-1, NAE-6, PC-14, PE-25, PG-6, PI-5, PS-8, ST-6, TG-19	DG-27, PE-25	CL-7.2
	Decrease		44	CER-2, DG-2, DGGA-1, PC-2, PE-7, ST-2, TG-27	TG-27	TG-2.8
21 DAI						
ATC vs. ATP	Increase	21		CER-1, CL-5, LPE-1, NAE-1, PE-9, PG-3, ST-1	PE-9	CL-6.4
	Decrease	32		DG-1, DGDG-3, DGGA-1, PC-7, PE-3, PI-1, TG-16	TG-16	TG-2.1
HTC vs. HTP	Increase		51	CER-3, CL-5, DG-3, DGDG-2, DGGA-2, HEXCER-2, LPC-1, LPE-3, MG-1, MGDG-1, PC-6, PE-12, PG-3, PI-1, SQDG-1, ST-3, TG-2.	PE-12	CL-8.1
	Decrease		110	CER-1, CL-1, DG-9, DGDG-4, DGGA-1, NAE-1, PC-6, PE-8, PG-1, PI-5, PS-3, ST-1, TG-69	TG-69	TG-5.3

4.3.6. Comparison of lipid profiles of ambient-grown and heat-stressed roots at different time points.

To isolate the effect of high temperature on roots, a separate analysis was conducted by comparing the treatments ATC (ambient – control) and HTC (high temperature – control) across three time points. **Figures 4.10 to 4.13** were generated to illustrate these effects. PCA score plot analysis (**Figure 4.10**) clearly showed a distinct separation between control (7-ATC, 14-ATC, and 21-ATC) and heat-stressed roots (7-HTC, 14-HTC, and 21-HTC) indicating the consistent influence of temperature on the root lipid profiles through time. ANOVA result (**Figure 4.11**) revealed a large number of significantly affected lipids between ambient and heat-stressed roots through time. **Figure 4.12** showed two distinct main group clustering, supporting the separation previously shown by the PCA score plot. The volcano plot analysis (**Figure 4.13**) and the resulting summary of fold change analysis (**Table 8**) allowed for the synthesis of further information including the 1) total number of lipid species that were affected by high temperature, the 2) lipid classes and categories they belong to, as well as the 3) lipid class with the greatest number of altered species, and the 4) magnitude of the fold changes detected. Whether increasing or decreasing, high temperatures significantly affected different lipid species at different time points: increasing the peak intensities of 257, 103, and 174 lipid species; and decreasing the peak intensities of 93, 320, and 236 lipid species – both at 7, 14, and 21 DAI, respectively. A prominent trend was shown by the consistent number of highly increased lipid species of TG, and the somewhat opposite trend by DG (with the highest number of decreased lipid species), although only shown at 14 and 21 DAI.

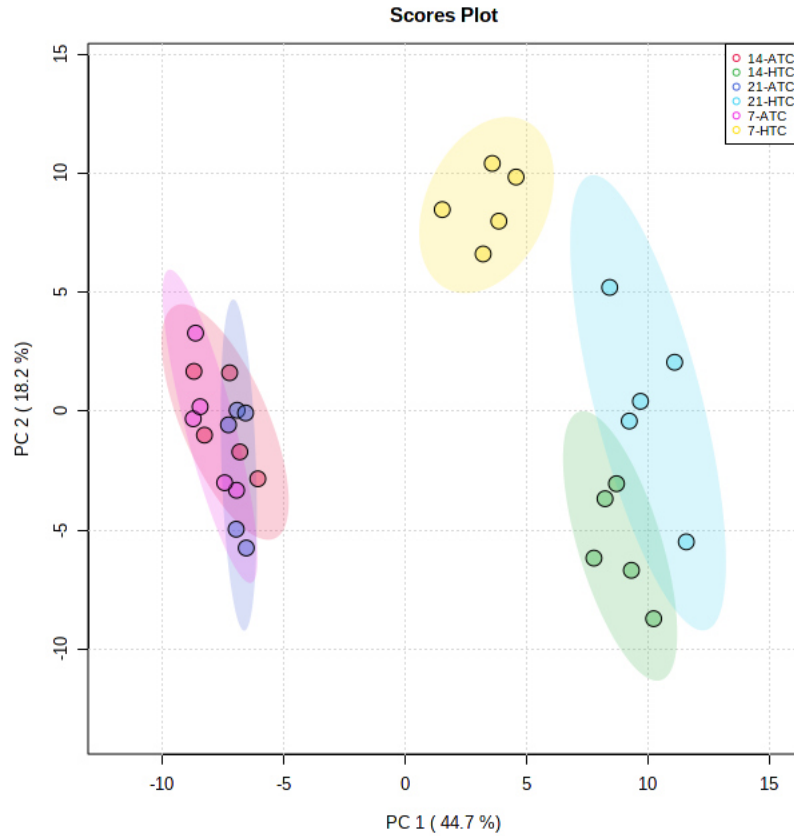


Figure 4. 10 Principal component analysis (PCA) plots between ambient-grown and heat-stressed roots at three timepoints. Treatments: ATC – ambient-control and HTC – high temperature- control. Measurements were taken at 7, 14, and 21 days after inoculation (DAI). Coloured ellipses around samples display 95% confidence areas.

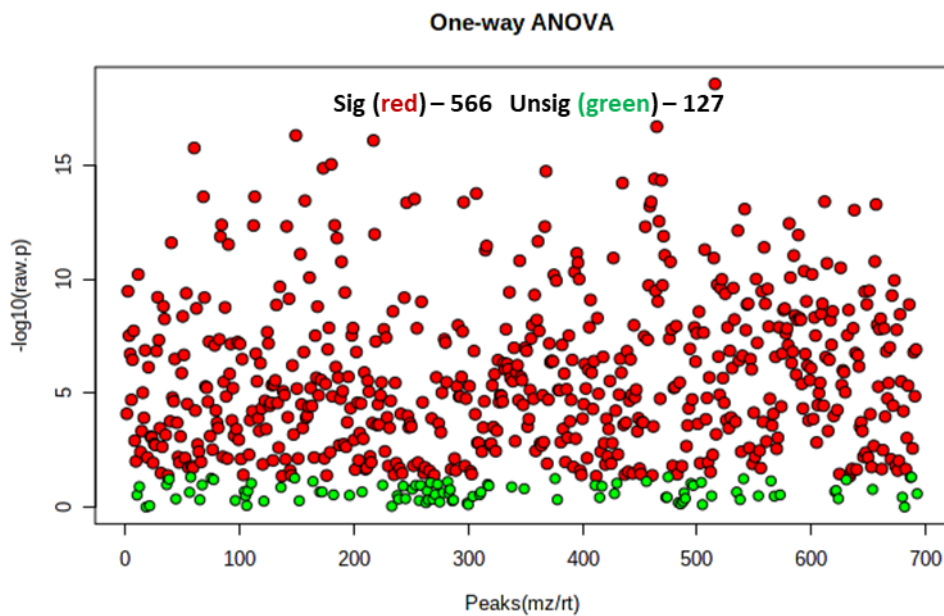


Figure 4. 11 Analysis of variance (ANOVA) between ambient-grown and heat stressed roots at all three time points. Red dots – lipid species showing significant differences, green dots – lipid species showing no significant differences.

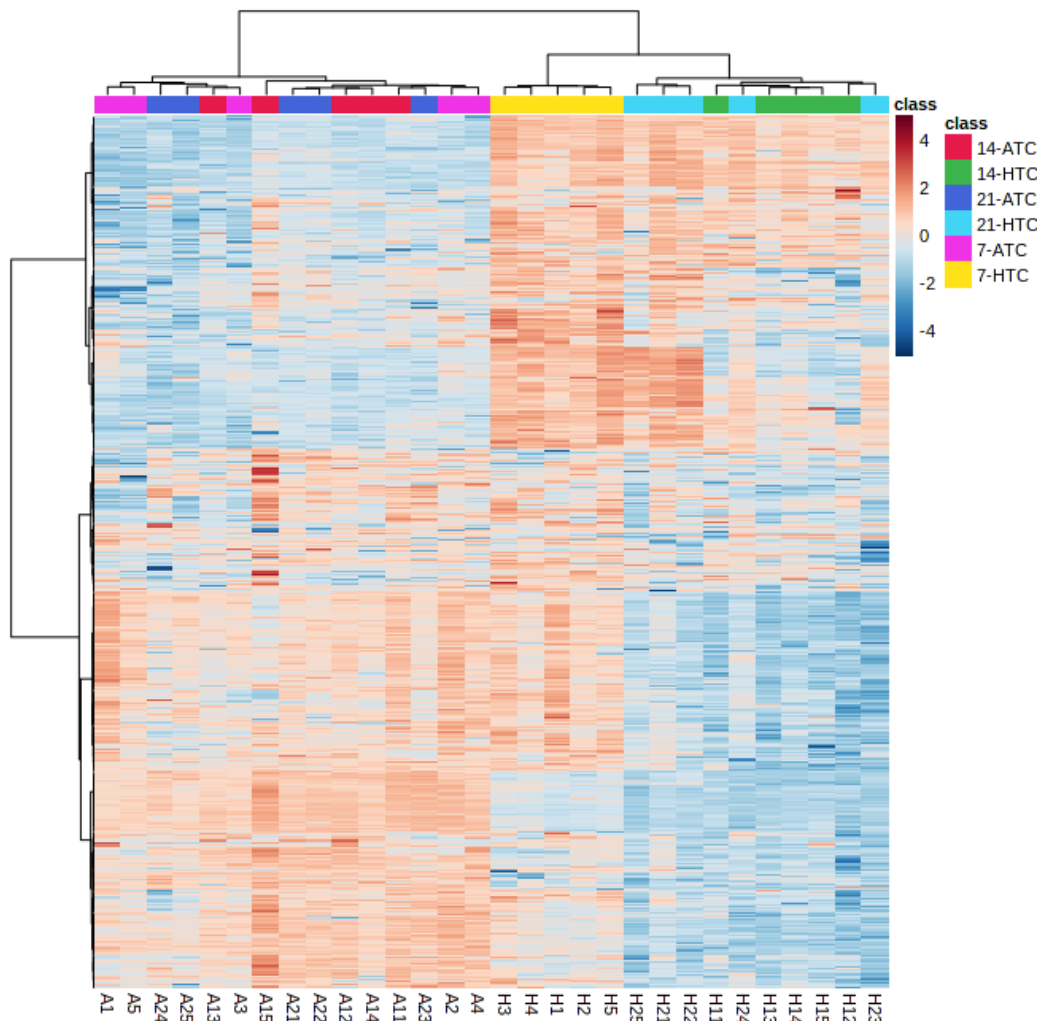


Figure 4. 12 Hierarchical clustering coupled with heatmap between ambient-grown and heat-stressed roots at three different timepoints. Treatments: ATC – ambient-control and HTC – high temperature-control. Measurements were taken at 7, 14, and 21 days after inoculation (DAI). Label at the bottom refers to the replicates; and for each replicate (column), blue and red colours signify the lower and higher abundance of specific lipids as compared to the other replicates, with darker colours indicating more pronounced differences. Dendrogram at the top indicates the main lipid clusters represented with branches of different colours.

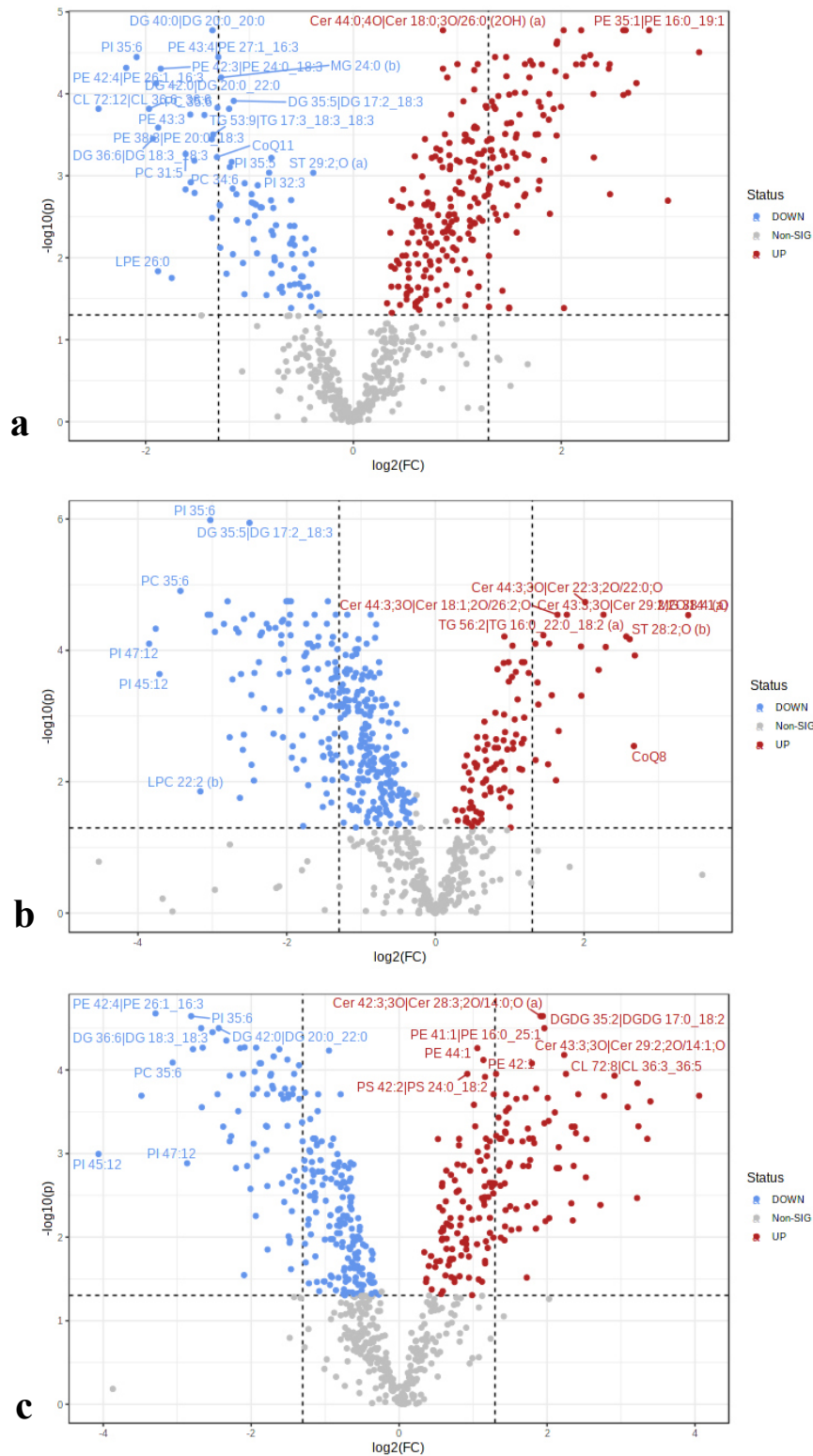


Figure 4. 13 Volcano plots of significantly altered lipids in the comparison between ambient-grown and heat-stressed roots taken at 7 (a), 14 (b), and 21 (c) DAI. Fold change direction is HTC/ATC. Horizontal axis plots the fold change between two groups (on a log₂ scale), while vertical axis shows the $P < 0.05$ for a t-test differences between samples (on a negative log scale). Red dots represent significantly increased lipid species with an FC threshold of 1.2, while blue dots represent significantly decreased lipid species, based on the two-factor t-test $P > 0.05$.

Table 4. 8 Number of significantly changed (increased or decreased) lipid species (with a $P < 0.05$ and ≥ 1.2 -fold change) corresponding to the peak areas between ambient-grown and heat-stressed roots at three time points. Treatments: ATC – ambient-control and HTC – high temperature-control.

Treatment combination		Total number of lipid species changed by ≥ 1.2 -fold at $P < 0.05$		Lipid classes increased or decreased (and number of lipid species per class)	Highest number of changed species	Highest $\text{Log}_2(\text{Fold Change})$
		Ambient	High-temperature			
7DAI						
ATC vs. HTC	Increase	257		CER-40, CL-5, CoQ-1, DG-21, DGDG-15, DGGGA-1, HEXCER-10, LPC-2, LPE-1, MG-2, MGDG-4, NAE-1, PC-27, PE-28, PG-5, PI-5, PS-3, SQDG-3, ST-5, TG-78	TG-78	CL- 3.3
	Decrease	93		CER-2, CL-1, CoQ-1, DG-12, DGDG-1, DGGGA-3, HEXCER-2, LPE-1, MG-2, NAE-1, PC-14, PE-23, PG-2, PI-6, PS-7, ST-4, TG-11	PE-23	CL- 2.5
14 DAI						
ATC vs. HTC	Increase	103		CER-28, CL-1, CoQ-2, DG-4, DGDG-5, HEXCER-4, MG-1, MGDG-2, PC-11, PE-4, PG-1, PI-2, PS- 1, SQDG-2, ST-3, TG-32	TG-32	MG-3.4
	Decrease	320		CER-38, CL-2, CoQ-1, DG-59, DGDG-5, DGGGA-8, HEXCER-6, LPC-7, LPE-5, MG-12, MGDG-2, NAE-18, PC-31, PE-37, PG-7, PI-14, PS-17, SQDG-1, ST-16, TG-34	DG-59	PI-3.8
21 DAI						
ATC vs. HTC	Increase	174		CER-33, CL-3, DG-5, DGDG-8, HEXCER-6, MG-2, MGDG-2, PC-14, PE-16, PG-1, PI-5, PS-3, SQDG-2, ST-3, TG-71	TG-71	TG-4.1
	Decrease	236		CER-30, CL-3, CoQ-1, DG-42, DGDG-4, DGGGA-7, HEXCER_4, LPC-5, LPE-3, MG-7, MGDG- 1, NAE-15, PC-26, PE-34, PG-6, PI-11, PS-13, ST-11, TG-13	DG-42	PI-4.0

4.4. Discussion

With scientific and technological advances in different fields comes the wide range of breakthrough studies on plants. Whether driven by the need to expand scientific information and fill knowledge gaps or the necessity to address current crop production and environmental sustainability issues, research on plants have been diverse and ranges from genetic and molecular to the whole plant level. However, whilst there are many investigations utilising DNA, RNA, and proteins, not many have looked into the intrinsic metabolic nature and biochemical interaction of plants with their surroundings. In this study we looked into the lipidomic profile of plants, particularly roots, which are not only essential parts for plant growth, but are also critical components of the underground ecosystem that are subjected to environmental stress such as high temperatures. To do so, a microcosm of plant-microbe niche was simulated to observe the development of the plants under biotic and abiotic influence and characterize the root lipidomic responses.

Arabidopsis Col-0 roots were grown on modified agar plates and treated with either mock inoculant or PsJN bacterial inoculum and then both were subjected to either ambient (22°C/18°C) or high temperatures (30°C /24°C) from germination until 21 days of growth. At three time points in their development (7, 14, and 21 days), roots were harvested and extracted for lipids, after which, the extracts were subjected to MS-based untargeted data acquisition. This study's discovery-based analysis of the lipid compounds extracted from control and PsJN-inoculated roots subjected to different temperatures and measured at different time points of their development provided several insights into the lipid profiles. Firstly, the annotated lipid species in the roots have shown dynamic changes in response to bacterial inoculation, elevated temperatures, and developmental stages. Although, the unknown features detected could not provide specific details, their huge number that mirrored the results of annotated lipids provided insights into how they would have potentially affected the lipid profiles of the treated roots. Secondly, high temperature strongly influenced the lipid profile of both control and PsJN-inoculated roots at all stages of development, showing different effects on different lipid species (variations in magnitude and directionality) at all time points. Thirdly, the effect of bacterial inoculation was clearly shown under high temperatures, with higher magnitude of changes observed in different lipid species at different time points. Finally, the levels of some specific lipid classes strongly increased or decreased as induced by bacterial inoculation and/or high temperatures.

4.4.1. High temperature altered several annotated lipid species and manifested similar dynamic changes in unknown features

The effects of high temperature on plant lipids have been previously investigated. Many of these studies looked into either whole plant tissues, or that located aboveground, such as leaves (Narayanan et al., 2016), pollen (Narayanan et al., 2018), flowers/parts of (Zoong Lwe et al., 2020), seeds (Chebrolu et al., 2016), and fruits (Wang & Lin, 2006). Other studies, like the one by Wang and Lin (2006), investigated the effect of high temperature on the leaves, flowers, and roots of strawberry. Furthermore, a recent study by Kehelpannala et al. (2021) provided a comprehensive profiling of lipids from different tissues of Arabidopsis Col-0 plants such as flowers, seeds, siliques, leaves, stems, and roots, although this did not include a heat stress treatment. In general, there are not many studies on plants roots, even more so on their metabolic and lipidomic profiles, particularly when paired with environmental factors.

As shown in the PCA score plots (**Figure 4.3**) and hierarchical clustering with heatmaps (**Figure 4.4**), high temperature significantly affected the lipid profiles of both control and PsJN-inoculated roots. Clear separation between ambient (ATC and ATP) and high temperature (HTC and HTP) treatments across three time points showed that the effect of constant high temperature from germination has consistent, perhaps even cumulative (as with long-term effects of high temperature on plants (Wahid et al., 2007)), effect on the modification of the lipid profiles. This effect was observed on both annotated lipids and unknown features. In addition, more information was extracted from the annotated data due to specific details such as the molecular name and number of lipid species, which made possible the comparison of the level and direction of changes induced by the treatments. Assessment of the lipid species that were involved in the heat stress analysis has shown the involvement of several lipid categories, mainly GPs, GLs, and SPs (**Table 8**). In particular, the consistent effect of high temperature on TG and DG has been highlighted in this experiment.

Many lipid species have been implicated in plant responses to high temperatures, including, GP, which are main components of biological membranes, such as PC, PE, PG, PI, and PS (Liu et al., 2019). In the lipid study presented here, which was performed on roots, many of the GPs have been detected, which being either increased or decreased under high temperatures. Present in highest number were PE species, although PC, PI, and PS species were also detected in lower quantities (**Figure 4.9, Table 7**). This result also coincides with the root lipid profiles found by Kehelpannala et al. (2021) and the study conducted by Devaiah et al. (2006), except for PGs 32 and 34:2 which were not detected in their studies.

Plants regulate their lipid metabolism as a response to high-temperature exposure. This highly involves the cell membranes, which influence the plant's ability to survive and flourish through the maintenance of membrane fluidity and permeability. One typical metabolic response is the decrease in unsaturation of fatty acids in membrane lipids (Higashi et al., 2015; Murakami et al., 2000; Shiva et al., 2020). At high temperatures, it has been proposed that reduced desaturation of newly synthesized fatty acids and increased lipid head group turnover are likely to contribute to the maintenance of membrane fluidity (Shiva et al., 2020; Zheng et al., 2011). The reduction of the degree of unsaturation under high temperatures was observed in *Arabidopsis* plants grown at 36°C having a double bond index (DBI) of 1.46 as opposed to the DBI of 2.39 of plants grown at 17°C, which illustrated a decrease of 39% (Falcone et al., 2004). As part of this, the dominant component of thylakoid membranes, GLs (e.g., DGDG, MGDG) increased their trienoic fatty acids more than the other membrane phospholipids, making them major contributors to membrane unsaturation in leaves (Murakami et al., 2000). These lipids, which are components of photosynthetic systems (Hölzl & Dörmann, 2007), were also found in roots, although in lower numbers.

Further changes to lipids under high temperatures include the increases in TG species, particularly those containing 18:3 (Mueller et al., 2017; Narayanan et al., 2016). According to Mueller et al. (2017), the accumulation of TG is partly dependent on the transfer of an acyl chain from PC to DG, which then forms into TG. Therefore, under high temperatures, the levels of PC, DG, and TG, including those of acylated MGDG and DGDG, are increased (Mueller et al., 2017). A study of changes occurring in membrane lipids of *C. reinhardtii* after exposure to brief heat stress followed by recovery (Légeret et al., 2016), has also shown the degradation of membrane lipids and the direct conversion of MGDG to DG, simultaneous with accumulation of the polyunsaturated TG (Hemme et al., 2014). This increase in TG was prominently observed in the current study. However, although there were observed increases in some DGs, most of the DG species were actually decreased, as with the result at 14 and 21 DAI (**Table 8**). It could be that although many of the observed lipid species have shown decreased intensities, the peak intensities of the few increased species may actually be higher when individually analysed, thus, it is recommended to perform further lipid identification to verify the associated specific DG species of interest. Moreover, most of the studies previously conducted were of aboveground plant parts and therefore, this response may be unique to roots.

Another implicated lipid class under heat stress found in this study are sterol lipids. Increases in the levels of sterol glucosides (SG) and acyl sterol glucosides (aSG) occur when plants are under high-temperature stress (Mishra et al., 2015). Sterol glucosyltransferases

synthesize SGs and catalyses the formation of glycosidic bonds between glucose and a free hydroxyl group on a sterol molecule. In plants, a mixture of sterol lipids such as sitosterol, stigmasterol, and campesterol, are synthesized. Recent works on increased SG and aSGs found during high-temperature stress hint at a potential for improving heat stress response in plants (Mishra et al., 2015; Shiva et al., 2020). This may partly explain the better response of the Arabidopsis plants in the current study to the otherwise detrimental high temperature effects. Moreover, this makes this particular lipid category/class of interest for future targeted lipidomic studies involving plant tolerance or adaptation to high temperature stress.

Aside from their functions as critical components of the plant plasma and endomembranes, the particular structure of sphingolipids makes them important contributors to the fluidity and biophysical order of the membranes (Huby et al., 2020). As these cell properties are subject to environmental fluctuations, sphingolipids also serve crucial functions in plant responses to temperature stress as signaling mediators. Several studies have previously reported the roles of sphingolipids in response to temperature stress. In particular, acclimation capacity was correlated with changes in the contents of MGDG, DGDG, TGs, and glycosylceramides (GlcCer) (Degenkolbe et al., 2012). However, most of these studies, e.g., on oat, rye, and Arabidopsis lipid profiles described acclimation responses to cold temperature, as with the decrease in GlcCer contents in the plasma membrane and unchanged property in microdomains (Minami et al., 2009; Takahashi et al., 2016). There have been no characterized functions for sphingolipids in tolerance of high temperature except for the high concentration of trienoic acids in the thylakoid membranes shown to be involved in both cold and high-temperature tolerance (Murakami et al., 2000; Routaboul et al., 2012). It was also shown that exogenous LCB-phosphate contributed to heat stress tolerance in Arabidopsis cell cultures (Alden et al., 2011). In our study, we found Cer and HexCer species that either increased or decreased under high temperatures. These lipids, however, have been implicated in hypoxia and oxidative stress (Xie et al., 2015).

It is noteworthy that many of the plant lipid studies are conducted simultaneously with drought in chickpea (Khan et al., 2019), cold in wheat (Cheong et al., 2019), salinity in barley (Gupta et al., 2019), nutrient stress in *Brachypodium* (Schillaci, Kehelpannala, et al., 2021), and other environmental stressors. Although considered a huge detrimental agricultural and environmental issue, with potential for further aggravated side effects due to climate change, high temperature or heat stress has received relatively lower attention. Moreover, lipid studies on temperature effects are mostly targeted at the leaves or photosynthetic parts. Only a few

lipid studies were conducted on roots, making the current study timely and a candidate for further exploration of interesting lipids that are subject to changes under high temperatures.

4.4.2. Bacteria-induced changes to the lipid profile is prominent under high temperature

PGPRs are beneficial soil microbes that colonize both the rhizosphere and develop close physical and biochemical interactions with plant roots (Lugtenberg & Kamilova, 2009). They are known to act as either biofertilizers, directly affecting plants by promoting growth and nutrient management, or as biocontrols, indirectly assisting plants by increasing resistance against pathogens. Some functions of PGPRs that have been documented include plant growth stimulation through production of phytohormones and siderophores (Hayat et al., 2010) and reinforcement of plant protection through production of antibiotic and hydrolytic enzymes (Niazi et al., 2014). These beneficial growth effects ultimately lead to increased biomass and yield. The effects of the plant and microbe interactions on the lipid profile have also been documented, although many of these were based on pathogenicity, and not many on beneficial soil microbes. Examples of studies that looked into lipid characterization of the interaction of plants and beneficial microbes are those from Gupta et al. (2019) and Schillaci, Kehelpannala, et al. (2021).

This study, focused on the lipid profile of *Arabidopsis* roots and the modifications under the influence of the bacteria PSJN, particularly its effect on roots when subjected to high temperature stress. The comparison of the peak areas of individual lipid species between control and PsJN-inoculated roots under two temperature conditions revealed that, whilst the effect of bacterial inoculation was significant under high temperature (HTC vs. HTP), this effect of inoculation was not consistent under ambient (ATC vs. ATP), with a group separation only found at 21 DAI for annotated lipids and at 7 DAI for unknown features. This separation of the treatment groups was observed through the PCA score plots (**Figure 4.3**) and hierarchical clustering with heatmaps (**Figure 4.4**).

Statistical analysis using ANOVA (**Figure 4.5**) has shown the number of lipid species that were significantly different among the four treatments, for both annotated and unknown features, and at different time points. This analysis also revealed that, aside from the large difference between annotated and unknown features, there was an observed decrease in the ratio between significant and non-significant lipid species from 7 to 21 DAI. Breaking down into pairs, the comparison of lipid classes revealed additional information such as the loadings

or specific lipid species responsible for the spread or clustering of the samples and the fold changes of significantly affected lipid species by the bacterization and temperature treatments. However, although we could quantify the changes in the levels of the lipid classes between control and PsJN-inoculated roots, there was no discernible trend. This could potentially be because the effect of both bacteria and heat are manifested on the species level within a lipid class. Therefore, pairwise analyses (volcano plots) of the treatments in the full annotated data were performed (**Figure 4.9**). This provided a more comprehensive result with distinct outcomes and trends on the lipid profiles as summarized in **Table 7**.

Under ambient conditions, several root lipids were affected by the inoculation of PsJN. Whilst some lipid classes were up-regulated as shown from the increases in the peak areas of lipid species relative to the control plants, other lipid species were also down-regulated. Following the outcome from the PCA plot where, the observed separation between control and PsJN-inoculated roots were only seen at 21 DAI, thus, we will focus on this time point. Significant increase in the levels of Cer, CL, LPE, some membrane lipids (PE, PG), and ST were observed. On the other hand, decreases in the levels of GL species, as well as TG were also observed (**Table 7**).

Sphingolipids, which are diverse lipids comprised of small molecules as well as large glycosylated lipids, are essential for membrane integrity and raft formation (Siebers et al., 2016). Ceramides serve as substrate for the synthesis of two major sphingolipid classes in plants, glucosylceramides (GlcCer) and glycosylinositol phosphoceramides (GIPC), both of which are abundant components of the plasma membrane, tonoplast, and the ER membrane involved in raft formation. HexCer belongs to the simple GcCer series. As with other membrane lipids, the increase in these lipid compounds, also shown in this study, may indicate their involvement in the reorganization and maintenance of plasma membrane integrity during the interaction with beneficial microbe (Cassim et al., 2019).

Lysophospholipids, which are small molecules that are minor components of plant membranes subject to tight regulation, were recently identified as signalling components mediating plant defense responses (Kimberlin et al., 2013; Luttgeharm et al., 2015). These lipid molecules interact with phospholipase Ds (PLDs) or phosphatidic acid (PA) in regulating enzyme activity, biosynthesis and signalling, particularly during plant defense response (Zhao, 2015). PGPRs can stimulate the plant immune system, resulting in induced systemic resistance (ISR), which shares common signalling components (Pieterse et al., 2014). Both LPC and LPE, which are products of plant phospholipase A2 (PLA2), are involved in systemic responses,

including with wounding (Jang et al., 2012). Both of these explanations are plausible reasons for the detected increases in these molecules in the current study.

Sterol lipids are synthesized via isoprenoid pathway in the cytosol of plant cells. The major sterols in plants (phytosterol) are stigmasterol, B-sitosterol, and campesterol, with cholesterol in low abundance (Wewer et al., 2011). It has been observed by Bhat et al. (2005), using sterol-specific filipin staining, that sterol lipids aggregated at the tip of appressorial germ tubes and the septum of *B. graminis* after germination on barley leaves. This aggregation indicated the enhanced production and also formation of lipid rafts in the plasma membrane by the sterol lipids. Although not in huge quantity, there has been some increases observed from ST species under bacterial inoculation in this study.

The noticeable increase of other compounds in inoculated roots can potentially be attributed to the contribution of the bacteria such as PSJN, the membrane lipids of which are generally consist of GPs, PG, CL, and PE (López-Lara et al., 2003). In addition, a subset of bacteria can also possess the methylated derivatives of PE, monomethylphosphatidylethanolamine, dimethylphosphatidylethanolamine, and phosphatidylcholine PC (López-Lara et al., 2003). The large increases in these lipid species found in PsJN-inoculated roots under ambient, only shows the significant contribution of the bacterial lipids in the overall lipid profile detected through untargeted analysis. This can potentially account for why the effect of inoculation with PsJN was only significant at 21 days (PCA result in Figure 4.3), since phenotypic response of bacterized plants in a closed-plate system mainly manifested bacteria-imparted root grown promotion at later stages.

Aside from their plant growth-promoting roles, PGPRs are also known to assist and impart tolerance against abiotic environmental stressors such as high temperature (heat stress). A range of studies have documented the various mechanisms that PGPRs employ leading to plant heat stress tolerance and improved plant performance. Some of these mechanisms include the production of phytohormones and plant growth regulators (Choudhary et al., 2016; Khan et al., 2020), induction of heat shock proteins (McLellan et al., 2007), mediation of ROS (Abd El-Daim et al., 2014; Maitra et al., 2021), moderation of protective molecules (Basu et al., 2021; Bista et al., 2018), and regulation of nutrient and water uptake (Bista et al., 2018). However, only a few studies investigated the plant 1) lipid response to microbial inoculation, 2) particularly in tandem with high temperature (as opposed to studies on salinity, drought, and cold stresses), and specifically 3) in roots, which are considered more sensitive to temperature than the shoots (Heckathorn et al., 2013), but are less studied due to their hidden nature.

The effects of bacterial inoculation under high temperatures were evident and consistent throughout the plant development, from 7 to 21 DAI (see PCA on **Figure 4.3**). Here we have observed almost similar trends in the increases of the same lipid species affected with bacterial inoculation, but with more classes detected and higher number of lipid species per class (**Table 8**). Lipids from almost all lipid classes were changed, even showing increases and decreases of lipid species within the same lipid class – which can potentially be resolved by further lipid identification, through MS/MS spectra analysis and targeting lipids of interests in future experiments. Lipids that were upregulated by bacteria PsJN at ambient seemed to be even more increased under high temperatures as observed during 14 and 21 DAI, while those downregulated were also further decreased.

Lipid classes that were increased and could have potentially been useful in imparting heat tolerance to plants were the membrane lipids PC, PE, PG, and PI – maintaining the organization and integrity of the membrane as an intrinsic plant response to high temperature stress, which could have also been enhanced by the PsJN bacteria. Other lipids involved include sphingolipid species as with Cer and HexCer, which have specific responses to high temperature that may have been enhanced by the bacteria. Sterol esters which are normally of low abundance have increased their contents due to both abiotic and biotic stimuli (Wewer et al., 2011). One new lipid class affected by both bacteria and high temperature was NAE, which are also small signalling molecules, as are lysophospholipids and sphingolipids (Jang et al., 2012). They are fatty acid amides derived from the hydrolysis of the membrane component N-acylphosphatidylethanolamine by PLD, which have been shown to be elicitor-activated during plant defense (Tripathy et al., 2003). Based on the analysis of fold changes, specific lipid classes showed prominent increasing or decreasing response to bacterial inoculation and high temperatures.

4.4.3. Specific lipid species with specific behaviour and fold change comparison of control and inoculated roots.

A very evident result (shown in **Table 8**) was the highest number of changed lipid species as well as the highest log₂ fold change values. We can see that, except for 14 DAI under ambient, PE consistently have the highest number of species with increased peak intensities, under ambient and high temperature conditions. This can very well be due to the contribution of the bacterial membranes which, as in the case of *Escherichia coli*, is majorly composed of phospholipids such as PG, PE, and CL (Gill & Suisted, 1978; Shukla & Turner, 1980). In the

same manner, although only a few of its species were affected, CL showed the highest fold change increase consistently throughout (except at 14 DAI ambient) the plant root development. CLs are key phospholipids in mitochondrial membranes, which plays significant roles in the maintenance of its functional integrity and dynamics of the mitochondria. CLs have also been known to play roles in plant responses to heat and extended darkness stresses that induce programmed cell death (Pan et al., 2014). This adds to the fact that this lipid class is an abundant component of bacterial membranes, which could have been the reason why CL showed the highest fold change increase, even at high temperatures.

One surprising result was with the bacterial inoculation effect on TG, which showed considerable decreases under both ambient and high temperature conditions. This outcome is not yet supported in any literature and was in fact the opposite expected effect due to the plant's mechanistic response of producing more TG under heat stress, and the bacteria's affinity for generating and storing more lipids in the form of TGs as endogenous carbon and energy sources (Kalscheuer et al., 2007). However, it is to be noted that this experiment was conducted only on roots and said observations of increased TGs under high temperature and were based on above-ground lipid studies. This further supports the novelty of the study and the potential for the elucidation of not only new lipids species, but also of more tissue-specific lipid functions, particularly under the influence of beneficial microbes and high temperature stress.

It is also highly possible that the annotation and identification of lipids from the unknown features may either shift the result of the current study or further strengthen its outcome. This is because some affected lipids might be hidden among the features that were not yet identified by the currently available lipid libraries and databases. As observed in the initial analysis comparing all the treatments between annotated lipids and unknown features, aside from the latter having considerably higher number of features (**Figure 4.5**), this also magnified the trend and differences found from the annotated lipid data, such as the consistent effect of bacterial inoculation under high temperature, and to some extent, the bacterial effect under ambient temperature (**Figure 4.3** and **4.4**). Whilst not all of these features may be real lipids and are instead lipid fragments, contaminants, noise, or artifacts, a number of them could very well be novel lipid species not yet documented in any available libraries. Comprehensive libraries and databases are not yet final (Gika, 2018) but are instead open to further addition of newly discovered lipids. Together with further lipid annotation using the MS/MS spectra, these improved and updated libraries can be used to newly annotate the unknown features found in

this study. This will hopefully characterize further lipid species influenced by *P. phytofirmans* PsJN in Arabidopsis roots under high temperature perturbation.

4.5. Conclusion

The utilization of an untargeted lipid approach enabled the profiling of existing and annotation of yet-to-be-identified lipids in Arabidopsis roots in interaction with varying temperatures and plant developmental stages. With the annotated lipid data, high temperature was shown to influence the magnitude and directionality of change in the peak intensities (areas), as well as the number of various lipid species. Exposure to constant high temperature has also seen modifications in the glycerophospholipids, glycerolipids, and sphingolipid species (essential membrane lipids), with quantified changes in the levels of lipid species or class. The effect of bacterial inoculation is also more prominent under high temperatures, as shown in the increases in the levels and number of lipid species affected by temperature, indicating their potential for manipulation for further heat tolerance studies.

Although the untargeted approach utilised in this study has generated some insights on the potential behaviour and changes in the plant root lipid profile when subjected to bacteria and high temperature, much could still be investigated following lipid identification. It is recommended that further annotation be conducted using MS/MS spectra analysis to fully characterize and determine the novelty of the lipid species upon identification. Succeeding studies could also use more biological replicates to increase the accuracy of the results.

Because of their immense structural diversity, the use of discovery-based lipidomics as a single analytical approach for profiling and quantifying lipids is challenging. What makes it even more complicated is that lipids have a large concentration range, with the occurrence of many isomeric and isobaric species that introduce uncertainty in their detection and identification. Therefore, to confirm the detection and identity of lipids, targeted experiments must be conducted, following untargeted lipid analysis.

It should, however, be emphasized that in plants, interpretation of data on the effects of high temperature on lipids may be difficult due to the variations in the experimental plant material (i.e., different species and different tissue types) under analysis, the different methods employed by different laboratories for the preparation of the plant tissues, as well as whether the reported results are about total lipids (untargeted approach) or particular lipid species (targeted approach). In any case, understanding the relationship between temperature and plant

root-microbe lipid responses can be beneficial in the cultivation of agricultural crops and protection against environmental damages.

CHAPTER 5

General discussion and conclusion

5.1. Introduction

Climate change, which is mainly driven by the rise of atmospheric CO₂, is characterized by elevated global temperatures that are adversely affecting plant health, growth, and productivity. This scenario is accompanied by longer and more intense heat waves, which are weakening the plant's natural defense systems against environmental challenges. Aside from directly impacting the plant's physiological functions and development throughout their ontogeny, climate change also affects other factors external to plants like availability of nutrients and water, and influencing the rhizomicrobiome, which in return influence the plant's well-being (Barnes & Tringe, 2022; Bassirirad, 2000). Amidst their global impact, elevated temperatures only receiving partial interest when compared with other environmental stressors such as drought and salinity.

Temperature is an essential factor in plant growth (Hatfield et al., 2011), however, exposure to supra-optimal temperatures beyond the growth range for plants can cause severe damage (Wahid et al., 2007). The effect of high temperatures can be manifested outwardly through root and shoot morphological modifications such as changes in leaf orientation, sunburns and discolorations, and leaf curling (Vollenweider & Günthardt-Goerg, 2005), as well as changes in the root structure (Calleja-Cabrera et al., 2020). Beyond what's perceivable from their physical exterior, high temperatures also elicit other responses involving changes in the plant's anatomy, phenology, physiological processes, and biochemical and molecular components (Hasanuzzaman et al., 2013; Wahid et al., 2012). As sessile organisms that are incapable of moving away from environmental challenges such as heat stress, plants have developed specific mechanisms to protect themselves. Plants employ adaptation mechanisms that can either be through short-term acclimation (e.g. adjustments of gas exchange parameters (Végh et al., 2018)) and avoidance (e.g. early maturation of crops (Prasad et al., 2006) or long-term induction of heat tolerance through mechanisms such as induction of osmoprotectants, antioxidant defenses, signaling cascades and transcriptional controls (Rodríguez et al., 2005). Another mechanism proposed to be utilized by plants against heat stress though studies are still in their infancy, are cell membrane reorganization and changes in the lipid levels (Cassim et al., 2019; Török et al., 2014).

Several strategies have been employed to address the challenges of high-temperature stress, either through field crop application or individual plant studies. These strategies include crop and resource management such as the utilization of the planting and harvest calendar, use of crop rotation, and variation in cropping schemes (Raza, Razzaq, et al., 2019). Other strategies

involve conventional breeding techniques, such as plant breeding (Blum, 2018) and genetic engineering and biotechnology, such as genome-wide association studies (GWAS) (Manolio, 2010), genome selection (GS) (Kumar et al., 2018), and omics-led breeding and marker-assisted selection (MAS) (Stinchcombe & Hoekstra, 2008). However, the still wide knowledge gap on the complex mechanisms behind heat stress tolerance in plants and the difficulties in targeting specific alleles and genetically modifying them, pose challenges to creating climate-resilient and high-yielding genotypes (Bhatnagar-Mathur et al., 2008). Even more so, the fact that most transgenic plant experiments are conducted within controlled environments and are rarely executed in the fields, hinders the potential breakthroughs in molecular and breeding techniques for bringing promising results to farmers, not to mention that these techniques can be laborious, time-, and resource-intensive (Etesami et al., 2015). Therefore, there is a need for less invasive and more sustainable strategies that can bring desired results with a quick turnover, thus, the proposal for the use of natural, plant-inhabiting beneficial microbes, specifically the plant growth-promoting ones.

Plant roots, which perform essential functions such as anchorage, water uptake, nutrient absorption, and storage of essential compounds (Smith, 2007), thrive in the abundance of and in complex interactions with their surrounding ecosystem. Plant roots are very responsive to environmental perturbations, such as high temperatures (Mc Michael & Burke, 2002), even more so than plant shoots, which are normally affected first by environmental fluctuations (Calleja-Cabrera et al., 2020). An important feature of the root, to cope with heterogeneously distributed nutrients in the soil, is its architecture. Dynamic root system architecture (RSA), which is also described as the topological and geometric measure of the root shape, is characterized by the spatial configuration of the root parts or the explicit deployment of root axes (Bucksch et al., 2017). The RSA is dynamic and responds to a wide range of stimuli, including the microbial colonization of the root tissues and increasing air/soil temperatures, making it a good target for trait-based breeding of resilient and high-producing crops (Tracy et al., 2020). However, although many studies involved measurements of root characteristics, only a few have conducted root-focused studies with an in-depth characterization of root morphological responses under different external stimuli.

For a long time, this plant organ has received little attention due to its hidden nature and the challenges of sampling and preparing, phenotyping or imaging, and its characterization, depending on the nature of the research. Root traits, such as root depth and width, root angle, fine root diameter, specific root area and length, root numbers, and root length density are some of the considered useful traits for improving plant productivity under heat stress conditions. It

is important to study plants and their interactions with the environment, and root phenotyping provides a huge advantage in this area. Due to advancements in technologies, many tools and platforms have been developed for root phenotyping, gaining more interest in root studies. According to Wasaya et al. (2018), phenotyping the roots is one of the heat stress management tools due to the roots' vulnerability to elevated soil temperatures, their essential roles in plant nutrient and water uptake, and their part in carrying out several metabolic and molecular functions for the plants. Different 2-D and 3-D techniques are now available, and among all of these, each has advantages and drawbacks. It is imperative to assess the objectives, experimental design, types of biological samples, the type of cultivation system, and the desired parametric traits to choose the appropriate phenotyping and imaging technology.

Finally, to understand plant responses to biotic and abiotic environments, observed physical and morphological responses must be linked with other omics-based studies to elucidate the mechanisms underlying such responses. Based on the accepted central dogma of biology, the focus of scientific research for a long time has been on DNA, RNA, and proteins (Stephenson et al., 2017). Recently, the study and characterization of metabolites have gained traction, mainly attributed to the progress in mass spectrometry technology. However, as primary metabolites with diverse functions in plant cells and the maintenance of cellular homeostasis, studies on lipids have been relatively fewer (Shevchenko & Simons, 2010). Lipids, which are a group of highly diverse and multi-function compounds, play essential roles, such as in the maintenance of structural integrity of the plasma and endomembranes (Quinn et al., 1989), as efficient energy and carbon storage (Welte & Gould, 2017), as mediators in cell signaling pathways (Wang, 2004), and as regulators of plant responses to soil microorganisms and environmental stressors (Okazaki & Saito, 2014). The roles of lipids in plant's various forms of interactions with microbes have been documented, ranging from being the chemical language that drives the rhizosphere interactions (Venturi & Keel, 2016), to being the elicitors and effectors of plant immune defenses during microbial adhesion and colonization of the root tissues (Siebers et al., 2016), to modulating the alterations in its structure and components upon the establishment of symbiosis (whether that be pathogenic or mutualistic) and in response to environmental conditions. The structural diversity of lipids made them so abundant in nature that, even with several thousand already identified species with their associated functions, there are still many more to be discovered, with functions yet to be elucidated in different biological systems under variable conditions. How plant root lipids behave during plant root–beneficial bacteria interactions under high temperatures is a relatively new frontier, especially when done in tandem with root phenotypic characterization, as was attempted in this study.

5.2. Relevance of the study

This study aspires to fill some of the gaps mentioned in the earlier part of the introduction. First, the use of high temperature as the environmental stressor for this study makes this one of the relatively few that investigate this abiotic factor in conjunction with other less studied areas in plant biology. Temperature affects all organisms, from microbes to plants, whether underground or aboveground and depending on the plant's ontogeny. It is therefore timely and essential to understand how increasing temperatures can impact the biotic interactions between plants and bacteria and their interconnectivity as components of the ecosystem. Second, as with the need for sustainable approaches to addressing high-temperature stress, this study made use of a PGPR, which has been shown to impart not only growth-promoting benefits but also heat tolerance capability to plants. Although there are already multitudes of studies on beneficial microbes spanning different omics fields, this current study investigated two uncommon parameters affected by bacterial application in plant roots, i.e., the morphological changes in the root system architecture and the lipidomic profile of the roots. Plant morphological responses to increased temperatures are very dynamic and can elicit prominent responses from roots. For example, Calleja-Cabrera et al. (2020) provided a review of the morphological changes in the RSA under a climate change scenario. The morphological responses of the RSA against combined bacterial application and high temperatures have also been recently dissected in an in-depth root phenotyping study by Macabuhay, Arsova, Watt, et al. (2022). Third, the root morphological characterization portion of this study introduced a new non-invasive high-throughput phenotyping platform, which attempted to address the pitfalls of existing phenotyping platforms, although still conducted in a 2D agar-plate system that still needs further validation of results in soil/field experiments. Finally, the characterization and profiling of plant lipids, particularly of the roots, when subjected to both bacterization and high temperatures, is relatively new and with only a few studies in precedence. It is rare to see a combination of root morphology with lipidomic phenomics studies, which can reveal not only novel lipids and functions but also the complex nature of the tripartite interaction between plant roots x beneficial bacteria x high temperatures, to elucidate how plants can tolerate high-temperature stress with the help of bacteria.

5.3. Thesis outline and main insights

The first sections (**sections 1.1 – 1.4**) of **Chapter 1** of this study attempted to enlighten the topic of climate change, which is a global environmental issue that threatens the agricultural

sector, in particular, the global crop production. This section describes the drivers as well as the implications of the changes in climate, mainly characterized by elevated global atmospheric temperatures, to crop production and plants in general. Described here as well are the plant and microbe-specific responses to high temperatures, the various mechanisms they employ to adapt in times of environmental stress, as well as the different strategies already utilized to address the problem of heat stress or heat waves in the field, including the use of soil microbe inoculants. Next, this section shed light on the nature of the hidden underground interactions between plant roots and the rhizomicrobiome. This provided a justification for harnessing the soil microbes, especially the plant growth-promoting microbes, not just in imparting growth benefits to plants under normal conditions, but more importantly, in imparting tolerance to high-temperature stress. The second section (**sections 1.5 – 1.5.6**) of this chapter, which has been published as a compressed review in Trends in Plants Science with the title “Modulators or facilitators? Roles of lipids in plant root-microbe interactions” (Macabuhay, Arsova, Watt, et al., 2022) described the biochemical nature of the plant root-microbe interactions. This mentioned the intrinsic roles of lipids in the plasma membrane as the interface for interaction, and the diverse lipid roles in the various stages of the rhizosphere interactions: from rhizodeposition, to signal perception and responses, and the establishment of either mutualistic or pathogenic interactions. The remaining sections depicted the advances in mass spectrometry for lipid visualization and characterization, as well as the steps in the lipidomics workflow. The significance and objectives of the study, including the biological samples used, were then explained. Finally, a synopsis of each thesis chapter was provided at the end of this chapter.

Chapter 2 explained the development of the methods employed in growing the Arabidopsis plants and the bacteria *P. phytofirmans* PsJN individually as well as their co-cultivation, in an atypical methods format. This also described the optimization of the two contrasting plant cultivation systems depending on the availability of the imaging and phenotyping platform in the current research groups involved in the joint PhD program, at the University of Melbourne or the Forschungszentrum Juelich in Germany. The two systems utilized in this study were the “closed-plate” or closed-agar plate system, where both the shoots and the roots are grown inside the plate and are illuminated throughout the plant growth, and the “open-top” system, which, as the name implies has an open top portion of the plate that allows for the unobstructed growth of the shoots in open air and light, while maintaining the roots in the dark environment.

This chapter addressed the first objective of the research which was to develop an optimized system for the co-cultivation of plants and microbes that is conducive to periodic imaging and

non-invasive plant phenotyping. Described here was the rationale behind the experimental design and the different considerations for selecting the appropriate type of growth system (after the selection of biological samples from the previous chapter). In concurrence with the location where the experiments were conducted, this chapter was divided into three sections: 1) Establishment of protocols for optimized plant and bacterial growth and co-cultivation using the traditional “closed-plate” system at the University of Melbourne, 2) Optimization methods for the “open-top” system using the phenotyping platform GrowScreen-Agar II at the Forschungszentrum Juelich (FZJ), and 3) Optimization methods to replicate the “open-top” system at the FZJ but using conventional agar-plate approaches. It is to be noted that the third optimization at UoM only happened due to the COVID-19 virus pandemic leading to the urgent return to Australia with unfinished final experiments at the FZJ.

Chapter 3 focused on the experiments conducted at the FZJ which also addressed the second objective of the study, i.e., to characterize and quantify the dynamics of microbe-imparted growth promotion in plants under ambient and high-temperature conditions through measurement of root and shoot morphological responses. Arabidopsis seeds sown on the top holes of the closed, customized plates (for the GrowScreen-Agar II platform) were inoculated with either mock inoculants or with the PsJN bacterial inoculum, after which, the plates were transferred to two growth chambers with either ambient temperature (22°C/18°C) or high-temperature (30°C/24°C) conditions. At several time points (5, 7, 9, 12, 14, 16, 19, and 21), the plates were imaged and the plants were subjected to phenotyping. Generated data by associated software GrowScreen-Root was then subjected to analysis generating results for several roots and shoot trait parameters.

The results indicated that the bacteria PsJN strongly influences Arabidopsis plants whether in a traditional “closed-plate” or an “open-top” cultivation system, with the latter allowing natural plant growth and more efficient shoot and, even more so, root phenotypic characterization (Fig. S5, Fig. 1). Testing for colonization of the rhizoplane and root tissues showed the presence of the bacteria in inoculated Arabidopsis roots and its absence in non-inoculated ones (Fig. S4); while colony PCR and 16s rRNA genomic sequencing confirmed the identity of the strain *P. phytofirmans* PsJN. The intensity of the bacteria-imparted growth promotion on the root system architecture varied depending on the specific root type and was influenced by temperature. That is, the effect of the bacterial inoculation was significant under ambient conditions; however, this growth stimulation was greater under high temperatures as was observed from the root lengths, growth rates, and the number of lateral roots (Fig. 2). The

overall root system traits particularly highlighted the strong deleterious effect of high temperature on the roots (Fig. 3). Our study was also able to shed light on the distribution of the roots across different depths from the top agar surface during their gravitropic growth. The development and increase in the total root lengths across a specific depth and time were affected by the bacteria PsJN and temperature; however, these changes affecting the density of the roots were resolved by scrutinizing the emergence and contribution of the 1st and 2nd order lateral roots (Fig. 4). Contrary to the bacterial effects on root traits, where growth promotion was stronger under high temperature, bacterial effects in shoots were prominently observed under ambient condition during the later stages of plant development (Fig. 5a). Shoot dry weights indicated the deleterious effect of high temperature and how bacterial inoculation ameliorated this effect, particularly under ambient condition (Fig. 5b). Finally, all manifested root and shoot growth promotion, as well as bacteria-imparted thermotolerance effects, were time- and tissue-specific. In roots, the stimulation effects of the bacteria were found during the early growth stage but declined from certain points in time depending on the root type. In shoots, the effect of the bacteria was only significantly detected towards the end of the growing period (Fig. 2 and 5).

Chapter 4 of the thesis hinted at the biochemical nature of the plant root-microbe interactions, by revealing the behaviour of plant lipids, during plant root-microbe interactions subjected to high-temperature conditions. This chapter addressed the last objectives of the study, which were to generate the lipidomics profiles of both control and PsJN-inoculated roots under ambient and high temperatures and to determine specific lipid species particularly affected by this tripartite interaction. The analysis for lipids also provided an additional factor, time, which revealed some time-dependent alterations in the lipid classes and species.

This study was able to annotate several hundreds of lipid species although further data processing is required to fully identify novel lipid species. Lipids were annotated based on their mass accuracy and the retention time patterns provided through the MS-Dial lipid database, which uses libraries from MassBank (Horai et al., 2010) and LipidBlast (Kind et al., 2013). The retention time pattern was taken into consideration to diminish false annotations due to interferences that arise from in-source fragmentation and isobaric/isomeric compounds (Yu et al., 2018). To validate the annotated lipids, their corresponding MS/MS spectra identified by the MS-Dial software, should be examined individually for characteristic fragmentation patterns. Currently, several lipid species covering multiple lipid classes were annotated from the 13,886 detected mass spectrometric peaks in roots (**Figure 4.1**).

Because of the challenges involved in quantifying a large number of lipids using a single statistical method (Khoury et al., 2018), most of the conducted untargeted LC-MS-based analyses rely on the comparison of mass spectrometric responses and fold change analyses (Breitkopf et al., 2017; Millner et al., 2020; Zhang et al., 2020). This method of data assessment, when performed with substantial statistical analysis, can provide meaningful and comprehensive comparisons between biological tissues or samples (Wang 2017) and various treatment comparisons with external factors. In this study, we used ANOVA to determine statistical differences among the four treatments, but mainly used fold change analyses paired with Student's *t*-test and volcano plots to compare and quantify the peak areas of lipid classes and individual lipid species between control and PsJN-inoculated roots under different conditions. Whilst further analysis can deliver additional information, this generated data already provided useful insights on the behavior of lipids when subjected to external perturbations as with the addition of a beneficial plant growth-promoting bacteria and the stress induced by elevated temperatures. Both annotated lipids and unknown features were analyzed; and based on univariate and multivariate statistical analyses, indications of specific behaviors in *Arabidopsis* roots against temperature, bacterization, and time were elucidated.

The bacteria PsJN has induced significant changes in the annotated lipid profile of *Arabidopsis* roots, under both temperatures, although with a stronger and more consistent effect under high temperatures. This trend was also observed in the unknown features, with a higher quantity of potentially hiding novel lipid species. The effect of high temperature on the lipid profile was significantly evident and affected almost all of the lipid classes throughout the plant development. The high number of increased TG species under high temperatures supports existing studies on the inherent response of plant root membranes to temperature stress, including the responses of other lipid classes such as GP, GL, and SP, which are the components of the cell membrane. However, contrary to previous findings, which indicated a similar increase of DG and TG (due to the former's conversion to TG), a high number of DG species was decreased in this study. Bacterial inoculation effects also showed changes in SP (Cer and HexCer), lysophospholipids (LPC and LPE), and ST lipids. It also highlighted the alterations in the extracted root lipids which are abundant components of bacterial membranes such as GPs, CL, PC, and PE. Being an abundant component of the bacterial membrane may potentially explain the highest number of increased PE species and the highest fold change increase in CL that was observed throughout the plant development (except at 14 DAI ambient). Surprisingly, TG under bacterial inoculation has decreased which is in contrast to the previously accounted plant response to high temperature (which is to increase TG) and the

bacteria's tendency of storing TG as an endogenous carbon source. Further analysis needs to be performed to confirm this result, but otherwise, the fact that most of the existing literature on plant lipids and high-temperature studies are conducted in above-ground plant parts may potentially account for the differences in results.

5.4. Synthesis

Since the experiments were conducted separately three times at different locations and with different technological resources, optimization of the utilized systems has therefore also been conducted thrice. All growth protocols and methods, including the objectives behind every development, were discussed in **Chapter 2**.

From the first experiment at UoM with the “closed-plate” system, the bacterial inoculation effect, though non-significant at the time (potentially due to the low number of plant samples), already indicated the growth promotion effects of bacteria through some root trait parameters such as total, primary, and branched root length, and also shoot dry weight (**Chapter 3, Figure S1**). In agreement with these, the calculation of the growth rates parameter also showed similar trends, with the percentage difference between control and PsJN-inoculated roots increasing as time progressed (max at 21 DAI). It could be that after this period, the bacterial stimulation effect would have been high enough to be significantly different from the control counterparts. This showed that for this particular system, the effect of bacterial application manifested at a later stage of plant development, and factors such as light (since both roots and shoots were illuminated), airflow within, and the material of the plate may have influenced the root and shoot morphological response. The particular skewing behavior of *Arabidopsis* roots grown in conventional agar Petri plates (Oliva & Dunand, 2007) that has been puzzling researchers was also observed, which indicated other factors (e.g. gravity and growth media surface) that could have influenced the bacterial effects. Nonetheless, the growth stimulation trend was indicated and this served as the basis for the larger scale, high throughput phenotyping at the FZJ using the “open-top” system.

Chapter 3 of the thesis is firstly an outcome of an optimized co-cultivation system for both *Arabidopsis* plants and PsJN bacteria, which was detailed also detailed in **Chapter 2**. The use of the GrowScreen-Agar II significantly increased the capability for root characterization for the following reasons: 1) The associated open-air and light-exposed growing of the shoot, with the darkened undisturbed root condition, allowed for a more “natural” plant growth as

compared to the traditional enclosed growing of the whole plants within a plate. 2) The manual tracing of the individual root type, though laborious at this time (may have the potential for automation and machine learning) especially at the later stages when the roots are extensively branched and covering the entire plate, has allowed for closer inspection of the root growth. This manual tracing, however, is compensated by the capacity of the software to superimpose older traced roots with new root images, which saved a considerable amount of time and maintained the accuracy of tracing. 3) The feature of this software allowed for the identification of the root types, therefore their associated traits, and the division of the analyzed root area into several sections to look at root length distribution per section. The full automation of this platform is something to look forward to. This will provide further advantages to its different pipelines – the plant cultivation system, the imaging capability, and the root and shoot trait characterization.

Because of this system, many conclusions were drawn, though restricted to 2D artificial environmental conditions. We are already aware of the plasticity of roots as regulated by their inherent properties such as cell division and differentiation, which affect the post-embryonic root development of primary roots as well as the development of other root types. However, this intrinsic plasticity was hijacked and manipulated by the tissue colonizer, bacteria PsJN to impart different root behaviors, which were mostly leading to the enhancement of growth. This was observed in the enhanced root lengths, growth rates, number of the 1st and 2nd lateral roots, as well as root length distribution. This alteration of the RSA could be attributed to a multitude of mechanisms such as the production of phytohormones (e.g. jasmonic acid, salicylic acid, gibberellins, indole-3-acetic acid (IAA), exopolysaccharides, and 1-aminocyclopropane 1-carboxylic acid (ACC) deaminase)), production of cell wall degrading enzymes, antibiotics, hydrogen cyanide, siderophores, and induction of quorum quenching. In other root parameters such as the root system depth, width, convex hull, and branching angle, the absence of the effect of bacterial inoculation could be because of the homogeneity of the agar media, where nutrients were well distributed, therefore the branching roots did not need to expand and the primary root did not need to elongate, more than what their growth required, even with the bacteria's growth promoting presence.

The effect of high temperatures was detrimental in all aspects of root and shoot morphological development – significantly inhibiting the root lengths (total, primary, and 1st and 2nd order laterals) and growth rates, reducing the number of both lateral roots, and prominently affecting the root system spread and distribution. The decrease in the number and length of lateral roots may have caused the likewise decreased distribution of the root system.

The heat-stressed roots appeared adversely affected, with values far below all the three other treatments in both root and shoot traits. On a good note, the bacterial treatment under high-temperature conditions has shown promising results of amelioration of the latter's otherwise negative effects. In almost all trait parameters, the difference between control and inoculated plants under high temperatures is almost double that of ambient. This indicates that, although bacteria have significant growth-promotion effects at ambient or normal conditions, their stimulatory benefits increase when applied at stressful temperatures.

Both the effects of high temperatures alone and bacterial inoculation at high temperatures on the root lipid profile described in **Chapter 4** follow the morphologic phenotype observed in the RSA. Clearly, high temperature has detrimental effects on the root lipids, as shown by a large number of down-regulated or decreased peak intensities of lipid species. This also coincides with the consistent lower values of HTC, which are control plants under high temperatures. As the initial perception of temperature fluctuations happens in the plasma membrane, and the succeeding responses involve changes in the structure and components of the membrane lipids, most of the affected lipids also belonged to the GP category, which is mainly comprised of membrane lipids such as PC, PE, PI, PG, and PS, with also some components from the GLs, and SPs. Almost all lipid classes were increased under high temperatures, however, specific lipid classes have shown some notable modifications as well, as with TG and DG, both connected and part of the synthesis and production of TGs. Bacterial inoculation under high temperatures has also shown some notable trends and behavior of lipid classes. There was a relatively lower number of total changed species, however, there were distinct outcomes deduced from the analysis showing specific lipids with highlighted involvement. This shows the consistent appearance of PE as an increased lipid class with the highest number of lipid species. Contrary to this is the result on TG, which was the opposite of high-temperature effects, showing decreases instead, showing both the highest number of changed lipid species with the highest fold change decrease as well. Finally, the lipid class CL appeared to be highly upregulated by bacterial inoculation as it has the highest fold change increases.

5.4. Concluding remarks and future perspectives

This study validated the plant growth-promoting and heat tolerance effects of *Paraburkholderia phytofirmans* PsJN on Arabidopsis plants subjected to ambient and a constant high temperature of 30°C, which is beyond the optimum growth range for the wildtype

Arabidopsis. Successful co-cultivation of the bacteria and the plants entailed optimal growth protocols for both species and an optimized microcosm system that also catered for the other requirements of the study, i.e., periodic, non-invasive imaging and phenotyping and time-specific root tissue harvest for lipidomics analyses.

The phenotyping platform GrowScreen-Agar II utilized in this study has proven that high-resolution phenotyping and root-and-shoot trait characterization can elucidate not just the morphological changes in these parts, but also the dynamics of changes in the bacteria-induced growth stimulation under ambient and high temperatures. The pipelines of this platform were efficient, in that, firstly, the plant growth system allowed for a more simulated growth of plants, i.e., shoots outside, in open air and light, with roots undisturbed in the dark. Secondly, the high throughput and resolution of the imaging system captured all the features of the roots, allowing for the efficient tracing of the different root types of Arabidopsis. Thirdly, the root and shoot associated analysis software GrowScreen-Root and Colour segmentation, respectively, have been powerful tools in the dissection of the different traits of both tissues, particularly the roots; allowing for in-depth, tissue- and time-specific characterization in a single analysis. It is highly recommended that future experiments utilize the shoot growth orientation (for potential physiological measurements) and imaging component (the use of side imaging especially for blade-leaf plants like *Brachypodium* and other cereals) to maximize the use of this technology.

Many different measured root traits allowed for the intensive characterization and quantification of the dynamics of bacteria-imparted growth promotion as was seen from the enhancement of root length and growth rates, and the increase in branching and number of lateral roots, which are useful for plant uptake and scavenging of nutrients. This analysis also quantified the magnitude of bacterial stimulation between the two temperature conditions and confirmed the excellent benefit of the PsJN bacteria in ameliorating the detrimental heat stress effects on plants. Although these generated results concretized the mechanisms of morphological growth-promotion induced by the bacteria PsJN in roots, it is still an artificial system; therefore, the results need to be validated in soil and field conditions. This type of experimentation would potentially require separate optimization and growth protocols for both plants and bacteria, as soil media is characteristically different from agar, and would require a larger space that will be more prone for contamination. Soil and pot studies would also require a different imaging system, potentially 3D tomographic imaging (e.g. X-ray CT and MRI) due to the opaque nature of the soil, in as much as a different root and shoot analysis software.

Finally, the untargeted lipidomics analysis employed in this study corresponded with the morphological effects of high temperature alone, and the bacterial effect under both ambient

and high-temperature conditions. The decreased or inhibited growth of the different root types and traits related to the downregulation of several lipid classes under high temperature, whereas, the enhanced characteristics of the roots under bacterial application were also shown in the upregulation of several lipid classes, under ambient, and even more so under high temperatures. The annotated data may have shown considerable trends in the changes of the plant root lipid profile under the influence of bacteria, temperature, and time. However, these results can be enhanced further by focussing efforts to annotate the unknown features generated by MS-Dial to determine any more underlying lipid species that may verify the results and trends from the annotated lipids.

The structural characterization of lipids is essential for the thorough analysis of their biological functions within plant cells and tissues, as both bioactivity and functions of lipids depend significantly on their chemical structures (Claes et al., 2021). The development of a comprehensive and widely accessible workflow that will allow isomer resolution and determine double bond locations and sn-positions, is a key challenge still faced in lipidomics analysis (Claes et al., 2021).

It is recommended that lipids be considered as part of an integrated system with enzymes and metabolites, within the context of plant function, in order to identify and investigate new lipids necessary for plant growth and survival (Kehelpannala et al., 2021). Lipidomics studies should also be linked and integrated with other “omics” studies such as metabolomics, proteomics, transcriptomics, and genomics to explain genetic mechanisms underlying the modifications in lipid responses to environmental cues (Cheong et al., 2021). This would require the development of web-accessible databases collating “omics” acquired data that would be particularly useful for lipid studies, which still lag behind other omics studies.

We are facing current challenges due to a changing climate, with elevated temperatures that are bound to increase further by the middle of this century. This poses serious threats that are already felt in all economic sectors. Added to the challenges of the warming climate is the increasing demand to enhance crop production, amid decreasing availability of fertile agricultural lands, to feed the increasing human population, which is projected to reach about 9 Billion by 2050. Given all these conditions, there is a need to address global food security while maintaining environmental sustainability. Plant growth-promoting rhizobacteria (PGPR) are potential solutions to assisting plants against environmental stressors while boosting productivity. This study explored this potential by investigating the mechanisms of bacteria-imparted growth promotion and heat tolerance in plants through morphological and biochemical phenotyping. Knowledge gained from this study can inform research agenda of

future directions for microbial studies as likely agricultural and biotechnological solutions in the endeavor to address global food security under climate change.

Appendices

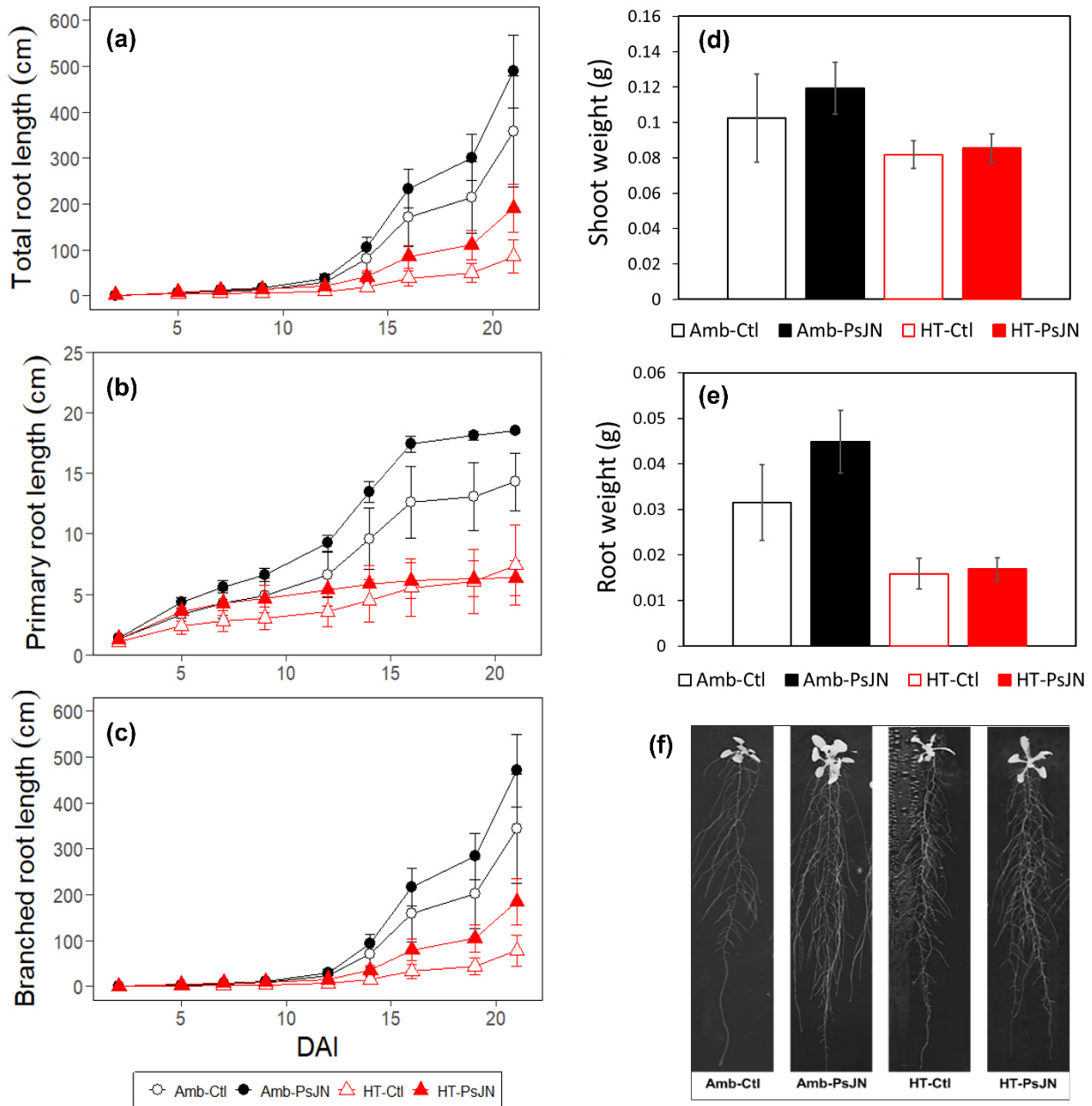


Figure S 1 WinRhizo analysed root lengths and root and shoot biomass. Root lengths quantified using WinRhizo analysis in a closed-plate experiment: (a) Total root lengths, (b) primary root length, and (c) branched root lengths. Temperature - black and circle symbol (ambient), red and triangle symbol (high temperature); bacterial application – empty symbol (control), filled symbol (PsJN-inoculated). Plant biomass taken at harvest: (d) shoot dry weight and (e) root dry weight. (f) Sample images of 16-day old seedlings from each of the four treatments. Treatments: Amb-Ctl (control plants under ambient), Amb-PsJN (PsJN-inoculated plants under ambient), HT-Ctl (control plants under high temperature), and HT-PsJN (PsJN-inoculated plants under high temperature). All points are the mean \pm standard error of $n=6$ samples within each treatment. Asterisks: Black – significant difference between mean of PsJN-inoculated and control plants under ambient condition, red - significant difference

between mean of PsJN-inoculated and control plants under high temperature condition, based on the Student's t-test with $p < 0.05$.

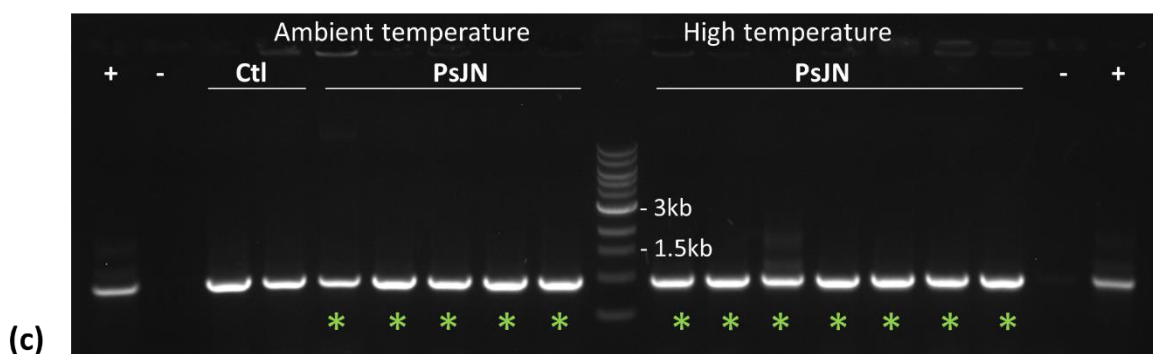
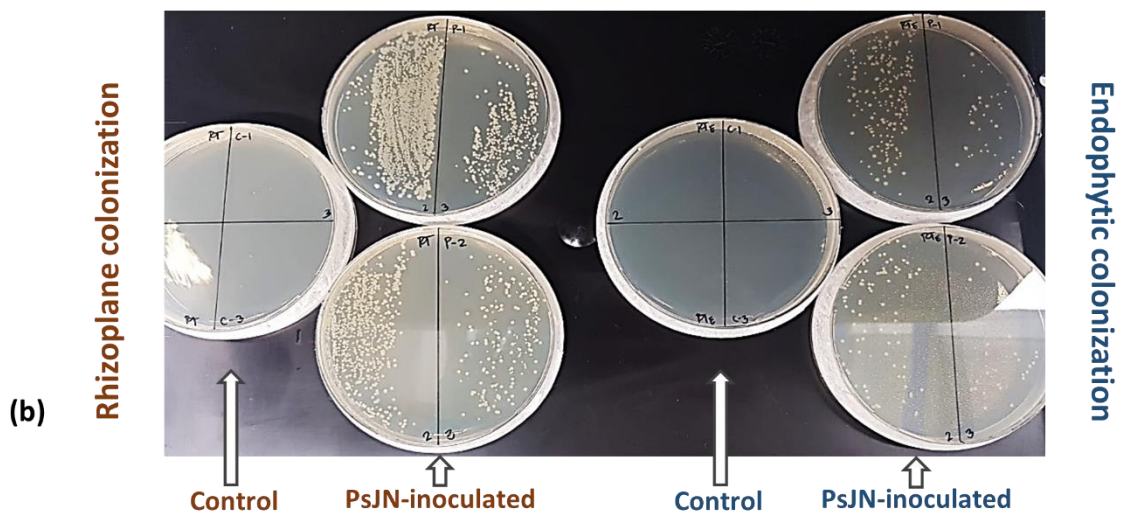
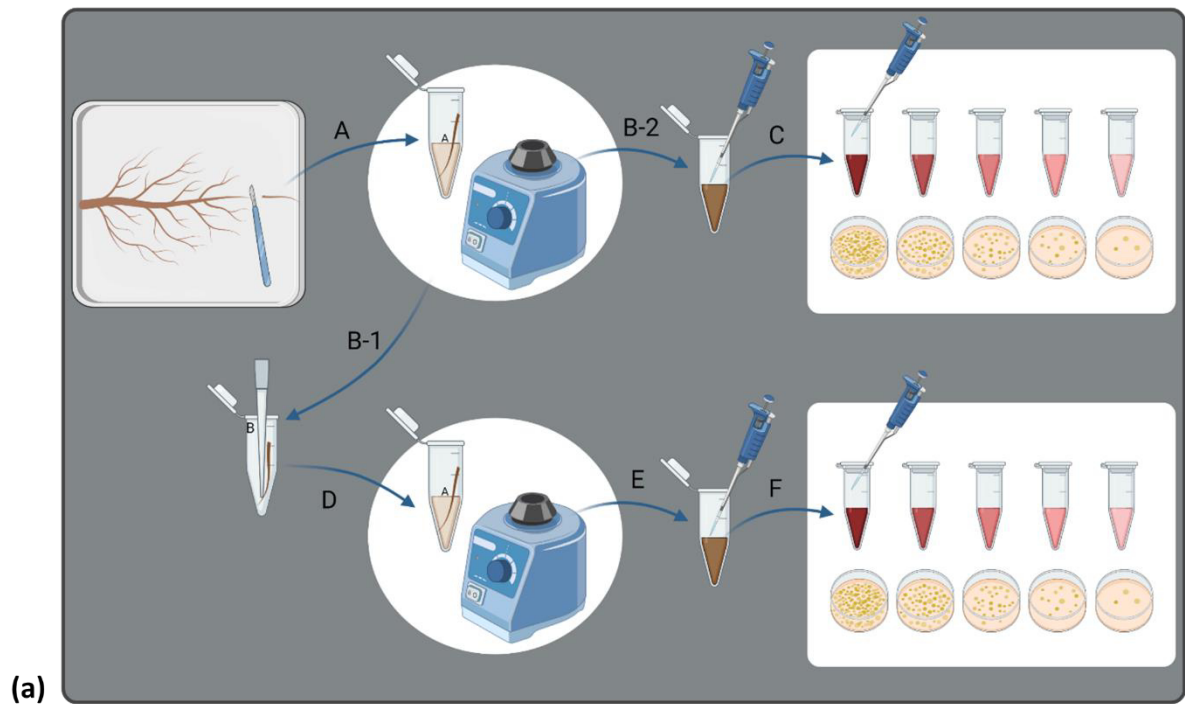


Figure S 2 Root sampling and bacterial colonization confirmation. (a) Brief procedure for sampling of root tissues for the determination of bacterial colonization. (A) Cutting about 1-2 cm of the root tip, placing into pre-prepared Eppendorf tube with LB (no NaCl) media, and washing/agitating the root using a vortex to get the root surface bacteria. (B-2) Aliquoting from the LB surface washing fraction. (C) Performing serial dilution of the bacterial inoculum, aliquoting from each dilution, and plating. (B-1) Removal of the washed root and transfer into a separate clean tube for maceration. (D) Adding LB media (no NaCl) to the macerated root and mixing using a vortex to extract the bacteria inside the root tissue. (E) Aliquoting from the washing to transfer to tubes for serial dilution and then plating each of the dilutions (F). (C) corresponds to **rhizoplane** colonization while (F) yields **endophytic** colonization of bacteria (image created with BioRender.com). (b) Sample plated dilutions at 21 DAI. Left two columns show rhizoplane colonization and right two columns show endophytic colonization of the bacteria. 1st and 3rd columns are from non-inoculated roots showing no growth, indicating sterility of system; while 2nd and 4th are from inoculated roots, showing growth from the bacterial strain PsJN. (c) PCR of single bacterial colonies from macerated root tips which have been plated out on LB media. The PCR products were sequenced, and the ones identified as *Parabulkoholderia* sp. are indicated with a green asterix “*”. Minimum of 3 plants of each treatment were sampled. Note that the three high temperature control roots and one ambient temperature control root showed no colonies at all on the plate - thus no PCR products, whereas the products in the 2 ambient temperature controls was identified as a *Paenibacillus* sp. “+”- positive control for the universal bacterial primers, “-“ – negative control for the PCR reaction, Ctl- control, PsJN- Roots inoculated with PsJN bacteria.

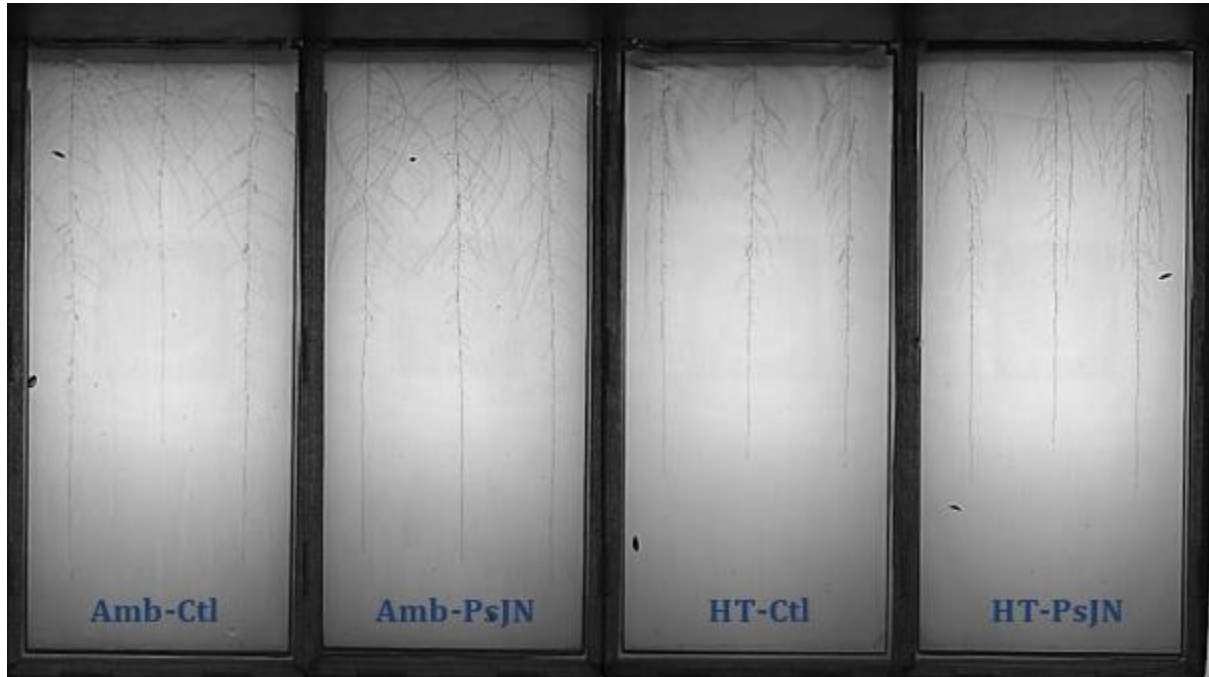


Figure S 3 Sample root images generated by the GrowScreen-Agar II. Images of plant roots from the four treatments at 16 DAI taken by the root camera of the GrowScreen-Agar II imaging system. Treatments (from left to right): Amb-Ctl (control or non-inoculated plants under ambient), Amb-PsJN (PsJN-inoculated plants under ambient), HT-Ctl (control or non-inoculated plants under high temperature), and HT-PsJN (PsJN-inoculated plants under high temperature).

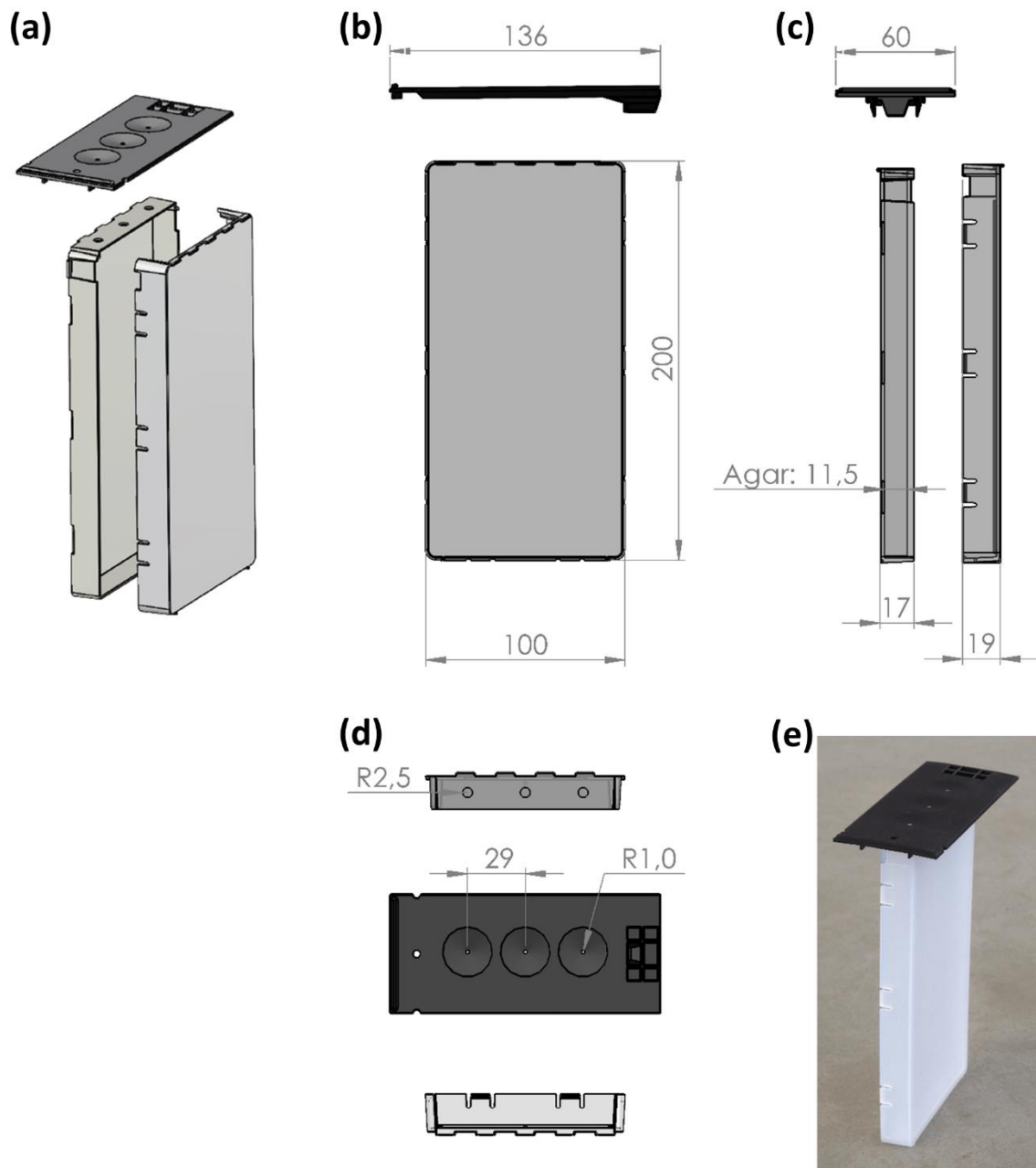


Figure S 4 Agar plates for GrowScreen-Agar II. Technical drawings of three components of the agar plate: 1) an opaque cover with an anti-fog agent which prevents water droplets, 2) a transparent back plate with holes on top which allows root imaging and the shoot to grow outside of the plate, and 3) a black top part (“collar”) also with three holes as background for shoot imaging, keeping light out of the root zone and mechanical support for leaves. The technical drawings show the assembly of the three components **(a)**, different side views **(b, c)**, top view **(d)**, while figure e) shows an original photo of the assembled plate. The dimensions are given in mm **(b-d)**. ‘Agar: 11,5’ represents the filling height of the agar **(c)** and ‘R’ the radius of the holes **(d)**.

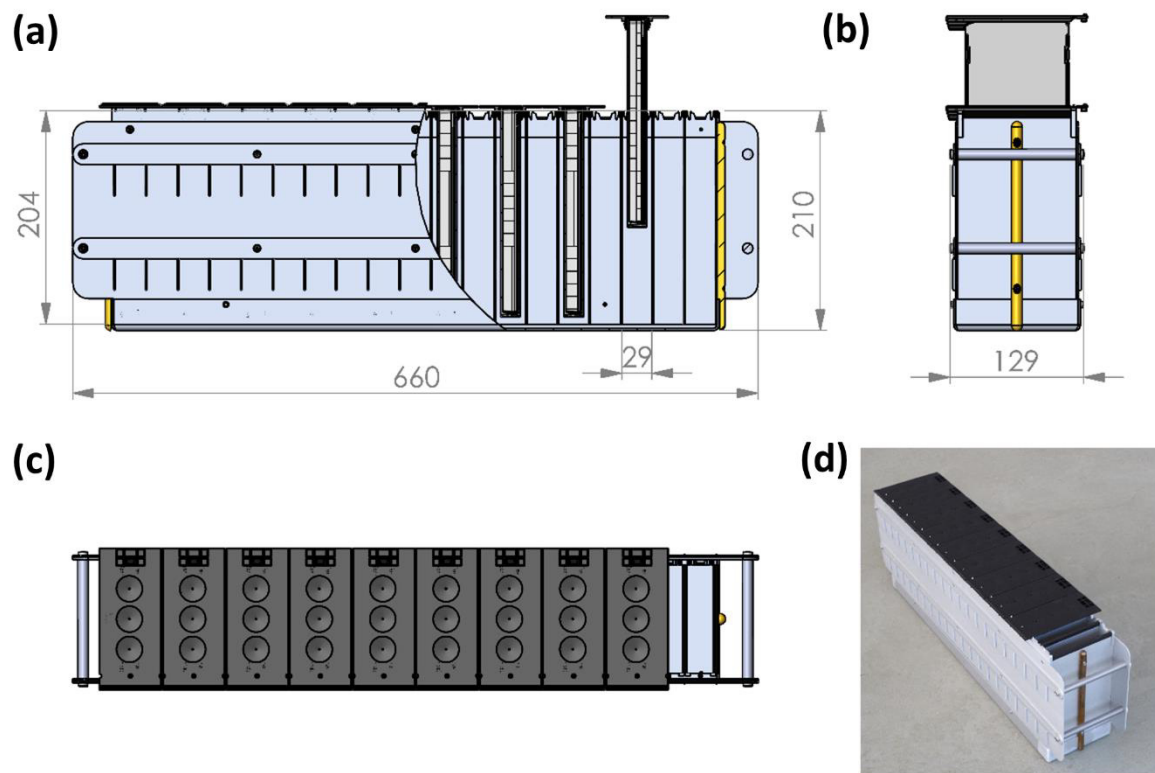


Figure S 5 Magazines for GrowScreen-Agar II. The plates are positioned vertically and maintained for plant cultivation in fabricated metal magazines accommodating up to 10 plates. The design of the magazines allows the roots to grow in the dark. The technical drawings show a side view **(a)**, top view **(b)**, and front view **(c)** of the magazine, while figure **(d)** shows an original photo of the magazine, each loaded with 9 plates and 1 open slot. In figure **(a)** the side wall of the magazine is partly removed to show the plates inside the magazine and one plate is lifted in **(a)** and **(b)**. The dimensions are given in mm.

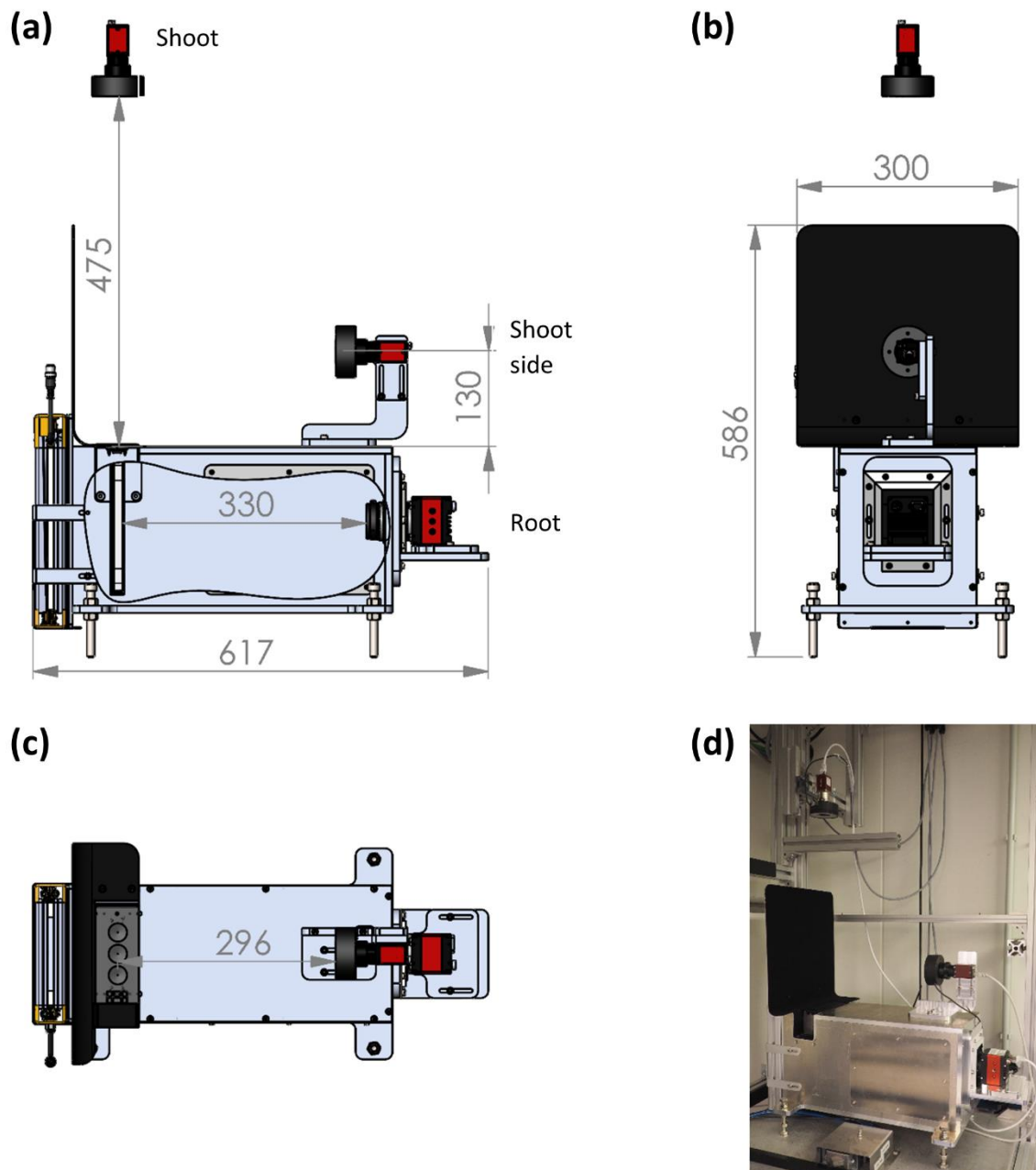





Figure S 6 Imaging station of GrowScreen-Agar II. For imaging roots and shoots, the plates are placed in the imaging station of the phenotyping platform GrowScreen-Agar II. The imaging system features a metal housing equipped with one root and two shoot cameras aiming at a slot for inserting the plate. The root camera takes images of the whole agar area (20 x 10 cm) while the shoot cameras take a side view and a top view image of the shoots. The technical drawings show a side view (a), top view (b), and front view (c) of the imaging station, while the original photo shows nearly a side view (d). The black background (c, d) provides a good contrast for shoot image analysis. Root illumination is achieved from the back while leaves are illuminated for imaging by using LED rings placed around the objective lenses of the shoot camera (a-d)

Figure S 7 Published section of Chapter 1 (section 1.5 to 1.5.6) in the journal Trends in Plant Science with the title “Modulators or facilitators? Roles of lipids in plant root–microbe interactions. (Macabuhay, A., Arsova, B., Walker, R., Johnson, A., Watt, M., & Roessner, U. (2022, 2022/02/01). Modulators or facilitators? Roles of lipids in plant root–microbe interactions. Trends in Plant Science, 27(2), 180-190. <https://doi.org/https://doi.org/10.1016/j.tplants.2021.08.004>).

(Next sections)

Review

Modulators or facilitators? Roles of lipids in plant root–microbe interactions

Allene Macabuhay ^{1,3,*} Borjana Arsova,² Robert Walker,¹ Alexander Johnson,¹ Michelle Watt ¹ and Ute Roessner ¹

Lipids have diverse functions in regulating the plasma membrane's cellular processes and signaling mediation. Plasma membrane lipids are also involved in the plant's complex interactions with the surrounding microorganisms, with which plants are in various forms of symbiosis. The roles of lipids influence the whole microbial colonization process, thus shaping the rhizomicrobiome. As chemical signals, lipids facilitate the stages of rhizospheric interactions – from plant root to microbe, microbe to microbe, and microbe to plant root – and modulate the plant's defense responses upon perception or contact with either beneficial or phytopathogenic microorganisms. Although studies have come a long way, further investigation is needed to discover more lipid species and elucidate novel lipid functions and profiles under various stages of plant root–microbe interactions.

How lipids are involved in rhizosphere interactions

Lipids (see [Glossary](#)), a ubiquitous class of biomolecules and major constituents of eukaryotic and prokaryotic cell membranes, are essential for a complete study of cell biology and functions. Lipids serve as structural components of plasma and intracellular membranes, provide energy and carbon storage, mediate cell signaling pathways, and regulate stress responses [1–3]. Because of their diverse roles, lipid homeostasis and lipid metabolism have systemic effects that can influence plant development and performance [4].

Numerous studies on aboveground plant–microbe interactions have already been documented; however, investigations of the **rhizosphere** have been restricted due to limitations in the application of ‘omics’ techniques [5] and difficulties in simulating a natural underground ecosystem [6]. These interactions have been investigated mostly at metabolic and transcriptomic levels, but there are still many questions on the biochemical exchange and communication between the involved organisms. Rhizosphere-related phenomena such as rhizodeposition and plant–microbe signaling are critical underground processes that still need to be further explored [7] and in which lipids are highly involved [8,9]. In the rhizosphere, whenever plant roots communicate with or contact microbes, molecular information is exchanged. Microbe recognition occurs at the plasma membrane (PM), which acts as the interface, either allowing advantageous resource exchange or inhibiting interaction through downstream signaling cascades [10,11]. Although the cell wall is the outermost border of the plant body that provides general resistance upon microbe penetration [12], the PM serves as the critical player in signaling responses to external stimuli, initial microbe recognition, and multiple downstream responses, which the microbes attempt to manipulate to suppress plant defense responses to colonize and procure nutrients [10,11,13]. As major components of the PM, lipids establish the physical barriers on the living cell surfaces, influence the communication between the host and microbe, and serve as signaling molecules or providers of elicitors for recognition, thereby influencing the establishment or prevention of microbial colonization [8,14–16].

Highlights

Lipids have diverse functions across the different stages in the formation of plant root–microbe interactions, commencing from the shaping of the rhizomicrobiome to the establishment of symbiosis.

Plant rhizodeposition and microbe-generated signals involve lipid substances, which act as chemical signals that are exchanged for successful microbe recruitment or phytopathogen defense.

The plasma membrane, as the interface for plant roots and microbes, is where lipids' intrinsic functions modulate and facilitate interactions.

¹School of BioSciences, Faculty of Science, The University of Melbourne, Parkville, Victoria, 3010, Australia

²Institute for Bio- & Geosciences, Plant Sciences (IBG-2), Forschungszentrum Jülich GmbH, Jülich, 52428, Germany

³<https://roessnerlab.science.unimelb.edu.au/>

*Correspondence: amacabuhay@student.unimelb.edu.au (A. Macabuhay).



This review highlights the various roles of lipids *in planta* and at the different stages of plant root–microbe interactions, from (i) signaling and resource exchange; to (ii) pattern recognition, signal transduction, and downstream defense mechanisms during perception and contact; and to (iii) the establishment of **sybiosis** that can either impart plant growth promotion and stress tolerance or cause death. For reference to specific lipid species mentioned throughout the review, we follow the LIPID MAPS comprehensive classification system for lipids. This classification organizes lipids, covering eukaryotic and prokaryotic sources, into eight well-defined categories (Box 1 and Figure 1) [17] and hereafter is referred to in italicized square brackets (*[]*) with abbreviated names to classify uncommonly known lipids.

Plant root PM and the lipids regulating its functions

The PM is a highly ordered fundamental biological structure that separates the interior of a living cell from the extracellular environment. It functions like a sensor that regulates cellular activities with an intricate pathway that orchestrates reception, signal transduction, and appropriate response mechanisms against a continuously changing environment [18].

Lipids, which compose and maintain the structural integrity of the PM, largely contribute to maintaining its essential processes and facilitating abiotic stress adaptation, intra- and intercellular communication, and nutrient exchange during an interaction [18]. The main lipid

Glossary

Induced systemic resistance (ISR):

plant defense response induced by beneficial and mutualistic colonizing microbes such as plant growth–promoting rhizobacteria and fungi against foliar pathogens and leaf-feeding insects, which initiate JA and SA signaling pathways.

Lipidomics: the science that analyzes the complete set of lipid species in a cell, tissue, or biological system (called the ‘lipidome’) through the application of analytical chemistry principles and techniques such as chromatography, spectroscopy, and mass spectrometry.

Lipids: various organic compounds that are insoluble in water but soluble in nonpolar solvents such as ether and chloroform. They are one of the macromolecules (carbohydrate, protein, nucleic acid, containing hydrocarbons), which are the principal structural components of living cells.

Lipid peroxidation: the oxidative degradation of lipids, which occurs when free radicals abstract an electron from an unsaturated fatty acid in the cell membrane, creating unstable lipid radicals that can react with oxygen, leading to cell damage. This process can be mediated via enzymatic pathways (lipoygenase) or nonenzymatic pathways (reactive oxygen species).

Mass spectrometry (MS): a powerful technique used to quantify known and identify unknown compounds by elucidating the structure and chemical properties of different molecules by measuring the mass and charge of those molecules or their fragments after ionization. Mass spectrometry (MS) often is hyphenated with chromatographic separation techniques. A typical MS-based workflow consists of biological sample collection, sample pretreatment and extraction, data acquisition, data processing and analysis, and biological interpretation.

Priming: a plant’s innate immune and physiological response triggered by beneficial microbes that helps the plant react more rapidly and/or robustly against future biotic and abiotic stimuli.

Quorum sensing (QS): a cell density–dependent signaling mechanism that regulates important bacterial biological processes, including bioluminescence, DNA transfer, antibiotic resistance, motility, biofilm formation, and virulence.

Rhizodeposits: a collective term for C-containing compounds released by the

Box 1. Lipid categories and description (refer to structure in Figure 1)

Fatty acyls [*FA*] represent the primary building blocks of complex lipids and therefore are one of the most fundamental categories of biological lipids. They are characterized by a series of methylene groups imparting their hydrophobic characteristic and are subdivided depending on double bonds in their hydrocarbon chains. Common examples include fatty acid esters such as wax monoesters and diesters and lactones.

Glycerolipids [*GL*] are mainly composed of mono-, di-, and trisubstituted glycerols, the most well known of which are the fatty acid esters of glycerol or acylglycerols. They comprise the bulk of oil storage in plant tissues.

Glycerophospholipids [*GPP*], also known as ‘phospholipids’, are amphipathic molecules with a polar head consisting of glycerol and a phosphate group and a nonpolar tail made of hydrocarbon chains. As critical components of the PM bilayer, they act as binding sites for intra- and intercellular proteins and are involved in cell metabolism and signaling.

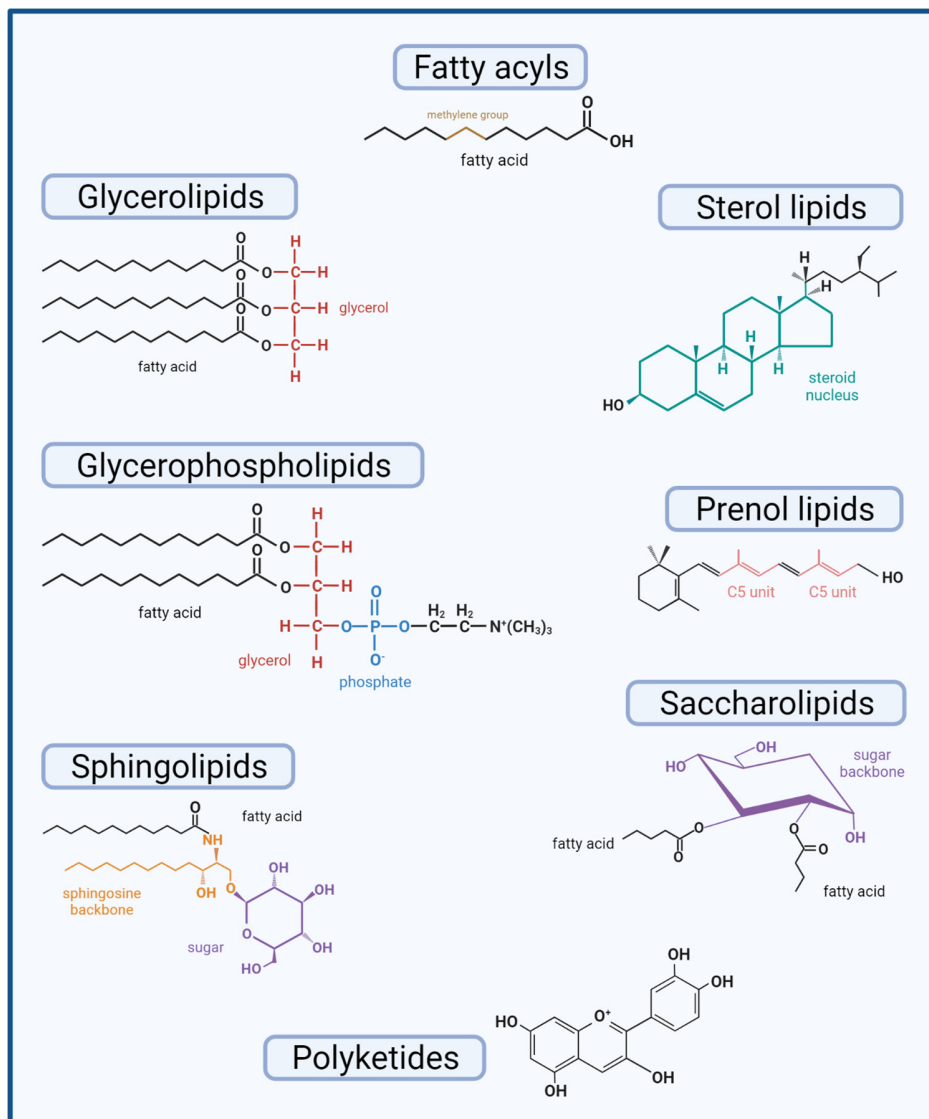
Sphingolipids [*SP*] are a family of compounds sharing a common structural feature – a sphingoid base backbone synthesized *de novo* from serine and a long-chain fatty acyl–coenzyme A then converted into products such as ceramides, phosphosphingolipids, glycosphingolipids, and other derivative species. They have protective functions and play important roles in cellular signaling.

Sterol lipids [*ST*] are important components of the cell membrane, participating in signal transduction. The most well-known examples are phytosterol in plants and cholesterol and derivatives, such as steroids with specific roles as hormones and signaling molecules.

Prenol lipids [*PR*] are synthesized from the 5-carbon precursors, isopentenyl diphosphate and dimethyl diphosphate, which are mainly produced via the mevalonic acid pathway. They are essential for immune response and some regulatory functions, such as carotenoids that function as antioxidants and precursors of vitamins A and E.

Saccharolipids [*SL*] are composed of a fatty acid linked to a sugar backbone, forming structures that are compatible with membrane lipid bilayers. They can be found in the lipid A component of lipopolysaccharides in gram-negative bacteria as acylated glucosamine precursors.

Polyketides [*PK*] have great structural diversity and compose many secondary metabolites. They are often cyclic molecules whose backbones are further modified by glycosylation, methylation, hydroxylation, oxidation, and other processes. PKs are found in many antimicrobial, antiparasitic, and anticancer agents, including PK derivatives such as erythromycins, tetracyclines, and avermectins [17,84,85].



Created with BioRender.com

Trends in Plant Science

Figure 1. Representative structure for each lipid category. The LIPID MAPS consortium has subdivided lipids into eight principal categories based on their functions, chemical characteristics, and specificities. A more consistent format for representing lipid structures has been proposed by Fahy *et al.* [84], in which, in the simplest case of the fatty acid derivatives, the acid group (or equivalent) is drawn on the right hand and the hydrophobic hydrocarbon chain is on the left, with some notable exceptions. Fatty acyls [FA] have an aliphatic chain of methylene groups and can be subdivided into saturated or unsaturated. Glycerolipids [GL] are characterized by the number of glycerol groups. Glycerophospholipids [GP] are amphipathic with a polar glycerol and phosphate group and nonpolar hydrocarbon. Sphingolipids [SP] have a sphingoid backbone. Sterol lipids [ST] have a sterol nucleus composed of four tightly fused carbon rings and a hydroxyl group attached to the first ring. Prenol lipids [PR] are synthesized from the five-carbon precursors (isopentyl diphosphate and dimethylallyl diphosphate). Saccharolipids [SL] have fatty acid and a sugar backbone. Polyketides [PK] have various structural forms, often as cyclic molecules with modifications such as methyl group or hydroxyl groups. Descriptions of each lipid category are provided in Box 1. Image created with BioRender.com.

roots, which can have various origins: at root apices, from sloughed-off root cells, border cells, and tissues; mucilage released from the root caps and root hairs; root exudates; volatile organic compounds; lysates released by senescing epidermal and cortical cells; and altered root-derived C by microbes or symbionts.

Rhizosphere: soil influenced by roots in terms of the microorganisms, caused by chemical changes in the soil due to the presence of the root and its secretions, including primary metabolites (e.g., carbohydrates, organic and amino acids) and secondary metabolites (e.g., alkaloids, terpenoids, and phenolics).

Symbiosis: any type of close and long-term ecological interaction between organisms from two different species, which usually benefits one or both organisms involved, be it mutualistic, commensalism, parasitic, or pathogenic.

Systemic acquired resistance (SAR): a 'whole-plant' resistance response that is activated by exposure to elicitors of virulent, avirulent, or nonpathogenic microbes or artificial chemical stimuli such as chitosan that triggers SA signaling.



components found in the PM are glycerophospholipids [GP], glycerolipids [GL], sphingolipids [SP], and sterol lipids [ST] [14]. GP, which have different head groups, make up its principal constituent, with phosphatidylcholine (PC) and phosphatidylethanolamine (PE) as major components and phosphatidylglycerol (PG), phosphatidylinositol (PI), phosphatidic acid (PA), and phosphatidylserine (PS) as minor components [14]. Phosphatidylinositol phosphates (PIPs), composed of a PI backbone with up to three phosphorylations on the inositol moiety, represent a minor fraction of GP. They are involved in many regulatory processes such as cell signaling and intracellular trafficking. GP are characterized by different lengths and the degree of unsaturation of their fatty acyl chains [14]. GL neutral lipids such as diacylglycerols (DAGs) have been found to be present at the PM of root epidermal cells in the transition zone and the apex of growing root hairs [19], whereas digalactosyldiacylglycerols (DGDGs) in the PM are found particularly as a phosphate deprivation response [20]. SP in plants are grouped into four classes: glycosyl inositolphosphoceramides (GIPCs), glucosylceramides, ceramides, and free long-chain bases, representing 64%, 34%, 2%, and 5% of total sphingolipids in *Arabidopsis*, respectively [21]. Just recently, GIPC SP have been shown to have essential roles in PM organization as necrosis and ethylene-inducing peptide 1-like (NLP) toxin receptors [22]. Over 250 different phytosterols have been identified in plants, with sitosterol being the dominant form in most of them, followed by isofucosterol (delta-5 avenasterol) also found in many plant species, and a few notable examples such as stigmasterol in tobacco and spinasterol in *Medicago* [23].

Lipids are vital components in the plant PM's physiological functions, such as regulating hormone signaling and transport, abiotic stress responses, plasmodesmata functions, and plant–microbe interactions [14]. For example, sterols are involved in endocytosis and recycling at the PM of PIN-FORMED (PIN) auxin carriers. This subcellular localization of sterol-mediated auxin carriers impacts the auxin distribution at the tissue level, affecting plant development such as the response of roots to gravity [24]. The length of the SP acyl chains (very-long-chain fatty acids) is also involved in the secretory sorting of the efflux phytohormone auxin carrier PIN2 and auxin redistribution during root gravitropism [25]. During abiotic stress responses, certain lipids function as secondary messengers. Phospholipase-derived PA, oxylipins, PIPs, SP, fatty acids, lysophospholipids, *N*-acylethanolamines, and galactolipids have been found to function in this manner [26,27]. A study on plasmodesmata by Grison [28] identified the role of sterols in modulating cell-to-cell connectivity by potentially establishing the positional specificity of callose-modifying glycosylphosphatidylinositol-anchored proteins at the PD, which also brought attention to the potential roles of GIPC and GL. Plants detect microbes by sensing non-self and modified-self molecules via cell surface and intracellular localized immune receptors [29]. Plant PM lipids and lipid-derived metabolites have been shown to facilitate the plant immune signaling response. For example, after sensing a pathogen, phospholipid-hydrolyzing enzymes are mobilized to trigger signaling cascades vital for cellular responses. As such, crucial messenger molecules, such as oxylipins, jasmonates, and notably PA, that regulate the activity of defense-associated proteins are generated by phospholipases [30]. Other PM lipid compounds involved in plant defense are phosphoinositides and lysophospholipids, which include lysophosphatidic acid (LPA), lysophosphatidylcholine, sphingosylphosphorylcholine, and sphingosine-1-phosphate. Several factors control the signaling activity or specificity of these compounds, such as the length and position of the acyl chain, the degree of saturation, and the presence of the phosphate head group [31]. As core components of membranes accumulating in the PM, plant sterols serve as conserved regulators of its organization, such as an increase in membrane stability and a decrease in membrane permeability, both associated with defense induction against phytopathogenic fungi [32].

Lipids in action

Rhizospheric interactions and signaling: Lipids as chemical language

Plant roots are contained within and highly influenced by the rhizosphere [33]. Because of their organotrophic nature, microorganisms such as bacteria, fungi, and protists populate this area – potentially extending the plant's performance and capacity to adapt to the environment or using nutrients at the plant's expense through niche colonization [8]. The behavior and impact of these microbes are believed to rely heavily on soil compounds in a process known in general terms as 'signaling or communication highways', 'underground interactions', 'rhizosphere chemical language', or 'complex plant–microbe interactions' [7,9]. The rhizospheric interactions can be grouped into three signaling categories: signaling from plant roots to microbes, microbial intra- and interspecies signaling, and signaling from microbes to plants [16] (Figure 2A, Key figure).

Plant root to microbe signaling through rhizodeposition

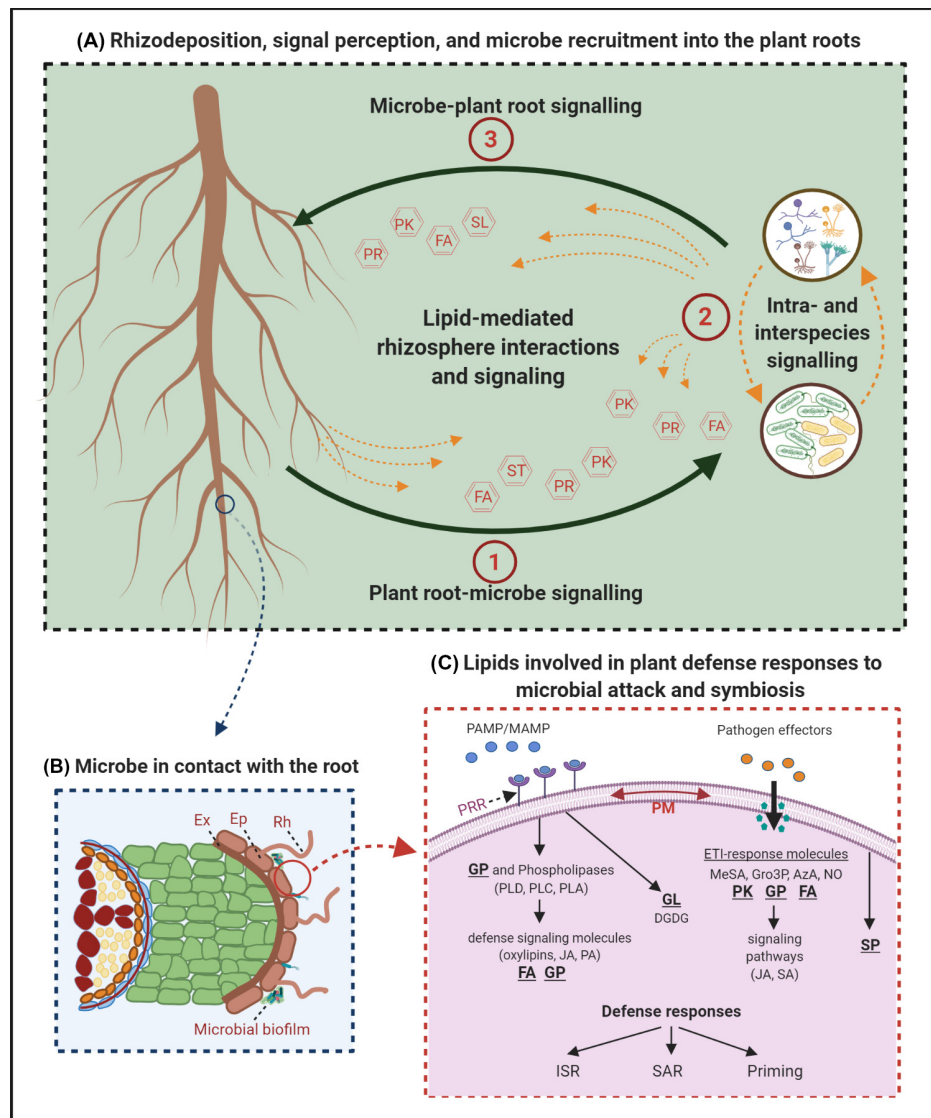
The first stage in a rhizospheric interaction is the recruitment of the rhizobiome into the plant vicinity, which is mediated by **rhizodeposits**. The release of rhizodeposits comes with a wide variety of substances, such as sugars, amino acids, organic acids, enzymes, growth factors and vitamins, flavanones and purines/nucleotides, and miscellaneous substances [34]. Lipids in various forms, such as fatty acids and sterols, are also among these compounds that enrich the rhizosphere chemistry [34]. Plants initiate an interaction by secreting these chemical signals into the rhizosphere. Some examples are plant-produced flavonoids [PK] such as 2-phenyl-1,4-benzopyrone derivatives involved in root nodule formation [35]; inhibitory flavonoids such as phytoalexin, medicarpin, and glyceollin [36]; and the volatile organic compound (VOC) (E)- β -caryophyllene [PR] that functions as a plant bioprotectant against herbivores and pathogens and as an attractant for organisms preying on root-feeding herbivores from maize roots [37,38]. These chemotactic attractors can facilitate the recruitment, nutrition, shaping, and tuning of the microbial communities from a reservoir of microorganisms present in the soil by encouraging, limiting, or inhibiting microbial activity and proliferation [8,9,36] (Figure 2A-1).

Microbe perception of plant root–released compounds and other microbial signals

The second stage of the rhizosphere interaction is the perception or detection of low-molecular-weight compounds, such as lipid molecules, released by the plant roots (or other microbes) by microbes, resulting in catabolism, transformation, or rejection of the perceived compound [16]. Perception of these compounds then leads to the stimulation of regulatory or signaling cascades that cause various responses in the microbes. Root-secreted substances have been thought to influence the gene expression of different microorganisms in the rhizosphere, which are not in proximity to and associated with plants [36]. Chemical communication (cell–cell signaling) with signal molecules called 'autoinducers' that increase in concentration as a function of cell density, found in bacteria [39] and recently in fungi [40], coordinate a wide range of activities within and between different species as a function of population density. The regulation of gene expression in response to fluctuations in microbial cell population density is done via **quorum sensing (QS)** [41]. QS is a widespread process using autoinducing chemical signals that coordinate diverse cooperative functions [39]. This governing mechanism is instrumental in regulating a wide array of physiological activities and microbial phenotypes such as biofilm formation, pathogenicity, conjugation, secretion of hydrolytic enzymes, and production of antibiotic and secondary metabolites, increasing rhizosphere competence that leads to successful colonization [42]. Common examples of lipids that act as QS signals are N-acyl homoserine lactones (AHL) [FA] [39], diffusible signal factor (DSF) family [FA], and the more recently discovered pyrones and dialkylresorcinols [PK] from gram-negative bacteria [43–46]. There are also antimicrobial lipids released at low concentrations, as well as alcohols from fungal species (mostly *Ascomycetes*), which are associated with developmental processes [34,47]. Some VOCs, such as aldehyde and ketone [FA] and terpene

Key Figure

Lipid roles in the microbial colonization of roots



Trends in Plant Science

Figure 2. (A) During the different stages in rhizosphere interactions (plant root to microbe, microbe to microbe, microbe to plant root), lipids act as chemical signals that facilitate signaling: from the release of rhizodeposits from the roots that comes with a variety of substances (through rhizodeposition), to the perception of these substances by microbes to regulate intra- and interspecies behavior, and to the release of microbial substances back to the plants that can influence plant gene expression, hormonal balance, development, metabolism, and stress responses. Some of the known lipid molecules involved in rhizosphere signaling belong to the categories of fatty acyls [FA], sterol lipids [ST], prenol lipids [PR], saccharolipids [SL], and polyketides [PK]. (B) Successful attachment and colonization of microbes lead to the formation of microbial biofilms on root surfaces. (C) Different lipid species perform various functions during the signal reception at the PM, transduction, and downstream defense mechanism of plants in response to microbial attack or beneficial symbiosis, which can be induced systemic resistance (ISR), systemic (Figure legend continued at the bottom of the next page.)

[*PK*], which are released by a wide range of bacterial and fungal species, can play crucial roles in long-distance rhizosphere interactions [48]. Some can act like ‘chemical weapons’ that inhibit microbial activity or interfere with other QS systems (interspecies). Moreover, they can coordinate gene expression and influence intraspecies behaviors such as biofilm formation, virulence, and stress tolerance [49]. All these QS signals and VOCs released by microorganisms can also act as interkingdom signals, influencing plant gene expression and immunity and affecting plant root architecture, growth, and development [16,48] (Figure 2A2).

Signaling response from microbes back to the plant

The third stage in the rhizosphere interaction involves the release of diverse signaling molecules from microorganisms to their plant host as a response to signals perceived from among themselves (intraspecies), other microorganisms (interspecies), or plants. Conserved microbe-specific molecules known as pathogen- or microbe-associated molecular patterns (PAMP/MAMP), such as lipopolysaccharides (which have the active lipid A), peptidoglycans, flagellin, and chitin, are detected by dedicated pattern recognition receptors (PRR) from plants [50]. These signals trigger a local basal systemic defense response controlled by regulatory networks that involve signaling pathways via plant hormones, including salicylic acid (SA), jasmonic acid (JA), and ethylene [51,52]. The defense response of plants can be **induced systemic resistance (ISR)** [52], **systemic acquired resistance (SAR)** [51], or **priming** [53]. Although these mechanisms are designed to prevent potential attacks, beneficial rhizosphere microbes have developed countermeasures for immune recognition, leading to successful plant colonization [50]. Molecules such as QS signals and VOCs used for intra- and interspecies signaling also act as interkingdom signals, influencing plants [16,48]. Examples of microorganism-released QS molecules are AHL from plant growth-promoting rhizobacteria (PGPR) and DSF from *Xanthomonas*. Certain antimicrobials at sub-inhibitory concentrations, such as 2,4-diacetylphloroglucinol [*PK*] from rhizosphere pseudomonads, can induce ISR responses (via SA and ethylene signaling) against fungal and bacterial leaf pathogens [54] and affect root development via an auxin-dependent signaling pathway [55,56]. They can change the gene expression and protein profiles of plant roots and shoots; influence root development, plant defense, and stress responses; and regulate metabolic activity and hormonal balance [57,58]. Other microbial signaling molecules belong to VOCs, which can act as plant growth promoters or inhibitors and as priming agents or elicitors of plant defense and stress tolerance (Figure 2A3).

Plant root lipids during pathogenic and symbiotic interactions with microorganisms

Apart from acting as chemical signals in rhizosphere signaling, lipids are also involved in diverse functions during pathogen attack or infection and mutualistic interactions with beneficial microorganisms. Specific lipids in the PM have particular functions, such as in host-specific pathogen recognition, signaling in the cells from the site of infection or interaction, and transfer of infection signals to distal organs of the plants during defense responses [2,31,59,60]. Signal-inducing compounds from microbes or elicitors are recognized by the plant’s innate immune system, which results in the induction of defense responses [59] or invasion of host tissues [13].

acquired resistance (SAR), and priming. Lipids that are particularly involved belong to the categories of glycerophospholipids [*GP*], glycerolipids [*GL*], sphingolipids [*SP*], fatty acyls [*FA*], and polyketides [*PK*]. Abbreviations: AzA, azelaic acid; Ep, epidermis; ETI, effector-triggered immunity; Ex, exodermis; Gro3P, glycerol-3-phosphate; JA, jasmonic acid; MeSA, methylsalicylic acid; NO, nitric oxide; PA, phosphatidic acid; PAMP/MAMP, pathogen-/microbe-associated molecular pattern; PLA, phospholipase A; PLC, phospholipase C; PLD, phospholipase D; PM, plasma membrane; PRR, pattern recognition receptor; RH, root hair; SA, salicylic acid. Image created with BioRender.com.



Lipids in the PM play essential roles in plant cell responses to microbial attack and interactions with beneficial microbes. These lipids are synthesized, modified, or reallocated upon the upregulation of genes encoding enzymes of lipid metabolism. Lipid-modifying enzymes regulate the spatial and temporal production of lipid metabolites involved in signaling and membrane proliferation to establish intracellular compartments or compositional changes of the bilayer [59]. During plant–pathogen interaction, phospholipid-hydrolyzing enzymes induce the production of defense-signaling molecules such as oxylipins, including JA and the potent second messenger PA [61]. For example, phospholipase D (PLD), which forms PA, is involved in lipid metabolism and hormone signaling in plant defense responses [62]. Plant-derived PA regulate a range of different physiological processes, such as activities of kinases, phosphatases, phospholipases, and proteins involved in membrane trafficking, Ca^{2+} signaling, or the oxidative burst [62]. They also act as precursors for lipid intermediates LPA, DAG, and free fatty acids, which are involved in plant defense signaling [63]. Activation of phospholipase C (PLC) or the DAG kinase pathway is triggered by PAMP recognition, also leading to the accumulation of PA [64]. Phospholipase A (PLA), which yields FA and lysophospholipids, the latter of which are involved in systemic responses after wounding, is involved in growth regulation, root and pollen development, stress responses, defense signaling, and plant immunity because of its roles in oxylipin and JA biosynthesis [65]. Phosphoinositides have also been implicated in the modulation of mutualistic interactions between plants and beneficial microorganisms and is known to involve ionic and cytoskeletal changes [26,66,67]. Lipid kinases in plants, particularly the phosphatidylinositol 3-kinase (PI3K) family, regulate various physiological functions, such as the innate immune response, intracellular trafficking, autophagy, and senescence, including symbiosis of leguminous plants with rhizobia and arbuscular mycorrhizal fungi [68–70].

At the site of infection during pathogen attack, small molecules that serve as initial signals of the effector-triggered immunity (ETI) response, such as methylsalicylic acid (MeSA), are produced and then moved to the distal plant organs, where they are hydrolyzed into SA that trigger SAR. Other signal molecules, such as glycerol-3-phosphate (Gro3P), azelaic acid (AzA), and nitric oxide (NO), function as inducers of SAR [42]. However, mutualistic or symbiotic interactions with beneficial plant growth-promoting microorganisms can stimulate the plant immune system, which results in ISR, mainly based on the activities of JA [52] that mediate resistance to a wide array of diseases. Galactolipids also have essential roles in signal transduction, cell communication, and pathogen response. For example, galactolipids have different functions in SAR, with monogalactosyldiacylglycerol (MGDG) regulating the biosynthesis of AzA and Gro3P and with DGDG affecting the biosynthesis of NO and SA [71]. In roots specifically, the accumulation of DGDG in the peribacteroid membrane of nodules helps to save phosphate because of reduced requirements for phospholipids during root–nodule symbiosis [72]. During arbuscular mycorrhizal formation (AMF), genes encoding enzymes for fatty acids from plastid and GL synthesis are upregulated, indicating the increased production of lipids during root mycorrhization [73]. This lipid demand might be explained by the requirements of phospholipids to establish a large surface of the periarbuscular membrane and by the accumulation of triacylglycerol in the fungus [59]. Lipid-derived signals by reduced arbuscular mycorrhiza 2 (RAM2) such as Gro3P acyltransferase (GPAT), involved in the synthesis of fatty acids associated with suberin and cutin, were also found to be involved in AMF formation [74,75].

A process that plays an important role in signal transduction and programmed cell death (PCD), which can be induced by both biotic and abiotic stresses, is **lipid peroxidation**. Lipids that can be subjected to peroxidation are galactolipids, free fatty acids, or acyl groups bound to triacylglycerol (TAG), leading to the generation of JA during defense response [76]. JA is mainly produced during wounding, such as after herbivore attack and microbe infection, and is vital for defense response to different fungal and bacterial pathogens [77]. Because some fungi, such as

Aspergillus spp., produce a set of oxylipins related to that of plants, it is speculated that plants and fungi 'communicate' via the oxylipin language [78]. AMF colonization leading to the accumulation of JA in barley roots also showed upregulation of the expression of JA biosynthetic genes (allene oxide cyclase, AOC; allene oxide synthase, AOS) [79]. SP have also been implicated in PCD, which is a defense reaction against pathogen attack [80]. For example, the expression of ceramide synthases in *Arabidopsis* (longevity assurance gene one homologs LOH1, LOH2, and LOH3) showed that although overexpression of LOH1 and LOH3 increases plant growth, overexpression of LOH2 results in dwarfing and the constitutive expression of hypersensitive response (HR) genes and PCD [81]. Moreover, an aspect in many studies is the accumulation of SA in SP mutants, which led to the proposal of a putative interaction between SP metabolism and SA signaling during PCD and HR [82].

The many essential functions of lipids can be assigned to distinct lipid categories (Figure 2) with unique chemical characteristics that allow a wide range of performances. This ability for specificity could be the reason that lipids evolved as signal molecules for communication between host plants and microorganisms in pathogenic and mutualistic interactions. Comprehensive lipid studies are necessary to further identify additional lipid chemistry that may be involved in plant root-microbe interactions. With substantial room for improvement in analytical techniques, much can still be done in plant lipid research, which can further our understanding of plant lipid metabolism and its interaction with the biotic environment.

Concluding remarks and future perspectives

Several research studies have shown the complex underground interactions that occur between plant roots and soil microorganisms through lipids. It has become apparent that plant lipids actively shape the microbiome inhabiting the rhizosphere and the subsequent colonization of their root tissues. We have presented lipid exchange in plant root-microbe interactions in three main stages: plant root to microbe, microbe to microbe, and microbe to plant root. On all accounts of these interactions, lipids have been shown to play essential roles as the 'chemical language' that facilitates the exchange of resources and modulates the cell responses by inhibiting pathogen attack or enhancing microbial symbiosis. There are many more currently unknown lipids with their corresponding signaling functions that are likely to exist which play a pivotal role in determining or shaping the rhizomicrobiome. Our understanding will become clearer through detecting, identifying, and quantifying the plant and microbial lipids *in situ* and while in interaction. This will shed light on their vital functions and how they behave, react, and transform in response to various stimuli. This knowledge will be greatly enhanced by continuous developments in analytical techniques, which will allow an effective qualitative and quantitative approach that can further our insights into lipid diversity and functions. **Lipidomics**, which is largely attributed to advances in its enabling technology, **mass spectrometry (MS)**, has been a powerful tool in the characterization of the structures of lipid species; quantification of the level of individual lipid species in biological samples; and determination of interactions of individual species with other lipids, metabolites, and proteins *in vivo* [83]. The large-scale analysis of the lipid compounds can then be combined with transcriptomic and genomic studies to begin to uncover the genes involved in the signaling and various stages of the interactions. These integrated 'omics' studies will be useful in the holistic interpretation of biological systems such as plants and how they respond to environmental biotic and abiotic stressors.

As part of rhizospheric signaling and interaction studies, research on lipids will therefore open new avenues to increase crop productivity and tolerance to environmental stresses. Harnessing the use of beneficial microorganisms and understanding the mechanisms of pathogenicity and symbiosis could reduce the use of agrochemicals. Microbial solutions can

Outstanding questions

Are specific interactions between plants and microbes common occurrences in the rhizosphere, or are they limited to a few organisms?

How do environmental abiotic stressors such as high or cold temperature, drought or flooding, metal toxicity, and salinity affect the underground, lipid-mediated plant-microbe interactions?

To what extent will lipidomics and other omic technologies contribute to discovering novel lipid molecules involved with *in planta* and *ex planta* functions and understanding the molecular mechanisms involved in signaling and rhizosphere interactions?

How conserved are lipid signaling mechanisms between various plant and microbial species?

How transferable will knowledge gained from the relatively few investigated cases of lipids in the rhizosphere be to application to improve plant performance in field conditions?

then be used for more sustainable agriculture to enrich the rhizomicrobiome for beneficial microbes, thereby improving plant performance and resistance to biotic and abiotic stresses. From a broader perspective, lipid research on plant–microbe interactions can also provide biotechnological solutions, as with the broad spectrum of antimicrobial lipids isolated from plants, which can be used as promising alternatives to control microbial infections. This can be applied in various economic sectors aside from agriculture, such as the pharmaceutical, cosmetic, and food industries (see [Outstanding questions](#)).

Acknowledgments

A.M. thanks the Jülich–University of Melbourne Postgraduate Academy (JUMPA) program for the joint PhD scholarship. M.W. holds the Adrienne Clarke Professorial Chair of Botany, which is supported through the University of Melbourne Botany Foundation.

Declaration of interests

The authors have no interests to declare.

References

- van Meer, G. *et al.* (2008) Membrane lipids: where they are and how they behave. *Nat. Rev. Mol. Cell Biol.* 9, 112
- Ruelland, E. and Valentova, O. (2016) Editorial: Lipid signaling in plant development and responses to environmental stresses. *Front. Plant Sci.* 7, 324
- Okazaki, Y. and Saito, K. (2014) Roles of lipids as signaling molecules and mitigators during stress response in plants. *Plant J.* 79, 584–596
- Boutte, Y. and Jaillais, Y. (2020) Metabolic cellular communications: Feedback mechanisms between membrane lipid homeostasis and plant development. *Dev. Cell* 54, 171–182
- Downie, H.F. *et al.* (2015) Challenges and opportunities for quantifying roots and rhizosphere interactions through imaging and image analysis. *Plant Cell Environ.* 38, 1213–1232
- Sergaki, C. *et al.* (2018) Challenges and approaches in microbiome research: From fundamental to applied. *Front. Plant Sci.* 9, 1205
- Mendes, R. *et al.* (2013) The rhizosphere microbiome: Significance of plant beneficial, plant pathogenic, and human pathogenic microorganisms. *FEMS Microbiol. Rev.* 37, 634–663
- van Dam, N.M. and Bouwmeester, H.J. (2016) Metabolomics in the rhizosphere: Tapping into belowground chemical communication. *Trends Plant Sci.* 21, 256–265
- Bais, H.P. *et al.* (2004) How plants communicate using the underground information superhighway. *Trends Plant Sci.* 9, 26–32
- Elmore, J.M. and Coaker, G. (2011) The role of the plasma membrane H⁺-ATPase in plant–microbe interactions. *Mol. Plant* 4, 416–427
- Boller, T. and Felix, G. (2009) A renaissance of elicitors: Perception of microbe-associated molecular patterns and danger signals by pattern-recognition receptors. *Annu. Rev. Plant Biol.* 60, 379–406
- Rich, M.K. *et al.* (2014) The role of the cell wall compartment in mutualistic symbioses of plants. *Front. Plant Sci.* 5, 238
- Rossi, C. *et al.* (2020) Bacterial adherence to plant and animal surfaces via adhesion–lipid interactions. In *Health Consequences of Microbial Interactions with Hydrocarbons, Oils, and Lipids* (Goldfine, H., ed.), pp. 145–164. Springer International Publishing
- Cassim, A.M. *et al.* (2019) Plant lipids: Key players of plasma membrane organization and function. *Prog. Lipid Res.* 73, 1–27
- Martínez, E. *et al.* (2019) Oxylipins mediate cell-to-cell communication in *Pseudomonas aeruginosa*. *Commun. Biol.* 2, 66
- Venturi, V. and Keel, C. (2016) Signaling in the rhizosphere. *Trends Plant Sci.* 21, 187–198
- Fahy, E. *et al.* (2009) Update of the LIPID MAPS comprehensive classification system for lipids. *J. Lipid Res.* 50, S9–S14
- Niu, Y. and Xiang, Y. (2018) An overview of biomembrane functions in plant responses to high-temperature stress. *Front. Plant Sci.* 9, 915
- Vermeer, J.E.M. *et al.* (2017) In Vivo imaging of diacylglycerol at the cytoplasmic leaflet of plant membranes. *Plant Cell Physiol.* 58, 1196–1207
- Andersson, M.X. *et al.* (2005) Phosphate-limited oat: the plasma membrane and the tonoplast as major targets for phospholipid-to-glycolipid replacement and stimulation of phospholipases in the plasma membrane. *J. Biol. Chem.* 280, 27578–27586
- Reszczyńska, E. and Hanaka, A. (2020) Lipids composition in plant membranes. *Cell Biochem. Biophys.* 78, 401–414
- Lenařič, T. *et al.* (2017) Eudicot plant-specific sphingolipids determine host selectivity of microbial NLP cytolysins. *Science* 358, 1431–1434
- Moreau, R.A. *et al.* (2018) Phytosterols and their derivatives: Structural diversity, distribution, metabolism, analysis, and health-promoting uses. *Prog. Lipid Res.* 70, 35–61
- Men, S. *et al.* (2008) Sterol-dependent endocytosis mediates post-cytokinetic acquisition of PIN2 auxin efflux carrier polarity. *Nat. Cell Biol.* 10, 237–244
- Wattelet-Boyer, V. *et al.* (2016) Enrichment of hydroxylated C24- and C26-acyl-chain sphingolipids mediates PIN2 apical sorting at trans-Golgi network subdomains. *Nat. Commun.* 7, 12788
- Xue, H.-W. *et al.* (2009) Function and regulation of phospholipid signaling in plants. *Biochem. J.* 421, 145–156
- Heilmann, M. and Heilmann, I. (2015) Plant phosphoinositides – complex networks controlling growth and adaptation. *Biochim. Biophys. Acta* 1851, 759–769
- Grison, M.S. *et al.* (2015) Specific membrane lipid composition is important for plasmodesmata function in Arabidopsis. *Plant Cell* 27, 1228–1250
- Jones, J.D. and Dangl, J.L. (2006) The plant immune system. *Nature* 444, 323–329
- Pokotylo, I. *et al.* (2018) The phosphatidic acid paradox: Too many actions for one molecule class? Lessons from plants. *Prog. Lipid Res.* 71, 43–53
- Lim, G.-H. *et al.* (2017) Fatty acid- and lipid-mediated signaling in plant defense. *Annu. Rev. Phytopathol.* 55, 505–536
- Michaelson, L.V. *et al.* (2016) Plant sphingolipids: Their importance in cellular organization and adaptation. *Biochim. Biophys. Acta* 1861, 1329–1335
- Verbon, E.H. and Liberman, L.M. (2016) Beneficial microbes affect endogenous mechanisms controlling root development. *Trends Plant Sci.* 21, 218–229
- Andersson, D.I. and Hughes, D. (2014) Microbiological effects of sublethal levels of antibiotics. *Nat. Rev. Microbiol.* 12, 465–478
- Mallet, F. *et al.* (2011) Fungal lipochitooligosaccharide symbiotic signals in arbuscular mycorrhiza. *Nature* 469, 58–63
- Costa, S.R. *et al.* (2021) Interaction of symbiotic rhizobia and parasitic root-knot nematodes in legume roots: From molecular regulation to field application. *Mol. Plant-Microbe Interact.* 34, 470–490

37. Dudareva, N. *et al.* (2006) Plant volatiles: recent advances and future perspectives. *Crit. Rev. Plant Sci.* 25, 417–440
38. Degenhardt, J. *et al.* (2009) Restoring a maize root signal that attracts insect-killing nematodes to control a major pest. *Proc. Natl. Acad. Sci. U. S. A.* 106, 13213–13218
39. Schuster, M. *et al.* (2013) Acyl-homoserine lactone quorum sensing: from evolution to application. *Annu. Rev. Microbiol.* 67, 43–63
40. Mehmood, A. *et al.* (2019) Fungal quorum-sensing molecules and inhibitors with potential antifungal activity: A review. *Molecules* 24, 1950
41. Miller, M.B. and Bassler, B.L. (2001) Quorum sensing in bacteria. *Annu. Rev. Microbiol.* 55, 165–199
42. Gao, Q.-M. *et al.* (2014) Mono- and digalactosyldiacylglycerol lipids function nonredundantly to regulate systemic acquired resistance in plants. *Cell Rep.* 9, 1681–1691
43. Ferluga, S. *et al.* (2008) N-acyl homoserine lactone quorum sensing in Gram-negative rhizobacteria. In *Secondary Metabolites in Soil Ecology* (Karlovsy, P., ed.), pp. 69–90, Springer
44. Brameyer, S. *et al.* (2015) Languages and dialects: bacterial communication beyond homoserine lactones. *Trends Microbiol.* 23, 521–523
45. Ryan, R.P. *et al.* (2015) The DSF family of cell-cell signals: An expanding class of bacterial virulence regulators. *PLoS Pathog.* 11, e1004986
46. Monnet, V. *et al.* (2016) Peptide conversations in Gram-positive bacteria. *Crit. Rev. Microbiol.* 42, 339–351
47. Leeder, A.C. *et al.* (2011) The social network: Deciphering fungal language. *Nat. Rev. Microbiol.* 9, 440–451
48. Bitas, V. *et al.* (2013) Sniffing on microbes: Diverse roles of microbial volatile organic compounds in plant health. *Mol. Plant-Microbe Interact.* 26, 835–843
49. Audrain, B. *et al.* (2015) Role of bacterial volatile compounds in bacterial biology. *FEMS Microbiol. Rev.* 39, 222–233
50. Zamioudis, C. and Pieterse, C.M. (2012) Modulation of host immunity by beneficial microbes. *Mol. Plant-Microbe Interact.* 25, 139–150
51. Vos, I.A. *et al.* (2013) Costs and benefits of hormone-regulated plant defences. *Plant Pathol.* 62, 43–55
52. Pieterse, C.M.J. *et al.* (2014) Induced systemic resistance by beneficial microbes. *Annu. Rev. Phytopathol.* 52, 347–375
53. Balmer, A. *et al.* (2015) The ‘prime-ome’: Towards a holistic approach to priming. *Trends Plant Sci.* 20, 443–452
54. Weller, D.M. *et al.* (2012) Induced systemic resistance in *Arabidopsis thaliana* against *Pseudomonas syringae* pv. tomato by 2,4-diacetylphloroglucinol-producing *Pseudomonas fluorescens*. *Phytopathology* 102, 403–412
55. Ortiz-Castro, R. *et al.* (2014) Pyocyanin, a virulence factor produced by *Pseudomonas aeruginosa*, alters root development through reactive oxygen species and ethylene signaling in *Arabidopsis*. *Mol. Plant-Microbe Interact.* 27, 364–378
56. Powers, M.J. *et al.* (2015) Inhibition of cell differentiation in *Bacillus subtilis* by *Pseudomonas protegens*. *J. Bacteriol.* 197, 2129–2138
57. Sieper, T. *et al.* (2014) N-acyl-homoserine lactone uptake and systemic transport in barley rest upon active parts of the plant. *New Phytol.* 201, 545–555
58. Grandclément, C. *et al.* (2016) Quorum quenching: role in nature and applied developments. *FEMS Microbiol. Rev.* 40, 86–116
59. Siebers, M. *et al.* (2016) Lipids in plant-microbe interactions. *Biochim Biophys Acta* 1861, 1379–1395
60. Mandal, S.M. *et al.* (2010) Phenolic acids act as signaling molecules in plant-microbe symbioses. *Plant Signal. Behav.* 5, 359–368
61. Canonne, J. *et al.* (2011) Phospholipases in action during plant defense signaling. *Plant Signal. Behav.* 6, 13–18
62. Zhao, J. (2015) Phospholipase D and phosphatidic acid in plant defence response: From protein-protein and lipid-protein interactions to hormone signalling. *J. Exp. Bot.* 66, 1721–1736
63. Wang, X. (2004) Lipid signaling. *Curr. Opin. Plant Biol.* 7, 329–336
64. Arisz, S.A. and Munnik, T. (2013) Distinguishing phosphatidic acid pools from de novo synthesis, PLD, and DGK. In *Plant Lipid Signaling Protocols* (Munnik, T. and Heilmann, I., eds), pp. 55–62, Springer
65. Rietz, S. *et al.* (2010) Roles of *Arabidopsis patatin*-related phospholipases a in root development are related to auxin responses and phosphate deficiency. *Mol. Plant* 3, 524–538
66. Oldroyd, G.E. (2013) Speak, friend, and enter: signalling systems that promote beneficial symbiotic associations in plants. *Nat. Rev. Microbiol.* 11, 252–263
67. Peleg-Grossman, S. *et al.* (2007) Root hair curling and Rhizobium infection in *Medicago truncatula* are mediated by phosphatidylinositol-regulated endocytosis and reactive oxygen species. *J. Exp. Bot.* 58, 1637–1649
68. Lee, Y. *et al.* (2008) The *Arabidopsis* phosphatidylinositol 3-kinase is important for pollen development. *Plant Physiol.* 147, 1886–1897
69. Kale, S.D. *et al.* (2010) External lipid PI3P mediates entry of eukaryotic pathogen effectors into plant and animal host cells. *Cell* 142, 284–295
70. Estrada-Navarrete, G. *et al.* (2016) An autophagy-related kinase is essential for the symbiotic relationship between *Phaseolus vulgaris* and both rhizobia and arbuscular mycorrhizal fungi. *Plant Cell* 28, 2326–2341
71. Hölzl, G. and Dörmann, P. (2007) Structure and function of glycolipids in plants and bacteria. *Prog. Lipid Res.* 46, 225–243
72. Gaude, N. *et al.* (2004) The galactolipid digalactosyldiacylglycerol accumulates in the peribacteroid membrane of nitrogen-fixing nodules of soybean and Lotus. *J. Biol. Chem.* 279, 34624–34630
73. Wewer, V. *et al.* (2014) Fatty acid synthesis and lipid metabolism in the obligate biotrophic fungus *Rhizophagus irregularis* during mycorrhization of *Lotus japonicus*. *Plant J.* 79, 398–412
74. Wang, E. *et al.* (2012) A common signaling process that promotes mycorrhizal and oomycete colonization of plants. *Curr. Biol.* 22, 2242–2246
75. Vijayakumar, V. *et al.* (2016) Integrated multi-omics analysis supports role of lysophosphatidylcholine and related glycerophospholipids in the *Lotus japonicus*–*Glomus intraradices* mycorrhizal symbiosis. *Plant Cell Environ.* 39, 393–415
76. Nakashima, A. *et al.* (2011) Monogalactosyl diacylglycerol is a substrate for lipoxygenase: Its implications for oxylipin formation directly from lipids. *J. Plant Interact.* 6, 93–97
77. Scalschi, L. *et al.* (2015) Silencing of OPR3 in tomato reveals the role of OPDA in callose deposition during the activation of defense responses against *Botrytis cinerea*. *Plant J.* 81, 304–315
78. Christensen, S.A. and Kolomiets, M.V. (2011) The lipid language of plant–fungal interactions. *Fungal Genet. Biol.* 48, 4–14
79. Isayenkov, S. *et al.* (2005) Suppression of allene oxide cyclase in hairy roots of *Medicago truncatula* reduces jasmonate levels and the degree of mycorrhization with *Glomus intraradices*. *Plant Physiol.* 139, 1401–1410
80. Dickman, M.B. and Fluhr, R. (2013) Centrality of host cell death in plant-microbe interactions. *Annu. Rev. Phytopathol.* 51, 543–570
81. Luttgeharm, K.D. *et al.* (2015) Overexpression of *Arabidopsis* ceramide synthases differentially affects growth, sphingolipid metabolism, programmed cell death, and mycotoxin resistance. *Plant Physiol.* 169, 1108–1117
82. Sánchez-Rangel, D. *et al.* (2015) Deciphering the link between salicylic acid signaling and sphingolipid metabolism. *Front. Plant Sci.* 6, 125
83. Correia, B.S.B. *et al.* (2018) Analytical tools for lipid assessment in biological assays. In *Advances in Lipid Metabolism* (Valenzuela Baez, R., ed.), IntechOpen
84. Fahy, E. *et al.* (2005) A comprehensive classification system for lipids. *Eur. J. Lipid Sci. Technol.* 107, 337–364
85. Liebisch, G. *et al.* (2020) Update on LIPID MAPS classification, nomenclature, and shorthand notation for MS-derived lipid structures. *J. Lipid Res.* 61, 1539–1555

Table S 1 Mean values and standard error of different root type morphological traits

Root trait	DAI	Mean values \pm standard error							
		Amb-Ctl		Amb-PsJN		HT-Ctl		HT-PsJN	
1. Length - Total	5	2.23	\pm 0.20	4.29	\pm 0.34	1.43	\pm 0.07	3.31	\pm 0.46
	7	3.50	\pm 0.29	7.08	\pm 0.45	1.96	\pm 0.11	4.39	\pm 0.44
	9	8.65	\pm 0.84	18.47	\pm 1.31	3.93	\pm 0.36	11.35	\pm 0.87
	12	32.41	\pm 3.14	65.92	\pm 4.37	14.06	\pm 1.65	42.46	\pm 4.13
	14	87.21	\pm 11.73	130.38	\pm 6.84	31.05	\pm 3.74	80.96	\pm 5.10
	16	212.74	\pm 20.75	249.04	\pm 11.06	61.35	\pm 7.62	139.61	\pm 9.89
	19	458.45	\pm 31.98	486.62	\pm 22.99	150.48	\pm 17.88	264.15	\pm 25.57
	21	647.27	\pm 40.54	798.84	\pm 38.75	242.07	\pm 27.04	366.98	\pm 36.10
2. Length - Primary	5	1.11	\pm 0.10	2.15	\pm 0.17	0.60	\pm 0.09	1.66	\pm 0.23
	7	1.65	\pm 0.12	3.53	\pm 0.23	0.90	\pm 0.10	2.20	\pm 0.22
	9	2.90	\pm 0.17	6.41	\pm 0.55	1.82	\pm 0.15	4.68	\pm 0.32
	12	5.26	\pm 0.25	10.79	\pm 0.64	3.64	\pm 0.24	10.17	\pm 1.11
	14	8.82	\pm 1.02	13.85	\pm 0.66	5.01	\pm 0.27	14.17	\pm 1.41
	16	12.26	\pm 1.20	16.70	\pm 0.75	6.38	\pm 0.27	16.44	\pm 1.49
	19	13.94	\pm 1.11	18.36	\pm 0.70	8.33	\pm 0.25	18.71	\pm 1.57
	21	14.02	\pm 1.09	18.36	\pm 0.70	9.45	\pm 0.24	19.58	\pm 1.56
3. Length - 1st Lateral	5	0.06	\pm 0.00						
	7	0.30	\pm 0.06	0.29	\pm 0.00				
	9	3.11	\pm 0.50	5.65	\pm 0.68	0.43	\pm 0.07	1.98	\pm 0.58
	12	21.78	\pm 2.68	44.25	\pm 3.73	7.40	\pm 1.12	22.13	\pm 3.59
	14	66.01	\pm 10.14	99.05	\pm 5.95	20.85	\pm 3.22	51.06	\pm 3.83
	16	165.73	\pm 16.26	190.65	\pm 9.02	47.12	\pm 6.87	97.05	\pm 7.33
	19	316.12	\pm 20.13	327.71	\pm 14.01	119.29	\pm 14.80	181.66	\pm 15.16
	21	416.80	\pm 24.49	451.21	\pm 16.32	180.06	\pm 19.35	236.24	\pm 17.69
4. Length - 2nd Lateral	5								
	7								
	9								
	12	0.23	\pm 0.06	0.43	\pm 0.07				
	14	4.27	\pm 1.07	3.64	\pm 0.43	0.45	\pm 0.09	1.78	\pm 0.89
	16	22.49	\pm 4.57	24.99	\pm 2.01	1.97	\pm 0.74	9.67	\pm 4.24
	19	114.46	\pm 13.24	122.19	\pm 9.76	14.53	\pm 4.64	45.07	\pm 13.51
	21	202.42	\pm 17.82	310.90	\pm 24.86	43.11	\pm 10.63	91.57	\pm 23.91
5. Growth rate - Total	5	0.45	\pm 0.04	0.86	\pm 0.07	0.29	\pm 0.01	0.66	\pm 0.09
	7	0.63	\pm 0.05	1.39	\pm 0.16	0.33	\pm 0.04	0.54	\pm 0.36
	9	2.57	\pm 0.29	5.69	\pm 0.56	1.06	\pm 0.09	3.48	\pm 0.40
	12	7.92	\pm 0.83	15.82	\pm 1.26	3.38	\pm 0.44	10.37	\pm 1.24
	14	27.40	\pm 4.75	32.23	\pm 1.71	8.49	\pm 1.09	19.25	\pm 0.86
	16	62.76	\pm 4.97	59.33	\pm 2.50	15.15	\pm 1.96	29.32	\pm 3.03
	19	81.90	\pm 4.67	118.79	\pm 7.39	29.71	\pm 3.45	41.51	\pm 5.71
	21	94.41	\pm 6.34	156.11	\pm 9.41	45.79	\pm 4.62	51.41	\pm 6.29
6. Growth rate - Primary	5	0.45	\pm 0.04	0.86	\pm 0.07	0.29	\pm 0.01	0.66	\pm 0.09
	7	0.54	\pm 0.02	1.38	\pm 0.16	0.33	\pm 0.04	0.54	\pm 0.36
	9	1.25	\pm 0.04	2.88	\pm 0.43	0.92	\pm 0.07	2.49	\pm 0.28
	12	1.58	\pm 0.12	2.92	\pm 0.26	1.21	\pm 0.07	3.65	\pm 0.64
	14	3.56	\pm 0.98	3.05	\pm 0.28	1.37	\pm 0.03	4.00	\pm 0.74
	16	3.44	\pm 0.45	2.86	\pm 0.28	1.37	\pm 0.02	2.27	\pm 0.27
	19	1.12	\pm 0.20	1.66	\pm 0.12	1.30	\pm 0.03	1.52	\pm 0.17
	21	1.01	\pm 0.00	0.04	\pm 0.00	1.11	\pm 0.03	0.87	\pm 0.08
7. Growth rate - 1st Lateral	5	0.01	\pm 0.00						
	7	0.14	\pm 0.03	0.15	\pm 0.00				
	9	1.45	\pm 0.23	2.81	\pm 0.34	0.22	\pm 0.03	0.99	\pm 0.29
	12	6.31	\pm 0.75	12.87	\pm 1.11	2.36	\pm 0.35	6.72	\pm 1.03
	14	22.11	\pm 4.02	27.40	\pm 1.51	7.04	\pm 1.04	14.47	\pm 0.71
	16	49.86	\pm 3.33	45.80	\pm 1.94	13.14	\pm 1.84	23.00	\pm 2.45
	19	50.13	\pm 2.31	68.53	\pm 3.97	24.05	\pm 2.69	28.20	\pm 3.12
	21	50.34	\pm 3.38	61.75	\pm 1.85	30.39	\pm 2.43	27.29	\pm 1.40
8. Growth rate - 2nd Lateral	5								
	7								
	9								
	12	0.08	\pm 0.02	0.14	\pm 0.02				
	14	2.08	\pm 0.53	1.78	\pm 0.21	0.22	\pm 0.04	0.89	\pm 0.44
	16	9.47	\pm 1.85	10.67	\pm 0.84	0.86	\pm 0.33	4.06	\pm 1.76
	19	30.66	\pm 3.04	48.60	\pm 4.28	4.35	\pm 1.34	11.80	\pm 3.38
	21	43.98	\pm 3.73	94.36	\pm 8.68	14.29	\pm 3.06	23.25	\pm 5.68
9. Number of 1st lateral roots	5	1.00	\pm 0.00						
	7	2.25	\pm 0.34	1.00	\pm 0.00				
	9	11.27	\pm 1.13	13.60	\pm 1.19	2.75	\pm 0.34	6.88	\pm 1.83
	12	32.25	\pm 2.94	50.20	\pm 3.78	17.82	\pm 1.83	44.25	\pm 6.27
	14	63.58	\pm 6.35	99.87	\pm 6.55	45.00	\pm 5.82	77.00	\pm 7.08
	16	121.42	\pm 9.81	159.67	\pm 7.95	65.08	\pm 7.62	119.38	\pm 8.57
	19	199.08	\pm 11.67	234.67	\pm 9.77	118.83	\pm 12.45	181.25	\pm 13.64
	21	238.83	\pm 13.23	297.07	\pm 10.18	152.25	\pm 13.89	214.88	\pm 14.29
10. Number of 2nd lateral roots	5								
	7								
	9								
	12	1.20	\pm 0.13	2.00	\pm 0.45				
	14	13.80	\pm 2.62	14.87	\pm 1.48	4.00	\pm 0.68	4.43	\pm 1.06
	16	46.33	\pm 8.09	65.07	\pm 4.66	10.78	\pm 2.81	19.63	\pm 5.83
	19	187.58	\pm 21.49	238.93	\pm 17.60	61.83	\pm 13.96	85.38	\pm 16.51
	21	324.67	\pm 29.34	605.27	\pm 44.47	160.75	\pm 29.07	181.38	\pm 29.63

Table S 2 Mean values and standard error of different root system traits describing distribution and spread

Root trait	DAI	Mean values \pm standard error											
		Amb-Ctl			Amb-PsJN			HT-Ctl			HT-PsJN		
1. Root system depth	5	2.25	\pm	0.20	2.32	\pm	0.06	1.43	\pm	0.07	1.59	\pm	0.08
	7	3.32	\pm	0.25	3.35	\pm	0.08	1.97	\pm	0.10	2.28	\pm	0.10
	9	5.83	\pm	0.34	5.66	\pm	0.12	3.55	\pm	0.29	4.30	\pm	0.14
	12	10.28	\pm	0.42	9.83	\pm	0.18	7.00	\pm	0.46	8.16	\pm	0.16
	14	13.52	\pm	0.46	13.08	\pm	0.20	9.66	\pm	0.52	10.96	\pm	0.16
	16	16.59	\pm	0.43	16.27	\pm	0.19	12.33	\pm	0.54	13.65	\pm	0.18
	19	19.02	\pm	0.18	19.27	\pm	0.02	16.10	\pm	0.50	17.28	\pm	0.24
	21	19.19	\pm	0.07	19.27	\pm	0.02	18.28	\pm	0.47	19.00	\pm	0.12
2. Root system width	5	0.11	\pm	0.02	0.12	\pm	0.01	0.08	\pm	0.01	0.08	\pm	0.01
	7	0.20	\pm	0.04	0.14	\pm	0.01	0.09	\pm	0.01	0.10	\pm	0.01
	9	0.96	\pm	0.13	1.25	\pm	0.12	0.22	\pm	0.04	0.37	\pm	0.04
	12	2.97	\pm	0.28	3.05	\pm	0.15	1.15	\pm	0.16	1.27	\pm	0.09
	14	4.21	\pm	0.31	4.08	\pm	0.18	1.87	\pm	0.24	2.08	\pm	0.15
	16	5.70	\pm	0.30	5.38	\pm	0.26	2.49	\pm	0.28	2.62	\pm	0.13
	19	7.31	\pm	0.26	7.00	\pm	0.37	3.18	\pm	0.28	3.45	\pm	0.20
	21	7.96	\pm	0.27	7.61	\pm	0.35	3.62	\pm	0.28	3.64	\pm	0.20
3. Convex hull area	5	28.47	\pm	3.80	28.56	\pm	2.20	14.00	\pm	1.30	18.01	\pm	1.96
	7	102.31	\pm	20.31	60.68	\pm	5.29	22.47	\pm	2.08	30.46	\pm	3.68
	9	904.58	\pm	137.17	1081.86	\pm	116.43	123.61	\pm	20.17	245.27	\pm	31.25
	12	4911.60	\pm	561.84	4832.34	\pm	278.58	1326.81	\pm	197.74	1644.98	\pm	140.32
	14	9749.58	\pm	837.04	8928.15	\pm	470.15	3050.44	\pm	409.82	3741.92	\pm	298.15
	16	16172.80	\pm	1097	15340.91	\pm	752.41	5362.50	\pm	613.27	6117.01	\pm	376.52
	19	26699.98	\pm	1041	26073.98	\pm	1177	9411.44	\pm	905.49	11132.84	\pm	914.97
	21	32662.63	\pm	954.99	32044.74	\pm	1336	12529.62	\pm	1099	13249.36	\pm	741.05
4. Branching angle of lateral roots	5												
	7	74.63	\pm	4.01	26.69	\pm	0.00						
	9	62.88	\pm	3.08	55.01	\pm	4.92	37.54	\pm	3.30	60.39	\pm	9.08
	12	59.10	\pm	2.11	59.95	\pm	2.03	56.13	\pm	3.74	55.75	\pm	3.84
	14	61.09	\pm	1.16	57.10	\pm	1.62	52.38	\pm	3.97	56.09	\pm	3.37
	16	61.84	\pm	2.94	55.05	\pm	1.23	55.09	\pm	2.70	56.69	\pm	2.28
	19	61.78	\pm	3.11	55.70	\pm	1.40	52.68	\pm	1.81	52.66	\pm	0.86
	21	60.54	\pm	2.81	54.95	\pm	1.38	51.73	\pm	1.55	50.57	\pm	1.09

References

- Abd El-Daim, I. A., Bejai, S., & Meijer, J. (2014, June 01). Improved heat stress tolerance of wheat seedlings by bacterial seed treatment [journal article]. *Plant and Soil*, 379(1), 337-350. <https://doi.org/10.1007/s11104-014-2063-3>
- Abdel-Mawgoud, A. M., & Stephanopoulos, G. (2018, 2018/03/01/). Simple glycolipids of microbes: Chemistry, biological activity and metabolic engineering. *Synthetic and Systems Biotechnology*, 3(1), 3-19. <https://doi.org/https://doi.org/10.1016/j.synbio.2017.12.001>
- Abeer, H., Abdallah, E., Alqarawi, A., Al-Huqail, A. A., Alshalawi, S., Wirth, S., & Dilfuza, E. (2015). Impact of plant growth promoting *Bacillus subtilis* on growth and physiological parameters of *Bassia indica* (Indian bassia) grown under salt stress. *Pak. J. Bot*, 47(5), 1735-1741.
- Adams, S., Cockshull, K., & Cave, C. (2001). Effect of temperature on the growth and development of tomato fruits. *Annals of Botany*, 88(5), 869-877.
- Adesemoye, A., Torbert, H., & Kloepper, J. (2009). Plant growth-promoting rhizobacteria allow reduced application rates of chemical fertilizers. *Microbial ecology*, 58(4), 921-929.
- Adu, M. O., Chatot, A., Wiesel, L., Bennett, M. J., Broadley, M. R., White, P. J., & Dupuy, L. X. (2014). A scanner system for high-resolution quantification of variation in root growth dynamics of *Brassica rapa* genotypes. *Journal of Experimental Botany*, 65(8), 2039-2048. <https://doi.org/10.1093/jxb/eru048>
- Agmon, E., & Stockwell, B. R. (2017, 2017/08/01/). Lipid homeostasis and regulated cell death. *Current Opinion in Chemical Biology*, 39, 83-89. <https://doi.org/https://doi.org/10.1016/j.cbpa.2017.06.002>
- Ahammed, G. J., & Yu, J.-Q. (2016). *Plant hormones under challenging environmental factors*. Springer.
- Ahmadian, M., Duncan, R. E., Jaworski, K., Sarkadi-Nagy, E., & Sook Sul, H. (2007, 2007/04/01). Triacylglycerol Metabolism In Adipose Tissue. *Future Lipidology*, 2(2), 229-237. <https://doi.org/10.2217/17460875.2.2.229>
- Aidoo, M. K., Bdolach, E., Fait, A., Lazarovitch, N., & Rachmilevitch, S. (2016). Tolerance to high soil temperature in foxtail millet (*Setaria italica* L.) is related to shoot and root growth and metabolism. *Plant Physiology and Biochemistry*, 106, 73-81.
- Ait Barka, E., Nowak, J., & Clément, C. (2006). Enhancement of chilling resistance of inoculated grapevine plantlets with a plant growth-promoting rhizobacterium, *Burkholderia phytofirmans* strain PsJN. *Applied and Environmental Microbiology*, 72(11), 7246-7252.
- Akhtar, T. A., Surowiecki, P., Siekierska, H., Kania, M., Van Gelder, K., Rea, K. A., Virta, L. K. A., Vatta, M., Gawarecka, K., Wojcik, J., Danikiewicz, W., Buszewicz, D., Swiezewska, E., & Surmacz, L. (2017). Polyprenols Are Synthesized by a Plastidial

- cis-Prenyltransferase and Influence Photosynthetic Performance. *The Plant Cell*, 29(7), 1709-1725. <https://doi.org/10.1105/tpc.16.00796>
- Akiyama, K., Matsuzaki, K.-i., & Hayashi, H. (2005). Plant sesquiterpenes induce hyphal branching in arbuscular mycorrhizal fungi. *Nature*, 435(7043), 824-827.
- Alberts, B., Johnson, A., Lewis, J., Morgan, D., Raff, M., Roberts, K., & Walter, P. (2002). *Molecular Biology of the Cell* (4th edition ed.). Garland Science. <https://www.ncbi.nlm.nih.gov/books/NBK26871/>
- Alden, K. P., Dhondt-Cordelier, S., McDonald, K. L., Reape, T. J., Ng, C. K. Y., McCabe, P. F., & Leaver, C. J. (2011). Sphingolipid long chain base phosphates can regulate apoptotic-like programmed cell death in plants. *Biochemical and biophysical research communications*, 410(3), 574-580. <https://doi.org/https://doi.org/10.1016/j.bbrc.2011.06.028>
- Alder, A., Jamil, M., Marzorati, M., Bruno, M., Vermathen, M., Bigler, P., Ghisla, S., Bouwmeester, H., Beyer, P., & Al-Babili, S. (2012). The Path from β -Carotene to Carlactone, a Strigolactone-Like Plant Hormone. *Science*, 335(6074), 1348-1351. <https://doi.org/10.1126/science.1218094>
- Alexander, J. M., Diez, J. M., & Levine, J. M. (2015). Novel competitors shape species' responses to climate change. *Nature*, 525(7570), 515-518.
- Ali, S., & Kim, W.-C. (2018, 2018-May-25). Plant Growth Promotion Under Water: Decrease of Waterlogging-Induced ACC and Ethylene Levels by ACC Deaminase-Producing Bacteria [Mini Review]. *Frontiers in Microbiology*, 9. <https://doi.org/10.3389/fmicb.2018.01096>
- Amato, M., Basso, B., Celano, G., Bitella, G., Morelli, G., & Rossi, R. (2008). In situ detection of tree root distribution and biomass by multi-electrode resistivity imaging. *Tree physiology*, 28(10), 1441-1448.
- Andersson, D. I., & Hughes, D. (2014). Microbiological effects of sublethal levels of antibiotics. *Nature Reviews Microbiology*, 12(7), 465-478.
- Araus, J. L., Slafer, G. A., Royo, C., & Serret, M. D. (2008). Breeding for yield potential and stress adaptation in cereals. *Critical Reviews in Plant Science*, 27(6), 377-412.
- Arias, P. A., N. Bellouin, E. Coppola, R.G. Jones, G. Krinner, J. Marotzke, V. Naik, M.D. Palmer, G.-K. Plattner, J. Rogelj, M. Rojas, J. Sillmann, T. Storelvmo, P.W. Thorne, B. Trewin, K. Achuta Rao, B. Adhikary, R.P. Allan, K. Armour, G. Bala, R. Barimalala, S. Berger, J.G. Canadell, C. Cassou, A. Cherchi, W. Collins, W.D. Collins, S.L. Connors, S. Corti, F. Cruz, F.J. Dentener, C. Dereczynski, A. Di Luca, A. Diongue Niang, F.J. Doblas-Reyes, A. Dosio, H. Douville, F. Engelbrecht, V. Eyring, E. Fischer, P. Forster, B. Fox-Kemper, J.S. Fuglestedt, J.C. Fyfe, N.P. Gillett, L. Goldfarb, I. Gorodetskaya, J.M. Gutierrez, R. Hamdi, E. Hawkins, H.T. Hewitt, P. Hope, A.S. Islam, C. Jones, D.S. Kaufman, R.E. Kopp, Y. Kosaka, J. Kossin, S. Krakovska, J.-Y. Lee, J. Li, T. Mauritsen, T.K. Maycock, M. Meinshausen, S.-K. Min, P.M.S. Monteiro, T. Ngo-Duc, F. Otto, I. Pinto, A. Pirani, K. Raghavan, R. Ranasinghe, A.C. Ruane, L.

- Ruiz, J.-B. Sallée, B.H. Samset, S. Sathyendranath, S.I. Seneviratne, A.A. Sörensson, S. Szopa, I. Takayabu, A.-M. Tréguier, B. van den Hurk, R. Vautard, K. von Schuckmann, S. Zaehle, X. Zhang, and K. Zickfeld. (2021). Technical Summary. In V. Masson-Delmotte, P. Zhai, A. Pirani, S.L. Connors, C. Péan, S. Berger, N. Caud, Y. Chen, L. Goldfarb, M.I. Gomis, M. Huang, K. Leitzell, E. Lonnoy, J.B.R. Matthews, T.K. Maycock, T. Waterfield, O. Yelekçi, R. Yu, and B. Zhou (Ed.), *Climate Change 2021: The Physical Science Basis. Contribution of Working Group I to the Sixth Assessment Report of the Intergovernmental Panel on Climate Change*. Cambridge University Press, Cambridge, United Kingdom and New York, NY, USA, pp. 33–144.
- Arisz, S. A., & Munnik, T. (2013). Distinguishing phosphatidic acid pools from de novo synthesis, PLD, and DGK. In *Plant lipid signaling protocols* (pp. 55-62). Springer.
- Arisz, S. A., Testerink, C., & Munnik, T. (2009). Plant PA signaling via diacylglycerol kinase. *Biochimica et Biophysica Acta (BBA)-Molecular and Cell Biology of Lipids*, 1791(9), 869-875.
- Armengaud, P. (2009). EZ-Rhizo software: the gateway to root architecture analysis. *Plant signaling & behavior*, 4(2), 139-141.
- Arrigo, A.-P. (1998). Small stress proteins: chaperones that act as regulators of intracellular redox state and programmed cell death. *Biological chemistry*, 379(1), 19-26.
- Arsova, B., Foster, K. J., Shelden, M. C., Bramley, H., & Watt, M. (2019). Dynamics in plant roots and shoots minimise stress, save energy and maintain water and nutrient uptake. *New Phytologist*.
- Asari, S., Tarkowská, D., Rolčík, J., Novák, O., Palmero, D. V., Bejai, S., & Meijer, J. (2017, January 01). Analysis of plant growth-promoting properties of *Bacillus amyloliquefaciens* UCMB5113 using *Arabidopsis thaliana* as host plant [journal article]. *Planta*, 245(1), 15-30. <https://doi.org/10.1007/s00425-016-2580-9>
- Ashraf, M., & Hafeez, M. (2004). Thermotolerance of pearl millet and maize at early growth stages: growth and nutrient relations. *Biologia plantarum*, 48(1), 81-86.
- Ashraf, M. A., Akbar, A., Askari, S. H., Iqbal, M., Rasheed, R., & Hussain, I. (2018). Recent Advances in Abiotic Stress Tolerance of Plants Through Chemical Priming: An Overview. In A. Rakshit & H. B. Singh (Eds.), *Advances in Seed Priming* (pp. 51-79). Springer Singapore. https://doi.org/10.1007/978-981-13-0032-5_4
- Asseng, S., Ewert, F., Martre, P., Rotter, R. P., Lobell, D. B., Cammarano, D., Kimball, B. A., Ottman, M. J., Wall, G. W., White, J. W., Reynolds, M. P., Alderman, P. D., Prasad, P. V. V., Aggarwal, P. K., Anothai, J., Basso, B., Biernath, C., Challinor, A. J., De Sanctis, G., Doltra, J., Fereres, E., Garcia-Vile, M., Gayler, S., Hoogenboom, G., Hunt, L. A., Izaurralde, R. C., Jabloun, M., Jones, C. D., Kersebaum, K. C., Koehler, A. K., Muller, C., Kumar, S. N., Nendel, C., O'Leary, G., Olesen, J. E., Palosuo, T., Priesack, E., Rezaei, E. E., Ruane, A. C., Semenov, M. A., Shcherbak, I., Stockle, C., Stratonovitch, P., Streck, T., Supit, I., Tao, F., Thorburn, P. J., Waha, K., Wang, E., Wallach, D., Wolf, I., Zhao, Z., & Zhu, Y. (2015, Feb). Rising temperatures reduce global wheat

production [Article]. *Nature Climate Change*, 5(2), 143-147.
<https://doi.org/10.1038/nclimate2470>

- Atkinson, J. A., Lobet, G., Noll, M., Meyer, P. E., Griffiths, M., & Wells, D. M. (2017). Combining semi-automated image analysis techniques with machine learning algorithms to accelerate large-scale genetic studies. *GigaScience*, 6(10), gix084.
- Atkinson, J. A., Pound, M. P., Bennett, M. J., & Wells, D. M. (2019). Uncovering the hidden half of plants using new advances in root phenotyping. *Current Opinion in Biotechnology*, 55, 1-8.
- Audrain, B., Farag, M. A., Ryu, C.-M., & Ghigo, J.-M. (2015). Role of bacterial volatile compounds in bacterial biology. *FEMS Microbiology Reviews*, 39(2), 222-233.
- Aufrecht, J. A., Ryan, J. M., Hasim, S., Allison, D. P., Nebenführ, A., Doktycz, M. J., & Retterer, S. T. (2017). Imaging the root hair morphology of Arabidopsis seedlings in a two-layer microfluidic platform. *JoVE (Journal of Visualized Experiments)*(126), e55971.
- Bago, B., Pfeffer, P. E., & Shachar-Hill, Y. (2000). Carbon Metabolism and Transport in Arbuscular Mycorrhizas. *Plant Physiology*, 124(3), 949-958.
<https://doi.org/10.1104/pp.124.3.949>
- Bai, Y., Müller, D. B., Srinivas, G., Garrido-Oter, R., Potthoff, E., Rott, M., Dombrowski, N., Münch, P. C., Spaepen, S., Remus-Emsermann, M., Hüttel, B., McHardy, A. C., Vorholt, J. A., & Schulze-Lefert, P. (2015, 12/02/online). Functional overlap of the Arabidopsis leaf and root microbiota [Article]. *Nature*, 528, 364.
<https://doi.org/10.1038/nature16192>
<https://www.nature.com/articles/nature16192#supplementary-information>
- Bailly, A., Groenhagen, U., Schulz, S., Geisler, M., Eberl, L., & Weisskopf, L. (2014). The inter-kingdom volatile signal indole promotes root development by interfering with auxin signalling. *The Plant Journal*, 80(5), 758-771.
- Bais, H. P., Park, S.-W., Weir, T. L., Callaway, R. M., & Vivanco, J. M. (2004, 2004/01/01/). How plants communicate using the underground information superhighway. *Trends in Plant Science*, 9(1), 26-32. <https://doi.org/https://doi.org/10.1016/j.tplants.2003.11.008>
- Bais, H. P., Weir, T. L., Perry, L. G., Gilroy, S., & Vivanco, J. M. (2006). The role of root exudates in rhizosphere interactions with plants and other organisms. *Annu. Rev. Plant Biol.*, 57, 233-266.
- Balmer, A., Pastor, V., Gamir, J., Flors, V., & Mauch-Mani, B. (2015). The 'prime-ome': towards a holistic approach to priming. *Trends in Plant Science*, 20(7), 443-452.
- Balogh, G., Péter, M., Glatz, A., Gombos, I., Török, Z., Horváth, I., Harwood, J. L., & Vigh, L. (2013, 2013/06/27/). Key role of lipids in heat stress management. *FEBS Letters*, 587(13), 1970-1980. <https://doi.org/https://doi.org/10.1016/j.febslet.2013.05.016>

- Bañon, S., Fernandez, J., Franco, J., Torrecillas, A., Alarcón, J., & Sánchez-Blanco, M. J. (2004). Effects of water stress and night temperature preconditioning on water relations and morphological and anatomical changes of *Lotus creticus* plants. *Scientia Horticulturae*, *101*(3), 333-342.
- Barnabas, B., Jager, K., & Feher, A. (2008, Jan). The effect of drought and heat stress on reproductive processes in cereals [Review]. *Plant Cell and Environment*, *31*(1), 11-38. <https://doi.org/10.1111/j.1365-3040.2007.01727.x>
- Barnes, E. M., & Tringe, S. G. (2022). Exploring the roles of microbes in facilitating plant adaptation to climate change. *Biochemical Journal*, *479*(3), 327-335.
- Barrero-Sicilia, C., Silvestre, S., Haslam, R. P., & Michaelson, L. V. (2017). Lipid remodelling: Unravelling the response to cold stress in *Arabidopsis* and its extremophile relative *Eutrema salsugineum*. *Plant Science*, *263*, 194-200.
- Bashan, Y., Alcaraz-Melendez, L., & Toledo, G. (1992). Responses of soybean and cowpea root membranes to inoculation with *Azospirillum brasilense*. *Symbiosis*.
- Bassirirad, H. (2000). Kinetics of nutrient uptake by roots: responses to global change. *The New Phytologist*, *147*(1), 155-169.
- Basu, A., Prasad, P., Das, S. N., Kalam, S., Sayyed, R., Reddy, M., & El Enshasy, H. (2021). Plant growth promoting rhizobacteria (PGPR) as green bioinoculants: recent developments, constraints, and prospects. *Sustainability*, *13*(3), 1140.
- Beccaccioli, M., Reverberi, M., & Scala, V. (2019, Jan). Fungal lipids: biosynthesis and signalling during plant-pathogen interaction [Article]. *Frontiers in Bioscience-Landmark*, *24*, 172-185. <https://doi.org/10.2741/4712>
- Becker, S., & Kastenholz, B. (2020). Plant cultivation in agar-Petri dishes. *Forschungszentrum Juelich*.
- Behl, R., Heise, K., & Moawad, A. (1996). High temperature tolerance in relation to changes in lipids in mutant wheat. *Der Tropenlandwirt-Journal of Agriculture in the Tropics and Subtropics*, *97*(2), 131-135.
- Bellstaedt, J., Trenner, J., Lippmann, R., Poeschl, Y., Zhang, X., Friml, J., Quint, M., & Delker, C. (2019). A mobile auxin signal connects temperature sensing in cotyledons with growth responses in hypocotyls. *Plant Physiology*, *180*(2), 757-766.
- Bensalim, S., Nowak, J., & Asiedu, S. K. (1998, May 01). A plant growth promoting rhizobacterium and temperature effects on performance of 18 clones of potato [journal article]. *American Journal of Potato Research*, *75*(3), 145-152. <https://doi.org/10.1007/bf02895849>
- Berry, J., & Bjorkman, O. (1980). Photosynthetic response and adaptation to temperature in higher plants. *Annual review of plant physiology*, *31*(1), 491-543.

- Bhat, R. A., Miklis, M., Schmelzer, E., Schulze-Lefert, P., & Panstruga, R. (2005). Recruitment and interaction dynamics of plant penetration resistance components in a plasma membrane microdomain. *Proceedings of the National Academy of Sciences*, *102*(8), 3135-3140.
- Bhatnagar-Mathur, P., Vadez, V., & Sharma, K. K. (2008, 2008/03/01). Transgenic approaches for abiotic stress tolerance in plants: retrospect and prospects. *Plant Cell Reports*, *27*(3), 411-424. <https://doi.org/10.1007/s00299-007-0474-9>
- Bilgin, M., Born, P., Fezza, F., Heimes, M., Mastrangelo, N., Wagner, N., Schultz, C., Maccarrone, M., Eaton, S., & Nadler, A. (2016). Lipid discovery by combinatorial screening and untargeted LC-MS/MS. *Scientific Reports*, *6*(1), 1-6.
- Bista, D. R., Heckathorn, S. A., Jayawardena, D. M., Mishra, S., & Boldt, J. K. (2018). Effects of drought on nutrient uptake and the levels of nutrient-uptake proteins in roots of drought-sensitive and-tolerant grasses. *Plants*, *7*(2), 28.
- Bitá, C. E., & Gerats, T. (2013). Plant tolerance to high temperature in a changing environment: scientific fundamentals and production of heat stress-tolerant crops. *Frontiers in Plant Science*, *4*, 273.
- Bitas, V., Kim, H.-S., Bennett, J. W., & Kang, S. (2013). Sniffing on microbes: diverse roles of microbial volatile organic compounds in plant health. *Molecular Plant-Microbe Interactions*, *26*(8), 835-843.
- Bligh, E. G., & Dyer, W. J. (1959). A rapid method of total lipid extraction and purification. *Canadian journal of biochemistry and physiology*, *37*(8), 911-917.
- Blum, A. (2018). *Plant breeding for stress environments*. CRC press.
- Boden, T. A., Marland, G., & Andres, R. J. (2017). National CO2 emissions from fossil-fuel burning, cement manufacture, and gas flaring: 1751-2014. *Carbon Dioxide Information Analysis Center, Oak Ridge National Laboratory, US Department of Energy*.
- Bohnert, H. J., Gong, Q., Li, P., & Ma, S. (2006). Unraveling abiotic stress tolerance mechanisms—getting genomics going. *Current opinion in plant biology*, *9*(2), 180-188.
- Boon, J. M., & Smith, B. D. (2002). Chemical control of phospholipid distribution across bilayer membranes. *Medicinal Research Reviews*, *22*(3), 251-281. <https://doi.org/10.1002/med.10009>
- Bose, J., Rodrigo-Moreno, A., & Shabala, S. (2014). ROS homeostasis in halophytes in the context of salinity stress tolerance. *Journal of Experimental Botany*, *65*(5), 1241-1257.
- Boutte, Y., & Jaillais, Y. (2020, Jul). Metabolic Cellular Communications: Feedback Mechanisms between Membrane Lipid Homeostasis and Plant Development. *Developmental cell*, *54*(2), 171-182. <https://doi.org/10.1016/j.devcel.2020.05.005>
- Bowen-Forbes, C., & Goldson-Barnaby, A. (2017). Fats. In *Pharmacognosy* (pp. 425-441). Elsevier.

- Boyes, D. C., Zayed, A. M., Ascenzi, R., McCaskill, A. J., Hoffman, N. E., Davis, K. R., & Görlach, J. (2001). Growth stage-based phenotypic analysis of Arabidopsis: a model for high throughput functional genomics in plants. *The Plant Cell*, *13*(7), 1499-1510.
- Brameyer, S., Bode, H. B., & Heermann, R. (2015). Languages and dialects: bacterial communication beyond homoserine lactones. *Trends in microbiology*, *23*(9), 521-523.
- Breitkopf, S. B., Ricoult, S. J., Yuan, M., Xu, Y., Peake, D. A., Manning, B. D., & Asara, J. M. (2017). A relative quantitative positive/negative ion switching method for untargeted lipidomics via high resolution LC-MS/MS from any biological source. *Metabolomics*, *13*(3), 1-21.
- Brown, D. A., & London, E. (2000). Structure and function of sphingolipid-and cholesterol-rich membrane rafts. *Journal of Biological Chemistry*, *275*(23), 17221-17224.
- Brown, K. M. (1997). Ethylene and abscission. *Physiologia Plantarum*, *100*(3), 567-576. <https://doi.org/https://doi.org/10.1111/j.1399-3054.1997.tb03062.x>
- Brown, M., Antle, J., Backlund, P., Carr, E., Easterling, B., Walsh, M., Ammann, C., Attavanich, W., Barrett, C., & Bellemare, M. (2015). Climate change, global food security and the US food system.
- Buchanan, B., Gruissem, W., & Jones, R. (2002). *Biochemistry & molecular biology of plants*. Rockville, MD. USA: John Wiley & Sons.
- Bucksch, A., Atta-Boateng, A., Azihou, A. F., Battogtokh, D., Baumgartner, A., Binder, B. M., Braybrook, S. A., Chang, C., Coneva, V., DeWitt, T. J., Fletcher, A. G., Gehan, M. A., Diaz-Martinez, D. H., Hong, L., Iyer-Pascuzzi, A. S., Klein, L. L., Leiboff, S., Li, M., Lynch, J. P., Maizel, A., Maloof, J. N., Markelz, R. J. C., Martinez, C. C., Miller, L. A., Mio, W., Palubicki, W., Poorter, H., Pradal, C., Price, C. A., Puttonen, E., Reese, J. B., Rellán-Álvarez, R., Spalding, E. P., Sparks, E. E., Topp, C. N., Williams, J. H., & Chitwood, D. H. (2017, 2017-June-09). Morphological Plant Modeling: Unleashing Geometric and Topological Potential within the Plant Sciences [Review]. *Frontiers in Plant Science*, *8*. <https://doi.org/10.3389/fpls.2017.00900>
- Bucksch, A., Burrridge, J., York, L. M., Das, A., Nord, E., Weitz, J. S., & Lynch, J. P. (2014). Image-based high-throughput field phenotyping of crop roots. *Plant Physiology*, *166*(2), 470-486.
- Bulgarelli, D., Garrido-Oter, R., Münch, P. C., Weiman, A., Dröge, J., Pan, Y., McHardy, A. C., & Schulze-Lefert, P. (2015). Structure and function of the bacterial root microbiota in wild and domesticated barley. *Cell Host Microbe*, *17*. <https://doi.org/10.1016/j.chom.2015.01.011>
- Bulgarelli, D., Schlaeppi, K., Spaepen, S., Themaat, E. V. L. v., & Schulze-Lefert, P. (2013). Structure and Functions of the Bacterial Microbiota of Plants. *Annual review of plant biology*, *64*(1), 807-838. <https://doi.org/10.1146/annurev-arplant-050312-120106>

- Burgos, A., Szymanski, J., Seiwert, B., Degenkolbe, T., Hannah, M. A., Giavalisco, P., & Willmitzer, L. (2011). Analysis of short-term changes in the Arabidopsis thaliana glycerolipidome in response to temperature and light. *The Plant Journal*, *66*(4), 656-668.
- Busby, P. E., Soman, C., Wagner, M. R., Friesen, M. L., Kremer, J., Bennett, A., Morsy, M., Eisen, J. A., Leach, J. E., & Dangl, J. L. (2017). Research priorities for harnessing plant microbiomes in sustainable agriculture. *PLoS biology*, *15*(3), e2001793.
- Busch, W., Moore, B. T., Martsberger, B., Mace, D. L., Twigg, R. W., Jung, J., Pruteanu-Malinici, I., Kennedy, S. J., Fricke, G. K., & Clark, R. L. (2012). A microfluidic device and computational platform for high-throughput live imaging of gene expression. *Nature Methods*, *9*(11), 1101-1106.
- Cabrera, J., Conesa, C. M., & del Pozo, J. C. (2022). May the dark be with roots: a perspective on how root illumination may bias in vitro research on plant–environment interactions. *New Phytologist*, *233*(5), 1988-1997. <https://doi.org/10.1111/nph.17936>
- Cacas, J.-L., Buré, C., Grosjean, K., Gerbeau-Pissot, P., Lherminier, J., Rombouts, Y., Maes, E., Bossard, C., Gronnier, J., Furt, F., Fouillen, L., Germain, V., Bayer, E., Cluzet, S., Robert, F., Schmitter, J.-M., Deleu, M., Lins, L., Simon-Plas, F., & Mongrand, S. (2016). Revisiting Plant Plasma Membrane Lipids in Tobacco: A Focus on Sphingolipids. *Plant Physiology*, *170*(1), 367-384. <https://doi.org/10.1104/pp.15.00564>
- Cajka, T., & Fiehn, O. (2016). Toward merging untargeted and targeted methods in mass spectrometry-based metabolomics and lipidomics. *Analytical Chemistry*, *88*(1), 524-545.
- Calleja-Cabrera, J., Boter, M., Oñate-Sánchez, L., & Pernas, M. (2020, 2020-May-08). Root Growth Adaptation to Climate Change in Crops [Review]. *Frontiers in Plant Science*, *11*(544). <https://doi.org/10.3389/fpls.2020.00544>
- Camejo, D., Jiménez, A., Alarcón, J. J., Torres, W., Gómez, J. M., & Sevilla, F. (2006). Changes in photosynthetic parameters and antioxidant activities following heat-shock treatment in tomato plants. *Functional Plant Biology*, *33*(2), 177-187.
- Caradus, J., & Woodfield, D. (1998). Genetic control of adaptive root characteristics in white clover. In *Root Demographics and Their Efficiencies in Sustainable Agriculture, Grasslands and Forest Ecosystems* (pp. 651-662). Springer.
- Carmen, B., & Roberto, D. (2011). Soil bacteria support and protect plants against abiotic stresses. *Abiotic stress in plants-Mechanisms and daptations, Italy*, 143-170.
- Carrera, D. Á., Oddsson, S., Grossmann, J., Trachsel, C., & Streb, S. (2018). Comparative proteomic analysis of plant acclimation to six different long-term environmental changes. *Plant and Cell Physiology*, *59*(3), 510-526.
- Casal, J. J., & Balasubramanian, S. (2019). Thermomorphogenesis. *Annual review of plant biology*, *70*(1), 321-346. <https://doi.org/10.1146/annurev-arplant-050718-095919>

- Casanovas, E. M., Barassi, C. A., & Sueldo, R. J. (2002, 2002/09/01). Azospirillum Inoculation Mitigates Water Stress Effects in Maize Seedlings. *Cereal Research Communications*, 30(3), 343-350. <https://doi.org/10.1007/BF03543428>
- Casares, D., Escribá, P. V., & Rosselló, C. A. (2019). Membrane Lipid Composition: Effect on Membrane and Organelle Structure, Function and Compartmentalization and Therapeutic Avenues. *International Journal of Molecular Sciences*, 20(9), 2167. <https://www.mdpi.com/1422-0067/20/9/2167>
- Cassim, A. M., Gouguet, P., Gronnier, J., Laurent, N., Germain, V., Grison, M., Boutte, Y., Gerbeau-Pissot, P., Simon-Plas, F., & Mongrand, S. (2019, Jan). Plant lipids: Key players of plasma membrane organization and function [Review]. *Progress in lipid research*, 73, 1-27. <https://doi.org/10.1016/j.plipres.2018.11.002>
- Castanheira, N. L., Dourado, A. C., Pais, I., Semedo, J., Scotti-Campos, P., Borges, N., Carvalho, G., Crespo, M. T. B., & Fareleira, P. (2017). Colonization and beneficial effects on annual ryegrass by mixed inoculation with plant growth promoting bacteria. *Microbiological research*, 198, 47-55.
- Chanda, B., Venugopal, S. C., Kulshrestha, S., Navarre, D. A., Downie, B., Vaillancourt, L., Kachroo, A., & Kachroo, P. (2008). Glycerol-3-phosphate levels are associated with basal resistance to the hemibiotrophic fungus *Colletotrichum higginsianum* in *Arabidopsis*. *Plant Physiology*, 147(4), 2017-2029.
- Chang, C.-H., & Yang, S.-S. (2009). Thermo-tolerant phosphate-solubilizing microbes for multi-functional biofertilizer preparation. *Bioresource Technology*, 100(4), 1648-1658.
- Chebrolu, K. K., Fritschi, F. B., Ye, S., Krishnan, H. B., Smith, J. R., & Gillman, J. D. (2016). Impact of heat stress during seed development on soybean seed metabolome. *Metabolomics*, 12(2), 1-14.
- Cheng, Y. T., Zhang, L., & He, S. Y. (2019). Plant-microbe interactions facing environmental challenge. *Cell host & microbe*, 26(2), 183-192.
- Cheong, B. E., Beine-Golovchuk, O., Gorka, M., Ho, W. W. H., Martinez-Seidel, F., Firmino, A. A. P., Skiryecz, A., Roessner, U., & Kopka, J. (2021). *Arabidopsis* REI-LIKE proteins activate ribosome biogenesis during cold acclimation. *Scientific Reports*, 11(1), 1-25.
- Cheong, B. E., Ho, W. W. H., Biddulph, B., Wallace, X., Rathjen, T., Rupasinghe, T. W., Roessner, U., & Dolferus, R. (2019). Phenotyping reproductive stage chilling and frost tolerance in wheat using targeted metabolome and lipidome profiling. *Metabolomics*, 15(11), 144.
- Chochois, V., Vogel, J. P., & Watt, M. (2012). Application of *Brachypodium* to the genetic improvement of wheat roots. *Journal of Experimental Botany*, 63(9), 3467-3474.
- Choudhary, D. K., Kasotia, A., Jain, S., Vaishnav, A., Kumari, S., Sharma, K. P., & Varma, A. (2016). Bacterial-mediated tolerance and resistance to plants under abiotic and biotic stresses. *Journal of Plant Growth Regulation*, 35(1), 276-300.

- Christensen, S. A., & Kolomiets, M. V. (2011). The lipid language of plant–fungal interactions. *Fungal Genetics and Biology*, 48(1), 4-14.
- Claes, B. S., Bowman, A. P., Poad, B. L., Young, R. S., Heeren, R. M., Blanksby, S. J., & Ellis, S. R. (2021). Mass spectrometry imaging of lipids with isomer resolution using high-pressure ozone-induced dissociation. *Analytical Chemistry*, 93(28), 9826-9834.
- Clark, R. T., MacCurdy, R. B., Jung, J. K., Shaff, J. E., McCouch, S. R., Aneshansley, D. J., & Kochian, L. V. (2011). Three-dimensional root phenotyping with a novel imaging and software platform. *Plant Physiology*, 156(2), 455-465.
- Cohen, A. C., Bottini, R., Pontin, M., Berli, F. J., Moreno, D., Boccanlandro, H., Travaglia, C. N., & Piccoli, P. N. (2015). Azospirillum brasilense ameliorates the response of Arabidopsis thaliana to drought mainly via enhancement of ABA levels. *Physiologia Plantarum*, 153(1), 79-90. <https://doi.org/doi:10.1111/ppl.12221>
- Colin, L. A., & Jaillais, Y. (2020). Phospholipids across scales: lipid patterns and plant development. *Current opinion in plant biology*, 53, 1-9.
- Compant, S., Reiter, B., Sessitsch, A., Nowak, J., Clément, C., & Barka, E. A. (2005). Endophytic colonization of Vitis vinifera L. by plant growth-promoting bacterium Burkholderia sp. strain PsJN. *Applied and Environmental Microbiology*, 71(4), 1685-1693.
- Cooper, G. M., Hausman, R. E., & Hausman, R. E. (2007). *The cell: a molecular approach* (Vol. 4). ASM press Washington, DC.
- Correia, B. S. B., Torrinhas, R. S., Ohashi, W. Y., & Tasic, L. (2018). Analytical Tools for Lipid Assessment in Biological Assays. In R. V. Baez (Ed.), *Advances in Lipid Metabolism*. IntechOpen. <https://doi.org/DOI: 10.5772/intechopen.81523>
- Costa, S. R., Ng, J. L. P., & Mathesius, U. (2021). Interaction of Symbiotic Rhizobia and Parasitic Root-Knot Nematodes in Legume Roots: From Molecular Regulation to Field Application. *Molecular Plant-Microbe Interactions®*, 34(5), 470-490. <https://doi.org/10.1094/mpmi-12-20-0350-fi>
- Crafts-Brandner, S. J., & Salvucci, M. E. (2002). Sensitivity of photosynthesis in a C4 plant, maize, to heat stress. *Plant Physiology*, 129(4), 1773-1780.
- Craine, J. M., Lee, W. G., Bond, W. J., Williams, R. J., & Johnson, L. C. (2005). Environmental constraints on a global relationship among leaf and root traits of grasses. *Ecology*, 86(1), 12-19.
- D'Alessandro, M., Erb, M., Ton, J., Brandenburg, A., Karlen, D., Zopfi, J., & Turlings, T. C. (2014). Volatiles produced by soil-borne endophytic bacteria increase plant pathogen resistance and affect tritrophic interactions. *Plant, Cell & Environment*, 37(4), 813-826.
- Dai Vu, L., Gevaert, K., & De Smet, I. (2019). Feeling the heat: Searching for plant thermosensors. *Trends in Plant Science*, 24(3), 210-219.

- Daleke, D. L. (2003). Regulation of transbilayer plasma membrane phospholipid asymmetry. *Journal of lipid research*, 44(2), 233-242.
- Degenhardt, J., Hiltpold, I., Köllner, T. G., Frey, M., Gierl, A., Gershenzon, J., Hibbard, B. E., Ellersieck, M. R., & Turlings, T. C. (2009). Restoring a maize root signal that attracts insect-killing nematodes to control a major pest. *Proceedings of the National Academy of Sciences*, 106(32), 13213-13218.
- Degenkolbe, T., Giavalisco, P., Zuther, E., Seiwert, B., Hinch, D. K., & Willmitzer, L. (2012). Differential remodeling of the lipidome during cold acclimation in natural accessions of *Arabidopsis thaliana*. *The Plant Journal*, 72(6), 972-982.
- Dennis, P. G., Miller, A. J., & Hirsch, P. R. (2010). Are root exudates more important than other sources of rhizodeposits in structuring rhizosphere bacterial communities? *FEMS Microbiology Ecology*, 72(3), 313-327. <https://doi.org/doi:10.1111/j.1574-6941.2010.00860.x>
- Devaiah, S. P., Roth, M. R., Baughman, E., Li, M., Tamura, P., Jeannotte, R., Welti, R., & Wang, X. (2006). Quantitative profiling of polar glycerolipid species from organs of wild-type *Arabidopsis* and a PHOSPHOLIPASE Dα1 knockout mutant. *Phytochemistry*, 67(17), 1907-1924.
- Di Paolo, G., & De Camilli, P. (2006, 2006/10/01). Phosphoinositides in cell regulation and membrane dynamics. *Nature*, 443(7112), 651-657. <https://doi.org/10.1038/nature05185>
- Dickman, M. B., & Fluhr, R. (2013). Centrality of host cell death in plant-microbe interactions. *Annual review of phytopathology*, 51, 543-570.
- Diercks, H., Semeniuk, A., Gisch, N., Moll, H., Duda, K. A., & Hölzl, G. (2015). Accumulation of novel glycolipids and ornithine lipids in *Mesorhizobium loti* under phosphate deprivation. *Journal of bacteriology*, 197(3), 497-509.
- Dimkpa, C., Weinand, T., & Asch, F. (2009). Plant-rhizobacteria interactions alleviate abiotic stress conditions. *Plant, Cell & Environment*, 32(12), 1682-1694. <https://doi.org/doi:10.1111/j.1365-3040.2009.02028.x>
- Dodd, I. C., & Pérez-Alfocea, F. (2012). Microbial amelioration of crop salinity stress. *Journal of Experimental Botany*, 63(9), 3415-3428.
- Dormann, P., Kim, H., Ott, T., Schulze-Lefert, P., Trujillo, M., Wewer, V., & Huckelhoven, R. (2014, Dec). Cell-autonomous defense, re-organization and trafficking of membranes in plant-microbe interactions [Review]. *New Phytologist*, 204(4), 815-822. <https://doi.org/10.1111/nph.12978>
- Dowhan, W., & Bogdanov, M. (2002). Functional roles of lipids in membranes. In *New comprehensive biochemistry* (Vol. 36, pp. 1-35). Elsevier.

- Downie, H. F., Adu, M. O., Schmidt, S., Otten, W., Dupuy, L. X., White, P. J., & Valentine, T. A. (2015). Challenges and opportunities for quantifying roots and rhizosphere interactions through imaging and image analysis. *Plant, Cell & Environment*, *38*(7), 1213-1232. <https://doi.org/10.1111/pce.12448>
- Dreccer, M. F., Wockner, K. B., Palta, J. A., McIntyre, C. L., Borgognone, M. G., Bourgault, M., Reynolds, M., & Miralles, D. J. (2014). More fertile florets and grains per spike can be achieved at higher temperature in wheat lines with high spike biomass and sugar content at booting [Article]. *Functional Plant Biology*, *41*(5), 482-495. <https://doi.org/10.1071/fp13232>
- Dubey, R. K., Tripathi, V., Dubey, P. K., Singh, H., & Abhilash, P. (2016). Exploring rhizospheric interactions for agricultural sustainability: the need of integrative research on multi-trophic interactions. *Journal of Cleaner Production*, *115*, 362-365.
- Dudareva, N., Negre, F., Nagegowda, D. A., & Orlova, I. (2006). Plant volatiles: recent advances and future perspectives. *Critical Reviews in Plant Sciences*, *25*(5), 417-440.
- Ehlers, J., & Hall, A. (1998). Heat tolerance of contrasting cowpea lines in short and long days. *Field Crops Research*, *55*(1-2), 11-21.
- Eichler, J., & Guan, Z. (2017, Jun). Lipid sugar carriers at the extremes: The phosphodolichols Archaea use in N-glycosylation. *Biochim Biophys Acta Mol Cell Biol Lipids*, *1862*(6), 589-599. <https://doi.org/10.1016/j.bbali.2017.03.005>
- el Zahar Haichar, F., Heulin, T., Guyonnet, J. P., & Achouak, W. (2016). Stable isotope probing of carbon flow in the plant holobiont. *Current Opinion in Biotechnology*, *41*, 9-13.
- Ellis, S. R., Paine, M. R. L., Eijkel, G. B., Pauling, J. K., Husen, P., Jervelund, M. W., Hermansson, M., Ejsing, C. S., & Heeren, R. M. A. (2018, 2018/07/01). Automated, parallel mass spectrometry imaging and structural identification of lipids. *Nature Methods*, *15*(7), 515-518. <https://doi.org/10.1038/s41592-018-0010-6>
- Enebe, M. C., & Babalola, O. O. (2018, 2018/09/01). The influence of plant growth-promoting rhizobacteria in plant tolerance to abiotic stress: a survival strategy. *Applied microbiology and biotechnology*, *102*(18), 7821-7835. <https://doi.org/10.1007/s00253-018-9214-z>
- Esmael, Q., Miotto, L., Rondeau, M., Leclere, V., Clement, C., Jacquard, C., Sanchez, L., & Barka, E. A. (2018, Aug). Paraburkholderia phytofirmans PsJN-Plants Interaction: From Perception to the Induced Mechanisms [Review]. *Frontiers in Microbiology*, *9*, 14, Article 2093. <https://doi.org/10.3389/fmicb.2018.02093>
- Etesami, H., Alikhani, H. A., & Hosseini, H. M. (2015, 2015/01/01/). Indole-3-acetic acid (IAA) production trait, a useful screening to select endophytic and rhizosphere competent bacteria for rice growth promoting agents. *MethodsX*, *2*, 72-78. <https://doi.org/https://doi.org/10.1016/j.mex.2015.02.008>
- Fahad, S., Bajwa, A. A., Nazir, U., Anjum, S. A., Farooq, A., Zohaib, A., Sadia, S., Nasim, W., Adkins, S., Saud, S., Ihsan, M. Z., Alharby, H., Wu, C., Wang, D., & Huang, J. (2017,

- 2017-June-29). Crop Production under Drought and Heat Stress: Plant Responses and Management Options [Review]. *Frontiers in Plant Science*, 8. <https://doi.org/10.3389/fpls.2017.01147>
- Fahy, E., Cotter, D., Sud, M., & Subramaniam, S. (2011, 2011/11/01/). Lipid classification, structures and tools. *Biochimica et Biophysica Acta (BBA) - Molecular and Cell Biology of Lipids*, 1811(11), 637-647. <https://doi.org/https://doi.org/10.1016/j.bbali.2011.06.009>
- Fahy, E., Subramaniam, S., Brown, H. A., Glass, C. K., Merrill Jr, A. H., Murphy, R. C., Raetz, C. R., Russell, D. W., Seyama, Y., & Shaw, W. (2005). A comprehensive classification system for lipids. *European journal of lipid science and technology*, 107(5), 337-364.
- Fahy, E., Subramaniam, S., Murphy, R. C., Nishijima, M., Raetz, C. R., Shimizu, T., Spener, F., van Meer, G., Wakelam, M. J., & Dennis, E. A. (2009). Update of the LIPID MAPS comprehensive classification system for lipids. *Journal of lipid research*, 50(Supplement), S9-S14.
- Falcone, D. L., Ogas, J. P., & Somerville, C. R. (2004, September 17). Regulation of membrane fatty acid composition by temperature in mutants of Arabidopsis with alterations in membrane lipid composition [journal article]. *BMC Plant Biology*, 4(1), 17. <https://doi.org/10.1186/1471-2229-4-17>
- Farmer, E. E., Alméras, E., & Krishnamurthy, V. (2003). Jasmonates and related oxylipins in plant responses to pathogenesis and herbivory. *Current opinion in plant biology*, 6(4), 372-378.
- Ferguson, B. J., & Mathesius, U. (2014, 2014/07/01). Phytohormone Regulation of Legume-Rhizobia Interactions. *Journal of Chemical Ecology*, 40(7), 770-790. <https://doi.org/10.1007/s10886-014-0472-7>
- Ferluga, S., Steindler, L., & Venturi, V. (2008). N-acyl homoserine lactone quorum sensing in Gram-negative rhizobacteria. In *Secondary metabolites in soil ecology* (pp. 69-90). Springer.
- Ferris, R., Ellis, R. H., Wheeler, T. R., & Hadley, P. (1998). Effect of High Temperature Stress at Anthesis on Grain Yield and Biomass of Field-grown Crops of Wheat [Article]. *Annals of Botany*, 82(5), 631-639. <https://ezp.lib.unimelb.edu.au/login?url=https://search.ebscohost.com/login.aspx?direct=true&db=eih&AN=44659889&scope=site>
- Finkel, O. M., Castrillo, G., Paredes, S. H., González, I. S., & Dangl, J. L. (2017). Understanding and exploiting plant beneficial microbes. *Current opinion in plant biology*, 38, 155-163.
- Fitter, A. H., & Hay, R. K. (2012). *Environmental physiology of plants*. Academic press.
- Flemming, H.-C., & Wingender, J. (2001). Relevance of microbial extracellular polymeric substances (EPSs)-Part I: Structural and ecological aspects. *Water science and technology*, 43(6), 1-8.

- Folch, J., Lees, M., & Stanley, G. S. (1957). A simple method for the isolation and purification of total lipides from animal tissues. *Journal of Biological Chemistry*, 226(1), 497-509.
- Fonseca de Lima, C. F., Kleine-Vehn, J., De Smet, I., & Feraru, E. (2021). Getting to the root of belowground high temperature responses in plants. *Journal of Experimental Botany*, 72(21), 7404-7413.
- Foolad, M. (2005). Breeding for abiotic stress tolerance in tomato. In M. Ashraf & P. J. C. Harris (Eds.), *Abiotic stresses: Plant resistance through breeding and molecular approaches*. The Haworth Press Inc.
- Franche, C., Lindström, K., & Elmerich, C. (2009). Nitrogen-fixing bacteria associated with leguminous and non-leguminous plants. *Plant and Soil*, 321(1), 35-59.
- Frommel, M. I., Nowak, J., & Lazarovits, G. (1991). Growth Enhancement and Developmental Modifications of in Vitro Grown Potato (*Solanum tuberosum* spp. *tuberosum*) as Affected by a Nonfluorescent *Pseudomonas* sp. 1. *Plant Physiology*, 96(3), 928-936. <https://doi.org/10.1104/pp.96.3.928>
- Fuqua, W. C., Winans, S. C., & Greenberg, E. P. (1994). Quorum sensing in bacteria: the LuxR-LuxI family of cell density-responsive transcriptional regulators. *Journal of bacteriology*, 176(2), 269.
- Galkovskyi, T., Mileyko, Y., Bucksch, A., Moore, B., Symonova, O., Price, C. A., Topp, C. N., Iyer-Pascuzzi, A. S., Zurek, P. R., & Fang, S. (2012). GiA Roots: software for the high throughput analysis of plant root system architecture. *BMC Plant Biology*, 12(1), 1-12.
- Gao, J., Sasse, J., Lewald, K. M., Zhalnina, K., Cornmesser, L. T., Duncombe, T. A., Yoshikuni, Y., Vogel, J. P., Firestone, M. K., & Northen, T. R. (2018, 2018/04/10/). Ecosystem Fabrication (EcoFAB) Protocols for The Construction of Laboratory Ecosystems Designed to Study Plant-microbe Interactions. *JoVE*(134), e57170. <https://doi.org/doi:10.3791/57170>
- Gao, L., Cazenave-Gassiot, A., Burla, B., Wenk, M. R., & Torta, F. (2020). Dual mass spectrometry as a tool to improve annotation and quantification in targeted plasma lipidomics. *Metabolomics*, 16(5), 1-12.
- Gao, Q.-m., Yu, K., Xia, Y., Shine, M., Wang, C., Navarre, D., Kachroo, A., & Kachroo, P. (2014). Mono- and digalactosyldiacylglycerol lipids function nonredundantly to regulate systemic acquired resistance in plants. *Cell reports*, 9(5), 1681-1691.
- Gathungu, R. M., Larrea, P., Sniatynski, M. J., Marur, V. R., Bowden, J. A., Koelmel, J. P., Starke-Reed, P., Hubbard, V. S., & Kristal, B. S. (2018). Optimization of electrospray ionization source parameters for lipidomics to reduce misannotation of in-source fragments as precursor ions. *Analytical Chemistry*, 90(22), 13523-13532.
- Gaude, N., Tippmann, H., Flemetakis, E., Katinakis, P., Udvardi, M., & Dörmann, P. (2004). The galactolipid digalactosyldiacylglycerol accumulates in the peribacteroid membrane

of nitrogen-fixing nodules of soybean and Lotus. *Journal of Biological Chemistry*, 279(33), 34624-34630.

[Record #2018 is using a reference type undefined in this output style.]

Gill, C., & Suisted, J. (1978). The effects of temperature and growth rate on the proportion of unsaturated fatty acids in bacterial lipids. *Microbiology*, 104(1), 31-36.

Gioia, T., Galinski, A., Lenz, H., Müller, C., Lentz, J., Heinz, K., Briese, C., Putz, A., Fiorani, F., & Watt, M. (2016). GrowScreen-PaGe, a non-invasive, high-throughput phenotyping system based on germination paper to quantify crop phenotypic diversity and plasticity of root traits under varying nutrient supply. *Functional Plant Biology*, 44(1), 76-93.

Giri, A., Heckathorn, S., Mishra, S., & Krause, C. (2017). Heat stress decreases levels of nutrient-uptake and-assimilation proteins in tomato roots. *Plants*, 6(1), 6.

Glick, B. R. (2004). Bacterial ACC deaminase and the alleviation of plant stress. *Advances in applied microbiology*, 56, 291-312.

Glick, B. R., Penrose, D. M., & Li, J. (1998). A model for the lowering of plant ethylene concentrations by plant growth-promoting bacteria. *Journal of theoretical biology*, 190(1), 63-68.

González, J. F., & Venturi, V. (2013). A novel widespread interkingdom signaling circuit. *Trends in Plant Science*, 18(3), 167-174.

Grandclément, C., Tannières, M., Moréra, S., Dessaux, Y., & Faure, D. (2016). Quorum quenching: role in nature and applied developments. *FEMS Microbiology Reviews*, 40(1), 86-116.

Gray, E., & Smith, D. (2005). Intracellular and extracellular PGPR: commonalities and distinctions in the plant–bacterium signaling processes. *Soil Biology and Biochemistry*, 37(3), 395-412.

Grieneisen, V. A., Xu, J., Marée, A. F., Hogeweg, P., & Scheres, B. (2007). Auxin transport is sufficient to generate a maximum and gradient guiding root growth. *Nature*, 449(7165), 1008.

Grisson, M. S., Brocard, L., Fouillen, L., Nicolas, W., Wewer, V., Dörmann, P., Nacir, H., Benitez-Alfonso, Y., Claverol, S., & Germain, V. (2015). Specific membrane lipid composition is important for plasmodesmata function in Arabidopsis. *The Plant Cell*, 27(4), 1228-1250.

Gronnier, J., Gerbeau-Pissot, P., Germain, V., Mongrand, S., & Simon-Plas, F. (2018, 2018/10/01). Divide and Rule: Plant Plasma Membrane Organization. *Trends in Plant Science*, 23(10), 899-917. <https://doi.org/https://doi.org/10.1016/j.tplants.2018.07.007>

- Grossmann, G., Guo, W.-J., Ehrhardt, D. W., Frommer, W. B., Sit, R. V., Quake, S. R., & Meier, M. (2011). The RootChip: an integrated microfluidic chip for plant science. *The Plant Cell*, *23*(12), 4234-4240.
- Grover, M., Ali, S. Z., Sandhya, V., Rasul, A., & Venkateswarlu, B. (2011, May 01). Role of microorganisms in adaptation of agriculture crops to abiotic stresses [journal article]. *World Journal of Microbiology and Biotechnology*, *27*(5), 1231-1240. <https://doi.org/10.1007/s11274-010-0572-7>
- Grover, M., Bodhankar, S., Sharma, A., Sharma, P., Singh, J., & Nain, L. (2021, 2021-January-08). PGPR Mediated Alterations in Root Traits: Way Toward Sustainable Crop Production [Review]. *Frontiers in Sustainable Food Systems*, *4*. <https://doi.org/10.3389/fsufs.2020.618230>
- Guilioni, L., Wéry, J., & Lecoœur, J. (2003). High temperature and water deficit may reduce seed number in field pea purely by decreasing plant growth rate. *Functional Plant Biology*, *30*(11), 1151-1164.
- Guo, Q., Liu, L., & Barkla, B. J. (2019). Membrane lipid remodeling in response to salinity. *International Journal of Molecular Sciences*, *20*(17), 4264.
- Gupta, D., Pena, L. B., Romero-Puertas, M. C., Hernández, A., Inouhe, M., & Sandalio, L. M. (2017). NADPH oxidases differentially regulate ROS metabolism and nutrient uptake under cadmium toxicity. *Plant, Cell & Environment*, *40*(4), 509-526.
- Gupta, S., & Pandey, S. (2019, 2019-July-09). ACC Deaminase Producing Bacteria With Multifarious Plant Growth Promoting Traits Alleviates Salinity Stress in French Bean (*Phaseolus vulgaris*) Plants [Original Research]. *Frontiers in Microbiology*, *10*. <https://doi.org/10.3389/fmicb.2019.01506>
- Gupta, S., & Rashotte, A. M. (2012). Down-stream components of cytokinin signaling and the role of cytokinin throughout the plant. *Plant Cell Reports*, *31*(5), 801-812.
- Gupta, S., Schillaci, M., Walker, R., Smith, P., Watt, M., & Roessner, U. (2021). Alleviation of salinity stress in plants by endophytic plant-fungal symbiosis: Current knowledge, perspectives and future directions. *Plant and Soil*, *461*(1), 219-244.
- Gupta, S. V. K., Rupasinghe, T. W. T., Callahan, D. L., Natera, S. H., Smith, P. M., Hill, C. B., Roessner, U., & Boughton, B. A. (2019). Spatio-Temporal Metabolite and Elemental Profiling of Salt Stressed Barley Seeds During Initial Stages of Germination by MALDI-MSI and μ -XRF Spectrometry. *Frontiers in Plant Science*, *10*, 1139.
- Gururani, M. A., Upadhyaya, C. P., Baskar, V., Venkatesh, J., Nookaraju, A., & Park, S. W. (2013). Plant growth-promoting rhizobacteria enhance abiotic stress tolerance in *Solanum tuberosum* through inducing changes in the expression of ROS-scavenging enzymes and improved photosynthetic performance. *Journal of Plant Growth Regulation*, *32*(2), 245-258.
- Hall, A. E. (1992). Breeding for heat tolerance. *Plant Breed. Rev.*, *10*(2), 129-168.

- Hao, D. C., & Xiao, P. G. (2017, Jul). Rhizosphere Microbiota and Microbiome of Medicinal Plants: From Molecular Biology to Omics Approaches [Review]. *Chinese Herbal Medicines*, 9(3), 199-217. [https://doi.org/10.1016/s1674-6384\(17\)60097-2](https://doi.org/10.1016/s1674-6384(17)60097-2)
- Harayama, T., & Riezman, H. (2018). Understanding the diversity of membrane lipid composition. *Nature Reviews Molecular Cell Biology*, 19(5), 281-296.
- Harkewicz, R., & Dennis, E. A. (2011). Applications of mass spectrometry to lipids and membranes. *Annual Review of Biochemistry*, 80, 301.
- Hartler, J., Tharakan, R., Köfeler, H. C., Graham, D. R., & Thallinger, G. G. (2013). Bioinformatics tools and challenges in structural analysis of lipidomics MS/MS data. *Briefings in bioinformatics*, 14(3), 375-390.
- Hartmann, A., Schmid, M., Tuinen, D. v., & Berg, G. (2009). Plant-driven selection of microbes. *Plant and Soil*, 321(1), 235-257.
- Hartmann, M.-A. (1998). Plant sterols and the membrane environment. *Trends in Plant Science*, 3(5), 170-175.
- Harwood, J. L., & Harwood, J. L. (1998). *Plant lipid biosynthesis: fundamentals and agricultural applications* (Vol. 67). Cambridge University Press.
- Hasanuzzaman, M., Nahar, K., Alam, M. M., Roychowdhury, R., & Fujita, M. (2013). Physiological, Biochemical, and Molecular Mechanisms of Heat Stress Tolerance in Plants. *International Journal of Molecular Sciences*, 14(5), 9643-9684. <https://www.mdpi.com/1422-0067/14/5/9643>
- Hatfield, J. L., Boote, K. J., Kimball, B. A., Ziska, L. H., Izaurralde, R. C., Ort, D., Thomson, A. M., & Wolfe, D. (2011). Climate Impacts on Agriculture: Implications for Crop Production. *Agronomy Journal*, 103(2), 351-370. http://sfx.unimelb.hosted.exlibrisgroup.com/sfxlcl41?url_ver=Z39.88-2004&url_ctx_fmt=info%3Aofi%2Ffmt%3Akev%3Amtx%3Actx&rft_val_fmt=info%3Aofi%2Ffmt%3Akev%3Amtx%3Ajournal&rft.atitle=Climate%20Impacts%20on%20Agriculture%3A%20Implications%20for%20Crop%20Production&rft.aufirst=J.%20L.&rft.aulast=Hatfield&rft.date=2011&rft.epage=370&rft.genre=article&rft.issn=0002-1962&rft.issue=2&rft.jtitle=AGRONOMY%20JOURNAL&rft.pages=351-370&rft.spage=351&rft.stitle=AGRON%20J&rft.volume=103&rfr_id=info%3Asid%2Fwww.isinet.com%3AWoK%3AUA&rft.au=Boote%2C%20K.%20J.&rft.au=Kimb all%2C%20B.%20A.&rft.au=Ziska%2C%20L.%20H.&rft.au=Izaurralde%2C%20R.%20C.&rft_id=info%3Adoi%2F10.2134%2Fagronj2010.0303
- Hawes, M. C., Bengough, G., Cassab, G., & Ponce, G. (2002). Root caps and rhizosphere. *Journal of Plant Growth Regulation*, 21(4), 352-367.
- Hayat, R., Ali, S., Amara, U., Khalid, R., & Ahmed, I. (2010). Soil beneficial bacteria and their role in plant growth promotion: a review. *Annals of Microbiology*, 60(4), 579-598.
- Heckathorn, S. A., Giri, A., Mishra, S., & Bista, D. (2013). Heat stress and roots. *Climate change and plant abiotic stress tolerance*, 109-136.

- Hedden, P., & Thomas, S. G. (2012). Gibberellin biosynthesis and its regulation. *Biochemical Journal*, 444(1), 11-25.
- Hemme, D., Veyel, D., Mühlhaus, T., Sommer, F., Jüppner, J., Unger, A.-K., Sandmann, M., Fehrle, I., Schönfelder, S., & Steup, M. (2014). Systems-wide analysis of acclimation responses to long-term heat stress and recovery in the photosynthetic model organism *Chlamydomonas reinhardtii*. *The Plant Cell*, 26(11), 4270-4297.
- Hetu, M. F., Tremblay, L. J., & Lefebvre, D. D. (2005, Sep). High root biomass production in anchored *Arabidopsis* plants grown in axenic sucrose supplemented liquid culture [Article]. *Biotechniques*, 39(3), 345-+. <https://doi.org/10.2144/05393st02>
- Heydarian, Z., Yu, M., Gruber, M., Glick, B. R., Zhou, R., & Hegedus, D. D. (2016, 2016-December-16). Inoculation of Soil with Plant Growth Promoting Bacteria Producing 1-Aminocyclopropane-1-Carboxylate Deaminase or Expression of the Corresponding *acdS* Gene in Transgenic Plants Increases Salinity Tolerance in *Camelina sativa* [Original Research]. *Frontiers in Microbiology*, 7. <https://doi.org/10.3389/fmicb.2016.01966>
- Higashi, Y., Okazaki, Y., Myouga, F., Shinozaki, K., & Saito, K. (2015). Landscape of the lipidome and transcriptome under heat stress in *Arabidopsis thaliana*. *Scientific Reports*, 5, 10533.
- Higashi, Y., & Saito, K. (2019, 2019/07/01/). Lipidomic studies of membrane glycerolipids in plant leaves under heat stress. *Progress in lipid research*, 75, 100990. <https://doi.org/https://doi.org/10.1016/j.plipres.2019.100990>
- Hözl, G., & Dörmann, P. (2007, 2007/09/01/). Structure and function of glycolipids in plants and bacteria. *Progress in lipid research*, 46(5), 225-243. <https://doi.org/https://doi.org/10.1016/j.plipres.2007.05.001>
- Horai, H., Arita, M., Kanaya, S., Nihei, Y., Ikeda, T., Suwa, K., Ojima, Y., Tanaka, K., Tanaka, S., & Aoshima, K. (2010). MassBank: a public repository for sharing mass spectral data for life sciences. *Journal of mass spectrometry*, 45(7), 703-714.
- Horn, A., & Jaiswal, J. K. (2019). Chapter Four - Structural and signaling role of lipids in plasma membrane repair. In L. O. Andrade (Ed.), *Current Topics in Membranes* (Vol. 84, pp. 67-98). Academic Press. <https://doi.org/https://doi.org/10.1016/bs.ctm.2019.07.001>
- Hou, Q., Ufer, G., & Bartels, D. (2016). Lipid signalling in plant responses to abiotic stress. *Plant, Cell & Environment*, 39(5), 1029-1048. <https://doi.org/https://doi.org/10.1111/pce.12666>
- Howarth, C. J. (2005). of Tolerance to High Temperature. *Abiotic stresses: Plant resistance through breeding and molecular approaches*, 1920.

- Hsiao, A.-S., Haslam, R. P., Michaelson, L. V., Liao, P., Napier, J. A., & Chye, M.-L. (2014). Gene Expression in Plant Lipid Metabolism in Arabidopsis Seedlings. *PLoS ONE*, 9(9), e107372. <https://doi.org/10.1371/journal.pone.0107372>
- Hsieh, E.-J., Cheng, M.-C., & Lin, T.-P. (2013). Functional characterization of an abiotic stress-inducible transcription factor AtERF53 in Arabidopsis thaliana. *Plant Molecular Biology*, 82(3), 223-237.
- Hu, C., Luo, W., Xu, J., & Han, X. (2022). Recognition and avoidance OF ION source-generated artifacts IN lipidomics analysis. *Mass spectrometry reviews*, 41(1), 15-31.
- Hu, J., Mitchum, M. G., Barnaby, N., Ayele, B. T., Ogawa, M., Nam, E., Lai, W.-C., Hanada, A., Alonso, J. M., Ecker, J. R., Swain, S. M., Yamaguchi, S., Kamiya, Y., & Sun, T.-p. (2008). Potential Sites of Bioactive Gibberellin Production during Reproductive Growth in Arabidopsis *The Plant Cell*, 20(2), 320-336. <https://doi.org/10.1105/tpc.107.057752>
- Hu, T., & Zhang, J.-L. (2018). Mass-spectrometry-based lipidomics. *Journal of Separation Science*, 41(1), 351-372. <https://doi.org/10.1002/jssc.201700709>
- Huby, E., Napier, J. A., Baillieux, F., Michaelson, L. V., & Dhondt-Cordelier, S. (2020). Sphingolipids: towards an integrated view of metabolism during the plant stress response. *New Phytologist*, 225(2), 659-670. <https://doi.org/https://doi.org/10.1111/nph.15997>
- Hunter, P. (2016). Plant microbiomes and sustainable agriculture: deciphering the plant microbiome and its role in nutrient supply and plant immunity has great potential to reduce the use of fertilizers and biocides in agriculture. *EMBO reports*, 17(12), 1696-1699.
- Hurd, E. (1974). Phenotype and drought tolerance in wheat. *Agricultural Meteorology*, 14(1-2), 39-55.
- Illston, B. G., & Fiebrich, C. A. (2017). Horizontal and vertical variability of observed soil temperatures. *Geoscience Data Journal*, 4(1), 40-46. <https://doi.org/https://doi.org/10.1002/gdj3.47>
- IPCC. (2013). *Summary for Policymakers. In: Climate Change 2013: The Physical Science Basis. Contribution of Working Group I to the Fifth Assessment Report of the Intergovernmental Panel on Climate Change [Stocker, T.F., D. Qin, G.-K. Plattner, M. Tignor, S.K. Allen, J. Boschung, A. Nauels, Y. Xia, V. Bex and P.M. Midgley (eds.)]*.
- IPCC. (2014). *Climate Change 2014: Impacts, Adaptation, and Vulnerability. Part A: Global and Sectoral Aspects. Contribution of Working Group II to the Fifth Assessment Report of the Intergovernmental Panel on Climate Change (C. B. Field, V.R. Barros, D.J. Dokken, K.J. Mach, M.D. Mastrandrea, T.E. Bilir, M. Chatterjee, K.L. Ebi, Y.O. Estrada, R.C. Genova, B. Girma, E.S. Kissel, A.N. Levy, S. MacCracken, P.R. Mastrandrea, and L.L.White, Ed.)*. Cambridge University Press, Cambridge, United Kingdom and New York, NY, USA, 1132 pp.

- IPCC. (2021). *Climate Change 2021: The Physical Science Basis. Contribution of Working Group I to the Sixth Assessment Report of the Intergovernmental Panel on Climate Change* (V. Masson-Delmotte, P. Zhai, A. Pirani, S.L. Connors, C. Péan, S. Berger, N. Caud, Y. Chen, L. Goldfarb, M.I. Gomis, M. Huang, K. Leitzell, E. Lonnoy, J.B.R. Matthews, T.K. Maycock, T. Waterfield, O. Yelekçi, R. Yu, and B. Zhou, Ed.). Cambridge University Press, Cambridge, United Kingdom and New York, NY, USA, 2391 pp.
- Isayenkov, S., Mrosk, C., Stenzel, I., Strack, D., & Hause, B. (2005). Suppression of allene oxide cyclase in hairy roots of *Medicago truncatula* reduces jasmonate levels and the degree of mycorrhization with *Glomus intraradices*. *Plant Physiology*, *139*(3), 1401-1410.
- Issa, A., Esmaeel, Q., Sanchez, L., Courteaux, B., Guise, J.-F., Gibon, Y., Ballias, P., Clément, C., Jacquard, C., Vaillant-Gaveau, N., & Aït Barka, E. (2018, 2018-October-18). Impacts of *Paraburkholderia phytofirmans* Strain PsJN on Tomato (*Lycopersicon esculentum* L.) Under High Temperature [Original Research]. *Frontiers in Plant Science*, *9*. <https://doi.org/10.3389/fpls.2018.01397>
- Issartel, J., & Coiffard, C. (2011, 2011/01/01). Extreme longevity in trees: live slow, die old? *Oecologia*, *165*(1), 1-5. <https://doi.org/10.1007/s00442-010-1807-x>
- Jagadish, K. S. V., Kadam, N. N., Xiao, G., Melgar, R. J., Bahuguna, R. N., Quinones, C., Tamilselvan, A., Prasad, P. V. V., & Sparks, D. L. (2014). *Agronomic and Physiological Responses to High Temperature, Drought, and Elevated CO2 Interactions in Cereals. Advances in Agronomy* (Vol. 127). http://sfx.unimelb.hosted.exlibrisgroup.com/sfxlcl41?url_ver=Z39.88-2004&url_ctx_fmt=info%3Aofi%2Ffmt%3Akev%3Amtx%3Actx&rft_val_fmt=info%3Aofi%2Ffmt%3Akev%3Amtx%3Abook&rft.atitle=Agronomic%20and%20Physiological%20Responses%20to%20High%20Temperature%2C%20Drought%2C%20and%20Elevated%20CO2%20Interactions%20in%20Cereals&rft.aufirst=Krishna%20S.%20V.&rft.aulast=Jagadish&rft.btitle=ADVANCES%20IN%20AGRONOMY%2C%20VOL%20127&rft.date=2014&rft.epage=156&rft.genre=bookitem&rft.isbn=978-0-12-800131-8&rft.issn=0065-2113&rft.pages=111-156&rft.place=SAN%20DIEGO&rft.pub=ELSEVIER%20ACADEMIC%20PRESS%20INC&rft.series=Advances%20in%20Agronomy&rft.spage=111&rft.tpages=46&rft.volume=127&rft_id=info%3Aasid%2Fwww.isinet.com%3AWoK%3AUA&rft.au=Kadam%2C%20Niteen%20N.&rft.au=Xiao%2C%20Gui&rft.au=Melgar%2C%20Reeeliza%20Jean&rft.au=Bahuguna%2C%20Rajeev%20N.&rft_id=info%3Adoi%2F10.1016%2FB978-0-12-800131-8.00003-0
- Jang, J.-H., Lee, C. S., Hwang, D., & Ryu, S. H. (2012). Understanding of the roles of phospholipase D and phosphatidic acid through their binding partners. *Progress in lipid research*, *51*(2), 71-81.
- Janssen, P. H. (2006). Identifying the Dominant Soil Bacterial Taxa in Libraries of 16S rRNA and 16S rRNA Genes. *Applied and Environmental Microbiology*, *72*(3), 1719-1728. <https://doi.org/doi:10.1128/AEM.72.3.1719-1728.2006>

- Jeudy, C., Adrian, M., Baussard, C., Bernard, C., Bernaud, E., Bourion, V., Busset, H., Cabrera-Bosquet, L., Cointault, F., & Han, S. (2016). RhizoTubes as a new tool for high throughput imaging of plant root development and architecture: test, comparison with pot grown plants and validation. *Plant Methods*, *12*(1), 1-18.
- Jia, J., Zhou, J., Shi, W., Cao, X., Luo, J., Polle, A., & Luo, Z.-B. (2017). Comparative transcriptomic analysis reveals the roles of overlapping heat-/drought-responsive genes in poplars exposed to high temperature and drought. *Scientific Reports*, *7*(1), 1-17.
- Jiang, H., Xu, Z., Aluru, M. R., & Dong, L. (2014). Plant chip for high-throughput phenotyping of Arabidopsis. *Lab on a Chip*, *14*(7), 1281-1293.
- Jin, H., & Zhu, Z. (2019). Dark, Light, and Temperature: Key Players in Plant Morphogenesis. *Plant Physiology*, *180*(4), 1793-1802. <https://doi.org/10.1104/pp.19.00331>
- Jones, D. L., Nguyen, C., & Finlay, R. D. (2009, 2009/08/01). Carbon flow in the rhizosphere: carbon trading at the soil–root interface. *Plant and Soil*, *321*(1), 5-33. <https://doi.org/10.1007/s11104-009-9925-0>
- Jones, J. D., & Dangl, J. L. (2006). The plant immune system. *Nature*, *444*(7117), 323.
- Jones, L. L., McDonald, D. A., & Borum, P. R. (2010, Jan). Acylcarnitines: role in brain. *Prog Lipid Res*, *49*(1), 61-75. <https://doi.org/10.1016/j.plipres.2009.08.004>
- Kachroo, P., Venugopal, S. C., Navarre, D. A., Lapchyk, L., & Kachroo, A. (2005). Role of salicylic acid and fatty acid desaturation pathways in ssi2-mediated signaling. *Plant Physiology*, *139*(4), 1717-1735.
- Kalscheuer, R., Stöveken, T., Malkus, U., Reichelt, R., Golyshin, P. N., Sabirova, J. S., Ferrer, M., Timmis, K. N., & Steinbüchel, A. (2007). Analysis of storage lipid accumulation in *Alcanivorax borkumensis*: evidence for alternative triacylglycerol biosynthesis routes in bacteria. *Journal of bacteriology*, *189*(3), 918-928.
- Kandel, S. L., Joubert, P. M., & Doty, S. L. (2017). Bacterial endophyte colonization and distribution within plants. *Microorganisms*, *5*(4), 77.
- Kasim, W. A., Gaafar, R. M., Abou-Ali, R. M., Omar, M. N., & Hewait, H. M. (2016, 2016/12/01/). Effect of biofilm forming plant growth promoting rhizobacteria on salinity tolerance in barley. *Annals of Agricultural Sciences*, *61*(2), 217-227. <https://doi.org/https://doi.org/10.1016/j.aos.2016.07.003>
- Kehelpannala, C., Rupasinghe, T., Pasha, A., Esteban, E., Hennessy, T., Bradley, D., Ebert, B., Provart, N. J., & Roessner, U. (2021). An Arabidopsis lipid map reveals differences between tissues and dynamic changes throughout development [<https://doi.org/10.1111/tpj.15278>]. *The Plant Journal*, *107*(1), 287-302. <https://doi.org/https://doi.org/10.1111/tpj.15278>
- Kehelpannala, C., Rupasinghe, T. W. T., Hennessy, T., Bradley, D., Ebert, B., & Roessner, U. (2020, 2020/12/03). A comprehensive comparison of four methods for extracting lipids

from Arabidopsis tissues. *Plant Methods*, 16(1), 155. <https://doi.org/10.1186/s13007-020-00697-z>

- Khan, A. G. (2005). Role of soil microbes in the rhizospheres of plants growing on trace metal contaminated soils in phytoremediation. *Journal of Trace Elements in Medicine and Biology*, 18(4), 355-364.
- Khan, M. A., Asaf, S., Khan, A. L., Jan, R., Kang, S.-M., Kim, K.-M., & Lee, I.-J. (2020). Thermotolerance effect of plant growth-promoting *Bacillus cereus* SA1 on soybean during heat stress. *BMC microbiology*, 20(1), 1-14.
- Khan, M. A., Gemenet, D. C., & Villordon, A. (2016, 2016-November-01). Root System Architecture and Abiotic Stress Tolerance: Current Knowledge in Root and Tuber Crops [Review]. *Frontiers in Plant Science*, 7. <https://doi.org/10.3389/fpls.2016.01584>
- Khan, N., & Bano, A. (2019). Exopolysaccharide producing rhizobacteria and their impact on growth and drought tolerance of wheat grown under rainfed conditions. *PLoS ONE*, 14(9), e0222302.
- Khan, N., Bano, A., & Babar, M. A. (2019). Metabolic and physiological changes induced by plant growth regulators and plant growth promoting rhizobacteria and their impact on drought tolerance in *Cicer arietinum* L. *PLoS ONE*, 14(3), e0213040.
- Khoury, S., Canlet, C., Lacroix, M. Z., Berdeaux, O., Jouhet, J., & Bertrand-Michel, J. (2018). Quantification of lipids: model, reality, and compromise. *Biomolecules*, 8(4), 174.
- Kimberlin, A. N., Majumder, S., Han, G., Chen, M., Cahoon, R. E., Stone, J. M., Dunn, T. M., & Cahoon, E. B. (2013). Arabidopsis 56-amino acid serine palmitoyltransferase-interacting proteins stimulate sphingolipid synthesis, are essential, and affect mycotoxin sensitivity. *The Plant Cell*, 25(11), 4627-4639.
- Kind, T., Liu, K.-H., Lee, D. Y., DeFelice, B., Meissen, J. K., & Fiehn, O. (2013). LipidBlast in silico tandem mass spectrometry database for lipid identification. *Nature Methods*, 10(8), 755-758.
- Kinet, J. M., & Peet, M. M. (1997). Tomato. In H. C. Wien (Ed.), *The Physiology of Vegetable Crops* (pp. 207-258). CAB International.
- Koelmel, J. P., Kroeger, N. M., Gill, E. L., Ulmer, C. Z., Bowden, J. A., Patterson, R. E., Yost, R. A., & Garrett, T. J. (2017). Expanding lipidome coverage using LC-MS/MS data-dependent acquisition with automated exclusion list generation. *Journal of the American Society for Mass Spectrometry*, 28(5), 908-917.
- Koevoets, I. T., Venema, J. H., Elzenga, J. T. M., & Testerink, C. (2016, 2016-August-31). Roots Withstanding their Environment: Exploiting Root System Architecture Responses to Abiotic Stress to Improve Crop Tolerance [Review]. *Frontiers in Plant Science*, 7. <https://doi.org/10.3389/fpls.2016.01335>

- Kono, N., & Arai, H. (2015, 2015/01/01). Intracellular Transport of Fat-Soluble Vitamins A and E [<https://doi.org/10.1111/tra.12231>]. *Traffic*, *16*(1), 19-34. <https://doi.org/https://doi.org/10.1111/tra.12231>
- Kopischke, M., Westphal, L., Schneeberger, K., Clark, R., Ossowski, S., Wewer, V., Fuchs, R., Landtag, J., Hause, G., & Dörmann, P. (2013). Impaired sterol ester synthesis alters the response of *Arabidopsis thaliana* to *Phytophthora infestans*. *The Plant Journal*, *73*(3), 456-468.
- Kost, T., Stopnisek, N., Agnoli, K., Eberl, L., & Weisskopf, L. (2014). Oxalotrophy, a widespread trait of plant-associated Burkholderia species, is involved in successful root colonization of lupin and maize by Burkholderia phytofirmans. *Frontiers in Microbiology*, *4*, 421.
- Kozlov, M. M., Campelo, F., Liska, N., Chernomordik, L. V., Marrink, S. J., & McMahon, H. T. (2014). Mechanisms shaping cell membranes. *Current opinion in cell biology*, *29*, 53-60.
- Kuang, W., Sanow, S., Kelm, J. M., Müller Linow, M., Andeer, P., Kohlheyer, D., Northen, T., Vogel, J. P., Watt, M., & Arsova, B. (2022). N-dependent dynamics of root growth and nitrate and ammonium uptake are altered by the bacterium *Herbaspirillum seropedicae* in the cereal model *Brachypodium distachyon*. *Journal of Experimental Botany*. <https://doi.org/10.1093/jxb/erac184>
- Kuijken, R. C., van Eeuwijk, F. A., Marcelis, L. F., & Bouwmeester, H. J. (2015). Root phenotyping: from component trait in the lab to breeding. *Journal of Experimental Botany*, *66*(18), 5389-5401.
- Kulkarni, G., Busset, N., Molinaro, A., Gargani, D., Chaintreuil, C., Silipo, A., Giraud, E., & Newman, D. K. (2015). Specific hopanoid classes differentially affect free-living and symbiotic states of *Bradyrhizobium diazoefficiens*. *MBio*, *6*(5).
- Kumar, A., & Verma, J. P. (2018, 2018/03/01). Does plant—Microbe interaction confer stress tolerance in plants: A review? *Microbiological research*, *207*, 41-52. <https://doi.org/https://doi.org/10.1016/j.micres.2017.11.004>
- Kumar, S., Muthusamy, S. K., Mishra, C. N., Gupta, V., & Venkatesh, K. (2018). Importance of genomic selection in crop improvement and future prospects. *Advanced Molecular Plant Breeding: Meeting the Challenge of Food Security*; CRC Press: Boca Raton, FL, USA,
- Laha, N. P., Giehl, R. F. H., Riemer, E., Qiu, D., Pullagurla, N. J., Schneider, R., Dhir, Y. W., Yadav, R., Mihiret, Y. E., Gaugler, P., Gaugler, V., Mao, H., Zheng, N., von Wirén, N., Saiardi, A., Bhattacharjee, S., Jessen, H. J., Laha, D., & Schaaf, G. (2022). INOSITOL (1,3,4) TRIPHOSPHATE 5/6 KINASE1-dependent inositol polyphosphates regulate auxin responses in *Arabidopsis*. *Plant Physiology*. <https://doi.org/10.1093/plphys/kiac425>

- Larkindale, J., & Huang, B. (2004). Thermotolerance and antioxidant systems in *Agrostis stolonifera*: involvement of salicylic acid, abscisic acid, calcium, hydrogen peroxide, and ethylene. *Journal of Plant Physiology*, *161*(4), 405-413.
- Larsson, C., Sommarin, M., & Widell, S. (1994). [44] Isolation of highly purified plant plasma membranes and separation of inside-out and right-side-out vesicles. In *Methods in Enzymology* (Vol. 228, pp. 451-469). Academic Press. [https://doi.org/https://doi.org/10.1016/0076-6879\(94\)28046-0](https://doi.org/https://doi.org/10.1016/0076-6879(94)28046-0)
- LaRue, T., Lindner, H., Srinivas, A., Exposito-Alonso, M., Lobet, G., & Dinneny, J. R. (2022). Uncovering natural variation in root system architecture and growth dynamics using a robotics-assisted phenomics platform. *eLife*, *11*, e76968.
- Le Bot, J., Serra, V., Fabre, J., Draye, X., & Adamowicz, S. (2010). DART: a software to analyse root system architecture and development from captured images. *Plant and Soil*, *326*(1), 261-273.
- Le Marié, C., Kirchgessner, N., Flütsch, P., Pfeifer, J., Walter, A., & Hund, A. (2016). RADIX: rhizoslide platform allowing high throughput digital image analysis of root system expansion. *Plant Methods*, *12*(1), 1-15.
- Lee, H.-C., & Yokomizo, T. (2018, 2018/10/07/). Applications of mass spectrometry-based targeted and non-targeted lipidomics. *Biochemical and biophysical research communications*, *504*(3), 576-581. <https://doi.org/https://doi.org/10.1016/j.bbrc.2018.03.081>
- Leeder, A. C., Palma-Guerrero, J., & Glass, N. L. (2011). The social network: deciphering fungal language. *Nature Reviews Microbiology*, *9*(6), 440-451.
- Leff, J. W., Del Tredici, P., Friedman, W. E., & Fierer, N. (2015). Spatial structuring of bacterial communities within individual Ginkgo biloba trees. *Environ Microbiol*, *17*. <https://doi.org/10.1111/1462-2920.12695>
- Légeret, B., Schulz-Raffelt, M., Nguyen, H., Auroy, P., Beisson, F., Peltier, G., Blanc, G., & Li-Beisson, Y. (2016). Lipidomic and transcriptomic analyses of *Chlamydomonas reinhardtii* under heat stress unveil a direct route for the conversion of membrane lipids into storage lipids. *Plant, Cell & Environment*, *39*(4), 834-847.
- Lerouge, P., Roche, P., Faucher, C., Maillet, F., Truchet, G., Promé, J. C., & Dénarié, J. (1990). Symbiotic host-specificity of *Rhizobium meliloti* is determined by a sulphated and acylated glucosamine oligosaccharide signal. *Nature*, *344*(6268), 781-784.
- Li, Q., Zheng, Q., Shen, W., Cram, D., Fowler, D. B., Wei, Y., & Zou, J. (2015). Understanding the biochemical basis of temperature-induced lipid pathway adjustments in plants. *The Plant Cell*, tpc. 114.134338.
- Liang, H., Yao, N., Song, J. T., Luo, S., Lu, H., & Greenberg, J. T. (2003). Ceramides modulate programmed cell death in plants. *Genes & development*, *17*(21), 2636-2641.

- Lim, G.-H., Singhal, R., Kachroo, A., & Kachroo, P. (2017). Fatty acid–and lipid-mediated signaling in plant defense. *Annual review of phytopathology*, *55*, 505-536.
- Lin, Z., Zhong, S., & Grierson, D. (2009). Recent advances in ethylene research. *Journal of Experimental Botany*, *60*(12), 3311-3336.
- Liu, J., & Conboy, J. C. (2005). 1, 2-diacyl-phosphatidylcholine flip-flop measured directly by sum-frequency vibrational spectroscopy. *Biophysical journal*, *89*(4), 2522-2532.
- Liu, W., Zhou, X., Li, G., Li, L., Kong, L., Wang, C., Zhang, H., & Xu, J.-R. (2011). Multiple plant surface signals are sensed by different mechanisms in the rice blast fungus for appressorium formation. *PLoS Pathog*, *7*(1), e1001261.
- Liu, X., Dong, X., & Leskovar, D. I. (2016). Ground penetrating radar for underground sensing in agriculture: a review. *International Agrophysics*, *30*(4).
- Liu, X., & Huang, B. (2000). Heat stress injury in relation to membrane lipid peroxidation in creeping bentgrass. *Crop Science*, *40*(2), 503-510.
- Liu, X. X., Ma, D. K., Zhang, Z. Y., Wang, S. W., Du, S., Deng, X. P., & Yin, L. N. (2019). Plant lipid remodeling in response to abiotic stresses [Review]. *Environmental and Experimental Botany*, *165*, 174-184. <https://doi.org/10.1016/j.envexpbot.2019.06.005>
- Liu, Z., Pillay, V., & Nowak, J. (1993). In vitro culture of watermelon and cantaloupe with and without beneficial bacterium. International Symposium on Cultivar Improvement of Horticultural Crops. Part 1: Vegetable Crops 402,
- Lobell, D. B., & Gourdjji, S. M. (2012, Dec). The Influence of Climate Change on Global Crop Productivity [Article]. *Plant Physiology*, *160*(4), 1686-1697. <https://doi.org/10.1104/pp.112.208298>
- Lobet, G., Pagès, L., & Draye, X. (2011). A novel image-analysis toolbox enabling quantitative analysis of root system architecture. *Plant Physiology*, *157*(1), 29-39.
- Lodish, H., Berk, A., Kaiser, C. A., Krieger, M., Scott, M. P., Bretscher, A., Ploegh, H., & Matsudaira, P. (2008). *Molecular cell biology*. Macmillan.
- Löfgren, L., Ståhlman, M., Forsberg, G.-B., Saarinen, S., Nilsson, R., & Hansson, G. I. (2012). The BUMÉ method: a novel automated chloroform-free 96-well total lipid extraction method for blood plasma. *Journal of lipid research*, *53*(8), 1690-1700.
- López-Bascón, M. A., Calderón-Santiago, M., & Priego-Capote, F. (2016). Confirmatory and quantitative analysis of fatty acid esters of hydroxy fatty acids in serum by solid phase extraction coupled to liquid chromatography tandem mass spectrometry. *Analytica chimica acta*, *943*, 82-88.
- López-Bucio, J., Acevedo-Hernández, G., Ramírez-Chávez, E., Molina-Torres, J., & Herrera-Estrella, L. (2006). Novel signals for plant development. *Current opinion in plant biology*, *9*(5), 523-529.

- López-Lara, I. M., Sohlenkamp, C., & Geiger, O. (2003). Membrane lipids in plant-associated bacteria: their biosyntheses and possible functions. *Molecular Plant-Microbe Interactions*, *16*(7), 567-579.
- López-Ráez, J. A., Verhage, A., Fernández, I., García, J. M., Azcón-Aguilar, C., Flors, V., & Pozo, M. J. (2010). Hormonal and transcriptional profiles highlight common and differential host responses to arbuscular mycorrhizal fungi and the regulation of the oxylipin pathway. *Journal of Experimental Botany*, *61*(10), 2589-2601.
- Lube, V., Noyan, M. A., Przybysz, A., Salama, K., & Blilou, I. (2022). MultipleXLab: A high-throughput portable live-imaging root phenotyping platform using deep learning and computer vision. *Plant Methods*, *18*(1), 1-22.
- Lugtenberg, B., & Kamilova, F. (2009). Plant-growth-promoting rhizobacteria. *Annual review of microbiology*, *63*, 541-556.
- Luo, H., Xu, H., Chu, C., He, F., & Fang, S. (2020, 2020-February-26). High Temperature can Change Root System Architecture and Intensify Root Interactions of Plant Seedlings [Original Research]. *Frontiers in Plant Science*, *11*. <https://doi.org/10.3389/fpls.2020.00160>
- Luttgeharm, K. D., Chen, M., Mehra, A., Cahoon, R. E., Markham, J. E., & Cahoon, E. B. (2015). Overexpression of Arabidopsis Ceramide Synthases Differentially Affects Growth, Sphingolipid Metabolism, Programmed Cell Death, and Mycotoxin Resistance. *Plant Physiology*, *169*(2), 1108-1117. <https://doi.org/10.1104/pp.15.00987>
- Lynch, J. (1995). Root architecture and plant productivity. *Plant Physiology*, *109*(1), 7.
- Lynch, J. P. (2007). Roots of the second green revolution. *Australian Journal of Botany*, *55*(5), 493-512.
- Lynch, J. P. (2022). Harnessing root architecture to address global challenges. *The Plant Journal*, *109*(2), 415-431. <https://doi.org/https://doi.org/10.1111/tpj.15560>
- Lynch, J. P., & Brown, K. M. (2012). New roots for agriculture: exploiting the root phenome. *Philosophical Transactions of the Royal Society B: Biological Sciences*, *367*(1595), 1598-1604.
- Lynch, J. P., & Clair, S. B. S. (2004). Mineral stress: the missing link in understanding how global climate change will affect plants in real world soils. *Field Crops Research*, *90*(1), 101-115.
- Macabuhay, A., Arsova, B., Walker, R., Johnson, A., Watt, M., & Roessner, U. (2022, 2022/02/01). Modulators or facilitators? Roles of lipids in plant root-microbe interactions. *Trends in Plant Science*, *27*(2), 180-190. <https://doi.org/https://doi.org/10.1016/j.tplants.2021.08.004>
- Macabuhay, A., Arsova, B., Watt, M., Nagel, K. A., Lenz, H., Putz, A., Adels, S., Müller-Linow, M., Kelm, J., & Johnson, A. A. (2022). Plant Growth Promotion and Heat Stress Amelioration in Arabidopsis Inoculated with Paraburkholderia phytofirmans PsJN

- Rhizobacteria Quantified with the GrowScreen-Agar II Phenotyping Platform. *Plants*, *11*(21), 2927.
- Macabuhay, A., Houshmandfar, A., Nuttall, J., Fitzgerald, G. J., Tausz, M., & Tausz-Posch, S. (2018). Can elevated CO₂ buffer the effects of heat waves on wheat in a dryland cropping system? *Environmental and Experimental Botany*, *155*, 578-588.
- Macková, H., Hronková, M., Dobrá, J., Turečková, V., Novák, O., Lubovská, Z., Motyka, V., Haisel, D., Hájek, T., & Prášil, I. T. (2013). Enhanced drought and heat stress tolerance of tobacco plants with ectopically enhanced cytokinin oxidase/dehydrogenase gene expression. *Journal of Experimental Botany*, *64*(10), 2805-2815.
- Maestri, E., Klueva, N., Perrotta, C., Gulli, M., Nguyen, H. T., & Marmiroli, N. (2002). Molecular genetics of heat tolerance and heat shock proteins in cereals. *Plant Molecular Biology*, *48*(5), 667-681.
- Maillet, F., Poinot, V., André, O., Puech-Pagès, V., Haouy, A., Gueunier, M., Cromer, L., Giraudet, D., Formey, D., & Niebel, A. (2011). Fungal lipochitoooligosaccharide symbiotic signals in arbuscular mycorrhiza. *Nature*, *469*(7328), 58-63.
- Maitra, S., Pramanick, B., Dey, P., Bhadra, P., Shankar, T., & Anand, K. (2021). Thermotolerant Soil Microbes and Their Role in Mitigation of Heat Stress in Plants. In A. N. Yadav (Ed.), *Soil Microbiomes for Sustainable Agriculture: Functional Annotation* (pp. 203-242). Springer International Publishing. https://doi.org/10.1007/978-3-030-73507-4_8
- Mandal, M. K., Chandra-Shekara, A., Jeong, R.-D., Yu, K., Zhu, S., Chanda, B., Navarre, D., Kachroo, A., & Kachroo, P. (2012). Oleic acid-dependent modulation of NITRIC OXIDE ASSOCIATED1 protein levels regulates nitric oxide-mediated defense signaling in Arabidopsis. *The Plant Cell*, *24*(4), 1654-1674.
- Mandal, S. M., Chakraborty, D., & Dey, S. (2010, 2010/04/01). Phenolic acids act as signaling molecules in plant-microbe symbioses. *Plant signaling & behavior*, *5*(4), 359-368. <https://doi.org/10.4161/psb.5.4.10871>
- Manolio, T. A. (2010). Genomewide association studies and assessment of the risk of disease. *New England journal of medicine*, *363*(2), 166-176.
- Marchant, R., Franzetti, A., Pavlostathis, S. G., Tas, D. O., Erdbrügger, I., Únyayar, A., Mazmanci, M. A., & Banat, I. M. (2008). Thermophilic bacteria in cool temperate soils: are they metabolically active or continually added by global atmospheric transport? *Applied microbiology and biotechnology*, *78*(5), 841-852.
- Martínez, E., Cosnahan, R. K., Wu, M., Gadila, S. K., Quick, E. B., Mobley, J. A., & Campos-Gómez, J. (2019, 2019/02/15). Oxylipins mediate cell-to-cell communication in *Pseudomonas aeruginosa*. *Communications Biology*, *2*(1), 66. <https://doi.org/10.1038/s42003-019-0310-0>
- Martins, S., Montiel-Jorda, A., Cayrel, A., Huguet, S., Roux, C. P.-L., Ljung, K., & Vert, G. (2017, 2017/08/21). Brassinosteroid signaling-dependent root responses to prolonged

- elevated ambient temperature. *Nature Communications*, 8(1), 309. <https://doi.org/10.1038/s41467-017-00355-4>
- Matyash, V., Liebisch, G., Kurzchalia, T. V., Shevchenko, A., & Schwudke, D. (2008). Lipid extraction by methyl-tert-butyl ether for high-throughput lipidomics. *Journal of lipid research*, 49(5), 1137-1146.
- Maurel, C., Boursiac, Y., Luu, D.-T., Santoni, V., Shahzad, Z., & Verdoucq, L. (2015). Aquaporins in plants. *Physiological reviews*, 95(4), 1321-1358.
- Mc Michael, B. L., & Burke, J. J. (2002). Temperature effects on root growth. In *Plant Roots* (pp. 1120-1138). CRC Press.
- McLellan, C. A., Turbyville, T. J., Wijeratne, E. M. K., Kerschen, A., Vierling, E., Queitsch, C., Whitesell, L., & Gunatilaka, A. A. L. (2007). A Rhizosphere Fungus Enhances Arabidopsis Thermotolerance through Production of an HSP90 Inhibitor. *Plant Physiology*, 145(1), 174-182. <https://doi.org/10.1104/pp.107.101808>
- McMichael, B., & Burke, J. (1994). Metabolic activity of cotton roots in response to temperature. *Environmental and Experimental Botany*, 34(2), 201-206.
- Meena, K. K., Sorty, A. M., Bitla, U. M., Choudhary, K., Gupta, P., Pareek, A., Singh, D. P., Prabha, R., Sahu, P. K., Gupta, V. K., Singh, H. B., Krishanani, K. K., & Minhas, P. S. (2017, 2017-February-09). Abiotic Stress Responses and Microbe-Mediated Mitigation in Plants: The Omics Strategies [Review]. *Frontiers in Plant Science*, 8(172). <https://doi.org/10.3389/fpls.2017.00172>
- Meinke, D. W., Cherry, J. M., Dean, C., Rounsley, S. D., & Koornneef, M. (1998). Arabidopsis thaliana: a model plant for genome analysis. *Science*, 282(5389), 662-682.
- Melnik, A. V., da Silva, R. R., Hyde, E. R., Aksenov, A. A., Vargas, F., Bouslimani, A., Protsyuk, I., Jarmusch, A. K., Tripathi, A., & Alexandrov, T. (2017). Coupling targeted and untargeted mass spectrometry for metabolome-microbiome-wide association studies of human fecal samples. *Analytical Chemistry*, 89(14), 7549-7559.
- Men, Y., Yu, Q., Chen, Z., Wang, J., Huang, Y., & Guo, H. (2012). A high-throughput imaging system to quantitatively analyze the growth dynamics of plant seedlings. *Integrative Biology*, 4(8), 945-952. <https://doi.org/10.1039/c2ib20020a>
- Mendes, R., Garbeva, P., & Raaijmakers, J. M. (2013). The rhizosphere microbiome: significance of plant beneficial, plant pathogenic, and human pathogenic microorganisms. *FEMS Microbiology Reviews*, 37(5), 634-663. <https://doi.org/10.1111/1574-6976.12028>
- Metcalf, N. B., & Monaghan, P. (2003, 2003/09/01/). Growth versus lifespan: perspectives from evolutionary ecology. *Experimental Gerontology*, 38(9), 935-940. [https://doi.org/https://doi.org/10.1016/S0531-5565\(03\)00159-1](https://doi.org/https://doi.org/10.1016/S0531-5565(03)00159-1)

- Millner, A., Lizardo, D. Y., & Atilla-Gokcumen, G. E. (2020). Untargeted lipidomics highlight the depletion of deoxyceramides during therapy-induced senescence. *Proteomics*, *20*(10), 2000013.
- Minami, A., Fujiwara, M., Furuto, A., Fukao, Y., Yamashita, T., Kamo, M., Kawamura, Y., & Uemura, M. (2009). Alterations in detergent-resistant plasma membrane microdomains in *Arabidopsis thaliana* during cold acclimation. *Plant and Cell Physiology*, *50*(2), 341-359.
- Miotto-Vilanova, L., Jacquard, C., Courteaux, B., Wortham, L., Michel, J., Clément, C., Barka, E. A., & Sanchez, L. (2016). Burkholderia phytofirmans PsJN confers grapevine resistance against Botrytis cinerea via a direct antimicrobial effect combined with a better resource mobilization. *Frontiers in Plant Science*, *7*, 1236.
- Mishkind, M., Vermeer, J. E. M., Darwish, E., & Munnik, T. (2009). Heat stress activates phospholipase D and triggers PIP2 accumulation at the plasma membrane and nucleus. *The Plant Journal*, *60*(1), 10-21. <https://doi.org/https://doi.org/10.1111/j.1365-313X.2009.03933.x>
- Mishra, M. K., Singh, G., Tiwari, S., Singh, R., Kumari, N., & Misra, P. (2015). Characterization of *Arabidopsis* sterol glycosyltransferase TTG15/UGT80B1 role during freeze and heat stress. *Plant signaling & behavior*, *10*(12), e1075682.
- Mitchell-Olds, T. (2001). *Arabidopsis thaliana* and its wild relatives: a model system for ecology and evolution. *Trends in Ecology & Evolution*, *16*(12), 693-700. [https://doi.org/https://doi.org/10.1016/S0169-5347\(01\)02291-1](https://doi.org/https://doi.org/10.1016/S0169-5347(01)02291-1)
- Mittler, R., & Blumwald, E. (2010). Genetic engineering for modern agriculture: challenges and perspectives. *Annual review of plant biology*, *61*(1), 443-462.
- Mohammadi, M., Burbank, L., & Roper, M. C. (2012). Biological role of pigment production for the bacterial phytopathogen *Pantoea stewartii* subsp. *stewartii*. *Applied and Environmental Microbiology*, *78*(19), 6859-6865.
- Monnet, V., Juillard, V., & Gardan, R. (2016). Peptide conversations in Gram-positive bacteria. *Critical reviews in microbiology*, *42*(3), 339-351.
- Morcillo, R. J., & Manzanera, M. (2021). The effects of plant-associated bacterial exopolysaccharides on plant abiotic stress tolerance. *Metabolites*, *11*(6), 337.
- Mosblech, A., Feussner, I., & Heilmann, I. (2009, 2009/06/01/). Oxylipins: Structurally diverse metabolites from fatty acid oxidation. *Plant Physiology and Biochemistry*, *47*(6), 511-517. <https://doi.org/https://doi.org/10.1016/j.plaphy.2008.12.011>
- Moubayidin, L., Di Mambro, R., Sozzani, R., Pacifici, E., Salvi, E., Terpstra, I., Bao, D., Van Dijken, A., Ioio, R. D., & Perilli, S. (2013). Spatial coordination between stem cell activity and cell differentiation in the root meristem. *Developmental cell*, *26*(4), 405-415.

- Mueckler, M., & Thorens, B. (2013). The SLC2 (GLUT) family of membrane transporters. *Molecular aspects of medicine*, 34(2-3), 121-138.
- Mueller, S. P., Unger, M., Guender, L., Fekete, A., & Mueller, M. J. (2017). Phospholipid: diacylglycerol acyltransferase-mediated triacylglycerol synthesis augments basal thermotolerance. *Plant Physiology*, 175(1), 486-497.
- Müller-Linow, M. (2022). A versatile tool for semantic plant segmentation via color space thresholding. <https://doi.org/https://doi.org/10.5281/zenodo.6443757>
- Müller-Linow, M., Pinto-Espinosa, F., Scharr, H., & Rascher, U. (2015, 2015/02/26). The leaf angle distribution of natural plant populations: assessing the canopy with a novel software tool. *Plant Methods*, 11(1), 11. <https://doi.org/10.1186/s13007-015-0052-z>
- Munnik, T. (2010). *Lipid signaling in plants. [electronic resource]* [Bibliographies Non-fiction Electronic document]. Heidelberg ; New York : Springer, 2010. <https://ezp.lib.unimelb.edu.au/login?url=https://search.ebscohost.com/login.aspx?direct=true&db=cat00006a&AN=melb.b4312536&site=eds-live&scope=site> <http://dx.doi.org.ezp.lib.unimelb.edu.au/10.1007/978-3-642-03873-0>
- Munnik, T., & Testerink, C. (2009). Plant phospholipid signaling:“in a nutshell”. *Journal of lipid research*, 50, S260-S265.
- Munns, R., James, R. A., & Läuchli, A. (2006). Approaches to increasing the salt tolerance of wheat and other cereals. *Journal of Experimental Botany*, 57(5), 1025-1043.
- Munns, R., James, R. A., Xu, B., Athman, A., Conn, S. J., Jordans, C., Byrt, C. S., Hare, R. A., Tyerman, S. D., & Tester, M. (2012). Wheat grain yield on saline soils is improved by an ancestral Na⁺ transporter gene. *Nature biotechnology*, 30(4), 360-364.
- Murakami, Y., Tsuyama, M., Kobayashi, Y., Kodama, H., & Iba, K. (2000). Trienoic Fatty Acids and Plant Tolerance of High Temperature. *Science*, 287(5452), 476-479. <https://doi.org/10.1126/science.287.5452.476>
- Murate, M., & Kobayashi, T. (2016, 2016/01/01/). Revisiting transbilayer distribution of lipids in the plasma membrane. *Chemistry and Physics of Lipids*, 194, 58-71. <https://doi.org/https://doi.org/10.1016/j.chemphyslip.2015.08.009>
- Nafees, M., Ali, S., Naveed, M., & Rizwan, M. (2018, 2018/03/01). Efficiency of biogas slurry and Burkholderia phytofirmans PsJN to improve growth, physiology, and antioxidant activity of Brassica napus L. in chromium-contaminated soil. *Environmental Science and Pollution Research*, 25(7), 6387-6397. <https://doi.org/10.1007/s11356-017-0924-z>
- Nagel, K. A., Kastenholz, B., Jahnke, S., Van Dusschoten, D., Aach, T., Mühlich, M., Truhn, D., Scharr, H., Terjung, S., & Walter, A. (2009). Temperature responses of roots: impact on growth, root system architecture and implications for phenotyping. *Functional Plant Biology*, 36(11), 947-959.

- Nagel, K. A., Lenz, H., Kastenholz, B., Gilmer, F., Averagesch, A., Putz, A., Heinz, K., Fischbach, A., Scharr, H., Fiorani, F., Walter, A., & Schurr, U. (2020, 2020/06/23). The platform GrowScreen-Agar enables identification of phenotypic diversity in root and shoot growth traits of agar grown plants. *Plant Methods*, *16*(1), 89. <https://doi.org/10.1186/s13007-020-00631-3>
- Nagel, K. A., Putz, A., Gilmer, F., Heinz, K., Fischbach, A., Pfeifer, J., Faget, M., Blossfeld, S., Ernst, M., Dimaki, C., Kastenholz, B., Kleinert, A.-K., Galinski, A., Scharr, H., Fiorani, F., & Schurr, U. (2012). GROWSCREEN-Rhizo is a novel phenotyping robot enabling simultaneous measurements of root and shoot growth for plants grown in soil-filled rhizotrons. *Functional Plant Biology*, *39*(11), 891-904. <https://doi.org/https://doi.org/10.1071/FP12023>
- Nakamoto, H., & Hiyama, T. (1999). Heat-shock proteins and temperature stress. *Handbook of plant and crop stress*. Marcel Dekker, New York, 399-416.
- Nakamura, Y., Teo, N. Z. W., Shui, G., Chua, C. H. L., Cheong, W.-F., Parameswaran, S., Koizumi, R., Ohta, H., Wenk, M. R., & Ito, T. (2014). Transcriptomic and lipidomic profiles of glycerolipids during Arabidopsis flower development. *New Phytologist*, *203*(1), 310-322. <https://doi.org/10.1111/nph.12774>
- Nakashima, A., Iijima, Y., Aoki, K., Shibata, D., Sugimoto, K., Takabayashi, J., & Matsui, K. (2011). Monogalactosyl diacylglycerol is a substrate for lipoxygenase: its implications for oxylipin formation directly from lipids. *Journal of Plant Interactions*, *6*(2-3), 93-97.
- Napier, J. A., Haslam, R. P., Beaudoin, F., & Cahoon, E. B. (2014, 2014/06/01/). Understanding and manipulating plant lipid composition: Metabolic engineering leads the way. *Current opinion in plant biology*, *19*, 68-75. <https://doi.org/https://doi.org/10.1016/j.pbi.2014.04.001>
- Narasimhan, R., Wang, G., Li, M., Roth, M., Welti, R., & Wang, X. (2013). Differential changes in galactolipid and phospholipid species in soybean leaves and roots under nitrogen deficiency and after nodulation. *Phytochemistry*, *96*, 81-91.
- Narayanan, S., Prasad, P. V., & Welti, R. (2016). Wheat leaf lipids during heat stress: II. Lipids experiencing coordinated metabolism are detected by analysis of lipid co-occurrence. *Plant, Cell & Environment*, *39*(3), 608-617.
- Narayanan, S., Prasad, P. V. V., & Welti, R. (2018). Alterations in wheat pollen lipidome during high day and night temperature stress. *Plant, Cell & Environment*, *41*(8), 1749-1761. <https://doi.org/doi:10.1111/pce.13156>
- Naseem, H., & Bano, A. (2014). Role of plant growth-promoting rhizobacteria and their exopolysaccharide in drought tolerance of maize. *Journal of Plant Interactions*, *9*(1), 689-701.
- Nathoo, N., Bernards, M. A., MacDonald, J., & Yuan, Z.-C. (2017, 2017/07/22/). A Hydroponic Co-cultivation System for Simultaneous and Systematic Analysis of

Plant/Microbe Molecular Interactions and Signaling. *JoVE*(125), e55955.
<https://doi.org/doi:10.3791/55955>

- Naveed, M., Hussain, M. B., Zahir, Z. A., Mitter, B., & Sessitsch, A. (2014). Drought stress amelioration in wheat through inoculation with Burkholderia phytofirmans strain PsJN. *Plant Growth Regulation*, 73(2), 121-131.
- Naveed, M., Qureshi, M. A., Zahir, Z. A., Hussain, M. B., Sessitsch, A., & Mitter, B. (2015). L-Tryptophan-dependent biosynthesis of indole-3-acetic acid (IAA) improves plant growth and colonization of maize by Burkholderia phytofirmans PsJN. *Annals of Microbiology*, 65(3), 1381-1389.
- Newton, J., & Fray, R. (2004). Integration of environmental and host-derived signals with quorum sensing during plant-microbe interactions. *Cellular microbiology*, 6(3), 213-224.
- Nezhad, A. S. (2014). Microfluidic platforms for plant cells studies. *Lab on a Chip*, 14(17), 3262-3274.
- Niazi, A., Manzoor, S., Asari, S., Bejai, S., Meijer, J., & Bongcam-Rudloff, E. (2014, 08/13 04/16/received 07/10/accepted). Genome Analysis of *Bacillus amyloliquefaciens* Subsp. *plantarum* UCMB5113: A Rhizobacterium That Improves Plant Growth and Stress Management. *PLoS ONE*, 9(8), e104651. <https://doi.org/10.1371/journal.pone.0104651>
- Niklas, K. J. (1994). *Plant allometry: the scaling of form and process*. University of Chicago Press.
- Nilsson, A. K., Johansson, O. N., Fahlberg, P., Kommuri, M., Töpel, M., Bodin, L. J., Sikora, P., Modarres, M., Ekengren, S., & Nguyen, C. T. (2015). Acylated monogalactosyl diacylglycerol: prevalence in the plant kingdom and identification of an enzyme catalyzing galactolipid head group acylation in *Arabidopsis thaliana*. *The Plant Journal*, 84(6), 1152-1166.
- Niu, Y., & Xiang, Y. (2018, 2018-July-03). An Overview of Biomembrane Functions in Plant Responses to High-Temperature Stress [Review]. *Frontiers in Plant Science*, 9(915). <https://doi.org/10.3389/fpls.2018.00915>
- Nollen, E. A., & Morimoto, R. I. (2002). Chaperoning signaling pathways: molecular chaperones as stress-sensing heat shock proteins. *Journal of cell science*, 115(14), 2809-2816.
- Nowak, J., Sharma, V., & A'Hearn, E. (2002). Endophyte enhancement of transplant performance in tomato, cucumber and sweet pepper. XXVI International Horticultural Congress: Issues and Advances in Transplant Production and Stand Establishment Research 631,
- Nuria, F.-B., Lourdes, F.-C., Alfonso, M., René, T., P., M. H., & Mar, C. M. (2018). HOP family plays a major role in long-term acquired thermotolerance in *Arabidopsis*. *Plant, Cell & Environment*, 41(8), 1852-1869. <https://doi.org/doi:10.1111/pce.13326>

- Oburger, E., Dell'mour, M., Hann, S., Wieshammer, G., Puschenreiter, M., & Wenzel, W. W. (2013). Evaluation of a novel tool for sampling root exudates from soil-grown plants compared to conventional techniques. *Environmental and Experimental Botany*, *87*, 235-247.
- Ogawa, S., Valencia, M. O., Ishitani, M., & Selvaraj, M. G. (2014). Root system architecture variation in response to different NH₄⁺ concentrations and its association with nitrogen-deficient tolerance traits in rice. *Acta physiologiae plantarum*, *36*(9), 2361-2372.
- Ogbonnaya, F., Subrahmanyam, N., Moullet, O., de Majnik, J., Eagles, H., Brown, J., Eastwood, R., Kollmorgen, J., Appels, R., & Lagudah, E. (2001). Diagnostic DNA markers for cereal cyst nematode resistance in bread wheat. *Australian Journal of Agricultural Research*, *52*(12), 1367-1374.
- Okazaki, Y., & Saito, K. (2014). Roles of lipids as signaling molecules and mitigators during stress response in plants. *The Plant Journal*, *79*(4), 584-596. <https://doi.org/https://doi.org/10.1111/tpj.12556>
- Okazaki, Y., & Saito, K. (2018). Plant Lipidomics Using UPLC-QTOF-MS. In C. António (Ed.), *Plant Metabolomics: Methods and Protocols* (pp. 157-169). Springer New York. https://doi.org/10.1007/978-1-4939-7819-9_11
- Oldroyd, G. E. (2013). Speak, friend, and enter: signalling systems that promote beneficial symbiotic associations in plants. *Nature Reviews Microbiology*, *11*(4), 252-263.
- Oliva, M., & Dunand, C. (2007). Waving and skewing: how gravity and the surface of growth media affect root development in Arabidopsis. *New Phytologist*, *176*(1), 37-43. <https://doi.org/https://doi.org/10.1111/j.1469-8137.2007.02184.x>
- Ortiz-Castro, R., Díaz-Pérez, C., Martínez-Trujillo, M., del Río, R. E., Campos-García, J., & López-Bucio, J. (2011). Transkingdom signaling based on bacterial cyclodipeptides with auxin activity in plants. *Proceedings of the National Academy of Sciences*, *108*(17), 7253-7258.
- Ortiz-Castro, R., Pelagio-Flores, R., Méndez-Bravo, A., Ruiz-Herrera, L. F., Campos-García, J., & López-Bucio, J. (2014). Pyocyanin, a virulence factor produced by *Pseudomonas aeruginosa*, alters root development through reactive oxygen species and ethylene signaling in Arabidopsis. *Molecular Plant-Microbe Interactions*, *27*(4), 364-378.
- Overvoorde, P., Fukaki, H., & Beeckman, T. (2010). Auxin control of root development. *Cold Spring Harbor perspectives in biology*, *2*(6), a001537.
- Ozga, J. A., Kaur, H., Savada, R. P., & Reinecke, D. M. (2017). Hormonal regulation of reproductive growth under normal and heat-stress conditions in legume and other model crop species. *Journal of Experimental Botany*, *68*(8), 1885-1894. <https://doi.org/10.1093/jxb/erw464>

- Pacifici, E., Polverari, L., & Sabatini, S. (2015). Plant hormone cross-talk: the pivot of root growth. *Journal of Experimental Botany*, *66*(4), 1113-1121. <https://doi.org/10.1093/jxb/eru534>
- Pan, R., Jones, A. D., & Hu, J. (2014). Cardiolipin-mediated mitochondrial dynamics and stress response in Arabidopsis. *The Plant Cell*, *26*(1), 391-409.
- Panchuk, I. I., Volkov, R. A., & Schöffl, F. (2002). Heat stress-and heat shock transcription factor-dependent expression and activity of ascorbate peroxidase in Arabidopsis. *Plant Physiology*, *129*(2), 838-853.
- Pardales Jr, J., Kono, Y., & Yamauchi, A. (1992). Epidermal cell elongation in sorghum seminal roots exposed to high root-zone temperature. *Plant Science*, *81*(2), 143-146.
- Parida, A. K., & Das, A. B. (2005). Salt tolerance and salinity effects on plants: a review. *Ecotoxicology and environmental safety*, *60*(3), 324-349.
- Parniske, M. (2008). Arbuscular mycorrhiza: the mother of plant root endosymbioses. *Nature Reviews Microbiology*, *6*(10), 763-775.
- Parsons, J. B., & Rock, C. O. (2013, 2013/07/01/). Bacterial lipids: Metabolism and membrane homeostasis. *Progress in lipid research*, *52*(3), 249-276. <https://doi.org/https://doi.org/10.1016/j.plipres.2013.02.002>
- Pata, M. O., Hannun, Y. A., & Ng, C. K. Y. (2010). Plant sphingolipids: decoding the enigma of the Sphinx. *New Phytologist*, *185*(3), 611-630.
- Paterson, E., Gebbing, T., Abel, C., Sim, A., & Telfer, G. (2007). Rhizodeposition shapes rhizosphere microbial community structure in organic soil. *New Phytologist*, *173*(3), 600-610.
- Penfield, S. (2008). Temperature perception and signal transduction in plants. *New Phytologist*, *179*(3), 615-628.
- Péret, B., De Rybel, B., Casimiro, I., Benková, E., Swarup, R., Laplaze, L., Beeckman, T., & Bennett, M. J. (2009, 2009/07/01/). Arabidopsis lateral root development: an emerging story. *Trends in Plant Science*, *14*(7), 399-408. <https://doi.org/https://doi.org/10.1016/j.tplants.2009.05.002>
- Pereyra, M. A., Zalazar, C. A., & Barassi, C. A. (2006). Root phospholipids in Azospirillum-inoculated wheat seedlings exposed to water stress. *Plant Physiology and Biochemistry*, *44*(11-12), 873-879.
- Perrotta, C., Treglia, A., Mita, G., Giangrande, E., Rampino, P., Ronga, G., Spano, G., & Marmiroli, N. (1998). Analysis of mRNAs from ripening wheat seeds: the effect of high temperature. *Journal of Cereal Science*, *27*(2), 127-132.
- Pettersson, M., & Bååth, E. (2003). Temperature-dependent changes in the soil bacterial community in limed and unlimed soil. *FEMS Microbiology Ecology*, *45*(1), 13-21.

- Philippot, L., Raaijmakers, J. M., Lemanceau, P., & Van Der Putten, W. H. (2013). Going back to the roots: the microbial ecology of the rhizosphere. *Nature Reviews Microbiology*, *11*(11), 789-799.
- Picard, D. (2002). Heat-shock protein 90, a chaperone for folding and regulation. *Cellular and Molecular Life Sciences CMLS*, *59*(10), 1640-1648.
- Pieterse, C. M. J., Does, D. V. d., Zamioudis, C., Leon-Reyes, A., & Wees, S. C. M. V. (2012). Hormonal Modulation of Plant Immunity. *Annual Review of Cell and Developmental Biology*, *28*(1), 489-521. <https://doi.org/10.1146/annurev-cellbio-092910-154055>
- Pieterse, C. M. J., Zamioudis, C., Berendsen, R. L., Weller, D. M., Wees, S. C. M. V., & Bakker, P. A. H. M. (2014). Induced Systemic Resistance by Beneficial Microbes. *Annual review of phytopathology*, *52*(1), 347-375. <https://doi.org/10.1146/annurev-phyto-082712-102340>
- Pillay, V., & Nowak, J. (1997). Inoculum density, temperature, and genotype effects on in vitro growth promotion and epiphytic and endophytic colonization of tomato (*Lycopersicon esculentum* L.) seedlings inoculated with a pseudomonad bacterium. *Canadian journal of microbiology*, *43*(4), 354-361.
- Pinedo, I., Ledger, T., Greve, M., & Poupin, M. J. (2015, 2015-June-23). Burkholderia phytofirmans PsJN induces long-term metabolic and transcriptional changes involved in Arabidopsis thaliana salt tolerance [Original Research]. *Frontiers in Plant Science*, *6*(466). <https://doi.org/10.3389/fpls.2015.00466>
- Pini, F., Galardini, M., Bazzicalupo, M., & Mengoni, A. (2011). Plant-bacteria association and symbiosis: are there common genomic traits in Alphaproteobacteria? *Genes*, *2*(4), 1017-1032.
- Pizarro, C., Arenzana-Rámila, I., Pérez-del-Notario, N., Pérez-Matute, P., & González-Sáiz, J. M. J. A. C. A. (2016). Thawing as a critical pre-analytical step in the lipidomic profiling of plasma samples: new standardized protocol. *912*, 1-9.
- Platre, M. P., Bayle, V., Armengot, L., Bareille, J., Marquès-Bueno, M. d. M., Creff, A., Maneta-Peyret, L., Fiche, J.-B., Nollmann, M., & Miège, C. (2019). Developmental control of plant Rho GTPase nano-organization by the lipid phosphatidylserine. *Science*, *364*(6435), 57-62.
- Pleskot, R., Li, J., Žárský, V., Potocký, M., & Staiger, C. J. (2013). Regulation of cytoskeletal dynamics by phospholipase D and phosphatidic acid. *Trends in Plant Science*, *18*(9), 496-504.
- Plett, J. M., Daguerre, Y., Wittulsky, S., Vayssières, A., Deveau, A., Melton, S. J., Kohler, A., Morrell-Falvey, J. L., Brun, A., & Veneault-Fourrey, C. (2014). Effector MiSSP7 of the mutualistic fungus *Laccaria bicolor* stabilizes the *Populus* JAZ6 protein and represses jasmonic acid (JA) responsive genes. *Proceedings of the National Academy of Sciences*, *111*(22), 8299-8304.

[Record #1387 is using a reference type undefined in this output style.]

- Pound, M. P., French, A. P., Atkinson, J. A., Wells, D. M., Bennett, M. J., & Pridmore, T. (2013). RootNav: navigating images of complex root architectures. *Plant Physiology*, *162*(4), 1802-1814.
- Poupin, M. J., Timmermann, T., Vega, A., Zuniga, A., & Gonzalez, B. (2013, Jul). Effects of the Plant Growth-Promoting Bacterium Burkholderia phytofirmans PsJN throughout the Life Cycle of Arabidopsis thaliana [Article]. *PLoS ONE*, *8*(7), 15, Article e69435. <https://doi.org/10.1371/journal.pone.0069435>
- Powers, M. J., Sanabria-Valentín, E., Bowers, A. A., & Shank, E. A. (2015). Inhibition of cell differentiation in Bacillus subtilis by Pseudomonas protegens. *Journal of bacteriology*, *197*(13), 2129-2138.
- Prados-Rosales, R. C., Aragonese-Cazorla, G., Estevez, H., Garcia-Calvo, E., Machuca, A., & Luque-Garcia, J. L. (2019). Strategies for Membrane Protein Analysis by Mass Spectrometry. In A. G. Woods & C. C. Darie (Eds.), *Advancements of Mass Spectrometry in Biomedical Research* (pp. 289-298). Springer International Publishing. https://doi.org/10.1007/978-3-030-15950-4_16
- Prasad, P. V. V., Boote, K., Allen, L. H., & Allen, L. H. (2006). Adverse high temperature effects on pollen viability, seed-set, seed yield and harvest index of grain-sorghum [Sorghum bicolor (L.) Moench] are more severe at elevated carbon dioxide due to higher tissue temperatures. *Agricultural and Forest Meteorology*, *139*(3-4), 237-251. http://sfx.unimelb.hosted.exlibrisgroup.com/sfxlcl41?url_ver=Z39.88-2004&url_ctx_fmt=info%3Aofi%2Ffmt%3Akev%3Amtx%3Actx&rft_val_fmt=info%3Aofi%2Ffmt%3Akev%3Amtx%3Ajournal&rft.atitle=Adverse%20high%20temperature%20effects%20on%20pollen%20viability%2C%20seed-set%2C%20seed%20yield%20and%20harvest%20index%20of%20grain-sorghum%20%5BSorghum%20bicolor%20%28L.%29%20Moench%5D%20are%20more%20severe%20at%20elevated%20carbon%20dioxide%20due%20to%20higher%20tissue%20temperatures&rft.aufirst=P.%20V.%20Vara&rft.aulast=Prasad&rft.date=2006&rft.epage=251&rft.genre=article&rft.issn=0168-1923&rft.issue=3-4&rft.jtitle=AGRICULTURAL%20AND%20FOREST%20METEOROLOGY&rft.pages=237-251&rft.spage=237&rft.stitle=AGR%20FOREST%20METEOROL&rft.volume=139&rft_id=info%3Asid%2Fwww.isinet.com%3AWoK%3AUA&rft.au=Boote%2C%20Kenneth%20J.&rft.au=Allen%2C%20L.%20Hartwell%2C%20Jr.&rft_id=info%3Adoi%2F10.1016%2Fj.agrformet.2006.07.003
- Pratt, W. B., & Toft, D. O. (2003). Regulation of signaling protein function and trafficking by the hsp90/hsp70-based chaperone machinery. *Experimental biology and medicine*, *228*(2), 111-133.
- Pregitzer, K. S., Zak, D. R., Maziasz, J., DeForest, J., Curtis, P. S., & Lussenhop, J. (2000). Interactive effects of atmospheric CO₂ and soil-N availability on fine roots of Populus tremuloides. *Ecological Applications*, *10*(1), 18-33.

- Qin, H., He, L., & Huang, R. (2019, 2019-July-10). The Coordination of Ethylene and Other Hormones in Primary Root Development [Mini Review]. *Frontiers in Plant Science*, *10*. <https://doi.org/10.3389/fpls.2019.00874>
- Queitsch, C., Sangster, T. A., & Lindquist, S. (2002). Hsp90 as a capacitor of phenotypic variation. *Nature*, *417*(6889), 618-624.
- Quinn, P., Joo, F., & Vigh, L. (1989). The role of unsaturated lipids in membrane structure and stability. *Progress in biophysics and molecular biology*, *53*(2), 71-103.
- Quinn, P. J. (1988). Effects of temperature on cell membranes. *Symposia of the Society for Experimental Biology*, *42*, 237-258. <http://europepmc.org/abstract/MED/3077859>
- Quint, M., Delker, C., Franklin, K. A., Wigge, P. A., Halliday, K. J., & van Zanten, M. (2016, 2016/01/06). Molecular and genetic control of plant thermomorphogenesis. *Nature plants*, *2*(1), 15190. <https://doi.org/10.1038/nplants.2015.190>
- Radville, L., McCormack, M. L., Post, E., & Eissenstat, D. M. (2016). Root phenology in a changing climate. *Journal of Experimental Botany*, *67*(12), 3617-3628. <https://doi.org/10.1093/jxb/erw062>
- Ray, J. D., Gesch, R. W., Sinclair, T. R., & Hartwell Allen, L. (2002). The effect of vapor pressure deficit on maize transpiration response to a drying soil. *Plant and Soil*, *239*(1), 113-121.
- Raza, A., Mehmood, S. S., Ashraf, F., & Khan, R. S. A. (2019). Genetic diversity analysis of Brassica species using PCR-based SSR markers. *Gesunde Pflanzen*, *71*(1), 1-7.
- Raza, A., Razaq, A., Mehmood, S. S., Zou, X., Zhang, X., Lv, Y., & Xu, J. (2019, Jan 30). Impact of Climate Change on Crops Adaptation and Strategies to Tackle Its Outcome: A Review. *Plants (Basel)*, *8*(2). <https://doi.org/10.3390/plants8020034>
- Rellán-Álvarez, R., Lobet, G., Lindner, H., Pradier, P.-L., Sebastian, J., Yee, M.-C., Geng, Y., Trontin, C., LaRue, T., & Schragger-Lavelle, A. (2015). GLO-Roots: an imaging platform enabling multidimensional characterization of soil-grown root systems. *eLife*, *4*, e07597.
- Reynolds, H. L., Packer, A., Bever, J. D., & Clay, K. (2003). Grassroots ecology: plant–microbe–soil interactions as drivers of plant community structure and dynamics. *Ecology*, *84*(9), 2281-2291.
- Reynolds, M., Tattaris, M., Cossani, C. M., Ellis, M., Yamaguchi-Shinozaki, K., & Pierre, C. S. (2015). Exploring genetic resources to increase adaptation of wheat to climate change. In *Advances in wheat genetics: From genome to field* (pp. 355-368). Springer, Tokyo.
- Ribeiro, P. R., Fernandez, L. G., de Castro, R. D., Ligterink, W., & Hilhorst, H. W. (2014). Physiological and biochemical responses of *Ricinus communis* seedlings to different temperatures: a metabolomics approach. *BMC Plant Biology*, *14*(1), 1-14.

- Richards, R., & Passioura, J. (1989). A breeding program to reduce the diameter of the major xylem vessel in the seminal roots of wheat and its effect on grain yield in rain-fed environments. *Australian Journal of Agricultural Research*, 40(5), 943-950.
- Rietz, S., Dermendjiev, G., Oppermann, E., Tafesse, F. G., Effendi, Y., Holk, A., Parker, J. E., Teige, M., & Scherer, G. F. (2010). Roles of Arabidopsis patatin-related phospholipases a in root development are related to auxin responses and phosphate deficiency. *Molecular Plant*, 3(3), 524-538.
- Rodríguez, H., & Fraga, R. (1999). Phosphate solubilizing bacteria and their role in plant growth promotion. *Biotechnology Advances*, 17(4-5), 319-339.
- Rodríguez, M., Canales, E., & Borrás-Hidalgo, O. (2005). Molecular aspects of abiotic stress in plants. *Biotecnología Aplicada*, 22(1), 1-10.
- Rogers, E. D., & Benfey, P. N. (2015, Apr). Regulation of plant root system architecture: implications for crop advancement. *Curr Opin Biotechnol*, 32, 93-98. <https://doi.org/10.1016/j.copbio.2014.11.015>
- Rossi, C., Cazzola, H., Holden, N. J., & Rossez, Y. (2020). Bacterial Adherence to Plant and Animal Surfaces via Adhesin-Lipid Interactions. In H. Goldfine (Ed.), *Health consequences of microbial interactions with hydrocarbons, oils, and lipids* (pp. 145-164). Springer International Publishing. https://doi.org/10.1007/978-3-030-15147-8_13
- Routaboul, J.-M., Skidmore, C., Wallis, J. G., & Browse, J. (2012). Arabidopsis mutants reveal that short-and long-term thermotolerance have different requirements for trienoic fatty acids. *Journal of Experimental Botany*, 63(3), 1435-1443.
- Rupasinghe, T. W. T., & Roessner, U. (2018). Extraction of Plant Lipids for LC-MS-Based Untargeted Plant Lipidomics. In C. António (Ed.), *Plant Metabolomics: Methods and Protocols* (pp. 125-135). Springer New York. https://doi.org/10.1007/978-1-4939-7819-9_9
- Rustam, Y. H., & Reid, G. E. (2018, 2018/01/02). Analytical Challenges and Recent Advances in Mass Spectrometry Based Lipidomics. *Analytical Chemistry*, 90(1), 374-397. <https://doi.org/10.1021/acs.analchem.7b04836>
- Ruyter-Spira, C., Al-Babili, S., Van Der Krol, S., & Bouwmeester, H. (2013). The biology of strigolactones. *Trends in Plant Science*, 18(2), 72-83.
- Ryan, R. P., An, S.-q., Allan, J. H., McCarthy, Y., & Dow, J. M. (2015). The DSF family of cell-cell signals: an expanding class of bacterial virulence regulators. *PLoS pathogens*, 11(7), e1004986.
- Ryu, C.-M., Hu, C.-H., Locy, R. D., & Kloepper, J. W. (2005). Study of mechanisms for plant growth promotion elicited by rhizobacteria in Arabidopsis thaliana. *Plant and Soil*, 268(1), 285-292.

- Sairam, R., & Tyagi, A. (2004). Physiology and molecular biology of salinity stress tolerance in plants. *Current science*, 407-421.
- Saleem, A. R., Brunetti, C., Khalid, A., Della Rocca, G., Raio, A., Emiliani, G., De Carlo, A., Mahmood, T., & Centritto, M. (2018). Drought response of *Mucuna pruriens* (L.) DC. inoculated with ACC deaminase and IAA producing rhizobacteria. *PLoS ONE*, 13(2), e0191218. <https://doi.org/10.1371/journal.pone.0191218>
- Samarakoon, T., Shiva, S., Lowe, K., Tamura, P., Roth, M. R., & Welti, R. (2012). Arabidopsis thaliana Membrane Lipid Molecular Species and Their Mass Spectral Analysis. In J. Normanly (Ed.), *High-Throughput Phenotyping in Plants: Methods and Protocols* (pp. 179-268). Humana Press. https://doi.org/10.1007/978-1-61779-995-2_13
- Sánchez-Rangel, D., Vicente, R.-S., de la Torre-Hernández, M. E., Nájera-Martínez, M., & Plasencia, J. (2015). Deciphering the link between salicylic acid signaling and sphingolipid metabolism. *Frontiers in Plant Science*, 6, 125.
- Sandhya, V., SK Z, A., Grover, M., Reddy, G., & Venkateswarlu, B. (2009). Alleviation of drought stress effects in sunflower seedlings by the exopolysaccharides producing *Pseudomonas putida* strain GAP-P45. *Biology and Fertility of Soils*, 46(1), 17-26.
- Sangam, D., Hari, U., Subudhi, P., Gehring, C., Bajic, V., & Ortiz, R. (2009). Enhancing abiotic stress tolerance in cereals through breeding and transgenic interventions. *Plant Breeding Reviews*, 33, 31-114.
- Santana, M., & Gonzalez, J. (2015). High temperature microbial activity in upper soil layers. *FEMS Microbiology Letters*, 362(22).
- Santi, C., Molesini, B., Guzzo, F., Pii, Y., Vitulo, N., & Pandolfini, T. (2017). Genome-wide transcriptional changes and lipid profile modifications induced by *Medicago truncatula* N5 overexpression at an early stage of the symbiotic interaction with *Sinorhizobium meliloti*. *Genes*, 8(12), 396.
- Sarabia, L. D., Boughton, B. A., Rupasinghe, T., Callahan, D. L., Hill, C. B., & Roessner, U. (2019). Comparative spatial lipidomics analysis reveals cellular lipid remodelling in different developmental zones of barley roots in response to salinity. *Plant, Cell & Environment*.
- Sarker, A., Ansary, M. W. R., Hossain, M. N., & Islam, T. (2021). Prospect and Challenges for Sustainable Management of Climate Change-Associated Stresses to Soil and Plant Health by Beneficial Rhizobacteria. *Stresses*, 1(4), 200-222. <https://www.mdpi.com/2673-7140/1/4/15>
- Sasaki, T., Yamamoto, Y., Delhaize, E., Ryan, P., Ariyoshi, M., & Matsumoto, H. (2005). Overexpression of wheat ALMT1 gene confers aluminum tolerance in plants. *Plant and Cell Physiology*, 46, S158.
- Sattar, A., Sher, A., Ijaz, M., Ul-Allah, S., Rizwan, M. S., Hussain, M., Jabran, K., & Cheema, M. A. (2020). Terminal drought and heat stress alter physiological and biochemical attributes in flag leaf of bread wheat. *PLoS ONE*, 15(5), e0232974.

- Sattelmacher, B., Marschner, H., & Kühne, R. (1990). Effects of the temperature of the rooting zone on the growth and development of roots of potato (*Solanum tuberosum*). *Annals of Botany*, 65(1), 27-36.
- Savchenko, T., Kolla, V. A., Wang, C.-Q., Nasafi, Z., Hicks, D. R., Phadungchob, B., Chehab, W. E., Brandizzi, F., Froehlich, J., & Dehesh, K. (2014). Functional convergence of oxylipin and abscisic acid pathways controls stomatal closure in response to drought. *Plant Physiology*, 164(3), 1151-1160.
- Sawana, A., Adeolu, M., & Gupta, R. S. (2014). Molecular signatures and phylogenomic analysis of the genus *Burkholderia*: proposal for division of this genus into the emended genus *Burkholderia* containing pathogenic organisms and a new genus *Paraburkholderia* gen. nov. harboring environmental species. *Frontiers in genetics*, 5, 429.
- Sayed, O. (1996). Adaptational responses of *Zygophyllum qatarense* Hadidi to stress conditions in a desert environment. *Journal of Arid Environments*, 32(4), 445-452.
- Scalschi, L., Sanmartín, M., Camañes, G., Troncho, P., Sánchez-Serrano, J. J., García-Agustín, P., & Vicedo, B. (2015). Silencing of OPR3 in tomato reveals the role of OPDA in callose deposition during the activation of defense responses against *Botrytis cinerea*. *The Plant Journal*, 81(2), 304-315.
- Scandalios, J. G. (1993). Oxygen stress and superoxide dismutases. *Plant Physiology*, 101(1), 7.
- Schenk, S. T., Stein, E., Kogel, K.-H., & Schikora, A. (2012, 2012/02/01). Arabidopsis growth and defense are modulated by bacterial quorum sensing molecules. *Plant signaling & behavior*, 7(2), 178-181. <https://doi.org/10.4161/psb.18789>
- Scheres, B., Benfey, P., & Dolan, L. (2002). Root development. *The Arabidopsis book/American Society of Plant Biologists*, 1.
- Schillaci, M., Arsova, B., Walker, R., Smith, P. M. C., Nagel, K. A., Roessner, U., & Watt, M. (2021, 2021/01/01). Time-resolution of the shoot and root growth of the model cereal *Brachypodium* in response to inoculation with *Azospirillum* bacteria at low phosphorus and temperature. *Plant Growth Regulation*, 93(1), 149-162. <https://doi.org/10.1007/s10725-020-00675-4>
- Schillaci, M., Kehelpannala, C., Martinez-Seidel, F., Smith, P. M. C., Arsova, B., Watt, M., & Roessner, U. (2021). The Metabolic Response of *Brachypodium* Roots to the Interaction with Beneficial Bacteria Is Affected by the Plant Nutritional Status. *Metabolites*, 11(6), 358. <https://www.mdpi.com/2218-1989/11/6/358>
- Schmidt, R., & Schippers, J. H. (2015). ROS-mediated redox signaling during cell differentiation in plants. *Biochimica et Biophysica Acta (BBA)-General Subjects*, 1850(8), 1497-1508.

- Schöffl, F., Prandl, R., & Reindl, A. (1999). Molecular responses to heat stress. *Molecular responses to cold, drought, heat and salt stress in higher plants*, 83, 93.
- Schuster, M., Sexton, D. J., Diggle, S. P., & Greenberg, E. P. (2013). Acyl-Homoserine Lactone Quorum Sensing: From Evolution to Application. *Annual review of microbiology*, 67(1), 43-63. <https://doi.org/10.1146/annurev-micro-092412-155635>
- Seelig, A., & Seelig, J. (1977). Effect of a single cis double bond on the structure of a phospholipid bilayer. *Biochemistry*, 16(1), 45-50.
- Seiler, G. J. (1998). Influence of temperature on primary and lateral root growth of sunflower seedlings. *Environmental and Experimental Botany*, 40(2), 135-146.
- Sergaki, C., Lagunas, B., Lidbury, I., Gifford, M. L., & Schäfer, P. (2018, 2018-August-17). Challenges and Approaches in Microbiome Research: From Fundamental to Applied [Review]. *Frontiers in Plant Science*, 9(1205). <https://doi.org/10.3389/fpls.2018.01205>
- Sessitsch, A., Howieson, J., Perret, X., Antoun, H., & Martinez-Romero, E. (2002). Advances in Rhizobium research. *Critical Reviews in Plant Sciences*, 21(4), 323-378.
- Shanmugam, S., Kjaer, K. H., Ottosen, C. O., Rosenqvist, E., Kumari Sharma, D., & Wollenweber, B. (2013). The Alleviating Effect of Elevated CO₂ on Heat Stress Susceptibility of Two Wheat (*Triticum aestivum* L.) Cultivars. *Journal of Agronomy and Crop Science*, 199(5), 340-350. <https://doi.org/10.1111/jac.12023>
- Shanmugavel, P., Rajaprakasam, S., Chockalingam, V., Ramasamy, G., Thiyagarajan, K., & Marimuthu, R. (2020). Breeding Mechanisms for High Temperature Tolerance in Crop Plants. In *Plant Breeding - Current and Future Views*. IntechOpen. <https://doi.org/10.5772/intechopen.94693>
- Shevchenko, A., & Simons, K. (2010, 07/07/online). Lipidomics: coming to grips with lipid diversity [Perspective]. *Nature Reviews Molecular Cell Biology*, 11, 593. <https://doi.org/10.1038/nrm2934>
- Shinozaki, K., & Yamaguchi-Shinozaki, K. (1999). *Molecular responses to cold, drought, heat and salt stress in higher plants* (Vol. 1). RG Landes Company Austin, TX.
- Shiva, S., Enniful, R., Roth, M. R., Tamura, P., Jagadish, K., & Welti, R. (2018). An efficient modified method for plant leaf lipid extraction results in improved recovery of phosphatidic acid. *Plant Methods*, 14(1), 14.
- Shiva, S., Samarakoon, T., Lowe, K. A., Roach, C., Vu, H. S., Colter, M., Porras, H., Hwang, C., Roth, M. R., Tamura, P., Li, M., Schrick, K., Shah, J., Wang, X., Wang, H., & Welti, R. (2020). Leaf Lipid Alterations in Response to Heat Stress of *Arabidopsis thaliana*. *Plants*, 9(7), 845. <https://www.mdpi.com/2223-7747/9/7/845>
- Shrivastava, P., & Kumar, R. (2015). Soil salinity: A serious environmental issue and plant growth promoting bacteria as one of the tools for its alleviation. *Saudi journal of biological sciences*, 22(2), 123-131.

- Shukla, S. D., & Turner, J. M. (1980). Microbial metabolism of amino alcohols. Biosynthetic utilization of ethanolamine for lipid synthesis by bacteria. *Biochemical Journal*, *186*(1), 13-19.
- Shulaev, V., & Chapman, K. D. (2017, 2017/08/01/). Plant lipidomics at the crossroads: From technology to biology driven science. *Biochimica et Biophysica Acta (BBA) - Molecular and Cell Biology of Lipids*, *1862*(8), 786-791. <https://doi.org/https://doi.org/10.1016/j.bbalip.2017.02.011>
- Siddique, K., Loss, S., Regan, K., & Jettner, R. (1999). Adaptation and seed yield of cool season grain legumes in Mediterranean environments of south-western Australia. *Australian Journal of Agricultural Research*, *50*(3), 375-388.
- Siebers, M., Brands, M., Wewer, V., Duan, Y., Holzl, G., & Dormann, P. (2016, Sep). Lipids in plant-microbe interactions [Article]. *Biochim Biophys Acta*, *1861*(9 Pt B), 1379-1395. <https://doi.org/10.1016/j.bbalip.2016.02.021>
- Sieper, T., Forczek, S., Matucha, M., Krämer, P., Hartmann, A., & Schröder, P. (2014). N-acetyl-homoserine lactone uptake and systemic transport in barley rest upon active parts of the plant. *New Phytologist*, *201*(2), 545-555.
- Silipo, A., Vitiello, G., Gully, D., Sturiale, L., Chaintreuil, C., Fardoux, J., Gargani, D., Lee, H.-I., Kulkarni, G., Busset, N., Marchetti, R., Palmigiano, A., Moll, H., Engel, R., Lanzetta, R., Paduano, L., Parrilli, M., Chang, W.-S., Holst, O., Newman, D. K., Garozzo, D., D'Errico, G., Giraud, E., & Molinaro, A. (2014, 2014/10/30). Covalently linked hopanoid-lipid A improves outer-membrane resistance of a Bradyrhizobium symbiont of legumes. *Nature Communications*, *5*(1), 5106. <https://doi.org/10.1038/ncomms6106>
- Singh, J. S. (2013). Plant growth promoting rhizobacteria. *Resonance*, *18*(3), 275-281.
- Singh, R., Masurkar, P., Pandey, S. K., & Kumar, S. (2019). Rhizobacteria–plant interaction, alleviation of abiotic stresses. In *Plant Growth Promoting Rhizobacteria for Sustainable Stress Management* (pp. 345-353). Springer.
- Slovak, R., Göschl, C., Su, X., Shimotani, K., Shiina, T., & Busch, W. (2014). A Scalable Open-Source Pipeline for Large-Scale Root Phenotyping of Arabidopsis *The Plant Cell*, *26*(6), 2390-2403. <https://doi.org/10.1105/tpc.114.124032>
- Smith, A. (2000). *Oxford dictionary of biochemistry and molecular biology: Revised Edition*. Oxford University Press.
- Smith, F. A. (2007). Plant roots. Growth, activity and interaction with soils.
- Sobol, S., Chayut, N., Nave, N., Kafle, D., Hegele, M., Kaminetsky, R., Wünsche, J. N., & Samach, A. (2014). Genetic variation in yield under hot ambient temperatures spotlights a role for cytokinin in protection of developing floral primordia. *Plant, Cell & Environment*, *37*(3), 643-657.

- Sohlenkamp, C., & Geiger, O. (2015). Bacterial membrane lipids: diversity in structures and pathways. *FEMS Microbiology Reviews*, 40(1), 133-159. <https://doi.org/10.1093/femsre/fuv008>
- Sohrabi, R., Ali, T., Harinantenaina Rakotondraibe, L., & Tholl, D. (2017). Formation and exudation of non-volatile products of the arabioidol triterpenoid degradation pathway in Arabidopsis roots. *Plant signaling & behavior*, 12(1), e1265722.
- Sollars, V., Lu, X., Xiao, L., Wang, X., Garfinkel, M. D., & Ruden, D. M. (2003). Evidence for an epigenetic mechanism by which Hsp90 acts as a capacitor for morphological evolution. *Nature Genetics*, 33(1), 70-74.
- Stephenson, D. J., Hoeflerlin, L. A., & Chalfant, C. E. (2017, 2017/11/01/). Lipidomics in translational research and the clinical significance of lipid-based biomarkers. *Translational Research*, 189, 13-29. <https://doi.org/https://doi.org/10.1016/j.trsl.2017.06.006>
- Stinchcombe, J. R., & Hoekstra, H. E. (2008). Combining population genomics and quantitative genetics: finding the genes underlying ecologically important traits. *Heredity*, 100(2), 158-170.
- Stone, J., & Taylor, H. (1983). Temperature and the Development of the Taproot and Lateral Roots of Four Indeterminate Soybean Cultivars 1. *Agronomy Journal*, 75(4), 613-618.
- Stone, P. (2001). The effects of heat stress on cereal yield and quality hexaploid wheat. *Euphytica*, 126, 275-282.
- Stryer, L. (1995). *Biochemistry* (Fourth ed.). W.H. Freeman and Company.
- Subramanian, R., Spalding, E. P., & Ferrier, N. J. (2013). A high throughput robot system for machine vision based plant phenotype studies. *Machine Vision and Applications*, 24(3), 619-636.
- Sud, M., Fahy, E., Cotter, D., Brown, A., Dennis, E. A., Glass, C. K., Merrill Jr, A. H., Murphy, R. C., Raetz, C. R., & Russell, D. W. (2007). Lmsd: Lipid maps structure database. *Nucleic Acids Research*, 35(suppl_1), D527-D532.
- Sukumar, P., LEGUÉ, V., VAYSSIÈRES, A., MARTIN, F., TUSKAN, G. A., & KALLURI, U. C. (2013). Involvement of auxin pathways in modulating root architecture during beneficial plant–microorganism interactions. *Plant, Cell & Environment*, 36(5), 909-919. <https://doi.org/https://doi.org/10.1111/pce.12036>
- Sun, A.-Z., & Guo, F.-Q. (2016). Chloroplast retrograde regulation of heat stress responses in plants. *Frontiers in Plant Science*, 7, 398.
- Sun, Y., Cheng, Z., & Glick, B. (2009). The role of 1-aminocyclopropane-1-carboxylate (ACC) deaminase in plant growth promotion by the endophytic bacterium Burkholderia phytofirmans PsJN. *FEMS Microbiol Lett*, 296, 131-136.

- Sung, D.-Y., Kaplan, F., Lee, K.-J., & Guy, C. L. (2003). Acquired tolerance to temperature extremes. *Trends in Plant Science*, 8(4), 179-187.
- Suzuki, K., Yano, A., Nishiuchi, T., Nakano, T., Kodama, H., Yamaguchi, K., & Shinshi, H. (2007). Comprehensive analysis of early response genes to two different microbial elicitors in tobacco cells. *Plant Science*, 173(3), 291-301.
- Szabados, L., & Savouré, A. (2010). Proline: a multifunctional amino acid. *Trends in Plant Science*, 15(2), 89-97.
- Takahashi, D., Imai, H., Kawamura, Y., & Uemura, M. (2016). Lipid profiles of detergent resistant fractions of the plasma membrane in oat and rye in association with cold acclimation and freezing tolerance. *Cryobiology*, 72(2), 123-134.
- Takahashi, H. (1997). Hydrotropism: the current state of our knowledge. *Journal of plant research*, 110(2), 163.
- Takahashi, H., & Pradal, C. (2021). Root phenotyping: important and minimum information required for root modeling in crop plants. *Breeding science*, 71(1), 109-116. <https://doi.org/10.1270/jsbbs.20126>
- Talanova, V., Akimova, T., & Titov, A. (2003). Effect of whole plant and local heating on the ABA content in cucumber seedling leaves and roots and on their heat tolerance. *Russian journal of plant physiology*, 50(1), 90-94.
- Tang, R.-S., Zheng, J.-C., Jin, Z.-Q., Zhang, D.-D., Huang, Y.-H., & Chen, L.-G. (2008). Possible correlation between high temperature-induced floret sterility and endogenous levels of IAA, GAs and ABA in rice (*Oryza sativa* L.). *Plant Growth Regulation*, 54(1), 37-43.
- Tang, X., Zhou, Y., Zhang, J., Ming, H., Nie, G.-X., Yang, L.-L., Tang, S.-K., & Li, W.-J. (2012). *Actinokineospora soli* sp. nov., a thermotolerant actinomycete isolated from soil, and emended description of the genus *Actinokineospora*. *International Journal of Systematic and Evolutionary Microbiology*, 62(Pt_8), 1845-1849.
- Tewolde, H., Fernandez, C., & Erickson, C. (2006). Wheat cultivars adapted to post-heading high temperature stress. *Journal of Agronomy and Crop Science*, 192(2), 111-120.
- Theodoridis, G., Gika, H., Franceschi, P., Caputi, L., Arapitsas, P., Scholz, M., Masuero, D., Wehrens, R., Vrhovsek, U., & Mattivi, F. (2012). LC-MS based global metabolite profiling of grapes: solvent extraction protocol optimisation. *Metabolomics*, 8(2), 175-185.
- Tian, T., Reverdy, A., She, Q., Sun, B., & Chai, Y. (2020). The role of rhizodeposits in shaping rhizomicrobiome. *Environmental Microbiology Reports*, 12(2), 160-172.
- Tindall, J. A., Mills, H., & Radcliffe, D. (1990). The effect of root zone temperature on nutrient uptake of tomato. *Journal of Plant Nutrition*, 13(8), 939-956.

- Topp, C. N., Iyer-Pascuzzi, A. S., Anderson, J. T., Lee, C.-R., Zurek, P. R., Symonova, O., Zheng, Y., Bucksch, A., Mileyko, Y., & Galkovskyi, T. (2013). 3D phenotyping and quantitative trait locus mapping identify core regions of the rice genome controlling root architecture. *Proceedings of the National Academy of Sciences*, *110*(18), E1695-E1704.
- Török, Z., Crul, T., Maresca, B., Schütz, G. J., Viana, F., Dindia, L., Piotto, S., Brameshuber, M., Balogh, G., & Péter, M. (2014). Plasma membranes as heat stress sensors: from lipid-controlled molecular switches to therapeutic applications. *Biochimica et Biophysica Acta (BBA)-Biomembranes*, *1838*(6), 1594-1618.
- Trachsel, S., Kaeppler, S. M., Brown, K. M., & Lynch, J. P. (2011). Shovelomics: high throughput phenotyping of maize (*Zea mays* L.) root architecture in the field. *Plant and Soil*, *341*(1), 75-87.
- Tracy, S. R., Nagel, K. A., Postma, J. A., Fassbender, H., Wasson, A., & Watt, M. (2020, 2020/01/01/). Crop Improvement from Phenotyping Roots: Highlights Reveal Expanding Opportunities. *Trends in Plant Science*, *25*(1), 105-118. <https://doi.org/https://doi.org/10.1016/j.tplants.2019.10.015>
- Trépanier, M., Bécard, G., Moutoglis, P., Willemot, C., Gagné, S., Avis, T. J., & Rioux, J.-A. (2005). Dependence of Arbuscular-Mycorrhizal Fungi on Their Plant Host for Palmitic Acid Synthesis. *Applied and Environmental Microbiology*, *71*(9), 5341-5347. <https://doi.org/10.1128/aem.71.9.5341-5347.2005>
- Tripathy, D., Mohanty, P., Dhindsa, S., Syed, T., Ghanim, H., Aljada, A., & Dandona, P. (2003). Elevation of free fatty acids induces inflammation and impairs vascular reactivity in healthy subjects. *Diabetes*, *52*(12), 2882-2887.
- Trivedi, P., Batista, B. D., Bazany, K. E., & Singh, B. K. (2022). Plant–microbiome interactions under a changing world: Responses, consequences and perspectives. *New Phytologist*.
- Tsugawa, H., Cajka, T., Kind, T., Ma, Y., Higgins, B., Ikeda, K., Kanazawa, M., VanderGheynst, J., Fiehn, O., & Arita, M. (2015). MS-DIAL: data-independent MS/MS deconvolution for comprehensive metabolome analysis. *Nature Methods*, *12*(6), 523-526.
- Tsugawa, H., Hanada, A., Ikeda, K., Isobe, Y., Senoo, Y., & Senoo, M. (2018). High-throughput lipid profiling with SWATH® acquisition and MS-DIAL. *Biomarkers and Omics Sciex, RUO-MKT-02-8536-A*, 1-5.
- Tsukaguchi, T., Kawamitsu, Y., Takeda, H., Suzuki, K., & Egawa, Y. (2003). Water status of flower buds and leaves as affected by high temperature in heat-tolerant and heat-sensitive cultivars of snap bean (*Phaseolus vulgaris* L.). *Plant Production Science*, *6*(1), 24-27.
- Tugizimana, F., Steenkamp, P. A., Piater, L. A., & Dubery, I. A. (2014). Multi-Platform Metabolomic Analyses of Ergosterol-Induced Dynamic Changes in *Nicotiana tabacum* Cells. *PLoS ONE*, *9*(1), e87846. <https://doi.org/10.1371/journal.pone.0087846>

- Uemura, M., Tominaga, Y., Nakagawara, C., Shigematsu, S., Minami, A., & Kawamura, Y. (2006). Responses of the plasma membrane to low temperatures. *Physiologia Plantarum*, *126*(1), 81-89.
- Uren, N. C. (2007). Types, amounts, and possible functions of compounds released into the rhizosphere by soil-grown plants. In R. Pinton, Z. Varanini, & P. Nannipieri (Eds.), *The rhizosphere: biochemistry and organic substances at the soil-plant interface* (Vol. 2, pp. 1-21). CRC Press.
- USGCRP. (2017). *Climate Science Special Report: Fourth National Climate Assessment, Volume I*.
- Vacheron, J., Desbrosses, G., Bouffaud, M.-L., Touraine, B., Moëgne-Loccoz, Y., Muller, D., Legendre, L., Wisniewski-Dyé, F., & Prigent-Combaret, C. (2013, 2013-September-17). Plant growth-promoting rhizobacteria and root system functioning [Review]. *Frontiers in Plant Science*, *4*(356). <https://doi.org/10.3389/fpls.2013.00356>
- van Dam, N. M., & Bouwmeester, H. J. (2016). Metabolomics in the rhizosphere: tapping into belowground chemical communication. *Trends in Plant Science*, *21*(3), 256-265.
- Van Der Heijden, M. G., & Hartmann, M. (2016). Networking in the plant microbiome. *PLoS biology*, *14*(2), e1002378.
- Van der Krift, T., & Berendse, F. (2002). Root life spans of four grass species from habitats differing in nutrient availability. *Functional Ecology*, 198-203.
- van Dusschoten, D., Metzner, R., Kochs, J., Postma, J. A., Pflugfelder, D., Bühler, J., Schurr, U., & Jahnke, S. (2016). Quantitative 3D analysis of plant roots growing in soil using magnetic resonance imaging. *Plant Physiology*, *170*(3), 1176-1188.
- van Meer, G. (2005). Cellular lipidomics. *The EMBO journal*, *24*(18), 3159-3165.
- van Meer, G., Voelker, D. R., & Feigenson, G. W. (2008, 02/01/online). Membrane lipids: where they are and how they behave [Review Article]. *Nature Reviews Molecular Cell Biology*, *9*, 112. <https://doi.org/10.1038/nrm2330>
- Van Ruyskensvelde, V., Van Breusegem, F., & Van Der Kelen, K. (2018). Post-transcriptional regulation of the oxidative stress response in plants. *Free Radical Biology and Medicine*, *122*, 181-192.
- Végh, B., Marček, T., Karsai, I., Janda, T., & Darkó, É. (2018). Heat acclimation of photosynthesis in wheat genotypes of different origin. *South African journal of botany*, *117*, 184-192.
- Venturi, V., & Keel, C. (2016, 2016/03/01/). Signaling in the Rhizosphere. *Trends in Plant Science*, *21*(3), 187-198. <https://doi.org/https://doi.org/10.1016/j.tplants.2016.01.005>
- Venugopal, S. C., Chanda, B., Vaillancourt, L., Kachroo, A., & Kachroo, P. (2009). The common metabolite glycerol-3-phosphate is a novel regulator of plant defense signaling. *Plant signaling & behavior*, *4*(8), 746-749.

- Verbon, E. H., & Liberman, L. M. (2016). Beneficial microbes affect endogenous mechanisms controlling root development. *Trends in Plant Science*, 21(3), 218-229.
- Verbruggen, N., & Hermans, C. (2008). Proline accumulation in plants: a review. *Amino acids*, 35(4), 753-759.
- Verma, S., Kumar, N., Verma, A., Singh, H., Siddique, K. H. M., & Singh, N. P. (2020, 2020/12/01). Novel approaches to mitigate heat stress impacts on crop growth and development. *Plant Physiology Reports*, 25(4), 627-644. <https://doi.org/10.1007/s40502-020-00550-4>
- Vessey, J. K. (2003, 2003/08/01). Plant growth promoting rhizobacteria as biofertilizers. *Plant and Soil*, 255(2), 571-586. <https://doi.org/10.1023/A:1026037216893>
- Vierling, E. (1991). The roles of heat shock proteins in plants. *Annual review of plant biology*, 42(1), 579-620.
- Vijayakumar, V., Liebisch, G., Buer, B., Xue, L., Gerlach, N., Blau, S., Schmitz, J., & Bucher, M. (2016). Integrated multi-omics analysis supports role of lysophosphatidylcholine and related glycerophospholipids in the Lotus japonicus–Glomus intraradices mycorrhizal symbiosis. *Plant, Cell & Environment*, 39(2), 393-415. <https://doi.org/10.1111/pce.12624>
- Vincent, C., & Gregory, P. (1989). Effects of temperature on the development and growth of winter wheat roots. *Plant and Soil*, 119(1), 87-97.
- Vinocur, B., & Altman, A. (2005). Recent advances in engineering plant tolerance to abiotic stress: achievements and limitations. *Current Opinion in Biotechnology*, 16(2), 123-132.
- Vishwakarma, K., Upadhyay, N., Kumar, N., Yadav, G., Singh, J., Mishra, R. K., Kumar, V., Verma, R., Upadhyay, R., & Pandey, M. (2017). Abscisic acid signaling and abiotic stress tolerance in plants: a review on current knowledge and future prospects. *Frontiers in Plant Science*, 8, 161.
- Vollenweider, P., & Günthardt-Goerg, M. S. (2005). Diagnosis of abiotic and biotic stress factors using the visible symptoms in foliage. *Environmental Pollution*, 137(3), 455-465.
- Vos, I. A., Pieterse, C. M., & Van Wees, S. C. (2013). Costs and benefits of hormone-regulated plant defences. *Plant Pathology*, 62, 43-55.
- Vossen, J. H., Abd-El-Haliem, A., Fradin, E. F., Van Den Berg, G. C., Ekengren, S. K., Meijer, H. J., Seifi, A., Bai, Y., Ten Have, A., & Munnik, T. (2010). Identification of tomato phosphatidylinositol-specific phospholipase-C (PI-PLC) family members and the role of PLC4 and PLC6 in HR and disease resistance. *The Plant Journal*, 62(2), 224-239.
- Vu, H. S., Shiva, S., Roth, M. R., Tamura, P., Zheng, L., Li, M., Sarowar, S., Honey, S., McElhiney, D., Hinkes, P., Seib, L., Williams, T. D., Gadbury, G., Wang, X., Shah, J.,

- & Welti, R. (2014). Lipid changes after leaf wounding in *Arabidopsis thaliana*: expanded lipidomic data form the basis for lipid co-occurrence analysis. *The Plant Journal*, *80*(4), 728-743. <https://doi.org/doi:10.1111/tpj.12659>
- Wahid, A., Farooq, M., Hussain, I., Rasheed, R., & Galani, S. (2012). Responses and Management of Heat Stress in Plants. In P. Ahmad & M. N. V. Prasad (Eds.), *Environmental Adaptations and Stress Tolerance of Plants in the Era of Climate Change* (pp. 135-157). Springer New York. https://doi.org/10.1007/978-1-4614-0815-4_6
- Wahid, A., Gelani, S., Ashraf, M., & Foolad, M. R. (2007, 2007/12/01/). Heat tolerance in plants: An overview. *Environmental and Experimental Botany*, *61*(3), 199-223. <https://doi.org/https://doi.org/10.1016/j.envexpbot.2007.05.011>
- Waldie, T., McCulloch, H., & Leyser, O. (2014). Strigolactones and the control of plant development: lessons from shoot branching. *The Plant Journal*, *79*(4), 607-622.
- Wallis, J. G., & Browse, J. (2002). Mutants of *Arabidopsis* reveal many roles for membrane lipids. *Progress in lipid research*, *41*(3), 254-278.
- Walter, M. (2013). Role of Carotenoid Metabolism in the Arbuscular Mycorrhizal Symbiosis. In *Molecular Microbial Ecology of the Rhizosphere* (pp. 513-524). <https://doi.org/10.1002/9781118297674.ch48>
- Wang, B., Mei, C., & Seiler, J. R. (2015). Early growth promotion and leaf level physiology changes in Burkholderia phytofirmans strain PsJN inoculated switchgrass. *Plant Physiology and Biochemistry*, *86*, 16-23.
- Wang, E., Schornack, S., Marsh, J. F., Gobbato, E., Schwessinger, B., Eastmond, P., Schultze, M., Kamoun, S., & Oldroyd, G. E. (2012). A common signaling process that promotes mycorrhizal and oomycete colonization of plants. *Current Biology*, *22*(23), 2242-2246.
- Wang, J., Wang, C., & Han, X. (2019). Tutorial on lipidomics. *Analytica chimica acta*, *1061*, 28-41. <https://doi.org/https://doi.org/10.1016/j.aca.2019.01.043>
- Wang, J. W., Zheng, L. P., Wu, J. Y., & Tan, R. X. (2006). Involvement of nitric oxide in oxidative burst, phenylalanine ammonia-lyase activation and Taxol production induced by low-energy ultrasound in *Taxus yunnanensis* cell suspension cultures. *Nitric Oxide*, *15*(4), 351-358.
- Wang, K., Senthil-Kumar, M., Ryu, C.-M., Kang, L., & Mysore, K. S. (2012). Phytosterols play a key role in plant innate immunity against bacterial pathogens by regulating nutrient efflux into the apoplast. *Plant Physiology*, *158*(4), 1789-1802.
- Wang, M., Wang, C., Han, R. H., & Han, X. (2016). Novel advances in shotgun lipidomics for biology and medicine. *Progress in lipid research*, *61*, 83-108.
- Wang, M., Wang, C., & Han, X. (2017). Selection of internal standards for accurate quantification of complex lipid species in biological extracts by electrospray ionization mass spectrometry—What, how and why? *Mass spectrometry reviews*, *36*(6), 693-714.

- Wang, R., Zhang, Y., Kieffer, M., Yu, H., Kepinski, S., & Estelle, M. (2016). HSP90 regulates temperature-dependent seedling growth in Arabidopsis by stabilizing the auxin co-receptor F-box protein TIR1. *Nature Communications*, 7(1), 1-11.
- Wang, S. Y., & Lin, H.-S. (2006, 2006/03/16/). Effect of plant growth temperature on membrane lipids in strawberry (*Fragaria×ananassa* Duch.). *Scientia Horticulturae*, 108(1), 35-42. <https://doi.org/https://doi.org/10.1016/j.scienta.2006.01.005>
- Wang, W., Vinocur, B., & Altman, A. (2003). Plant responses to drought, salinity and extreme temperatures: towards genetic engineering for stress tolerance. *Planta*, 218(1), 1-14.
- Wang, W., Vinocur, B., Shoseyov, O., & Altman, A. (2004). Role of plant heat-shock proteins and molecular chaperones in the abiotic stress response. *Trends in Plant Science*, 9(5), 244-252.
- Wang, X. (2004, 2004/06/01/). Lipid signaling. *Current opinion in plant biology*, 7(3), 329-336. <https://doi.org/https://doi.org/10.1016/j.pbi.2004.03.012>
- Wang, Y.-S., Shrestha, R., Kilaru, A., Wiant, W., Venables, B. J., Chapman, K. D., & Blancaflor, E. B. (2006). Manipulation of Arabidopsis fatty acid amide hydrolase expression modifies plant growth and sensitivity to N-acylethanolamines. *Proceedings of the National Academy of Sciences*, 103(32), 12197-12202.
- Warnecke, D., & Heinz, E. (2003, 2003/05/01). Recently discovered functions of glucosylceramides in plants and fungi. *Cellular and Molecular Life Sciences CMLS*, 60(5), 919-941. <https://doi.org/10.1007/s00018-003-2243-4>
- Wasaya, A., Zhang, X., Fang, Q., & Yan, Z. (2018). Root phenotyping for drought tolerance: a review. *Agronomy*, 8(11), 241.
- Wasson, A., Bischof, L., Zwart, A., & Watt, M. (2016). A portable fluorescence spectroscopy imaging system for automated root phenotyping in soil cores in the field. *Journal of Experimental Botany*, 67(4), 1033-1043.
- Weaich, K., Bristow, K. L., & Cass, A. (1996). Modeling preemergent maize shoot growth: I. physiological temperature conditions. *Agronomy Journal*, 88(3), 391-397.
- Weller, D. M., Mavrodi, D. V., van Pelt, J. A., Pieterse, C. M., van Loon, L. C., & Bakker, P. A. (2012). Induced systemic resistance in Arabidopsis thaliana against Pseudomonas syringae pv. tomato by 2, 4-diacetylphloroglucinol-producing Pseudomonas fluorescens. *Phytopathology*, 102(4), 403-412.
- Welte, M. A., & Gould, A. P. (2017). Lipid droplet functions beyond energy storage. *Biochimica et Biophysica Acta (BBA)-Molecular and Cell Biology of Lipids*, 1862(10), 1260-1272.
- Welti, R., Li, W., Li, M., Sang, Y., Biesiada, H., Zhou, H.-E., Rajashekar, C., Williams, T. D., & Wang, X. (2002). Profiling membrane lipids in plant stress responses role of

- phospholipase D α in freezing-induced lipid changes in Arabidopsis. *Journal of Biological Chemistry*, 277(35), 31994-32002.
- Welti, R., Shah, J., Li, W., Li, M., Chen, J., Burke, J., Fauconnier, M.-L., Chapman, K., Chye, M., & Wang, X. (2007). Plant lipidomics: discerning biological function by profiling plant complex lipids using mass spectrometry. *Frontiers in bioscience: a journal and virtual library*, 12.
- Welti, R., & Wang, X. (2004). Lipid species profiling: a high-throughput approach to identify lipid compositional changes and determine the function of genes involved in lipid metabolism and signaling. *Current opinion in plant biology*, 7(3), 337-344.
- Wewer, V., Brands, M., & Dörmann, P. (2014). Fatty acid synthesis and lipid metabolism in the obligate biotrophic fungus *Rhizophagus irregularis* during mycorrhization of *Lotus japonicus*. *The Plant Journal*, 79(3), 398-412. <https://doi.org/10.1111/tpj.12566>
- Wewer, V., Dombrink, I., vom Dorp, K., & Dörmann, P. (2011). Quantification of sterol lipids in plants by quadrupole time-of-flight mass spectrometry. *Journal of lipid research*, 52(5), 1039-1054.
- Wheeler, T., & von Braun, J. (2013). Climate Change Impacts on Global Food Security. *Science*, 341(6145), 508-513. <https://doi.org/10.1126/science.1239402>
- Whipps, J. M. (2001). Microbial interactions and biocontrol in the rhizosphere. *Journal of Experimental Botany*, 52(suppl_1), 487-511.
- WHO. (2018). *The state of food security and nutrition in the world 2018: building climate resilience for food security and nutrition*. Food & Agriculture Org.
- Wilhelm, E. P., Mullen, R. E., Keeling, P., & Singletary, G. (1999). Heat stress during grain filling in maize: effects on kernel growth and metabolism. *Crop Science*, 39(6), 1733-1741.
- Williams, P., Winzer, K., Chan, W. C., & Cámara, M. (2007). Look who's talking: communication and quorum sensing in the bacterial world. *Philosophical Transactions of the Royal Society B: Biological Sciences*, 362(1483), 1119-1134. <https://doi.org/doi:10.1098/rstb.2007.2039>
- Willits, D., & Peet, M. (1998). The effect of night temperature on greenhouse grown tomato yields in warm climates. *Agricultural and Forest Meteorology*, 92(3), 191-202.
- Wise, R., Olson, A., Schrader, S., & Sharkey, T. (2004). Electron transport is the functional limitation of photosynthesis in field-grown Pima cotton plants at high temperature. *Plant, Cell & Environment*, 27(6), 717-724.
- Wissuwa, M., Kretzschmar, T., & Rose, T. J. (2016). From promise to application: root traits for enhanced nutrient capture in rice breeding. *Journal of Experimental Botany*, 67(12), 3605-3615.

- Wollenweber, B., Porter, J. R., & Schellberg, J. (2003). Lack of Interaction between Extreme High-Temperature Events at Vegetative and Reproductive Growth Stages in Wheat. *Journal of Agronomy and Crop Science*, 189(3), 142-150. <https://doi.org/10.1046/j.1439-037X.2003.00025.x>
- Woodfield, H. K., Sturtevant, D., Borisjuk, L., Munz, E., Guschina, I. A., Chapman, K., & Harwood, J. L. (2017). Spatial and temporal mapping of key lipid species in Brassica napus seeds. *Plant Physiology*, 173(4), 1998-2009.
- Wu, Z., Bagarolo, G. I., Thoro-Boveleth, S., & Jankowski, J. (2020, Jun 14). "Lipidomics": Mass spectrometric and chemometric analyses of lipids. *Adv Drug Deliv Rev*. <https://doi.org/10.1016/j.addr.2020.06.009>
- Xie, L.-J., Chen, Q.-F., Chen, M.-X., Yu, L.-J., Huang, L., Chen, L., Wang, F.-Z., Xia, F.-N., Zhu, T.-R., & Wu, J.-X. (2015). Unsaturation of very-long-chain ceramides protects plant from hypoxia-induced damages by modulating ethylene signaling in Arabidopsis. *PLoS genetics*, 11(3), e1005143.
- Xu, S., Li, J., Zhang, X., Wei, H., & Cui, L. (2006). Effects of heat acclimation pretreatment on changes of membrane lipid peroxidation, antioxidant metabolites, and ultrastructure of chloroplasts in two cool-season turfgrass species under heat stress. *Environmental and Experimental Botany*, 56(3), 274-285.
- Xue, H.-W., Chen, X., & Mei, Y. (2009). Function and regulation of phospholipid signalling in plants. *Biochemical Journal*, 421(2), 145-156. <https://doi.org/10.1042/bj20090300>
- Yaeno, T., Matsuda, O., & Iba, K. (2004). Role of chloroplast trienoic fatty acids in plant disease defense responses. *The Plant Journal*, 40(6), 931-941.
- Yang, J., Kloepper, J. W., & Ryu, C.-M. (2009). Rhizosphere bacteria help plants tolerate abiotic stress. *Trends in Plant Science*, 14(1), 1-4.
- Yang, N. J., & Hinner, M. J. (2015). Getting Across the Cell Membrane: An Overview for Small Molecules, Peptides, and Proteins. In A. Gautier & M. J. Hinner (Eds.), *Site-Specific Protein Labeling: Methods and Protocols* (pp. 29-53). Springer New York. https://doi.org/10.1007/978-1-4939-2272-7_3
- Yang, X., Dong, G., Palaniappan, K., Mi, G., & Baskin, T. I. (2017). Temperature-compensated cell production rate and elongation zone length in the root of Arabidopsis thaliana. *Plant, Cell & Environment*, 40(2), 264-276.
- Yu, D., Rupasinghe, T. W., Boughton, B. A., Natera, S. H., Hill, C. B., Tarazona, P., Feussner, I., & Roessner, U. (2018). A high-resolution HPLC-QqTOF platform using parallel reaction monitoring for in-depth lipid discovery and rapid profiling. *Analytica chimica acta*, 1026, 87-100.
- Yu, K., Soares, J. M., Mandal, M. K., Wang, C., Chanda, B., Gifford, A. N., Fowler, J. S., Navarre, D., Kachroo, A., & Kachroo, P. (2013). A feedback regulatory loop between G3P and lipid transfer proteins DIR1 and AZI1 mediates azelaic-acid-induced systemic immunity. *Cell reports*, 3(4), 1266-1278.

- Yu, P., Hochholdinger, F., & Li, C. (2019, 2019-March-29). Plasticity of Lateral Root Branching in Maize [Mini Review]. *Frontiers in Plant Science*, 10. <https://doi.org/10.3389/fpls.2019.00363>
- Zamioudis, C., & Pieterse, C. M. (2012). Modulation of host immunity by beneficial microbes. *Molecular Plant-Microbe Interactions*, 25(2), 139-150.
- Zhalnina, K., Louie, K. B., Hao, Z., Mansoori, N., da Rocha, U. N., Shi, S. J., Cho, H. J., Karaoz, U., Loque, D., Bowen, B. P., Firestone, M. K., Northen, T. R., & Brodie, E. L. (2018, Apr). Dynamic root exudate chemistry and microbial substrate preferences drive patterns in rhizosphere microbial community assembly [Article]. *Nature Microbiology*, 3(4), 470-480. <https://doi.org/10.1038/s41564-018-0129-3>
- Zhang, A., Sun, H., Xu, H., Qiu, S., & Wang, X. (2013, 2013/10/01). Cell Metabolomics. *OMICS: A Journal of Integrative Biology*, 17(10), 495-501. <https://doi.org/10.1089/omi.2012.0090>
- Zhang, G., Ahmad, M. Z., Chen, B., Manan, S., Zhang, Y., Jin, H., Wang, X., & Zhao, J. (2020). Lipidomic and transcriptomic profiling of developing nodules reveals the essential roles of active glycolysis and fatty acid and membrane lipid biosynthesis in soybean nodulation. *The Plant Journal*, 103(4), 1351-1371.
- Zhang, J. H., HUANG, W. D., LIU, Y. P., & PAN, Q. H. (2005). Effects of temperature acclimation pretreatment on the ultrastructure of mesophyll cells in young grape plants (*Vitis vinifera* L. cv. Jingxiu) under cross-temperature stresses. *Journal of Integrative Plant Biology*, 47(8), 959-970.
- Zhao, J. (2015). Phospholipase D and phosphatidic acid in plant defence response: from protein-protein and lipid-protein interactions to hormone signalling. *Journal of Experimental Botany*, 66(7), 1721-1736. <https://doi.org/10.1093/jxb/eru540>
- Zhao, J., Devaiah, S. P., Wang, C., Li, M., Welti, R., & Wang, X. (2013). Arabidopsis phospholipase D β 1 modulates defense responses to bacterial and fungal pathogens. *New Phytologist*, 199(1), 228-240.
- Zhao, Y.-Y., Cheng, X.-l., & Lin, R.-C. (2014). Lipidomics applications for discovering biomarkers of diseases in clinical chemistry. In *International review of cell and molecular biology* (Vol. 313, pp. 1-26). Elsevier.
- Zheng, G., Tian, B., Zhang, F., Tao, F., & Li, W. (2011). Plant adaptation to frequent alterations between high and low temperatures: remodelling of membrane lipids and maintenance of unsaturation levels. *Plant, Cell & Environment*, 34(9), 1431-1442. <https://doi.org/doi:10.1111/j.1365-3040.2011.02341.x>
- Zhou, R., Yu, X., Ottosen, C.-O., Rosenqvist, E., Zhao, L., Wang, Y., Yu, W., Zhao, T., & Wu, Z. (2017). Drought stress had a predominant effect over heat stress on three tomato cultivars subjected to combined stress. *BMC Plant Biology*, 17(1), 1-13.

- Ziska, L., Crimmins, A., Auclair, A., DeGrasse, S., Garofalo, J., Khan, A., Loladze, I., de León, A., Showler, A., & Thurston, J. (2016). Ch. 7: Food safety, nutrition, and distribution. *The impacts of climate change on human health in the United States: a scientific assessment*, 189-216.
- Ziska, L. H., Blumenthal, D. M., Runion, G. B., Hunt, E. R., & Diaz-Soltero, H. (2011). Invasive species and climate change: an agronomic perspective. *Climatic Change*, 105(1), 13-42.
- Zoong Lwe, Z. S., Welti, R., Anco, D., Naveed, S., Rustgi, S., & Narayanan, S. (2020). Heat stress elicits remodeling in the anther lipidome of peanut. *Scientific Reports*, 10(1), 1-18.
- Zúñiga, A., Poupin, M. J., Donoso, R., Ledger, T., Guiliani, N., Gutiérrez, R. A., & González, B. (2013). Quorum sensing and indole-3-acetic acid degradation play a role in colonization and plant growth promotion of *Arabidopsis thaliana* by *Burkholderia* phytofirmans PsJN. *Molecular Plant-Microbe Interactions*, 26(5), 546-553.